EMERGING
INFECTIOUS DISEASES®

Vectorborne Infectious Diseases

August 2021

EMERGING INFECTIOUS DISEASES®

EDITOR-IN-CHIEF
D. Peter Drotman

On the Cover

Jonas Lie (1880–1940) *The Conquerors* (*Culebra Cut, Panama Canal*), **1913**. Oil on canvas, 60 in x 50 in/ 152.4 cm x 127 cm. Image copyright © The Metropolitan Museum of Art, New York, NY, United States. Image source: Art Resource, New York, NY, United States.

About the Cover p. 2244

2020

Dispatches

2027

2164

EMERGING INFECTIOUS DISEASES®

Letters

Books and Media

About the Cover

Etymologia

Research Letters

2209

⊘DPDx

Diagnostic Assistance and Training in Laboratory Identification of Parasites

A free service of CDC available to laboratorians, pathologists, and other health professionals in the United States and abroad

Diagnosis from photographs of worms, histological sections, fecal, blood, and other specimen types

Expert diagnostic review

Formal diagnostic laboratory report

Submission of samples via secure file share

Visit the DPDx website for information on laboratory diagnosis, geographic distribution, clinical features, parasite life cycles, and training via Monthly Case Studies of parasitic diseases.

Considerations for Establishing Successful Coronavirus Disease Vaccination Programs in Africa

Victor Williams, Bassey Edem, Marianne Calnan, Kennedy Otwombe, Charles Okeahalam

The accelerated development of coronavirus disease (COVID-19) candidate vaccines is intended to achieve worldwide immunity. Ensuring COVID-19 vaccination is crucial to stemming the pandemic, reclaiming everyday life, and helping restore economies. However, challenges exist to deploying these vaccines, especially in resource-limited sub-Saharan Africa. In this article, we highlight lessons learned from previous efforts to scale up vaccine distribution and offer considerations for policymakers and key stakeholders to use for successful COVID-19 vaccination rollout in Africa. These considerations range from improving weak infrastructure for managing data and identifying adverse events after immunization to considering financing options for overcoming the logistical challenges of vaccination campaigns and generating demand for vaccine uptake. In addition, providing COVID-19 vaccination can be used to promote the adoption of universal healthcare, especially in sub-Saharan Africa countries.

The World Health Organization (WHO) declared the spread of severe acute respiratory syndrome coronavirus 2 (SARS-COV-2), the causative agent of coronavirus disease (COVID-19), a pandemic in March 2020 on the basis of the rapid rate of increase in infections across many countries. As of May 9, 2021, ≈157 million cases and 3.2 million deaths had been recorded globally (1), a figure that continues to grow. The COVID-19 pandemic, which originated in Wuhan, China, in late 2019, led to global shutdowns or restrictions of economic and social activities and has

Author affiliations: University of the Witwatersrand School of Public Health, Johannesburg, South Africa (V. Williams, K. Otwombe); Medical Research Council Unit The Gambia at London School of Hygiene and Tropical Medicine, Fajara, The Gambia (B. Edem); University Research Co., LLC, Manila, the Philippines (M. Calnan); University of the Witwatersrand Perinatal HIV Research Unit, Johannesburg (K. Otwombe);University of the Witwatersrand Graduate School for Business Administration, Johannesburg (C. Okeahalam)

caused an unprecedented strain on healthcare services. Although the initial infections were transmitted to local residents from travelers, community infections now make up the bulk of new infections despite ongoing use of preventive measures, including restricted movement, sanitization, face mask wearing, and social distancing based on guidelines or mandates enacted by various governments. New infections continue to occur daily, and many countries anticipate a third wave, which is already underway in a few places. Effectively rolling out programs to distribute available vaccines is urgently needed to complement these ongoing public health measures (2,3).

When we have limited knowledge of the epidemiology of an infectious disease, waiting to achieve global herd immunity without a vaccine comes at considerable cost because health systems need to increase their use of resources for unplanned expenses to address illness and death. Herd immunity is the indirect protection from an infectious disease acheived in a susceptible population when an adequate proportion of the population becomes immune to the infection (4,5). Ongoing research has demonstrated that persons who recover from the infection develop antibodies and cellular immune responses that might offer some protection; these findings form the basis for continuing development of COVID-19 vaccines (6,7). The duration of protection achieved postinfection, although uncertain, is estimated to be ≥6 months (4,6,8).

As of May 7, 2021, WHO had documented 183 candidate vaccines in preclinical evaluation stages and 97 in clinical evaluation, including 22 in phase 3 or 4 trials and ≥8 approved by different national regulatory authorities for emergency or full use (8–10). Consequently, vaccination of priority groups and the general population has begun on different scales globally including in countries in Africa. Unfortunately, the discovery of multiple COVID-19 variants has raised uncertainty about the efficacy of

the available vaccines. Variants have been detected in many countries: United States (B.1.526/B.1.526.1/B.1.427/B.1.429), South Africa (B.1.351), United Kingdom (B.1.1.7/B.1.525), Brazil (P.1/P.2), and India (B.1.617/B.1.617.1/B.1.617.2/B.1.617.3) (11).

Considering that successful candidate vaccines will require mass production to meet global demand, governments need to take immediate action to address potential barriers to establishing effective vaccination campaigns in Africa after vaccines are available. Data from WHO and the United Nations Children's Fund (UNICEF) indicate that, in 2019, Africa had the highest levels of unvaccinated children and the highest number (6.8 million) of children without any doses of the diptheria-pertussis-tetanus1 (DPT1) vaccine (12). These data illustrate the challenges facing individual country vaccine programs. However, previous successful vaccination campaigns in Africa provide models from which countries can draw best practices for evidence-informed decision making and planning. MenAfriVac campaigns, introduced in 2010 to provide meningococcal vaccines in the Africa meningitis belt, led to a substantial reduction in meningitis epidemics and a 99% reduction in group A meningococcal meningitis (13). The success can be attributed to commitments from multilateral stakeholders to develop and distribute the vaccine and affected countries to roll out vaccination campaigns with efficient surveillance systems simultaneously (13). Because the target population for COVID-19 vaccination is broader, country vaccination programs in Africa should consider both universal and unique potential challenges to this effort. Anticipating and understanding these challenges and addressing them through data-driven planning, will be vital to overcome barriers to establishing successful COVID-19 vaccination campaigns that include robust social behavior efforts targeted to residents (Table 1).

Vaccine Characteristics

Although many COVID-19 vaccines remain in clinical development, ≥8 vaccine candidates have completed phase 3 trials and received emergency authorization: Oxford-AstraZeneca (https://www.astrazeneca.com), Moderna (https://www.modernatx.com), Pfizer-BioNTech (https://www.pfizer.com), Gamaleya (Sputnik) (https://sputnikvaccine.com), Sinovac (CoronaVac) (http://www.sinovac.com), Sinopharm (http://www.sinopharm.com), Novavax (https://www.novavax.com), and Janssen (Johnson & Johnson) (https://www.jnj.com). Moderna and Pfizer report >90% efficacy and Oxford-AstraZeneca 62%–90% when recipients have been fully vaccinated (9,14–16). Candidate vaccines are mainly being developed from mRNA (e.g., Pfizer-BioNTech and Moderna), nonreplicating viral vector (e.g., Oxford-AstraZeneca, Gamaleya, and Janssen), or inactivated virus (e.g., Sinovac and Sinopharm). The logistic requirements vary for distributing different vaccines. Except for the Janssen vaccine, which requires only 1 dose, all of the vaccines require 2 intramuscular doses administered several days apart (9). The Pfizer-BioNTech and Moderna vaccines might be challenging to administer in Africa because each requires –70°C cold chain storage and transportation (14).

The WHO target product profile for COVID-19 vaccines specifies that target vaccines should be indicated for active immunization, administered in either a 1- or 2-dose regimen, viable for all age groups in an outbreak, including the elderly, and have a rapid onset of protection, preferably ≤2 weeks (17). Also, the vaccine must be prequalified in a multidose vial presentation and be thermostable, which can simplify vaccine distribution and eliminate the additional costs required for cold chain management. Distributing vaccines to target populations in mass campaigns, as postulated, requires a less complex administration route than other distribution strategies. However, mass vaccination campaigns might present some challenges. The elderly constitute an important target population, and inadequate immune response to vaccination in this age group is well documented; in addition, experience with routine immunization of this age group in Africa is limited (18).

Table 1. Key considerations for COVID-19 mass vaccination program development*	
Category	Key considerations
Vaccine characteristic	Vaccine thermostability and requirement for cold chain system; route of administration; no. doses/person; COVID-19 testing capacity; adverse event surveillance
Financing	Ability of low-and middle-income countries to pay for vaccines and deliver financing
Prioritizing beneficiaries	Priority populations: healthcare workers, first responders, essential services personnel, elderly persons, persons with coexisting conditions, children; use of phased approach with timelines
Vaccination policy and logistics	National policy to guide vaccination process and ensure availability of resources. Timelines for receiving and distributing vaccine from manufacturers after procurement
Communications	Effective communication about benefits of the vaccine to increase acceptability, especially with phased approaches
Vaccine data management systems	Track demographics of vaccinated persons, doses received, risk factors, and adverse events

*COVID-19, coronavirus disease.

Influenza and pneumonia are the vaccines most commonly recommended for elderly persons, and studies on the uptake and effectiveness of these vaccines in Africa are few. Studies from South Africa show that elderly populations at risk for high mortality rates have reduced uptake of the influenza vaccine, indicating the need for more effective approaches to increase uptake and ultimately achieve population-level immunity (19). Compared with the influenza vaccine, which showed an efficacy of 30%–50% among persons ≥65 years of age and 70%–90% in children and younger adults, available data from 2 leading vaccine candidates (Pfizer-BionTech and Oxford-AstraZeneca) indicate an efficacy >90% in persons ≥65 years of age (15,16,18). This notable improvement in vaccine design addresses reduced immune response among the elderly.

Program Monitoring

One challenge to establishing vaccination programs in Africa is that data from COVID-19 testing has been suboptimal, which might affect rollout of vaccination campaigns. Because of limited testing, information on the number of cases and patient demographics is lacking, further hindering effective planning. Therefore, countries in Africa need to increase testing capacity to better characterize and manage the pandemic.

Another planning consideration is the capacity to monitor adverse events following immunization (AEFI), which is imperative in the context of a COVID-19 vaccine rollout. First, these vaccines have undergone rapidly accelerated development. The adverse event profiles of the vaccines are not fully known, and early data from trials of 2 leading vaccine candidates suggested more adverse events occurred in the vaccine groups than in the control groups (15,16). After rollout of the vaccines, adverse events including rheumatoid symptoms, blood clots, severe headache, and fever were reported, but WHO guidance indicates that the benefits of the vaccine outweigh the risks (20). Phase 4 studies and robust postmarketing surveillance will strengthen risk profile characterization and help manufacturers and regulators effect risk minimization strategies, vital steps that might have been missed because of the accelerated development and licensing process (21).

South Africa is the only country in Africa that has thus far conducted COVID-19 vaccine trials, indicating that safety and efficacy data for the vaccines might be limited in these populations (14). AEFI reporting has historically been weak in Africa, using only passive monitoring systems that are restricted to tuberculosis (TB) and HIV. However, AEFI systems are being scaled up, as demonstrated in Malawi and the

Democratic Republic of the Congo, where officers are being trained on pharmacovigilance and AEFI with subsequent active follow-up to improve documentation of adverse events from medications and vaccines (22,23). This process has been recognized by WHO as a best practice and recommended for other countries in Africa. Multistakeholder collaborations are needed to sustain the strengthening of postlicensure AEFI monitoring (21) and the national immunization technical advisory groups in each country should identify and address policy issues related to COVID-19 vaccine rollout and administration (24).

Vaccination Logistics

Rollout of a COVID-19 vaccination campaign in Africa will require each country to formulate a national deployment plan, a document that will guide the overall allocation of resources for a successful campaign by ensuring the availability of personal protective equipment, vaccine supply, storage and transportation within a continuous cold chain system (if needed), human resources, security, and other prerequisites (24). It can be argued that some of these resources are already available from the WHO Expanded Program on Immunization (EPI) programs in different countries and that COVID-19 vaccination administration programs can easily be integrated. However, existing EPI programs target specific populations, mainly pregnant women and infants, and might not offer adequate resources to accommodate a large-scale population-based vaccination campaign. In addition, existing challenges encountered by EPI programs, such as lack of funding, human resources, logistics infrastructure, transportation to certain difficult-to-access terrains, and kidnappings and killings of EPI program staff in conflict zones in some Africa countries, further complicate the challenges brought by the COVID-19 pandemic (12). Therefore, careful assessment of the current state of each country's EPI will be required to identify critical deficiencies and necessary resources added before existing EPI infrastructures can be integrated into successful COVID-19 vaccination campaigns. Given that larger populations will need to be vaccinated compared with target groups in previous vaccination campaigns for other diseases, adopting a phased approach based on priorities for vaccinating different population groups in each country could prevent overburdening of existing EPI infrastructures and resources (13,25).

COVID-19 Vaccination Program Financing

To prepare for distributing licensed COVID-19 vaccines once they became available, the United States

and European Union committed funds for developing programmatic infrastructure and purchasing vaccine doses. Considering the cost of advanced candidate vaccines, uncertainty had been expressed about how developing countries would fund vaccine purchases (*26*). A coalition, COVID-19 Global Access (COVAX), led by the Global Alliance for Vaccines and Immunizations (Gavi), the Coalition for Epidemic Preparedness Innovation, and WHO, was tasked with ensuring equitable distribution of licensed COVID-19 vaccines to give developing countries access to the vaccines through the advance market commitment model (*27*). This model has been used to successfully distribute new vaccines, such as pneumococcal conjugate vaccines, in low- and middle-income countries. COVAX has been proposed to provide COVID-19 vaccine for 20% of the population of each country registered under the WHO fair allocation mechanism (*28*). Since February 2021, >41 Africa countries have received 18 million doses of the COVID-19 vaccine from COVAX to commence vaccination of priority populations; COVAX has committed to distributing additional doses to accommodate more vaccinations. So far, vaccinations in Africa constitute ≈1.5% of vaccinations globally. Observed challenges include low vaccine uptake because of poor administration and vaccine hesitancy, which have resulted in expiration of received vaccines in some countries (*29,30*).

Since 2001, the cost of the basic package of vaccines recommended by the United Nations for all children has risen >2,700% (from US $1.38 to $39.00) (*27*) even at the best possible price, paid by the most impoverished countries eligible for support from Gavi. For countries graduating from or not eligible for Gavi assistance, just adding 1 new vaccine to a national EPI program's mandate would cost US $0.54–$2.34 per person in resources above the vaccine purchase price (*31*). However, variations within and between countries and the uncertain price per dose and wastage rates for the candidate COVID-19 vaccines makes the actual administration costs difficult to predict (*32*). Countries need to develop a financial strategy that,

in addition to contributions from COVAX, enables them to procure adequate amounts of the vaccine to ensure access among the beneficiary populations. Considering the number of resources deployed to address the COVID-19 pandemic, reductions in development assistance for health, and economic activity lost because of widespread quarantine, each country needs to carefully identify the resources required for its COVID-19 vaccination program and where to find those resources. Resource requirements will depend on COVID-19 incidence, target vaccination coverage, size of at-risk populations, special demographic and geographic features, availability of existing infrastructure, and competing social priorities (*33*).

In line with the principles of universal health care, vaccination targets should be supported by financial mobilization in a way that ensures resources are available in a timely and reliable manner, do not burden the poor, minimize administrative costs, promote program efficiency, require accountability in resource use, and boost self-sufficiency (*34*). Countries need to consider the pros and cons of each funding source, whether private or public, domestic or external, when making reasoned choices for financing options to achieve vaccination goals of equity, access, use, quality, and safety. For example, depending on out-of-pocket fees to finance immunization services will burden the poor. The type and characteristics of funding mechanisms (Table 2) should also be considered. For example, although trust funds might generate a steady stream of financial resources that can be earmarked for vaccination, they can be administratively costly under certain circumstances.

Prioritizing Vaccine Recipients

Prioritizing who should receive the COVID-19 vaccine and in what order may create ethical dilemmas. COVID-19 vaccine strategies aim to achieve sufficient coverage to develop population-level immunity. However, the people most susceptible to severe COVID-19 infections are often nearing the end of their economic productivity, have underlying conditions,

Table 2. Sources of financing for administering COVID-19 mass vaccination programs*		
Type	Domestic	External
Public	Tax revenues (national or subnational) for current spending	Project grants from bilateral or multilateral agencies
	Tax revenues (national or subnational) for repaying domestically or internationally held debt	Grant portion of development loans
		Budget support
	Social health insurance (compulsory)	Debt relief proceeds
		Sectorwide approaches
Private	User fees (out of pocket, direct employer payment)	Vaccine fund
	Cross-subsidies	Project grants from philanthropic institutions
	Health insurance	Contributions (often in-kind) from vaccine manufacturers
*COVID-19, coronavirus disease.		

Table 3. Guiding ethical principles when considering who should receive COVID-19 vaccine (*35*)*

Principle	Description	Practical application
Equality	Equal interest of everyone unless good reasons to justify differential prioritization	May be most appropriate to guide allocation of scarce resources among persons or populations who can be expected to derive the same benefit from the resource (e.g., high-risk populations)
Best outcomes	Allocation according to capacity to do most good or minimize most harm (e.g., saving most possible lives)	May be most appropriate to guide the allocation of scarce resources that confer substantially different benefits to different persons (e.g., groups expected to derive the most benefit)
Prioritize highest risk	Allocation to persons most at risk	May be most appropriate to guide allocation of resources intended to protect those most at risk (e.g., groups most at risk for infection and severe illness)
Prioritize those tasked with helping others	Allocation to persons with certain skills that can save others or because of their participation in helping others (e.g., vaccine trial volunteers)	May be most appropriate to guide allocation of resources to health care workers, first responders, vaccine trial participants, etc.
*COVID-19, coronavirus disease.		

or both. Although these target populations may be prioritized to receive the vaccine, they often have the weakest immune responses (*18*). However, available data from 2 leading COVID-19 vaccine candidates indicates that, on the contrary, immune responses are similar across all age groups (*15,16*). Conversely, groups at high risk for exposure to the virus, such as healthcare providers, supermarket workers, and other frontline workers, are often young and healthy.

Questions persist about whether to prioritize specific population groups hardest hit by the virus. In sub-Saharan Africa, with its youthful populations, high HIV and TB rates, and inadequate resources, decision makers must make ethically justifiable decisions about who receives the COVID-19 vaccine and in what order (*35*) (Table 3). When identifying priority populations, countries should consider the effects of the availability of data in the immunization system on the criteria, such as age, used to identify potential recipients to ensure accurate tracking. Finally, along with the ethical justifications for which populations are prioritized, countries should consider what they need to achieve to maximize the benefit of the vaccine: preventing increased death and illness by vaccinating populations at highest risk for becoming infected and seriously ill or for transmitting the disease to others and maintaining reciprocal obligations with frontline or critical service providers, including those who volunteered to participate in vaccine development trials, to ensure continuity of services and encourage future participation.

Communicating Accurate Information about COVID-19 Vaccines

Rollout of COVID-19 vaccine programs shows that vaccine hesitancy exists regardless of the proven benefits of vaccination (*36,37*). In a 15-country survey on COVID-19 vaccine perceptions in Africa, 60% of respondents believed that the threat posed by CO-VID-19 is exaggerated, 42% reported that they have

been exposed to a lot of disinformation, and 18% (range 4%–38%) would not accept a COVID-19 vaccine (60% of those because they do not trust the safety of the vaccine and 15% because they claim the virus does not exist) (*37*). These concerns and others posed by the emergence of multiple variants of the virus urgently need to be addressed by providing appropriate information to potential vaccine recipients about the benefits of available vaccines, including offering protection against known variants (*38,39*).

Scale-up of programs to distribute antiretroviral medication to treat HIV has shown that continuous communication promoting benefits and debunking myths related to a particular treatment are needed to increase acceptance (*40*). Vaccines are preventive and do not have a prolonged course like HIV treatment and therefore urgently need widespread acceptance. Vaccine refusal because of stigma or differing personal, cultural, or religious beliefs has contributed to a resurgence in vaccine-preventable diseases, such as measles, which had been greatly reduced in different regions of the world (*41,42*); vaccine refusal poses a threat to COVID-19 vaccine uptake in Africa and other parts of the world. Mass advocacy and information campaigns are needed to address those concerns (*43,44*). In response to this need, WHO developed a COVID-19 vaccine communications plan to promote high vaccine acceptance globally. WHO is also partnering with global and regional organizations, scientific communities, civil societies, policy- and decision-makers, media, and the general public to achieve this by making regular and easily accessible communication available about potential benefits and risks of the vaccines (*21,45*). Countries in Africa should develop country- and culture-specific communication plans in appropriate languages and communication modes to address specific miscommunication and reinforce the use of preventive measures, such as social distancing, handwashing, and face masks, that have been shown to limit transmission of infection. Interim guidance

from WHO on risk communication and community engagement readiness and response to COVID-19 provides a step-by-step guide for country teams (*45*).

Vaccine Data Management Systems

Successful public health interventions require a robust data management system for efficient data collection, analysis, and interpretation to inform planning and admininstration. This necessity was demonstrated during the 2014 Ebola outbreak in West Africa and continues to be used when developing other public health interventions, including those for HIV, TB, and malaria (*46*,*47*). At the onset of the COVID-19 pandemic, different systems were developed by different countries and organizations to document and track the pandemic globally and locally (*1*,*48*). However, challenges arise from duplicate health information systems, systems not being linked to one another or not using unique identifiers for patients, or systems depending on outside donors that are specific to health programs that might not cover all populations in sub-Saharan Africa (*49*). A robust system in which data can be disaggregated into different sociodemographic indices is required for COVID-19 surveillance and tracking related demographics, doses of vaccine administered, adverse events, and underlying conditions in vaccinated persons. Any proposed COVID-19 vaccination data system should be integral to existing country immunization information systems and, where feasible, linked with laboratory information systems to easily verify COVID-19 test results and enhance case-based management (*50*). As COVID-19 vaccines are available, a COVID-19 vaccination certificate might become a requisite for international travel, pending the availability of a cure (*8*). Robust data systems with unique personal identifiers could be used to form a database for identifying and certifying vaccinated persons. Such systems could also support research on vaccine effectiveness. However, the number of doses required for specific vaccines must be considered during planning because of the need to follow up with persons who miss second or third doses. These vaccination information systems will be vital for monitoring, evaluating, and improving surveillance of and response to COVID-19 outbreaks.

Conclusions

The COVID-19 pandemic, although it has disrupted life and destabilized economies globally, has also presented an opportunity for global leaders to reassess basic healthcare infrastructure and preparedness for and capacity to respond to health emergencies in their countries. In many countries, the COVID-19 pandemic response has revealed weaknesses in leadership and disparities in the health infrastructure available to some residents that might be strengthened through collaboration, cooperation, and communication among all stakeholders.

The scientific community's ongoing research and efforts to develop vaccines in the shortest possible time is commendable and should receive maximum support from all stakeholders. Equitable access to these vaccines should be guaranteed and distribution and admininstration not hindered by cost or logistic challenges. In addition, each country should identify suitable funding mechanisms to procure the right number of vaccine doses and plan for how to deliver them to its target populations. Countries need to clearly define policies on who will be prioritized for vaccination and develop clear admininstration strategies to support the vaccination campaign. Adequate health information systems for documentation and data management are required to track progress, identify challenges, and provide evidence for admininstrators and policymakers. Communicating with intended beneficiaries of vaccination is of utmost importance and should be done through various media to address concerns and minimize miscommunication. Appropriate emphasis should also be placed on mass education about COVID-19 and vaccination campaign policies.

About the Author

Dr. Williams is a medical epidemiologist and a graduate of the University of the Witwatersrand School of Public Health. His research interests are emerging infectious diseases, tuberculosis, and vaccine-preventable diseases.

References

1. World Health Organization. WHO coronavirus disease (COVID-19) dashboard [cited 2021 May 9]. https://covid19.who.int
2. Altmann DM, Douek DC, Boyton RJ. What policy makers need to know about COVID-19 protective immunity. Lancet. 2020;395:1527–9. https://doi.org/10.1016/S0140-6736(20)30985-5
3. Horton R. Offline: COVID-19—a reckoning. Lancet. 2020;395:935. https://doi.org/10.1016/S0140-6736(20)30669-3
4. Kirkcaldy RD, King BA, Brooks JT. COVID-19 and postinfection immunity: limited evidence, many remaining questions. JAMA. 2020;323:2245–6. https://doi.org/10.1001/jama.2020.7869
5. Randolph HE, Barreiro LB. Herd Immunity: Understanding COVID-19. Immunity. 2020;52:737–41. https://doi.org/10.1016/j.immuni.2020.04.012
6. Sewell HF, Agius RM, Kendrick D, Stewart M. Covid-19 vaccines: delivering protective immunity. BMJ. 2020; 371:m4838. https://doi.org/10.1136/bmj.m4838

7. Suthar MS, Zimmerman MG, Kauffman RC, Mantus G, Linderman SL, Hudson WH, et al. Rapid generation of neutralizing antibody responses in COVID-19 patients. Cell Rep Med. 2020;1:100040. https://doi.org/10.1016/j.xcrm.2020.100040

8. Phelan AL. COVID-19 immunity passports and vaccination certificates: scientific, equitable, and legal challenges. Lancet. 2020;395:1595–8. https://doi.org/10.1016/S0140-6736(20)31034-5

9. World Health Organization. Draft landscape and tracker of COVID-19 candidate vaccines [cited 2020 Dec 20]. https://www.who.int/publications/m/item/draft-landscape-of-covid-19-candidate-vaccines

10. World Health Organization. COVID-19 vaccines [cited 2021 May 8]. https://www.who.int/emergencies/diseases/novel-coronavirus-2019/covid-19-vaccines

11. Centers for Disease Control and Prevention. SARS-CoV-2 variant classifications and definitions [cited 2021 May 9]. https://www.cdc.gov/coronavirus/2019-ncov/cases-updates/variant-surveillance/variant-info.html

12. World Health Organization and United Nations Children's Fund. Progress and challenges with achieving universal immunization coverage: 2019 WHO/UNICEF estimates of national immunization coverage [cited 2020 Aug 6]. https://www.who.int/immunization/monitoring_surveillance/who-immuniz.pdf

13. Trotter CL, Lingani C, Fernandez K, Cooper LV, Bita A, Tevi-Benissan C, et al. Impact of MenAfriVac in nine countries of the African meningitis belt, 2010-15: an analysis of surveillance data. Lancet Infect Dis. 2017;17:867–72. https://doi.org/10.1016/S1473-3099(17)30301-8

14. Mahase E. Covid-19: What do we know about the late stage vaccine candidates? BMJ. 2020;371:m4576. https://doi.org/10.1136/bmj.m4576

15. Polack FP, Thomas SJ, Kitchin N, Absalon J, Gurtman A, Lockhart S, et al.; C4591001 Clinical Trial Group. Safety and efficacy of the BNT162b2 mRNA Covid-19 vaccine. N Engl J Med. 2020;383:2603–15. https://doi.org/10.1056/NEJMoa2034577

16. Ramasamy MN, Minassian AM, Ewer KJ, Flaxman AL, Folegatti PM, Owens DR, et al.; Oxford COVID Vaccine Trial Group. Safety and immunogenicity of ChAdOx1 nCoV-19 vaccine administered in a prime-boost regimen in young and old adults (COV002): a single-blind, randomised, controlled, phase 2/3 trial. Lancet. 2021;396:1979–93. https://doi.org/10.1016/S0140-6736(20)32466-1

17. World Health Organization. WHO target product profiles for COVID-19 vaccines [cited 2021 May 7]. https://www.who.int/publications/m/item/who-target-product-profiles-for-covid-19-vaccines

18. Ciabattini A, Nardini C, Santoro F, Garagnani P, Franceschi C, Medaglini D. Vaccination in the elderly: The challenge of immune changes with aging. Semin Immunol. 2018;40:83–94. https://doi.org/10.1016/j.smim.2018.10.010

19. van Vuuren A, Rheeder P, Hak E. Effectiveness of influenza vaccination in the elderly in South Africa. Epidemiol Infect. 2009;137:994–1002. https://doi.org/10.1017/S0950268808001386

20. World Health Organization. Statement of the WHO Global Advisory Committee on Vaccine Safety (GACVS) COVID-19 subcommittee on safety signals related to the AstraZeneca COVID-19 vaccine [cited 2021 May 9]. https://www.who.int/news/item/19-03-2021-statement-of-the-who-global-advisory-committee-on-vaccine-safety-(gacvs)-covid-19-subcommittee-on-safety-signals-related-to-the-astrazeneca-covid-19-vaccine

21. World Health Organization. Global vaccine safety. Global Advisory Committee on Vaccine Safety, 27–28 May 2020 [cited 2021 May 9]. https://www.who.int/vaccine_safety/committee/reports/May_2020/en

22. Nzolo D, Kuemmerle A, Lula Y, Ntamabyaliro N, Engo A, Mvete B, et al. Development of a pharmacovigilance system in a resource-limited country: the experience of the Democratic Republic of Congo. Ther Adv Drug Saf. 2019;10:2042098619864853. https://doi.org/10.1177/2042098619864853

23. Jusot V, Chimimba F, Dzabala N, Menang O, Cole J, Gardiner G, et al. Enhancing pharmacovigilance in sub-Saharan Africa through training and mentoring: a GSK pilot initiative in Malawi. Drug Saf. 2020;43:583–93. Erratum in: Drug Saf. 2021;44:723. https://doi.org/10.1007/s40264-020-00925-4

24. Duclos P. National Immunization Technical Advisory Groups (NITAGs): guidance for their establishment and strengthening. Vaccine. 2010;28(Suppl 1):A18–25. https://doi.org/10.1016/j.vaccine.2010.02.027

25. Sarma H, Budden A, Luies SK, Lim SS, Shamsuzzaman M, Sultana T, et al. Implementation of the World's largest measles-rubella mass vaccination campaign in Bangladesh: a process evaluation. BMC Public Health. 2019;19:925. https://doi.org/10.1186/s12889-019-7176-4

26. Kupferschmidt K. 'Vaccine nationalism' threatens global plan to distribute COVID-19 shots fairly. Science [cited 2020 Aug 6]. https://www.sciencemag.org/news/2020/07/vaccine-nationalism-threatens-global-plan-distribute-covid-19-shots-fairly

27. Portnoy A, Ozawa S, Grewal S, Norman BA, Rajgopal J, Gorham KM, et al. Costs of vaccine programs across 94 low- and middle-income countries. Vaccine. 2015;33(Suppl 1):A99–108. https://doi.org/10.1016/j.vaccine.2014.12.037

28. World Health Organization. Fair allocation mechanism for COVID-19 vaccines through the COVAX facility [cited 2021 May 9]. https://www.who.int/publications/m/item/fair-allocation-mechanism-for-covid-19-vaccines-through-the-covax-facility

29. Holder J. Tracking coronavirus vaccinations around the world. The New York Times. Updated 2021 May 8 [cited 2021 May 9]. https://www.nytimes.com/interactive/2021/world/covid-vaccinations-tracker.html

30. Mwai P. British Broadcasting Corporation. Covid-19 Africa: What is happening with vaccines? Updated 2021 April 23 [cited 2021 May 9]. https://www.bbc.com/news/56100076.

31. Brew J, Sauboin C. A systematic review of the incremental costs of implementing a new vaccine in the expanded program of immunization in sub-Saharan Africa. MDM Policy Pract. 2019;4:2381468319894546. https://doi.org/10.1177/2381468319894546

32. Vaughan K, Ozaltin A, Mallow M, Moi F, Wilkason C, Stone J, et al. The costs of delivering vaccines in low- and middle-income countries: Findings from a systematic review. Vaccine X. 2019;2:100034. https://doi.org/10.1016/j.jvacx.2019.100034

33. Guignard A, Praet N, Jusot V, Bakker M, Baril L. Introducing new vaccines in low- and middle-income countries: challenges and approaches. Expert Rev Vaccines. 2019;18:119–31. https://doi.org/10.1080/14760584.2019.1574224

34. Kalantari N, Borisch B, Lomazzi M. Vaccination—a step closer to universal health coverage. J Public Health. 2020:s10389–020–01322-y.

35. World Health Organization. Global health ethics. Ethics and COVID-19: resource allocation and priority setting [cited

2021 May 8]. https://www.who.int/ethics/publications/ethics-and-covid-19-resource-allocation-and-priority-setting/en

36. Sallam M. COVID-19 vaccine hesitancy worldwide: a concise systematic review of vaccine acceptance rates. Vaccines (Basel). 2021;9:160. https://doi.org/10.3390/vaccines9020160

37. Africa Centres for Disease Control and Prevention. COVID-19 vaccine perceptions: a 15-country study [cited 2021 May 9]. https://africacdc.org/download/covid-19-vaccine-perceptions-a-15-country-study

38. Benenson S, Oster Y, Cohen MJ, Nir-Paz R. BNT162b2 mRNA Covid-19 vaccine effectiveness among health care workers. N Engl J Med. 2021;384:1775–7. https://doi.org/10.1056/NEJMc2101951

39. Abu-Raddad LJ, Chemaitelly H, Butt AA. Effectiveness of the BNT162b2 Covid-19 vaccine against the B.1.1.7 and B.1.351 variants. N Engl J Med. 2021 May 5 [Epub ahead of print]. https://doi.org/10.1056/NEJMc2104974

40. Stranix-Chibanda L, Brummel S, Pilotto J, Mutambanengwe M, Chanaiwa V, Mhembere T, et al.; PROMISE study team. Slow acceptance of universal antiretroviral therapy (ART) among mothers enrolled in IMPAACT PROMISE studies across the globe. AIDS Behav. 2019;23:2522–31. https://doi.org/10.1007/s10461-019-02624-3

41. Jegede AS. What led to the Nigerian boycott of the polio vaccination campaign? PLoS Med. 2007;4:e73. https://doi.org/10.1371/journal.pmed.0040073

42. Phadke VK, Bednarczyk RA, Salmon DA, Omer SB. Association between vaccine refusal and vaccine-preventable diseases in the United States: a review of measles and pertussis. JAMA. 2016;315:1149–58. https://doi.org/10.1001/jama.2016.1353

43. Krause NM, Freiling I, Beets B, Brossard D. Fact-checking as risk communication: the multi-layered risk of misinformation in times of COVID-19. J Risk Res. 2020; 23:1052–9. https://doi.org/10.1080/13669877.2020.1756385

44. Malecki KMC, Keating JA, Safdar N. Crisis communication and public perception of COVID-19 risk in the era of social media. Clin Infect Dis. 2021;72:697–702. https://doi.org/10.1093/cid/ciaa758

45. World Health Organization. Risk communication and community engagement readiness and response to coronavirus disease (COVID-19): interim guidance. Updated 2020 March 19 [cited 2021 May 8]. https://apps.who.int/iris/bitstream/handle/10665/331513/WHO-2019-nCoV-RCCE-2020.2-eng.pdf.

46. Fähnrich C, Denecke K, Adeoye OO, Benzler J, Claus H, Kirchner G, et al. Surveillance and Outbreak Response Management System (SORMAS) to support the control of the Ebola virus disease outbreak in West Africa. Euro Surveill. 2015;20:21071. https://doi.org/10.2807/1560-7917.ES2015.20.12.21071

47. Jobanputra K, Greig J, Shankar G, Perakslis E, Kremer R, Achar J, et al. Electronic medical records in humanitarian emergencies—the development of an Ebola clinical information and patient management system. F1000 Res. 2016;5:1477. https://doi.org/10.12688/f1000research.8287.1

48. Dong E, Du H, Gardner L. An interactive web-based dashboard to track COVID-19 in real time. Lancet Infect Dis. 2020;20:533–4. https://doi.org/10.1016/S1473-3099(20)30120-1

49. Mpofu M, Semo BW, Grignon J, Lebelonyane R, Ludick S, Matshediso E, et al. Strengthening monitoring and evaluation (M&E) and building sustainable health information systems in resource limited countries: lessons learned from an M&E task-shifting initiative in Botswana. BMC Public Health. 2014;14:1032. https://doi.org/10.1186/1471-2458-14-1032

50. World Health Organization. Overview of VPD surveillance principles [cited 2021 May 8]. https://www.who.int/immunization/monitoring_surveillance/burden/vpd/WHO_SurveillanceVaccinePreventable_01_Overview_R2.pdf

Address for correspondence: Victor Williams, School of Public Health, University of the Witwatersrand, 27 Saint Andrews Rd, Park Town 2193, Johannesburg, South Africa; email: victormw55@gmail.com

Comparison of Lyme Disease in the United States and Europe

Adriana R. Marques, Franc Strle, Gary P. Wormser

Lyme disease, or Lyme borreliosis, is the most common tickborne disease in the United States and Europe. In both locations, *Ixodes* species ticks transmit the *Borrelia burgdorferi* sensu lato bacteria species responsible for causing the infection. The diversity of *Borrelia* species that cause human infection is greater in Europe; the 2 *B. burgdorferi* s.l. species collectively responsible for most infections in Europe, *B. afzelii* and *B. garinii*, are not found in the United States, where most infections are caused by *B. burgdorferi* sensu stricto. Strain differences seem to explain some of the variation in the clinical manifestations of Lyme disease, which are both minor and substantive, between the United States and Europe. Future studies should attempt to delineate the specific virulence factors of the different species of *B. burgdorferi* s.l. responsible for these variations in clinical features.

Lyme disease, or Lyme borreliosis, is the most common tickborne disease in both the United States and Europe; an estimated ≈476,000 cases are diagnosed and treated per year in the United States and >200,000 cases per year in western Europe (*1–3*). The principal tick vector in the United States is *Ixodes scapularis*, followed by *I. pacificus*; in Europe, most cases are transmitted by *I. ricinus*, followed by *I. persulcatus* ticks (Table 1). The etiologic agent, *Borrelia burgdorferi*, was discovered in 1982 in the United States. Later, it became recognized that strains of *B. burgdorferi* in Europe were more heterogenous than strains in North America. *B. burgdorferi* sensu lato was then classified into 3 main genospecies. The originally discovered genospecies was named *B. burgdorferi* sensu stricto. The second genospecies was named *Borrelia garinii* sp. nov., and the third was named *Borrelia afzelii* sp. nov. Recently, the taxonomy of the family *Borreliaceae* (and the genus *Borrelia*) has been revised into 2 main genera, *Borrelia* and *Borreliella* (*4*). The spirochetes that cause relapsing fever retained the genus name *Borrelia,* and spirochetes that cause Lyme disease have been renamed *Borreliella* (hereafter referred to as Lyme borrelia). However, these changes have been challenged (*5*).

Most cases of Lyme disease in the United States occur in the mid-Atlantic, Northeast, and Upper Midwest regions. *B. burgdorferi* s.s., which also is found in Europe, causes most human infections in the United States (*1,2*); the newly recognized species *B. mayonii* (which is not known to exist in Europe) is an infrequent cause of human illness in the Upper Midwest region of the United States (*6*). The incidence of Lyme disease in Europe is highest in the Scandinavian and Baltic states in northern Europe and in Austria, the Czech Republic, Germany, and Slovenia in central Europe. *B. afzelii* and *B. garinii* are the genospecies most frequently detected in *I. ricinus* and *I. persulcatus* ticks and cause most cases of Lyme disease in Europe (*1,2*). Neither genospecies is found in the United States. Transmission of *B. burgdorferi* s.s. by *I. scapularis* or by *I. pacificus* ticks is very infrequent during the first 36 hours after tick attachment; in contrast, transmission of *B. afzelii* by *I. ricinus* ticks may occur within 24 hours (Table 1) (*7*).

Erythema Migrans and Other Skin Manifestations

After Lyme borrelia are deposited in the skin by the bite of an infected *Ixodes* tick, an infection is typically established at that site, which causes the characteristic skin lesion, erythema migrans (Figure 1). Erythema migrans is the most common clinical manifestation of Lyme disease in the United States and Europe, occurring in ≥80% of patients in both geographic areas (*2*). Overall, US patients with erythema migrans caused by *B. burgdorferi* s.s. are less likely than patients in Europe with erythema migrans caused by *B. afzelii* or *B. garinii* to remember a tick bite at the site of the lesion (25% vs. 60% for *B. afzelii* or 64% for *B. garinii*) but more likely to have concomitant systemic symptoms (69% vs. 38% or

Author affiliations: National Institutes of Health, Bethesda, Maryland, USA (A.R. Marques); University Medical Centre Ljubljana, Ljubljana, Slovenia (F. Strle); New York Medical College, Valhalla, New York, USA (G.P. Wormser)

Table 1. Lyme disease in the United States and Europe

Variable	United States	Europe
Tick vector	*Ixodes scapularis, I. pacificus*	*I. ricinus, I. persulcatus*
Lyme borrelia	Mostly *Borrelia burgdorferi* sensu stricto; *B. mayonii* may occur in the upper midwestern United States	Mostly *B. afzelii* and *B. garinii*, but several other species cause human disease, including *B. burgdorferi* s.s., *B. bavariensis*, *B. spielmanii*, and *B. lusitaniae*
Speed of tick transmission of Lyme borrelia	Rarely before 36 h	*I. ricinus* ticks may transmit *B. afzelii* within 24 h
Predominant patient sex	Male patients account for 56% of reported cases during 2001–2018; no manifestation is predominant among female patients	Most cases of erythema migrans and acrodermatitis chronica atrophicans occur in women; neuroborreliosis and arthritis are predominant in men
Coinfections	Risk depends on the geographic area; the most common co-infections are anaplasmosis and babesiosis.	Risk depends on the geographic area; the most common co-infection is tick-borne encephalitis

37%), multiple erythema migrans skin lesions (13% vs. 5% for both *B. afzelii* and *B. garinii*), and regional lymphadenopathy (29% vs. 8% or 3%) (*8–10*) (Table 2). Erythema migrans lesions in patients acquiring the infection in the United States have a shorter incubation period from tick bite to lesion development and are less likely to have central clearing at the time of diagnosis (*8–10*). The frequency of central clearing at least partially depends on the duration of the erythema migrans lesion before the diagnosis, and the duration is on average longer in Europe than in the United States (*8–10*). In Europe, the percentage of patients with multiple erythema migrans lesions is lower for adult patients than for children (*8–11*), whereas in the United States, multiple erythema migrans lesions occur with similar frequency in adults and children (*8,12–14*). Patients infected with *B. mayonii*, found in the Upper Midwest region of the United States, can exhibit multiple and very small erythema migrans lesions (*6*).

In the United States, an entity referred to as southern tick-associated rash illness (STARI) is associated with a skin lesion very similar to erythema migrans (Figure 2). STARI, however, occurs after the bite of ticks of a different species, *Amblyomma americanum*, and is not caused by Lyme borrelia. The etiology of STARI has not been determined. *A. americanum* ticks are most frequently found in the southeastern and south-central United States, but their range is spreading

to geographic areas where *I. scapularis* tick bites are common (*15*). The potential for diagnostic confusion clearly exists in areas such as Long Island, New York, where both tick species coexist. STARI does not occur in Europe, presumably because *A. americanum* ticks are not found in that geographic area. Available, but limited, data suggest that STARI can be distinguished from erythema migrans on the basis of different serum metabolic profiles (*16*).

Two clinical manifestations of Lyme disease involving the skin occur exclusively in infections acquired in Europe: borrelial lymphocytoma and acrodermatitis chronica atrophicans (ACA) (Figure 3). Borrelial lymphocytoma appears as a small area of skin induration that slowly enlarges to a solitary bluish-red nodule or plaque with a diameter of up to a few centimeters and is predominantly located on the ear lobe in children and on the breast in adults. It usually develops at the site of a tick bite and is often accompanied with an erythema migrans lesion (*17*). ACA is a late cutaneous manifestation of Lyme disease located primarily on the extensor parts of the distal extremities. It starts with reddish-blue discoloration and swelling of the skin (an inflammatory phase), which slowly enlarges and, if untreated, is followed by atrophic changes several months to years later. For some patients, ACA was known to have been preceded by an earlier manifestation of Lyme disease, such as erythema
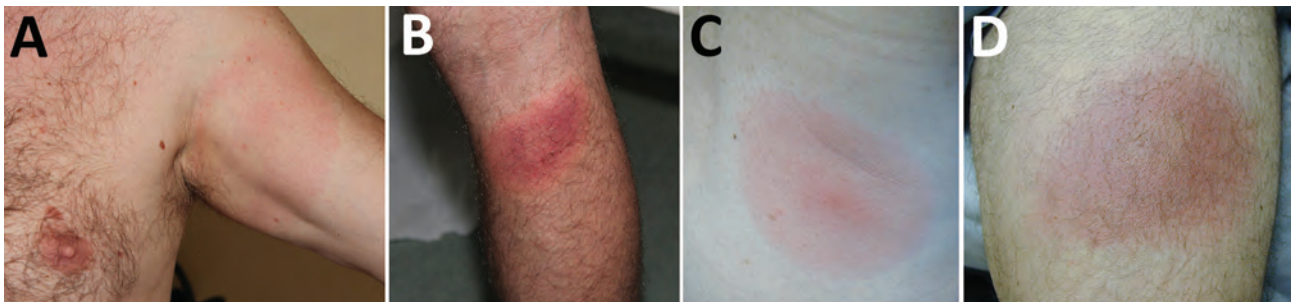
Figure 1. Erythema migrans skin lesions from patients in Europe (A, B) and the United States (C, D).

Table 2. Characteristics of erythema migrans in the United States and Europe

Characteristic	United States, % cases Borrelia burgdorferi sensu stricto*	Europe, % cases B. afzelii†	B. garinii‡
Tick bite at skin site	25	60	64
Central clearing	35	69	62
Systemic symptoms	69	38	37
Multiple erythema migrans lesions	13	5	5
Regional lymphadenopathy	29	8	3

*Data from culture-confirmed erythema migrans caused by *B. burgdorferi* sensu stricto from reference (*8*).
†Data combining patients with culture-confirmed erythema migrans caused by *B. afzelii* from references (*10*) and (*8*).
‡Data from culture-confirmed erythema migrans caused by *B. garinii* from reference (*9*).

migrans (*18*). The apparent explanation for the absence of these manifestations in the United States is that these skin infections are principally caused by *B. afzelii* (Table 3).

Neurologic Manifestations

The typical presentation of early Lyme neuroborreliosis is cranial nerve palsy, particularly facial nerve palsy, as well as lymphocytic meningitis and painful radiculitis. In the United States, the most common manifestation of early Lyme neuroborreliosis is facial palsy. Most cases of early Lyme neuroborreliosis in Europe are caused by *B. garinii* and *B. bavariensis*; in adult patients, painful meningoradiculitis is most common (*19,20*). In a study of 194 adult patients with Lyme neuroborreliosis in Denmark during 2015–2017, radicular pain affected 70% of the patients and facial nerve palsy 43%; intrathecal production of IgG or IgM against Lyme borrelia was found in 87% (*21*). Similar results were found in a retrospective series of 431 Lyme neuroborreliosis patients in Denmark, which included 126 children. Radicular pain (in 66%) and facial nerve palsy (in 41%) were the predominant symptoms; 84.5% of patients had evidence of intrathecal antibody production against Lyme borrelia (*22*). Although there are no comparable studies from the United States, it seems that adult US patients with early Lyme neuroborreliosis less frequently have severe radicular pain (*23*) (Table 3). Newer studies addressing Lyme neuroborreliosis in the United States would be a welcome addition for providing additional data on the frequency of particular symptoms and also on clarifying the frequency of intrathecal antibody production to *B. burgdorferi* s.s. at the time of symptom onset.

Late Lyme neuroborreliosis with encephalitis, myelitis, or encephalomyelitis has been reported in Europe but is very rare in the United States (*24*). On the other hand, 2 neurologic manifestations that have been reported to occur in the United States are now regarded as controversial. The first is Lyme encephalopathy, a poorly defined entity, which occurs in the absence of cerebrospinal fluid pleocytosis, intrathecal production of antiborrelial antibody, or direct microbiologic evidence of *B. burgdorferi* s.s. infection in the central nervous system. Symptoms include memory and concentration complaints. A now-recognized source of confusion with regard to this entity is that some patients with posttreatment Lyme disease syndrome in the United States report cognitive difficulties, and a subset of these patients have abnormal neurocognitive test results (*25,26*). Adding to the controversy, however, is the question of what constitutes dysfunction on such testing and the clinical significance of the test results (*27*).

The second controversial neurologic manifestation in the United States is a chronic distal symmetric sensory neuropathy. In Europe, distal axonal neuropathy in the context of Lyme disease is exclusively associated with ACA. In patients with ACA, the neuropathy is predominantly sensory, most often in the involved skin areas (*28*). Case series in adult patients in the United States reported a similar neuropathy but without evidence of ACA (*29,30*). The distribution of neurologic deficits, which is predominantly sensory, is distal and typically symmetric, but it can be asymmetric. The
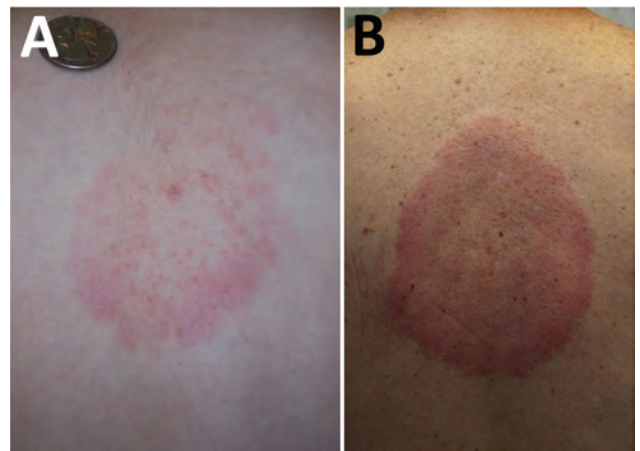
Figure 2. Southern tick-associated rash illness skin lesions. Adapted from Centers for Disease Control and Prevention, National Center for Emerging and Zoonotic Infectious Diseases, Division of Vector-Borne Diseases.
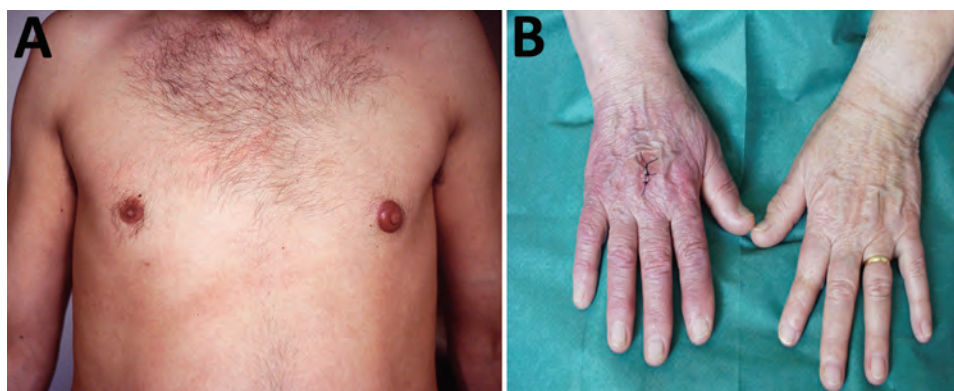
Figure 3. A) Borrelial lymphocytoma on nipple, showing local swelling and a remnant of erythema migrans on chest; at the time of diagnosis, the lesions had been noticed for 6 weeks. B) Acrodermatitis chronica atrophicans involving the right hand, showing red-purple discoloration, swelling, and skin atrophy; at the time of diagnosis, the lesions had been noticed for ≈2.5 years.

neuropathy is primarily axonal and thought to be a mononeuropathy multiplex, which can be confluent (*24*). Cerebrospinal fluid examination is usually unremarkable. Major concerns have been raised as to whether this entity has been appropriately validated as a manifestation of *B. burgdorferi* s.s. infection in the United States (*31*).

Overall, several factors have probably contributed to the belief that cognitive complaints or a chronic distal symmetric sensory peripheral neuropathy was attributable to Lyme disease in the United States (*31*). These factors include the use of diagnostic testing that is no longer considered valid, failure to appreciate that background seropositivity for antibodies to *B. burgdorferi* s.s. exists, and failure to include matched controls to determine if an association with cognitive complaints or peripheral neuropathy with a positive diagnostic assay for Lyme disease is higher than expected.

Lyme Arthritis

Lyme arthritis will develop in ≈60% of US patients with untreated erythema migrans over a 2-year period (*32*) and is said to comprise 28% of Lyme disease cases reported to the US Centers for Disease Control and Prevention that have data on symptoms available (*33*). Lyme arthritis seems to be less frequent in Europe (*34,35*), and for untreated patients in Europe, the interval between onset of erythema migrans and development of Lyme arthritis

may be shorter (*1*). Of note, *B. burgdorferi* s.s. was the most prevalent species of Lyme borrelia found in synovial fluid in a study of patients with Lyme arthritis in Europe (*36*). An acute manifestation of Lyme arthritis in children in the United States can mimic septic arthritis; this manifestation, however, does not seem to occur in children in Europe with Lyme arthritis (*37*).

With regard to demographics, Lyme disease in the United States is more common in male patients (56% of the patients reported during 2001–2018 were male) (*38*). Indeed, no clinical manifestation has been associated with a female predominance in the United States, whereas in Europe, most cases of erythema migrans and ACA occur in women (*39,40*). Many studies (but not all) demonstrated a male predominance for Lyme neuroborreliosis and Lyme arthritis (*22,35,36,41*).

Laboratory Diagnosis, Treatment, and Prophylaxis

In the United States and Europe, most laboratory tests performed to diagnose Lyme disease are based on detecting serum antibodies to Lyme borrelia. Because Lyme disease in Europe is caused by a more diverse group of Lyme borrelia, criteria for test interpretation were more challenging to standardize than in the United States. In the United States, the Centers for Disease Controland Prevention has recommended the

Table 3. Lyme disease clinical manifestations in the United States and Europe

Manifestation	United States	Europe
Radicular pain from Lyme neuroborreliosis	Less common in the United States*	More common in Europe
Lyme arthritis	More common in the United States in untreated patients with erythema migrans; may have septic arthritis-like presentation in children	Occurs in Europe; more commonly associated with *Borrelia burgdorferi* sensu stricto; septic arthritis-like manifestation in children seems to be rare
Acrodermatitis chronica atrophicans	No autochthonous US cases	Occurs in Europe (late manifestation)
Borrelial lymphocytoma	No autochthonous US cases	Occurs in Europe
Lyme encephalopathy	Controversial in the United States	Not recognized to occur
Diffuse axonal peripheral neuropathy	Controversial in the United States	Occurs but only in conjunction with acrodermatitis chronica atrophicans

*More studies, however, are needed.

standard 2-tier algorithm since 1995. This approach typically uses a sensitive enzyme immunoassay (EIA) as the initial step. A negative result requires no further testing. A positive or equivocal result is followed by supplemental testing using separate IgM and IgG immunoblots as the second-tier assay. The interpretation of immunoblot results uses standardized criteria (at least 2 of 3 signature bands for a positive IgM immunoblot and 5 of 10 signature bands for a positive IgG immunoblot). Results from the IgM immunoblot are only relevant when the duration of the illness is <30 days. Of note, testing performed in Europe is more likely to have positive results for patients who acquired Lyme disease in the United States than is testing performed in the United States to diagnose infection acquired in Europe (42). Recently, a 2-EIA approach has been approved as an alternative (or modified) 2-tier testing strategy (Figure 4). This new approach has higher sensitivity in early disease, similar specificity (43), greater ability for automation, and offers objective, quantitative values that leads to less variability in interpretation of the result. Also, the 2-EIA approach can be used in the United States and Europe. Moreover, it opens the door for a possible point-of-care test, a development that would be particularly helpful for patients with facial palsy, carditis, and pediatric patients with Lyme arthritis when septic arthritis is part of the differential diagnosis. A disadvantage is that the 2-EIA approach does not establish the extent of IgG seropositivity, which is essential knowledge for diagnosing late Lyme disease.

Recommendations for treating Lyme disease are generally very similar in guidelines for the United States and Europe. One difference is that phenoxymethylpenicillin (penicillin V) is recommended for treatment of erythema migrans and borrelial lymphocytoma by some of the guidelines in Europe but is not part of the treatment recommendations in the United States (1,44,45). Another difference is the recommendation by some authorities in Europe to use intravenous ceftriaxone to treat erythema migrans, as well as other manifestations of Lyme disease, in pregnant women; whereas in the United States, antimicrobial drug treatment of Lyme disease for pregnant women is the same as that for nonpregnant patients, except that doxycycline is not recommended for pregnant women (1,44,46). Postexposure antimicrobial prophylaxis with a single 200-mg dose of doxycycline has been shown to reduce the risk for Lyme disease after an *I. scapularis* tick bite and is recommended for consideration for tick bite prophylaxis in the United States (44). A recently published study conducted in Europe has also shown that a single 200-mg dose doxycycline successfully prevented Lyme disease after a tick bite (47). To what extent doxycycline will be used
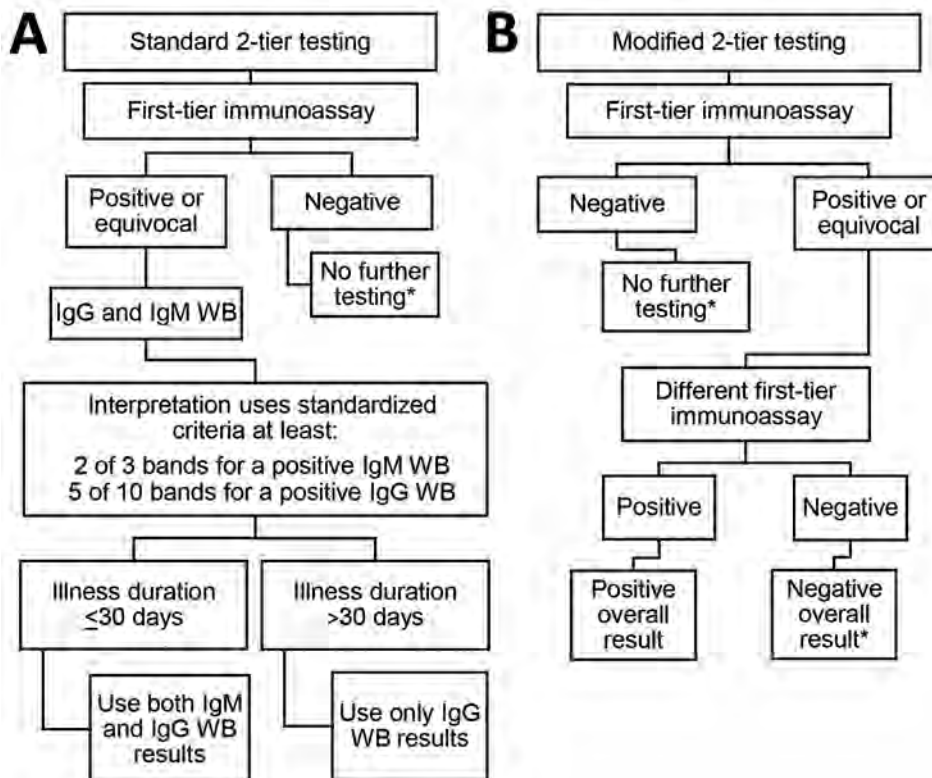
Figure 4. Standard 2-tier and modified 2-tier algorithms for serodiagnosis of Lyme disease. The US Centers for Disease Control and Prevention recommended a standard 2-tier algorithm (A) and the modified 2-tier algorithm (B). *For patients with signs or symptoms consistent with Lyme disease for ≤30 days, the provider may treat and follow up with a convalescent-phase serum sample. Patients with erythema migrans should receive treatment on the basis of the clinical diagnosis. WB, Western blot.

in Europe after a tick bite is unknown; the standard of care has been observation (*1*).

Lyme Borrelia Co-infections

Ixodes ticks can carry multiple pathogens, and a single tick bite may result in transmission of >2 infectious agents. Pathogens potentially transmitted by *I. scapularis* ticks to humans include *B. burgdorferi* s.s., *B. mayonii*, *B. miyamotoi*, *Anaplasma phagocytophilum*, *Babesia microti*, *Ehrlichia muris eauclairensis*, and the deer tick virus subtype of Powassan virus (*48*). The frequency of co-infections depends on the prevalence of the infectious agents in ticks, which will vary in different geographic areas. In the United States, *A. phagocytophilum* and *B. microti* are the most frequent co-infections in patients with Lyme disease (*49*). In the northeastern United States, ≈11% of patients infected with *B. miyamotoi*, a relapsing fever spirochete, are co-infected with *B. burgdorferi* s.s.; of note, *B. miyamotoi* infections per se can cause positive results on first-tier tests for Lyme disease, potentially leading to diagnostic confusion. Encephalitis caused by deer tick virus is relatively rare, but cases may be increasing. In Europe, in addition to Lyme borrelia, *I. ricinus* ticks can transmit tick-borne encephalitis virus, *A. phagocytophilum*, species of the bacterial genus *Rickettsia*, *B. miyamotoi*, and *Babesia* protozoans. Tick-borne encephalitis virus is well recognized as a cause of co-infection in patients with Lyme disease in Europe (*50*). More data are needed on the frequency of co-infections in both the United States and Europe.

Conclusions

Lyme disease is common in many areas of the United States and Europe and may have a variety of clinical manifestations. The duration of infection and the species of Lyme borrelia causing the infection can affect the clinical features of Lyme disease. In the United States, patients with erythema migrans more often have concomitant systemic symptoms than do patients in Europe. In Europe, Lyme arthritis is associated with *B. burgdorferi* s.s. and Lyme neuroborreliosis with *B. garinii*. Certain cutaneous manifestations of Lyme disease in Europe do not occur at all in the United States. It will be valuable to delineate the specific virulence factors of the different species of Lyme borrelia that contribute to these clinical differences.

About the Author

Dr. Marques is chief of the Lyme Disease Studies Unit, Laboratory of Clinical Immunology and Microbiology, Division of Intramural Research, at the National Institute of Allergy and Infectious Diseases, National Institutes of Health, Bethesda, MD. Her primary research interest is clinical research on Lyme disease and other tickborne illnesses.

References

1. Stanek G, Strle F. Lyme borreliosis-from tick bite to diagnosis and treatment. FEMS Microbiol Rev. 2018;42:233–58. https://doi.org/10.1093/femsre/fux047
2. Steere AC, Strle F, Wormser GP, Hu LT, Hovius JW, Branda JA, et al. Lyme borreliosis. Nat Rev Dis Primers. 2016;2:16090. https://doi.org/10.1038/nrdp.2016.90
3. Kugeler KJ, Schwartz AM, Delorey MJ, Mead PS, Hinckley AF. Estimating the frequency of lyme disease diagnoses, United States, 2010–2018. Emerg Infect Dis. 2021;27:616–9. https://doi.org/10.3201/eid2702.202731
4. Barbour AG, Gupta RS. The Family Borreliaceae (Spirochaetales), a diverse group in two genera of tick-borne spirochetes of mammals, birds, and reptiles. J Med Entomol. 2021:tjab055. https://doi.org/10.1093/jme/tjab055
5. Margos G, Castillo-Ramirez S, Cutler S, Dessau RB, Eikeland R, Estrada-Peña A, et al. Rejection of the name *Borreliella* and all proposed species comb. nov. placed therein. Int J Syst Evol Microbiol. 2020;70:3577–81. https://doi.org/10.1099/ijsem.0.004149
6. Pritt BS, Mead PS, Johnson DKH, Neitzel DF, Respicio-Kingry LB, Davis JP, et al. Identification of a novel pathogenic *Borrelia* species causing Lyme borreliosis with unusually high spirochaetaemia: a descriptive study. Lancet Infect Dis. 2016;16:556–64. https://doi.org/10.1016/S1473-3099(15)00464-8
7. Eisen L. Pathogen transmission in relation to duration of attachment by *Ixodes scapularis* ticks. Ticks Tick Borne Dis. 2018;9:535–42. https://doi.org/10.1016/j.ttbdis.2018.01.002
8. Strle F, Nadelman RB, Cimperman J, Nowakowski J, Picken RN, Schwartz I, et al. Comparison of culture-confirmed erythema migrans caused by *Borrelia burgdorferi* sensu stricto in New York State and by *Borrelia afzelii* in Slovenia. Ann Intern Med. 1999;130:32–6. https://doi.org/10.7326/0003-4819-130-1-199901050-00006
9. Strle F, Ružić-Sabljić E, Logar M, Maraspin V, Lotrič-Furlan S, Cimperman J, et al. Comparison of erythema migrans caused by *Borrelia burgdorferi* and *Borrelia garinii*. Vector

Borne Zoonotic Dis. 2011;11:1253–8. https://doi.org/10.1089/vbz.2010.0230

10. Logar M, Ruzić-Sabljić E, Maraspin V, Lotric-Furlan S, Cimperman J, Jurca T, et al. Comparison of erythema migrans caused by *Borrelia afzelii* and *Borrelia garinii*. Infection. 2004;32:15–9. https://doi.org/10.1007/s15010-004-3042-z

11. Arnez M, Pleterski-Rigler D, Luznik-Bufon T, Ruzic-Sabljić E, Strle F. Solitary and multiple erythema migrans in children: comparison of demographic, clinical and laboratory findings. Infection. 2003;31:404–9. https://doi.org/10.1007/s15010-003-4007-3

12. Wormser GP, Ramanathan R, Nowakowski J, McKenna D, Holmgren D, Visintainer P, et al. Duration of antibiotic therapy for early Lyme disease. A randomized, double-blind, placebo-controlled trial. Ann Intern Med. 2003;138:697–704. https://doi.org/10.7326/0003-4819-138-9-200305060-00005

13. Eppes SC, Childs JA. Comparative study of cefuroxime axetil versus amoxicillin in children with early Lyme disease. Pediatrics. 2002;109:1173–7. https://doi.org/10.1542/peds.109.6.1173

14. Gerber MA, Shapiro ED, Burke GS, Parcells VJ, Bell GL; Pediatric Lyme Disease Study Group. Lyme disease in children in southeastern Connecticut. N Engl J Med. 1996; 335:1270–4. https://doi.org/10.1056/NEJM199610243351703

15. Raghavan RK, Peterson AT, Cobos ME, Ganta R, Foley D. Current and future distribution of the lone star tick, *Amblyomma americanum* (L.) (Acari: Ixodidae) in North America. PLoS One. 2019;14:e0209082. https://doi.org/10.1371/journal.pone.0209082

16. Molins CR, Ashton LV, Wormser GP, Andre BG, Hess AM, Delorey MJ, et al. Metabolic differentiation of early Lyme disease from southern tick-associated rash illness (STARI). Sci Transl Med. 2017;9:eaal2717. https://doi.org/10.1126/scitranslmed.aal2717

17. Maraspin V, Nahtigal Klevišar M, Ružić-Sabljić E, Lusa L, Strle F. Borrelial lymphocytoma in adult patients. Clin Infect Dis. 2016;63:914–21. https://doi.org/10.1093/cid/ciw417

18. Ogrinc K, Maraspin V, Lusa L, Cerar Kišek T, Ružić-Sabljić E, Strle F. Acrodermatitis chronica atrophicans: clinical and microbiological characteristics of a cohort of 693 Slovenian patients. J Intern Med. 2021 Feb 7 [Epub ahead of print]. https://doi.org/10.1111/joim.13266

19. Coipan EC, Jahfari S, Fonville M, Oei GA, Spanjaard L, Takumi K, et al. Imbalanced presence of *Borrelia burgdorferi* s.l. multilocus sequence types in clinical manifestations of Lyme borreliosis. Infect Genet Evol. 2016;42:66–76. https://doi.org/10.1016/j.meegid.2016.04.019

20. Ogrinc K, Lusa L, Lotrič-Furlan S, Bogovič P, Stupica D, Cerar T, et al. Course and outcome of early European Lyme neuroborreliosis (Bannwarth syndrome): clinical and laboratory findings. Clin Infect Dis. 2016;63:346–53. https://doi.org/10.1093/cid/ciw299

21. Nordberg CL, Bodilsen J, Knudtzen FC, Storgaard M, Brandt C, Wiese L, et al.; DASGIB study group. Lyme neuroborreliosis in adults: a nationwide prospective cohort study. Ticks Tick Borne Dis. 2020;11:101411. https://doi.org/10.1016/j.ttbdis.2020.101411

22. Knudtzen FC, Andersen NS, Jensen TG, Skarphédinsson S. Characteristics and clinical outcome of Lyme neuroborreliosis in a high endemic area, 1995–2014: a retrospective cohort study in Denmark. Clin Infect Dis. 2017;65:1489–95. https://doi.org/10.1093/cid/cix568

23. Pachner AR, Steere AC. The triad of neurologic manifestations of Lyme disease: meningitis, cranial neuritis, and radiculoneuritis. Neurology. 1985;35:47–53. https://doi.org/10.1212/WNL.35.1.47

24. Halperin JJ. Diagnosis and management of Lyme neuroborreliosis. Expert Rev Anti Infect Ther. 2018;16:5–11. https://doi.org/10.1080/14787210.2018.1417836

25. Klempner MS, Hu LT, Evans J, Schmid CH, Johnson GM, Trevino RP, et al. Two controlled trials of antibiotic treatment in patients with persistent symptoms and a history of Lyme disease. N Engl J Med. 2001;345:85–92. https://doi.org/10.1056/NEJM200107123450202

26. Krupp LB, Hyman LG, Grimson R, Coyle PK, Melville P, Ahnn S, et al. Study and treatment of post Lyme disease (STOP-LD): a randomized double masked clinical trial. Neurology. 2003;60:1923–30. https://doi.org/10.1212/01.WNL.0000071227.23769.9E

27. Binder LM, Iverson GL, Brooks BL. To err is human: "abnormal" neuropsychological scores and variability are common in healthy adults. Arch Clin Neuropsychol. 2009;24:31–46. https://doi.org/10.1093/arclin/acn001

28. Kindstrand E, Nilsson BY, Hovmark A, Pirskanen R, Asbrink E. Peripheral neuropathy in acrodermatitis chronica atrophicans—a late *Borrelia* manifestation. Acta Neurol Scand. 1997;95:338–45. https://doi.org/10.1111/j.1600-0404.1997.tb00222.x

29. Logigian EL, Steere AC. Clinical and electrophysiologic findings in chronic neuropathy of Lyme disease. Neurology. 1992;42:303–11. https://doi.org/10.1212/WNL.42.2.303

30. Halperin JJ, Little BW, Coyle PK, Dattwyler RJ. Lyme disease: cause of a treatable peripheral neuropathy. Neurology. 1987;37:1700–6. https://doi.org/10.1212/WNL.37.11.1700

31. Wormser GP, Strle F, Shapiro ED, Dattwyler RJ, Auwaerter PG. A critical appraisal of the mild axonal peripheral neuropathy of late neurologic Lyme disease. Diagn Microbiol Infect Dis. 2017;87:163–7. https://doi.org/10.1016/j.diagmicrobio.2016.11.003

32. Steere AC, Malawista SE, Snydman DR, Shope RE, Andiman WA, Ross MR, et al. Lyme arthritis: an epidemic of oligoarticular arthritis in children and adults in three Connecticut communities. Arthritis Rheum. 1977;20:7–17. https://doi.org/10.1002/art.1780200102

33. Centers for Disease Control and Prevention. Lyme disease charts and figures: historical data [cited 2020 Nov 15]. https://www.cdc.gov/lyme/stats/graphs.html

34. Enkelmann J, Böhmer M, Fingerle V, Siffczyk C, Werber D, Littmann M, et al. Incidence of notified Lyme borreliosis in Germany, 2013-2017. Sci Rep. 2018;8:14976. https://doi.org/10.1038/s41598-018-33136-0

35. Strle F, Wormser GP, Mead P, Dhaduvai K, Longo MV, Adenikinju O, et al. Gender disparity between cutaneous and non-cutaneous manifestations of Lyme borreliosis. PLoS One. 2013;8:e64110. https://doi.org/10.1371/journal.pone.0064110

36. Grillon A, Scherlinger M, Boyer PH, De Martino S, Perdriger A, Blasquez A, et al. Characteristics and clinical outcomes after treatment of a national cohort of PCR-positive Lyme arthritis. Semin Arthritis Rheum. 2019;48:1105–12. https://doi.org/10.1016/j.semarthrit.2018.09.007

37. Huppertz HI, Karch H, Suschke HJ, Döring E, Ganser G, Thon A, et al.; The Pediatric Rheumatology Collaborative Group. Lyme arthritis in European children and adolescents. Arthritis Rheum. 1995;38:361–8. https://doi.org/10.1002/art.1780380310

38. Centers for Disease Control and Prevention. Lyme disease charts and figures: most recent year [cited 2020 Nov 15]. https://www.cdc.gov/lyme/datasurveillance/charts-figures-recent.html

39. Sajanti E, Virtanen M, Helve O, Kuusi M, Lyytikäinen O, Hytönen J, et al. Lyme borreliosis in Finland, 1995–2014. Emerg Infect Dis. 2017;23:1282–8. https://doi.org/10.3201/eid2308.161273

40. Bennet L, Stjernberg L, Berglund J. Effect of gender on clinical and epidemiologic features of Lyme borreliosis. Vector Borne Zoonotic Dis. 2007;7:34–41. https://doi.org/10.1089/vbz.2006.0533

41. Rojko T, Bogovič P, Lotrič-Furlan S, Ogrinc K, Cerar-Kišek T, Glinšek Biškup U, et al. *Borrelia burgdorferi* sensu lato infection in patients with peripheral facial palsy. Ticks Tick Borne Dis. 2019;10:398–406. https://doi.org/10.1016/j.ttbdis.2018.11.019

42. Wormser GP, Tang AT, Schimmoeller NR, Bittker S, Cooper D, Visintainer P, et al. Utility of serodiagnostics designed for use in the United States for detection of Lyme borreliosis acquired in Europe and vice versa. Med Microbiol Immunol (Berl). 2014;203:65–71. https://doi.org/10.1007/s00430-013-0315-0

43. Marques AR. Revisiting the Lyme disease serodiagnostic algorithm: the momentum gathers. J Clin Microbiol. 2018;56:e00749–18. https://doi.org/10.1128/JCM.00749-18

44. Lantos PM, Rumbaugh J, Bockenstedt LK, Falck-Ytter YT, Aguero-Rosenfeld ME, Auwaerter PG, et al. Clinical Practice Guidelines by the Infectious Diseases Society of America (IDSA), American Academy of Neurology (AAN), and American College of Rheumatology (ACR): 2020 Guidelines for the Prevention, Diagnosis and Treatment of Lyme Disease. Clin Infect Dis. 2021;72:1–8.

45. Wormser GP, Strle F. Evaluation of the role of oral penicillin for treating Lyme disease patients with erythema migrans in the United States. Diagn Microbiol Infect Dis. 2020;97:115071. https://doi.org/10.1016/j.diagmicrobio.2020.115071

46. Maraspin V, Lusa L, Blejec T, Ružić-Sabljić E, Pohar Perme M, Strle F. Course and outcome of erythema migrans in pregnant women. J Clin Med. 2020;9:E2364. https://doi.org/10.3390/jcm9082364

47. Harms MG, Hofhuis A, Sprong H, Bennema SC, Ferreira JA, Fonville M, et al. A single dose of doxycycline after an *Ixodes ricinus* tick bite to prevent Lyme borreliosis: an open-label randomized controlled trial. J Infect. 2021;82:98–104. https://doi.org/10.1016/j.jinf.2020.06.032

48. Nelder MP, Russell CB, Sheehan NJ, Sander B, Moore S, Li Y, et al. Human pathogens associated with the blacklegged tick *Ixodes scapularis*: a systematic review. Parasit Vectors. 2016;9:265. https://doi.org/10.1186/s13071-016-1529-y

49. Centers for Disease Control and Prevention. Nationally notifiable infectious diseases and conditions, United States: annual tables. Annual data for 2018. Tables 1, 2c, 2e [cited 2020 Nov 15]. https://wonder.cdc.gov/nndss/nndss_annual_tables_menu.asp?mmwr_year=2018

50. Velušček M, Blagus R, Cerar Kišek T, Ružić-Sabljić E, Avšič-Županc T. F Bajrović F, et al. Antibiotic use and long-term outcome in patients with tick-borne encephalitis and co-infection with *Borrelia Burgdorferi* sensu lato in central Europe. A retrospective cohort study. J Clin Med. 2019;8:E1740. https://doi.org/10.3390/jcm8101740

Address for correspondence: Adriana Marques. Laboratory of Clinical Immunology and Microbiology, National Institute of Allergy and Infectious Diseases, National Institutes of Health, 10/12C118 10 Center Dr, Bethesda, MD 20892, USA; email: amarques@niaid.nih.gov

Mycobacterium microti Infections in Free-Ranging Red Deer (*Cervus elaphus*)

Giovanni Ghielmetti, Anne M. Kupca, Matthias Hanczaruk, Ute Friedel, Hubert Weinberger,
Sandra Revilla-Fernández, Erwin Hofer, Julia M. Riehm, Roger Stephan, Walter Glawischnig

Infections with *Mycobacterium microti*, a member of the *M. tuberculosis* complex, have been increasingly reported in humans and in domestic and free-ranging wild animals. At postmortem examination, infected animals may display histopathologic lesions indistinguishable from those caused by *M. bovis* or *M. caprae*, potentially leading to misidentification of bovine tuberculosis. We report 3 cases of *M. microti* infections in free-ranging red deer (*Cervus elaphus*) from western Austria and southern Germany. One diseased animal displayed severe pyogranulomatous pleuropneumonia and multifocal granulomas on the surface of the pericardium. Two other animals showed alterations of the lungs and associated lymph nodes compatible with parasitic infestation. Results of the phylogenetic analysis including multiple animal strains from the study area showed independent infection events, but no host-adapted genotype. Personnel involved in bovine tuberculosis–monitoring programs should be aware of the fastidious nature of *M. microti*, its pathogenicity in wildlife, and zoonotic potential.

Tuberculosis (TB) is one of the most prevalent zoonotic diseases worldwide and remains the leading cause of death from a single infectious agent (*1*). The causative pathogens of TB in humans and animals are a group of closely related acid-fast bacilli commonly known as the *Mycobacterium tuberculosis* complex (MTBC). One animal-adapted sublineage within the complex, *M. microti*, was first isolated from field voles (*Microtus agrestis*) that had granulomatous tuberculosis-like lesions (*2*). Although wild rodents, such as bank voles (*Myodes glareolus*), wood mice (*Apodemus sylvaticus*), and shrews

Author affiliations: Institute for Food Safety and Hygiene, Section of Veterinary Bacteriology, Vetsuisse Faculty University of Zurich, Zurich, Switzerland (G. Ghielmetti, U. Friedel, R. Stephan); Bavarian Health and Food Safety Authority, Oberschleissheim, Germany (A.M. Kupca, M. Hanczaruk, J.M. Riehm); Institute for Veterinary Disease Control, Austrian Agency for Health and Food Safety (AGES), Innsbruck and Mödling, Austria (H. Weinberger, S. Revilla-Fernández, E. Hofer, W. Glawischnig)

(*Sorex araneus*), are considered to be primary reservoirs for *M. microti*, several other hosts have been identified, including domestic and wild animals (*3,4*). Overall, cats (*5,6*), New World camelids (*7*), and free-ranging wild boar (*8–10*) seem to be prone to *M. microti* infections; humans (*11–14*) and other animal species, including pigs (*15*), goats (*16*), cattle (*17,18*), dogs (*19*), captive meerkats (*20*), squirrel monkeys (*21*), and ferrets (*14*), are most likely incidental hosts.

This broad host range, however, highlights the pathogenic potential of *M. microti* and the need to reveal its virulence mechanisms. Comparative genomics studies have identified >100 genes whose presence are facultative and differ among members of MTBC. Many of these genes occur in chromosomal regions of difference (RD) that have been deleted from certain species and that may confer differences in phenotype, host range, and virulence (*22*). Isolates of the animal-adapted ecotype defined as *M. microti* are characterized by the deletion of the RD1[mic] in the RD1 region, which includes open reading frame coding for well-known virulence factors, such as early secreted antigenic target (ESAT) 6, locus tag Rv3875, and CFP-10, a culture filtrate protein encoded by the neighboring gene Rv3874 (*23*). Strains lacking RD1 are likely to be less virulent or pathogenic than other members of the MTBC possessing an intact locus (*22*). However, pulmonary and disseminated *M. microti* infections have been described in both immunocompromised and immunocompetent human patients in different countries in Europe (*11,12,14,24*). Until recently, reports of *M. microti* infections were geographically restricted to continental Europe and the United Kingdom. However, a recent study from South Africa revealed the presence of this *Mycobacterium* species in 1.9% of local human tuberculosis cases (*25*). These findings highlight the potential of *M. microti* to cause clinical illness in immunocompetent patients and suggest that the pathogenicity of certain strains is higher than previously estimated.

Therefore, it is crucial to identify clinical MTBC isolates at the species level, and the zoonotic risk posed by *M. microti* should be further evaluated.

The mode of infection of *M. microti* can only be speculated for humans, animals, and in particular herbivores, such as free-ranging red deer. Similar to that for *M. caprae*, transmission of *M. microti* is likely to occur indirectly through a contaminated environment. Wounds in the oral cavity may play an important role as entry ports for *M. microti*; involvement of the lungs, heart, and eventually additional organs is most likely a consequence of bacteremia, as it is in other animal species (*3,5*). The first confirmed *M. caprae* TB case in deer in western Austria was recorded in 1998. Subsequent infections in cattle, deer, and humans were reported in the same area (*26*). As a consequence, an ongoing wildlife surveillance program monitoring *M. caprae* in deer was started in 2008 (*27*). Furthermore, Germany in 2007 and Switzerland in 2013 reported anecdotal outbreaks in cattle (*28,29*). During 2011–2013, a monitoring program coordinated by the EMIDA ERA-Net (Coordination of European Research on Emerging and Major Infectious Diseases of Livestock European Research Area Networks) partnership and including specific regions of Austria, Switzerland, Germany, and Italy was conducted with the aim of investigating the prevalence of bovine tuberculosis (bTB) in red deer and additional wildlife species such as wild boar, chamois, and roe deer (*30,31*). We report 3 TB cases in red deer identified within the framework of these monitoring programs.

Study Material and Methods

Cases
Three cases of natural *M. microti* infections in red deer were identified (Table 1). The deer in case 1, a highly emaciated 9-year-old stag from the province of Vorarlberg, Austria, was humanely killed by a local game warden, who submitted the lungs, heart, and lymphatic tissues (including medial retropharyngeal, tracheobronchial, and mediastinal lymph nodes) fresh for pathoanatomic inspection. Thereafter, histologic examination and mycobacterial analysis of the lungs were performed. The deer in case 2 was a stag 1–3 years of age and in case 3 a hind >2 years of age, both in the province of Miesbach, Germany, where deer are regularly hunted. The heads, lungs, intestines, and associated lymph nodes were macroscopically inspected; subsequently, histopathologic and bacteriologic examinations of the lungs and lymph nodes were performed.

Mycobacterial Analyses and Histologic Examination
We isolated mycobacteria following a standardized protocol as described elsewhere (*32*). In brief, 2–3 g of minced tissue samples were homogenized in 5 mL 0.9% NaCl solution by using a rotating-blade macerator system (Ultra-Turrax IKA, https://www.ika.com). The suspension was decontaminated by using 1% N-acetyl-L-cystein-NaOH solution and neutralized with 20 mL phosphate buffer (pH 6.8). We centrifuged the solution for 20 min at 3300 × *g* and plated the obtained pellet on 2 growth media: Löwenstein-Jensen medium with glycerin and PACT (polymyxin B, amphotericin B, carbenicillin, and trimethoprim) and Stonebrink medium with pyruvate and PACT (BD, https://www.bd.com). Cultures of lung and lymph node specimens on solid Stonebrink medium yielded growth of suspicious mycobacterial colonies after 4–6 wk of incubation at 37°C. The isolates were identified by using GenoType MTBC reversed line blotting (Hain Lifescience, https://www.hain-lifescience.de). For histologic examination, we fixed tissue samples in 10% nonbuffered formalin for ≈48 h, then trimmed and routinely embedded them in paraffin wax. Sections of 3–4 μm were prepared and stained with hematoxylin and eosin (HE) and Ziehl Neelsen (ZN) or modified ZN (*33*).

Investigation of Phylogenetic Relationships
DVR spoligotyping (direct variable repeat spacer oligonucleotide typing) was performed using a commercial microarray system (Alere Technologies, https://www.globalpointofcare.abbott) with integrated data analysis as described elsewhere (*29*). Multilocus variable-number tandem repeats analysis (MLVA) was conducted based on the 24-loci panel standardized for *M. tuberculosis* typing (*34*). We amplified the single markers by endpoint PCR and subsequently analyzed them by using a capillary electrophoresis device (*29*). To investigate the phylogenetic relationships between the 3 isolates from red deer, we analyzed 8 additional strains isolated from different wild and domestic hosts that originated from the regions bordering Germany, Austria, and Switzerland by MLVA (Table 2). We calculated a neighbor-joining

Table 1. Overview of 3 cases of tuberculosis caused by *Mycobacterium microti* in red deer, Austria and Germany

Case	Age, y/sex	Year isolated	Main findings	Country
1	9/M	2017	Severe pyogranulomatous pleuropneumonia, multifocal to coalescing granulomas on the epicardium	Austria
2	1–3/M	2013	Moderate focal nonpurulent pneumonia	Germany
3	>2/F	2013	Moderate purulent bronchitis and bronchiolitis, fibroblastic pleuritis, lungworms	Germany

phylogenic tree based on the copy numbers of the tested loci using the MIRU-VNTR*plus* (https://www.miru-vntrplus.org/MIRU) server and exported it using MEGAX version 10.11 (*35*).

Results

Case 1
Postmortem examination of the stag revealed multiple enlarged lymph nodes exhibiting a whitish cut surface. The lung tissue showed severe pyogranulomatous pleuropneumonia with multifocal to confluent cavernous granulomas of 2–10 mm diameter (Figure 1, panel A). Multifocal to coalescing granulomas of 4–25 mm diameter were observed on the surface of the epicardium (Figure 1, panel B). Histopathologic examination of the lung revealed a severe chronic multifocal to coalescing pyogranulomatous pneumonia with focal areas of fibrosis, central areas of necrosis and mineralization, surrounded by numerous epithelioid macrophages and a few multinucleated Langhans giant cells. Lymphocytes, plasma cells and occasionally well-differentiated fibroblasts surrounded the granulomas (Figure 1, panel C). Few extracellular and intracellular acid-fast bacilli were identified in the pulmonary lesions by using ZN staining (Figure 1, panel D).

Case 2
Macroscopically, a single yellowish, pinhead-sized focus in the left dorsal main lobe of the lung of this

Table 2. Multilocus variable-number tandem-repeat analysis of 8 *Mycobacterium microti* strains used in study of tuberculosis caused by *M. microti* in red deer, Austria and Germany

Strain	Year isolated	Host	Country	Reference
TG 481	2010	Wild boar	Switzerland	(*31*)
TG 435	2010	Wild boar	Switzerland	(*31*)
TI 17–1545	2017	Wild boar	Switzerland	(*9*)
TG 15–1955	2015	Cat	Switzerland	(*5*)
TG 15–294	2015	Cat	Switzerland	This study
ZH 1522744	2016	Cat	Switzerland	(*5*)
18–2304	2016	Red fox	Austria	This study
SG 17–2287	2017	Alpaca	Switzerland	This study

stag was observed. Lymph nodes and intestines did not display any abnormalities. Histologically, the pulmonary focus consisted of macrophages and lymphocytes with single multinucleated Langhans-type giant cells in the lesion, surrounded by eosinophilic lymphocytes (Figure 2). Numerous eosinophilic granulocytes were seen in the pulmonary lymph node. These findings were compatible with a parasitic infestation. Intracellular acid-fast bacilli could not be identified by using modified ZN staining.

Case 3
The caudal part of the main lobes of the lung of this hind showed multiple whitish foci ≤0.5 cm in size. Enlarged pulmonary lymph nodes and multifocal fibroblastic pleuritis were observed. The histologic examination revealed moderate purulent bronchitis and bronchiolitis with several intraluminal stages of lungworms and infiltration of numerous eosinophilic

Figure 1. Macroscopic and histopathologic features in the red deer in case 1 in study of tuberculosis caused by *Mycobacterium microti* in red deer, Austria and Germany. A) Gross picture of the cutting surface of the lungs with severe pyogranulomatous pleuropneumonia with multifocal to confluent cavernous granulomas, 2–10 mm diameter. B) Multifocal to coalescing granulomas 4–25 mm diameter on the surface of the epicardium. C) Chronic multifocal to coalescing pyogranulomatous pneumonia in lungs with central areas of necrosis and mineralization surrounded by numerous epithelioid macrophages and a few multinucleated Langhans giant cells. Single lymphocytes and plasma cells were observed around the periphery and between the granulomas, hematoxylin and eosin stain. Scale bar = 20 μm. D) Numerous macrophages and epithelioid cells containing solitary or multiple acid-fast bacilli. Ziehl Neelsen stain. Scale bar = 10 μm.
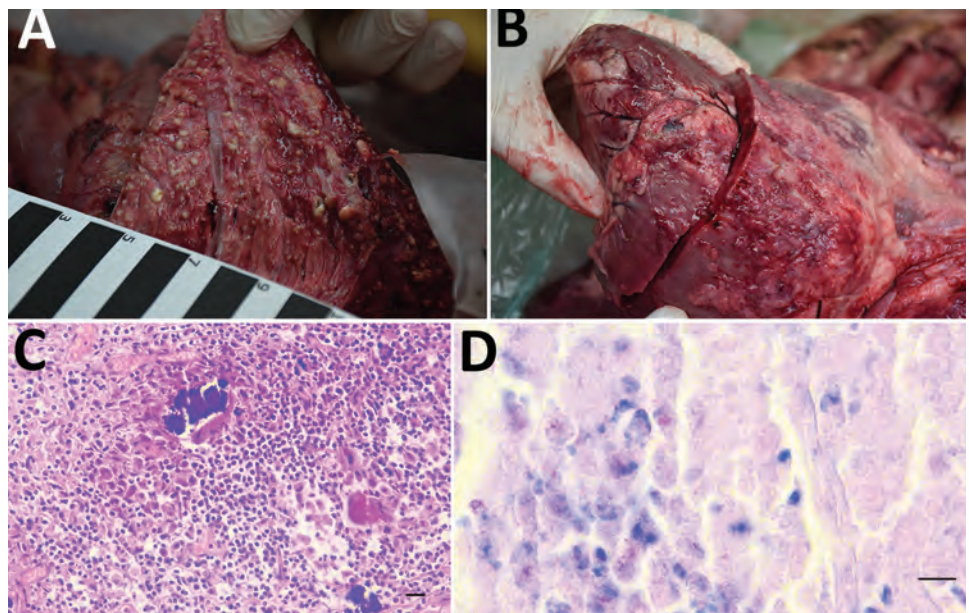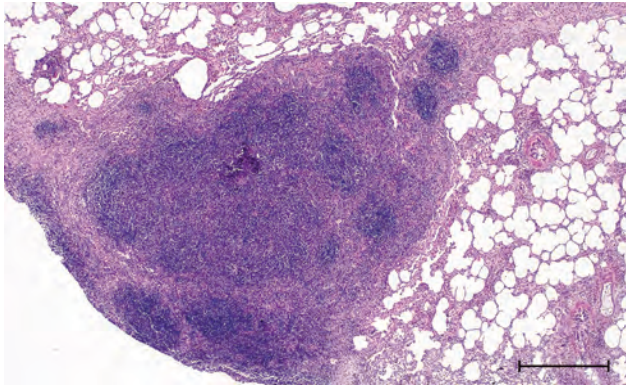
Figure 2. Histopathologic features in red deer in case 2 in study of tuberculosis caused by *Mycobacterium microti* in red deer, Austria and Germany. Lung tissue highly infiltrated by round cells, predominantly lymphocytes and some macrophages, single multinucleated Langhans-type giant cells, hematoxylin and eosin stain. Scale bar = 500 µm.

granulocytes. We observed very few multinucleated Langhans-type giant cells (Figure 3) and could identify no intracellular acid-fast bacilli in the lesions using modified ZN staining.

Investigation of Phylogenetic Relationships

The isolates from 11 animals (3 wild boars, 3 cats, 1 alpaca, and 1 red fox), integrated for further comparative genotyping, exhibited the same spoligotype signature, SB0118, characterized by the presence of spacers 37–38 (https://www.mbovis.org). The same signature is also registered in the international spoligotyping database SpolDB4 as ST 539 and is characteristic
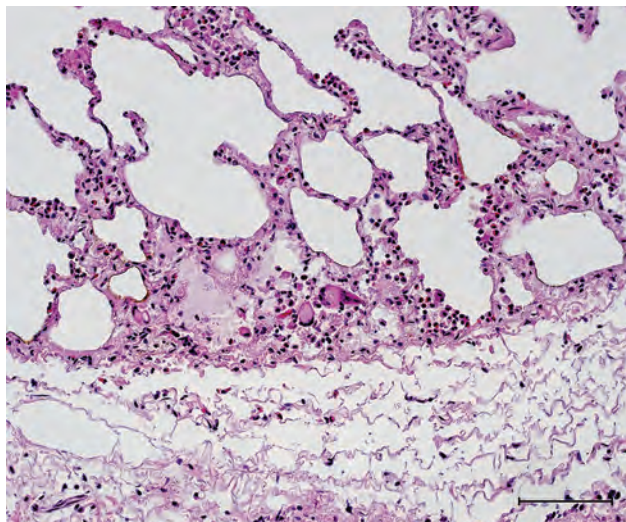
Figure 3. Histopathologic features in red deer in case 3 in study of tuberculosis caused by *Mycobacterium microti* in red deer, Austria and Germany. Lung tissue with granulocytic infiltration and some multinucleated Langhans-type giant cells, hematoxylin and eosin stain. Scale bar = 100 µm.

of *M. microti* (*36*). MLVA showed 2 distinct genotypes (Figure 4; Appendix, https://wwwnc.cdc.gov/EID/article/27/8/21-0634-App1.xlsx), 1 for the 2 identical isolates from the red deer from Germany and 1 for the red deer isolate from Austria. Of interest, the isolates from Germany were closely related to isolates from Switzerland, whereas 2 isolates from Austria, originating from a red deer (case 1) and a red fox, were genetically more distant despite their geographic proximity (Figure 5).

Discussion

Case 1 in this study reported an *M. microti*–positive stag killed in the alpine region in western Austria manifesting clinical signs of tuberculosis. Tuberculosis caused by *M. caprae* has been described several times in domestic animals and wildlife in this area (*26,30*). Specifically, red deer represent a reservoir and a possible source of infection with *M. caprae* for cattle in Austria, Germany, Italy, and Switzerland (*26,28,29,37*). *M. microti* has been isolated only once in Austria, from a red fox without visible lesions (Table 2). This fox was located at a distance of ≈30 km from the site where the *M. microti*–positive stag in case 1 was found. Clear evidence proving transmission of *M. microti* between individual animals of the same species or between species is missing. Human-to-human transmission regarding this pathogen has previously been investigated and the possibility cannot be dismissed (*14*). However, ingesting feed or water from contaminated sources, for example, might play an important role in transmitting mycobacteria to wildlife. In fact, recent reports suggest that *M. microti* infections might often occur through oral ingestion and that direct transmission between animals is less likely (*9,20*).

The presence of MTBC in wild red deer seems to depend on multiple factors, such as population density, TB prevalence in nearby cattle or other wildlife species, and the morphologic structure of the habitat. Observations made from infected wild deer in New Zealand showed that *M. bovis* prevalence decreased substantially after control of TB-infected possums, suggesting that wild deer may be spillover hosts that can be regularly reinfected by possums (*38*). In fact, considering the high levels (>50%) of bTB in cattle in Europe before eradication campaigns, sporadic transmissions to wildlife populations might have occurred. It is, however, surprising to note that as a result of successfully lowering the prevalence in cattle, the disease has been eradicated from wild deer populations, such as in Switzerland (*38*). The situation is considerably different for deer in captivity or in high-density

populations, which could be the origin of TB dissemination to other species (*39*). Of interest, the virulence of *M. microti* seems to vary greatly both between host species and within the same species. Most visible lesions compatible with TB diagnosed in *M. bovis*– and *M. caprae*–infected red deer are located in the lymph nodes, particularly the medial retropharyngeal and mesenteric lymph nodes, suggesting oral rather than aerosol transmission. The respiratory tract, including the lungs and associated lymph nodes, seems to be affected by MTBC in a secondary phase of the infection, which is also likely for *M. microti* infections in red deer (*30*).

DVR spoligotyping analysis is a popular technique worldwide for molecular characterization of MTBC of animal origin with excellent resolution and cost-benefit ratio (*40,41*), but the discriminatory power is too low to prove any link on an epidemiologic

level or even minute transmission patterns among *M. microti* lineages. The molecular background of *M. microti* seems highly conserved, and traceback analyses are delicate. The 11 isolates included in this study were collected over an 8-year period from regions bordering Austria, Germany, and Switzerland (Table 2). These strains originated from 5 different wild and domestic animal species, and most of the animals in these cases showed severe TB lesions. Although the number of isolates investigated was small, in accordance with previous studies, no correlation between host species and *M. microti* genotypes was observed (*4,42*). Moreover, even though the isolates from Switzerland were genetically close, genetic variation determined by MLVA did not correlate with the relative geographic distance of their origin. In fact, the isolates from red deer in Germany were genetically closer to the strains from Switzerland, whereas the 2 isolates
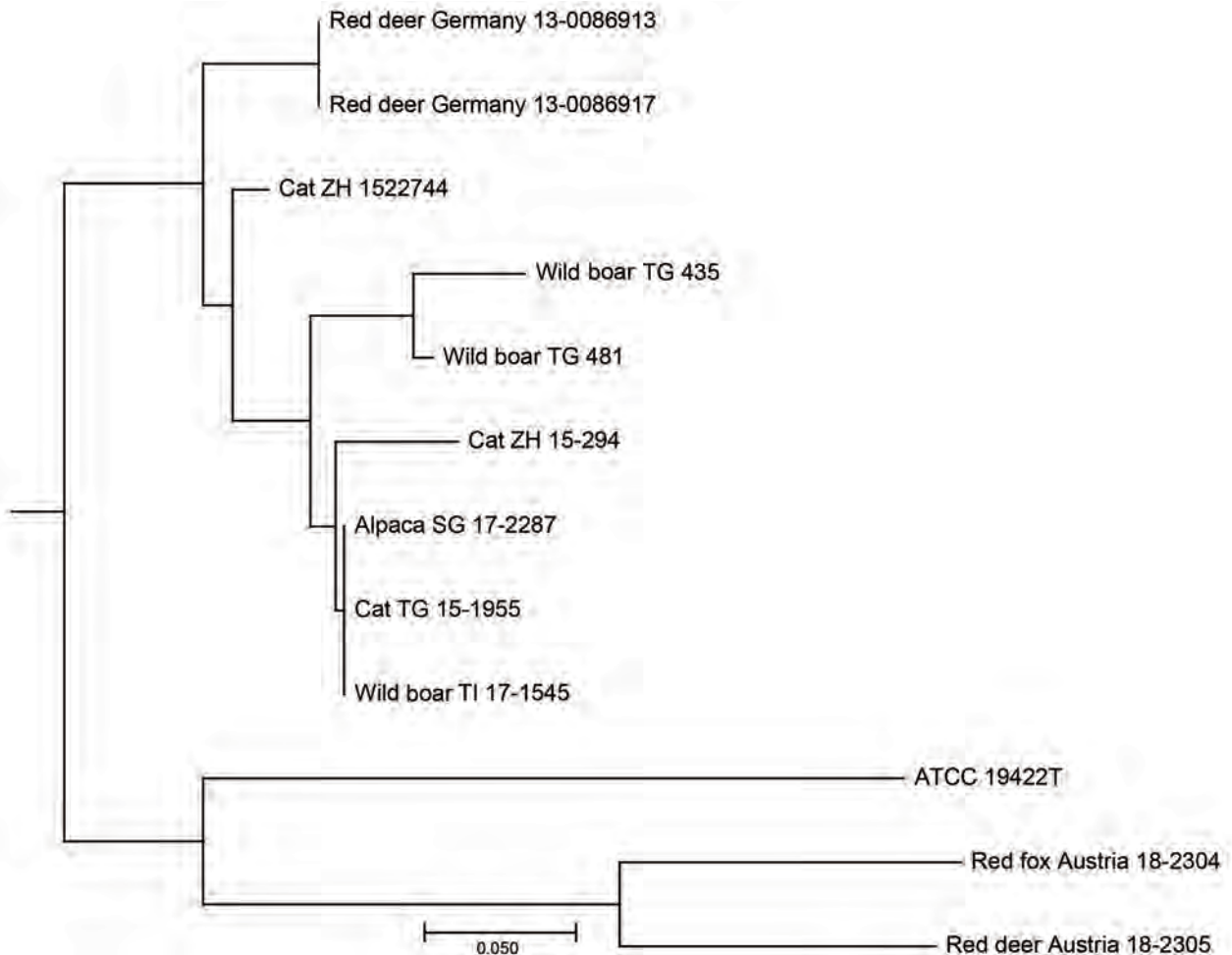
Figure 4. Neighbor-joining tree based on the copy numbers of 24-loci mycobacterial interspersed repetitive unit variable-number tandem-repeat analysis derived from 11 *Mycobacterium microti* clinical isolates and type strain *M. microti* Reed ATCC 19422^T in study of tuberculosis caused by *M. microti* in red deer, Austria and Germany. We calculated the tree using the MIRU-VNTR*plus* server (https:// www.miru-vntrplus.org; Appendix, https://wwwnc.cdc.gov/EID/article/27/8/21-0634-App1.xlsx) and exported it using MEGAX version 10.11 (https://www.megasoftware.net). Scale bar indicates substitutions per site.
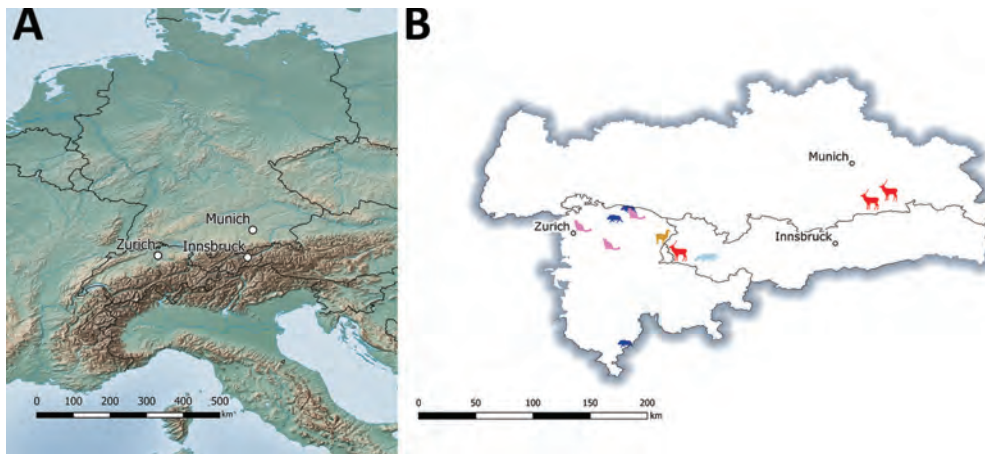
Figure 5. Geographic distribution of tuberculosis cases caused by *Mycobacterium microti* in different animal species over 8 years from study of tuberculosis caused by *M. microti* in red deer, Austria and Germany. Central Europe (left) and the region bordering Germany, Austria, and Switzerland (right) are shown. Animals are shaped and colored: red deer, red; cats, pink; wild boar, dark blue; alpaca, orange; and red fox, light blue.

from Austria, originating in the border region shared with Switzerland, were genetically more distant (Figures 4, 5), which suggests that the circulation of host-adapted *M. microti* genetic lineages is unlikely. MLVA has been successfully used worldwide as an ancillary tool for animal TB epidemiologic surveillance and outbreak investigations in multihost scenarios (*27,43–45*). However, the discriminatory capacity of whole-genome sequencing has elsewhere been shown to be superior for identifying MTBC strains belonging to the same regional clonal complex, which may apply to *M. microti* as well (*39,46*). Under certain specific circumstances, such as for formalin-fixed, paraffin-embedded samples or extremely fastidious strains, MLVA represents a valid alternative to whole-genome sequencing.

These findings highlight the wide host range of *M. microti* and suggest that it might be an opportunistic pathogen rather than a host-adapted MTBC member, such as *M. tuberculosis*. In the past, similar to *Mycobacterium bovis* BCG strains, certain vole strains of *M. microti* have been used to develop live attenuated human TB vaccines in the United Kingdom and the former Czechoslovakia (*47–49*). Therefore, marked virulence differences between *M. microti* strains are likely to exist (*50*).

Some seemingly feasible theories about the natural transmission route of *M. microti* suggest that the natural foci and reservoirs of this animal-adapted lineage are small rodents and that the pathogen subsequently infects predators, such as cats or foxes, through ingestion; the mode of infection for herbivores, such as red deer or alpacas, remains ill defined. The lesions we observed in the lungs of the deer in case 1, however, provide strong evidence of bacterial shedding, which might occur either as a consequence of inflammatory processes that break into the airways or by infection of alveolar macrophages that are part

of the exudate (*5*), which result in environmental contamination and further transmission of the pathogen (*3*). It is therefore alarming that animal species, such as red deer, that can cover long distances in short periods of time might contribute to the spread of *M. microti*, an MTBC agent.

Because of the potential zoonotic risk related to MTBC members, rapidly and accurately identifying the mycobacterial species causing disease in animals hunted for human consumption is crucial. Once MTBC is detected, determining whether *M. bovis* or *M. caprae* is present is of primary importance for veterinary and public health authorities. To date, molecular testing of cultured bacteria remains the preferred method for differentiating MTBC species. Because of the fastidious nature of *M. microti* and the extremely slow growth rate of specific animal strains, this differentiation can take several months or remain incomplete in cases where the mycobacterium cannot be cultured. On the basis of published data, it can be assumed that a large proportion of *M. microti* infections remain culture negative, even if the incubation time is prolonged to 18 weeks (*8*). Therefore, identifying species using molecular methods on native samples is recommended.

These findings show the morphologic versatility of lesions induced by *M. microti* in red deer. Given the absence of typical pulmonary lesions in some cases, such as in the red deer in cases 2 and 3, diagnostic pathologists must remain highly alert. Incidence of this pathogen should be monitored within the framework of bTB surveillance programs and suspicious cases differentiated from classical bTB caused by *M. bovis* and *M. caprae*. The actual occurrence of *M. microti* in wildlife may be underestimated, and personnel involved in bTB monitoring programs should be aware of its pathogenicity and zoonotic potential.

Therefore, molecular methods to differentiate this member of the MTBC should be included in the diagnostic workflow of bTB reference laboratories.

About the Author

Dr. Ghielmetti is a researcher at the Institute for Food Safety and Hygiene, Section of Veterinary Bacteriology, University of Zurich, Switzerland. His research interests include the molecular characterization and epidemiology of zoonotic pathogens.

References

1. World Health Organization. Global tuberculosis report 2020. Geneva: World Health Organization. 2020 [cited 2021 Mar 17]. https://www.who.int/publications/i/item/9789240013131
2. Wells AQ, Robb-Smith AHT. The murine type of tubercle bacillus (the vole acid-fast bacillus); with notes on the morphology of infection by the vole acid-fast bacillus. London: H.M. Stationery Office; 1946.
3. Kipar A, Burthe SJ, Hetzel U, Rokia MA, Telfer S, Lambin X, et al. *Mycobacterium microti* tuberculosis in its maintenance host, the field vole (*Microtus agrestis*): characterization of the disease and possible routes of transmission. Vet Pathol. 2014;51:903–14. https://doi.org/10.1177/0300985813513040
4. Smith NH, Crawshaw T, Parry J, Birtles RJ. *Mycobacterium microti*: More diverse than previously thought. J Clin Microbiol. 2009;47:2551–9. https://doi.org/10.1128/JCM.00638-09
5. Peterhans S, Landolt P, Friedel U, Oberhänsli F, Dennler M, Willi B, et al. *Mycobacterium microti*: not just a coincidental pathogen for cats. Front Vet Sci. 2020;7:590037. https://doi.org/10.3389/fvets.2020.590037
6. Rüfenacht S, Bögli-Stuber K, Bodmer T, Jaunin VF, Jmaa DC, Gunn-Moore DA. *Mycobacterium microti* infection in the cat: a case report, literature review and recent clinical experience. J Feline Med Surg. 2011;13:195–204. https://doi.org/10.1016/j.jfms.2011.01.012
7. Oevermann A, Pfyffer GE, Zanolari P, Meylan M, Robert N. Generalized tuberculosis in llamas (*Lama glama*) due to *Mycobacterium microti*. J Clin Microbiol. 2004;42:1818–21. https://doi.org/10.1128/JCM.42.4.1818-1821.2004
8. Boniotti MB, Gaffuri A, Gelmetti D, Tagliabue S, Chiari M, Mangeli A, et al. Detection and molecular characterization of *Mycobacterium microti* isolates in wild boar from northern Italy. J Clin Microbiol. 2014;52:2834–43. https://doi.org/10.1128/JCM.00440-14
9. Ghielmetti G, Hilbe M, Friedel U, Menegatti C, Bacciarini L, Stephan R, et al. Mycobacterial infections in wild boars (*Sus scrofa*) from southern Switzerland: diagnostic improvements, epidemiological situation and zoonotic potential. Transbound Emerg Dis. 2021;68:573–86. https://doi.org/10.1111/tbed.13717
10. Pérez de Val B, Sanz A, Soler M, Allepuz A, Michelet L, Boschiroli ML, et al. *Mycobacterium microti* infection in free-ranging wild boar, Spain, 2017–2019. Emerg Infect Dis. 2019;25:2152–4. https://doi.org/10.3201/eid2511.190746
11. Niemann S, Richter E, Dalügge-Tamm H, Schlesinger H, Graupner D, Königstein B, et al. Two cases of *Mycobacterium microti* derived tuberculosis in HIV-negative immunocompetent patients. Emerg Infect Dis. 2000;6:539–42. https://doi.org/10.3201/eid0605.000516
12. Panteix G, Gutierrez MC, Boschiroli ML, Rouviere M, Plaidy A, Pressac D, et al. Pulmonary tuberculosis due to *Mycobacterium microti*: a study of six recent cases in France. J Med Microbiol. 2010;59:984–9. https://doi.org/10.1099/jmm.0.019372-0
13. van de Weg CAM, de Steenwinkel JEM, Miedema JR, Bakker M, van Ingen J, Hoefsloot W. The tough process of unmasking the slow-growing mycobacterium: case report of *Mycobacterium microti* infection. Access Microbiol. 2019;2:acmi000074.
14. van Soolingen D, van der Zanden AGM, de Haas PEW, Noordhoek GT, Kiers A, Foudraine NA, et al. Diagnosis of *Mycobacterium microti* infections among humans by using novel genetic markers. J Clin Microbiol. 1998;36:1840–5. https://doi.org/10.1128/JCM.36.7.1840-1845.1998
15. Taylor C, Jahans K, Palmer S, Okker M, Brown J, Steer K. *Mycobacterium microti* isolated from two pigs. Vet Rec. 2006;159:59–60. https://doi.org/10.1136/vr.159.2.59-a
16. Michelet L, de Cruz K, Phalente Y, Karoui C, Hénault S, Beral M, et al. *Mycobacterium microti* infection in dairy goats, France. Emerg Infect Dis. 2016;22:569–70. https://doi.org/10.3201/eid2203.151870
17. Jahans K, Palmer S, Inwald J, Brown J, Abayakoon S. Isolation of *Mycobacterium microti* from a male Charolais-Hereford cross. Vet Rec. 2004;155:373–4.
18. Michelet L, de Cruz K, Tambosco J, Hénault S, Boschiroli ML. *Mycobacterium microti* interferes with bovine tuberculosis surveillance. Microorganisms. 2020;8:1850. https://doi.org/10.3390/microorganisms8121850
19. Deforges L, Boulouis HJ, Thibaud JL, Boulouha L, Sougakoff W, Blot S, et al. First isolation of *Mycobacterium microti* (Llama-type) from a dog. Vet Microbiol. 2004;103:249–53. https://doi.org/10.1016/j.vetmic.2004.06.016
20. Palgrave CJ, Benato L, Eatwell K, Laurenson IF, Smith NH. *Mycobacterium microti* infection in two meerkats (*Suricata suricatta*). J Comp Pathol. 2012;146:278–82. https://doi.org/10.1016/j.jcpa.2011.06.001
21. Henrich M, Moser I, Weiss A, Reinacher M. Multiple granulomas in three squirrel monkeys (*Saimiri sciureus*) caused by *Mycobacterium microti*. J Comp Pathol. 2007;137:245–8. https://doi.org/10.1016/j.jcpa.2007.06.005
22. Pym AS, Brodin P, Brosch R, Huerre M, Cole ST. Loss of RD1 contributed to the attenuation of the live tuberculosis vaccines *Mycobacterium bovis* BCG and *Mycobacterium microti*. Mol Microbiol. 2002;46:709–17. https://doi.org/10.1046/j.1365-2958.2002.03237.x
23. Berthet FX, Rasmussen PB, Rosenkrands I, Andersen P, Gicquel B. A *Mycobacterium tuberculosis* operon encoding ESAT-6 and a novel low-molecular-mass culture filtrate protein (CFP-10). Microbiology (Reading). 1998;144:3195–203. https://doi.org/10.1099/00221287-144-11-3195
24. Emmanuel FX, Seagar A-L, Doig C, Rayner A, Claxton P, Laurenson I. Human and animal infections with *Mycobacterium microti*, Scotland. Emerg Infect Dis. 2007;13:1924–7. https://doi.org/10.3201/eid1312.061536
25. Maguga-Phasha NTC, Munyai NS, Mashinya F, Makgatho ME, Mbajiorgu EF. Genetic diversity and distribution of *Mycobacterium tuberculosis* genotypes in Limpopo, South Africa. BMC Infect Dis. 2017;17:764. https://doi.org/10.1186/s12879-017-2881-z
26. Prodinger WM, Eigentler A, Allerberger F, Schönbauer M, Glawischnig W. Infection of red deer, cattle, and humans with *Mycobacterium bovis* subsp. *caprae* in western Austria.

J Clin Microbiol. 2002;40:2270–2. https://doi.org/10.1128/JCM.40.6.2270-2272.2002

27. Schoepf K, Prodinger WM, Glawischnig W, Hofer E, Revilla-Fernandez S, Hofrichter J, et al. A two-years' survey on the prevalence of tuberculosis caused by *Mycobacterium caprae* in red deer (*Cervus elaphus*) in the Tyrol, Austria. ISRN Vet Sci. 2012;2012:245138. https://doi.org/10.5402/2012/245138

28. Dorn-In S, Körner T, Büttner M, Hafner-Marx A, Müller M, Heurich M, et al. Shedding of *Mycobacterium caprae* by wild red deer (*Cervus elaphus*) in the Bavarian alpine regions, Germany. Transbound Emerg Dis. 2020;67:308–17. https://doi.org/10.1111/tbed.13353

29. Ghielmetti G, Scherrer S, Friedel U, Frei D, Suter D, Perler L, et al. Epidemiological tracing of bovine tuberculosis in Switzerland, multilocus variable number of tandem repeat analysis of *Mycobacterium bovis* and *Mycobacterium caprae.* PLoS One. 2017;12:e0172474. https://doi.org/10.1371/journal.pone.0172474

30. Fink M, Schleicher C, Gonano M, Prodinger WM, Pacciarini M, Glawischnig W, et al. Red deer as maintenance host for bovine tuberculosis, Alpine region. Emerg Infect Dis. 2015;21:464–7. https://doi.org/10.3201/eid2103.141119

31. Schöning JM, Cerny N, Prohaska S, Wittenbrink MM, Smith NH, Bloemberg G, et al. Surveillance of bovine tuberculosis and risk estimation of a future reservoir formation in wildlife in Switzerland and Liechtenstein. PLoS One. 2013;8:e54253. https://doi.org/10.1371/journal.pone.0054253

32. Leth C, Varadharajan A, Mester P, Fischaleck M, Rossmanith P, Schmoll F, et al. Matrixlysis, an improved sample preparation method for recovery of *Mycobacteria* from animal tissue material. PLoS One. 2017;12:e0181157. https://doi.org/10.1371/journal.pone.0181157

33. Fite GL, Cambre PJ, Turner MH. Procedure for demonstrating lepra bacilli in paraffin sections. Arch Pathol (Chic). 1947;43:624–5.

34. Supply P, Allix C, Lesjean S, Cardoso-Oelemann M, Rüsch-Gerdes S, Willery E, et al. Proposal for standardization of optimized mycobacterial interspersed repetitive unit-variable-number tandem repeat typing of *Mycobacterium tuberculosis.* J Clin Microbiol. 2006; 44:4498–510. https://doi.org/10.1128/JCM.01392-06

35. Allix-Béguec C, Harmsen D, Weniger T, Supply P, Niemann S. Evaluation and strategy for use of MIRU-VNTR*plus*, a multifunctional database for online analysis of genotyping data and phylogenetic identification of *Mycobacterium tuberculosis* complex isolates. J Clin Microbiol. 2008;46:2692–9. https://doi.org/10.1128/JCM.00540-08

36. Brudey K, Driscoll JR, Rigouts L, Prodinger WM, Gori A, Al-Hajoj SA, et al. *Mycobacterium tuberculosis* complex genetic diversity: mining the fourth international spoligotyping database (SpolDB4) for classification, population genetics and epidemiology. BMC Microbiol. 2006;6:23. https://doi.org/10.1186/1471-2180-6-23

37. Chiari M, Zanoni M, Alborali LG, Zanardi G, Avisani D, Tagliabue S, et al. Isolation of *Mycobacterium caprae* (Lechtal genotype) from red deer (*Cervus elaphus*) in Italy. J Wildl Dis. 2014;50:330–3. https://doi.org/10.7589/2013-06-135

38. Griffin JFT, Mackintosh CG. Tuberculosis in deer: perceptions, problems and progress. Vet J. 2000;160:202–19. https://doi.org/10.1053/tvjl.2000.0514

39. Michelet L, Conde C, Branger M, Cochard T, Biet F, Boschiroli ML. Transmission network of deer-borne *Mycobacterium bovis* infection revealed by a WGS approach. Microorganisms. 2019;7:687. https://doi.org/10.3390/microorganisms7120687

40. Javed MT, Aranaz A, de Juan L, Bezos J, Romero B, Alvarez J, et al. Improvement of spoligotyping with additional spacer sequences for characterization of *Mycobacterium bovis* and *M. caprae* isolates from Spain. Tuberculosis (Edinb). 2007;87:437–45. https://doi.org/10.1016/j.tube.2007.04.002

41. Rodríguez S, Romero B, Bezos J, de Juan L, Alvarez J, Castellanos E, et al.; Spanish Network on Surveillance and Monitoring of Animal Tuberculosis. High spoligotype diversity within a *Mycobacterium bovis* population: clues to understanding the demography of the pathogen in Europe. Vet Microbiol. 2010;141:89–95. https://doi.org/10.1016/j.vetmic.2009.08.007

42. Michelet L, de Cruz K, Zanella G, Aaziz R, Bulach T, Karoui C, et al. Infection with *Mycobacterium microti* in animals in France. J Clin Microbiol. 2015;53:981–5. https://doi.org/10.1128/JCM.02713-14

43. Boniotti MB, Gaffuri A, Gelmetti D, Tagliabue S, Chiari M, Mangeli A, et al. Detection and molecular characterization of *Mycobacterium microti* isolates in wild boar from northern Italy. J Clin Microbiol. 2014;52:2834–43. https://doi.org/10.1128/JCM.00440-14

44. Hauer A, De Cruz K, Cochard T, Godreuil S, Karoui C, Henault S, et al. Genetic evolution of *Mycobacterium bovis* causing tuberculosis in livestock and wildlife in France since 1978. PLoS One. 2015;10:e0117103. https://doi.org/10.1371/journal.pone.0117103

45. Réveillaud É, Desvaux S, Boschiroli ML, Hars J, Faure É, Fediaevsky A, et al. Infection of wildlife by *Mycobacterium bovis* in France assessment through a national surveillance system, Sylvatub. Front Vet Sci. 2018;5:262. https://doi.org/10.3389/fvets.2018.00262

46. Hauer A, Michelet L, Cochard T, Branger M, Nunez J, Boschiroli ML, et al. Accurate phylogenetic relationships among *Mycobacterium bovis* strains circulating in France based on whole genome sequencing and single nucleotide polymorphism analysis. Front Microbiol. 2019;10:955. https://doi.org/10.3389/fmicb.2019.00955

47. Hart PD, Sutherland I. BCG and vole bacillus vaccines in the prevention of tuberculosis in adolescence and early adult life. BMJ. 1977;2:293–5. https://doi.org/10.1136/bmj.2.6082.293

48. Sula L, Radkovský I. Protective effects of *M. microti* vaccine against tuberculosis. J Hyg Epidemiol Microbiol Immunol. 1976;20:1–6.

49. Wells AQ. Vaccination with the murine type of tubercle bacillus (vole bacillus). Lancet. 1949;2:53–5. https://doi.org/10.1016/S0140-6736(49)91043-0

50. Orgeur M, Frigui W, Pawlik A, Clark S, Williams A, Ates LS, et al. Pathogenomic analyses of *Mycobacterium microti,* an ESX-1-deleted member of the *Mycobacterium tuberculosis* complex causing disease in various hosts. Microb Genom. 2021;7:7. https://doi.org/10.1099/mgen.0.000505

Address for correspondence: Giovanni Ghielmetti DVM, Institute for Food Safety and Hygiene, Section of Veterinary Bacteriology, Winterthurerstrasse 270 CH-8057 Zurich, Vetsuisse Faculty, University of Zurich, Zurich, Switzerland; email: giovanni.ghielmetti@vetbakt.uzh.ch

Plague Transmission from Corpses and Carcasses

Sophie Jullien, Nipun Lakshitha de Silva, Paul Garner

Knowing whether human corpses can transmit plague will inform policies for handling the bodies of those who have died of the disease. We analyzed the literature to evaluate risk for transmission of *Yersinia pestis*, the causative agent of plague, from human corpses and animal carcasses. Because we could not find direct evidence of transmission, we described a transmission pathway and assessed the potential for transmission at each step. We examined 3 potential sources of infection: body fluids of living plague patients, infected corpses and carcasses, and body fluids of infected corpses. We concluded that pneumonic plague can be transmitted by intensive handling of the corpse or carcass, presumably through the inhalation of respiratory droplets, and that bubonic plague can be transmitted by blood-to-blood contact with the body fluids of a corpse or carcass. These findings should inform precautions taken by those handling the bodies of persons or animals that died of plague.

Plague is an ancient disease that has killed millions of persons including one third of the population of Europe during the Black Death pandemic in the 14th century (*1*). Plague remains a threat in many parts of the world (*2*) and has been categorized by the World Health Organization as a reemerging disease (*3*). Caused by *Yersinia pestis*, a nonmotile, gram-negative coccobacillus, this zoonotic disease has its main reservoir in rodents (*4,5*). Humans become infected by *Y. pestis* through bites from infected fleas or animals, handling or ingesting infected animals or humans, or inhaling aerosolized droplets from infected tissues (Figure 1) (*6–10*). Plague has 3 main clinical syndromes: bubonic plague, which is characterized by inflammation of lymph nodes after a flea bite or scratch from an infected animal (*11,12*); pneumonic plague, which is spread by inhalation of droplets from infected humans or animals; and septicemic plague, which results from the hematogenous spread of bubonic or pneumonic plague (*13*).

To inform World Health Organization recommendations on personal protective equipment (PPE) for healthcare workers, we evaluated whether corpses of plague patients might be infectious. Little is known about the potential infectiousness of corpses, the duration of risk for infection to humans handling corpses, or possible transmission routes. Information on infectiousness of human corpses can guide development of protective measures for healthcare staff and relatives who might not use PPE during traditional funeral rituals (*14*). We know of 3 possible transmission routes: direct contact with infectious body fluids, such as through open wounds or inhalation; indirect contact through contaminated clothing; and bites from infected fleas from corpses or their clothes. In this review, we sought to estimate the risk for *Y. pestis* transmission from body fluids of corpses. Because little direct evidence for plague transmission from corpses exists, we assessed evidence for potential transmission by body fluids of living plague patients, corpses and carcasses, and body fluids of corpses and carcasses. We also analyzed the potential duration of infectiousness of body fluids from corpses and carcasses (Figure 2) (*15*).

Methods

We used different inclusion criteria for each potential transmission pathway (Table 1). Because we assumed that the consumption of human corpses was rare, we excluded cases caused by the consumption of infected meat. We also excluded cases caused by transmission from vectors, such as fleas.

We searched PubMed, Embase, Science Citation Index, and Scopus for literature published by May 20, 2019, and identified all relevant studies regardless of language, publication status, or publication date (Appendix, https://wwwnc.cdc.gov/EID/article/27/8/20-0136-App1.pdf). We also manually

Author affiliations: University of Barcelona, Barcelona, Spain (S. Jullien); Liverpool School of Tropical Medicine, Liverpool, UK (S. Jullien, P. Garner); General Sir John Kotelawala Defence University, Colombo, Sri Lanka (N.L. de Silva)
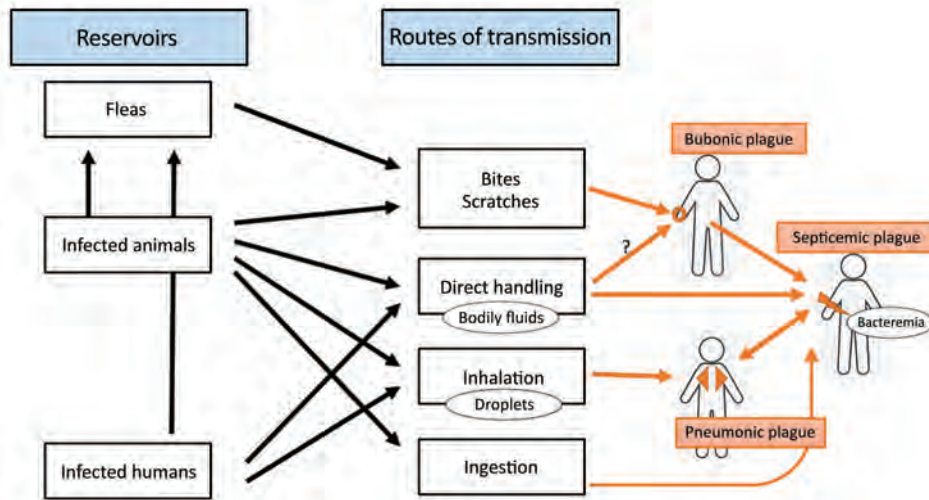
Figure 1. Reservoirs of *Yersinia pestis* and transmission routes leading to different forms of plague. Black arrows indicate links between infection sources and transmission routes. Orange arrows indicate causality of different plague syndromes according to transmission routes.

searched the reference lists of all identified papers and contacted relevant researchers.

Study Selection

First, we (2 review authors) independently screened the abstracts of articles retrieved by the search strategy and classified them using predefined eligibility criteria (Table 1). For the second stage of screening, we retrieved full-text copies and applied the same criteria. We assessed manuscripts in French, Russian, German, and Chinese with the help of native-speaking authors and plague experts or through online translation. We resolved any discrepancies through discussion and excluded studies that did not meet the inclusion criteria (Figure 3; Appendix Table 1).

Data Extraction, Bias Assessment, and Analysis

For each included study, we (2 review authors) extracted data on protocol and other characteristics (Appendix Tables 4–57). We also considered each study's limitations by assessing risk for bias using 6 questions

modified from the quality appraisal tool developed by Cho et al. (*16*) (Appendix Table 3). We did not find suitable data for statistical analysis.

Results

We identified 644 studies (616 in the literature search, after removal of duplicates, and 28 in the manual search) and used 25 in the final review (Figure 3). Ten studies addressed potential transmission by body fluids of living persons who had plague, 16 addressed potential transmission from corpses and carcasses, and 2 addressed potential transmission from body fluids of human corpses and animal carcasses. Three studies addressed ≥1 research question.

Infectiousness of Body Fluids of Living Plague Patients

Study Descriptions

We found 10 studies that documented direct human-to-human transmission of *Y. pestis* (Appendix Table
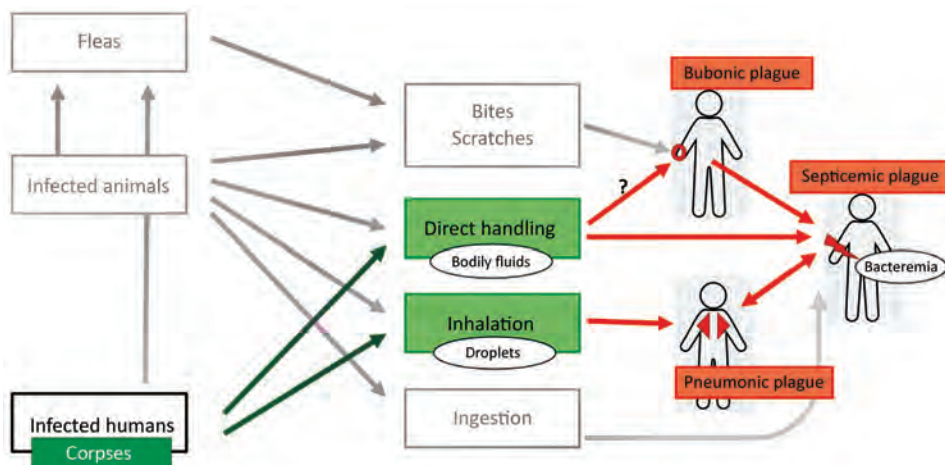
Figure 2. Potential plague transmission routes from human corpses. Black arrows indicate links between infection sources and transmission routes. Orange arrows indicate causality of different plague syndromes according to transmission routes.

Table 1. Inclusion criteria for literature review on transmission of plague from human corpses

Research topic	Infectiousness of body fluids of living plague patients	Infections acquired from corpses and carcasses	Infectiousness of body fluids of corpses and carcasses
Study type	Descriptive (including surveillance data, case series, and case reports)	Descriptive (including case series and case reports)	Descriptive (including case series and case reports)
Participants	Persons who have laboratory-confirmed plague	Persons or animals that died of laboratory-confirmed plague	Persons or animals that died of laboratory-confirmed plague
Outcomes	New case of confirmed plague attributed to direct transmission from an infected human (i.e., human-to-human transmission)	New case of confirmed plague attributed to direct transmission from an infected corpse or carcass	New case of confirmed plague attributed to direct transmission from an infected corpse or carcass, with a specified period between the time of death of the plague victim and time of contact with corpse Isolation of *Yersinia pestis* by culture from body fluids from an infected corpse or carcass, with a specified period between the time of death of the plague victim and the time of *Y. pestis* identification
Exclusion criteria	None	Studies reporting only cases of plague attributed to consumption of infected meat, or cases transmitted by vectors such as fleas	Studies examining the persistence of *Y. pestis* DNA in corpses or carcasses that were previously buried, in the soil, or on environmental surfaces

4). In total, 4 studies described plague cases during the 20th century in Brazil (*17*), South Africa (*18*), and the United States (*19,20*) and 6 reported outbreaks during 1997–2017 in Madagascar (*21–24*), Uganda (*25*), and the Democratic Republic of the Congo (*26*). Altogether, the 10 studies described 2,388 plague cases caused by direct human-to-human contact, including 1,861 cases documented during an outbreak in Madagascar (*21*). Nearly all the patients had primary pneumonic plague, except for 4 patients who had septicemic plague (*18,26*) and 6 who had a mixed form described as probable pneumonic affectation secondary to buboes (*18*).

Risk for Bias

Six studies included adequate descriptions of patient characteristics such as age, sex, and form of plague; 3 had inadequate descriptions; and 1 did not provide such information. Four studies described efforts to trace contacts from the index case, suggesting a perception of contagiousness. All 10 studies met our inclusion criterion by providing a description of laboratory methods used to confirm cases, although 2 studies included only partial descriptions. We used the quality appraisal tool to judge whether the suggested transmission route and causative relationship to infection was plausible for 8 studies. We could not
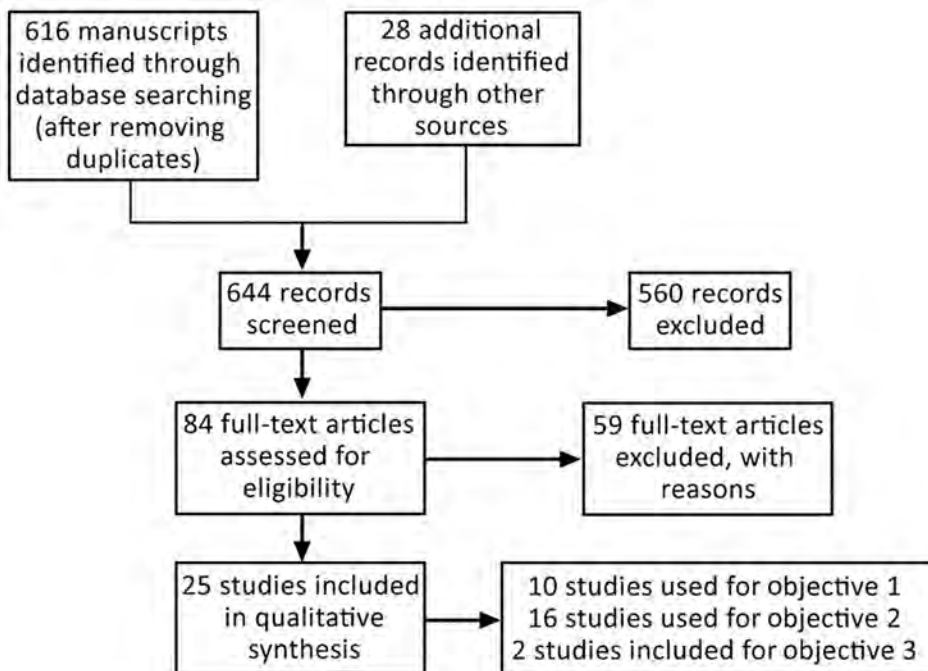
Figure 3. Flowchart of study on plague transmission from human corpses. Study examined 3 potential sources of infection: body fluids of living plague patients (objective 1), infected corpses and carcasses (objective 2), and body fluids of infected corpses (objective 3).

make definitive judgements for 2 studies that comprised 50 cases but lacked sufficient data (Table 2; Appendix Tables 6, 8, 10, 12, 14, 16, 18, 20, 22, 24).

Findings

Various studies reported bloody sputum from the index patient (23,25), infected contacts (18,22), or both (24). Transmission was attributed to respiratory droplets for 1,893 combined cases (20,21,23,25) and to aerosolized bacteria for 311 combined cases (24,26). A combination of 3 studies found that 63 cases were consistent with human-to-human transmission, but the studies did not provide further details (17,19,22).

To assess the contagiousness of plague patients, we extracted data about uninfected contacts. Across 4 studies that provided such information, a total of 51 contacts were infected by 5 index patients (although however, some infected contacts then acted as index patients for additional infections), whereas 341 contacts of those 5 index patients did not become ill (22–25). The study authors estimated incidence proportions of 8%, 8.4%, and 55% (23–25). One study estimated the transmission rate to be 0.41 susceptible persons/day (22). Some studies reported that infected contacts had close and prolonged exposure to index patients (18,20,23–25). Four studies from South Africa and Madagascar attributed plague transmission to funerary activities, such as preparing bodies for funerals or active participation in the funerals (18,21–23). Uninfected contacts included family members who slept in the same bed as the patient until the night before the patient's death (24,25); some of these contacts slept with their heads <2 meters from the coughing plague patient (25).

Summary

In total, 6 studies described 2,204 cases of direct *Y. pestis* transmission through infective cough droplets from living plague patients. Some direct transmission occurred only after close and prolonged exposure. We found no publication describing human-to-human transmission of plague through other body fluids, such as blood (although patients with pneumonic plague can produce respiratory droplets from bloody sputum), urine, feces, sweat, or bubo pus.

Plague Transmitted by Corpses and Carcasses

Study Descriptions

We analyzed 16 retrospective case reports and series published during 1930–2019 (Appendix Tables 25–57). The studies documented a total of 250 cases in 7 countries: 114 in China (27–29), 96 in the United States (8,19,30–35), 17 in Libya (36), 12 in Kazakhstan (37), 9 in Madagascar (23), 1 in South Africa (38), and 1 in Saudi Arabia (39). Plague was more common among men than women, and patient ages ranged from 1–69 years. The combined studies reported 125 cases of primary bubonic plague (mostly with axillary buboes), 70 of primary pneumonic plague, 8 of primary septicemic plague, and 2 of primary intestinal plague.

Risk for Bias

Ten studies adequately described the main characteristics of participants (Table 3; Appendix Tables 27, 29, 31, 33, 35, 37, 39, 41, 43, 45, 47, 49, 51, 53, 55, 57). Twelve studies did not describe efforts to trace all contacts of the index patient. These studies provided no information on whether other persons were exposed but did not get infected, complicating our assessment of corpse contagiousness. Eight studies had missing or partial descriptions of laboratory methods used for defining confirmed cases of plague; however, patients with unconfirmed infection were highly suspected to have plague because of clinical and epidemiologic data. Using the quality appraisal toll, we judged the proposed transmission route and causative relationship to infection to be highly

Table 2. Risk for bias in studies on human-to-human transmission of plague*

Study	Were patient characteristics adequately reported?	Was there some effort to trace all contacts from the index case?	Were the methods used for tracing contacts adequate?	Were the laboratory methods used for defining a confirmed case of plague reliable?	Was the route of transmission plausible?	Was the cause-effect of transmission plausible?
Almeida et al. (17)	Partial	Unknown	NA	Yes	No	Unknown
Begier et al. (25)	Yes	Yes	Yes	Partial	Yes	Yes
Bertherat et al. (26)	No	Partial	Unknown	Yes	Yes	Yes
Evans et al. (18)	Yes	Unknown	NA	Yes	Yes	Yes
Kellogg et al. (20)	Yes	Unknown	NA	Yes	Yes	Yes
Kugeler 2015 (19)	Partial	Unknown	NA	Yes	Unknown	Unknown
Rabaan et al. (21)	Partial	Partial	Unknown	Yes	Yes	Yes
Ramasindrazana et al. (22)	Yes	Yes	Yes	Yes	Yes	Yes
Ratsitorahina et al. (23)	Yes	Yes	Unknown	Partial	Yes	Yes
Richard et al. (24)	Yes	Yes	Unknown	Yes	Yes	Yes

*NA, not applicable.

Table 3. Risk for bias summary in studies on plague acquired from corpses and carcasses*

Study ID	Were patient characteristics adequately reported?	Was there some effort to trace all contacts from the index case?	Were the methods used for tracing contacts adequate?	Were the laboratory methods used for defining a confirmed case of plague reliable?	Was the route of transmission plausible?	Was the cause-effect of transmission plausible?
Centers for Disease Control and Prevention (*30*)	Yes	Unknown	NA	Yes	Yes	Yes
Christie et al. (case series 1; *37*)	Partial	Unknown	NA	Partial	Yes	Yes
Christie et al. (case series 2; *37*)	Partial	Unknown	NA	Partial	Partial	Partial
Gage et al. (*31*)	Yes	Unknown	NA	Yes	Yes	Yes
Ge et al. (case report; *27*)	Yes	Yes	Yes	Yes	Yes	Yes
Ge et al. (case series; *27*)	Partial	Unknown	NA	Unknown	Partial	Partial
Kartman et al. (*33*)	Partial	Unknown	NA	No	Yes	Yes
Kartman et al. (*32*)	Partial	Unknown	NA	Unknown	Yes	Yes
Kugeler et al. (*34*)	No	Unknown	NA	Unknown	Partial	Partial
Mitchell et al. (*39*)	Yes	Unknown	NA	Unknown	Yes	Yes
Poland et al. (*35*)	Yes	Yes	Yes	Yes	Yes	Yes
Ratsitorahina et al. (*23*)	Yes	Yes	Unknown	Yes	Yes	Partial
Saeed et al. (*40*)	Yes	Yes	Yes	Yes	Yes	Yes
Sagiev et al. (*38*)	No	Unknown	NA	Unknown	Unknown	Unknown
Von Reyn et al. (*36*)	Yes	Yes	Yes	Yes	Yes	Yes
Wong et al. (*8*)	Yes	Yes	Yes	Yes	Yes	Yes
Wu et al. (*28*)	Yes	Unknown	NA	Yes	Yes	Partial
Zhang et al. (*29*)	Partial	Unknown	NA	Partial	Unknown	Partial

*ID, identification; NA, not applicable.

plausible in 11 studies. Although the remaining 5 studies and case series described in an additional 2 sources also proposed transmission routes, they lacked the information needed to judge plausibility. Furthermore, some case series could not fully exclude fleaborne transmission in all patients.

Findings

Corpses were described as the source of exposure in 3 studies comprising up to 42 cases (*23,38*). Axillary bubonic plague developed in 1 patient after he had conducted a postmortem examination of 2 infected corpses during the 1920s (*38*). It is unclear whether the examiner had skin lesions on the hands, was wearing PPE during the autopsy, or how soon the autopsies were conducted after death. The second study described 9 persons who contracted pneumonic plague after attending the funeral of someone who died of plague (*23*). Eight of these contacts had lodged at the house of the deceased person for 2 days after the patient's death and might have had contact with the deceased person's wife and son, who also died of plague shortly after. Although the authors concluded that "infection resulted from active participation in the funeral ceremonies and attendance on patients," it is difficult to distinguish between human-to-human and corpse-to-human transmission in this scenario (*23*). The third study reported 32 persons infected by contact with plague patients or corpses; this study

provided no disaggregated data nor further details on the route of transmission (*29*).

The remaining 13 studies reported 208 cases of plague transmitted by carcasses of camels, goats, cats, a bobcat, a fox, a coyote, a mountain lion, Tibetan sheep, marmots, dogs, rabbits, squirrels, and other rodents. Most exposures consisted of carcass-related activities, such as killing the animal, skinning the carcass, or conducting a necropsy, all of which require relatively long and close exposure to the infection source.

Only 1 study directly specified the duration of time between the death of the infected animal and exposure, a period of ≈35 hours (*8*). Three studies described a total of 11 cases in which exposure occurred <24 hours after the death of the infected animal (*23,34,39*). In addition, 3 other studies described 26 patients who had killed the infected animal, implying immediate exposure (*32,33,36*).

Of the patients who had bubonic plague, 5 had open skin lesions on their hands or arms while they handled the carcass with bare hands (*33,34,35,39*). Other persons who had no skin lesions were exposed to the same infection source but were not infected (*34,35*). Most cases of bubonic plague were axillary, consistent with the inoculation of *Y. pestis* through cuts in the hands or arms. Two studies attributed transmission of primary pneumonic plague to inhalation of aerosols generated by handling the carcass,

including 1 study that theorized aerosol inhalation during necropsy (*8,27*).

Summary

Limited evidence exists for plague transmission from human corpses. Ten studies reported plague transmission through direct skin contact with blood from animal carcasses, leading to 121 cases of bubonic plague. Persons who had cuts or skin abrasions had an increased risk of contracting plague. The potential infectiousness of other body fluids remains unknown. It is possible that pneumonic plague might be spread by actions that cause aerosolization of infected body fluids, but this process would require considerable manipulation of the corpse or carcass.

Infectiousness of Body Fluids of Corpses or Carcasses

We identified 2 studies that detailed the infectious period of plague-infected animal carcasses; however, we could not find any studies documenting the duration of infectiousness of human corpses. One experimental study from Madagascar published in 1965 isolated *Y. pestis* from rodents that died of septicemic plague and were buried in laterite alone or in laterite enriched with manure to simulate local conditions (*40*). *Y. pestis* was successfully isolated after 5 and 10 days, but not 15 days, after the death and burial of the rodents. Another study reported the case of a wildlife biologist who was in contact with a mountain lion carcass ≈35 hours after the animal had died (*8*). The time of death was identified from a mortality signal transmitted from the animal's radio-collar after recording no movement for 6 hours. *Y. pestis* was isolated by culture of the animal's tissues and subtyped by pulsed-field gel electrophoresis. The same strain was later isolated from the biologist, indicating that the mountain lion was the source of the biologist's infection. We judged both studies to be at low risk for bias.

In summary, we do not know how long *Y. pestis* can survive in the body fluids of persons that die of plague, and thus we do not know how long the human corpse might be contagious. Because 1 study documented transmission from an animal 35 hours after death, we surmise the risk for infection from animal carcasses period might extend beyond 24 hours (*8*).

Discussion

Historical narratives of plague outbreaks suggest that human-to-human transmission is common for pneumonic plague, but more modern researchers have contested this claim (*41*). Kool (*42*) summarized data from historical records and contemporary experiences and used qualitative analysis to conclude that "pneumonic plague is not easily transmitted from one person to another." Some analysts have estimated transmission potential of plague using mathematical models based on historical data (*43,44*). The studies in this review, which examine mostly modern plague outbreaks (many earlier reports did not provide sufficient detail to meet our inclusion criteria), provide evidence that pneumonic plague is transmissible from human to human, but only after close and prolonged exposure. Historical records that did not meet inclusion criteria also provided useful information on the transmissibility of pneumonic plague. For example, some excluded studies demonstrated the isolation of *Y. pestis* from sputum of patients who had pneumonic plague (*45,46*), suggesting the potential for transmission of plague through inhalation of infected sputum.

We found that bloody sputum was clearly reported as the source of plague transmission in several studies. In studies describing plague transmitted from corpses, the types of contaminated body fluids causing plague transmission, although presumably blood, were not clearly described. Activities reported as the cause of infection included skinning, butchering, and flaying carcasses, as well as conducting postmortem examinations, all of which result in contact with blood. However, transmission could potentially occur through other body fluids, such as urine, feces, gastric content, or bubo pus.

We did not find evidence that plague can be transmitted by body fluids other than sputum and blood. In addition, the length of time that *Y. pestis* can survive in body fluids or that the corpse is contagious is unknown. We found only 1 study describing plague transmission from an animal that had been dead for ≈35 hours before patient exposure.

The studies in this review described 2 main routes of transmission. The first is the inhalation of particles, which can result in pneumonic plague. Plague patients generate contaminated droplets by coughing, which is associated with bloody sputum. Corpses do not produce contaminated droplets by cough, but handling the corpse in preparation for autopsy or funeral can generate contaminated droplets of body fluids, mainly blood. Regardless, a close and prolonged exposure is probably needed for disease transmission.

The second route of transmission is through the handling of corpses, such as prolonged exposure during invasive procedures. Some studies documented skin cuts or abrasions on the hands of the persons who became infected, although other studies have not commented on the presence of open wounds. Thus, it is difficult to know whether transmission
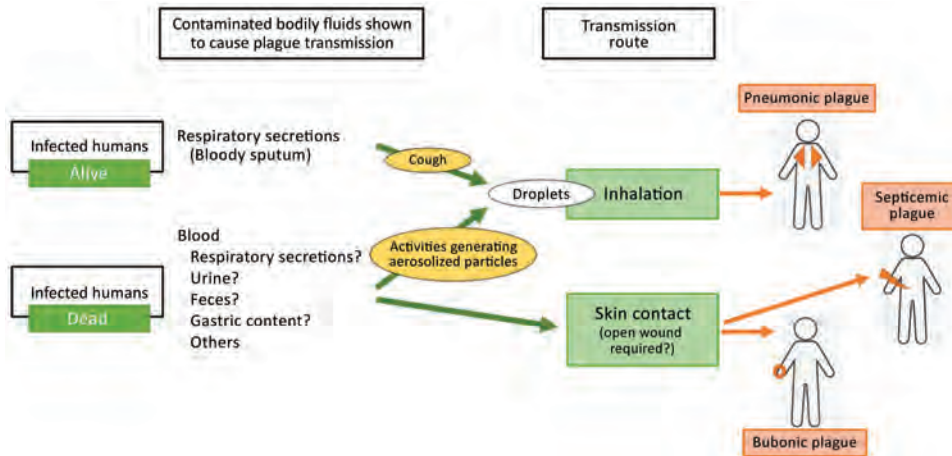
Figure 4. Summary of the transmission routes described in study on plague transmission from human corpses.

through intact skin can occur, although such transmission seems improbable. We did not find any study describing plague acquired through contact with mucosa.

In some cases, we could not distinguish between transmission routes from corpses, such as whether transmission occurred through body fluids, clothing contaminated with body fluids, or fleas on the body or clothing from the corpse. Our examination of documented plague transmission from the body fluids of living plague patients found that all such reports were of primary pneumonic plague, suggesting the inhalation of particles as the transmission route. Our examination of the infectiousness of body fluids of corpses and carcasses showed that it is difficult to totally exclude the possibility that some cases of bubonic plague were transmitted by fleas. Although most patients were infected by animals (thus excluding the possibility of fleas carried on clothes), the corpses themselves might have had fleas. However, our inclusion criteria limited the likelihood of fleaborne transmission, and we appraised the plausibility of the proposed transmission route for each study. We excluded studies associated with fleas or unknown sources of transmission (*30*). We noted instances when studies reported an absence of flea bites (*33*) or when fleaborne transmission might not have been fully excluded (*19*).

In summary, we provide evidence for plague transmission from human corpses (Figure 4). Inhalation of respiratory droplets produced by intense manipulation of the corpse or carcass could result in pneumonic plague, especially after close and prolonged exposure. Direct skin contact with infected body fluids (mainly blood; it is unclear whether other body fluids might also be infectious) could cause bubonic plague, or when a person has cuts on their hands, eventually septicemic plague. These findings suggest that persons handling the corpses of those who have died of plague should use PPE, including an adequate mask, gloves, and gown.

Acknowledgments

About the Author

Dr. Jullien is a pediatrician at the Barcelona Institute for Global Health in Barcelona, Spain. Her primary research interests include infectious diseases, public health, and evidence-based practice.

References

1. Rasmussen S, Allentoft ME, Nielsen K, Orlando L, Sikora M, Sjögren KG, et al. Early divergent strains of *Yersinia pestis* in Eurasia 5,000 years ago. Cell. 2015;163:571–82. https://doi.org/10.1016/j.cell.2015.10.009
2. World Health Organization. Interregional meeting on prevention and control of plague. 2008 [cited 2019 Oct 21]. https://www.who.int/csr/resources/publications/WHO_HSE_EPR_2008_3w.pdf
3. World Health Organization, Regional Office for South-East Asia, Operational guidelines on plague surveillance, diagnosis, prevention and control. 2009 [cited 2019 Oct 21]. https://apps.who.int/iris/handle/10665/205593

4. Eisen RJ, Gage KL. Adaptive strategies of *Yersinia pestis* to persist during inter-epizootic and epizootic periods. Vet Res. 2009;40:1–14. https://doi.org/10.1051/vetres:2008039

5. Pollitzer R. Plague (World Health Organization Monograph Series). Geneva: World Health Organization; 1954.

6. Centers for Disease Control and Prevention. Fatal laboratory-acquired infection with an attenuated *Yersinia pestis* strain—Chicago, Illinois, 2009. MMWR Morb Mortal Wkly Rep. 2011;60:201–5.

7. Weniger BG, Warren AJ, Forseth V, Shipps GW, Creelman T, Gorton J, et al. Human bubonic plague transmitted by a domestic cat scratch. JAMA. 1984;251:927–8. https://doi.org/10.1001/jama.1984.03340310041017

8. Wong D, Wild MA, Walburger MA, Higgins CL, Callahan M, Czarnecki LA, et al. Primary pneumonic plague contracted from a mountain lion carcass. Clin Infect Dis. 2009;49:e33–8. https://doi.org/10.1086/600818

9. Centers for Disease Control and Prevention. Plague. 2019 [cited 2019 Apr 15]. https://www.cdc.gov/plague/index.html

10. Bramanti B, Stenseth NC, Walloe L, Lei X. Plague: a disease which changed the path of human civilization. In: Yang R, Anisimov A, editors. *Yersinia pestis*: retrospective and perspective. Dordrecht (Netherlands): Springer; 2016. p. 11–5.

11. Arifuzzaman M, Ang WXG, Choi HW, Nilles ML, St John AL, Abraham SN. Necroptosis of infiltrated macrophages drives *Yersinia pestis* dispersal within buboes. JCI Insight. 2018;3:e122188. https://doi.org/10.1172/jci.insight.122188

12. Prentice MB, Rahalison L. Plague. Lancet. 2007;369:1196–207. https://doi.org/10.1016/S0140-6736(07)60566-2

13. Center for Infectious Disease Research and Policy. Plague: agent and pathogenesis. 2013 [cited 2019 Apr 15]. https://www.cidrap.umn.edu/infectious-disease-topics/plague

14. Poleykett B. Ethnohistory and the dead: cultures of colonial epidemiology. Med Anthropol. 2018;37:472–85. https://doi.org/10.1080/01459740.2018.1453507

15. Jullien S, da Silva NL, Garner P. Risk of plague transmission from human cadavers. National Institute for Health Research. 2019 [cited 2019 Jan 13]. https://www.crd.york.ac.uk/PROSPERO/display_record.php?RecordID=133786

16. Cho MK, Bero LA. Instruments for assessing the quality of drug studies published in the medical literature. JAMA. 1994;272:101–4. https://doi.org/10.1001/jama.1994.03520020027007

17. Almeida CR, Almeida AR, Vieira JB, Guida U, Butler T. Plague in Brazil during two years of bacteriological and serological surveillance. Bull World Health Organ. 1981;59:591–7.

18. Evans CM, Egan JR, Hall I. Pneumonic plague in Johannesburg, South Africa, 1904. Emerg Infect Dis. 2018;24:95–102. https://doi.org/10.3201/eid2401.161817

19. Kugeler KJ, Staples JE, Hinckley AF, Gage KL, Mead PS. Epidemiology of human plague in the United States, 1900–2012. Emerg Infect Dis. 2015;21:16–22. https://doi.org/10.3201/eid2101.140564

20. Kellogg WH. An epidemic of pneumonic plague. Am J Public Health (N Y). 1920;10:599–605. https://doi.org/10.2105/AJPH.10.7.599

21. Rabaan AA, Al-Ahmed SH, Alsuliman SA, Aldrazi FA, Alfouzan WA, Haque S. The rise of pneumonic plague in Madagascar: current plague outbreak breaks usual seasonal mould. J Med Microbiol. 2019;68:292–302. https://doi.org/10.1099/jmm.0.000915

22. Ramasindrazana B, Andrianaivoarimanana V, Rakotondramanga JM, Birdsell DN, Ratsitorahina M, Rajerison M. Pneumonic plague transmission, Moramanga, Madagascar, 2015. Emerg Infect Dis. 2017;23:521–4. https://doi.org/10.3201/eid2303.161406

23. Ratsitorahina M, Chanteau S, Rahalison L, Ratsifasoamanana L, Boisier P. Epidemiological and diagnostic aspects of the outbreak of pneumonic plague in Madagascar. Lancet. 2000;355:111–3. https://doi.org/10.1016/S0140-6736(99)05163-6

24. Richard V, Riehm JM, Herindrainy P, Soanandrasana R, Ratsitoharina M, Rakotomanana F, et al. Pneumonic plague outbreak, Northern Madagascar, 2011. Emerg Infect Dis. 2015;21:8–15. https://doi.org/10.3201/eid2101.131828

25. Begier EM, Asiki G, Anywaine Z, Yockey B, Schriefer ME, Aleti P, et al. Pneumonic plague cluster, Uganda, 2004. Emerg Infect Dis. 2006;12:460–7. https://doi.org/10.3201/eid1203.051051

26. Bertherat E, Thullier P, Shako JC, England K, Koné ML, Arntzen L, et al. Lessons learned about pneumonic plague diagnosis from two outbreaks, Democratic Republic of the Congo. Emerg Infect Dis. 2011;17:778–84. https://doi.org/10.3201/eid1705.100029

27. Ge P, Xi J, Ding J, Jin F, Zhang H, Guo L, et al. Primary case of human pneumonic plague occurring in a Himalayan marmot natural focus area Gansu Province, China. Int J Infect Dis. 2015;33:67–70. https://doi.org/10.1016/j.ijid.2014.12.044

28. Wu K, Wang Y, Wang M. Epidemiologic analysis on Tibetan sheep plague from 1975 to 2005 in Qinghai Province. Chinese Journal of Endemiology. 2009;28:665–7.

29. Zhang H, Wang S, Wu D, Liang X. Dynamic analysis of human plague epidemic situation in Gansu. Chinese Journal of Endemiology. 2007;26:82–4.

30. Centers for Disease Control and Prevention. Plague—United States, 1992. MMWR Morb Mortal Wkly Rep 1992;41:787–90.

31. Gage KL, Dennis DT, Orloski KA, Ettestad P, Brown TL, Reynolds PJ, et al. Cases of cat-associated human plague in the Western US, 1977–1998. Clin Infect Dis. 2000;30:893–900. https://doi.org/10.1086/313804

32. Kartman L. Historical and oecological observations on plague in the United States. Trop Geogr Med. 1970;22:257–75.

33. Kartman L. The role of rabbits in sylvatic plague epidemiology, with special attention to human cases in New Mexico and use of the fluorescent antibody technique for detection of *Pasteurella pestis* in field specimens. Zoonoses Res. 1960;1:1–27.

34. Poland JD, Barnes AM, Herman JJ. Human bubonic plague from exposure to a naturally infected wild carnivore. Am J Epidemiol. 1973;97:332–7. https://doi.org/10.1093/oxfordjournals.aje.a121513

35. von Reyn CF, Barnes AM, Weber NS, Quan T, Dean WJ. Bubonic plague from direct exposure to a naturally infected wild coyote. Am J Trop Med Hyg. 1976;25:626–9. https://doi.org/10.4269/ajtmh.1976.25.626

36. Christie AB, Chen TH, Elberg SS. Plague in camels and goats: their role in human epidemics. J Infect Dis. 1980;141:724–6. https://doi.org/10.1093/infdis/141.6.724

37. Sagiev Z, Meka-Mechenko T, Kunitsa T, Musagalieva R, Ismailova A, Kulbaeva M, et al. Diseases of human plague in 1974–2003 in Kazakhstan. Ekoloji. 2019;28:39–48.

38. Mitchell JA, Pirie JH, Rhodes WF, Powell W. Epizootic among veld rodents in De Aar and neighbouring districts of the Northern Cape province. J Hyg (Lond). 1930; 29:394–414.

39. Saeed AA, Al-Hamdan NA, Fontaine RE. Plague from eating raw camel liver. Emerg Infect Dis. 2005;11:1456–7. https://doi.org/10.3201/eid1109.050081

40. Brygoo E, Dodin A. Apropos of telluric plague and burrow plague: Madagascan data [in French]. Bull Soc Pathol Exot. 1965;1:14–7.

41. Chernin E. Richard Pearson Strong and the Manchurian epidemic of pneumonic plague, 1910–1911. J Hist Med Allied Sci. 1989;44:296–319. https://doi.org/10.1093/jhmas/44.3.296

42. Kool JL. Risk of person-to-person transmission of pneumonic plague. Clin Infect Dis. 2005;40:1166–72. https://doi.org/10.1086/428617

43. Didelot X, Whittles LK, Hall I. Model-based analysis of an outbreak of bubonic plague in Cairo in 1801. J R Soc Interface. 2017;14:20170160. https://doi.org/10.1098/rsif.2017.0160

44. Whittles LK, Didelot X. Epidemiological analysis of the Eyam plague outbreak of 1665–1666. Proc Biol Sci. 2016;283:20160618. https://doi.org/10.1098/rspb.2016.0618

45. Teh W, Chun W, Pollitzer R. Plague in Manchuria: I. observations made during and after the second Manchurian plague epidemic of 1920–21, II. The rôle of the tarabagan in the epidemiology of plague.. J Hyg (Lond). 1923;21:307–58. https://doi.org/10.1017/S0022172400031521

46. Strong R, Teague O. Studies on pneumonic plague and plague immunisation. II the method of transmission of the infection in pneumonic plague and manner of spread of the disease during the epidemic. The Philippine Journal of Tropical Medicine. 1912;7:137–56.

Address for correspondence: Sophie Jullien, Institute of Global Health, University of Barcelona, Carrer Rosselló 132, 5-2, 08036 Barcelona, Spain; email: sophjullien@gmail.com

etymologia

Culex quinquefasciatus [ˈkyo͞o leks ˈkwinkwə fa she ˈah tus]

Sarah Anne J. Guagliardo, Rebecca S. Levine

In 1823, the American entomologist Thomas Say described *Culex* (Latin for "gnat") *quinquefasciatus*, which he collected along the Mississippi River. Originally written as "C. 5-fasciatus," the name refers to 5 ("quinque") black, broad, transverse bands ("fasciatus" or "fasciae") on the mosquito's dorsal abdomen. The name remains despite later revelations of more than 5 fasciae, thanks to improved microscopy. Although quinquefasciatus is the official scientific name, there are at least 5 synonymous names for this species.

Say described this species as "exceedingly numerous and troublesome." "Quinx" are among the world's most abundant peridomestic mosquitoes, earning the nickname "southern house mosquito." *Cx. quinquefasciatus* is found throughout subtropical and tropical areas worldwide, except for exceedingly dry or cold regions. This mosquito is a principal vector of many pathogens, transmitting the phlebovirus Rift Valley fever virus and the 2 flaviviruses St. Louis encephalitis virus and West Nile virus, in addition to filarial worms and avian malarial parasites.

Figure. Female *Culex quinquefasciatus* mosquito. Image credit: CDC Public Health Image Library, 1976.

Sources

1. Belkin J. *Quinquefasciatus* or *Fatigans* for the tropical (Southern) house mosquito (Diptera: Culicidae). Proc Entomol Soc Wash. 1977;79:45–52.

2. Farajollahi A, Fonseca DM, Kramer LD, Marm Kilpatrick A. "Bird biting" mosquitoes and human disease: a review of the role of *Culex pipiens* complex mosquitoes in epidemiology. Infect Genet Evol. 2011;11:1577–85. https://doi.org/10.1016/j.meegid.2011.08.013

3. Harrison BA, Byrd BD, Sither CB, Whitt PB. The Mosquitoes of the Mid-Atlantic Region: An Identification Guide. Cullowhee (NC): Western Carolina University; 2016.

4. Say T. Descriptions of dipterous insects of the United States. Journal of the Academy of Natural Sciences. 1823;3:9–54.

5 University of Florida, Department of Entomology and Nematology. Featured creatures. [cited 2021 Mar 3]. http://entnemdept.ufl.edu/creatures/aquatic/southern_house_mosquito.htm

Address for correspondence: Sarah Anne J. Guagliardo, Centers for Disease Control and Prevention, 1600 Clifton Rd NE, Atlanta, GA 30327-4027, USA; email: sguagliardo@cdc.gov

Four Human Cases of Eastern Equine Encephalitis in Connecticut, USA, during a Larger Regional Outbreak, 2019

Stacy C. Brown,[1,2] Justine Cormier,[1] Jessica Tuan, Audun J. Lier, Declan McGuone,
Philip M. Armstrong, Firas Kaddouh,[3] Sunil Parikh, Marie Louise Landry, Kevin T. Gobeske

Medscape ACTIVITY
EDUCATION

In support of improving patient care, this activity has been planned and implemented by Medscape, LLC and Emerging Infectious Diseases. Medscape, LLC is jointly accredited by the Accreditation Council for Continuing Medical Education (ACCME), the Accreditation Council for Pharmacy Education (ACPE), and the American Nurses Credentialing Center (ANCC), to provide continuing education for the healthcare team.

Medscape, LLC designates this Journal-based CME activity for a maximum of 1.00 **AMA PRA Category 1 Credit(s)™**. Physicians should claim only the credit commensurate with the extent of their participation in the activity.

Successful completion of this CME activity, which includes participation in the evaluation component, enables the participant to earn up to 1.0 MOC points in the American Board of Internal Medicine's (ABIM) Maintenance of Certification (MOC) program. Participants will earn MOC points equivalent to the amount of CME credits claimed for the activity. It is the CME activity provider's responsibility to submit participant completion information to ACCME for the purpose of granting ABIM MOC credit.

All other clinicians completing this activity will be issued a certificate of participation. To participate in this journal CME activity: (1) review the learning objectives and author disclosures; (2) study the education content; (3) take the post-test with a 75% minimum passing score and complete the evaluation at http://www.medscape.org/journal/eid; and (4) view/print certificate. For CME questions, see page 2248.

Release date: July 21, 2021; Expiration date: July 21, 2022

Learning Objectives

Upon completion of this activity, participants will be able to:

• Examine the clinical findings and diagnostic challenges in an outbreak of 4 eastern equine encephalitis cases seen at a single Connecticut institution within a 3-week period in 2019

• Assess the epidemiologic patterns in an outbreak of 4 eastern equine encephalitis cases seen at a single Connecticut institution within a 3-week period in 2019

• Evaluate the clinical and public health implications of diagnostic challenges, clinical findings, and epidemiologic patterns in an outbreak of 4 eastern equine encephalitis cases seen at a single Connecticut institution within a 3-week period in 2019

CME Editor

Amy J. Guinn, BA, MA, Copyeditor, Emerging Infectious Diseases. *Disclosure: Amy J. Guinn, BA, MA, has disclosed no relevant financial relationships.*

CME Author

Laurie Barclay, MD, freelance writer and reviewer, Medscape, LLC. *Disclosure: Laurie Barclay, MD, has disclosed no relevant financial relationships.*

Authors

Disclosures: **Stacy C. Brown, MD; Justine Cormier, MD; Jessica J. Tuan, MD, MS; Audun J. Lier, MD, MPH; Declan McGuone, MD; Philip M. Armstrong, ScD; Firas Kaddouh, MD; Sunil Parikh MD, MPH; Marie Louise Landry, MD;** and **Kevin T. Gobeske, MD, PhD, MPH,** *have disclosed no relevant financial relationships.*

Author affiliations: Yale University, New Haven, Connecticut, USA (S.C. Brown, J. Cormier, J. Tuan, A.J. Lier, D. McGuone, F. Kaddouh, S. Parikh, M.L. Landry, K.T. Gobeske); Connecticut Agricultural Experiment Station, New Haven (P.M. Armstrong)

[1]These authors contributed equally to this article.
[2]Current affiliation: University of Hawai'i, Honolulu, Hawaii, USA.
[3]Current affiliation: University of Texas Health Science Center, San Antonio, Texas, USA.

During 3 weeks in 2019, 4 human cases of Eastern equine encephalitis (EEE) were diagnosed at a single hospital in Connecticut, USA. The cases coincided with notable shifts in vector–host infection patterns in the northeastern United States and signified a striking change in EEE incidence. All 4 cases were geographically clustered, rapidly progressive, and neurologically devastating. Diagnostic tests conducted by a national commercial reference laboratory revealed initial granulocytic cerebrospinal fluid pleocytosis and false-negative antibody results. EEE virus infection was diagnosed only after patient samples were retested by the arbovirus laboratory of the Centers for Disease Control and Prevention in Fort Collins, Colorado, USA. The crucial diagnostic challenges, clinical findings, and epidemiologic patterns revealed in this outbreak can inform future public health and clinical practice.

Eastern equine encephalitis virus (EEEV) is a single-stranded, positive-sense RNA arbovirus within the *Alphavirus* genus of the *Togaviridae* family. EEEV is maintained in enzootic cycles between ornithophilic *Culiseta melanura* mosquitoes and passerine birds in hardwood swamps in the northeast region of the United States (1). Epizootic cycles develop when virus infects mammal-biting bridge vector mosquitoes and then spreads to dead-end hosts, such as humans or husbanded animals (2,3). Mechanisms of viral or ecologic changes that could sustain epizootic patterns are of great public health interest.

Human Eastern equine encephalitis (EEE) disease develops 4–10 days after arboviral transmission (4). Neuroinvasive EEE occurs in just 5% of cases, but mortality rates exceed 30% and neurologic effects are widespread (5). Animal studies suggest that central nervous system (CNS) invasion occurs by neuro-olfactory spread or by crossing the blood–brain barrier during peak viremia (6). Neuronal injury occurs via direct viral toxicity or secondarily through CNS vasculitis, in which the basal ganglia, thalamus, and cortex commonly are affected (7). Histopathologic traits include tissue infiltration of neutrophils and mononuclear cells, perivascular cuffing, inclusion bodies, and neuronal necrosis (6–8). Like other alphaviruses, EEEV can antagonize components of innate and adaptive immunity to enable rapid propagation in brain tissue (9). Inflammatory cascades and direct cytopathy continue to amplify cerebral injury, leading to progressive fever, confusion, coma, cerebral edema, and death (6,10–12).

Thus far, the epidemiologic significance of EEE in the United States has been relatively small, and only 4–8 human cases are diagnosed nationally in a typical year; before 2019, Connecticut had only 1 human case, in 2013 (13–15). However, during 2019, human cases climbed to 38 nationally, and 19 of these were in New England, representing the largest EEE outbreak in 50 years (5,16). Experts are closely tracking whether the increased EEE cases reflect similar patterns occurring in West Nile virus (WNV), Powassan virus, Zika virus, and other arboviruses undergoing shifts in background prevalence (11–14). We describe the diagnosis, clinical features, and epidemiology of 4 human EEE cases from Connecticut, USA, that illustrate lessons for emerging viral disease.

Cases and Objective Findings

Case 1

A 77-year-old woman with prior breast cancer and treatment for Lyme disease arrived at the emergency department with acute fever, headache, weakness, and confusion (Appendix Figure 1, https://wwwnc.cdc.gov/EID/article/27/8/20-3730-App1.pdf). Cerebrospinal fluid (CSF) studies revealed mild protein elevation with monocytic pleocytosis (Table). Standard infectious workup was performed, along with WNV testing and an immunofluorescence assay (IFA) arboviral panel that included EEE, Western equine encephalitis, Saint Louis encephalitis, and California encephalitis; all results were negative (Appendix Table).

Despite empiric meningitis treatment, her illness progressed swiftly, involving seizures, coma, flaccid paralysis, and refractory shock, marking an especially severe case (Appendix Figure 1). CSF counts on day 7 and 13 shifted to a lymphocytic pleocytosis with escalating protein level, yet infectious workup results remained negative (Table; Appendix Figure 2). Secondary inflammatory pathology was treated with methylprednisolone, plasma exchange, and intravenous immunoglobulin (IVIg), yielding fleeting small improvements (Appendix Figure 1).

Computed tomography (CT) imaging on day 2 of illness showed nonspecific subcortical changes (Figure 1), but magnetic resonance imaging (MRI) on day 4 showed diffuse T2 signal throughout the forebrain, thalamus, cerebellum, and brainstem (Figure 2). Repeat MRI on days 12 and 18 revealed expansion of bilateral frontotemporal edema and injury, consistent with progression of inflammatory mechanisms (Figure 2; Appendix Figure 2).

Recent mosquito surveillance and reported equine cases of EEE, plus the patient's temporal and geographic proximity to these reports, environmental exposures, and current symptom progression, all suggested arboviral disease. Thus, we also sent initial CSF samples to the Arbovirus Diagnostic Laboratory,

Table. Clinical and laboratory findings of 4 patients hospitalized with Eastern equine encephalitis, Connecticut, 2019*

Characteristics and diagnostic testing	Case 1			Case 2			Case 3		Case 4		
Age, y/sex	77/F			73/M			64/M		42/M		
Date of illness onset	Aug 28			Sep 11			Sep 12		Aug 21		
Signs and symptoms	Fever, confusion, headache, shock, coma, seizures, flaccid paralysis			Stupor, left-sided weakness			Fever, right arm clumsiness; rapid progression to coma		Neck pain, fever, dysarthria, confusion, seizures		
Day of brain MRI; result	Day 4; diffuse T2 hyperintensity cerebrum, cerebellum, brainstem			Day 4; hyperintensity bilateral basal ganglia, right occipital regions			Day 5; left thalamic enhancement, T2 hyperintensity temporal lobe		Day 3; leptomeningeal enhancement right frontal and parietal lobes, T1 hyperintense signal globi pallidi		
	Days postadmission										
Laboratory findings	3	7	13	2	4	9	2†	4	2	9	21
CSF values											
Protein, mg/dL	90	238	94	112	119	174	108	146	236	288	ND
Glucose, mg/dL	57	74	53	62	64	81	65	78	225	79	ND
Leukocytes/mm^3	60‡	13	9	428	62	40	1,162	33	343	142	13
Neutrophils, %	22	2	0	86	9	0	76	8	80	0	2
Lymphocytes, %	38	73	100	9	78	85	11	87	14	89	79
Immunoassay, CSF											
Reference lab§											
IgM IFA	−	ND	ND	ND	−	ND	ND	−	ND	−	ND
IgG IFA	−	ND	ND	ND	−	ND	ND	−	ND	−	ND
CDC											
IgM MIA	+	ND	ND	ND	+	ND	ND	+	ND	+	+
PRNT¶	1:4	ND	ND	ND	1:32	ND	ND	1:16	ND	ND	1:4,096#
Immunoassay, serum											
Reference lab**								Day 7			
IgM IFA	−	ND	ND	ND	ND	ND	ND	−	ND	ND	ND
IgG IFA	−	ND	ND	ND	ND	ND	ND	+; 1:16	ND	ND	ND
CDC								Day 6			
IgM MIA	ND	ND	ND	ND	ND	ND	ND	+	ND	ND	ND
PRNT#	ND	ND	ND	ND	ND	ND	ND	ND	ND	ND	ND
Outcome	Death on day 22			Death on day 10			Death on day 8		Severe sequelae		

*CDC, Centers for Disease Control and Prevention; CSF, cerebrospinal fluid; IFA, indirect immunofluorescence assay; lab, laboratory; MIA, microparticle immunoassay; ND, not done; PRNT, plaque reduction neutralization test; −, negative; +, positive.
†CSF from outside hospital laboratory before transfer.
‡CSF with 40% mononuclear cells.
§CSF IFA ≥1:4 is positive.
¶CSF PRNT ≥1:2 is positive.
#CSF contaminated with blood.
**Serum IFA ≥1:16 positive.

part of the Division of Vector-Borne Diseases, National Center for Emerging and Zoonotic Infectious Diseases, at the Centers for Disease Control and Prevention (CDC) in Fort Collins, Colorado, USA. On day 18 of the patient's illness, CDC reported microsphere-based immunoassay (MIA) IgM screening for EEEV was positive and confirmed by plaque-reduction neutralization test (PRNT) titers. Given the patient's grave brain injury, her family elected to pursue comfort-focused care strategies, and she died on day 22 of her illness (Appendix Figure 1).

Case 2

A 73-year-old man who enjoyed feeding wild animals around his wooded home was found unresponsive after reporting new dizziness, paresthesia, and confusion the previous day. In the emergency department he was stuporous, with left-sided weakness, but neuroimaging results were negative. His CSF samples had a granulocytic pleocytosis and elevated protein on day 2 of illness (Table). Despite empiric treatment, he experienced abnormal neuromuscular tone, brainstem dysfunction, coma, and respiratory failure requiring mechanical ventilation (Appendix Figure 1). Subsequent CSF studies on days 4 and 9 of illness revealed lymphocytic pleocytosis and persistent protein elevation (Table). Commercial EEEV IFA on CSF collected on day 4 was negative, as were further infectious studies. IVIg was started on day 9 without improvement. MRI on day 4 showed diffuse patchy enhancement, edema, and injury (Figure 2).

Retesting of CSF by CDC demonstrated positive EEEV IgM MIA results, confirmed by PRNT on day 9 of illness. Understanding the gravity of his injury, his family requested a comfort-centered care transition, and he died on day 10 after compassionate extubation (Figure 1). At autopsy, gross and microscopic pathology of the brain showed ischemic changes, vascular

congestion, inflammatory cell infiltration and microgliosis (Figure 2; Appendix Figure 3), although viral inclusions were not found.

Case 3

A 64-year-old man with Parkinson's disease and rheumatoid arthritis was admitted with fever and right arm clumsiness that rapidly progressed to coma and ventilator dependence by day 2. Despite antimicrobial and steroid immunosuppressant treatments, his function declined persistently (Appendix Figure 1). MRI on day 2 and 5 showed progressive enhancement and T2 hyperintensity in limbic, thalamic, and striatal regions, advancing to severe edema and compression (Figure 2).

Initial CSF studies showed elevated protein and granulocytic pleocytosis, shifting to lymphocytic predominance and higher protein by day 4 (Table). New seizures on day 4 were controlled with levetiracetam, but the cooccurring sympathetic and neuromuscular instability remained intractable, signifying especially severe disease (Appendix Figure 1). IVIg was started on day 6 without improvement. On day 8, the patient had acute loss of brainstem reflexes, and a CT showed global cerebral edema and brainstem compression (Figure 1). Hypertonic therapy was started; however, his family soon elected for a comfort-centered focus, and he was compassionately extubated that day.

Reference laboratory EEEV IFA from serum on illness day 6 was negative. Day 4 CSF was retested by CDC; 12 days postmortem, the sample tested positive for EEEV IgM, which was confirmed by PRNT with a 1:16 titer (Table; Appendix Figure 1). Postmortem pathology studies revealed severe ischemic, inflammatory, and compressive injury (Figure 2).

Case 4

A 42-year-old man with hepatitis C and childhood ventriculoperitoneal shunt placement arrived at the emergency department with neck pain, fever, dysarthria, and confusion. His neurologic function declined rapidly, and he experienced refractory seizures that required intubation and multidrug treatment (Appendix Figure 1). CSF also showed granulocytic to lymphocytic shift of pleocytosis and elevated protein on days 2 and 9 (Table). We confirmed his shunt was nonfunctional; we removed it because of the concern of infection and started the patient on broad-spectrum antimicrobial drugs. Results of autoimmune panels, WNV serology, and EEEV IFA for IgG and IgM from CSF on day 9 were negative (Appendix Table).

Right frontal lobe brain biopsy on day 15 showed cortical necrosis and inflammation of unclear etiology (Appendix Figure 2). He received empiric IVIg on days 23–27 per regular protocols for neuroinflammatory pathologies but showed no clinical or radiographic improvement. His ongoing hospital course remained complicated (Appendix Figure 1). MRI studies revealed spreading patchy cortical hyperintensity, gyriform enhancement, and mild subcortical injury (Figure 2; Appendix Figure 1, panel C).

On day 40, CDC testing of CSF collected on day 21 of his illness returned positive results for EEEV IgM, confirmed by PRNT titer of 1:4,096. Subsequent CDC retesting of the stored day 9 CSF sample also returned positive results. After 6 weeks, the patient was discharged to inpatient hospice, where he became more alert and regained language comprehension. He moved to a rehab facility and continued to have slow improvement but remained dependent on skilled care.

Figure 1. Representative computed tomography axial sections showing early gray-white boundary changes among patients with Eastern equine encephalitis, Connecticut, USA, 2019. A) Axial section showing early gray-white boundary changes on day 3 of illness. B) Axial section with advancing subcortical edema on day 5 of illness. C) Axial section showing diffuse edema with mass effect on adjacent structures and risk of herniation syndromes after 7 days of infection.
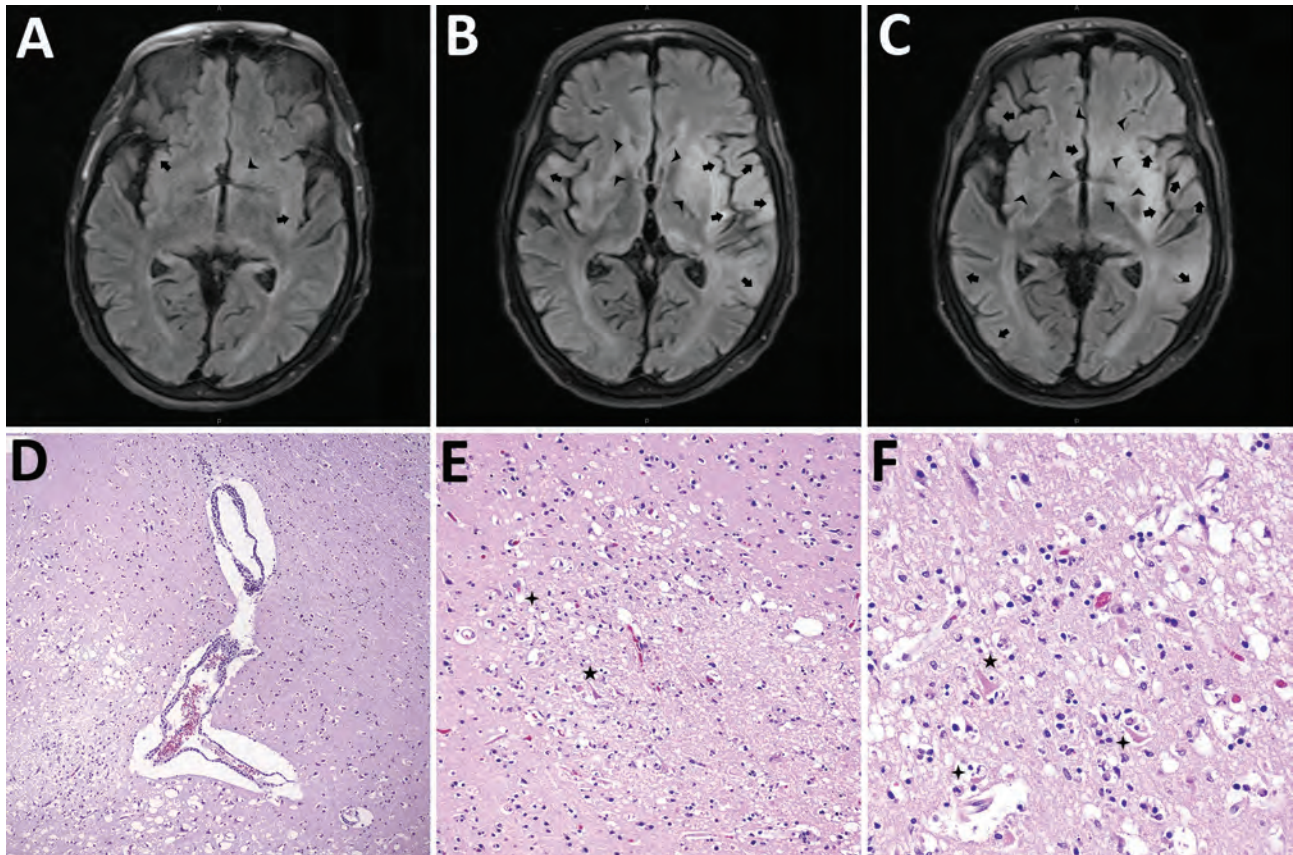
Figure 2. Mechanisms of injury in 4 human cases of Eastern equine encephalitis, Connecticut, USA, 2019. A) Magnetic resonance imaging (MRI) representative axial section from day 2 of a patient's illness shows early development of edema around the thalamus, basal ganglia, and limbic cortical (arrows) and subcortical (arrowheads) regions. B) Representative MRI axial section from day 4 of a patient's illness shows progression of injury in these regions and the diencephalon, basal forebrain, and subcortical areas (arrowheads). C) MRI axial section after 1 week of a patient's illness shows expanding patchy and confluent cortical edema (arrows) and diffuse swelling in basal regions (arrowheads). D) Hematoxylin and eosin (HE)–stained photomicrograph shows the gray-white matter interface with perivascular lymphocytic cuffing and hypoxic-ischemic change in adjacent cortex. Original magnification ×40. E) HE-stained photomicrograph shows a recent gray matter microinfarction, including ischemic neurons with red cell change (5-pointed star) and perineuronal vacuolation (4-pointed star). Original magnification ×200. F) HE-stained photomicrograph shows details of acute hypoxemic-ischemic change with perineuronal (4-pointed stars) and nonspecific vacuolation, red neurons (5-pointed star), rarefaction, and pyknotic cellular debris. Original magnification ×400.

Diagnostic Testing

Epidemiologic and clinical features, together with knowledge of unprecedented prevalence of EEEV-positive mosquitoes in the state, prompted our virology laboratory to contact CDC's Arbovirus Diagnostic Laboratory to have case 1 retested with expedited processing. After this positive test result, the Connecticut Department of Public Health (DPH) and CDC approved submission of subsequent samples directly to CDC for priority testing. Turnaround was improved from 3–4 weeks to <10 days. Connecticut DPH subsequently validated an in-house EEEV IgM MIA test for rapid and sensitive screening for future outbreaks.

Reference laboratory EEEV IFA testing of CSF at 1:4 dilution was negative for IgM for all cases in samples spanning day 3, 4, 6, and 9 of illness. Upon learning of false-negative results, the commercial laboratory retested 3 of the CSF samples undiluted, but results remained negative. Thus, for our samples, IFA IgM findings did not correlate with the duration of illness or concentration as shown by PRNT titer.

Local Epidemiology

During June–October 2019, mosquitoes were trapped and tested for arbovirus infection at 92 fixed-trapping sites in Connecticut as a part of the statewide surveillance program. During the season, mosquitoes are collected weekly at each location by using CDC light traps baited with dry ice and gravid traps baited with a hay-lactalbumin infusion. Sample preparation and EEEV detection was consistent for all sites and

between years. Connecticut surveillance sites first collected EEEV-positive mosquitoes in late July 2019, ≈4 weeks earlier than other years having EEEV (*17*,*18*). Equine EEEV infections surfaced in early August and continued through September. Numbers of EEEV-positive mosquitoes peaked by late August, but numbers remained elevated through mid-October. The 4 human cases occurred in late August and early September within a localized region of southeastern Connecticut where equine and vector involvement also were highest. Shortly before the incidence in humans, numbers of *Cs. melanura* mosquitoes and mammal-biting bridge vectors carrying EEEV both rose distinctly (Figure 3, panel A). Climate conditions in the preceding months had shown temperatures 2.4°F above average through the summer and 2.6°F warmer during the winter; the region had 11 inches more precipitation than normal (*19*,*20*). Concordantly,

21,880 *Cs. melanura* mosquitoes were collected in Connecticut during 2019, which is 2.4 times the annual average during 2001–2018 (Figure 3, panel B). All human and equine EEE cases were tightly clustered geographically and coincided with temperature and vector population rises (Figure 4).

Discussion

The cases we report represent a notable diversion from the background incidence and clinical severity of EEE in this region. This single-state experience is striking individually but becomes more salient in relation to patterns occurring contemporaneously in nearby states and possibly in the future (Appendix Figure 5). Recognizing and controlling epidemics requires dependable diagnostic methods and coordination between clinicians, health departments, and surveillance programs. Viral neuroinvasive infections
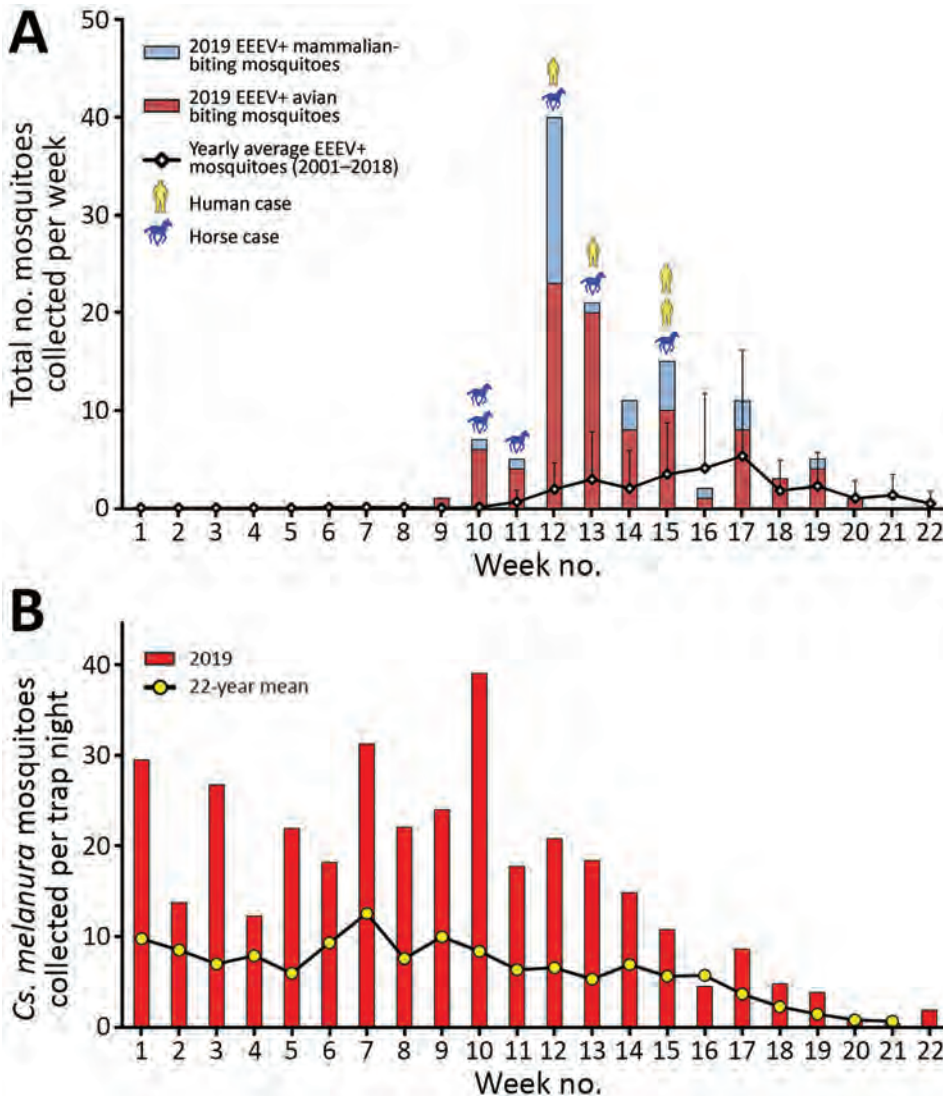
Figure 3. Epidemiology of EEE and mosquito vector populations, Connecticut, USA, June 2–November 2, 2019. A) Epidemic curve of EEE in Connecticut in mosquito populations, horses, and humans. Error bars indicate 95% CIs. B) Weekly collection of *Culiseta melanura* mosquitoes during 2019 compared with long-term historical averages. EEE, Eastern equine encephalitis; EEEV, EEE virus; +, positive.
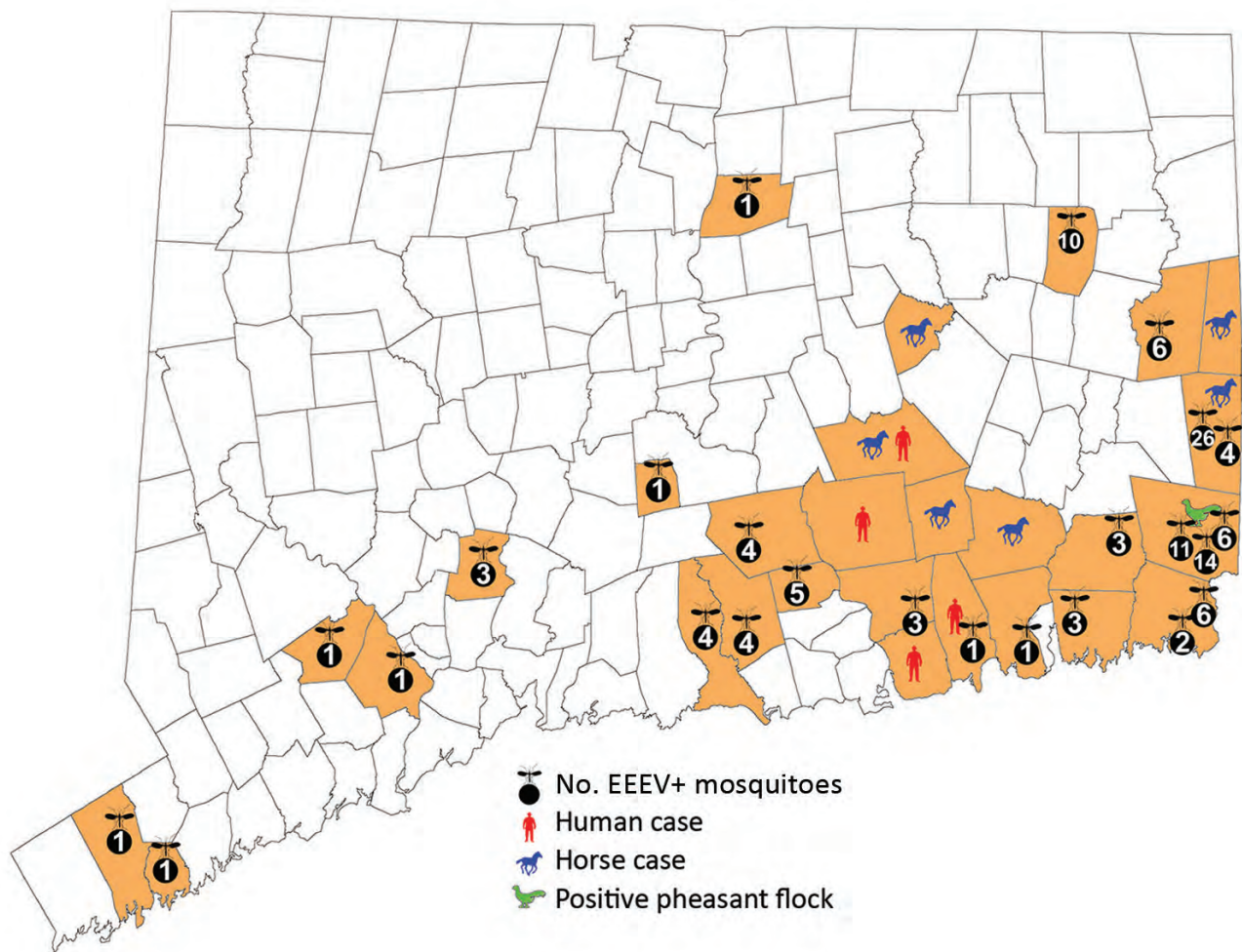
Figure 4. Geographic distribution of EEE in mosquitoes, humans, horses, and pheasant flocks, Connecticut, USA, 2019. EEE, Eastern equine encephalitis; EEEV, EEE virus; +, positive.

can pose even greater challenges because our best diagnostic efforts reveal an etiology in only one third of encephalitis cases (*21*). Our experience demonstrates the importance of unified efforts in recognizing a new epidemic and avoiding public health pitfalls.

Because virus rarely is present in specimens when patients are symptomatic, EEEV assays target host antibodies produced against viral epitopes. EEEV IgM usually becomes measurable 3–8 days after infection (*22*). Assay processing time can further extend the lag time from clinical onset to initiation of secondary injury mechanisms and the ability to make diagnostically informed decisions. The cases we report demonstrate the challenges of mismatched timeframes for analytic pathways versus critical periods for intervention in patient care and community education. Assessment of data needed for decision-making becomes crucial, especially when considerations

involve rapidly devastating illness, expensive treatments, or time-sensitive community interventions. Our experience exemplified the need for prompt compilation and synthesis of findings to guide decisions, such as whether and when to begin IVIg or plasma exchange treatments during case 1 and to postpone outdoor school sporting events statewide during case 4. Future ability to establish evidence-based treatments or targeted protocols likewise will depend on improved timing of diagnosis and decision-making.

Shared clinical features from our patients also highlight patterns to alert practitioners of EEEV infection as the etiology of encephalitis. We noted rapid shifts in CSF profiles from granulocytic to lymphocytic predominance. Seizures, secondary inflammatory injury, cerebral edema, rapid deterioration, and clinical considerations for starting immunomodulatory treatments all should be signals prompting outreach

to public health and laboratory medicine colleagues. Other features of severe disease that were especially prominent in our patients, and possibly underrecognized as elements of critical neuroinvasive EEE overall, included refractory shock with adrenergic insensitivity and neuromuscular instability with either flaccid paralysis or rigidity.

Diagnosing EEE in our patients was unexpectedly challenging because the commercially available arbovirus IFA test failed to detect EEEV antibodies in all cases. Yet, all 4 CSF samples tested positive at the CDC laboratory by the more recently developed MIA to screen for EEEV IgM and confirmatory PRNT. Whereas older IFA methods use spots of virus-infected cells affixed to slide wells, MIA uses microbeads coated with EEEV envelope proteins as the antigen-presenting substrate incubated with a patient's CSF or serum, then secondary IgM for detection (23). For PRNT, IgM-reactive samples are serially diluted, each dilution is mixed with infectious virus, then inoculated into cell culture. If present, virus-specific neutralizing antibodies will reduce the number of virus-induced plaques observed after a designated incubation period. Of note, the virus strain EEE New Jersey 60 is used in all 3 methods and does not appear to explain the discrepancy.

Because only 1 test in the United States, DxSelect Arbovirus IFA IgM/IgG (Focus Diagnostics, https://www.focusdx.com), has been cleared by the Food and Drug Administration for diagnosing EEEV, Western equine encephalitis virus, St. Louis encephalitis virus, and California encephalitis/La Crosse virus, all commercial reference laboratories use the same IFA kits for arbovirus antibody detection. Many potential variables exist within IFA testing, including slide and reagent manufacturing, manual processing of antibody application steps, microscopy techniques and equipment, and subjective reading of results. Nevertheless, no other false-negative IFA results have been reported to date. Of note, arboviral IFA kits are approved by the Food and Drug Administration only for serum testing at an initial dilution of 1:16; CSF testing must be validated independently at each commercial laboratory, including ascertaining the starting dilution. Because of the failure to detect antibody at a 1:4 screening dilution in our 4 cases, the reference laboratory now screens all CSF samples undiluted.

Because only 4–8 cases occur nationally in a typical year, EEE is a rarely diagnosed infection, and large reference laboratories might receive few to no positive samples annually. The infrequent positivity rates among samples provides little opportunity to verify diagnostic assays by using clinical specimens or for comparison between IFA and other methods; we found no such reports in the literature. Nonetheless, MIA clearly was more sensitive than IFA as a screening test in our patients. A specific reason for the failure of IFA testing in these cases was not identified, but the presumed lower sensitivity of IFA methods should remain a consideration in future epidemics. Regardless of the cause, the discovery of systematic false-negative results highlights the need to think broadly about testing strategies for arboviral disease in a public health context, and particularly for cases of infectious encephalitis.

Crucial epidemiologic and viral ecologic factors also shed light on regional EEE emergence and could provide warnings for EEE risk in future years. Historically, EEEV has cyclic years of high amplification; Connecticut saw spikes in 2003 and 2009 and in 2013, when the only prior human case was recorded (15,18). However, closer examination of mosquito surveillance during high-activity years reveals patterns associated with the emergence of epidemics (Figure 3; Appendix Figure 4). High-activity years had exceptional increases of EEEV carriage by *Culiseta* mosquitoes, after which greater infection of mammal-biting vectors was reported. When human or equine cases emerged, temporal and geographic correlation were noted after the upsurges (Figures 3, 4). Mechanisms for human spillover from vector–host cycles remain unclear; studies also show direct transmission from primary enzootic vectors to mammalian and human hosts during larger EEE epizootic events (1–3,24–27). Therefore, prevention must be informed by recognition of earlier seasonal escalation of *Cs. melanura* populations and rapid rise of EEEV within enzootic or epizootic vectors (24).

Locally, the Connecticut River Valley has abundant densely wooded freshwater swamps, creating ideal habitat for EEEV enzootic vectors and hosts, and likely models conditions elsewhere (1,17). Weather patterns preceding our cases increased the productivity of mosquito larval environments and might have fostered *Cs. melanura* mosquitoes overwintering and early reproduction, per our trap collection timelines (1,2,18–20,27). Indeed, EEEV-positive mosquito counts were greater than any other arbovirus in our region, reaching 20 times normal in Connecticut and 200 times normal in Massachusetts (Appendix Figure 4). As the climate warms, the risk for EEE outbreaks could increase because of emergence of EEEV into optimized environments and from late-season persistence of infected vectors. Additional studies assessing

population genetics of the virus and vectors are needed to illuminate the triggers and evolution of such epidemics (2,5,25–27).

In the face of climatic and global changes, including warmer temperatures and human population growth and interaction with vector ecologies, future arboviral epidemics are certain, and the likelihood of an increasing burden of EEE is high. Coordination between public health and hospital settings to improve surveillance, clinical detection, and community education will be essential for gaining control of this potentially devastating neuroinvasive disease. Of note, awareness to reappraise and navigate diagnostic testing through local and reference laboratories has become a crucial skill for early detection of EEE cases and management of a local epidemic. Our state's experience shows the importance of bringing together public health, healthcare, diagnostic systems, and vector-control agencies, as well as community education and diagnostic systems, to mitigate risk for EEE among the public.

Acknowledgments

About the Author

Dr. Brown completed her fellowship training in neurocritical care and emergency neurology at Yale New Haven Hospital, Yale School of Medicine, in 2020 and currently serves as a neurointensivist at The Queen's Medical Center and Assistant Professor at the University of Hawai'i John A. Burns School of Medicine, Honolulu, Hawaii. Her research aims to understand and address population disparities in access to emergent neurologic care and brain injury support.

References

1. Molaei G, Thomas MC, Muller T, Medlock J, Shepard JJ, Armstrong PM, et al. Dynamics of vector-host Interactions in avian communities in four Eastern equine encephalitis virus foci in the Northeastern U.S. PLoS Negl Trop Dis. 2016;10:e0004347. https://doi.org/10.1371/journal.pntd.0004347
2. Arrigo NC, Adams AP, Weaver SC. Evolutionary patterns of Eastern equine encephalitis virus in North versus South America suggest ecological differences and taxonomic revision. J Virol. 2010;84:1014–25. https://doi.org/10.1128/JVI.01586-09
3. Heberlein-Larson LA, Tan Y, Stark LM, Cannons AC, Shilts MH, Unnasch TR, et al. Complex epidemiological dynamics of Eastern equine encephalitis virus in Florida. Am J Trop Med Hyg. 2019;100:1266–74. https://doi.org/10.4269/ajtmh.18-0783
4. Gill CM, Beckham JD, Piquet AL, Tyler KL, Pastula DM. Five emerging neuroinvasive arboviral diseases: Cache Valley, Eastern equine encephalitis, Jamestown Canyon, Powassan, and Usutu. Semin Neurol. 2019;39:419–27. https://doi.org/10.1055/s-0039-1687839
5. Morens DM, Folkers GK, Fauci AS. Eastern equine encephalitis virus—another emergent arbovirus in the United States. N Engl J Med. 2019;381:1989–92. https://doi.org/10.1056/NEJMp1914328
6. Vogel P, Kell WM, Fritz DL, Parker MD, Schoepp RJ. Early events in the pathogenesis of Eastern equine encephalitis virus in mice. Am J Pathol. 2005;166:159–71. https://doi.org/10.1016/S0002-9440(10)62241-9
7. Calisher CH. Medically important arboviruses of the United States and Canada. Clin Microbiol Rev. 1994;7:89–116. https://doi.org/10.1128/CMR.7.1.89
8. Roy CJ, Reed DS, Wilhelmsen CL, Hartings J, Norris S, Steele KE. Pathogenesis of aerosolized Eastern equine encephalitis virus infection in guinea pigs. Virol J. 2009;6:170. https://doi.org/10.1186/1743-422X-6-170
9. Trobaugh DW, Klimstra WB. Alphaviruses suppress host immunity by preventing myeloid cell replication and antagonizing innate immune responses. Curr Opin Virol. 2017;23:30–4. https://doi.org/10.1016/j.coviro.2017.02.004
10. Deresiewicz RL, Thaler SJ, Hsu L, Zamani AA. Clinical and neuroradiographic manifestations of Eastern equine encephalitis. N Engl J Med. 1997;336:1867–74. https://doi.org/10.1056/NEJM199706263362604
11. Hollidge BS, González-Scarano F, Soldan SS. Arboviral encephalitides: transmission, emergence, and pathogenesis. J Neuroimmune Pharmacol. 2010;5:428–42. https://doi.org/10.1007/s11481-010-9234-7
12. Zacks MA, Paessler S. Encephalitic alphaviruses. Vet Microbiol. 2010;140:281–6. https://doi.org/10.1016/j.vetmic.2009.08.023
13. Lindsey NP, Staples JE, Fischer M. Eastern equine encephalitis virus in the United States, 2003–2016. Am J Trop Med Hyg. 2018;98:1472–7. https://doi.org/10.4269/ajtmh.17-0927
14. McDonald E, Martin SW, Landry K, Gould CV, Lehman J, Fischer M, et al. West Nile virus and other domestic nationally notifiable arboviral diseases—United States, 2018. MMWR Morb Mortal Wkly Rep. 2019;68:673–8. https://doi.org/10.15585/mmwr.mm6831a1
15. Nelson R, Ciesielski T, Andreadis T, Armstrong PM. Human case of Eastern equine encephalitis–Connecticut, 2013. Connecticut Epidemiologst. 2014;34:9–10 [cited 2020 Aug 8]. https://portal.ct.gov/-/media/Departments-and-Agencies/DPH/dph/infectious_diseases/CTEPINEWS/Vol34No3pdf.pdf
16. Lindsey NP, Martin SW, Staples JE, Fischer M. Notes from the field: multistate outbreak of Eastern equine encephalitis virus—United States, 2019. MMWR Morb Mortal Wkly Rep. 2020;69:50–1. https://doi.org/10.15585/mmwr.mm6902a4
17. Skaff NK, Armstrong PM, Andreadis TG, Cheruvelil KS. Wetland characteristics linked to broad-scale patterns in *Culiseta melanura* abundance and Eastern equine encephalitis virus infection. Parasit Vectors. 2017;10:501. https://doi.org/10.1186/s13071-017-2482-0
18. The Connecticut Agricultural Experiment Station. State of Connecticut mosquito trapping and arbovirus testing program. 2019 Oct 22 [cited 2020 March 28]. https://portal.ct.gov/CAES/Mosquito-Testing/Introductory/State-of-Connecticut-Mosquito-Trapping-and-Arbovirus-Testing-Program
19. Mermel LA. Association of human Eastern equine encephalitis with precipitation levels in Massachusetts.

JAMA Netw Open. 2020;3:e1920261. https://doi.org/10.1001/jamanetworkopen.2019.20261

20. National Oceanic and Atmospheric Administration. 1981–2010 U.S. climate normals. 2018 Nov 5 [cited 2020 Mar 8]. https://www.ncdc.noaa.gov/data-access/land-based-station-data/land-based-datasets/climate-normals/1981-2010-normals-data

21. Bloch KC, Glaser CA. Encephalitis surveillance through the emerging infections program, 1997–2010. Emerg Infect Dis. 2015;21:1562–7. https://doi.org/10.3201/eid2109.150295

22. Centers for Disease Control and Prevention. Arboviral diseases, neuroinvasive and non-neuroinvasive case definition 2015; updated 2017 Aug 2 [cited 2020 March 20]. https://wwwn.cdc.gov/nndss/conditions/eastern-equine-encephalitis-virus-disease/case-definition/2015

23. Johnson AJ, Noga AJ, Kosoy O, Lanciotti RS, Johnson AA, Biggerstaff BJ. Duplex microsphere-based immunoassay for detection of anti-West Nile virus and anti-St. Louis encephalitis virus immunoglobulin m antibodies. Clin Diagn Lab Immunol. 2005;12:566–74. https://doi.org/10.1128/CDLI.12.5.566-574.2005

24. Molaei G, Armstrong PM, Graham AC, Kramer LD, Andreadis TG. Insights into the recent emergence and expansion of Eastern equine encephalitis virus in a new focus in the Northern New England USA. Parasit Vectors. 2015;8:516. https://doi.org/10.1186/s13071-015-1145-2

25. Soghigian J, Andreadis TG, Molaei G. Population genomics of *Culiseta melanura*, the principal vector of Eastern equine encephalitis virus in the United States. PLoS Negl Trop Dis. 2018; 12:e0006698. https://doi.org/10.1371/journal.pntd.0006698

26. Shepard JJ, Andreadis TG, Thomas MC, Molaei G. Host associations of mosquitoes at eastern equine encephalitis virus foci in Connecticut, USA. Parasit Vectors. 2016;9:474. https://doi.org/10.1186/s13071-016-1765-1

27. Tan Y, Lam TT, Heberlein-Larson LA, Smole SC, Auguste AJ, Hennigan S, et al. Large-scale complete-genome sequencing and phylodynamic analysis of Eastern equine encephalitis virus reveals source-sink transmission dynamics in the United States. J Virol. 2018;92:e00074-18. https://doi.org/10.1128/JVI.00074-18

Address for correspondence: Kevin T. Gobeske, Division of Neurocritical Care and Emergency Neurology, Department of Neurology, Yale School of Medicine, 15 York St, Box 208018, New Haven, CT 06510, USA; email: kevin.gobeske@yale.edu

Transmission Dynamics of Severe Acute Respiratory Syndrome Coronavirus 2 in High-Density Settings, Minnesota, USA, March–June 2020

Nicholas B. Lehnertz, Xiong Wang, Jacob Garfin, Joanne Taylor, Jennifer Zipprich,
Brittany VonBank, Karen Martin, Dana Eikmeier, Carlota Medus, Brooke Wiedinmyer,
Carmen Bernu, Matthew Plumb, Kelly Pung, Margaret A. Honein, Rosalind Carter, Duncan MacCannell,
Kirk E. Smith, Kathryn Como-Sabetti, Kris Ehresmann, Richard Danila, Ruth Lynfield

Coronavirus disease has disproportionately affected persons in congregate settings and high-density workplaces. To determine more about the transmission patterns of severe acute respiratory syndrome coronavirus 2 (SARS-CoV-2) in these settings, we performed whole-genome sequencing and phylogenetic analysis on 319 (14.4%) samples from 2,222 SARS-CoV-2–positive persons associated with 8 outbreaks in Minnesota, USA, during March–June 2020. Sequencing indicated that virus spread in 3 long-term care facilities and 2 correctional facilities was associated with a single genetic sequence and that in a fourth long-term care facility, outbreak cases were associated with 2 distinct sequences. In contrast, cases associated with outbreaks in 2 meat-processing plants were associated with multiple SARS-CoV-2 sequences. These results suggest that a single introduction of SARS-CoV-2 into a facility can result in a widespread outbreak. Early identification and cohorting (segregating) of virus-positive persons in these settings, along with continued vigilance with infection prevention and control measures, is imperative.

In the United States, coronavirus disease (CO-VID-19) has disproportionately affected adults residing in long-term care facilities (LTCFs) (*1–5*). Outbreaks in LTCFs have caused high numbers of

Author affiliations: Minnesota Department of Health, St. Paul, Minnesota, USA (N. Lehnertz, X. Wang, J. Garfin, J. Zipprich, B. VonBank, K. Martin, D. Eikmeier, C. Medus, B. Wiedinmyer, C. Bernu, M. Plumb, K. Pung, K.E. Smith, K. Como-Sabetti, K. Ehresmann, R. Danila, R. Lynfield); Centers for Disease Control and Prevention, Atlanta, Georgia, USA (J. Taylor, M.A. Honein, R. Carter, D. MacCannell)

hospitalizations and deaths. Similar findings have been reported in correctional facilities, where severe acute respiratory syndrome coronavirus 2 (SARS-CoV-2) infection incidence among inmates and staff is ≈5 times greater and age-adjusted mortality rate 3 times greater than that of the general population (*6–8*). Workers in high-density workplaces (e.g., meat-processing plants) have similarly been heavily affected; minority populations have been disproportionately affected (*9–11*).

The first COVID-19 case in Minnesota was detected on March 6, 2020. Shortly thereafter, CO-VID-19 outbreaks occurred across the state, including in LTCFs (March 12, 2020) and meat-processing plants (March 15, 2020), followed shortly thereafter by correctional facilities (March 25, 2020). During March 6–June 30, 2020, the Minnesota Department of Health (MDH) identified and responded to 1,060 distinct outbreaks of COVID-19 in LTCFs, comprising 4,421 cases in residents and 3,002 in staff members. In addition, 4 discrete outbreaks in correctional facilities resulted in 382 cases, and 68 outbreaks in meat-processing plants resulted in ≈2,616 cases among employees (data only from persons interviewed and where workplace information was provided); outbreaks in these 3 settings accounted for 31.3% of all identified persons in Minnesota.

For outbreaks in congregate settings and high-density workplaces, confirming the temporal and relational aspects of SARS-CoV-2 transmission was difficult, and the role of intrafacility spread versus multiple introductions was difficult to disentangle on the basis of epidemiologic information alone.

Whole-genome sequencing (WGS) of specimens from outbreak case-patients can be used to determine transmission dynamics and relatedness of viral pathogens in infectious disease outbreaks (12–15). Unprecedented efforts to sequence SARS-CoV-2 genomes have occurred at the local, regional, national, and international levels to investigate potential reinfections (16–19), nosocomial transmission (20), patterns of community spread (G.K. Moreno et al., unpub. data, https://doi.org/10.1101/2020.07.09.20149104) (21,22), and sources of SARS-CoV-2 introduction without known epidemiologic links (23).

In Minnesota, as part of the Centers for Disease Control and Prevention (CDC) SARS-CoV-2 Sequencing for Public Health Emergency Response, Epidemiology and Surveillance (SPHERES) consortium, the Minnesota Molecular Surveillance of SARS-CoV-2 initiative solicited specimens from outbreak case-patients for sequencing and genetic variation analysis to determine virus transmission patterns in congregate settings and meat-processing plants. To supplement epidemiologic information, assess whether single or multiple introductions were likely to have occurred during a facility outbreak, and evaluate molecular relatedness, we performed WGS on a convenience sample of SARS-CoV-2–positive specimens associated with outbreaks.

Methods

We chose 3 types of outbreak settings for WGS (LTCFs, correctional facilities, and meat-processing plants) and selected specific facilities partly according to outbreak effect and severity, the need for further clarity regarding transmission patterns, and availability of samples. Selected outbreaks occurred during March 6–June 30, 2020, at 4 unique LTCFs (A–D), 2 correctional facilities (A and B), and 2 meat-processing plants (A and B); cases were identified in persons residing in the same county as meat-processing plant A (community samples A).

At LTCFs, an outbreak was defined as $\geq$1 confirmed COVID-19 case in a resident or staff member. At correctional facilities, an outbreak was defined as 1 of the following:

- $\geq$2 cases in the inmate population >7 days after intake to a new facility with an epidemiologic link (defined as residing in the same unit or ward within a 14-day period).
- $\geq$2 cases in correctional staff members with an epidemiologic link (defined as having the potential to have been within 6 feet for $\geq$15 minutes while working in the facility during the 14 days before symptom onset (e.g., worked on the same unit during the same shift). An epidemiologic link also requires that cases among correctional staff neither shared a household nor were identified as close contacts with each other outside the facility during the standard case investigation.
- $\geq$1 facility-acquired COVID-19 cases in an inmate (defined as a confirmed diagnosis $\geq$14 days after entry to the facility, without exposure during the previous 14 days to another setting where an outbreak was known or suspected).

At meat-processing facilities, an outbreak was defined as $\geq$3 laboratory-confirmed COVID-19 cases among facility workers who resided in separate households. On June 1, we added to the definition of an outbreak in meat-processing plants that case onset dates occurred within 14 days of each other.

We defined case-patients at all outbreak locations as persons with a positive SARS-CoV-2 result according to reverse transcription PCR (RT-PCR), determined by using the original CDC protocol (24). We collected epidemiologic data (sex, age, symptom status, symptom onset date, residence, occupation, and potential source of exposure) by interviewing persons with laboratory-confirmed SARS-CoV-2.

The MDH Public Health Laboratory (PHL) performed WGS on available specimens positive for SARS-CoV-2 by RT-PCR, collected March 6–June 30, 2020. Specimens were obtained from the nasopharynx, anterior nares, or oropharynx. SARS-CoV-2 RNA extracts were acquired either as residuals from clinical testing at the MDH PHL or from other clinical laboratories serving Minnesota residents. We created cDNA and tiled amplicons as described in the ARTIC Network nCoV-2019 sequencing protocol (25). We prepared Illumina sequencing libraries for next-generation sequencing according to the Nextera DNA Flex protocol created by the State Public Health Bioinformatics Group (StaPH-B) (26) and performed sequencing by using 2×250 bp Illumina V2 chemistry on MiSeq instruments (https://www.illumina.com). Consensus SARS-CoV-2 genome sequences for each specimen were generated with the StaPH-B Toolkit Monroe pipeline (https://staph-b.github.io/staphb_toolkit/workflow_docs/monroe). We individually reviewed assembled SARS-CoV-2 genomes in Geneious Prime 2019.2.1 (https://www.geneious.com) and discarded genomes with gaps >125 nt.

We used the Augur toolkit (27) to align SARS-CoV-2 genome consensus sequences, generate phylogenetic trees, and incorporate epidemiologic sequence metadata. We aligned genomes with MAFFT version

7.310 with options "–keeplength–reorder–anysymbol–nomemesave–adjustdirection" (*28*). Variation in sequences identified in the first 54 and last 67 bases of the Wuhan-Hu-1 reference sequence (GenBank accession no. MN908947.3) was masked during tree generation because of the inability of the tiled-amplicon sequencing approach to reliably generate sequence in those regions. We used IQ-TREE version 1.6.1 to create phylogenetic trees with parameters "-ninit 2 -n 2 -me 0.05" (*29*). Output from Augur was visualized by using Auspice as hosted by the nextstrain team (http://auspice.us) (*27*). The resulting trees were visualized with the Interactive Tree of Life (*30*); branch lengths rounded and scaled represent mutations from the reference. Pangolin lineages for all samples were retrieved after assemblies were submitted to GISAID (https://github.com/cov-lineages/pangolin) (*27,31*).

We defined genetically closely related sequences (i.e., clusters) as cases that were both associated epidemiologically with a known outbreak and that formed a monophyletic clade on the statewide phylogenetic tree. Branch lengths were scaled to represent the number of single-nucleotide mutations.

In accordance with federal human subjects protection regulations at 45 CFR §46.101c and §46.102d and with the Guidelines for Defining Public Health Research and Public Health Non-Research, a human subjects protection coordinator at CDC and the MDH reviewed the project. They determined it to be a non-research, public health response exempt from institutional review board evaluation.

Results

As of June 30, 2020, we had successfully conducted WGS and phylogenetic analysis of 468 total samples, 319 (68.2%) of which were associated with the 8 outbreaks, constituting 14.4% of the 2,222 total positive cases identified from outbreaks in Minnesota through June 2020. Specimens were obtained from staff and residents from 4 LTCFs (180 [35.6%] specimens from 505 case-patients were sequenced), staff and inmates from 2 correctional facilities (110 [20.2%] specimens from 544 case-patients were sequenced), and employees at 2 meat-processing plants, along with community case-patients (29 [2.5%] samples from 1,173 identified case-patients) (Table). Among most sequenced specimens, virus spread was associated with a single genetic sequence unique to each outbreak facility at 3 LTCFs and both correctional facilities. At a fourth LTCF, outbreak cases were associated with 2 distinct sequences. In contrast, cases associated with outbreaks in the 2 meat-processing plants were represented by multiple SARS-CoV-2 sequences. (Figure 1)

Single Cluster in LTCFs

During the COVID-19 outbreak at LTCF A (*3*), April 15–June 11 (Figure 2), infection was confirmed for 51/77 residents and 38/108 healthcare workers

Table. Features of outbreaks and convenience samples of specimens collected and characterized by whole-genome sequencing at LTCFs, correctional facilities, and meat-processing plants in Minnesota, USA, March 6–June 30, 2020*

Outbreak facility	Total confirmed outbreak cases at facility, no.	Total samples successfully sequenced from facility, no. (%)	Role at facility	Total outbreak cases at facility confirmed by role, no.	Total samples successfully sequenced by role, no. (%)
LTCF					
A	89	27 (30.3)	Staff	38	10 (26.3)
			Residents	51	17 (33.3)
B	190	82 (43.2)	Staff	76	5 (6.6)
			Residents	114	77 (67.5)
C	139	32 (23.0)	Staff	56	23 (41.0)
			Residents	83	9 (10.8)
D	74	39 (52.7)	Staff	21	3 (14.2)
			Residents	53	36 (67.9)
Correctional facility					
A	128	49 (38.3)	Staff	82	15 (18.3)
			Inmates	46	34 (73.9)
B	416	61 (14.7)	Staff	210	1 (0.5)
			Inmates	206	60 (29.1)
Meat-processing plant					
A	432	16 (3.7)	Employees	432	16 (3.7)
B	724	5 (0.7)	Employees	724	5 (0.7)
Community sample A	17	8 (47.1)	Known contact	9	2 (22.2)
			No known contact	8	6 (75.0)
Total	2,222	319 (14.4)	NA	NA	NA

*No cases or samples sequenced after June 30, 2020, are included in study. An outbreak is defined as closed if there are no new coronavirus disease cases for 28 days after the onset date of the last case. The outbreak at correctional facility A was considered closed as of July 20; the outbreak at correctional facility B was considered closed as of August 5. The outbreaks at processing plants A and B were considered ongoing as of November 6, 2020. LTCF, long-term care facility; NA, not applicable.
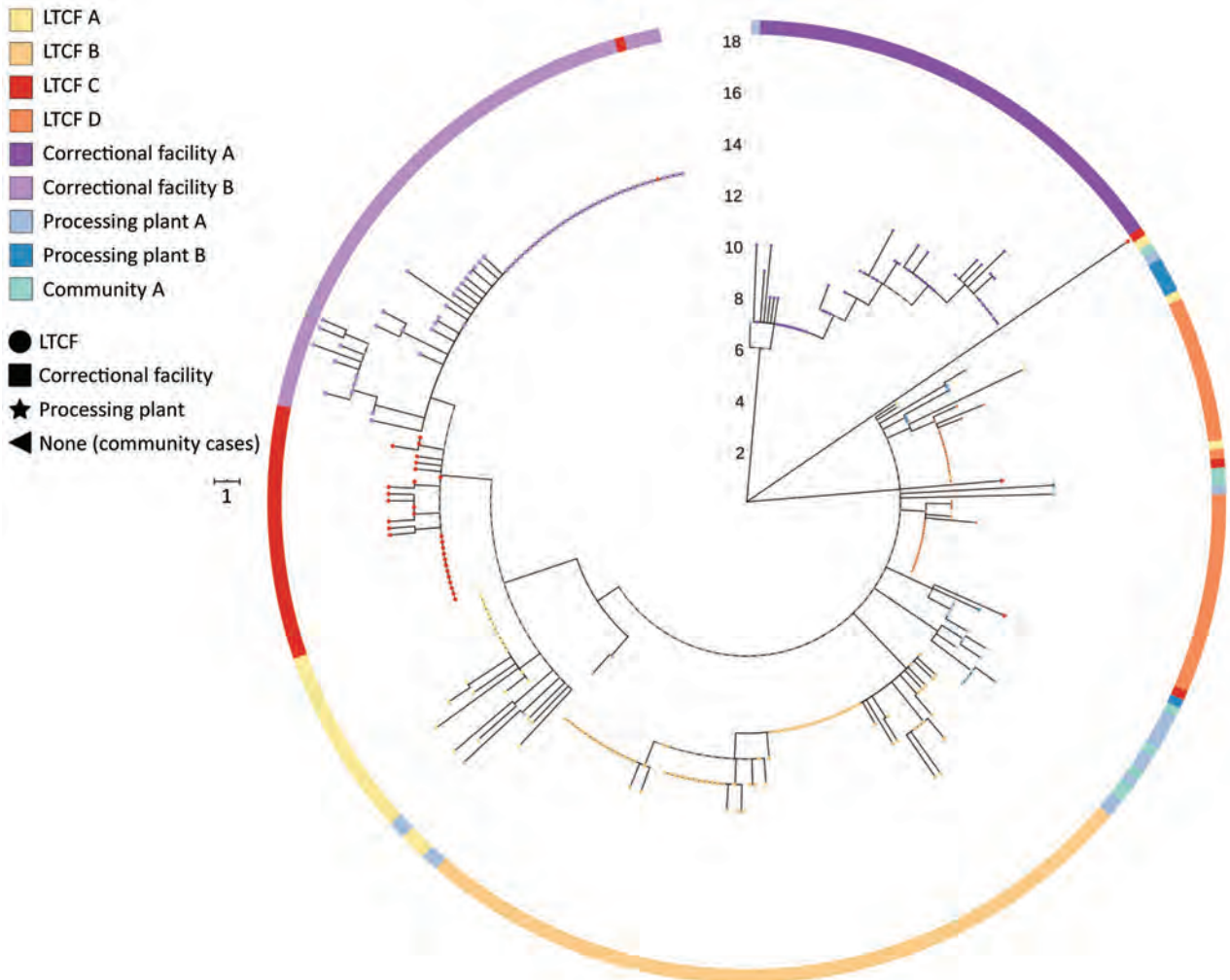
Figure 1. Phylogenetic tree of severe acute respiratory syndrome coronavirus 2 associated with selected outbreaks in Minnesota, USA, March 6–June 30, 2020. IQ-TREE (*29*) was used with the general time reversible substitution model for tree generation. Branch lengths were scaled to represent number of single-nucleotide mutations as shown in the scale key. LTCF, long-term care facility.

(HCWs) tested after identification of SARS-CoV-2–positive HCWs. Specimens from 17 residents (33.3% of case-patients) and 10 HCWs (26.3% of case-patients) were available for WGS. SARS-CoV-2 viral sequences from these 27 persons were genetically closely related (pangolin lineage B.1.2). Viral genomes from 2 HCWs (MN-MDH-1007 and MN-MDH-1016) sampled on April 30 and 1 resident (MN-MDH-1171) sampled on May 18 at LTCF A did not cluster with each other or the primary outbreak cluster, although all were a part of the broad pangolin lineage B.1.

In LTCF B (*3*) (Appendix Figure 1, https://wwwnc.cdc.gov/EID/article/27/8/20-4838-App1.pdf), during April 29–June 11, SARS-CoV-2 positivity was confirmed for 114 of 182 tested residents and 76 of 233 tested HCWs, after a SARS-CoV-2–positive resident

was identified on April 29. All 82 sequenced specimens from this facility, including those from 77 residents (67.5% of case-patients) and 5 HCWs (6.6% of case-patients), were closely related (pangolin lineage B.1.116).

The first COVID-19 case at LTCF C (Appendix Figure 2) was identified on April 24. Four positive HCWs and 3 symptomatic residents were identified by April 30. Throughout May and June, facilitywide testing was implemented; ≈941 residents and staff were tested and 80 SARS-CoV-2–positive residents and 52 SARS-CoV-2–positive staff members were identified. Phylogenetic analysis of the 32 successfully sequenced genomes, including those from 9 residents (10.8% of case-patients) and 23 staff members (41% of case-patients) showed that viruses from 29 of the 32 case-patients were closely related (pangolin lineage B.1.2). Viruses from the remaining 3

case-patients (pangolin lineages B.1 and B.4) were not closely related to each other nor identified with further transmission.

Two Distinct Clusters in an LTCF

LTCF D (Figure 3) is a 100-bed facility with ≈78 residents and 100 staff, where an outbreak began on April 17, 2020, with a symptomatic HCW. The first cases in residents and staff were identified on April 20, 2020; subsequent testing identified of 53 SARS-CoV-2–positive residents and 21 positive staff members. Although this outbreak was epidemiologically similar to outbreaks at other LTCFs, an analysis of the genetic relatedness among 39 sequenced isolates demonstrated that 2 distinct genetic clusters were in the facility during approximately the same period. In contrast to the outbreaks in LTCFs A, B, and C, viruses from both clusters at LTCF D seemed to circulate simultaneously throughout the facility, each contributing to the outbreak. All sequenced isolates from LTCF D belonged to the broad pangolin lineage B.1.

Single Cluster in Correctional Facilities

In late March 2020, an outbreak of SARS-CoV-2 was identified in correctional facility A (Figure 4). The first identified case-patient was an inmate who became symptomatic and had a positive SARS-CoV-2 test result on March 25. By March 30, a total of 7 confirmed cases and 6 suspected cases among the inmate population

were identified. During March 30–April 7, SARS-CoV-2 test results were positive for 15 staff members. Analysis of the genetic relatedness of the virus from 34 inmates (73.9% of case-patients) and 15 staff members (18.3% of case-patients) from correctional facility A were all closely related (pangolin lineage A.1).

In early June 2020, an outbreak was identified in correctional facility B (Appendix Figure 3). The investigation revealed that an employee had symptoms consistent with COVID-19 on May 13, had a positive SARS-CoV-2 test result on May 14, and was subsequently excluded from work and isolated at home. Approximately 2 weeks later, 3 additional case-patients (1 staff member and 2 inmates from the same unit as the index patient) had positive SARS-CoV-2 test results. A point-prevalence survey on June 1 in this unit revealed 63 SARS-CoV-2–positive inmates among the 87 tested. Subsequent facilitywide testing of both staff and inmates identified cases in other units, 83 new cases in inmates and 1 new case in a staff member, identified among the ≈2,200 persons tested. Test results were ultimately positive for 210 staff members and 206 inmates during this outbreak. Phylogenetic analysis of viruses from this outbreak among the 1 staff member (0.5% of staff case-patients) and 60 inmates (29.1% of inmate case-patients) at correctional facility B shows that all viruses were closely related (pangolin lineage B.1.2) and genetically identical to, or plausibly descended from, the sequence of SARS-CoV-2 from the index case-patient.

Figure 2. Phylogenetic tree of severe acute respiratory syndrome coronavirus 2 genome sequences associated with long-term care facility A, Minnesota, USA, April 15–June 11, 2020. Solid circles represent sequences in samples from residents; open circles represent sequences from samples from healthcare workers. IQ-TREE (29) was used with the general time reversible substitution model for tree generation. Branch lengths were scaled to represent number of single-nucleotide mutations, as shown in the scale. MDH, Minnesota Department of Health.
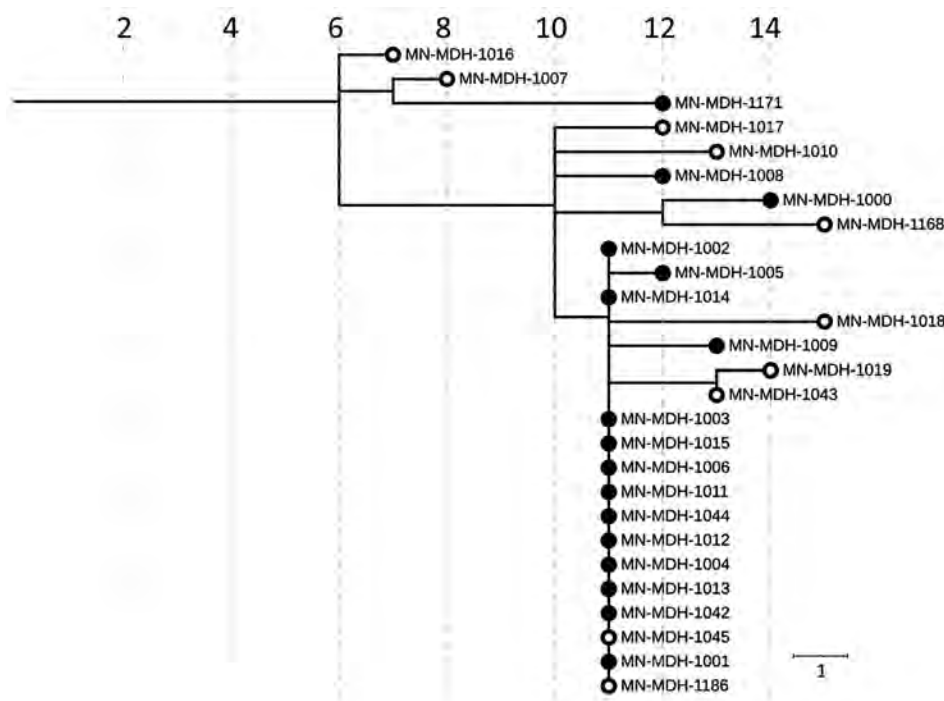
Figure 3. Phylogenetic tree of severe acute respiratory syndrome coronavirus 2 genome sequences associated with long-term care facility D, Minnesota, USA, April 17–May 15, 2020. Filled circles represent sequences taken from residents; open circles represent sequences from healthcare workers. IQ-TREE (*29*) was used with the general time reversible substitution model for tree generation. Branch lengths were scaled to represent number of single-nucleotide mutations, as shown in the scale. MDH, Minnesota Department of Health.
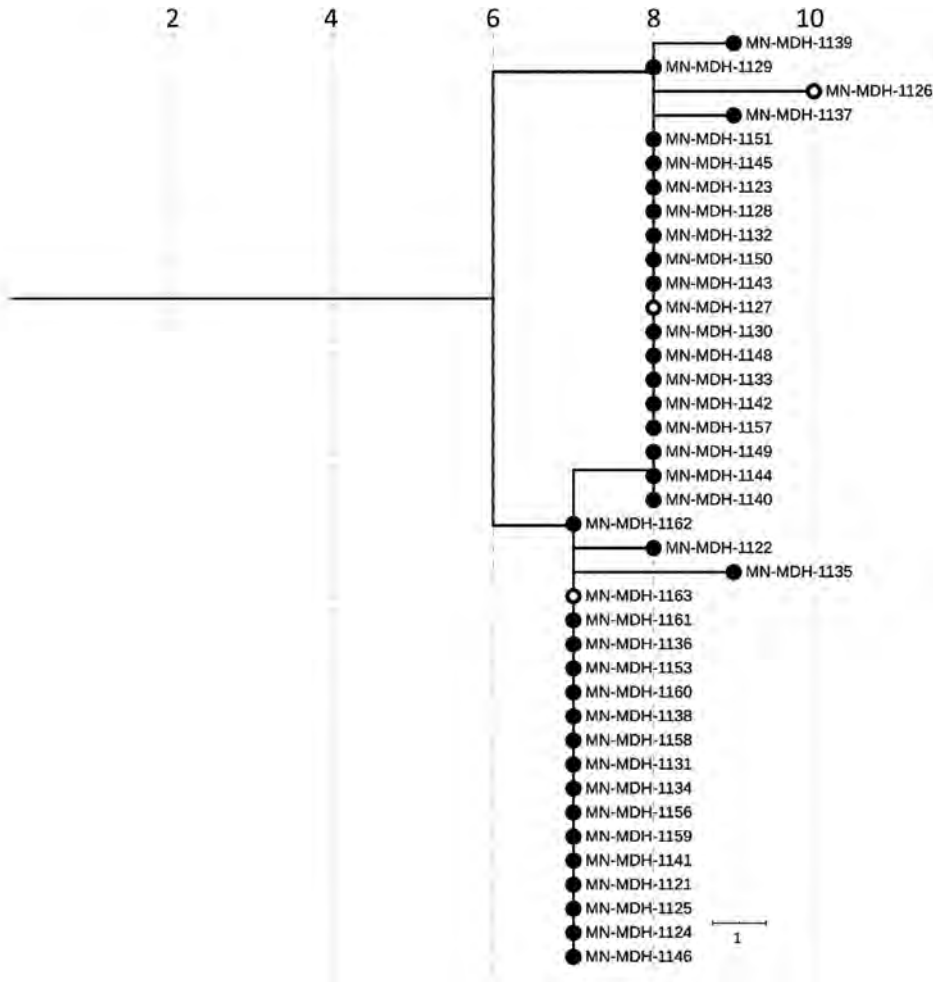
Linking LTCF C with Correctional Facility B

During the epidemiologic investigation at LTCF C, we learned that an HCW at LTCF C was a household contact of a correctional facility B employee. Both persons became symptomatic at the same time, and both subsequently had positive test results in mid-May. SARS-CoV-2 genome sequences recovered from these 2 household contacts were identical to each other and to the genomic sequences recovered from 32 inmates at correctional facility B (Figure 5). In addition, this genomic sequence differs by only a single mutation (G5617T) from isolates sequenced from 13 case-patients at LTCF C.

Multiple Clusters in Meat-Processing Plants

In early April 2020, an outbreak was detected at processing plant A (Figure 6), a large primary and secondary meat processor. This outbreak continued for several weeks until mid-May, when the number of cases among workers began to increase rapidly. During March 15–July 1, a total of 446 persons with confirmed cases who reported working at processing plant A, including 4 (1%) case-patients with positive test results in March (management and office staff), 5 (1%) in April, 211 (47%) in May, and 226 (51%) in June. Of the 16 samples (3.7% of case-patients) sequenced during March 15–June 3, at least 6 clusters or single cases were unrelated. Although most genomes sequenced from processing plant B belonged to pangolin lineages B.1, B1.2, B.1.26, one early case is genetically quite different (pangolin lineage A.1). An interview confirmed that this early case-patient had traveled out of the state during the exposure period (14 days before symptom onset).

During May 15–June 1, we sequenced samples obtained from 8 case-patients in the county where processing plant A is located (community samples A). From these 8 samples, we identified 5 clusters. Of the 8 samples, 5 were closely related with 3 clusters from processing plant A, while the remaining 3 samples formed 2 distinct clusters. Of the 5 sequences from community samples A that clustered with sequences from processing plant A, 4 had sequences that were identical to

sequences from processing plant A, and all 4 persons had no known contact with a verified case-patient.

In mid-April 2020, an outbreak was identified among employees at processing plant B (Appendix Figure 4), another large meat-processing plant. By May 1, a total of 649 cases among workers at processing plant B were confirmed. Sequencing of the 5 available samples from processing plant B (0.7% of cases) identified 1 cluster and 2 single genomes, all belonging to pangolin lineage B.1.

Discussion

WGS identified 3 primary patterns of genetic relatedness among cases in various outbreak settings:

outbreaks in which cases were part of 1 genetically related cluster; an outbreak with 2 unique clusters of cases, each contributing to the outbreak during the same period; and outbreaks for which multiple genetically distinct sequences were present. Phylogenetic analyses of the viral sequences from available specimens (Appendix Table 1) associated with outbreaks in LTCFs A, B, and C were all consistent with ≥1 primary cluster affecting each facility, suggesting that a single introduction of SARS-CoV-2 into a facility can result in a widespread outbreak. This finding is similar to previously reported findings, in which WGS has evidenced rapid spread in high-density settings as opposed to multiple introductions
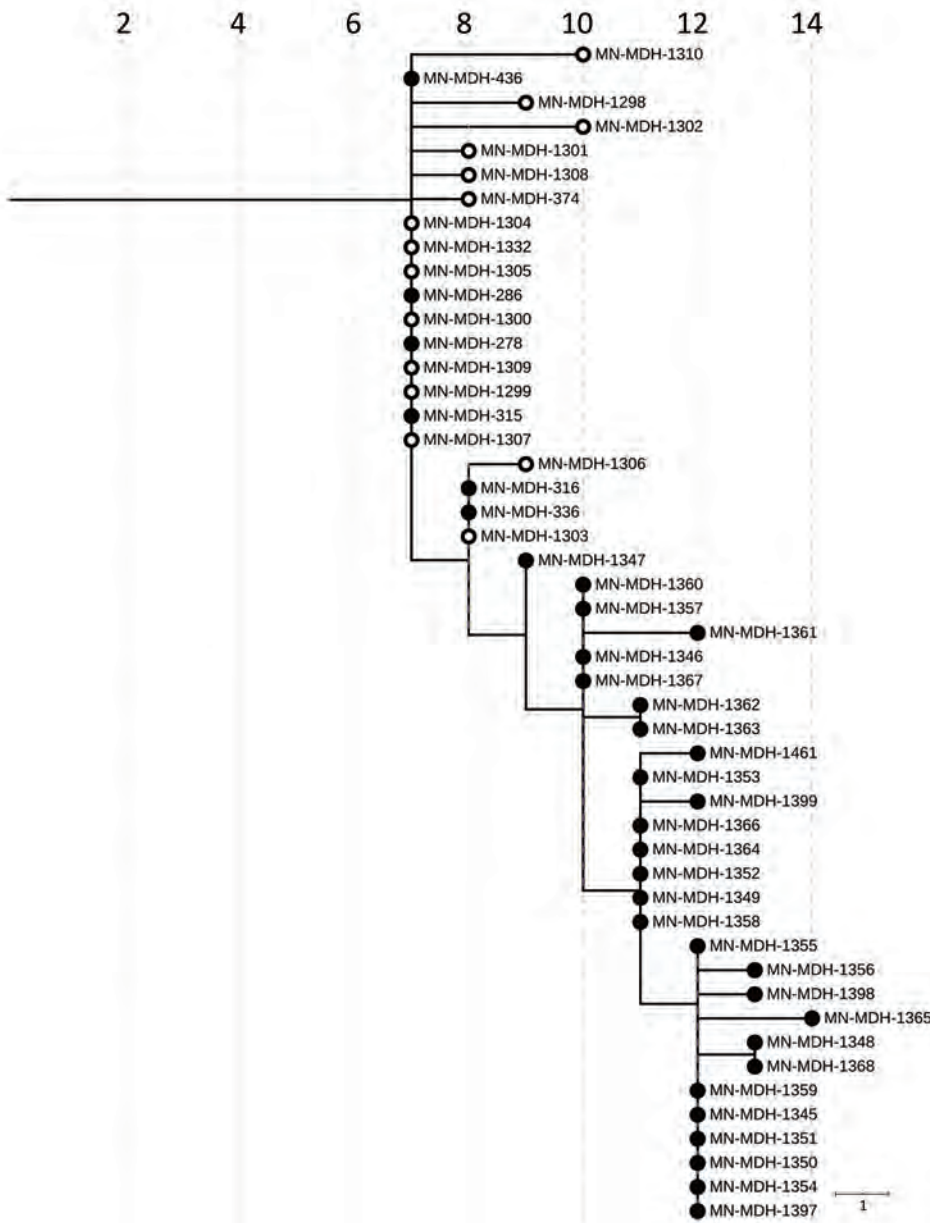
Figure 4. Phylogenetic tree of severe acute respiratory syndrome coronavirus 2 genome sequences associated with correctional facility A, Minnesota, USA, March 25–June 30, 2020. Filled circles represent sequences from samples from inmates, open circles represent sequences from samples from facility staff. IQ-TREE (29) was used with the general time reversible substitution model for tree generation. Branch lengths were scaled to represent number of single-nucleotide mutations, as shown in the scale. MDH, Minnesota Department of Health.
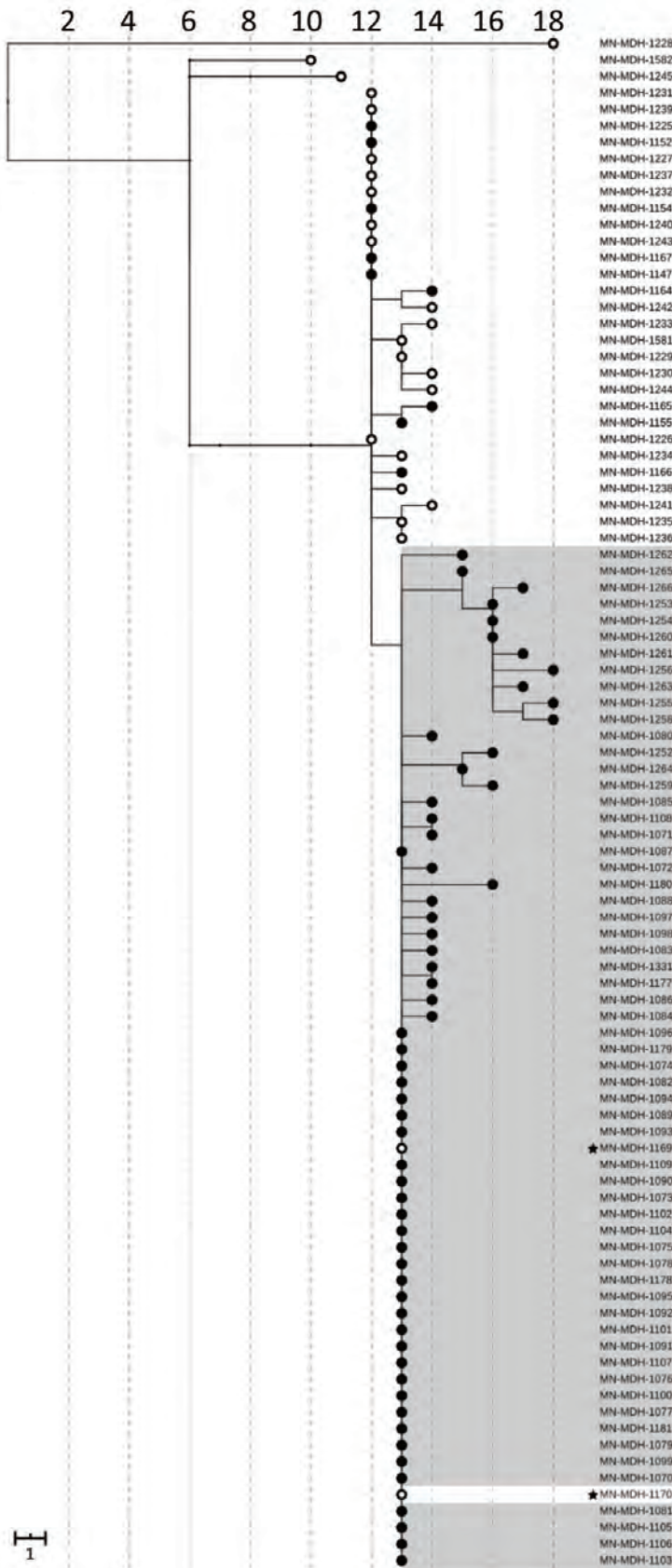
Figure 5. Phylogenetic tree of severe acute respiratory syndrome coronavirus 2 genome sequences associated with long-term care facility C and correctional facility B, Minnesota, US, April–June 2020. Filled circles represent sequences from samples from inmates or residents; open circles represent sequences from facility staff or healthcare workers. Sequences from long-term care facility C are shown on a white background; sequences from correctional facility B, on a gray background. Sequences from 2 household contacts are noted with stars. IQ-TREE (*29*) was used with the general time reversible substitution model for tree generation. Branch lengths were scaled to represent number of single-nucleotide mutations, as shown in the scale. MDH, Minnesota Department of Health.
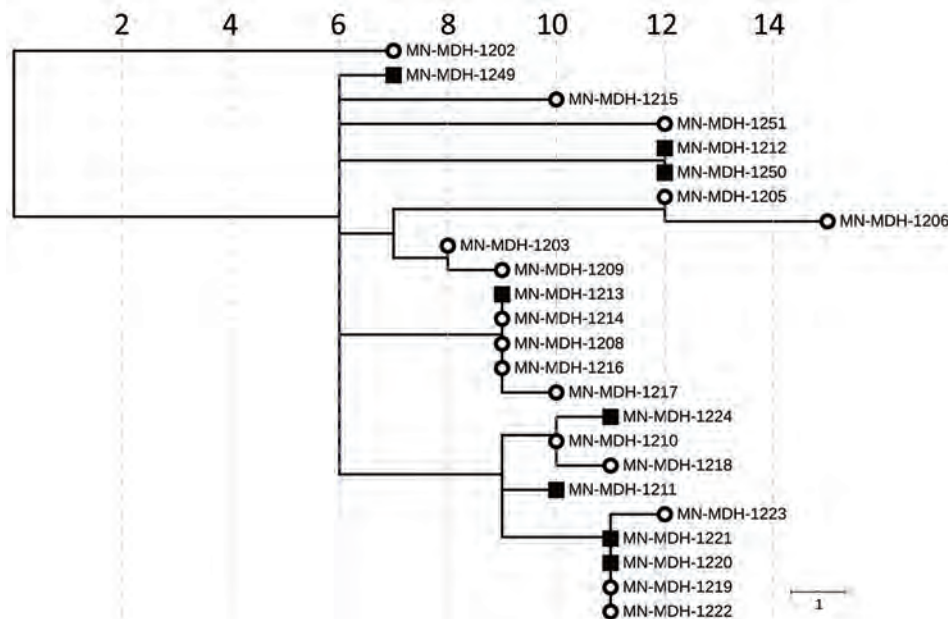
Figure 6. Phylogenetic tree of SARS-CoV-2 genome sequences associated with meat-processing plant A and the surrounding community, Minnesota, USA, March 15–June 30, 2020. Open circles represent sequences from samples from staff at processing plant A; squares represent sequences from samples from persons in the surrounding community. IQ-TREE (*29*) was used with the general time reversible substitution model for tree generation. Branch lengths were scaled to represent number of single-nucleotide mutations, as shown in the scale. MDH, Minnesota Department of Health.

contributing to the outbreak (*20*). Cases from LTCF D, in contrast, formed 2 distinct genetic clusters, 1 consisting of 17 related samples and the other consisting of 22 samples. This finding is consistent with a potential scenario in which there were 2 separate, independent introductions into the facility and subsequent parallel intrafacility spread of each individually distinct sequence.

Phylogenetic analysis conducted for LTCFs A and C also demonstrated outlier SARS-CoV-2 viral sequences that were not genetically closely related to the primary cluster in each facility. This finding suggests community-acquired infection and subsequent introduction of SARS-CoV-2 into the facility (*3*). Two of the 3 outlier case-patients at LTCF C had positive test results >1 month after the first identified case. Similarly, 2 of the 3 outlier case-patients identified at LTCF A were identified 10 days after the first identified case-patient, and the third had a positive test result 28 days later. It is not possible to determine whether these introductions of distinct genetic sequences resulted in additional spread, given that WGS characterization was not performed on all positive samples in each facility and not all HCWs or residents were tested. However, the timing of the identification of these outlier cases after the date of the first identified primary case suggests that mitigation strategies implemented after the initial identification of the outbreak, including cohorting strategies, infection prevention and control measures, and correct use of personal protective equipment (PPE), may have effectively prevented intrafacility transmission of these late outlier cases, as has been reported (*3,21,22*).

WGS identified a different genetic landscape in meat-processing plants, in which several distinct sequences contributed to the facility outbreak. This finding is despite sequencing of only 2.5% of SARS-CoV-2–positive samples from the processing plants, suggesting that increased sequencing may have identified even greater genetic diversity. In addition, several genomes identified at processing plant A were either identical or closely related to genomes in the surrounding community (community samples A). Of the 8 sequenced community samples (community sample A), 6 were from persons with no known epidemiologic link to a case-patient at processing plant A, strongly suggesting an unrecognized connection. The benefit of WGS for identifying previously unrecognized transmission patterns has been established (*20,32*). Although no definitive conclusions can be made regarding the direction of transmission, WGS provided strong evidence of worker/community member spread; hypothesized factors potentially contributing to this transmission pattern are communal housing, multigenerational families, and group transportation.

WGS has contributed to improved knowledge of an outbreak after retrospective analysis (G.K. Moreno et al., unpub. data, https://doi.org/10.1101/2020.07.09.20149104) (*3,20,21*), justification for specific public health measures (*21,22*), and added insight to transmission patterns in high-risk settings. Our work further supports use of WGS in these situations while

identifying several additional public health implications. WGS has demonstrated that outbreaks in LTCFs and correctional facilities can result from a single introduction. Continued vigilance, including facilitywide staff screening and subsequent exclusion of symptomatic HCWs or staff and those with known or suspected contacts, is imperative. WGS has demonstrated extensive intrafacility spread; closely related sequences comprise all or most cases contributing to the outbreak. Measures such as infection prevention and control, consistent and correct use of PPE, cohorting of known positive residents, and exclusion of positive HCWs must be maintained. WGS has also illuminated the transmission patterns in processing plants, including the multiple introductions identified through the multiple genetically distinct sequences identified and the related community strains. WGS has illustrated the need for community-level mitigation to prevent introductions in high-density worksites, including accessible communitywide testing, housing and transportation strategies, and facility-level measures to prevent unintended introduction into the workplace.

The first limitation of this study is that only a subset of specimens were available for sequencing because of different laboratory specimen retention policies. For example, at LTCF B, samples from only 5 staff members were available for sequencing. Similarly, in meat-processing plant B, only 5 samples were available because of a clinical testing laboratory protocol that resulted in the discarding of samples after ≈7 days. In addition, not all available samples could be successfully sequenced, primarily because of degraded quality or low concentrations of viral RNA.

Another limitation is that not all staff and employees at the LTCFs, correctional facilities, and processing plants agreed to be tested. Because of the incomplete genomic picture at each setting, definitive conclusions about single introductions in LTCFs A and D are speculative, and these individual introductions may have resulted in some virus transmission that was not identified in the study.

Last, we were not able to present sociodemographic data such as race or ethnicity associated with these outbreaks because of limitations in the case investigation process and incomplete case data. This limitation is particularly relevant because of the disproportionate effect of COVID-19 on those who are Black, indigenous, or other persons of color. Because those populations disproportionately experience incarceration and a high proportion of meat-processing plant employees are persons from immigrant communities, these settings can serve to amplify racial and ethnic health disparities related to COVID-19.

LTCFs, correctional facilities, and high-density workplace settings have many factors that are hypothesized to contribute to rapid transmission of SARS-CoV-2. These factors include insufficient resources and training in infection prevention and control, difficulties implementing social distancing because of close habitation or work environment, and delayed case detection and access to care (8,11,33). WGS results have demonstrated that many outbreaks in Minnesota were caused by single introductions of SARS-CoV-2, highlighting the value of consistent and correct PPE use, rigorous and systematic infection prevention and control, environmental control measures, and systematic testing of residents and staff to identify asymptomatic infected persons. As this pandemic continues, community mitigation strategies and strong enforcement of policies to reduce the risk of introducing SARS-CoV-2 virus into congregate settings are more crucial than ever. Similarly, infection prevention and control and aggressive containment practices are vital for mitigating the spread of SARS-CoV-2 after its introduction into a facility. WGS can be a useful tool for supplementing epidemiologic information and examining the role of facility and community factors contributing to SARS-COV-2 outbreaks in high-risk settings.

This article was preprinted at https://www.medrxiv.org/content/10.1101/2020.12.30.20248277v1

About the Author

Dr. Lehnertz is a medical specialist in infectious disease epidemiology, prevention, and control at the MDH. His current research involves the epidemiology of COVID-19 transmission patterns, clinical characteristics of presymptomatic COVID-19 infection in residents of LTCFs, and human belief systems surrounding COVID-19.

References

1. Arons MM, Hatfield KM, Reddy SC, Kimball A, James A, Jacobs JR, et al.; Public Health–Seattle and King County and CDC COVID-19 Investigation Team. Presymptomatic SARS-CoV-2 infections and transmission in a skilled nursing facility. N Engl J Med. 2020;382:2081–90. https://doi.org/10.1056/NEJMoa2008457
2. Kimball A, Hatfield KM, Arons M, James A, Taylor J, Spicer K, et al.; Public Health–Seattle and King County and

CDC COVID-19 Investigation Team. Asymptomatic and presymptomatic SARS-CoV-2 infections in residents of a long-term care skilled nursing facility—King County, Washington, March 2020. MMWR Morb Mortal Wkly Rep. 2020;69:377–81. https://doi.org/10.15585/mmwr.mm6913e1

3. Taylor J, Carter RJ, Lehnertz N, Kazazian L, Sullivan M, Wang X, et al.; Minnesota Long-Term Care COVID-19 Response Group. Serial testing for SARS-CoV-2 and virus whole genome sequencing inform infection risk at two skilled nursing facilities with COVID-19 outbreaks—Minnesota, April–June 2020. MMWR Morb Mortal Wkly Rep. 2020;69:1288–95. https://doi.org/10.15585/mmwr.mm6937a3

4. Dora AV, Winnett A, Jatt LP, Davar K, Watanabe M, Sohn L, et al. Universal and serial laboratory testing for SARS-CoV-2 at a long-term care skilled nursing facility for veterans–Los Angeles, California, 2020. MMWR Morb Mortal Wkly Rep. 2020;69:651–5. https://doi.org/10.15585/mmwr.mm6921e1

5. Ladhani SN, Chow JY, Janarthanan R, Fok J, Crawley-Boevey E, Vusirikala A, et al.; London Care Home Investigation Team. Increased risk of SARS-CoV-2 infection in staff working across different care homes: enhanced CoVID-19 outbreak investigations in London care homes. J Infect. 2020;81:621–4. https://doi.org/10.1016/j.jinf.2020.07.027

6. Wallace M, Hagan L, Curran KG, Williams SP, Handanagic S, Bjork A, et al. COVID-19 in correctional and detention facilities—United States, February–April 2020. MMWR Morb Mortal Wkly Rep. 2020;69:587–90. https://doi.org/10.15585/mmwr.mm6919e1

7. Montoya-Barthelemy AG, Lee CD, Cundiff DR, Smith EB. COVID-19 and the correctional environment: the American prison as a focal point for public health. Am J Prev Med. 2020;58:888–91. https://doi.org/10.1016/j.amepre.2020.04.001

8. Watson C, Warmbrod L, Vahey R, Cicero A, Inglesby T, Beyrer C, et al. COVID-19 and the US criminal justice system: evidence for public health measures to reduce risk. Baltimore: Johns Hopkins Center for Health Security; 2020.

9. Waltenburg MA, Victoroff T, Rose CE, Butterfield M, Jervis RH, Fedak KM, et al.; COVID-19 Response Team. Update: COVID-19 among workers in meat and poultry processing facilities—United States, April–May 2020. MMWR Morb Mortal Wkly Rep. 2020;69:887–92. https://doi.org/10.15585/mmwr.mm6927e2

10. Steinberg J, Kennedy ED, Basler C, Grant MP, Jacobs JR, Ortbahn D, et al. COVID-19 outbreak among employees at a meat-processing facility—South Dakota, March–April 2020. MMWR Morb Mortal Wkly Rep. 2020;69:1015–9. https://doi.org/10.15585/mmwr.mm6931a2

11. Waltenburg MA, Rose CE, Victoroff T, Butterfield M, Dillaha JA, Heinzerling A, et al.; CDC COVID-19 Emergency Response Team. Coronavirus disease among workers in food processing, food manufacturing, and agriculture workplaces. Emerg Infect Dis. 2021;27:243–9. https://doi.org/10.3201/eid2701.203821

12. Thielen BK, Bye E, Wang X, Maroushek S, Friedlander H, Bistodeau S, et al. Summer outbreak of severe RSV-B disease, Minnesota, 2017 associated with emergence of a genetically distinct viral lineage. J Infect Dis. 2020;222:288–97. https://doi.org/10.1093/infdis/jiaa075

13. Longmire AG, Sims S, Rytsareva I, Campo DS, Skums P, Dimitrova Z, et al. GHOST: global hepatitis outbreak and surveillance technology. BMC Genomics. 2017;18(Suppl 10):916. https://doi.org/10.1186/s12864-017-4268-3

14. Quick J, Loman NJ, Duraffour S, Simpson JT, Severi E, Cowley L, et al. Real-time, portable genome sequencing for Ebola surveillance. Nature. 2016;530:228–32. https://doi.org/10.1038/nature16996

15. Rounds JM, Taylor AJ, Eikmeier D, Nichols MM, Lappi V, Wirth SE, et al. Prospective *Salmonella* Enteritidis surveillance and outbreak detection using whole genome sequencing, Minnesota 2015–2017. Epidemiol Infect. 2020;148:e254. https://doi.org/10.1017/S0950268820001272

16. To KK, Hung IF, Ip JD, Chu AW, Chan WM, Tam AR, et al. COVID-19 re-infection by a phylogenetically distinct SARS-coronavirus-2 strain confirmed by whole genome sequencing. Clin Infect Dis. 2020 Aug 25 [Epub ahead of print]. https://doi.org/10.1093/cid/ciaa1275

17. Larson D, Brodniak SL, Voegtly LJ, Cer RZ, Glang LA, Malagon FJ, et al. A case of early re-infection with SARS-CoV-2. Clin Infect Dis. 2020 Sep 19 [Epub ahead of print]. https://doi.org/10.1093/cid/ciaa1436

18. Van Elslande J, Vermeersch P, Vandervoort K, Wawina-Bokalanga T, Vanmechelen B, Wollants E, et al. Symptomatic SARS-CoV-2 reinfection by a phylogenetically distinct strain. Clin Infect Dis. 2020 Sep 5[Epub ahead of print]. https://doi.org/10.1093/cid/ciaa1330

19. Gupta V, Bhoyar RC, Jain A, Srivastava S, Upadhayay R, Imran M, et al. Asymptomatic reinfection in two healthcare workers from India with genetically distinct SARS-CoV-2. Clin Infect Dis. 2020 Sep 23 [Epub ahead of print]. https://doi.org/10.1093/cid/ciaa1451

20. Lucey M, Macori G, Mullane N, Sutton-Fitzpatrick U, Gonzalez G, Coughlan S, et al. Whole-genome sequencing to track SARS-CoV-2 transmission in nosocomial outbreaks. Clin Infect Dis. 2020 Jun 1 [Epub ahead of print]. https://doi.org/10.1093/cid/ciaa1433

21. Oude Munnink BB, Nieuwenhuijse DF, Stein M, O'Toole Á, Haverkate M, Mollers M, et al. Dutch-Covid-19 response team. Rapid SARS-CoV-2 whole-genome sequencing and analysis for informed public health decision-making in the Netherlands. Nat Med. 2020;26:1405–10. https://doi.org/10.1038/s41591-020-0997-y

22. Seemann T, Lane CR, Sherry NL, Duchene S, Gonçalves da Silva A, Caly L, et al. Tracking the COVID-19 pandemic in Australia using genomics. Nat Commun. 2020;11:4376. https://doi.org/10.1038/s41467-020-18314-x

23. Rockett RJ, Arnott A, Lam C, Sadsad R, Timms V, Gray KA, et al. Revealing COVID-19 transmission in Australia by SARS-CoV-2 genome sequencing and agent-based modeling. Nat Med. 2020;26:1398–404. https://doi.org/10.1038/s41591-020-1000-7

24. US Food and Drug Administration. CDC 2019-novel coronavirus (2019-nCoV) real-time RT-PCR diagnostic panel [cited 2020 Dec 10]. https://www.fda.gov/media/134922/download

25. Quick J. nCoV-2019 sequencing protocol V.1 [cited 2020 Dec 10]. https://doi.org/10.17504/protocols.io.bbmuik6w

26. Sevinsky J, Nassiri A, Blankenship H, Young E, Libuit K, Oakeson K, et al. SARS-CoV-2 Sequencing on Illumina MiSeq using ARTIC protocol: part 2—Illumina DNA flex protocol V.1 [cited 2020 Dec 10]. https://doi.org/10.17504/protocols.io.bffyjjpw

27. Hadfield J, Megill C, Bell SM, Huddleston J, Potter B, Callender C, et al. Nextstrain: real-time tracking of pathogen evolution. Bioinformatics. 2018;34:4121–3. https://doi.org/10.1093/bioinformatics/bty407

28. Katoh K, Standley DM. MAFFT multiple sequence alignment software version 7: improvements in performance and usability. Mol Biol Evol. 2013;30:772–80. https://doi.org/10.1093/molbev/mst010

29. Nguyen LT, Schmidt HA, von Haeseler A, Minh BQ. IQ-TREE: a fast and effective stochastic algorithm for estimating maximum-likelihood phylogenies. Mol Biol Evol. 2015;32:268–74. https://doi.org/10.1093/molbev/msu300

30. Letunic I, Bork P. Interactive Tree Of Life (iTOL) v4: recent updates and new developments. Nucleic Acids Res. 2019;47(W1):W256–9. https://doi.org/10.1093/nar/gkz239

31. Elbe S, Buckland-Merrett G. Data, disease and diplomacy: GISAID's innovative contribution to global health. Glob Chall. 2017;1:33–46. https://doi.org/10.1002/gch2.1018

32. Gonzalez-Reiche AS, Hernandez MM, Sullivan MJ, Ciferri B, Alshammary H, Obla A, et al. Introductions and early spread of SARS-CoV-2 in the New York City area. Science.2020; 369:297–301. https://doi.org/10.1126/science.abc1917

33. Grabowski DC, Mor V. Nursing home care in crisis in the wake of COVID-19. JAMA. 2020;324:23–4. https://doi.org/10.1001/jama.2020.8524

Address for correspondence: Nicholas B. Lehnertz, Minnesota Department of Health, 625 Robert St N, St. Paul, MN 55164, USA; email: nick.lehnertz@state.mn.us

Intense and Mild First Epidemic Wave of Coronavirus Disease, The Gambia

Baderinwa Abatan, Orighomisan Agboghoroma, Fatai Akemoke, Martin Antonio, Babatunde Awokola,
Mustapha Bittaye, Abdoulie Bojang, Kalifa Bojang, Helen Brotherton, Carla Cerami, Ed Clarke,
Umberto D'Alessandro, Thushan de Silva, Mariama Drammeh, Karen Forrest, Natalie Hofmann,
Sherifo Jagne, Hawanatu Jah, Sheikh Jarju, Assan Jaye, Modou Jobe, Beate Kampmann,
Buba Manjang, Melisa Martinez-Alvarez, Nuredin Mohammed, Behzad Nadjm,
Mamadou Ousmane Ndiath, Esin Nkereuwem, Davis Nwakanma, Francis Oko, Emmanuel Okoh,
Uduak Okomo, Yekini Olatunji, Eniyou Oriero, Andrew M. Prentice, Charles Roberts, Anna Roca,
Babanding Sabally, Sana Sambou, Ahmadou Samateh, Ousman Secka, Abdul Karim Sesay,
Yankuba Singhateh, Bubacarr Susso, Effua Usuf, Aminata Vilane, Oghenebrume Wariri[1,2]

The severe acute respiratory syndrome coronavirus 2 (SARS-CoV-2) pandemic is evolving differently in Africa than in other regions. Africa has lower SARS-CoV-2 transmission rates and milder clinical manifestations. Detailed SARS-CoV-2 epidemiologic data are needed in Africa. We used publicly available data to calculate SARS-CoV-2 infections per 1,000 persons in The Gambia. We evaluated transmission rates among 1,366 employees of the Medical Research Council Unit The Gambia (MRCG), where systematic surveillance of symptomatic cases and contact tracing were implemented. By September 30, 2020, The Gambia had identified 3,579 SARS-CoV-2 cases, including 115 deaths; 67% of cases were identified in August. Among infections, MRCG staff accounted for 191 cases; all were asymptomatic or mild. The cumulative incidence rate among nonclinical MRCG staff was 124 infections/1,000 persons, which is >80-fold higher than estimates of diagnosed cases among the population. Systematic surveillance and seroepidemiologic surveys are needed to clarify the extent of SARS-CoV-2 transmission in Africa.

Author affiliations: Medical Research Council Unit The Gambia at the London School of Hygiene and Tropical Medicine, London, UK (B. Abatan, O. Agboghoroma, F. Akemoke, M. Antonio, B. Awokola, A. Bojang, K. Bojang, H. Brotherton, C. Cerami, E. Clarke, U. D'Alessandro, T. de Silva, K. Forrest, N. Hofmann, H. Jah, S. Jarju, A. Jaye, M. Jobe, B. Kampmann, M. Martinez-Alvarez, N. Mohammed, B. Nadjm, M.O. Ndiath, E. Nkereuwem, D. Nwakanma, F. Oko, E. Okoh, U. Okomo, Y. Olatunji, E. Oriero, A.M. Prentice, A. Roca, O. Secka, A.K. Sesay, B. Susso, E. Usuf, A. Vilane, O. Wariri); Ministry of Health, Banjul, The Gambia (M. Bittaye, M. Drammeh, S. Jagne, B. Manjang, C. Roberts, B. Sabally, A. Samateh, S. Sambou, Y. Singhateh)

By the end of October 2020, the severe acute respiratory syndrome coronavirus 2 (SARS-CoV-2) pandemic had spread to 6 continents and caused >45 million coronavirus disease (COVID-19) cases and 1.1 million deaths (1). Despite having 15.6% of the worldwide population (2), by October 31, 2020, Africa had only 3.9% (1.76 million) of the world's COVID-19 cases and 3.6% (42,233) of deaths during the pandemic (1). Data suggest that the pandemic is evolving differently in sub-Saharan Africa compared with the rest of the world and that the outbreak started later (3).

Of note, severe COVID-19 cases seem to occur less frequently in Africa than in the rest of the world (4). Several factors have been proposed to explain this. Age is likely a major factor because older persons are at higher risk for severe disease, but Africa has an extremely young population; >60% of persons are <25 years of age (5). However, variation of COVID-19 severity with age alone does not fully explain the observed differences (4). Clinical cases and deaths in Africa likely are underreported because systematic surveillance is limited and no systematic death registration exists; thus, the true SARS-CoV-2 burden probably is underestimated (4). Nevertheless, local health systems in Africa, which have a lower capacity to deal with COVID-19 patients than healthcare systems in high-resource settings, were not overwhelmed, even at the peak of the epidemic (6). Although potential

---

[1]Authors are listed in alphabetical order.

[2]All authors were part of the MRC/Gambian Government COVID-19 Working Group and contributed equally to this article.

avoidance of medical care during the pandemic, as described in other regions (*7*), could partly explain the low number of hospitalized patients, the milder COVID-19 disease severity reported appears to be genuine, and several biologic and environmental factors have been proposed as potential contributing factors (*8–10*).

Recent serosurveys conducted in Kenya, Malawi, and South Africa showed that community transmission was several times higher than that detected by surveillance; 5%–40% of the population had SARS-CoV-2 IgG (*11–13*). Such results highlight the need for robust epidemiologic studies to assess the extent of community transmission in different regions in Africa.

The Gambia is the smallest country in continental mainland Africa and is surrounded by Senegal, except for its narrow Atlantic coast. Although an imported case was identified in The Gambia on March 17, 2020, by June 30, 2020, only 48 additional cases had been detected. Nevertheless, a rapid increase in cases was seen in July 2020, and by the end of September 2020, 3,579 cases were reported (*1*). The trajectory of the epidemic in The Gambia is different from that in Senegal, which has a population ≈7 times larger than The Gambia. In Senegal, community transmission was reported in early April 2020, and almost 7,000 cases were recorded by the end of June (*1*). Systematic surveillance, testing, contact tracing for staff of the Medical Research Council Unit The Gambia (MRCG) at the London School of Hygiene and Tropical Medicine (https://www.mrc.gm) who had influenza-like symptoms was implemented during the pandemic; the first case among MCRG staff was identified on July 18. We considered MRCG staff as a cohort to provide additional insights into the nature of the COVID-19 epidemic in The Gambia.

Methods

Population Demographics, Climate, and Healthcare Structure
In 2020, The Gambia had a population of ≈2.42 million. The median age is 17.8 years, and ≈41.9% of the population are 20–64 years of age. About 95% of the population is Muslim. The illiteracy rate is high across the country. Around 59% of the population live in urban and peri-urban settings, mainly along the coast (Figure 1).

The climate is typical of the sub-Sahel region, including a long dry season during November–May and a short rainy season during June–October. Maximum temperature is high throughout the year, 30°C–34°C, and lowest during the rainy season; minimum temperatures range from 22°C–24°C during the rainy season to 16°C−20°C during the dry season (*14*). Humidity can be >80% during the rainy months (*15*).

The government of The Gambia is the main health provider, and healthcare delivery has 3 tiers, based on the primary healthcare strategy in which most healthcare delivery occurs at local health posts. The Gambia has 4 tertiary hospitals, 38 health centers at the secondary level, and 492 health posts at the primary level. The system is complemented by 34 private and nongovernmental organization clinics.

COVID-19 Response in The Gambia
Shortly after the first COVID-19 case was detected in The Gambia on March 19, 2020, the country closed its international land, sea, and air borders. On March 27, the country declared a state of emergency, which included closing schools, nonessential shops, places of worship, and many workplaces. Initial SARS-CoV-2 testing by PCR was focused on identifying imported cases and tracing and isolating case contacts, especially among travelers from Senegal. The Ministry of Health, supported by several international organizations, set up a hotline for the public, which persons, including those with suspected cases, could call to ask for advice or request the surveillance team to perform the SARS-CoV-2 test either at health facilities or at home.

As the epidemic progressed, the Ministry of Health established testing facilities at strategic locations in the most densely populated parts of the country, mainly the western urban areas. Persons were encouraged to go for testing if they were symptomatic or after contact with a confirmed COVID-19 case. Demand for testing services was not high, and attempts to raise awareness were unsuccessful. All identified cases were isolated in designated facilities regardless of symptoms until considered noninfectious as per World Health Organization (WHO) guidelines (*16*). Ministry of Health staff traced and quarantined contacts for 10 days in hotels during the early part of the outbreak, April–July 2020, after which persons were permitted to self-isolate for 10 days at home.

MRCG Unit
MRCG is a biomedical research institution that also provides outpatient and inpatient clinical care to the local population through its clinical services department (CSD). As of August 2020, MRCG had 1,336 employees. Staff were distributed as follows: 845 were along the coast, mainly in Fajara; 158 were in Keneba; 116 were in the Central River Division, mainly in Farafenni; and 217 were in the
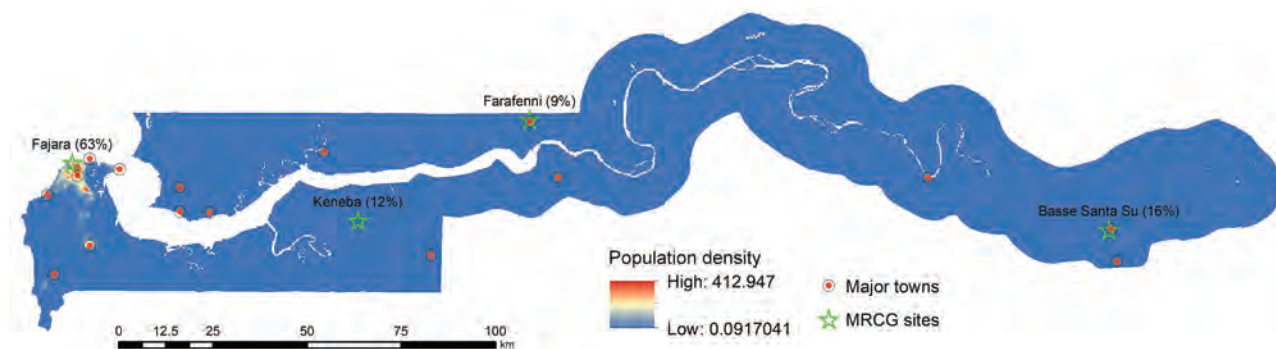
Figure 1. Population density of The Gambia, including Medical Research Council Unit The Gambia (MRCG) research sites distributed across the country.

Upper River Division, mainly Basse (Figure 1). MRCG staff work in different environments, including 715 (53.5%) field-based staff, such as drivers, community workers, nurses, and research clinicians; 334 (25.0%) office-based staff, including those in administrative, operations, data-management, and statistics positions; and 177 (13.2%) laboratory-based staff. Only 110 (8.2%) MRCG staff provide healthcare to the general population at the CSD.

CSD is 1 of 2 hospital facilities in The Gambia able to care for severe COVID-19 patients. CSD dedicated 42 beds for COVID-19 patients, including MRCG staff and the general population. From the start of the epidemic, all staff were trained to wear appropriate personal protective equipment (PPE) according to international guidelines (17).

MRCG staff underwent a clinician-administered risk assessment in the early phases of the epidemic. Staff deemed to be at high risk for severe disease were advised to work from home and were excluded from high-risk clinical areas.

Surveillance and Contact Tracing among MRCG Staff
In July 2020, MRCG established enhanced passive case detection by testing all staff exhibiting COVID-19 symptoms, such as cough, fever, headache, sore throat, nasal congestion, body pain, or other influenza-like symptoms. Families and contacts of symptomatic staff also were tested, as were staff known to have been exposed to confirmed cases. In addition, CSD staff were offered active weekly PCR-based testing, regardless of symptoms. MRCG set up a hotline manned by doctors from whom staff could receive answers to questions or concerns and get information on how to access services. Case contacts were called to confirm exposure and then tested 3–5 days after the last exposure. Regardless of negative test results, all exposed staff were quarantined for 14 days; SARS-CoV-2–positive staff isolated in their homes for 14

days, or at the MRCG site if at-home isolation was not possible, in line with WHO recommendations (18).

Sample Collection
Samples were collected via nasopharyngeal swab, oropharyngeal swab, or both by using FLOQSwabs (COPAN Diagnostics, https://www.copanusa.com). Samples were placed in single tubes containing universal transport medium (COPAN Diagnostics) and delivered to the laboratory within 24 hours. Sampling methods were comparable across cohorts with similar operational procedures and training.

Laboratory Methods for SARS-CoV-2 Detection
MRCG laboratories collaborated with national public health laboratories to support national testing throughout the country during the epidemic. MRCG and these laboratories used the same laboratory methods and assays. Because the outbreak was expected to spread to the West Africa subregion, MRCG staff attended an Africa Centres for Disease Control and Prevention (https://africacdc.org) regional training workshop on diagnosing COVID-19, which was held in February 2020 in Dakar, Senegal. Thereafter, The Gambia established laboratory protocols for processing and testing suspected SARS-CoV-2–infected samples according to WHO guidelines (19,20). The same procedures and assays were transferred to the laboratory.

The standard test for COVID-19 diagnosis in The Gambia is real-time reverse transcription PCR (RT-PCR) of SARS-CoV-2–specific viral gene sequences. In the early stages of the outbreak, RT-PCR diagnosis was made by using the Berlin Charité Laboratory protocol (21), which targets the RNA-dependent RNA polymerase and envelope protein gene. Subsequent tests kits, primarily the Da An Gene Nucleic Acid Extraction Kit (Da An Gene Co., Ltd., of Sun Yat-sen University, https://en.daangene.com) and Novel Coronavirus

(2019-nCoV) Nucleic Acid Diagnostic Kit (Sansure Biotech, Inc., http://eng.sansure.com.cn) were donated to the national public health libraries; both tests target the open reading frame 1ab and the nucleocapsid gene coding regions.

Sample inactivation and downstream RNA extraction were done by using commercially available kits according to the manufacturers' protocols. Initial extractions were performed manually by using the QIAamp Viral RNA Mini Kit (QIAGEN, https://www.qiagen.com) or the IndiSpin Pathogen Kit (INDICAL BIOSCIENCE, https://www.indical.com). When donations to the public health system became available, kits from the Da An Gene Co., Ltd., of Sun Yat-sen University and Sansure Biotech, Inc., were included. As the outbreak progressed and daily sample numbers increased, automated RNA extraction system on the QIAcube HT (QIAGEN) was implemented. In all cases, 200 μL of universal transport medium sample was processed, and the RNA eluted in 50–80 μL, depending on the extraction kit. RT-PCR analysis was conducted with 5 μL of extracted RNA in 25 μL of reaction mix containing reaction buffer, one-step reverse transcription enzyme, either the Takara One Step PrimeScript III RT-PCR Kit (TaKaRa Bio, Inc., http://www.takara-bio.com) or SuperScript III Platinum One-Step qRT-PCR Kit (Invitrogen, https://www.thermofisher.com), and the primer and probe mix.

Samples were defined as positive if amplification of any viral gene occurred after 40 cycles and with all the controls amplifying as appropriate. We defined a COVID-19 case as any person with a SARS-CoV-2–positive RT-PCR from a nasopharyngeal or oropharyngeal swab sample, regardless of symptomatology.

Statistical Analysis

We calculated rates of risk for COVID-19 per 1,000 persons among the population of The Gambia. For MRCG, we stratified rates by occupational clinical exposure for staff working at the CSD versus non-CSD staff. In addition to occupational clinical exposure, surveillance for CSD staff was more intense due to routine testing, regardless of symptoms or known exposure.

The Ministry of Health generated daily national data for The Gambia (22). We extracted compiled data from the publicly available Johns Hopkins University COVID-19 database (23). The Gambian Government/MRCG Joint Ethics committee approved the study (reference no. L2020.E37).

Results

Persons <25 years of age and persons >60 years of age are underrepresented in the MRCG cohort compared with the population of The Gambia, (Table). In addition, urban residents are overrepresented in the MRCG cohort; 67.6% of MRCG staff live in cities or towns compared with 59.4% of the overall population.

SARS-CoV-2 Positivity Rates

From the start of the epidemic through September 30, 2020, a total of 17,885 samples were tested in The Gambia; 20.1% (3,590) were SARS-CoV-2–positive. The positivity rate was lower before July (1.6%; 40/3,095 samples tested) and higher during July–September (23.7%; 3,499/14,790 samples tested) (19,20). The number of samples collected and the positivity rate were the highest during August–September 2020, during which time the number of daily swabs collected varied from 28 to 524/day (median 184/day) (Figure 2). Positivity rate also varied substantially, from <5% to >50%. Approximately 67% of confirmed cases were detected in August; overall, 60% of confirmed cases were among persons <40 years of age (20).

During July 1–September 30, a total of 937 samples were collected from the MRCG cohort; 191

Baseline characteristics	The Gambia, no. (%)	MRCG staff, no. (%)
Age groups, y†		
<25	1,549,084 (64.2)	51 (3.89)
25–34	367,334 (15.2)	450 (34.35)
35–44	217,500 (9.0)	381 (29.08)
45–54	132,917 (5.5)	307 (23.44)
55–64	72,500 (3.0)	113 (8.63)
>65	74,917 (3.1)	8 (0.61)
Median age, y	17.8	37.5
Sex		
M	1,193,834 (49.4)	915 (68.5)
F	1,220,418 (50.6)	421 (31.5)
Living in main towns or cities‡	1,420,600 (59.4)	903 (67.6)

Table. Epidemiologic and demographic characteristics of the population of The Gambia and staff of MRCG*

*MRCG, Medical Research Council Unit The Gambia at the London School of Hygiene and Tropical Medicine.
†Ages were missing for 6 MRCG staff.
‡For MRCG staff location, we considered the workplace rather than the living place.
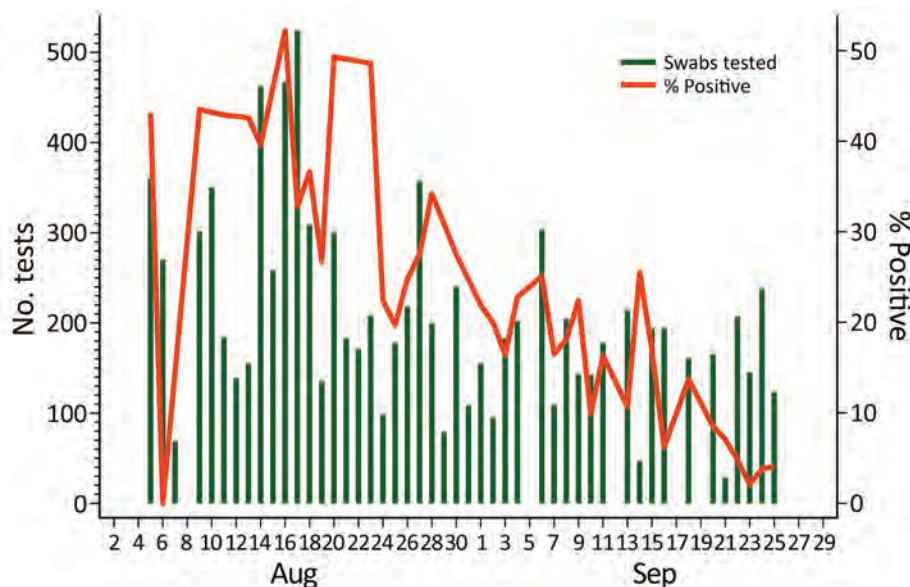
Figure 2. Number of daily nasopharyngeal and oropharyngeal swab samples tested for severe acute respiratory syndrome coronavirus 2 and percentage of positive samples in The Gambia during August–September 2020, the timeframe for the most intense transmission in the country.

(20.4%) were SARS-CoV-2–positive. Most (60%) confirmed cases were detected in August. The median age among MRCG staff with SARS-CoV-2–positive samples was 36 years.

Rates of Infection and Death

By the end of September 2020, the cumulative rate of infection among the population of The Gambia ≈1.5/1,000 persons (Figure 3, panel A). During the same period, 115 COVID-19 deaths were recorded across the country.

Among MRCG staff, stratified analysis showed that infection rates among CSD staff were 2.6 times higher than among non-CSD staff, whom we considered representative of the infection risk among the general population (Figure 3, panel B). By the end of September, the cumulative risk for infection among non-CSD MRCG staff was ≈124/1,000 persons (Figure 3, panel B). All 191 confirmed cases among MRCG staff were either asymptomatic or mildly symptomatic; no cases met WHO criteria for moderate or severe pneumonia and no deaths occurred in this cohort.

Discussion

The COVID-19 pandemic arrived in The Gambia in July 2020, later than in most countries in the world. The Gambia had a short and intense first wave; 67% of cases occurred in August, and most cases were asymptomatic or mild. Among our MRCG cohort, 1/7 (14.3%) persons were SARS-CoV-2–positive. During the epidemic peak, the SARS-CoV-2 positivity rate among the population of The Gambia was >20%.

The later start of the epidemic is probably the result of the early closure of national borders, including for air travel, and of the identification and isolation of infected persons who continued to enter the country from Senegal. These measures were complemented by contact tracing and by the provision of facilities for quarantine by the government. The relative effects of these measures, together with other measures implemented during the state of emergency, such as closure of schools, reduction of access to markets, banning of large gatherings including at religious festivals, and use of facemasks, are hard to quantify, as are behavioral changes, such as social distancing and handwashing. Nonetheless, these measures seem to have been key in preparing the country to respond and minimize potential harm.

The sudden increase of cases in August coincided with the major Muslim feast of Eid-Ul Adha, locally called Tobaski, on July 30, 2020, during which travel and family gatherings were common. However, the number of COVID-19 cases had already started to increase in July.

Although climate in The Gambia is hot throughout the year, the peak epidemic coincided with the months of highest daily humidity and highest minimum temperature but lowest maximum temperature (*14,15*). Data on how temperature and humidity affect transmission are contradictory (*24,25*). In The Gambia, climate conditions might have had an indirect effect on transmission because persons are more likely to spend time indoors during the rainy season. In The Gambia, the rainy season also occurs during the months with the highest respiratory virus transmission (*26*).

Through the systematic testing of the MRCG staff cohort, including asymptomatic contacts and mildly symptomatic cases, we might have more robust estimates of the actual rates of SARS-CoV-2 infection in The Gambia than are available from the general population. The rate of SARS-CoV-2 in MRCG staff outside the CSD (124 cases/1,000 persons) was >80-fold higher than that reported for the general population. Rates among MRCG staff remained ≥40-fold higher than the general population, even when we considered only the more intensely populated coastal area of The Gambia in the denominator. Assuming the urban adult population

had similar exposures and transmission as our MRCG cohort, we would expect ≥75,000 infections among the 601,394 persons 20–64 years of age who live in main towns. This estimation contrasts sharply with the 3,579 cases reported during the same period across the country and in all age groups, a discrepancy that could be partly explained by the high occurrence of asymptomatic or mildly symptomatic infections and the national testing strategy that used passive case detection and targeted symptomatic persons. Because >50% of the population is <20 years of age, we would expect a high frequency of asymptomatic
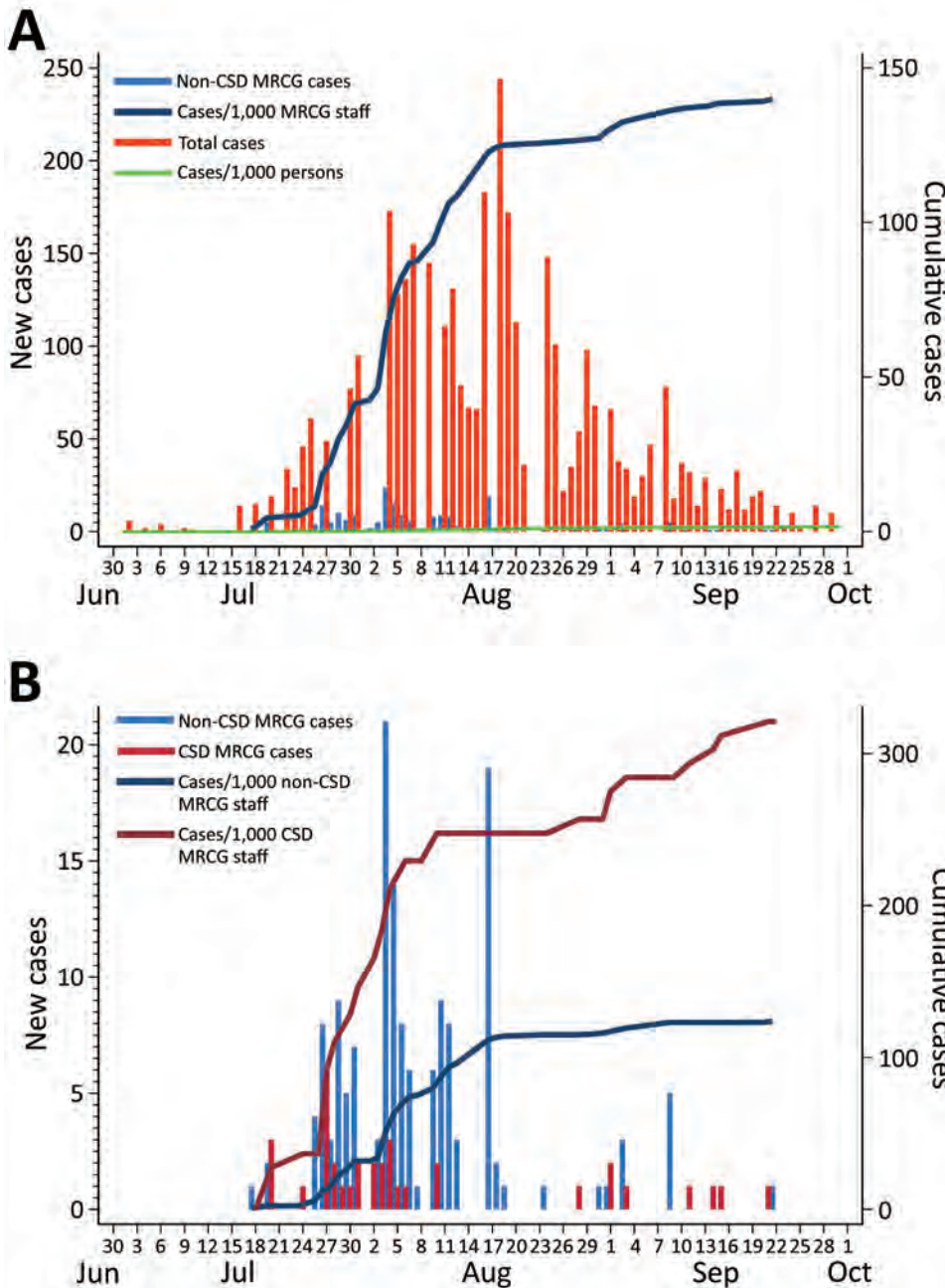
Figure 3. Daily COVID-19 cases and cumulative rates of SARS-CoV-2 infection per 1,000 persons among staff of Medical Research Council Unit The Gambia (MRCG) and the population of The Gambia, June 30–October 1, 2020. A) Case rates for MRCG staff outside the clinical service department and the population of The Gambia. We considered MRCG staff outside the clinical service department to be at the same risk for COVID-19 as the rest of the population. B) Risk for SARS-CoV-2 infection among MRCG staff stratified by potential occupational exposure risk. We considered clinical service department staff at highest risk for SARS-CoV-2 infection, and these staff were under more intense surveillance. Scales for the y-axes differ substantially to underscore patterns but do not permit direct comparisons. COVID-19, coronavirus disease; SARS-CoV-2, severe acute respiratory syndrome coronavirus 2.

infections in The Gambia. Indeed, the discrepancies between estimated and reported cases we noted are consistent with recent seroprevalence studies from eastern and southern Africa. Those studies suggest higher rates of community infection compared with those estimated by passive case surveillance. For instance, 3 weeks after the COVID-19 peak in South Africa, 40% of HIV-positive pregnant women had SARS-CoV-2 antibodies (*12*). In Kenya, a retrospective survey of blood donor samples collected during April–June 2020 found that 1 in 20 adults had SARS-CoV-2 antibodies (*13*). In Malawi, SARS-CoV-2 seroprevalence was 12.3% in a cohort of 500 healthcare workers sampled during May–June 2020; using the observed seroprevalence, the researchers concluded that the predicted number of deaths was 8 times the number of reported deaths (*11*). In a smaller study of 113 frontline healthcare workers in Nigeria, 45% had SARS-CoV-2 antibodies (*27*). In The Gambia, >30% of the CSD staff became infected by September 30, 2020. Rates among CSD staff were higher than the rest of the MRCG cohort, which probably reflects a combination of stronger surveillance and occupational clinical exposure exacerbated by traveling to work, but the weight of each factor is difficult to estimate. However, higher seroprevalence has been reported among healthcare workers in Europe (*28*).

The prevalence of mild disease also is reflected by the low occupancy of hospital beds reserved for severe COVID-19 patients. However, the fewer hospitalizations also could indicate avoidance of SARS-CoV-2 testing because of stigmatization, which has been observed in other regions (*7*). Indeed, among the 115 COVID-19 deaths counted in The Gambia, 30% of SARS-CoV-2 tests were performed postmortem on samples collected from patients hospitalized in non–COVID-19 health facilities. Without an official registration system for deaths, the overall toll of COVID-19–associated deaths is difficult to quantify, and the real number could be several times higher.

The low occurrence of severe disease in Africa compared with other continents underlines the importance of minimizing the potential collateral damage of the COVID-19 pandemic. Such damage includes diversion of financial and personnel resources from other services to the COVID-19 response, changes in healthcare seeking behavior, reduced availability of medicines for acute and chronic diseases, and disruption of routine vaccination services (*29–33*). The pandemic also has worsened the economic stability of households and increased food insecurity, particularly in low- and middle-income countries (*34*), and mitigating the short- and mid-term effects of the pandemic should be a priority. Use of COVID-19

restriction measures to control transmission must be carefully weighed against the economic effects these measures have on the population. Tackling fear and stigma will be essential to avoid decreases in health system use in future COVID-19 waves.

One limitation of our study is that, although cases in the general population and the MRCG cohort showed similar timelines and the size of the MRCG cohort is relatively large, MRCG cases could be considered a cluster. In addition, the level of education and the monthly income of MRCG staff is above that of the general population, thus, staff likely understand and are able to better implement prevention measures. MRCG staff live mainly in urban areas, where transmission tends to be higher (*35*), but they also live in less crowded environments with better access to water and sanitation, which could protect them from infection. MRCG also developed policies, launched many levels of staff education on COVID-19, and reinforced messages related to social distancing, handwashing, and the wearing of face masks at work and in the community. Given the nature of the MRCG's work, the level of understanding and background knowledge of infectious diseases, even among staff not directly involved in research, likely is higher than for the general population. The rapid identification and isolation of cases through the robust surveillance among MRCG staff should have further limited transmission. On the other hand, no moderate or severe COVID-19 cases occurred among the MRCG staff. The mild clinical manifestations among cases were not modified by treatment; for instance, no MRCG staff member met WHO criteria for hospitalization and fewer required oxygen supplementation or dexamethasone treatment. The prevalence of risk factors for severity should be similar between MRCG staff and the population, except the MCRG cohort had fewer persons >60 years of age, which is a primary risk factor for severe COVID-19 and death.

In conclusion, SARS-CoV-2 transmission in The Gambia was intense over a short period. Reassuringly, COVID-19 seems less severe in The Gambia than in high-income countries in Europe, North America, and Asia. It is unclear whether a second wave of infection will occur because the causes of the sudden increase of cases in July are unclear. We strongly encourage continuous protection of healthcare workers with appropriate PPE and strengthening of surveillance systems around the country to promptly detect another sudden increase of cases. Countrywide seroprevalence surveys would clarify the epidemiology of infection in different age groups and places. However, engaging with the community to mitigate

collateral damage of the pandemic should take priority. In addition, investigation is needed to define the major drivers that shape the epidemic so differently in Africa than in some high-income regions. Clarifying such drivers should help model adequate interventions for both low- and high-income countries.

References

1. Worldometers. Coronavirus updates [cited 2020 Oct 31]. https://www.worldometers.info/coronavirus
2. Worldometers. World population by region 2020 [cited 2020 Oct 31]. https://www.worldometers.info/world-population/#region
3. Martinez-Alvarez M, Jarde A, Usuf E, Brotherton H, Bittaye M, Samateh AL, et al. COVID-19 pandemic in west Africa. Lancet Glob Health. 2020;8:e631–2. https://doi.org/10.1016/S2214-109X(20)30123-6
4. Norton A, De La Horra Gozalo A, Feune de Colombi N, Alobo M, Mutheu Asego J, Al-Rawni Z, et al. The remaining unknowns: a mixed methods study of the current and global health research priorities for COVID-19. BMJ Glob Health. 2020;5:e003306. https://doi.org/10.1136/bmjgh-2020-003306
5. Visual Capitalist. Mapped: each region's median age since 1950 [cited 2020 Oct 31]. https://www.visualcapitalist.com/median-age-changes-since-1950
6. Adepoju P. COVID-19: the sky hasn't fallen yet in Africa. Health Policy Watch. 2020 Aug 15 [cited 2020 Oct 31]. https://healthpolicy-watch.news/covid-19-the-sky-hasnt-fallen-yet-in-africa
7. Czeisler ME, Marynak K, Clarke KEN, Salah Z, Shakya I, Thierry JM, et al. Delay or avoidance of medical care because of COVID-19–related concerns—United States, June 2020. MMWR Morb Mortal Wkly Rep. 2020;69:1250–7. https://doi.org/10.15585/mmwr.mm6936a4
8. Grant WB, Lahore H, McDonnell SL, Baggerly CA, French CB, Aliano JL, et al. Evidence that vitamin D supplementation could reduce risk of influenza and COVID-19 infections and deaths. Nutrients. 2020;12:988. https://doi.org/10.3390/nu12040988
9. Mbow M, Lell B, Jochems SP, Cisse B, Mboup S, Dewals BG, et al. COVID-19 in Africa: dampening the storm? Science. 2020;369:624–6. https://doi.org/10.1126/science.abd3902
10. O'Neill LAJ, Netea MG. BCG-induced trained immunity: can it offer protection against COVID-19? Nat Rev Immunol. 2020;20:335–7. https://doi.org/10.1038/s41577-020-0337-y
11. Chibwana MG, Jere KC, Kamng'ona R, Mandolo J, Katunga-Phiri V, Tembo D, et al. High SARS-CoV-2 seroprevalence in Health Care Workers but relatively low numbers of deaths in urban Malawi. Wellcome Open Res. 2020; 5:199. https://doi.org/10.12688/wellcomeopenres.16188.1
12. Shaw JA, Meiring M, Cummins T, Chegou NN, Claassen C, Du Plessis N, et al. Higher SARS-CoV-2 seroprevalence in workers with lower socioeconomic status in Cape Town, South Africa. PLoS One. 2021;16:e0247852. https://doi.org/10.1371/journal.pone.0247852
13. Uyoga S, Adetifa IMO, Karanja HK, Nyagwange J, Tuju J, Wanjiku P, et al. Seroprevalence of anti-SARS-CoV-2 IgG antibodies in Kenyan blood donors. Science. 2021;371:79–82. https://doi.org/0.1126/science.abe1916
14. Climatestotravel.com. Climate–Gambia [cited 2020 Oct 31]. https://www.climatestotravel.com/climate/gambia
15. World Weather & Climate Information. Average humidity in Banjul: the mean monthly relative humidity over the year in Banjul, Gambia [cited 2020 Oct 31]. https://weather-and-climate.com/average-monthly-Humidity-perc,Banyul,Gambia
16. World Health Organization. Clinical management of COVID-19 (Interim Guidance) 27 May 2020 [cited 2020 Oct 31]. https://www.who.int/publications-detail/clinical-management-of-covid-19
17. World Health Organization. Rational use of personal protective equipment (PPE) for coronavirus disease (COVID-19) (Interim Guidance) 19 March 2020 [cited 2020 Mar 19]. https://www.who.int/publications/i/item/rational-use-of-personal-protective-equipment-(ppe)-for-coronavirus-disease-(covid-19)
18. World Health Organization. Criteria for releasing COVID-19 patients from isolation (scientific brief) 17 June 2020 [cited 2020 Jun 17]. https://apps.who.int/iris/rest/bitstreams/1282284/retrieve
19. World Health Organization. Laboratory biosafety guidance related to the novel coronavirus disease 2019 (2019-nCoV): interim guidance, 12 Feb 2020 [cited 2020 Feb 12].

https://www.who.int/docs/default-source/coronaviruse/laboratory-biosafety-novel-coronavirus-version-1-1.pdf

20. World Health Organization. Laboratory testing for coronavirus disease 2019 (COVID-19) in suspected human cases: interim guidance, 2 March 2020 [cited 2020 Mar 2]. https://apps.who.int/iris/handle/10665/331329

21. Corman VM, Eckerle I, Bleicker T, Zaki A, Landt O, Eschbach-Bludau M, et al. Detection of a novel human coronavirus by real-time reverse-transcription polymerase chain reaction. Euro Surveill. 2012;17:20285. https://doi.org/10.2807/ese.17.39.20285-en

22. Ministry of Health. The Gambia. COVID-19 sitrep, 1 Oct 2020 [cited 2020 Oct 1] https://www.moh.gov.gm/wp-content/uploads/2020/10/Gambia_The_COVID-19_Sitrep-01st-Oct-2020-1.doc.pdf

23. Johns Hopkins University. COVID-19 data [cited 2020 Oct 9]. https://github.com/CSSEGISandData/COVID-19

24. Wu Y, Jing W, Liu J, Ma Q, Yuan J, Wang Y, et al. Effects of temperature and humidity on the daily new cases and new deaths of COVID-19 in 166 countries. Sci Total Environ. 2020; 729:139051. https://doi.org/10.1016/j.scitotenv.2020.139051

25. Yao Y, Pan J, Liu Z, Meng X, Wang W, Kan H, et al. No association of COVID-19 transmission with temperature or UV radiation in Chinese cities. Eur Respir J. 2020;55:2000517. https://doi.org/10.1183/13993003.00517-2020

26. Jarju S, Greenhalgh K, Wathuo M, Banda M, Camara B, Mendy S, et al. Viral etiology, clinical features and antibiotic use in children <5 years of age in The Gambia presenting with influenza-like illness. Pediatr Infect Dis J. 2020;39:925–30. https://doi.org/10.1097/INF.0000000000002761

27. Olayanju O, Bamidele O, Edem F, Eseile B, Amoo A, Nwaokenye J, et al. SARS-CoV-2 seropositivity in asymptomatic frontline health workers in Ibadan, Nigeria. Am J Trop Med Hyg. 2021;104:91–4. https://doi.org/10.4269/ajtmh.20-1235

28. Moncunill G, Mayor A, Santano R, Jimenez A, Vidal M, Tortajada M, et al. SARS-CoV-2 seroprevalence and antibody kinetics among health care workers in a Spanish hospital after three months of follow-up. J Infect Dis. 2021;223:62–71. https://doi.org/10.1093/infdis/jiaa696

29. How to stop COVID-19 fuelling a resurgence of AIDS, malaria and tuberculosis. Nature. 2020;584:169. https://doi.org/10.1038/d41586-020-02334-0

30. Amimo F, Lambert B, Magit A. What does the COVID-19 pandemic mean for HIV, tuberculosis, and malaria control? Trop Med Health. 2020;48:32. https://doi.org/10.1186/s41182-020-00219-6

31. Ogundele OA, Omotoso AA, Fagbemi AT. COVID-19 outbreak: a potential threat to routine vaccination programme activities in Nigeria. Hum Vaccin Immunother. 2021;17:661–3. https://doi.org/10.1080/21645515.2020.1815490

32. Roberton T, Carter ED, Chou VB, Stegmuller AR, Jackson BD, Tam Y, et al. Early estimates of the indirect effects of the COVID-19 pandemic on maternal and child mortality in low-income and middle-income countries: a modelling study. Lancet Glob Health. 2020;8:e901–8. https://doi.org/10.1016/S2214-109X(20)30229-1

33. Teboh-Ewungkem MI, Ngwa GA. COVID-19 in malaria-endemic regions: potential consequences for malaria intervention coverage, morbidity, and mortality. Lancet Infect Dis. 2021;21:5–6. https://doi.org/0.1016/S1473-3099(20)30763-5

34. World Health Organization. Impact of COVID-19 on people's livelihood their health and our food systems: joint statement by ILO, FAO, IFAD and WHO; 2020 Oct 13 [cited 2020 Oct 13]. https://www.who.int/news/item/13-10-2020-impact-of-covid-19-on-people%27s-livelihoods-their-health-and-our-food-systems

35. United Nations. UN-Habitat's COVID-19 response plan [cited 2020 Oct 31]. https://unhabitat.org/un-habitat-covid-19-response-plan

Address for correspondence: Anna Roca, MRC Unit The Gambia at the London School of Hygiene and Tropical Medicine, London, UK; Atlantic Road, PO Box 273, Fajara, The Gambia; email: aroca@mrc.gm

Peridomestic Mammal Susceptibility to Severe Acute Respiratory Syndrome Coronavirus 2 Infection

Angela M. Bosco-Lauth, J. Jeffrey Root, Stephanie M. Porter, Audrey E. Walker,
Lauren Guilbert, Daphne Hawvermale, Aimee Pepper, Rachel M. Maison,
Airn E. Hartwig, Paul Gordy, Helle Bielefeldt-Ohmann, Richard A. Bowen

Wild animals have been implicated as the origin of severe acute respiratory syndrome coronavirus 2 (SARS-CoV-2), but it is largely unknown how the virus affects most wildlife species and if wildlife could ultimately serve as a reservoir for maintaining the virus outside the human population. We show that several common peridomestic species, including deer mice, bushy-tailed woodrats, and striped skunks, are susceptible to infection and can shed the virus in respiratory secretions. In contrast, we demonstrate that cottontail rabbits, fox squirrels, Wyoming ground squirrels, black-tailed prairie dogs, house mice, and racoons are not susceptible to SARS-CoV-2 infection. Our results expand the knowledge base of susceptible species and provide evidence that human–wildlife interactions could result in continued transmission of SARS-CoV-2.

The rapid global expansion of severe acute respiratory syndrome coronavirus 2 (SARS-CoV-2), which causes coronavirus disease (COVID-19), has been unprecedented in modern history. Although the original human infection(s) were potentially linked to wild animals in a wet market (*1*), human-to-human transmission is currently the dominant mechanism of viral spread. Peridomestic animals, which are represented by wild and feral animals living near humans, represent key species to evaluate for SARS-CoV-2 epidemiology for multiple reasons. First, given their common associations with humans and anthropogenically modified habitats, they represent the wildlife species with the greatest chance

Author affiliations: Colorado State University, Fort Collins, Colorado, USA (A.M. Bosco-Lauth, S.M. Porter, A.E. Walker, L. Guilbert, D. Hawvermale, A. Pepper, R.M. Maison, A.E. Hartwig, P. Gordy, R.A. Bowen); US Department of Agriculture, Fort Collins (J.J. Root); The University of Queensland, St. Lucia, Queensland, Australia (H. Bielefeldt-Ohmann)

of exposure to the virus from humans (i.e., reverse zoonosis) or pets, such as cats. Second, should select peridomestic wildlife prove to be susceptible to the virus and have the capacity to replicate it to high viral titers, these species would have the potential to maintain the virus among conspecifics. Third, should some species possess the maintenance host criteria mentioned, they would represent wildlife species that would have the greatest chance (e.g., shedding ability and proximity to humans) to spread the virus back to humans. Wild rodents, cottontail rabbits (*Sylvilagus* sp.), raccoons (*Procyon lotor*), and striped skunks (*Mephitis mephitis*) can exhibit peridomestic tendencies in urban and suburban environments. Members of all those species/taxonomic groups have been shown to shed influenza A viruses after experimental inoculations (*2–4*), suggesting they might harbor productive infections when exposed to other human-pathogenic respiratory viruses.

Based upon protein analyses of amino acid residues of angiotensin-converting enzyme 2 (ACE2), transmembrane protease serine type 2, and spike protein, species susceptibility analyses suggested that, among other taxonomic groups, both carnivores and wild rodents are potentially high-risk groups (*5–7*). However, predicting susceptibility of specific species is more challenging. Looking at protein sequence analysis of ACE2 binding with the spike protein of SARS-CoV-2, one study indicated that raccoons could be ruled out as potential hosts for SARS-CoV-2 (*6*), and a different study based upon sequence analysis suggested that the western spotted skunks (*Spilogale gracilis*) had a low prediction of SARS-CoV-2 S binding propensity (*7*). Similarly, the same study also suggested that American mink (*Neovison vison*) have a similar prediction as western spotted skunks (*7*). However, over the past several months, outbreaks of SAR-CoV-2 in commercial mink farms have been

reported in Europe and more recently in the United States (*8,9*). Respiratory problems, rapid transmission, or unusually high mortality rates have been reported for this species in various regions (*8,10*), which suggests that those analyses have limitations.

Because rodents are the largest and most diverse order of mammals, it is not surprising that the susceptibility of rodents to SARS-CoV-2 varies by species. To date, only a handful of rodent species have been evaluated as potential reservoir hosts or animal models for SARS-CoV-2, and the results largely indicate that outbred species, including laboratory animals, are at most only moderately affected. Most nontransgenic laboratory mice (*Mus musculus*) are resistant to infection, but transgenic humanized mice and hamsters, including Syrian hamsters (*Mesocricetus auratus*) and dwarf hamsters (*Phodopus* sp.), are highly susceptible (*11,12*); 1 report described Roborovki dwarf hamsters becoming diseased and dying within 3 days of exposure (*13*). Other species, including deer mice (*Peromyscus maniculatus*), become infected and shed low titers of virus, but the infection is subclinical (A. Fagre, Colorado State University, pers. comm., 2020 Aug 7). Considering that there are >1,700 species of rodents worldwide, many of which exist closely at the human–wildlife interface, there remain many unanswered questions about SARS-CoV-2 and wild rodents.

Various lagomorphs exist as pets, livestock, and peridomestic wildlife, and as such are in a prime position to come into contact with SARS-CoV-2–infected humans. In 1 study, New Zealand white rabbits were experimentally infected and shed infectious virus for <7 days without signs of clinical disease (*14*). Wild rabbits, particularly cottontails in the United States, are prolific and commonly found around human dwellings, farms, and commercial buildings. Furthermore, as with rodents, wild rabbits are likely to be predated upon by domestic and wild felids and canids. Thus, the susceptibility of these animals must be determined to interpret the risk posed to them and by them from infection with SARS-CoV-2.

Among carnivores, felids and mustelids have been frequently linked to SARS-CoV-2 infections since the early stages of the pandemic. Domestic cats are highly susceptible to SARS-CoV-2 and are capable of transmitting the virus to other cats, suggesting that they could also potentially transmit virus to other animals (*15,16*). Although striped skunks are currently considered to be mephitids, they are highly related to mammals within the family Mustelidae and were formerly classified as mustelids. Thus, on the basis of findings for SARS-CoV-2 susceptibility in various mustelids,

we determined that the closely related mephitids are a logical candidate to evaluate for replication of this virus. Raccoons are notoriously associated with human environments and frequently interact with human trash and sewage; these interactions have been proposed as a potential indirect means for infected humans to transmit SARS-CoV-2 to mammalian wildlife (e.g., raccoons and select mustelids) (*17–19*). Thus, it is essential to determine the relative susceptibility of these common peridomestic carnivores and assess the likelihood that they could propagate infection.

In this study, we assessed 6 common peridomestic rodent species for susceptibility to SARS-CoV-2: deer mice, wild-caught house mice (*Mus musculus*), bushy-tailed woodrats (aka pack rats; *Neotoma cinerea*), fox squirrels (*Sciurus niger*), Wyoming ground squirrels (*Urocitellus elegans*), and black-tailed prairie dogs (*Cynomys ludovicianus*). These rodents are common in many parts of the United States, several of them frequently come into close contact with humans and human dwellings, and some are highly social animals, thus increasing the likelihood of pathogen transmission among conspecifics. In addition, we evaluated 3 other common peridomestic mammals: cottontail rabbits, raccoons, and striped skunks.

Materials and Methods

Animals
We evaluated the following mixed-sex animals for susceptibility to SARS-CoV-2: deer mice, house mice, bushy-tailed woodrats, Wyoming ground squirrels, black-tailed prairie dogs, fox squirrels, cottontail rabbits, striped skunks, and raccoons. Deer mice, house mice, and bushy-tailed woodrats were trapped by using Sherman traps (https://www.shermantraps.com) baited with grain. Wyoming ground squirrels, fox squirrels, black-tailed prairie dogs, and cottontails were trapped using Tomahawk live traps (https://www.livetrap.com) (e.g., 7 in × 7 in × 20 in or 7 in × 7 in × 24 in). All trapping was conducted in northern Colorado (Larimer, Jackson and Weld Counties) in accordance with Colorado wildlife regulations and with appropriate permits and Institutional Animal Care and Use Committee protocols in place. Skunks and raccoons were purchased from a private vendor. Animals were housed in an Animal Biosafety Level 3 facility at Colorado State University, in rooms (12 ft × 18 ft) that had natural lighting and controlled climate. Mice, black-tailed prairie dogs, and Wyoming ground squirrels were group housed by species with access to water and food ad libitum. All other animals were housed individually with access to food and water ad libitum.

Rodents were fed Teklad Rodent Diet (Enviro, https://www.envigo.com) supplemented with fresh fruit and occasional nuts. Rabbits were fed Manna Pro alfalfa pellets (https://www.mannapro.com) supplemented with grass hay and apples. Skunks and raccoons were fed Mazuri Omnivore Diet (https://www.mazuri.com) supplemented with fresh fruit and occasional eggs. Raccoons, striped skunks, and black-tailed prairie dogs were implanted with thermally sensitive microchips (Bio-Thermo Lifechips, http://destronfering.com) for identification and temperature measurement and deer mice were ear notched; all other animals were identified by cage number or distinct markings.

Virus

We obtained SARS-CoV-2 strain WA1/2020WY96 from BEI Resources (https://www.beiresources.org), passaged it twice in Vero E6 cells, and prepared stocks frozen at −80°C in Dulbecco modified Eagle medium containing 5% fetal bovine serum and antimicrobial drugs. We titrated the virus stock on Vero cells by using a standard double overlay plaque assay (15) and counted plaques 72 hours later to determine PFUs/mL.

Virus Challenge

Before challenge with SARS-CoV-2, we lightly anesthetized most animals as needed with 1–3 mg/kg xylazine and 10–30 mg/kg ketamine hydrochloride and collected a blood sample just before inoculation (day 0). We administered virus diluted in phosphate-buffered saline to all species into the nares by using a pipette (50 µL for deer and house mice, 100 µL for bushy-tailed woodrats, and 200 µL for all other species) and observed animals until they were fully recovered from anesthesia. Virus back-titration was performed on Vero cells immediately after inoculation, confirming that animals received 4.5–4.9 $\log_{10}$ PFU of SARS-CoV-2.

Sampling

We used groups of 3 animals from each species (2 ground squirrels) for preliminary studies to evaluate viral shedding and acute pathologic changes. For these animals, we obtained oral swab specimens prechallenge and on days 1–3 postchallenge, at which time animals were euthanized and the following tissues harvested for virus isolation and formalin fixation: trachea, nasal turbinates, lung, heart, liver, spleen, kidney, small intestine, and olfactory bulb. The exception to this process was raccoons, for which we euthanized only 1 animal at day 3; we kept the remaining 2 raccoons through day 28 to evaluate serologic response. We swabbed the remaining 3–6 animals/selected species daily from days 0–5 and 7 to further evaluate duration of viral shedding (if any). We sedated striped skunks and raccoons for all sampling and collected a nasal swab specimen in addition to the oral swab specimen. We evaluated tissues harvested from animals euthanized on day 7 as for the day 3 animals. We euthanized the remaining animals at 28 days postinfection (dpi), harvested tissues for histopathologic analysis, and collected serum for serologic analysis. We provide the necropsy scheme for each species (Table).

Clinical Observations

We clinically evaluated all animals daily and included assessment for temperament and any clinical signs of disease, such as ocular discharge, nasal discharge, ptyalism, coughing/sneezing, dyspnea, diarrhea, lethargy, anorexia, and moribund status. The stress of handling wild animals for sampling precluded the ability to obtain accurate body temperature measurements; as such, we excluded temperature in these preliminary studies for all species except skunks and raccoons, which were implanted with thermal microchips and could be measured under sedation during sampling.

Viral Assays

We performed plaque reduction neutralization assays as described (15). Serum samples were heat-inactivated for 30 min at 56°C, and 2-fold dilutions were prepared in Tris-buffered minimal essential

Table. Wildlife species evaluated for experimental infections with SARS-CoV-2 and day animals were euthanized*

Animals	No. euthanized at 3 dpi	No. euthanized at 7 dpi	No. euthanized at 28 dpi
Deer mice, n = 9	3	3	3
House mice, n =6	3	0	3
Bushy-tailed woodrats, n = 6	3	0	3
Fox squirrels, n = 3	3	0	0
Wyoming ground squirrels, n = 2	2	0	0
Black-tailed prairie dogs, n = 9	3	3	3
Cottontails, n = 3	3	0	0
Raccoons, n = 3	1	0	2
Striped skunks, n = 6	3	0	3

*dpi, days postinfection; SARS-CoV-2, severe acute respiratory syndrome coronavirus 2.

medium containing 1% bovine serum albumin starting at a 1:5 dilution and aliquoted onto 96-well plates. An equal volume of virus was added to the serum dilutions and incubated for 1 hour at 37°C. After incubation, serum–virus mixtures were plated onto Vero monolayers as described for virus isolation assays. We screened serum samples for antibodies specific to SARS-CoV-2 to ensure seronegative status before inoculation by using a cutoff value <50% viral neutralization. We recorded antibody titers as the reciprocal of the highest dilution in which >90% of virus was neutralized.

Serologic Analysis

We performed plaque reduction neutralization assays as described (15). We heat-inactivated serum samples for 30 min at 56°C, and prepared 2-fold dilutions in Tris-buffered minimal essential medium containing 1% bovine serum albumin starting at a 1:5 dilution and aliquoted onto 96-well plates. We added an equal volume of virus to the serum dilutions and incubated the serum dilutions for 1 hour at 37°C. After incubation, we plated serum–virus mixtures onto Vero monolayers as described for virus isolation assays. We screened serum samples for antibodies specific to SARS-CoV-2 to ensure seronegative status before inoculation by using a cutoff value <50% viral neutralization. We recorded antibody titers as the reciprocal of the highest dilution in which >90% of virus was neutralized.

Quantitative Reverse Transcription PCR

We picked plaques from culture plates from each positive animal to confirm SARS-CoV-2 viral shedding. We extracted RNA by using QiaAmp Viral RNA Mini Kits (QIAGEN, https://www.qiagen.com) according to the manufacturer's instructions. We performed reverse transcription PCR (RT-PCR) by using the E_Sarbeco primer probe sequence described by Corman et al. (20) and the Superscript III Platinum One-Step qRT-PCR System (Invitrogen, https://www.thermofisher.com) with the following modification: the initial reverse transcription was at 50°C. RNA standards for PCR were obtained from BEI Resources.

Histopathologic Analysis

We fixed animal tissues in 10% neutral-buffered formalin for 12 days and transferred them to 70% ethanol before processing for paraffin embedding and sectioning for staining with hematoxylin and eosin. Slides were read by a veterinary pathologist blinded to the treatments.

Results

Viral Shedding

Of the 9 species evaluated, 3 (deer mice, bushy-tailed woodrats, and striped skunks) shed infectious virus after challenge (Figure). Deer mice, which have previously been demonstrated to shed infectious SARS-CoV-2 experimentally (A. Fagre, Colorado State University, pers. comm., 2020 Aug 7), shed virus orally for $\leq$4 days and virus was isolated from lungs (3/3) and trachea (2/3) of animals tested at 3 dpi. All 9 inoculated deer mice shed virus on at $\geq$2 of the first 4 days after infection and had peak titers of 3.1 $\log_{10}$ PFU/swab specimen. Bushy-tailed woodrats shed virus orally for $\leq$5 days postinoculation (6/6), and virus was isolated from turbinates (2/3), trachea (1/3), and lung (1/3) from animals that underwent necropsy on 3 dpi. Peak titers from bushy-tailed woodrats reached 3.0 $\log_{10}$ PFU/swab specimen 3 dpi. The single bushy-tailed woodrat for which infectious virus was isolated from the lungs only shed 1.3 $\log_{10}$ PFU/swab specimen orally on the day of necropsy, but the lungs contained 5.2 $\log_{10}$ PFU/g of virus.

Striped skunks, which had to be handled under heavy sedation, were sampled on days 1–3, 5, and 7, during which time 3 of the 6 infected animals shed virus orally, nasally, or both, and 1 animal shed $\leq$7 dpi. Of the 3 skunks that underwent necropsy on 3 dpi, 2 had infectious virus in the turbinates but not in other tissues tested. One of those 2 animals had 3.2 $\log_{10}$ PFU/g of virus in the turbinates but did not shed detectable virus nasally or orally before euthanasia. In general, viral titers were slightly higher in nasal samples than oral samples, but overall peak titers in skunks were relatively low, with oral titers reaching 2 $\log_{10}$ PFU/swab specimen and nasal titers reaching 2.3 $\log_{10}$ PFU/swab specimen. All animals that had plaque assay–positive samples were confirmed as having SARS-CoV-2 by RT-PCR. Similarly, all animals that were negative by plaque assay were confirmed as negative for viral shedding by RT-PCR.

Seroconversion

All animals were seronegative against SARS-CoV-2 at the time of inoculation. On the basis of the lack of evidence of infection and the overall difficulty of maintaining wildlife, we opted not to hold subsets of squirrels or rabbits for additional time to assess seroconversion. We assessed neutralizing antibody titers in all animals euthanized at 28 dpi, which included deer mice, house mice, bushy-tailed woodrats, black-tailed prairie dogs, raccoons, and striped skunks. All species that had detectable viral infections (deer
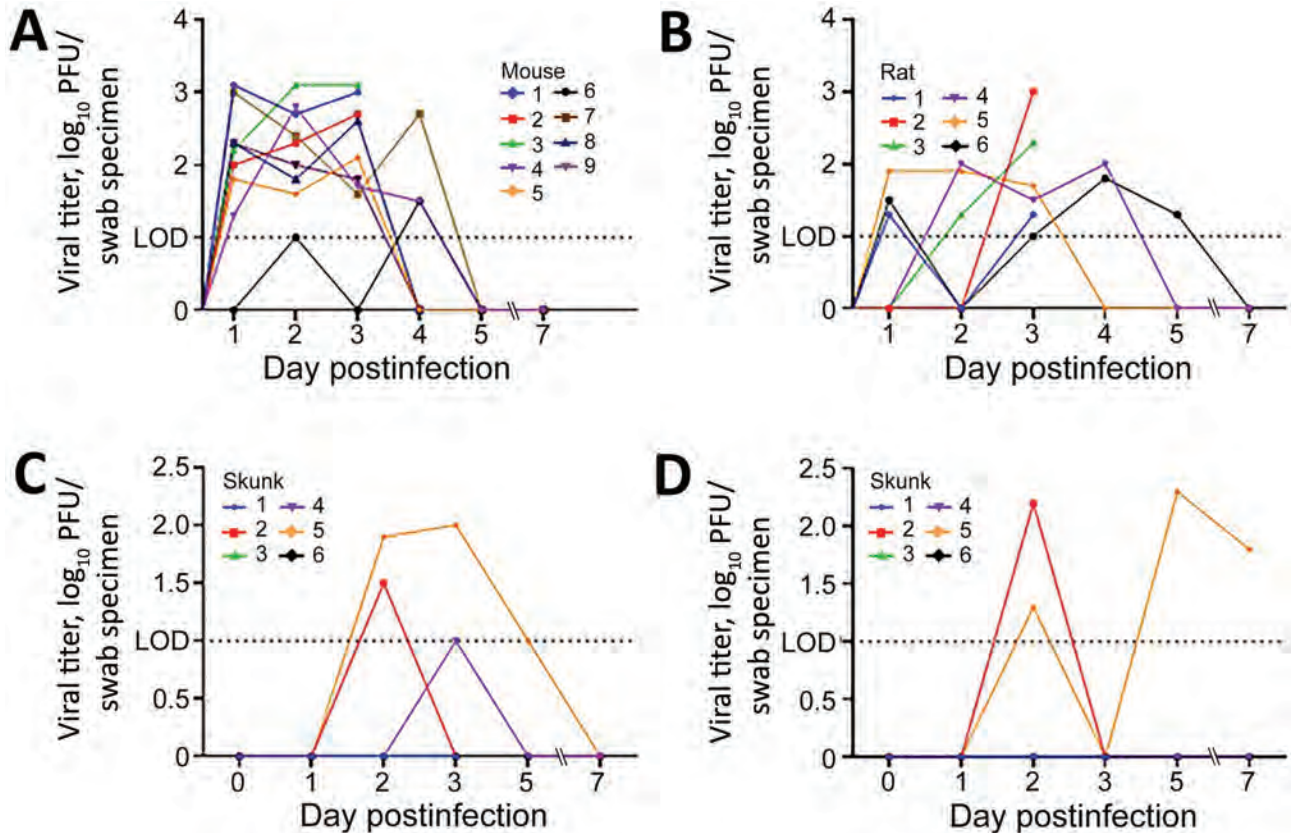
Figure. Oropharyngeal shedding of severe acute respiratory syndrome coronavirus 2 in deer mice (A), bushy-tailed woodrats (B), and striped skunks (C) and nasal shedding in striped skunks (D). LOD = 1 $\log_{10}$ PFU. LOD, limit of detection.

mice, skunks, and bushy-tailed woodrats) also had neutralizing antibodies develop, whereas the other species (house mice, raccoons, and black-tailed prairie dogs) did not. Deer mice and bushy-tailed woodrats reached or exceeded titers of 1:80, the 2 skunks that shed infectious virus reached or exceeded titers of 1:160, and the single skunk that did not shed virus had a titer of 1:10 at 28 dpi. We did not test animals euthanized at 3 dpi for seroconversion because previous investigations have demonstrated that neutralizing antibodies are typically not detectable during acute infection (*21*).

Clinical Disease
None of the animals exhibited clinical signs of disease (see Materials and Methods) at any time during the study. Skunks and raccoons, which were sedated for sampling procedures, did not display increased elevated temperatures at those times. In addition to monitoring clinical signs, we monitored behavior by observing animals through double-paned glass and assessing eating and response to provided enrichment (playing with toys, eating treats, using hides).

None of the animals behaved abnormally after infection compared with the acclimation period.

Pathology
None of the animals had gross lesions at the time of necropsy. At histopathologic examination of tissues harvested 3 dpi, rare, small foci of mild macrophage and neutrophil infiltration were noted in the lungs of 2 woodrats and 2 deer mice with one of the deer mice also having mild vasculitis. Two skunks had well-developed bronchioles associated lymphoid tissue, but inflammation was not apparent in the lungs or other tissues.

Discussion
COVID-19 has had a major impact on the human population globally, but so far little is known about how SARS-CoV-2 virus affects wildlife. Domestic cats and dogs have repeatedly been shown to be infected by SARS-CoV-2, but with few exceptions these infections are subclinical or animals show development of mild clinical disease (*15,22,23*). Conversely, farmed mink are not only susceptible

to infection but can also have fulminating fatal disease develop (*10,24*). In contrast, ferrets, which are closely related to mink, shed virus after infection, but the infection is subclinical (*25*). Raccoon dogs, which were heavily implicated in the severe acute respiratory syndrome outbreak during 2002–2004, are susceptible to SARS-CoV-2 infection, but infections remain subclinical (*26*). Experimentally, deer mice can be infected and shed the virus by oral secretions, as demonstrated by this study and others (A. Fagre, Colorado State University, pers. comm., 2020 Aug 7). However, other mice, including wild house mice and nontransgenic laboratory strains of this species, are not susceptible to infection by SARS-CoV-2 (*27*).

Studies in which bats and select small mammals were experimentally exposed to SARS-CoV-2 showed that some species (i.e., fruit bats [*Rousettus aegyptiacus*] and tree shrews [*Tupaia belangeri*]) are capable of minimal viral replication, but others (big brown bats [*Eptesicus fuscus*]) do not become infected, which suggests that although the virus might have originated in bats, they are unlikely to serve as reservoir hosts (*28–30*). The confounding clinical response to infection between closely related species makes predicting impacts on wildlife and their potential for reservoir maintenance difficult. Despite best attempts to predict host susceptibility on the basis of receptor similarity or other modeling approaches, experimental infections remain the standard for evaluating the susceptibility of an animal to infection and following the course of disease.

Our results demonstrate that several common peridomestic wildlife species, including deer mice, bushy-tailed woodrats, and striped skunks, are susceptible to SARS-CoV-2 infection and can shed infectious virus. Our results and the results of others indicate that so far, most exposed wildlife species show development of mild to no clinical disease and either did not shed virus or shed low levels for short durations (*26,28–30*). These experimental infections suggest that we can rule out several common rodents, selected wild lagomorphs, and raccoons as potential SARS-CoV-2 reservoirs. However, there are limitations to these experimental models, namely that the animals in our studies were directly exposed to high doses (e.g., $5 \log_{10}$ PFU) of virus, which is unlikely to be representative of an exposure in nature. In addition, experimental infections using low numbers of apparently healthy, immunocompetent animals do not generate sufficient data to fully characterize the risk posed to animals of varying ages and health status. However, results of this study and results of others, combined with the dramatic response to

infection seen in certain species, such as mink, indicate that SARS-CoV-2 might infect infecting wildlife, establishing a transmission cycle, and becoming endemic in nonhuman species. In particular, the relatively high titers observed in select woodrat tissues (e.g., $5.2 \log_{10}$ PFU/g of lung) suggests that a predator–prey transmission scenario among this rodent species and various small wild and domestic carnivore species is plausible, and experiments designed to capture oral transmission between prey and predator are a logical next step in determining the likelihood of this scenario.

The major outcomes of such an event include direct threat to the health of wildlife and establishment of a reservoir host, which could complicate control measures of this virus in human populations. Experimental studies to identify and characterize responses of species to SARS-CoV-2 infection help scientists classify those species that are at highest risk and enable implementation of prevention measures. For example, because deer mice and bushy-tailed woodrats are commonly found in barns and sheds near humans, when cleaning out sheds or attempting to rodent-proof barns, persons should consider wearing appropriate personal protective equipment to prevent exposure to the pathogens that rodents carry, as well as to prevent exposing wildlife to SARS-CoV-2. Persons whose occupations put them in contact with susceptible animals (biologists, veterinarians, rehabilitators) and COVID-19 patients who own cats and dogs should practice extra precaution when interacting with animals, including minimizing their pet's exposure to wildlife. Of note, a photo-monitoring study provided evidence that striped skunks can commonly use the same urban cover types (e.g., outbuildings and decks) as domestic cats (*31*). Intentionally available pet food and spilled bird feed, which were 2 of the attractants evaluated, produced instances where skunks and domestic cats were documented to be on study sites simultaneously or nearly simultaneously, which could lead to interspecies transmission of SARS-CoV-2.

Wildlife and SARS-CoV-2 are intricately involved, from the initial spillover event to potential reverse zoonotic transmission, and we will undoubtedly continue to discover more susceptible species as the search for zoonotic reservoirs continues. COVID-19 is just the latest in a series of examples of how the human–wildlife interface continues to drive the emergence of infectious disease. Using experimental research, field studies, surveillance, genomics, and modeling as tools for predicting outbreaks and epidemics should help provide the knowledge base and resources necessary to prevent future pandemics.

About the Author

Dr. Bosco-Lauth is an assistant professor in the Department of Biomedical Sciences, Colorado State University. Fort Collins, CO. Her research interests include pathogenesis, transmission, and ecology of infectious diseases.

References

1. Zhou P, Yang X-L, Wang X-G, Hu B, Zhang L, Zhang W, et al. A pneumonia outbreak associated with a new coronavirus of probable bat origin. Nature. 2020;579:270–3. https://doi.org/10.1038/s41586-020-2012-7
2. Root JJ, Bosco-Lauth AM, Bielefeldt-Ohmann H, Bowen RA. Experimental infection of peridomestic mammals with emergent H7N9 (A/Anhui/1/2013) influenza A virus: implications for biosecurity and wet markets. Virology. 2016;487:242–8. https://doi.org/10.1016/j.virol.2015.10.020
3. Shriner SA, VanDalen KK, Mooers NL, Ellis JW, Sullivan HJ, Root JJ, et al. Low-pathogenic avian influenza viruses in wild house mice. PLoS One. 2012;7:e39206. https://doi.org/10.1371/journal.pone.0039206
4. Romero Tejeda A, Aiello R, Salomoni A, Berton V, Vascellari M, Cattoli G. Susceptibility to and transmission of H5N1 and H7N1 highly pathogenic avian influenza viruses in bank voles (*Myodes glareolus*). Vet Res (Faisalabad). 2015;46:51. https://doi.org/10.1186/s13567-015-0184-1
5. Martínez-Hernández F, Isaak-Delgado AB, Alfonso-Toledo JA, Muñoz-García CI, Villalobos G, Aréchiga-Ceballos N, et al. Assessing the SARS-CoV-2 threat to wildlife: potential risk to a broad range of mammals. Perspect Ecol Conserv. 2020;18:223–34. https://doi.org/10.1016/j.pecon.2020.09.008
6. Luan J, Lu Y, Jin X, Zhang L. Spike protein recognition of mammalian ACE2 predicts the host range and an optimized ACE2 for SARS-CoV-2 infection. Biochem Biophys Res Commun. 2020;526:165–9. https://doi.org/10.1016/j.bbrc.2020.03.047
7. Damas J, Hughes GM, Keough KC, Painter CA, Persky NS, Corbo M, et al. Broad host range of SARS-CoV-2 predicted by comparative and structural analysis of ACE2 in vertebrates. Proc Natl Acad Sci U S A. 2020;117:22311–22. https://doi.org/10.1073/pnas.2010146117
8. Oreshkova N, Molenaar RJ, Vreman S, Harders F, Oude Munnink BB, Hakze-van der Honing RW, et al. SARS-CoV-2 infection in farmed minks, the Netherlands, April and May 2020. Euro Surveill. 2020;25. https://doi.org/10.2807/1560-7917.ES.2020.25.23.2001005
9. Shriner SA, Ellis JW, Root JJ, Roug A, Stopak SR, Wiscomb GW, et al. SARS-CoV-2 exposure in escaped mink, Utah, USA. Emerg Infect Dis. 2021;27:988–90. https://doi.org/10.3201/eid2703.204444
10. Molenaar RJ, Vreman S, Hakze-van der Honing RW, Zwart R, de Rond J, Weesendorp E, et al. Clinical and pathological findings in SARS-CoV-2 disease outbreaks in farmed mink (*Neovison vison*). Vet Pathol. 2020;57:653–7. https://doi.org/10.1177/0300985820943535
11. Younes S, Younes N, Shurrab F, Nasrallah GK. Severe acute respiratory syndrome coronavirus-2 natural animal reservoirs and experimental models: systematic review. Rev Med Virol. 2020;Nov 18:e2196.
12. Sia SF, Yan LM, Chin AW, Fung K, Choy KT, Wong AYL, et al. Pathogenesis and transmission of SARS-CoV-2 in golden hamsters. Nature. 2020;583:834–8. https://doi.org/10.1038/s41586-020-2342-5
13. Trimpert J, Vladimirova D, Dietert K, Abdelgawad A, Kunec D, Dökel S, et al. The Roborovski dwarf hamster is a highly susceptible model for a rapid and fatal course of SARS-CoV-2 infection. Cell Rep. 2020;33:108488. https://doi.org/10.1016/j.celrep.2020.108488
14. Mykytyn AZ, Lamers MM, Okba NM, Breugem TI, Schipper D, van den Doel PB, et al. Susceptibility of rabbits to SARS-CoV-2. Emerg Microbes Infect. 2021;10:1–7. https://doi.org/10.1080/22221751.2020.1868951
15. Bosco-Lauth AM, Hartwig AE, Porter SM, Gordy PW, Nehring M, Byas AD, et al. Experimental infection of domestic dogs and cats with SARS-CoV-2: Pathogenesis, transmission, and response to reexposure in cats. Proc Natl Acad Sci U S A. 2020;117:26382–8. https://doi.org/10.1073/pnas.2013102117
16. Shi J, Wen Z, Zhong G, Yang H, Wang C, Huang B, et al. Susceptibility of ferrets, cats, dogs, and other domesticated animals to SARS-coronavirus 2. Science. 2020;368:1016–20. https://doi.org/10.1126/science.abb7015
17. Gross J, Elvinger F, Hungerford LL, Gehrt SD. Raccoon use of the urban matrix in the Baltimore Metropolitan Area, Maryland. Urban Ecosyst. 2012;15:667–82. https://doi.org/10.1007/s11252-011-0218-z
18. Hoffmann CO, Gottschang JL. Numbers, distribution, and movements of a raccoon population in a suburban residential community. J Mammal. 1977;58:623–36. https://doi.org/10.2307/1380010
19. Franklin AB, Bevins SN. Spillover of SARS-CoV-2 into novel wild hosts in North America: a conceptual model for perpetuation of the pathogen. Sci Total Environ. 2020;733:139358. https://doi.org/10.1016/j.scitotenv.2020.139358
20. Corman VM, Landt O, Kaiser M, Molenkamp R, Meijer A, Chu DK, et al. Detection of 2019 novel coronavirus (2019-nCoV) by real-time RT-PCR. Euro Surveill. 2020;25. https://doi.org/10.2807/1560-7917.ES.2020.25.3.2000045
21. Kellam P, Barclay W. The dynamics of humoral immune responses following SARS-CoV-2 infection and the potential for reinfection. J Gen Virol. 2020;101:791–7. https://doi.org/10.1099/jgv.0.001439
22. Patterson EI, Elia G, Grassi A, Giordano A, Desario C, Medardo M, et al. Evidence of exposure to SARS-CoV-2 in cats and dogs from households in Italy. Nat Commun. 2020;11:6231. https://doi.org/10.1038/s41467-020-20097-0
23. de Morais HA, Dos Santos AP, do Nascimento NC, Kmetiuk LB, Barbosa DS, Brandão PE, et al. Natural infection by SARS-CoV-2 in companion animals: a review of case reports and current evidence of their role in the epidemiology of COVID-19. Front Vet Sci. 2020;7:591216. https://doi.org/10.3389/fvets.2020.591216
24. Hammer AS, Quaade ML, Rasmussen TB, Fonager J, Rasmussen M, Mundbjerg K, et al. SARS-CoV-2 transmission between mink (*Neovison vison*) and humans, Denmark. Emerg Infect Dis. 2021;27:547–51. https://doi.org/10.3201/eid2702.203794
25. Kim Y-I, Kim S-G, Kim S-M, Kim E-H, Park S-J, Yu K-M, et al. Infection and rapid transmission of SARS-CoV-2 in ferrets. Cell Host Microbe. 2020;27:704–709.e2. https://doi.org/10.1016/j.chom.2020.03.023

26. Freuling CM, Breithaupt A, Müller T, Sehl J, Balkema-Buschmann A, Rissmann M, et al. Susceptibility of raccoon dogs for experimental SARS-CoV-2 infection. Emerg Infect Dis. 2020;26:2982–5. https://doi.org/10.3201/eid2612.203733

27. Cohen J. From mice to monkeys, animals studied for coronavirus answers. Science. 2020;368:221–2. https://doi.org/10.1126/science.368.6488.221

28. Hall JS, Knowles S, Nashold SW, Ip HS, Leon AE, Rocke T, et al. Experimental challenge of a North American bat species, big brown bat (Eptesicus fuscus), with SARS-CoV-2. Transbound Emerg Dis. 2020;Dec 9:tbed.13949. https://doi.org/10.1111/tbed.13949

29. Schlottau K, Rissmann M, Graaf A, Schön J, Sehl J, Wylezich C, et al. SARS-CoV-2 in fruit bats, ferrets, pigs, and chickens: an experimental transmission study. Lancet Microbe. 2020;1:e218–25. https://doi.org/10.1016/S2666-5247(20)30089-6

30. Zhao Y, Wang J, Kuang D, Xu J, Yang M, Ma C, et al. Susceptibility of tree shrew to SARS-CoV-2 infection. Sci Rep. 2020;10:16007. https://doi.org/10.1038/s41598-020-72563-w

31. Weissinger MD, Theimer TC, Bergman DL, Deliberto TJ. Nightly and seasonal movements, seasonal home range, and focal location photo-monitoring of urban striped skunks (Mephitis mephitis): implications for rabies transmission. J Wildl Dis. 2009;45:388–97. https://doi.org/10.7589/0090-3558-45.2.388

Address for correspondence: Angela Bosco-Lauth, Department of Biomedical Sciences, Colorado State University, 1683 Campus Delivery, Fort Collins, CO 80523, USA; email: angela.bosco-lauth@colostate.edu
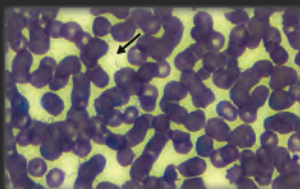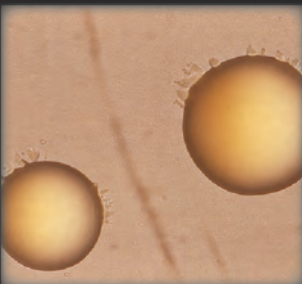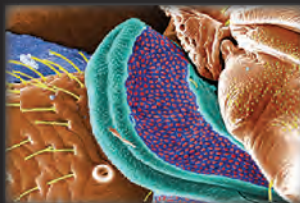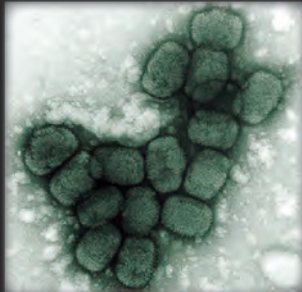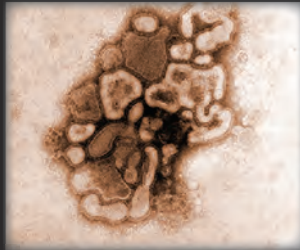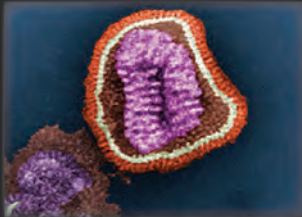
Effects of Patient Characteristics on Diagnostic Performance of Self-Collected Samples for SARS-CoV-2 Testing

Sarah E. Smith-Jeffcoat, Mitsuki Koh, Adam Hoffman, Paulina A. Rebolledo, Marcos C. Schechter, Halie K. Miller, Sadia Sleweon, Rebecca Rossetti, Vyjayanti Kasinathan, Talya Shragai, Kevin O'Laughlin, Catherine C. Espinosa, George M. Khalil, AdeSubomi O. Adeyemo, Anne Moorman, Brenda L. Bauman, Kahaliah Joseph, Michelle O'Hegarty, Nazia Kamal, Hany Atallah, Brooks L. Moore, Caitlin D. Bohannon, Bettina Bankamp, Claire Hartloge, Michael D. Bowen, Ashley Paulick, Amy S. Gargis, Christopher Elkins, Rebekah J. Stewart, Juliana da Silva, Caitlin Biedron, Jacqueline E. Tate, Yun F. Wang, Hannah L. Kirking, the CDC COVID-19 Response Team[1]

We evaluated the performance of self-collected anterior nasal swab (ANS) and saliva samples compared with healthcare worker–collected nasopharyngeal swab specimens used to test for severe acute respiratory syndrome coronavirus 2 (SARS-CoV-2). We used the same PCR diagnostic panel to test all self-collected and healthcare worker–collected samples from participants at a public hospital in Atlanta, Georgia, USA. Among 1,076 participants, 51.9% were men, 57.1% were ≥50 years of age, 81.2% were Black (non-Hispanic), and 74.9% reported ≥1 chronic medical condition. In total, 8.0% tested positive for SARS-CoV-2. Compared with nasopharyngeal swab samples, ANS samples had a sensitivity of 59% and saliva samples a sensitivity of 68%. Among participants tested 3–7 days after symptom onset, ANS samples had a sensitivity of 80% and saliva samples a sensitivity of 85%. Sensitivity varied by specimen type and patient characteristics. These findings can help physicians interpret PCR results for SARS-CoV-2.

Author affiliations: Centers for Disease Control and Prevention, Atlanta, Georgia, USA (S.E. Smith-Jeffcoat, M. Koh, H.K. Miller, S. Sleweon, R. Rossetti, T. Shragai, K. O'Laughlin, C.C. Espinosa, G.M. Khalil, A.O. Adeyemo, A. Moorman, B.L. Bauman, K. Joseph, M. O'Hegarty, N. Kamal, C.D. Bohannon, B. Bankamp, C. Hartlodge, M.D. Bowen, A. Paulick, A.S. Gargis, C. Elkins, R.J. Stewart, J. da Silva, C. Biedron, J.E. Tate, H.L. Kirking); Public Health Institute—CDC Global Health Fellowship Program, Atlanta (M. Koh); Emory University, Atlanta (A. Hoffman, P.A. Rebolledo, M.C. Schechter, V. Kasinathan, H. Atallah, B.L. Moore, Y.F. Wang); Grady Memorial Hospital, Atlanta (A. Hoffman, P.A. Rebolledo, M.C. Schechter, V. Kasinathan, H. Atallah, B.L. Moore, Y.F. Wang)

Detection of severe acute respiratory syndrome coronavirus 2 (SARS-CoV-2), the virus that causes coronavirus disease (COVID-19), originally relied mainly on nasopharyngeal swab (NPS) samples collected by healthcare workers (HCWs). However, NPS sample collection requires substantial amounts of time and personal protective equipment (PPE) that could be preferentially used for patient care. In light of >98 million confirmed COVID-19 cases globally as of January 27, 2021, relying solely on HCW-collected specimens for testing is not feasible (1). During the COVID-19 pandemic, many healthcare sites have experienced shortages of PPE and testing supplies. In addition, NPS sample collection often causes coughing or sneezing, which can generate infectious aerosols and thereby put the HCW at increased risk for exposure (2). Furthermore, NPS collection can cause discomfort and occasional nosebleeds, possibly affecting a patient's willingness to be retested. The use of self-collected saliva and anterior nasal swab (ANS) samples reduces HCW contact, limits need for PPE, and preserves transport media and other collection supplies needed for NPS samples.

Various upper respiratory specimen types, including saliva and oral swab samples, have demonstrated similar sensitivity to NPS samples in nucleic acid amplification tests for SARS-CoV-2 (3–6). However, most patients in these studies reported the recent onset of respiratory symptoms. Other investigations have shown that many infected persons, especially those who are young and otherwise healthy, are

asymptomatic or have mild symptoms (7–9). SARS-CoV-2 RNA has been detected in NPS samples nearly 2 months after initial detection; however, the performance of self-collected ANS and saliva samples of patients with prolonged viral shedding remains unclear (10,11). Understanding how these less invasive, self-collected specimens perform in a variety of contexts can inform testing strategies. We compared the diagnostic performance of self-collected ANS and saliva samples and HCW-collected NPS samples used in SARS-CoV-2–specific PCR by patient characteristics and symptom status.

Methods

We recruited patients from several inpatient and outpatient departments of Grady Memorial Hospital (Atlanta, GA, USA), where a high proportion of patients are uninsured (24%) or have Medicare/Medicaid insurance (57%) (12). Patients were eligible if their treating physician ordered collection of an NPS sample for SARS-CoV-2–specific reverse transcription PCR (RT-PCR) for any reason, including diagnostic (e.g., patients were symptomatic or exposed) or screening (e.g., preoperative requirement or before admission for non–COVID-19 reasons) purposes. Patients were excluded if they were unable to provide consent, declined consent, were <18 years of age, had a contraindicated NPS specimen (e.g., had a condition that prevented NPS sample collection), were unable to self-collect specimens, or had previously participated in this investigation. Trained interviewers used a standardized questionnaire to collect data on patient demographics, reason for visit, current and previous symptoms, and medical history (including previous SARS-CoV-2 testing). Each participant received a US $25 gift card.

During interviews, patients were given an infographic outlining steps for self-collection of saliva and ANS samples (Appendix Figure, https://wwwnc.cdc.gov/EID/article/27/8/21-0667-App1.pdf) (13). Patients self-collected raw (unenhanced) saliva in a 50-mL tube. Patients then inserted a miniature flocked-tip swab into 1 anterior naris, twirled the swab for 10 seconds, removed the swab and placed it directly into the other naris, and twirled it again for 10 seconds. Patients inserted the swab into 3 mL of viral transport media. After the interview and self-collection of specimens, a HCW collected an NPS sample from the participant and inserted the swab into 3 mL of viral transport media. Hospital laboratory staff conducted RT-PCR on the NPS sample on the same day; these results were used to inform clinical care and were not included in the performance analysis. NPS samples then were aliquoted and transferred to the Centers for Disease Control and Prevention (CDC) for RT-PCR. CDC staff extracted nucleic acid and tested samples using the CDC 2019-nCoV Real-Time Reverse Transcription PCR (rRT-PCR) Diagnostic Panel, which is selective for the SARS-CoV-2 nucleocapsid 1 (N1) and 2 (N2) genes, as per the Emergency Use Authorization Instructions for Use (14,15) (Appendix).

We entered and stored completed questionnaires and laboratory results in a REDCap version 10.0.8 (https://www.project-redcap.org) database hosted at CDC. We grouped patients according to COVID-19 symptom status: always asymptomatic participants reported no COVID-19 symptoms at specimen collection or in the previous 14 days; currently asymptomatic participants reported no COVID-19 symptoms at specimen collection but had symptoms in the previous 14 days; and currently symptomatic participants reported COVID-19 symptoms at specimen collection. We categorized symptoms according to previously defined case definitions (16–18) (Appendix). We calculated sample size using a 1-sided, 1-sample proportions test with a continuity correction to determine whether sensitivity of self-collected samples was $\geq$90% compared with HCW-collected NPS samples, assuming that NPS samples had a true sensitivity of 98% (3). Using $\alpha = 0.05$, 80% power, and 5% NPS percent positivity, we calculated the minimum sample size to be 920 and the required number of positive self-collected specimens to be 46.

We compiled demographic and clinical characteristics for patients according to the results of their NPS samples. To analyze the benefit of using both self-collected ANS and saliva specimens for diagnosis, we merged each patient's ANS and swab sample results to create a self-collected combination result. If $\geq$1 self-collected specimen was positive, we marked that patient's self-collected combination result as positive. If neither was positive and $\geq$1 was negative, then we marked that patient's self-collected combination result as negative. We calculated sensitivity, specificity, positive predictive value (PPV), and negative predictive value (NPV) of ANS, saliva, and self-collected combination samples compared with NPS samples for all patients who had a definitive (i.e., positive or negative) NPS result and $\geq$1 self-collected specimen. Because NPS samples do not show all SARS-CoV-2 infections, we reran the sensitivity analysis with a combined variable for any positive result from ANS, saliva, or NPS samples as the comparator. We compiled proportions of concordant and discordant results for each self-collected and HCW-collected sample and calculated Cohen's κ

coefficient to compare result agreement by specimen type. We calculated the sensitivity of self-collected specimens by patient characteristics and determined significant differences using a 1-sample, 2-sided test of proportions (p<0.05). We used the Pearson correlation coefficient to compare the cycle threshold (C_t) values of positive self-collected and HCW-collected specimens; we used the Mann-Whitney U test to compare the C_t values of NPS samples by patient characteristic. We analyzed the data in R version 4.0.2 (The R Project for Statistical Computing, https://www.r-project.org).

This investigation was reviewed by CDC and conducted in accordance with applicable federal law and CDC policy (e.g., 45 C.F.R. part 46, 21 C.F.R. part 56, 42 U.S.C.; 241(d); 5 U.S.C. 552a; 44 U.S.C. 3501 et seq.). This investigation was determined to be an exempt public health activity by the Emory University Institutional Review Board and Grady Memorial Hospital Research Oversight Committee.

Results

During August 31–November 23, 2020, a total of 1,096 patients consented to and enrolled in the study; 20 were excluded because they did not meet inclusion criteria (Figure 1). Among 1,076 participants, overall positivity of any specimen was 8.0%; NPS samples had 7.4% positivity, ANS samples had 4.4% positivity, and saliva samples had 4.8% positivity. Among the 1,076 participants, 51.9% (559) were men, 57.1% (614) were ≥50 years of age, 81.2% (874) were Black (non-Hispanic), and 74.9% (806) had ≥1 chronic medical condition (Table 1). Most (80.0%; 861) participants were enrolled in the emergency department: nearly half sought care for a COVID-19–related concern (18.2%; 196) or had a chief complaint including COVID-19–like symptoms (30.6%; 329). Over half (56.7%; 610) of participants had ≥1 current COVID-19 symptom; among currently symptomatic participants, 68.9% (420) reported symptom onset ≤1 week previously.
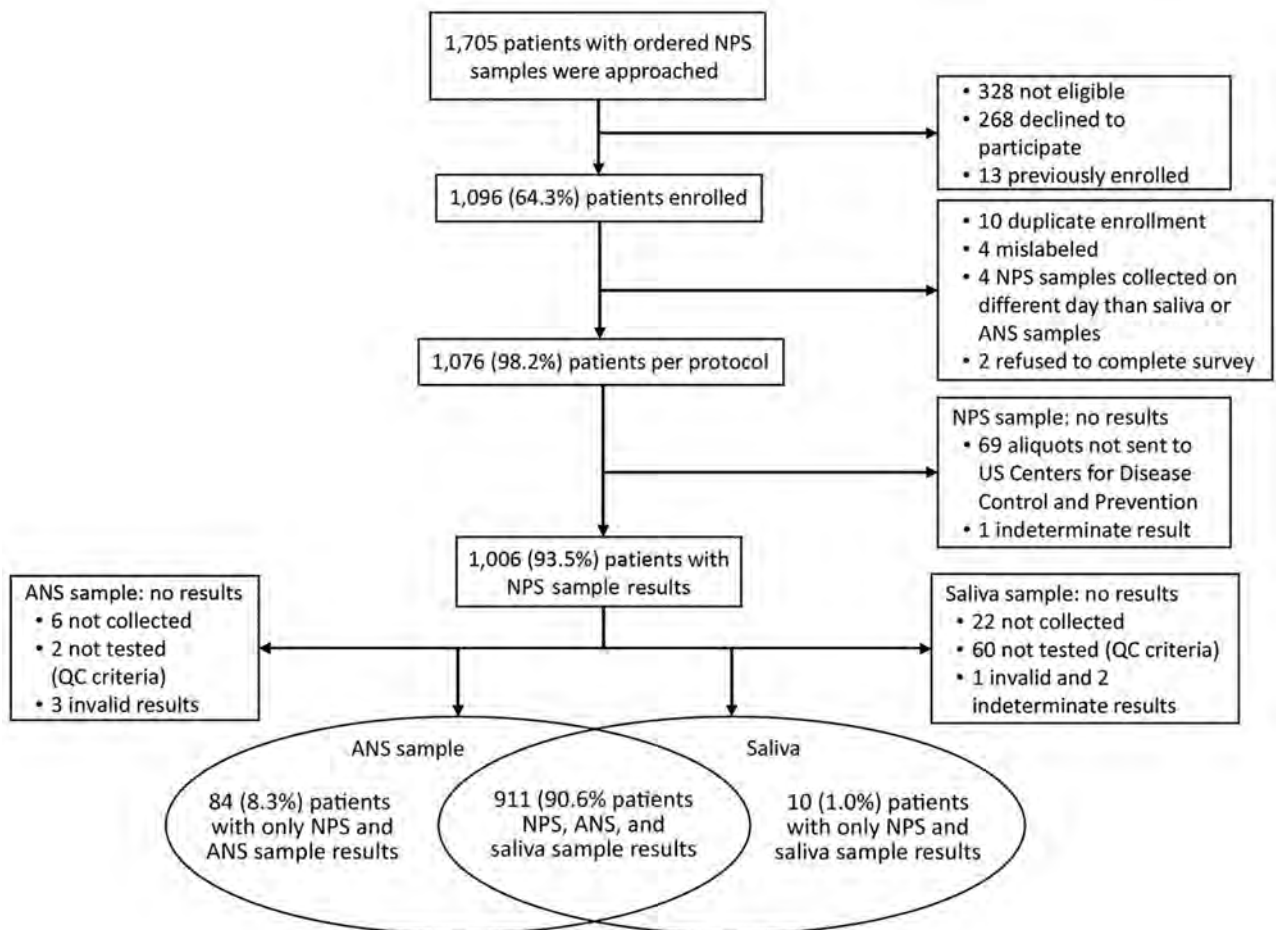

Figure 1. Flowchart of patient enrollment and sample results for investigation of the effects of patient characteristics on self-collected and healthcare worker–collected samples for severe acute respiratory syndrome coronavirus 2 testing, Atlanta, Georgia, USA. ANS, anterior nasal swab; NPS, nasopharyngeal swab; QC, quality control.

Most (93.5%; 1,006) participants provided an NPS sample, of which 8.0% (80/1,006) tested positive for SARS-CoV-2. A total of 911 participants had an RT-PCR result for all 3 specimens (i.e., saliva, ANS, and NPS samples), 10 participants had results for only saliva and NPS samples, and 84 participants had results for only ANS and NPS samples (Figure 1).

Performance of Self-Collected Sample Types

Among 995 participants who provided ANS and NPS samples that produced definitive results, 963 (96.8%) had concordant results (κ = 0.73, 95% CI 0.64–0.82). Compared with NPS samples, ANS samples had 59% sensitivity (95% CI 47%–70%), 100% specificity (95% CI 100%–100%), 100% PPV (95% CI 92%–100%), and 97% NPV (95% CI 95%–98%). Among 921 participants who provided saliva and NPS samples that produced definitive results, 894 (97.1%) had concordant results (κ = 0.76, 95% CI 0.67–0.85). Compared with NPS samples, saliva had 68% sensitivity (95% CI 55%–78%), 99% specificity (95% CI 99%–100%), 90% PPV (95% CI 79%–97%), and 97% NPV (95% CI 96%–98%).

To understand the benefit of using both self-collected specimens for diagnosis, we analyzed data from 1,005 participants who had definitive results for >1 self-collected specimen. We found that 977 (97.2%) had concordant results between the self-collected combination and NPS samples (κ = 0.79, 95% CI 0.71–0.86). Using NPS as the comparator, we found self-collected combination samples had 71% sensitivity (95% CI 60%–81%), 99% specificity (95% CI 99%–100%), 92% PPV (95% CI 82%–97%), and 98% NPV (95% CI 96%–98%). When any positive was used as the comparator, we observed little change in the overall findings: the overall sensitivity of the ANS swab sample decreased slightly, the sensitivity of saliva samples increased slightly, and sensitivity of self-collected combination samples increased slightly (Appendix Table 1).

Sensitivity by Patient Characteristics and Symptoms

Saliva and self-collected combination samples had higher overall sensitivities than ANS samples; this pattern was reflected among men, participants 18–29 years of age and 50–59 years of age, and Black (non-Hispanic) participants (Table 2). Among Hispanic/ Latinx participants, sensitivity was significantly lower for saliva and self-collected combination samples. Sensitivity was higher among those not reporting any chronic medical conditions, whose reason for hospital visit was a COVID-19–related concern or whose chief complaint included COVID-19–like symptoms, who

reported close contact to a COVID-19 patient during the previous ≤14 days, and who did not report a previous positive COVID-19 test. Sensitivity was lower among participants who reported a previous positive COVID-19 test (Table 2).

Sensitivity was higher among samples from currently symptomatic participants (62% for ANS, 72% for saliva, and 76% for self-collected combination) and was highest among samples from participants who provided samples 3–7 days after symptom onset (80% for ANS, 85% for saliva, and 88% for self-collected combination); these differences were statistically significant for ANS and self-collected combination samples (p<0.05). Sensitivity was higher for most individual symptoms, but highest among participants reporting measured fever, congestion or runny nose, new loss of smell, new loss of taste, cough, or subjective fever. Similarly, sensitivity was higher among participants who met most symptom case definitions, but highest among patients who had influenza-like illness, COVID-19–like symptoms, or upper respiratory symptoms accompanied by loss of smell or taste. Sensitivity was lower among patients with nonconstitutional symptoms (Table 2).

C_t Values

Among 46 participants with positive ANS and NPS samples, 85% (for PCR target N1) and 78% (for PCR target N2) had an ANS sample with a higher C_t value than that of its paired NPS sample (Figure 2, panels A, B). We observed a moderate positive correlation between the C_t values of ANS and NPS samples (r = 0.75 for N1, r = 0.71 for N2); both targets had median NPS C_t values of 22.8 (range 14.6–34.1 for N1, 14.7–35.0 for N2). Among 46 participants with positive saliva and NPS samples, 57% (N1) and 59% (N2) had a saliva sample with a higher C_t value than that of its paired NPS sample (Figure 2, panels C, D). We observed a low positive correlation between the C_t values of saliva and NPS samples (r = 0.53 for both N1 and N2); targets had median NPS C_t values of 23.1 (range 14.6–38.3) for N1 and 23.8 (range 14.7–37.7) for N2. When limiting the analysis to the 72 participants who had 3 definitive and ≥1 positive result, C_t values were lowest when all paired specimens were SARS-CoV-2–positive; for N1, the median C_t values were 27.2 for ANS, 24.9 for saliva, and 22.6 for NPS samples (Figure 3). When ≤2 specimens were positive, all specimens had median C_t values >30. Participants who did not have COVID-19 symptoms had higher median NPS C_t values (33.5 for N1, 34.4 for N2) than did those who reported ≥1 COVID-19 symptom (25.6 for N1, p = 0.03; 26.9 for N2, p = 0.03). Among those
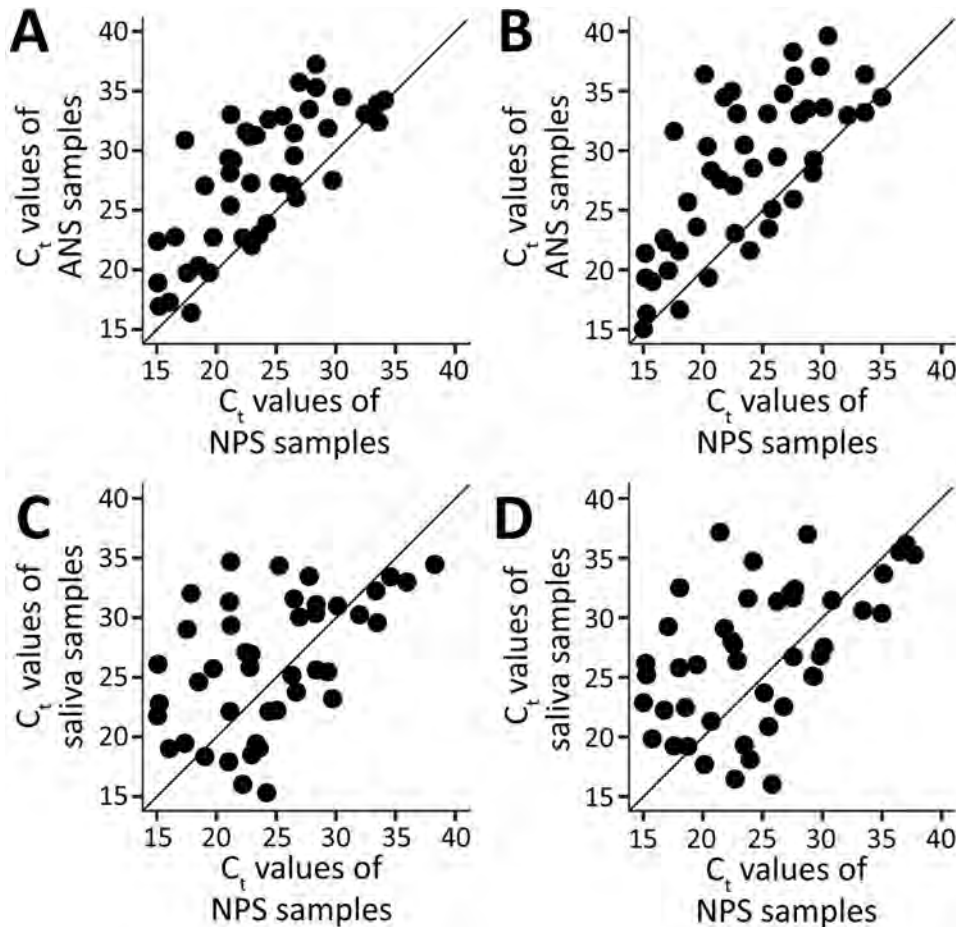
Figure 2. C_t values of self-collected and healthcare worker–collected samples for severe acute respiratory syndrome coronavirus 2 testing, Atlanta, Georgia, USA. PCR completed using CDC 2019-nCoV Real-Time Reverse Transcriptase PCR Diagnostic Panel (*15*). A) ANS and NPS samples at PCR target N1. B) ANS and NPS samples at PCR target N2. C) NPS and saliva samples at PCR target N1. D) NPS and saliva samples at PCR target N2. ANS, anterior nasal swab; C_t, cycle threshold; NPS, nasopharyngeal swab.

reporting COVID-19 symptoms, participants who had symptom onset ≤1 week before testing had the lowest median NPS C_t values (23.5 vs. 30.8 for N1, p<0.01; 24.2 vs. 33.3 for N2, p<0.01).

Discussion

In this investigation, we found that self-collected saliva samples had a higher sensitivity than self-collected ANS samples (68% vs. 59%) compared with HCW-collected NPS samples. However, each sample type had lower sensitivity than suggested by most previously published data (*3,6,19–21*). The self-collected combination had a higher sensitivity (71%) than NPS samples. We found that the sensitivity of self-collected samples (separately and in combination) differed according to patient characteristics. The presence of COVID-19 symptoms at time of specimen collection and the time since symptom onset affected sensitivity. We also noted differences in sensitivity across demographic groups, possibly reflecting differences in access to care or care-seeking behavior rather than differences in viral shedding. Our results illustrate that certain patient characteristics are associated

with the sensitivity of self-collected specimens used for RT-PCR.

We found lower sensitivities for saliva and ANS samples than those for most other published studies, including 2 recent meta-analyses that found saliva samples to have sensitivities of 83.2% and 86.9% (*21,22*). Many studies showing high sensitivity of self-collected specimens enrolled symptomatic patients who were recently hospitalized for confirmed CO-VID-19 or whose symptom onset was ≤1 week before sample collection (*3,4*). A strength of our investigation was that we included symptomatic and asymptomatic patients being tested for SARS-CoV-2 for screening and diagnostic purposes. Because a substantial proportion of patients infected with SARS-CoV-2 have asymptomatic or mild illness, physicians must be able to analyze results in the context of test sensitivity in patients with few or no symptoms. Sample sensitivity was highest among participants reporting symptom onset 3–7 days before sample collection. Similarly, another study found that the sensitivity of saliva samples was highest (95%) among symptomatic patients tested ≤1 week after symptom onset and lowest

(50%) among patients tested >1 week after symptom onset (*23*). The sample sensitivity differences among patients with different demographic characteristics might reflect differences in access to care or healthcare-seeking behavior. Delayed access to care might postpone specimen collection, decreasing the sensitivity of the samples. For example, Hispanic/Latinx participants who had a positive NPS sample had longer symptom duration compared with participants of other race/ethnicity categories (data not shown).

Using 2 self-collected specimens could increase overall test sensitivity, which reached 88% among participants whose symptoms began 3–7 days before sample collection. Similarly, Tan et al. (*24*) found that combining self-collected oropharynx and midturbinate swab and saliva results increased test sensitivity. Using multiple noninvasive specimens might improve SARS-CoV-2 detection in persons tested ≤1 week after symptom onset and reduce demand for PPE and HCW exposure. However, testing multiple specimens might put additional strain on laboratory systems that are already overburdened. Pooling self-collected specimens before testing might alleviate some of this additional strain on laboratories, but this practice should be investigated further for accuracy.

Similar to other studies, we found that most NPS samples had lower C_t values than did their paired saliva and ANS samples (*4,25,26*). We also found that median C_t values were lowest when all 3 specimens were SARS-CoV-2–positive; the median C_t value increased to >30 when ≤2 specimens were positive (Figure 3). The lower sensitivity in this investigation might be due to high C_t value discordant specimens, which can occur as infection subsides. We also found slightly higher overall median C_t values for NPS samples than reported in similar studies (*5,27*). However, many of these previous studies were implemented earlier in the pandemic when previous infection or exposure was less common. Our investigation began after the first 2 peaks in Atlanta; by the end of enrollment, Atlanta was entering its third peak. When the C_t value of the NPS sample is high, discordance with the self-collected specimens also could increase. Salvatore et al. (*28*) found that C_t values for NPS samples were lowest ≤1 week after symptom onset. Furthermore, Wolfel et al. (*29*) found viral subgenomic mRNA in throat swab specimens collected <5 days after symptom onset and in sputum samples taken 4–11 days after symptom onset, indicating active infection. Although C_t values are not directly correlated with viral load, they provide a semiquantitative assessment of viral RNA concentration.
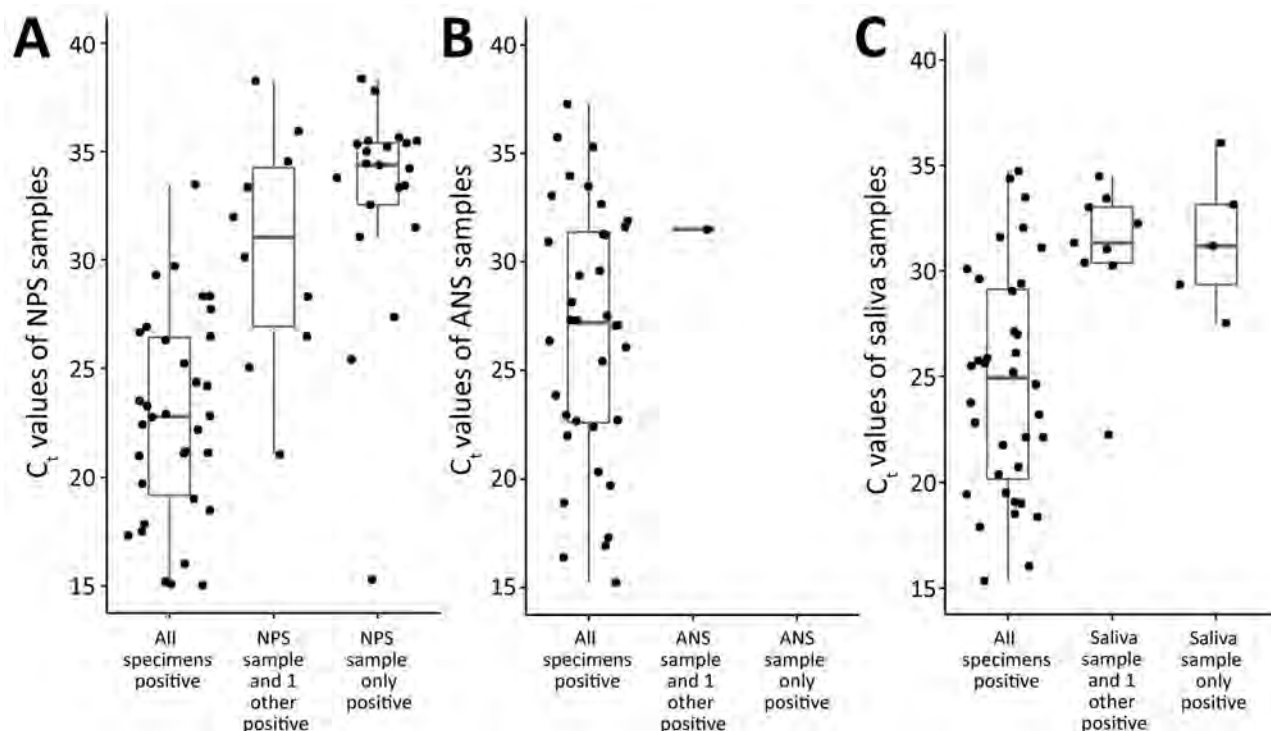
Figure 3. C_t values of self-collected and healthcare worker–collected samples for N1 target of severe acute respiratory syndrome coronavirus 2 PCR, Atlanta, Georgia, USA. PCR completed using CDC 2019-nCoV Real-Time Reverse Transcriptase PCR Diagnostic Panel (*15*). Horizontal lines within boxes indicate medians; box tops and bottoms indicate 25th and 75th percentiles; whiskers indicate the range. ANS, anterior nasal swab; C_t, cycle threshold; NPS, nasopharyngeal swab.

Specimen collection method might also affect sensitivity. Procop et al. (5) compared NPS and enhanced saliva samples (i.e., self-collected nasal secretions or mucus, phlegm, and saliva stored in a single tube) and found 100% positive agreement and 99.4% negative agreement. This method of saliva collection provides a mixture of upper and lower respiratory secretions, thereby enabling detection for a longer time after symptom onset. We used general spitting for saliva collection, which has the lowest sensitivity estimate in comparison with other saliva collection methods (22). General spitting does not require special devices or transport media, enabling our methods and results to be broadly applicable. The duration and pressure applied while swabbing the anterior nares also might affect ANS sample quality. The sequence of specimen collection, which was not always clear from published studies, could also affect sensitivity (19). In our investigation, saliva and ANS samples were collected before NPS samples. Collecting ANS samples after NPS samples could displace virus from nasopharyngeal tissue or midturbinate before the swab leaves the nares, thereby biasing self-collected ANS toward higher sensitivity.

The first limitation of our study is that because we used a cross-sectional design, we did not have information on whether patients were asymptomatic or presymptomatic at specimen collection; we also did not have data on disease severity. In presymptomatic patients, samples might have been collected too early to detect viral RNA in some or all specimen types. Second, we lacked the statistical power to detect significant differences in sensitivity by most variables because the initial sample size calculation assumed self-collected specimens to have $\geq$90% sensitivity. Third, all responses were self-reported and could have been affected by recall bias. Fourth, the CDC 2019-nCoV rRT-PCR Diagnostic Panel has a higher limit of detection than many commercially available, high-throughput assays (30), limiting our ability to detect lower concentrations of viral RNA. However, the clinical and public health utility of detecting these lower concentrations is unknown. Fifth, the CDC 2019-nCoV rRT-PCR Diagnostic Panel does not currently include saliva; instead, the assay was designed for qualitative detection of nucleic acid from SARS-CoV-2. Of 1,006 NPS samples, 64 aliquots did not meet storage requirements approved under the assay's instructions for use (samples should be stored at 4°C for $\leq$72 hours after collection) (15). Because some samples were stored for longer than recommended, viral RNA degradation might have affected the

assay's performance. Because the CDC RT-PCR results were not used for clinical care, excluding these specimens did not change sensitivity; furthermore, CDC RT-PCR results were in concordance with the hospital's RT-PCR results (data not shown). As a result, we decided to include these specimens in the analysis (Appendix). Our findings might not be generalizable to other assays or techniques. Sixth, heterogenous self-collection coaching techniques might have introduced differences in the quality of samples collected under the guidance of different interviewers. Finally, PCR does not indicate whether active replication is occurring. Therefore, we are unable to determine whether patients with positive NPS samples but negative saliva or ANS samples have older infections or if the self-collected specimens are less sensitive than NPS samples. Additional laboratory testing is required to clarify the viability of different specimen types and how viability affects clinical presentation and transmissibility. Our study highlights that the sensitivities of saliva and ANS samples are different than that of NPS samples. These findings show that physicians should consider the patient's clinical history, exposures, and time of symptom onset when interpreting PCR results.

Overall, the sensitivities of ANS and saliva samples were lower than that of NPS samples from patients being tested for SARS-CoV-2 for diagnostic and screening purposes. The sample sensitivity was highest among participants with symptom onset within 3–7 days of specimen collection, especially when the reason for the patient visit was COVID-19–related, and those not reporting a previous positive test. Encouraging persons to seek testing within a week of symptom onset could increase the accuracy and usefulness of self-collected specimens used for diagnosing SARS-CoV-2 infections. It is important that clinicians are aware of how differences in patient characteristics and specimen type can affect test sensitivity. Testing programs and clinical settings might consider patient characteristics, previous test results, and timing of symptom onset when determining which specimen types to use.

About the Author
Ms. Smith-Jeffcoat is an epidemiologist with the Respiratory Viruses Branch, Division of Viral Diseases, National Center for Immunization and Respiratory Diseases, Centers for Disease Control and Prevention, Atlanta, Georgia, USA. Her research interests include respiratory disease epidemiology and global tuberculosis epidemiology, especially drug-resistant tuberculosis.

References
1. World Health Organization. COVID-19 weekly epidemiological update—27 January 2021. 2021 Jan 27 [cited 2021 Feb 9]. https://www.who.int/publications/m/item/weekly-epidemiological-update---27-january-2021
2. Centers for Disease Control and Prevention. Interim guidelines for collecting, handling, and testing clinical specimens for COVID-19. 2021 [cited 2021 Jan 29]. https://www.cdc.gov/coronavirus/2019-ncov/lab/guidelines-clinical-specimens.html
3. Tu Y-P, Jennings R, Hart B, Cangelosi GA, Wood RC, Wehber K, et al. Swabs collected by patients or health care workers for SARS-CoV-2 testing. N Engl J Med. 2020;383:494–6. https://doi.org/10.1056/NEJMc2016321
4. McCormick-Baw C, Morgan K, Gaffney D, Cazares Y, Jaworski K, Byrd A, et al. Saliva as an alternate specimen source for detection of SARS-CoV-2 in symptomatic patients using Cepheid Xpert Xpress SARS-CoV-2. J Clin Microbiol. 2020;58:e01109–20. https://doi.org/10.1128/JCM.01109-20
5. Procop GW, Shrestha NK, Vogel S, Van Sickle K, Harrington S, Rhoads DD, et al. A direct comparison of enhanced saliva to nasopharyngeal swab for the detection of SARS-CoV-2 in symptomatic patients. J Clin Microbiol. 2020;58:e01946–20. https://doi.org/10.1128/JCM.01946-20
6. Hanson KE, Barker AP, Hillyard DR, Gilmore N, Barrett JW, Orlandi RR, et al. Self-collected anterior nasal and saliva specimens versus health care worker-collected nasopharyngeal swabs for the molecular detection of SARS-CoV-2. J Clin Microbiol. 2020;58:e01824–20. https://doi.org/10.1128/JCM.01824-20
7. Payne DC, Smith-Jeffcoat SE, Nowak G, Chukwuma U, Geibe JR, Hawkins RJ, et al.; CDC COVID-19 Surge Laboratory Group. SARS-CoV-2 infections and serologic responses from a sample of U.S. Navy service members—USS Theodore Roosevelt, April 2020. MMWR Morb Mortal Wkly Rep. 2020;69:714–21. https://doi.org/10.15585/mmwr.mm6923e4
8. Yousaf AR, Duca LM, Chu V, Reses HE, Fajans M, Rabold EM, et al. A prospective cohort study in nonhospitalized household contacts with severe acute respiratory syndrome coronavirus 2 infection: symptom profiles and symptom change over time. Clin Infect Dis. 2020 Jul 28 [Epub ahead of print]. https://doi.org/10.1093/cid/ciaa1072
9. Buitrago-Garcia D, Egli-Gany D, Counotte MJ, Hossmann S, Imeri H, Ipekci AM, et al. Occurrence and transmission potential of asymptomatic and presymptomatic SARS-CoV-2 infections: a living systematic review and meta-analysis. PLoS Med. 2020;17:e1003346. https://doi.org/10.1371/journal.pmed.1003346
10. Sun J, Xiao J, Sun R, Tang X, Liang C, Lin H, et al. Prolonged persistence of SARS-CoV-2 RNA in body fluids. Emerg Infect Dis. 2020;26:1834–8. PubMed https://doi.org/10.3201/eid2608.201097
11. COVID-19 Investigation Team. Clinical and virologic characteristics of the first 12 patients with coronavirus disease 2019 (COVID-19) in the United States. Nat Med. 2020;26:861–8. PubMed https://doi.org/10.1038/s41591-020-0877-5
12. Grady Health System. Grady fast facts. 2018 [cited 2021 Jan 29]. https://www.gradyhealth.org/wp-content/uploads/2018/07/Grady_Fast_Facts.pdf
13. Centers for Disease Control and Prevention. How to collect your anterior nasal swab sample for COVID-19 testing. 2020 [cited 2021 Feb 12]. https://www.cdc.gov/coronavirus/2019-ncov/testing/How-To-Collect-Anterior-Nasal-Specimen-for-COVID-19.pdf
14. Lu X, Wang L, Sakthivel SK, Whitaker B, Murray J, Kamili S, et al. US CDC real-time reverse transcription PCR panel for detection of severe acute respiratory syndrome coronavirus 2. Emerg Infect Dis. 2020;26:1654–65. https://doi.org/10.3201/eid2608.201246
15. United States Food and Drug Administration. Emergency use authorization: CDC 2019-nCoV Real-Time RT-PCR Diagnostic Panel. 2020 [cited 2021 Mar 2]. https://www.fda.gov/media/134919/download

16. Boehmer TK, DeVies J, Caruso E, van Santen KL, Tang S, Black CL, et al. Changing age distribution of the COVID-19 pandemic—United States, May–August 2020. MMWR Morb Mortal Wkly Rep. 2020;69:1404–9. https://doi.org/10.15585/mmwr.mm6939e1

17. Council of State and Territorial Epidemiologists. Update to the standardized surveillance case definition and national notification for 2019 novel coronavirus disease (COVID-19). 2020 [cited 2021 Jan 29]. https://cdn.ymaws.com/www.cste.org/resource/resmgr/ps/positionstatement2020/Interim-20-ID-02_COVID-19.pdf

18. World Health Organization. RSV surveillance case definitions. 2020 [cited 2021 January 29]; https://www.who.int/influenza/rsv/rsv_case_definition/en

19. Altamirano J, Govindarajan P, Blomkalns AL, Kushner LE, Stevens BA, Pinsky BA, et al. Assessment of sensitivity and specificity of patient-collected lower nasal specimens for severe acute respiratory syndrome coronavirus 2 testing [Erratum in: JAMA Netw Open. 2020;3: e2014910]. JAMA Netw Open. 2020;3:e2012005. https://doi.org/10.1001/jamanetworkopen.2020.12005

20. Kojima N, Turner F, Slepnev V, Bacelar A, Deming L, Kodeboyina S, et al. Self-collected oral fluid and nasal swabs demonstrate comparable sensitivity to clinician-collected nasopharyngeal swabs for the detection of SARS-CoV-2. Clin Infect Dis. 2020 Oct 19 [Epub ahead of print]. https://doi.org/10.1093/cid/ciaa1589

21. Butler-Laporte G, Lawandi A, Schiller I, Yao M, Dendukuri N, McDonald EG, et al. Comparison of saliva and nasopharyngeal swab nucleic acid amplification testing for detection of SARS-CoV-2: a systematic review and meta-analysis. JAMA Intern Med. 2021;181:353–60. https://doi.org/10.1001/jamainternmed.2020.8876

22. Bastos ML, Perlman-Arrow S, Menzies D, Campbell JR. The sensitivity and costs of testing for SARS-CoV-2 infection with saliva versus nasopharyngeal swabs: a systematic review and meta-analysis. Ann Intern Med. 2021;174:501–10. https://doi.org/10.7326/M20-6569

23. Migueres M, Mengelle C, Dimeglio C, Didier A, Alvarez M, Delobel P, et al. Saliva sampling for diagnosing SARS-CoV-2 infections in symptomatic patients and asymptomatic carriers. J Clin Virol. 2020;130:104580. https://doi.org/10.1016/j.jcv.2020.104580

24. Tan SY, Tey HL, Lim ETH, Toh ST, Chan YH, Tan PT, et al. The accuracy of healthcare worker versus self collected (2-in-1) oropharyngeal and bilateral mid-turbinate (OPMT) swabs and saliva samples for SARS-CoV-2. PLoS One. 2020;15:e0244417. https://doi.org/10.1371/journal.pone.0244417

25. Landry ML, Criscuolo J, Peaper DR. Challenges in use of saliva for detection of SARS CoV-2 RNA in symptomatic outpatients. J Clin Virol. 2020;130:104567. https://doi.org/10.1016/j.jcv.2020.104567

26. Van Vinh Chau N, Lam VT, Dung NT, Yen LM, Minh NNQ, Hung LM, et al.; Oxford University Clinical Research Unit COVID-19 Research Group. The natural history and transmission potential of asymptomatic severe acute respiratory syndrome coronavirus 2 infection. Clin Infect Dis. 2020;71:2679–87. https://doi.org/10.1093/cid/ciaa711

27. Williams E, Bond K, Zhang B, Putland M, Williamson DA. Saliva as a noninvasive specimen for detection of SARS-CoV-2. J Clin Microbiol. 2020;58:e00776–20. https://doi.org/10.1128/JCM.00776-20

28. Salvatore PP, Dawson P, Wadhwa A, Rabold EM, Buono S, Dietrich EA, et al. Epidemiological correlates of polymerase chain reaction cycle threshold values in the detection of SARS-CoV-2. Clin Infect Dis. 2020;72:e761–7. https://doi.org/10.1093/cid/ciaa1469

29. Wölfel R, Corman VM, Guggemos W, Seilmaier M, Zange S, Müller MA, et al. Virological assessment of hospitalized patients with COVID-2019 [Erratum in: Nature. 2020; 588:E35]. Nature. 2020;581:465–9. https://doi.org/10.1038/s41586-020-2196-x

30. Food and Drug Administration. Individual EUAs for molecular diagnostic tests for SARS-CoV-2. 2021 [cited 2021 Feb 2]. https://www.fda.gov/medical-devices/coronavirus-disease-2019-covid-19-emergency-use-authorizations-medical-devices/vitro-diagnostics-euas#individual-molecular

Address for correspondence: Sarah E. Smith-Jeffcoat, Centers for Disease Control and Prevention, 1600 Clifton Road NE, Mailstop H24-5, Atlanta, GA 30329-4027, USA; email: uyi7@cdc.gov

Fungemia and other Fungal Infections Associated with Use of *Saccharomyces boulardii* Probiotic Supplements

Juha Rannikko, Ville Holmberg, Matti Karppelin, Pertti Arvola, Reetta Huttunen, Eero Mattila, Niina Kerttula, Teija Puhto, Ülle Tamm, Irma Koivula, Risto Vuento, Jaana Syrjänen, Ulla Hohenthal

Author affiliations: Tampere University, Tampere, Finland (J. Rannikko); Tampere University Hospital, Tampere (J. Rannikko, M. Karppelin, P. Arvola, R. Huttunen, J. Syrjänen); University of Helsinki, Helsinki, Finland (V. Holmberg); Helsinki University Hospital, Helsinki (V. Holmberg, E. Mattila); Oulu University Hospital, Oulu, Finland (N. Kerttula, T. Puhto); Kuopio University Hospital; Kuopio Finland (Ü. Tamm, I. Koivula); Fimlab Laboratories, Tampere (R. Vuento); Turku University Hospital, Turku, Finland (U. Hohenthal)

Because of widespread use of probiotics, their safety must be guaranteed. We assessed use of *Saccharomyces boulardii* probiotic yeast from medical records for patients who had *Saccharomyces* fungemia or other clinical *Saccharomyces* culture findings. We evaluated all *Saccharomyces* sp. findings at 5 university hospitals in Finland during 2009–2018. We found 46 patients who had *Saccharomyces* fungemia; at least 20 (43%) were using *S. boulardii* probiotic. Compared with a control group that had bacteremia or candidemia, the odds ratio for use of an *S. boulardii* probiotic was 14 (95% CI 4–44). Of 1,153 nonblood culture findings, the history for 125 patients was checked; at least 24 (19%) were using the probiotic (odds ratio 10, 95% CI 3–32). This study adds to published fungemia cases linked to use of *S. boulardii* probiotic and sheds light on the scale of nonblood *Saccharomyces* culture findings that are also linked to use of this probiotic.

Probiotics are live microorganisms intended to provide health benefits when consumed (*1*). Typically, the endpoint in randomized controlled trials of probiotics has been the prevention of diarrhea or faster alleviation of diarrhea symptoms (*2*). Regarding their safety, serious adverse effects have been rare in probiotic studies (*3*). However, the adverse effects have not been fully reported (*4*). In 1 trial in which a multispecies probiotic preparation was given to patients who had severe acute pancreatitis, the mortality rate was higher in the probiotic arm (*5*). Nevertheless, the use of probiotics is common. According to the 2012 National Health Interview Survey in the United States, 1.6% of adults had used prebiotics or probiotics in the preceding 30 days (*6*).

Saccharomyces cerevisiae var. *boulardii* is a yeast that is used as a probiotic. In hospitals in the United States, the use of *S. cerevisiae* var. *boulardii* has been common, especially among elderly patients (*7*). This strain is difficult to distinguish microbiologically from *S. cerevisiae* because they have >99% genomic relatedness (*8*). Thus, in everyday clinical laboratory work, the *S. cerevisiae* var. *boulardii* strain is identified as either *Saccharomyces* sp. or *S. cerevisiae*. A review from 2005 considered *S. cerevisiae* var. *boulardii* to be the etiologic agent of *Saccharomyces* fungemia if the patient received treatment with a probiotic containing *S. cerevisiae* var. *boulardii* or if a molecular typing method confirmed the identification of this yeast (*9*). The authors found 37 cases in the literature. We found an additional 14 reports, including 22 cases of *Saccharomyces* fungemia with the same diagnostic method published after this review (*10–23*). Thus, before our study, 59 cases of fungemia with a link to the use of the probiotic had been published. All of these cases have been either individual cases or small cases series (<7 cases) without any systematic approach to quantify the problem.

Furthermore, besides fungemia, there are few reports on other clinically relevant microbiological findings for this yeast (i.e., in abscesses, ascites fluid, or the pleural cavity). The meta-analysis we mention listed 20 cases of findings other than fungemia (*9*). These findings are useful because they might also lead to a change in antimicrobial treatment.

We conducted a retrospective registry study (case series) at 5 university hospitals in Finland to evaluate the use of the *S. cerevisiae* var. *boulardii* probiotic in patients who had *Saccharomyces* fungemia or another clinical culture finding for this yeast. To evaluate the association between probiotic use and subsequent findings, we compared use of *S. cerevisiae* var. *boulardii* for patients who had a *Saccharomyces* infection with use of *S. cerevisiae* var. *boulardii* for patients who had an infection caused by another etiologic agent, such as bacteria or *Candida* sp.

Methods

Background

Finland has 5 university hospitals that are secondary referral centers of their catchment areas and tertiary referral centers for other hospital districts. Their combined catchment areas cover more than half population of Finland (3.29 million of 5.6 million persons). All university hospitals use the same register (SAI-registry; Neotide Ltd, https://www.neotide.fi), in which the local clinical microbial laboratory data are collected. These data cover all blood culture data and most of all other clinical microbial culture data of the catchment area of the university hospital.

Patient Data

At least 1 infectious diseases specialist in every university hospital collected the clinical data from the medical records for all blood culture-positive cases found in the register that were identified as *Saccharomyces* sp. or *S. cerevisiae*. The use of the *S. cerevisiae* var. *boulardii* probiotic was defined as use at the time of the positive culture or in the preceding 7 days. Data were collected on use during the preceding 3 months. If the medical record was not available, the case-patient was classified as not using a probiotic. The Quick SOFA score and the definition of septic shock were based on the Sepsis–3 definitions (*24*). The McCabe score was determined as reported by McCabe and Jackson (*25*). Data collected for case-patients who had nonblood cultures were age, sex,

malignancy, digestive tract disease, use of probiotics, use of antifungal medication at the time of the culture, and possible change of medication resulting from finding of *Saccharomyces* sp. The most recent 25 cases of nonblood culture findings in each hospital district were evaluated (excluding case-patients who had positive fecal samples). Isolates were obtained from routine laboratory bacterial and fungal cultures. The anatomic site of the culture was collected from the local hospital microbial registry (SAI) for all culture-positive cases. Abdominal sites were those in which culture was taken from, for example, ascites fluid, a biliary drainage catheter, or abscess drainage fluid, but not from skin or wound secretions. Oral and respiratory tract samples were from sinus drainage, bronchial lavage cultures, and pleural drainage. Other sites included samples from perianal abscesses, mediastinum, and urine.

Control Group

To evaluate the practice of probiotic use in the hospital ward in which the patient who had a *Saccharomyces* finding was given treatment, a control group was obtained from the same SAI register. For every *Saccharomyces* fungemia case-patient, 2 blood culture-positive patients (1 chronologically closest before and 1 after) from the same ward as the case were selected. For every clinical culture sample (other than blood), there was 1 chronologically closest positive culture sample from the same ward as the case-patient who served as a control. Data collected for the controls were date, ward, microbe, age, sex, malignancy, digestive tract disease, and *S. cerevisiae var. boulardii* probiotic use at the time of the positive culture or in the previous 3 months.

Statistical Analysis

We used SPSS version 22.0 software (IBM Corp., https://www.ibm.com) for statistical analyses. The study was centrally approved by the Ethics Committee of Tampere University Hospital, Tampere, Finland. The requirement for informed consent was waived.

Results

Blood Cultures

There were 46 patients with a positive blood culture for *Saccharomyces* in the 5 hospitals during between January 2009–December 2018. The median age of case-patients was 68 (range 30–93) years and a male predominance (63%). The most common underlying condition was a digestive tract disease (59%). There was a medical record confirming the use of the

S. cerevisiae var. *boulardii* probiotic on the day of the blood culture or during the preceding 7 days for 20 case-patients (43%). Medical records were not available for 10 case-patients (22%), and these patients were classified as nonusers.

Of the 20 case-patients, 17 were using *S. cerevisiae* var. *boulardii* probiotic on the day of the blood culture and 3 case-patients had already stopped using it (2 patients on the day before and 1 patient 5 days earlier). Five additional case-patients had used the probiotic in the preceding 3 months, of whom 1 patient had already stopped using it 26 days earlier. For 4 case-patients, the time when the use of the probiotic was terminated could not be determined. Most case-patients (16/20, 80%) received the *S. cerevisiae* var. *boulardii* probiotic in the hospital, 3 case-patients in some other facility, and 1 case-patient was using it at home. All *S. cerevisiae* var. *boulardii* probiotics found in the medical records were from the same strain (Precosa; Biocodex Ltd., https://www.biocodex.com). We provide characteristics, underlying diseases, and severity of the disease for these patients (Table 1, https://wwwnc.cdc.gov/EID/article/27/8/21-0018-T1.htm; Table 2).

Antimicrobial drugs were commonly used by the patients (72%) during 4 weeks preceding the fungemia. Antifungal treatment was commenced or changed because of *Saccharomyces* fungemia for 23 patients (50%). For an additional 8 patients (17%), the culture result came after the patient had died. Case-fatality rates by day 7 were 22% (10 patients) and by day 28 were 37% (17 patients). Of patients who died by day 28, 6 patients had an ultimately fatal disease (McCabe score 2) and 5 patients had a rapidly fatal disease (McCabe score 3).

Nonblood Cultures

There were 1,153 nonblood *Saccharomyces* culture findings (fecal samples excluded). There was considerable variation between hospital districts in numbers of the microbial cultures and anatomic sites from which cultures were obtained (Table 3). We evaluated use of probiotics for 125 case-patients. Medical records were not available for 6 of them. Use of *S. cerevisiae* var. *boulardii* probiotic was confirmed for 24 case-patients (19%). This finding was divided by the anatomic site as follows: 17 (21%) of 82 from the abdominal region, 4 (13%) of 30 from the oral or respiratory tract, and 3 (23%) of 13 from other sites. Antifungal medication was already in use at the time of culture for 38% (47/125, the medical record was not available for 1 case-patient) of the case-patients. This finding led to a modification of the antifungal

Table 2. Characteristics of 46 case-patients who had *Saccharomyces* fungemia in 5 hospital districts, Finland, January 1, 2009–December 31, 2018*

Characteristic	Value
No. patients	46
Median age, y (range)	68 (30–93)
Sex	
M	29 (63)
F	17 (37)
Use of *S. cerevisiae* var. *boulardii* probiotic in preceding 3 mo†	25/46 (54)
Use of *S. cerevisiae* var. *boulardii* probiotic in preceding 7 d†	20/46 (43)
Use of *S. cerevisiae* var. *boulardii* probiotic in preceding 7 d in control group‡	4/76 (5)
Central venous catheter	8 (17)
Use of antimicrobial drugs in preceding 4 weeks	33 (72)
Change in antimicrobial drugs because of fungemia	23 (50)
Underlying diseases	
Digestive tract	27 (59)
Neurologic	11 (24)
Cardiovascular	8 (17)
Solid tumor with metastasis	6 (13)
Diabetes mellitus (any type)	6 (13)
Pulmonary	5 (11)
Liver	4 (9)
Rheumatic	4 (9)
Chronic kidney§	3 (7)
McCabe score†	
No or nonfatal underlying disease	22 (48)
Ultimately fatal underlying diseases (<5 y)	9 (20)
Rapidly fatal underlying diseases (<1 y)	5 (11)
Severity of disease	
qSOFA score $\geq$2 at time of fungemia	16 (35)
Septic shock at time of fungemia	6 (13)
Death by day 7 after fungemia	10 (22)

*Values are no. (%) or no. positive/no. tested (%) unless otherwise indicated.
†Medical records were not available for 10 case-patients.
‡Medical records were not available for 6 control case-patients.
§History of creatinine level >120 μmol/L.

medication in for 35% (44/125, medical records not available for 2 case-patients) of the case-patients.

Controls

The controls for the fungemia case-patients (n = 76) were mostly bacteremic (n = 65), but there were 5 case-patients infected with *Candida* sp. Medical records were not available for 6 control case-patients. Median age for this group was 70 years (vs. 68 years for case-patients), 70% were males (versus 63% for the case-patients), 47% had digestive tract disease (vs. 59% of the case-patients), and 17% had a malignancy (vs. 13% of the case-patients) (data were available for 64 case-patients). Use of *S. cerevisiae* var. *boulardii* probiotic by the *Saccharomyces* fungemia group was 43% compared with 5% (4/76) for the control group (odds ratio [OR] 14, 95% CI 4–44).

Microbes detected for controls who had nonblood cultures (n = 123) were also mostly bacteria (n = 97), but *Candida* sp. or other yeasts (n = 51; with or without a concomitant bacterial finding) were more common than in blood cultures. Median age for this group was 65 years (vs. 64 years for case-patients), 44% were males (vs. 59% for case-patients), 70% had

digestive tract disease (vs. 69% of case-patients), and 28% had a malignancy (vs. 38% of case-patients) (data on underlying diseases were available for 100 controls). Use of *S. cerevisiae* var. *boulardii* probiotic was 19% (24/125) in the *Saccharomyces* culture-positive group compared with 2% (3/123) for the control group (OR 10, 95% CI 3–32).

Discussion

We report 20 cases of *Saccharomyces* fungemia in patients who used *S. cerevisiae* var. *boulardii* probiotic. These cases have increased the number of cases reported in the literature by 34%.

We evaluated 125 of 1,153 patients who had a nonblood *Saccharomyces* culture finding and confirmed use of *S. cerevisiae* var. *boulardii* probiotic by 19% of these case-patients. To our knowledge, the magnitude of findings other than fungemia has not been reported. Although some of these nonblood findings might represent colonization, positive *Saccharomyces* cultures led to a change in antimicrobial drugs for 44 (35%) patients who had evaluated cases.

We also evaluated use of *S. cerevisiae* var. *boulardii* probiotic for patients who had a *Saccharomyces* culture

finding and compared it with that of a control group who had different positive blood and nonblood cultures and were in the same ward around the same time. The *Saccharomyces* fungemia patients had an OR of 14 and nonblood culture-positive patients had an OR of 10 for use of this probiotic compared with respective controls. Moreover, case-patient 7 (Table 1) is an example of a patient in whom probiotic use unequivocally caused the fungemia. The patient had had a percutaneous endoscopic gastrostomy feeding tube inserted 2 days before the fungemia, had septic shock, and then died. The probiotic was administered at least once through the tube, and the tip of the tube was unintentionally displaced from its ventricular position, leading to an accidental peritoneal application of the probiotic.

Saccharomyces fungemias occurred most often in patients who had diseases of the gastrointestinal tract (59%). This finding is nearly identical to the amount reported in a meta-analysis (58%) (*9*). Furthermore, there are reports of *Saccharomyces* fungemias in patients not given pretreatment with a *S. cerevisiae* var. *boulardii* probiotic that have been believed to have been derived from contaminated central venous catheters (*26–28*).

Bacteremias and fungemias have not been encountered in clinical trials with probiotics in general. There were probiotic studies conducted with susceptible patients who did not have blood culture findings and who had hepatic encephalopathy (*29*). However, serious concurrent conditions have usually been an exclusion criterion; thus, the safety profile remains unclear. Furthermore, there are other reported safety issues with probiotics, such as contamination of a probiotic

supplement with a pathogenic microbe or possible transfer of an antimicrobial drug resistance gene from a probiotic microbe to pathogenic microbes (*30–32*).

Regarding the benefits of probiotics, is there evidence showing that adults should use *S. cerevisiae* var. *boulardii* probiotic in conjunction with antimicrobial drugs to prevent *Clostridioides difficile* infections (CDIs) that cause diarrhea? A meta-analysis during 2017 combined *S. cerevisiae* var. *boulardii* probiotic studies conducted in adult populations to prevent CDIs (*33*). There were 5 studies. All studies had a low number of CDIs (15 cases of CDI in control groups) and all had nonsignificant results (pooled risk ratio 0.63, 95% CI 0.29–1.37).

Currently, several companies sell *S. cerevisiae* var. *boulardii* yeast, but total consumption of this yeast in Finland is not known. Thus, we are not able to relate our study results to its use. However, nationwide consumption of probiotics does not reflect the risk for fungemia or nonblood culture findings, or use of this probiotic by susceptible patients in hospitals. Cautious use of *S. cerevisiae* var. *boulardii* probiotic in gastrointestinal surgery wards would probably be one of the most effective ways to decrease these culture findings.

Moreover, the benefits for the indication for which the probiotic is used need to be established. There are 2 recent US guidelines on administration of probiotics in general for primary prevention of CDI. The first guideline states that there are insufficient data to recommend the administration (*34*), and the second guideline states that in certain circumstances certain probiotics could be used, but the quality of evidence is low (*35*).

Table 3. *Saccharomyces* clinical culture findings (excluding fungemias), Finland, January 1, 2009–December 31, 2018*

Characteristic	All			University hospital district		
	Total	Helsinki	Tampere	Turku	Oulu	Kuopio
Catchment area in 2017	3,310,000	1,650,000	530,000	480,000	400,000	250,000
Inpatient days in 2017	1,814,183	784,252	307,484	294,834	191,612	236,001
Patients who had clinical findings	1,344	649	30	215	285	165
Abdominal region	205	67	21	8	76	33
Oral or respiratory tract	676	387	6	71	137	75
Fecal	191	53	1	130	4	3
Other or unspecified	272	142	2	6	68	54
Patients who had medical record of *Saccharomyces cerevisiae* var. *boulardii* probiotic per clinical finding†	24/125 (19)	3/25 (12)	6/25 (24)	4/25 (16)	4/25 (16)	7/25 (28)
Abdominal region	15	2	4	1	4	4
Oral or respiratory tract	4	0	1	3	0	0
Other or unspecified	5	1	1	0	0	3
Patients who had medical record of *S. cerevisiae* var. *boulardii* probiotic in control group	3/123 (2)	0/25 (0)	1/25 (4)	0/23 (0)	0/25 (0)	2/25 (8)
No. patients who had change of antimicrobial drugs because of finding of *Saccharomyces* sp.‡	44/125 (35)	11/25 (44)	3/25 (12)	8/25 (32)	13/25 (52)	9/25 (36)

*Values are no. or no. positive/no. tested (%).
†Fecal samples excluded. The most recent 25 case-patients per hospital district checked. Medical records not available for 6 case-patients. Kuopio last 3 mo of probiotic use, others last 7 d.
‡Medical records not available for 2 case-patients.

The first limitation of this study is that we were not able to obtain microbiological evidence that the fungal infections were caused by the *S. cerevisiae* var. *boulardii* probiotic strain and not by another strain. Furthermore, the retrospective design using medical records can lead to a bias in reporting. Only confirmed use of probiotics was reported in this study, and case-patients whose medical records were not available were defined as not using a probiotic. Thus, the percentage of probiotic users was the minimum estimate in all groups. All medications given to patients in the wards were documented in medical records of patients, but patients might have used these medications before they were admitted to the hospital. Moreover, most patients who had fungemia were given bacterial antimicrobial drugs, which could have decreased the routine of taking blood cultures. Recall bias (e.g., the *S. cerevisiae* var. *boulardii* probiotic would have been mentioned in the medical charts more often in case-patients than in control-patients because of *Saccharomyces* culture finding) was not a limitation in this study. For all but 1 case-patient, the probiotic was recorded in the charts before the culture result was complete.

S. cerevisiae var. *boulardii* probiotics are not recommended for patients who have indwelling catheters, are immunocompromised, or are critically ill. Our results indicate that use of *S. cerevisiae* var. *boulardii* probiotics should also be considered carefully for patients whose gastrointestinal tract integrity might be compromised. Furthermore, more data are needed to elucidate the health benefits of *S. cerevisiae* var. *boulardii* probiotics in general.

About the Author

Dr. Rannikko is an infectious diseases consultant at Tampere University Hospital, Tampere, Finland, and clinical instructor at Tampere University. One of his primary research interests is the role of the infection in postbacteremic deaths.

References

1. Hill C, Guarner F, Reid G, Gibson GR, Merenstein DJ, Pot B, et al. Expert consensus document. The International Scientific Association for Probiotics and Prebiotics consensus statement on the scope and appropriate use of the term probiotic. Nat Rev Gastroenterol Hepatol. 2014;11:506–14. https://doi.org/10.1038/nrgastro.2014.66

2. McFarland LV. From yaks to yogurt: the history, development, and current use of probiotics. Clin Infect Dis. 2015;60(Suppl 2):S85–90. https://doi.org/10.1093/cid/civ054

3. Sanders ME, Akkermans LM, Haller D, Hammerman C, Heimbach J, Hörmannsperger G, et al. Safety assessment of probiotics for human use. Gut Microbes. 2010;1:164–85. https://doi.org/10.4161/gmic.1.3.12127

4. Bafeta A, Koh M, Riveros C, Ravaud P. Harms reporting in randomized controlled trials of interventions aimed at modifying microbiota: a systematic review. Ann Intern Med. 2018;169:240–7. https://doi.org/10.7326/M18-0343

5. Besselink MG, van Santvoort HC, Buskens E, Boermeester MA, van Goor H, Timmerman HM, et al.; Dutch Acute Pancreatitis Study Group. Probiotic prophylaxis in predicted severe acute pancreatitis: a randomised, double-blind, placebo-controlled trial. Lancet. 2008;371:651–9. https://doi.org/10.1016/S0140-6736(08)60207-X

6. Clarke TC, Black LI, Stussman BJ, Barnes PM, Nahin RL. Trends in the use of complementary health approaches among adults: United States, 2002–2012. Natl Health Stat Report. 2015;Feb 10:1–16.

7. Yi SH, Jernigan JA, McDonald LC. Prevalence of probiotic use among inpatients: a descriptive study of 145 U.S. hospitals. Am J Infect Control. 2016;44:548–53. https://doi.org/10.1016/j.ajic.2015.12.001

8. Khatri I, Tomar R, Ganesan K, Prasad GS, Subramanian S. Complete genome sequence and comparative genomics of the probiotic yeast *Saccharomyces boulardii*. Sci Rep. 2017;7:371. https://doi.org/10.1038/s41598-017-00414-2

9. Enache-Angoulvant A, Hennequin C. Invasive *Saccharomyces* infection: a comprehensive review. Clin Infect Dis. 2005;41:1559–68. https://doi.org/10.1086/497832

10. Lolis N, Veldekis D, Moraitou H, Kanavaki S, Velegraki A, Triandafyllidis C, et al. *Saccharomyces boulardii* fungaemia in an intensive care unit patient treated with caspofungin. Crit Care. 2008;12:414. https://doi.org/10.1186/cc6843

11. Santino I, Alari A, Bono S, Teti E, Marangi M, Bernardini A, et al. *Saccharomyces cerevisiae* fungemia, a possible consequence of the treatment of *Clostridium difficile* colitis with a probioticum. Int J Immunopathol Pharmacol. 2014;27:143–6. https://doi.org/10.1177/039463201402700120

12. Fadhel M, Patel S, Liu E, Levitt M, Asif A. *Saccharomyces cerevisiae* fungemia in a critically ill patient with acute cholangitis and long term probiotic use. Med Mycol Case Rep. 2018;23:23–5. https://doi.org/10.1016/j.mmcr.2018.11.003

13. Kara I, Yıldırım F, Özgen Ö, Erganiş S, Aydoğdu M, Dizbay M, et al. *Saccharomyces cerevisiae* fungemia after probiotic treatment in an intensive care unit patient. J Mycol Med. 2018;28:218–21. https://doi.org/10.1016/j.mycmed.2017.09.003

14. Romanio MR, Coraine LA, Maielo VP, Abramczyc ML, Souza RL, Oliveira NF. *Saccharomyces cerevisiae* fungaemia in a pediatric patient after treatment with probiotics. Rev Paul Pediatr. 2017;35:361–4. https://doi.org/10.1590/1984-0462/;2017;35;3;00014

15. Appel-da-Silva MC, Narvaez GA, Perez LR, Drehmer L, Lewgoy J. *Saccharomyces cerevisiae* var. *boulardii* fungemia following probiotic treatment. Med Mycol Case Rep. 2017;18:15–7. https://doi.org/10.1016/j.mmcr.2017.07.007

16. Atıcı S, Soysal A, Karadeniz Cerit K, Yılmaz Ş, Aksu B, Kıyan G, et al. Catheter-related *Saccharomyces cerevisiae* fungemia following *Saccharomyces boulardii* probiotic treatment: in a child in intensive care unit and review of the literature. Med Mycol Case Rep. 2017;15:33–5. https://doi.org/10.1016/j.mmcr.2017.02.002

17. Roy U, Jessani LG, Rudramurthy SM, Gopalakrishnan R, Dutta S, Chakravarty C, et al. Seven cases of *Saccharomyces fungaemia* related to use of probiotics. Mycoses. 2017;60:375–80. https://doi.org/10.1111/myc.12604

18. Ellouze O, Berthoud V, Mervant M, Parthiot JP, Girard C. Septic shock due to *Saccharomyces boulardii*. Med Mal Infect. 2016;46:104–5. https://doi.org/10.1016/j.medmal. 2015.12.003

19. Landaburu MF, Lopez Daneri GA, Relloso S, Zarlenga LJ, Vinante MA, Mujica MT. Fungaemia following *Saccharomyces cerevisiae* var. *boulardii* probiotic treatment in an elderly patient. Rev Argent Microbiol. 2019.

20. Popiel KY, Wong P, Lee MJ, Langelier M, Sheppard DC, Vinh DC. Invasive *Saccharomyces cerevisiae* in a liver transplant patient: case report and review of infection in transplant recipients. Transpl Infect Dis. 2015;17:435–41. https://doi.org/10.1111/tid.12384

21. Chioukh FZ, Ben Hmida H, Ben Ameur K, Toumi A, Monastiri K. *Saccharomyces cerevisiae* fungemia in a premature neonate treated receiving probiotics [in French]. Med Mal Infect. 2013;43:359–60. https://doi.org/10.1016/j.medmal.2013.06.008

22. Thygesen JB, Glerup H, Tarp B. *Saccharomyces boulardii* fungemia caused by treatment with a probioticum. BMJ Case Rep. 2012;2012(mar26 1):bcr0620114412. https://doi.org/10.1136/bcr.06.2011.4412

23. Ventoulis I, Sarmourli T, Amoiridou P, Mantzana P, Exindari M, Gioula G, et al. Bloodstream infection by *Saccharomyces cerevisiae* in two COVID-19 patients after receiving supplementation of *Saccharomyces* in the ICU. J Fungi (Basel). 2020;6:98. https://doi.org/10.3390/jof6030098

24. Singer M, Deutschman CS, Seymour CW, Shankar-Hari M, Annane D, Bauer M, et al. The Third International Consensus Definitions for Sepsis and Septic Shock (Sepsis-3). JAMA. 2016;315:801–10. https://doi.org/10.1001/jama.2016.0287

25. McCabe W, Jackson G. Gram-negative bacteremia; I. Etiology and ecology. Arch Intern Med. 1962;110:847–55. https://doi.org/10.1001/archinte.1962.03620240029006

26. Hennequin C, Kauffmann-Lacroix C, Jobert A, Viard JP, Ricour C, Jacquemin JL, et al. Possible role of catheters in *Saccharomyces boulardii* fungemia. Eur J Clin Microbiol Infect Dis. 2000;19:16–20. https://doi.org/10.1007/s100960050003

27. Lherm T, Monet C, Nougière B, Soulier M, Larbi D, Le Gall C, et al. Seven cases of fungemia with *Saccharomyces boulardii* in critically ill patients. Intensive Care Med. 2002;28:797–801. https://doi.org/10.1007/s00134-002-1267-9

28. Cassone M, Serra P, Mondello F, Girolamo A, Scafetti S, Pistella E, et al. Outbreak of *Saccharomyces cerevisiae* subtype *boulardii* fungemia in patients neighboring those treated with a probiotic preparation of the organism. J Clin Microbiol. 2003;41:5340–3. https://doi.org/10.1128/JCM.41.11.5340-5343.2003

29. Dalal R, McGee RG, Riordan SM, Webster AC. Probiotics for people with hepatic encephalopathy. Cochrane Database Syst Rev. 2017;2:CD008716.

30. Cohen PA. Probiotic safety: no guarantees. JAMA Intern Med. 2018;178:1577–8. https://doi.org/10.1001/jamainternmed.2018.5403

31. Vallabhaneni S, Walker TA, Lockhart SR, Ng D, Chiller T, Melchreit R, et al.; Centers for Disease Control and Prevention (CDC). Notes from the field: fatal gastrointestinal mucormycosis in a premature infant associated with a contaminated dietary supplement—Connecticut, 2014. MMWR Morb Mortal Wkly Rep. 2015;64:155–6.

32. Egervärn M, Lindmark H, Olsson J, Roos S. Transferability of a tetracycline resistance gene from probiotic *Lactobacillus reuteri* to bacteria in the gastrointestinal tract of humans. Antonie van Leeuwenhoek. 2010;97:189–200. https://doi.org/10.1007/s10482-009-9401-0

33. Shen NT, Maw A, Tmanova LL, Pino A, Ancy K, Crawford CV, et al. Timely use of probiotics in hospitalized adults prevents *Clostridium difficile* infection: a systematic review with meta-regression analysis. Gastroenterology. 2017;152:1889–1900. e9. https://doi.org/10.1053/j.gastro.2017.02.003

34. McDonald LC, Gerding DN, Johnson S, Bakken JS, Carroll KC, Coffin SE, et al. Clinical Practice guidelines for *Clostridium difficile* infection in adults and children: 2017 update by the Infectious Diseases Society of America (IDSA) and Society for Healthcare Epidemiology of America (SHEA). Clin Infect Dis. 2018;66:987–94. https://doi.org/10.1093/cid/ciy149

35. Su GL, Ko CW, Bercik P, Falck-Ytter Y, Sultan S, Weizman AV, et al. AGA clinical practice guidelines on the role of probiotics in the management of gastrointestinal disorders. Gastroenterology. 2020;159:697–705. https://doi.org/10.1053/j.gastro.2020.05.059

Address for correspondence: Juha Rannikko, Department of Internal Medicine, Tampere University Hospital, Box 2000, FI-33521 Tampere, Finland; email: juha.rannikko@gmail.com

Estimates of Toxoplasmosis Incidence Based on Healthcare Claims Data, Germany, 2011–2016

Amrei Krings, Josephine Jacob, Frank Seeber, Uwe Pleyer, Jochen Walker, Klaus Stark, Hendrik Wilking

Toxoplasmosis is a zoonotic infection contracted through *Toxoplasma gondii*–contaminated food, soil, or water. Seroprevalence in Germany is high, but estimates of disease incidence are scarce. We investigated incidences for various toxoplasmosis manifestations using anonymized healthcare claims data from Germany for 2011–2016. Patients with a toxoplasmosis diagnosis during the annual observational period were considered incident. The estimated incidence was adjusted to the general population age/sex distribution. We estimated an annual average of 8,047 toxoplasmosis patients in Germany. The average incidence of non–pregnancy-associated toxoplasmosis patients was 9.6/100,000 population. The incidence was highest in 2011, at 10.6 (95% CI 9.4–12.6)/100,000 population, and lowest in 2016, at 8.0 (95% CI 7.0–9.4)/100,000 population. The average incidence of toxoplasmosis during pregnancy was 40.3/100,000 pregnancies. We demonstrate a substantial toxoplasmosis disease burden in Germany. Public health and food safety authorities should implement toxoplasmosis-specific prevention programs.

Toxoplasmosis is caused by infection with the protozoan parasite *Toxoplasma gondii*. Transmission of *T. gondii* can occur through food items and the environment. Main infection routes are the consumption of raw or undercooked meat or meat products containing *T. gondii* tissue cysts; ingestion of *T. gondii* oocysts through contaminated food items, such as fruits and vegetables; or ingestion of oocyst-contaminated soil or water (*1*). Most (80%–90%) infections in immune-competent persons are asymptomatic or manifest with mild influenza-like symptoms (*2*).

However, infections in immunocompromised persons can cause severe disease manifestations and often occur as a reactivation of latent *T. gondii* infections (*2*). Disease manifestations can include meningoencephalitis, conjunctivitis, chorioretinitis, myocarditis, pneumonitis, and hepatitis. A primary infection with *T. gondii* during pregnancy can cause severe sequelae, known as congenital toxoplasmosis, for neonates and fetuses; these manifestations may include developmental delay, blindness, epilepsy, spontaneous abortion, and stillbirth (*3,4*). Although *T. gondii* seroprevalence in several countries in Europe and the United States has slowly decreased over the past few decades (*5–8*), emerging collaborative and interdisciplinary One Health approaches may enable new prevention efforts that could substantially reduce the disease burden of toxoplasmosis.

In a systematic review, Torgerson et al. (*9*) estimated the global incidence and burden of disease for congenital toxoplasmosis as 190,100 (95% CI 179,300–206,300) cases/year, which translates into an incidence rate of 1.5 cases/1,000 live births and a burden of disease of 1.2 million disease-adjusted life years (DALYs)/year. For Europe, an incidence rate of 0.5/1,000 live births and a burden of disease of 2.8 DALYs/1,000 live births have been calculated (*9*). A meta-analysis reports a global incidence of acute toxoplasmosis during pregnancy as 1.1%, ranging from 0.5% in the European region to 2.5% in Eastern Mediterranean region (*10*).

In Germany, *T. gondii* seroprevalence was previously found to range from 20% among patients 18–29 years of age to 77% among patients 70–79 years of age (*11*). The same study estimated 345 incident congenital toxoplasmosis cases per year (*11*). In contrast, routine surveillance data in Germany from 2009–2018 identified a minimum of 6 notified cases in 2014 and maximum of 23 cases in 2008. Medical doctors are required to report congenital forms of toxoplasmosis to the Germany national surveillance

Author affiliations: Robert Koch Institute, Berlin, Germany
(A. Krings, F. Seeber, K. Stark, H. Wilking); European Centre for
Disease Prevention and Control, Stockholm, Sweden (A. Krings);
InGef–Institute for Applied Health Research Berlin GmbH, Berlin
(J. Jacob, J. Walker); Charité Universitätsmedizin Berlin, Berlin
(U. Pleyer)

system, but not other forms of the disease or its diagnosis for patients infected with HIV or receiving organ transplants. We assumed substantial underreporting of diagnosis and underascertainment, which describes the potential absence of a diagnosis (*12*). Consequently, in Germany no data are available for the incidence of toxoplasmosis manifestations other than for congenital toxoplasmosis. However, having such estimates is essential to assess the disease burden and advise on appropriate and targeted prevention measures. Toxoplasmosis testing during pregnancy is not covered by the statutory health insurance in Germany; general screening of pregnant women has been shown to be cost-effective, but self-financed screening leads to selective testing of mostly women of higher educational status (*13,14*). Although information about the risk for foodborne *T. gondii* infections during pregnancy is available to the public (*15*), there is no systematic monitoring of *T. gondii* in food products.

Disease surveillance of *T. gondii* is fragmented and unreliable; valid disease estimates could consequently inform and justify implementation of preventive measures. We aimed to estimate the annual incidence of different toxoplasmosis manifestations in Germany during 2012–2016. The method for using healthcare claims data in this study followed Lykins et al.'s approach for assessing toxoplasmosis estimates in the United States (*16*).

Methods

Data and Definitions

We obtained the study data from the anonymized healthcare claims database and provided by the Institute for Applied Health Research Berlin (InGef). Approximately 60 of the 123 statutory health insurance providers in Germany contribute to the database, which covers longitudinal data from ≈7 million of the 83 million Germany residents. The characteristics of this dataset and its external validity have been described (*17*). The authors showed that, compared with the general population, the database population was slightly younger and includes a smaller proportion of East Germany inhabitants. However, rates of hospitalization and overall mortality and drug prescription rates were similar to those of the general population. The overall illness rates were slightly lower in the database population.

The study period covered 2011–2016. To estimate the annual toxoplasmosis incidence rates, we used inclusion criteria of continuous insurance with one of the statutory health insurance providers for >8 quarters before the year analyzed and for all quarters of the year analyzed or until death (Figure 1). An exception was made for toxoplasmosis in mother and child, in which children needed to be insured since birth and pregnant women for >4 quarters before and during the entire pregnancy to be included (Table 1).
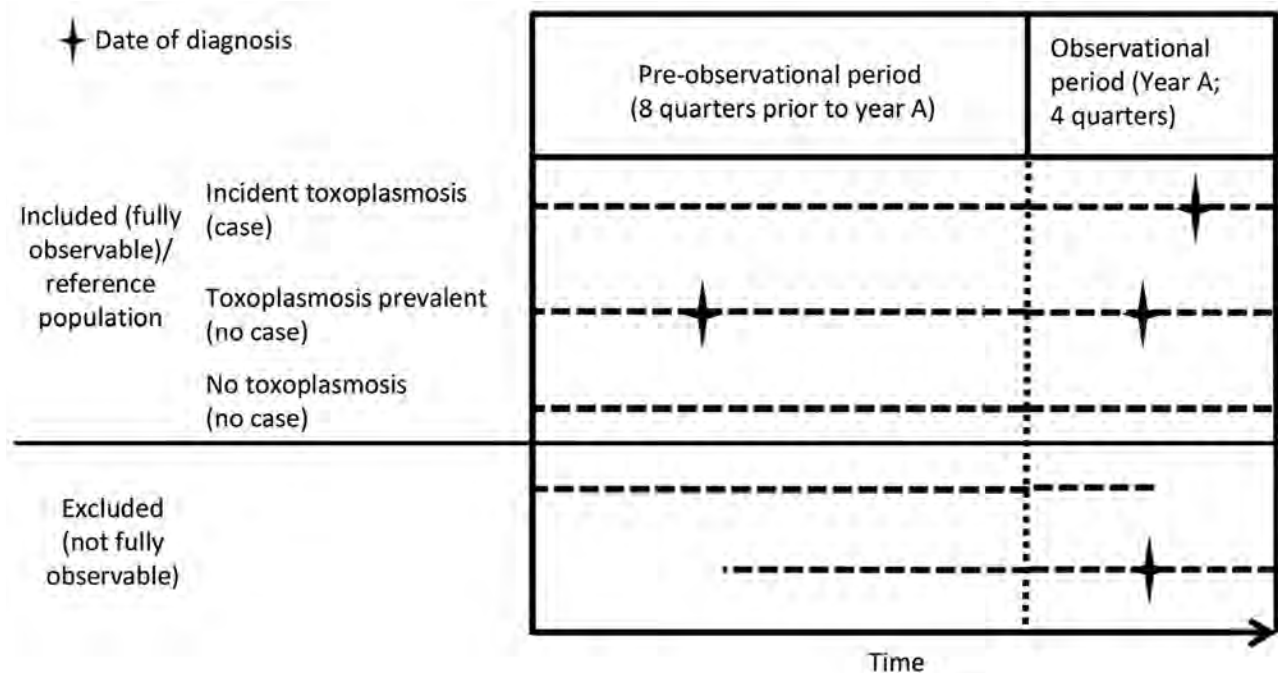

Figure 1. Visualization of different inclusion and exclusion definitions for study of toxoplasmosis incidence based on healthcare claims data, Germany, 2011–2016.

Table 1. Case definitions for toxoplasmosis disease manifestations used in analysis of healthcare claims, Germany*

Toxoplasmosis manifestation	Case definition
Non–pregnancy-associated	
Ocular toxoplasmosis	Patient with ICD-10 diagnosis code B58.0
Cerebral toxoplasmosis	Patient with ICD-10 diagnosis code B58.2
Hepatitis through toxoplasmosis	Patient with ICD-10 diagnosis code B58.1
Pneumonitis through toxoplasmosis	Patient with ICD-10 diagnosis code B58.3
Toxoplasmosis of other specified sites	Patient with ICD-10 diagnosis code B58.8
Unspecified toxoplasmosis	Patient with ICD-10 diagnosis code B58 or B58.9
Toxoplasmosis in mother and child	
Congenital toxoplasmosis†	Children <u><</u>12 mo of age with ICD-10 code P37.1 or B58.9
Toxoplasmosis during pregnancy‡	Pregnant woman with ICD-10 code B58
	AND 1 of the following laboratory tests: avidity testing (EBM 32640) or testing for *Toxoplasma gondii* in amniotic fluid or fetal blood (EBM 32833)
	AND who received 1 of the following treatments: spiramycin (before 16th week of pregnancy), pyrimethamine in combination with sulfadiazine/clindamycin/atovaquone (after 16th week of pregnancy), trimethoprim/sulfamethoxazole

*The reference population for incidence estimation for each form of toxoplasmosis was all patients in the healthcare database not fulfilling the case definition. ICD-10, International Classification of Diseases, 10th Revision.
†Reference population was children <1 year of age.
‡Reference population was female patients 15–50 y of age and pregnant. Pregnancy was defined based on ICD-10 diagnostic codes indicating birth, stillbirth, abortion, or miscarriage.

Case definitions for various toxoplasmosis manifestations were determined by diagnosis codes from the International Classification of Diseases, 10th Revision (ICD-10) (Table 1). The case definition for toxoplasmosis during pregnancy also includes toxoplasmosis-specific laboratory testing and therapy.

Estimates of Incidence

Toxoplasmosis patients are considered incident if they receive a diagnosis during the observational period but not in the preobservational period. For overall estimation of case numbers and incidence in Germany, we adjusted calculations in accordance with German Federal Statistical Office estimates for age, sex, and geographic distribution for each respective year. We calculated annual incidences for each toxoplasmosis manifestation separately and the average annual incidence as the arithmetic mean of the 6 yearly-determined incidence rates for 2011–2016. Patients identified in 2016, the most recent study period, were used for stratified analysis of geographic distribution of residence, sex, and age.

Recurring Medical Claims of Toxoplasmosis

To investigate potential toxoplasmosis relapse, we used recurring medical claims as an approximation. We defined any second medical toxoplasmosis claim as recurring if the patient had >2 quarters without an existing ICD-10 code for toxoplasmosis; if the patient had a diagnosis of a different toxoplasmosis manifestation than that previously recorded; or if the patient record showed >2 quarters without treatment while they still had the ICD-10 code. We differentiated rates of recurring medical claims per 100 person-years by relapse with the same or a different toxoplasmosis

manifestation. Criteria for inclusion were a fully insured 4-quarter preobservational period before the first medical claim and continuous insurance throughout the 2012–2016 study period (Figure 2). We analyzed patients with recurring medical claims as proportions of all toxoplasmosis patients.

Underlying Conditions in Patients with *T. gondii* Infection

For comparison, we used the scientifically reported and discussed underlying conditions provided in Lykins et al. (*16*) to analyze those conditions for Germany in this analysis (Appendix Table 1, https://wwwnc.cdc.gov/EID/article/27/8/20-3740-App1.pdf). We defined toxoplasmosis cases as described previously (*16*) (Table 1). Toxoplasmosis-negatives were cases insured without any recorded episode of toxoplasmosis. Inclusion criteria were similar to those for the assessment of recurring medical claims (Figure 2); we excluded pregnant women and children <12 months of age from this subanalysis. We matched the toxoplasmosis and reference groups 1:1 on the basis of age (by 5-year age groups), sex, and quarter of the diagnosis date of the underlying illness. Matching by quarter of diagnosis helped to avoid confounding due to seasonal variation of some underlying conditions. We calculated odds ratios for measure of association based on the frequencies of predefined conditions among the toxoplasmosis and reference group.

Results

Study Population

Of ≈7 million persons insured during 2011–2016, we determined that 4.8–5.2 million were eligible for inclusion in our analysis per year. We found 2,625
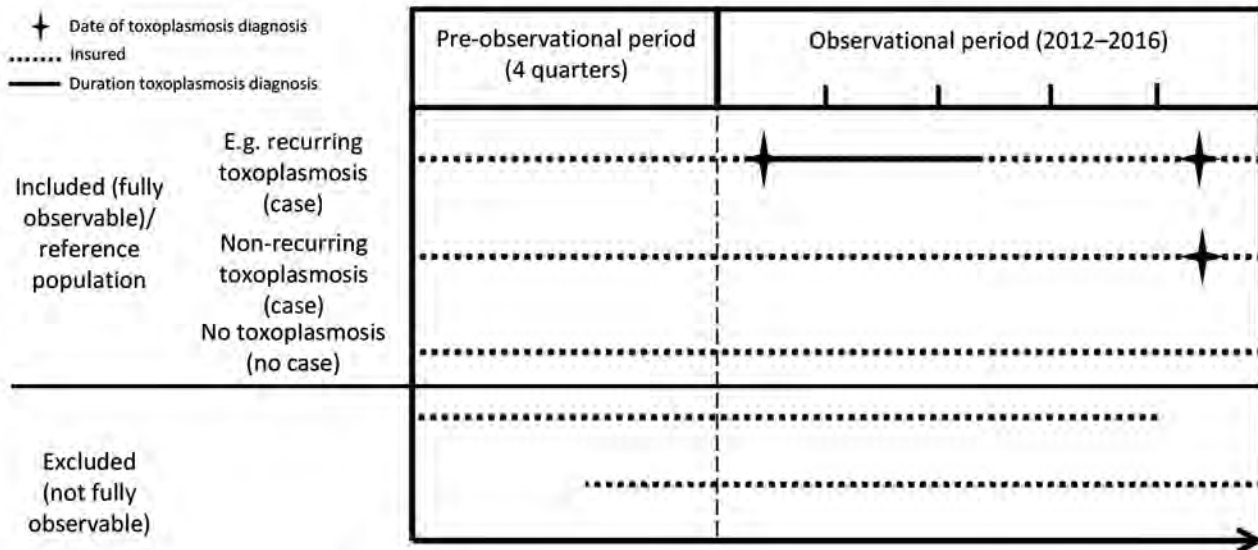
Figure 2. Visualization of different inclusion and exclusion definitions of recurring medical claims and identification of underlying conditions for study of toxoplasmosis incidence based on healthcare claims data, Germany, 2011–2016.

toxoplasmosis patients who met the case definitions in the database for these years, which is equivalent to 48,368 patients among ≈83 million Germany residents. This total corresponds to an average annual case number of 8,061 patients. For 950/2,625 (36%) of patients, a classification in one of the specific toxoplasmosis manifestations was possible; most patients had no specified toxoplasmosis manifestation.

Temporal and Geographic Distribution

Incidence for non–pregnancy-associated toxoplasmosis was as low as 8.0 (95% CI 7.0–9.4)/100,000 population in 2016 and as high as 10.6 (95% CI 9.4–12.6)/100,000 population in 2011. The average annual incidence of non–pregnancy-associated toxoplasmosis cases was 9.5/100,000 population. Geographically, in 2016, the incidence of 4.5 (95% CI 3.1–6.5)/100,000 population in Baden-Württemberg was significantly lower than the incidence of 12.5 (95% CI 6.6–25.1)/100,000 population in Berlin and 9.1 (95% CI: 6.7–12.2)/100,000 population in Lower Saxony (Figure 3).

Ocular Toxoplasmosis

We estimated an average annual case number of 1,601 cases of ocular toxoplasmosis and an average annual incidence of 2.0/100,000 population in Germany. The estimated incidence of ocular toxoplasmosis fluctuated between 1.5 (95% CI 1.1– 2.3) patients/100,000 population in 2016 and 2.5 (95% CI 2.0–3.8) patients/100,000 population in 2013 (Table 2). In 2016, the highest incidences of ocular toxoplasmosis were seen among women and in the 51–60-year age group (Table 3).

Cerebral Toxoplasmosis

The average annual number of cerebral toxoplasmosis patients in Germany was 142, and the average annual incidence was 0.18/100,000 population. Incidence for cerebral toxoplasmosis was 0.1 cases/100,000 population in 2012, 2013, and 2014 and 0.3 cases/100,000 population in 2015 (Table 2). Because very few cases were recorded in the database, we were unable to stratify estimates for most sociodemographic characteristics (Table 4).

Other Types and Nonspecified Types of Toxoplasmosis

The average annual number of patients with toxoplasmosis manifestations at other sites, including those with hepatitis or pneumonitis from toxoplasmosis, was 752 patients. The average annual number of unspecified toxoplasmosis patients was 5,202 and the average annual incidence was 6.4/100,000 population. In 2016, toxoplasmosis incidence was significantly higher among patients who were 21–40 years of age compared with patients <21 years or >40 years of age (p<0.05) (Table 5).

Congenital Toxoplasmosis

The average annual number of congenital toxoplasmosis patients was 8.2 and average annual incidence was 0.1/100,000 population in Germany. Incidence estimates ranged from 0.05 (95% CI 0.01–1.64)/100,000 pregnancies in 2012 to 0.14 (95% CI 0.05–1.07)/100,000 in 2015 (Table 2). Our ability to estimate stratified incidence was limited because the number of cases found was low (Appendix Table 2).

Toxoplasmosis during Pregnancy

The average annual number of patients with toxoplasmosis during pregnancy is 289 and average annual incidence is 40.3/100,000 pregnancies in Germany. Incidence of toxoplasmosis during pregnancy fluctuated between 29.3 (95% CI 16.7–56.4)/100,000 pregnancies in 2011 and 60.3 (95% CI 33.0–107.5)/100,000 pregnancies in 2015 (Table 2).

Stratification by age group and geographic region was partly limited because of low case numbers. Therefore, estimation was only possible for women 31–40 years of age, who had an estimated incidence rate of 52.7 (95% CI 24.1–138.1)/100,000 pregnancies. Stratification by region fluctuated between 34.4 (95% CI 17.7–71.9)/100,000 pregnancies in the western region of Germany and 58.2 (95% CI 17.2–177.9)/100,000 pregnancies in the northern region. No estimations are available for the middle and eastern regions (Table 6).

Recurring Medical Claims of Toxoplasmosis

Among all toxoplasmosis patients found in the dataset (n = 2,776), 722 (26%) had a recurring toxoplasmosis medical claim. The highest proportion of these (250/574; 44%) was seen among patients who initially received a diagnosis of ocular toxoplasmosis. The rate of recurring medical claims (termed rate of claims in this study) among initial ocular toxoplasmosis patients was 19.8/100 person-years for any type of toxoplasmosis.

Among these patients, the rate of claims in patients with an additional episode of ocular toxoplasmosis was 16.8/100 person-years; for other manifestations, the rate of claims was 3.0/100 person-years.

Underlying Conditions

We calculated odds ratios for statistically significant underlying conditions found among toxoplasmosis cases, compared with matched controls based on 5-year age groups and sex (Table 7). Conditions that were significantly associated with toxoplasmosis were anxiety, epilepsy, lymphadenopathy, and thrombocytopenia, as well as vision loss or blindness (all p<0.05). The conditions with <5 cases in the reference group but >10 cases in the toxoplasmosis group were HIV/AIDS; memory loss; and encephalitis, myelitis, or encephalomyelitis. We tested for other conditions that were not significantly associated with toxoplasmosis or affected <5 persons in either group (Appendix Table 1).

Discussion

Our study of toxoplasmosis incidence estimates and its manifestations, as determined from healthcare claims data, adds a valuable contribution to the evidence base. Most of the evidence on *T. gondii* infections and disease in Germany available to date is drawn either from serosurveys or from mandatory disease surveillance for congenital toxoplasmosis (*11,12*). Therefore, our estimation
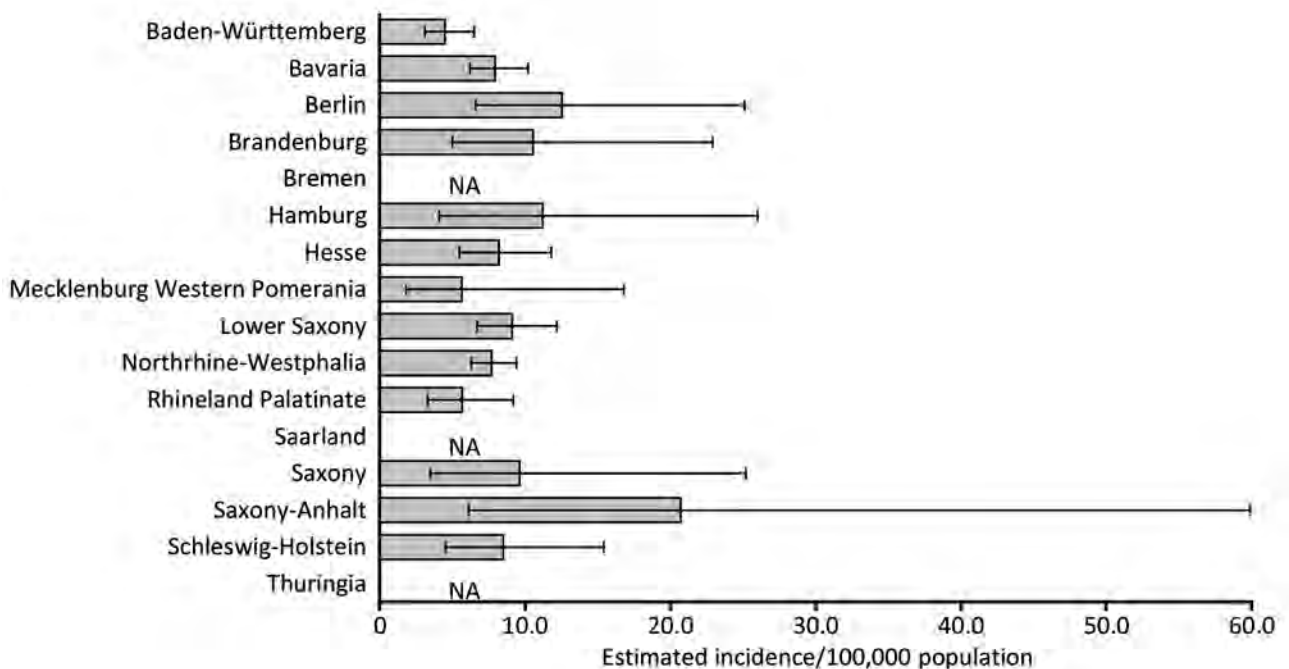

Figure 3. Toxoplasmosis disease incidence by federal state in Germany, 2016. Error bars indicate 95% CIs. No estimates were available for Bremen, Saarland, and Thüringen. NA, not available.

Table 2. Estimated incidence of toxoplasmosis manifestations by year, Germany, 2011–2016

Disease manifestation	Year	No. patients in database	No. patients identified	Estimated no. patients (95% CI)	Estimated cases/100,000 population (95% CI)
Ocular toxoplasmosis	2011	4,705,497	86	1,618 (1,253–2,940)	2.0 (1.6–3.7)
	2012	4,751,579	95	1,937 (1,522–3,189)	2.4 (1.9–4.0)
	2013	5,024,715	111	2,017 (1,623–3,029)	2.5 (2.0–3.8)
	2014	5,134,795	74	1,359 (1,015–2,241)	1.7 (1.3–2.8)
	2015	5,177,282	76	1,452 (1,035–2,342)	1.8 (1.3–2.9)
	2016	5,171,212	75	1,224 (941–1,931)	1.5 (1.1–2.3)
Cerebral toxoplasmosis	2011	4,705,497	8	144 (56–1,534)	0.2 (0.1–1.9)
	2012	4,751,579	6	114 (40–1,377)	0.1 (0.1–1.7)
	2013	5,024,715	5	97 (24–1,090)	0.1 (0.0–1.4)
	2014	5,134,795	6	80 (32–934)	0.1 (0.0–1.2)
	2015	5,177,282	13	218 (115–970)	0.3 (0.1–1.2)
	2016	5,171,212	10	200 (74–883)	0.2 (0.1–1.1)
Other types of toxoplasmosis†	2011	4,705,497	45	865 (NA)	NA
	2012	4,751,579	40	715 (NA)	NA
	2013	5,024,715	32	588 (NA)	NA
	2014	5,134,795	58	912 (NA)	NA
	2015	5,177,282	44	782 (NA)	NA
	2016	5,171,212	43	651 (NA)	NA
Nonspecified types of toxoplasmosis	2011	4,705,497	306	5,866 (5,093–7,406)	7.3 (6.3–9.2)
	2012	4,751,579	283	5,503 (4,703–6,981)	6.8 (5.8–8.7)
	2013	5,024,715	265	5,177 (4,483–6,389)	6.4 (5.6–7.9)
	2014	5,134,795	237	4,277 (3,686–5,327)	5.3 (4.5–6.6)
	2015	5,177,282	309	5,821 (5,070–6,936)	7.1 (6.2–8.4)
	2016	5,171,212	242	4,569 (3,862–5,628)	5.5 (4.7–6.8)
Congenital toxoplasmosis	2011	97,177	10	74 (32–1,478)	0.1 (0.0–1.8)
	2012	98,140	5	43 (8–1,321)	0.1 (0.0–1.6)
	2013	100,420	10	73 (32–1,066)	0.1 (0.0–1.3)
	2014	103,481	7	77 (16–934)	0.1 (0.0–1.2)
	2015	105,882	11	116 (41–879)	0.1 (0.1–1.1)
	2016	107,517	6	65 (25–751)	0.1 (0.0–0.9)
Toxoplasmosis during pregnancy	2011	63,102	18	252 (144–485)	29.3 (16.7–56.4)
	2012	53,178	14	226 (110–478)	32.0 (15.6–67.7)
	2013	53,476	16	324 (171–619)	44.4 (23.4–84.9)
	2014	52,951	21	296 (176–560)	40.5 (24.1–76.6)
	2015	53,900	21	450 (247–803)	60.3 (33.0–107.5)
	2016	37,302	14	186 (99–431)	35.3 (18.7–81.7)

*NA, not available.
†Other types include hepatitis, pneumonitis, other organs. Because the number of cases is summarized, no 95% CI and incidence estimation are available.

of ≈8,000 annual toxoplasmosis patients among 83 million residents of Germany offers a new assessment.

Our analysis indicates a potentially declining incidence of non–pregnancy-associated toxoplasmosis as well as toxoplasmosis during pregnancy in 2011–2016, except in 2015. This finding is in line with decreasing infections in the Netherlands (5) and France (6), as well as decreasing seroprevalence observed in Switzerland (7) and the United States (8). We hypothesize that, in France and the Netherlands, decreasing incidence is a result of improved practices in meat production, modern farming systems, increased use of frozen meat by consumers, or changes in food habits (5,6). Changing diets may also play a role in the decreasing incidence in our study; vegetarianism was shown to be negatively associated with *T. gondii* seropositivity in Germany (11). The observed nonsignificant increase of disease incidence in 2015 might be explained by a fluctuation of *T. gondii* exposure because, during this time, no programs were introduced by public health or veterinary health services that may have affected the number of diagnoses. We are not aware of potential changes from the healthcare sector regarding medical claims policies. Disease incidence in some Germany federal states seems higher, despite lacking statistical significance. Geographic differences in raw meat consumption in Germany, such as consumption of the regional specialty food Hackepeter, were previously shown in a cross-sectional survey (18). These observations are in line with the geographic differences of toxoplasmosis incidence found in our analysis.

For congenital toxoplasmosis the mandatory disease surveillance system reported 6–20 cases of congenital toxoplasmosis each year, 2011–2016 (12). Our analysis found 43–116 cases in Germany for the same years, confirming the suspicion that the surveillance system likely has underascertainment and underreporting. Our analysis, limited to children ≤12 months of age, might still underestimate the incidence of congenital

Table 3. Estimated incidence of ocular toxoplasmosis manifestations by age group, sex, and region, Germany, 2016*

Characteristic	No. patients in database	No. patients in country (95% CI)	No. cases/100,000 population (95% CI)
Sex			
M	34	516 (346–948)	1.3 (0.9–2.3)
F	41	707 (494–1,389)	1.7 (1.2–3.3)
Age group			
<1 y	<5	NA	NA
1–5 y	<5	NA	NA
6–10 y	<5	NA	NA
11–20 y	5	70 (22–329)	0.9 (0.3–4.1)
21–30 y	9	160 (73–432)	1.6 (0.7–4.3)
31–40 y	9	157 (65–421)	1.5 (0.6–4.1)
41–50 y	11	178 (81–430)	1.6 (0.7–3.7)
51–60 y	22	354 (212–653)	2.7 (1.6–5.1)
61–70 y	8	131 (56–399)	1.4 (0.6–4.2)
>71 y	5	94 (28–779)	0.8 (0.2–6.4)
Region			
East	6	172 (58–861)	1.1 (0.4–5.3)
West	69	1,052 (810–1,400)	1.6 (1.2–2.1)
North	20	415 (244–819)	2.0 (1.2–3.9)
Middle	33	492 (331–1,157)	1.7 (1.2–4.1)
South	22	317 (197–559)	1.1 (0.7–1.9)
Total	75	1,224 (941–1,931)	1.5 (1.1–2.3)

*Reference population N = 5,171,212. NA, not available.

toxoplasmosis compared with the postulated annual total of 345 neonates in Germany, because of potential development of clinical symptoms later in life (*11,19,20*). Another reason for an underestimation could be the lack of systematic screening of infants for congenital toxoplasmosis, which could prevent difficulties with diagnosis (*21*). Nevertheless, our analysis provides an improved estimation compared with the mandatory disease surveillance system.

Among non–pregnancy-associated toxoplasmosis, most patients were not further specified by disease manifestation, resulting in a large proportion of underascertainment; this phenomenon was similarly observed by Lykins et al. (*16*). Ocular toxoplasmosis was the non–pregnancy-associated disease manifestation with the highest incidence seen in our analysis, which is also in line with the results for the United States (*16*). The annual incidence in Germany of 2.0/100.000 population is roughly double the incidence reported by Lykins et al. in the United States. We would expect an even higher incidence in Germany, given the ≈4 times higher seroprevalence in Germany (49.1%) compared with the United States (12.4%) (*11,22*). The large number of patients in our

Table 4. Estimated incidence of cerebral toxoplasmosis manifestations by age group, sex, and region, Germany, 2016*

Characteristic	No. patients in database	No. patients in country (95% CI)	No. cases/100,000 population (95% CI)
Sex			
M	5	108 (24–533)	0.3 (0.1–1.3)
F	5	92 (25–778)	0.2 (0.1–1.9)
Age group, y			
<1 y	0	0	0
1–5 y	0	0	0
6–10 y	0	0	0
11–20 y	0	0	0
21–30 y	0	0	0
31–40 y	0	0	0
41–50 y	5	123 (29–395)	1.1 (0.3–3.4)
51–60 y	<5	NA	NA
61–70 y	<5	NA	NA
>71 y	<5	NA	NA
Region			
East	<5	NA	NA
West	8	113 (46–319)	0.2 (0.1–0.5)
North	<5	NA	NA
Middle	<5	NA	NA
South	<5	NA	NA
Total	10	200 (74–883)	0.2 (0.1–1.1)

*Reference population N = 5,171,212. NA, not available.

Table 5. Estimated incidence of other unspecified toxoplasmosis manifestations by age group, sex, and region, Germany, 2016*

Characteristic	No. patients in database	No. patients in country (95% CI)	No. cases/100,000 population (95% CI)
Sex			
M	64	1,181 (863–1,730)	2.9 (2.1–4.3)
F	221	4,039 (3,384–5,048)	9.7 (8.1–12.1)
Age group, y			
<1 y	0	0	0
1–5 y	0	0	0
6–10 y	<5	NA	NA
11–20 y	18	430 (226–812)	5.4 (2.8–10.1)
21–30 y	80	1,704 (1,306–2,247)	16.9 (12.9–22.2)
31–40 y	83	1,399 (1,083–1,846)	13.8 (10.7–18.2)
41–50 y	46	582 (422–865)	5.1 (3.7–7.5)
51–60 y	33	540 (356–873)	4.2 (2.8–6.8)
61–70 y	9	149 (68–419)	1.6 (0.7–4.5)
≥71 y	14	390 (102–1,235)	3.2 (0.8–10.1)
Region			
East	35	1,466 (932–2,430)	9.1 (5.8–15.0)
West	250	3,754 (3,292–4,314)	5.7 (5.0–6.5)
North	73	1,564 (1,203–2,116)	7.5 (5.7–10.1)
Middle	109	1,896 (1,413–2,773)	6.7 (5.0–9.7)
South	98	1,423 (1,152–1,795)	4.9 (4.0–6.2)
Total	242	4,569 (3,862–5,628)	5.5 (4.7–6.8)

*Reference population N = 5,171,212. NA, not available.

dataset with unspecified toxoplasmosis probably contributes to this remaining underestimation compared to seroprevalence in Germany.

Our data on disease relapse also reveal a high relapse for ocular toxoplasmosis. These results are not surprising because ocular toxoplasmosis is common in immune-competent patients (*24,25*), constituting most of the population. It can develop during childhood or adolescence even if infected neonates were born without symptoms for congenital toxoplasmosis (*19,20,26*). An estimated ≈2% of *T. gondii* infections lead to ocular toxoplasmosis (*23*); this would translate into 22 patients/100,000 population annually according to the seroprevalence seen in Germany in 2008 (*11*). We see a lower average annual incidence of 2 patients/100,000 population in this analysis, possibly resulting from underdiagnosis and missing specification of toxoplasmosis cases. We further suspect an underestimation of incidence for cerebral as well as other types of toxoplasmo-

sis, including pneumonitis and hepatitis or other organs affected, especially in immunocompromised patients; these are opportunistic infections among this group of patients and may therefore remain unrecognized.

Analysis of underlying conditions shows an association with psychiatric conditions (anxiety) and alternative diagnoses (visual loss, lymphadenopathy). Our analysis found an association with the known conditions HIV/AIDS and encephalitis, myelitis, or encephalomyelitis. However, we were unable to provide odds ratios for these conditions because of the low number of patients with HIV or encephalitis in our reference population. Directionality of conditions remains unclear from this analysis, and we were not able to confirm most associations found by Lykins et al. (*16*) on the basis of our dataset.

One limitation of this study is that healthcare claims are primarily intended for financial reimbursement rather than disease surveillance or clinical research.

Table 6. Estimated incidence of pregnancy-associated toxoplasmosis by age group and region for 2016, Germany

Characteristic	No. patients identified in database	No. patients in country (95% CI)	No. cases/100,000 pregnancies (95% CI)
Age group, y			
15–20 y	<5	NA	NA
21–30 y	<5	NA	NA
31–40 y	10	134 (61–351)	52.7 (24.1–138.1)
41–50 y	<5	NA	NA
Region			
East	<5	NA	NA
West	12	145 (75–303)	34.4 (17.7–71.9)
North	5	78 (23–238)	58.2 (17.2–177.9)
Middle	<5	NA	NA
South	6	73 (27–176)	37.3 (13.7–89.8)
Total	14	186 (99–431)	35.3 (18.7–81.7)

*Reference population N = 37,302 women 15–50 years of age. NA, not available.

Table 7. Underlying conditions among patients with ocular, cerebral, or other toxoplasmosis manifestations, Germany, 2012–2016

Condition	Odds ratio (95% CI)
Epilepsy	2.1 (1.3–3.3)
Visual loss, blindness, etc.	2.7 (1.7–4.3)
Anxiety	1.5 (1.2–1.8)
Thrombocytopenia	3.2 (1.7–6.1)
Lymphadenopathy	6.0 (3.9–9.3)

Therefore, the results rely on accurate coding and diagnosis and should be interpreted cautiously. Comparisons between the approaches in the United States and our data are hampered by the fundamental differences between the health systems, particularly in relation to medical claims. For similar reasons, an analysis based on toxoplasmosis-specific treatment as conducted by Lykins et al. was not possible due to different clinical guidelines. An estimate of annual toxoplasmosis incidence during pregnancy from this study (40.3/100,000 pregnancies) was restricted to women receiving toxoplasmosis-specific treatment. We can assume an unknown number of additional women need diagnostic clarification because of toxoplasmosis infection suspicion, which is likely to substantially burden the health system but is not accounted for in our incidence estimation. Although we tried to eliminate falsely diagnosed toxoplasmosis relapses by applying the criteria on patients with recurring medical claims, we need to interpret these results with caution, bearing in mind the nature of healthcare claims data and the purpose of claims. Although the estimates are adjusted for age, sex, and regional distribution, the selection of health insurance providers and the socioeconomic status of their target populations represented in this dataset may have a residual effect on these estimates that we cannot account for. Furthermore, as shown by Andersohn et al. (*17*), the overall death rate in the database population was slightly lower than the general population in Germany. This difference may also lead to an underestimation of toxoplasmosis illness rates in our analysis.

The incidence estimates for the different toxoplasmosis manifestations in this analysis provide a clearer picture of this disease's occurrence in Germany. The average annual number of ≈8,000 toxoplasmosis patients can be regarded as high, and even more undiagnosed cases are likely. Using healthcare claims data may also help other countries with improved assessments of their toxoplasmosis burden and renew the discussion for prevention measures in European Union countries and beyond. The incidence shown and the severity of symptoms and long-term sequelae of infections justify this urgent need.

Because *T. gondii* is a parasite with transmission and disease aspects affecting the veterinary, human, and environmental medicine sectors, an overall prevention program needs to target different levels, following an international One Health approach (*27*). Screening of pregnant women is one possible method of prevention, but its cost-effectiveness, health consequences for mother and child, and effectiveness of resulting treatment are debated in light of decreasing disease incidence (*28,29*). Although informing pregnant women of food- and animal-related risks is important, as is currently done in Germany, the incidence found in our analysis raises doubts about the effectiveness of this method. So far, insufficient evidence for effectiveness of educational efforts targeted at pregnant women has been published (*30*). Therefore, screening should be evaluated on the basis of the national health system structure and incidence in the country in question. Other preventive strategies currently debated include screening and implementing biosafety precautions for animal farms, as well as decontaminating meat products used for raw or undercooked consumption (*31*). A social cost–benefit analysis in the Netherlands has shown that freezing meat products is effective to reduce disease (*32*); freezing could be further implemented, especially for the production of meat products that are typically consumed raw in Germany.

About the Author

Dr. Krings is a researcher at the Robert Koch Institute in Berlin, Germany, involved in various data-for-action projects. Current research interests include hepatitis B, hepatitis C, and HIV in intravenous drug users.

References

1. Montoya JG, Liesenfeld O. Toxoplasmosis. Lancet. 2004;363:1965–76. https://doi.org/10.1016/S0140-6736 (04)16412-X

2. Robert Koch-Institut. RKI guide: toxoplasmosis. 2018 [cited 2021 Jun 21]. https://www.rki.de/DE/Content/Infekt/EpidBull/Merkblaetter/Ratgeber_Toxoplasmose.html

3. Jones JL, Lopez A, Wilson M, Schulkin J, Gibbs R. Congenital toxoplasmosis: a review. Obstet Gynecol Surv. 2001;56:296–305. https://doi.org/10.1097/00006254-200105000-00025

4. Pappas G, Roussos N, Falagas ME. Toxoplasmosis snapshots: global status of *Toxoplasma gondii* seroprevalence and implications for pregnancy and congenital toxoplasmosis. Int J Parasitol. 2009;39:1385–94. https://doi.org/10.1016/j.ijpara.2009.04.003

5. Hofhuis A, van Pelt W, van Duynhoven YT, Nijhuis CD, Mollema L, van der Klis FR, et al. Decreased prevalence and age-specific risk factors for *Toxoplasma gondii* IgG antibodies in the Netherlands between 1995–1996 and 2006–2007. Epidemiol Infect. 2011;139:530–8. https://doi.org/10.1017/S0950268810001044

6. Nogareda F, Le Strat Y, Villena I, De Valk H, Goulet V. Incidence and prevalence of *Toxoplasma gondii* infection in women in France, 1980–2020: model-based estimation. Epidemiol Infect. 2014;142:1661–70. https://doi.org/10.1017/S0950268813002756

7. Rudin C, Hirsch HH, Spaelti R, Schaedelin S, Klimkait T. Decline of seroprevalence and incidence of congenital toxoplasmosis despite changing prevention policy-three decades of cord-blood screening in north-western Switzerland. Pediatr Infect Dis J. 2018;37:1087–92. https://doi.org/10.1097/INF.0000000000001978

8. Jones JL, Kruszon-Moran D, Elder S, Rivera HN, Press C, Montoya JG, et al. *Toxoplasma gondii* infection in the United States, 2011–2014. Am J Trop Med Hyg. 2018;99:241–2

9. Torgerson PR, Mastroiacovo P. The global burden of congenital toxoplasmosis: a systematic review. Bull World Health Organ. 2013;91:501–8. https://doi.org/10.2471/BLT.12.111732

10. Rostami A, Riahi SM, Contopoulos-Ioannidis DG, Gamble HR, Fakhri Y, Shiadeh MN, et al. Acute toxoplasma infection in pregnant women worldwide: a systematic review and meta-analysis. PLoS Negl Trop Dis. 2019;13:e0007807. https://doi.org/10.1371/journal.pntd.0007807

11. Wilking H, Thamm M, Stark K, Aebischer T, Seeber F. Prevalence, incidence estimations, and risk factors of *Toxoplasma gondii* infection in Germany: a representative, cross-sectional, serological study. Sci Rep. 2016;6:22551. https://doi.org/10.1038/srep22551

12. Robert Koch-Institut. Epidemiological yearbook of notifiable infectious diseases 2017 [in German]. Berlin; The Institute: 2018.

13. Zylka-Menhorn V. Toxoplasmosis test: arguments for screening [in German]. Dtsch Arztebl Int. 2013;110:446. https://www.aerzteblatt.de/archiv/135207/Toxoplasmose-Test-Argumente-fuer-ein-Screening

14. Lange AE, Thyrian JR, Wetzka S, Flessa S, Hoffmann W, Zygmunt M, et al. The impact of socioeconomic factors on the efficiency of voluntary toxoplasmosis screening during pregnancy: a population-based study. BMC Pregnancy Childbirth. 2016;16:197. https://doi.org/10.1186/s12884-016-0966-0

15. Bundesinstitut für Risikobewertung. Toxoplasmosis underestimated danger [in German]. 2010 [cited 2021 Jun 4]. https://www.bfr.bund.de/de/presseinformation/2010/02/toxoplasmose__unterschaetzte_gefahr-32526.html

16. Lykins J, Wang K, Wheeler K, Clouser F, Dixon A, El Bissati K, et al. Understanding toxoplasmosis in the United States through "large data" analyses. Clin Infect Dis. 2016;63:468–75. https://doi.org/10.1093/cid/ciw356

17. Andersohn F, Walker J. Characteristics and external validity of the German Health Risk Institute (HRI) database. Pharmacoepidemiol Drug Saf. 2016;25:106–9. https://doi.org/10.1002/pds.3895

18. Bremer V, Bocter N, Rehmet S, Klein G, Breuer T, Ammon A. Consumption, knowledge, and handling of raw meat: a representative cross-sectional survey in Germany, March 2001. J Food Prot. 2005;68:785–9. https://doi.org/10.4315/0362-028X-68.4.785

19. Wallon M, Garweg JG, Abrahamowicz M, Cornu C, Vinault S, Quantin C, et al. Ophthalmic outcomes of congenital toxoplasmosis followed until adolescence. Pediatrics. 2014;133:e601–8. https://doi.org/10.1542/peds.2013-2153

20. Faucher B, Garcia-Meric P, Franck J, Minodier P, Francois P, Gonnet S, et al. Long-term ocular outcome in congenital toxoplasmosis: a prospective cohort of treated children. J Infect. 2012;64:104–9. https://doi.org/10.1016/j.jinf.2011.10.008

21. Wallon M, Peyron F. Congenital toxoplasmosis: a plea for a neglected disease. Pathogens. 2018;7:25. https://doi.org/10.3390/pathogens7010025

22. Jones JL, Kruszon-Moran D, Rivera HN, Price C, Wilkins PP. *Toxoplasma gondii* seroprevalence in the United States 2009–2010 and comparison with the past two decades. Am J Trop Med Hyg. 2014;90:1135–9. https://doi.org/10.4269/ajtmh.14-0013

23. Jones JL, Holland GN. Annual burden of ocular toxoplasmosis in the US. Am J Trop Med Hyg. 2010;82:464–5. https://doi.org/10.4269/ajtmh.2010.09-0664

24. Pleyer U, Gross U, Schlüter D, Wilking H, Seeber F. Toxoplasmosis in Germany. Dtsch Arztebl Int. 2019;116:435–44.

25. Maenz M, Schlüter D, Liesenfeld O, Schares G, Gross U, Pleyer U. Ocular toxoplasmosis past, present, and new aspects of an old disease. Prog Retin Eye Res. 2014;39:77–106. https://doi.org/10.1016/j.preteyeres.2013.12.005

26. Wallon M, Kodjikian L, Binquet C, Garweg J, Fleury J, Quantin C, et al. Long-term ocular prognosis in 327 children with congenital toxoplasmosis. Pediatrics. 2004;113:1567–72. https://doi.org/10.1542/peds.113.6.1567

27. Aguirre AA, Longcore T, Barbieri M, Dabritz H, Hill D, Klein PN, et al. The One Health approach to toxoplasmosis: epidemiology, control, and prevention strategies. EcoHealth. 2019;16:378–90. https://doi.org/10.1007/s10393-019-01405-7

28. Khoshnood B, De Vigan C, Goffinet F, Leroy V. Prenatal screening and diagnosis of congenital toxoplasmosis: a review of safety issues and psychological consequences for women who undergo screening. Prenat Diagn. 2007;27:395–403. https://doi.org/10.1002/pd.1715

29. Picone O, Fuchs F, Benoist G, Binquet C, Kieffer F, Wallon M, et al. Toxoplasmosis screening during pregnancy in France: opinion of an expert panel for the CNGOF. J Gynecol Obstet Hum Reprod. 2020;49:101814. https://doi.org/10.1016/j.jogoh.2020.101814

30. Di Mario S, Basevi V, Gagliotti C, Spettoli D, Gori G, D'Amico R, et al. Prenatal education for congenital toxoplasmosis. Cochrane Database Syst Rev. 2015;(10):CD006171.

31. Opsteegh M, Kortbeek TM, Havelaar AH, van der Giessen JW. Intervention strategies to reduce human *Toxoplasma gondii* disease burden. Clin Infect Dis. 2015;60:101–7. https://doi.org/10.1093/cid/ciu721

32. Suijkerbuijk AWM, Over EAB, Opsteegh M, Deng H, Gils PFV, Bonačić Marinović AA, et al. A social cost–benefit analysis of two One Health interventions to prevent toxoplasmosis. PLoS One. 2019;14:e0216615. https://doi.org/10.1371/journal.pone.0216615

Address for correspondence: Amrei Krings, Robert Koch Institute, Seestraße 10, 13353 Berlin, Germany; email: kringsa@rki.de

Modeling Immune Evasion and Vaccine Limitations by Targeted Nasopharyngeal *Bordetella pertussis* Inoculation in Mice

Illiassou Hamidou Soumana,[1,2] Bodo Linz,[1,3] Kalyan K. Dewan,[1] Demba Sarr,
Monica C. Gestal,[4] Laura K. Howard,[5] Amanda D. Caulfield, Balázs Rada, Eric T. Harvill

Conventional pertussis animal models deliver hundreds of thousands of *Bordetella pertussis* bacteria deep into the lungs, rapidly inducing severe pneumonic pathology and a robust immune response. However, human infections usually begin with colonization and growth in the upper respiratory tract. We inoculated only the nasopharynx of mice to explore the course of infection in a more natural exposure model. Nasopharyngeal colonization resulted in robust growth in the upper respiratory tract but elicited little immune response, enabling prolonged and persistent infection. Immunization with human acellular pertussis vaccine, which prevents severe lung infections in the conventional pneumonic infection model, had little effect on nasopharyngeal colonization. Our infection model revealed that *B. pertussis* can efficiently colonize the mouse nasopharynx, grow and spread within and between respiratory organs, evade robust host immunity, and persist for months. This experimental approach can measure aspects of the infection processes not observed in the conventional pneumonic infection model.

Less than a century ago, *Bordetella pertussis* was rampant worldwide, causing pertussis (whooping cough) that killed millions of persons every year, mostly infants and children (*1*). Whole-cell pertussis vaccines (wP), introduced in the mid-1950s, successfully controlled the disease, but concerns over side effects led many countries to replace wP vaccines with acellular pertussis (aP) vaccines in the mid-1990s (*2*). aP vaccines reduced side effects, but outbreaks of pertussis were still noted among highly aP-vaccinated populations (*3*), and the incidence of disease has been increasing among adults vaccinated with aP vaccines as children (*3–5*). In addition, experiments conducted with primates and rodents show that aP

vaccines prevent the symptoms of disease but do not prevent the spread of the bacterium (*6,7*). There is now consensus among researchers that aP vaccines confer good but short-lived protective immunity against disease but much less protection against colonization, shedding, and transmission (*6,7*).

Most of our knowledge of *B. pertussis* has been learned from animal models of pneumonic infection that were developed during an era guided by Koch's postulates (*8–19*). These animal experimental systems were designed to cause severe pathology and near-lethal virulence to simulate the most severe human disease. In pertussis models that emerged from this approach, large numbers of pathogen are introduced deep in the respiratory tract of animals, resembling extreme human infections in their severity and virulence but with more lung involvement than is generally clinically observed. In these models, high doses of *B. pertussis,* often 10^5–10^6 CFU, are delivered to the lungs of rodents (*20,21*). Larger primates, such as baboons, are inoculated by endotracheal intubation with even larger numbers, 10^8–10^{10} CFU (*6,22,23*).

High-dose pneumonic inoculations have provided several experimental benefits, including consistent colonization and growth of bacteria in the lungs, which induces severe pathology. Such inoculations served as assays to measure the contributions

[1]These authors contributed equally to this article.

[2]Current affiliation: University of British Columbia, Vancouver, British Columbia, Canada.

[3]Current affiliation: Friedrich Alexander University Erlangen-Nuremberg, Erlangen, Germany.

[4]Current affiliation: Louisiana State University Health Science Center, Shreveport, Louisiana, USA.

[5]Current affiliation: Augusta University, Augusta, Georgia, USA.

of individual virulence factors to severe disease and to develop effective vaccines. Delivery of large numbers of bacteria deep in the lungs predictably induces a vigorous and quantifiable immune response that begins to control infection within 2–3 weeks, reducing bacteria numbers below detectable levels within about 1 month (6,24) and providing an experimental system in which to develop and test vaccines to protect against such severe disease.

As valuable as conventional high-dose models have been, the bolus introduction of many bacteria deep into the lungs bypasses many key steps in the highly infectious catarrhal stage of pertussis, the prolonged period of early infection involving milder nonspecific upper respiratory tract symptoms. Of note, these aspects of early infection are most relevant to the current challenge of the ongoing circulation of *B. pertussis*. Indeed, recent work has revealed that a large proportion of human infections are asymptomatic and undiagnosed (25). Assays that specifically measure how colonization, early growth, and immunomodulation contribute to shedding and transmission during the catarrhal stage of infection, before and perhaps independent of lower respiratory tract infection, are critical for development of vaccines that can prevent transmission.

We describe a novel nasopharyngeal infection model in mice that efficiently establishes *B. pertussis* infections that mimic human infections, beginning with low numbers of pathogens colonizing the upper respiratory tract. Nasopharyngeal infections in our model revealed crucial aspects of *B. pertussis*–host interactions not observed in conventional pneumonic infection models and successfully demonstrating the failure of aP vaccines to prevent nasopharyngeal colonization. This nasopharyngeal infection system allows mechanistic study of several aspects of the early infectious process that usually are obscured by conventional pneumonic challenge. In addition, the model provided assays that are likely to be useful for development of new and improved vaccines to prevent *B. pertussis* colonization and transmission.

Materials and Methods

Bacterial Cultures and Inocula Preparation
We grew *B. pertussis* strain 536, a derivative of strain Tohama I, as previously described (12). We then pelleted bacteria by centrifugation and resuspended it in phosphate-buffered saline (PBS) to an optical density of 600 nm (OD_{600}) of 0.1 ($\approx 10^8$ CFU/mL). We serially diluted bacteria in PBS to obtain 500 CFU in 5 µL PBS for low-dose–low-volume (LDLV) nasopharyngeal inoculation or 5×10^5 CFU in 50 µL PBS for high-dose–high-volume (HDHV) pneumonic inoculation.

Mouse Experiments
We housed C57BL/6 female mice from Jackson Laboratories (https://www.jax.org) in the specific pathogen-free facility at the University of Georgia (Athens, Georgia, USA). We diluted veterinary grade antimicrobial drugs, including enrofloxacin (Baytril; Bayer, https://www.bayer.com) and gentamicin (GentaFuse; Henry Schein, https://www.henryschein.com), for intranasal delivery in 10 µL PBS to mice anesthetized by using 10% isoflurane. We optimized the amount of antimicrobial drug delivered to a single dose of 45 µg enrofloxacin per mouse. Twelve hours after antimicrobial drug treatment, we delivered 500 CFU *B. pertussis* in 5 µL PBS for LDLV nasopharyngeal infections or 5×10^5 CFU in 50 µL for HDHV pneumonic infections. Delivery of incula for both groups was by nasal inhalation under mild anesthesia. For vaccination experiments, we used intraperitoneal delivery, which is convenient and known to confer robust protection. In brief, we vaccinated 5-week-old mice on day 0 and gave a booster vaccine on day 28 by intraperitoneal injection of 200 µL PBS containing either wP vaccine (2×10^9 CFU of *B. pertussis* Tohama I heat-killed at 65°C for 30 min) (7), or one tenth of a human dose of commercial aP (Adacel TdaP; Sanofi Pasteur, https://www.sanofi.us). We inoculated mice 2 weeks after the booster vaccination (day 42 post vaccination). At indicated time points, we euthanized mice by CO_2 inhalation and excised nasal cavities, trachea, and lungs, which we homogenized in 1 mL sterile PBS by using Bead Mill 24 (Fisher Scientific, https://www.fishersci.com). We plated serial dilutions on Bordet-Gengou agar for bacterial enumeration.

Flow Cytometry
We prepared single-cell suspensions from collagenase-treated lungs, which we strained through 70 mm mesh and centrifuged through 44% Percoll (MP Biomedical, https://www.mpbio.com) in Gibco RPMI 1640 medium (Thermo Fischer Scientific, https://www.thermofisher.com), and then layered onto 67% Percoll in 1× PBS. We used TruStain FcX (Biolegend, https://www.biolegend.com) anti-mouse CD16/32 antibody to block Fc receptor cells and performed flow cytometry by using the LSR II system (BD Biosciences, https://www.bdbiosciences.com). We then stained surface markers with the

antibodies used to sort neutrophils, T cells, B cells, and natural killer (NK) cells. We used the following Biolegend products from Thermo Fischer Scientific: for neutrophils, CD11b (CD11b Antibody, PE-Cyanine 7), CD115 (CD115 Antibody, APC), lymphocyte antigen complex 6 locus G (Lys6G Antibody, AF488); for T cells, CD45 (CD45 Antibody, Alexa Fluor-700), CD3 (CD3 Antibody-APC); for B cells, B220 (B220 Antibody-PE-Cy7), and NK cells, NK1.1 (NK1.1 Antibody-PE) (Appendix Figure 1, https://wwwnc.cdc.gov/EID/article/27/8/20-3566-App1.pdf). We analyzed data by using FACS Diva version 8.0.1 (BD Biosciences) and determined percentage viability by using Zombie Aqua (Biolegend) live-dead dye.

Evaluation of Splenic Lymphocytes Responses
To analyze CD4 T cells and cytokines, including interleukin (IL) 17, IL-10, and IL-4, we collected spleens in ice chilled PBS (≈1°C–2°C) and then passed the mixture through a 40-μm cell strainer. We seeded 2×10^7 cells in a 96-well plate and stained cells according to standard protocols (*26*). We acquired data in the LSR II (BD Bioscience) and analyzed data with FlowJo 10.0 by using a standard gating strategy (*27*). In brief, we used Ghost Dye Red 710 (Tonbo Biosciences, https://tonbobio.com) for determining live cells, then gated CD45+ for total leukocytes and Thy1.2+ for T cells. We used CD4+ cells to evaluate levels of intracellular IL-17, IL-4, and IL-10.

B. pertussis–Specific Antibodies
We quantified serum antibodies by ELISA using Corning Costar 96-well EIA microtiter plates (Thermo Fischer Scientific) coated with heat-killed *B. pertussis* grown to an OD_{600} of 0.600 in Stanier Scholte medium. We coated plates by using sodium-carbonate buffer (0.1 mmol/L at pH 9.5) overnight at 4°C (*28*). We considered the IgG titer to be the reciprocal of the lowest dilution in which we obtained an OD ≥0.1.

We used 2-way analysis of variance and a paired 2-tailed Student *t*-test in Prism version 8.0.2 (GraphPad, https://www.graphpad.com) for statistical analyses between the pneumonic and nasopharyngeal groups. We performed animal experiments in accordance with recommendations in the Guide for the Care and Use of Laboratory Animals, National Research Council (https://www.nap.edu/read/12910). The study protocols were approved by the Institutional Animal Care and Use Committee at the University of Georgia (approval nos. A2016 02-010-Y3-A9 and A2016 04-019-Y3-A10).

Results

Nasopharyngeal Colonization
B. pertussis generally is considered to be specialized to its human host and to have lost the ability to efficiently colonize other animals (*29*). However, in a previous investigation, we noted that resident nasal microbiota in mice create a barrier to colonization and that perturbing the microbiota with antimicrobial drugs permitted low numbers of *B. pertussis* to efficiently colonize the nasal cavities (*30*). To repeat this experiment and demonstrate improved ability to colonize mice, we intranasally treated groups of C57BL/6 mice (n = 4) 3 times, at 8-hour intervals, with either 45 μg enrofloxacin in 10 μL PBS or PBS only for the control group. Twelve hours after the last treatment, we intranasally delivered 500 CFU of *B. pertussis* in 5 μL of PBS to localize the inoculum within the nasal cavity. After 3 day, no *B. pertussis* were recovered from the nasal cavities of PBS-treated control mice, but we found all mice treated with antimicrobial drugs were colonized with thousands of CFUs of *B. pertussis*, indicating that enrofloxacin treatment facilitated *B. pertussis* colonization (Figure 1, panel A). We performed a similar experiment using gentamicin, which showed a similar increase in *B. pertussis* colonization, indicating that the effect is not limited to enrofloxacin (Appendix Figure 2). We also found no notable difference in respiratory tract colonization at days 3 and 7 between C57Bl6/J and BALBC/J mice that were treated with antimicrobial drugs and inoculated (Appendix Figure 3), indicating that nasopharyngeal colonization largely was independent of the genetic background between the 2 mouse strains.

Further optimization experiments (Figure 1, panels B, C, D) showed that pretreatment with antimicrobial drugs reduced the infective dose from 10,000 CFU in untreated mice to <100 CFU in treated mice (Figure 1, panel B). The threshold for successful nasal colonization was 4.5–45 μg of enrofloxacin. Even a single enrofloxacin pretreatment allowed *B. pertussis* to efficiently colonize mice (Figure 1, panels C, D). We settled on this relatively simple single enrofloxacin pretreatment and LDLV inoculation regimen as the experimental nasopharyngeal inoculation model.

LDLV Nasopharyngeal Inoculation
We first assessed the course of infection in our model by comparing it with the conventional HDHV pneumonic model of *B. pertussis* infection. Groups of mice (4 per group) were either treated with enrofloxacin then nasopharyngeally inoculated with 500 CFU of *B. pertussis* in 5 μL PBS; or given the conventional
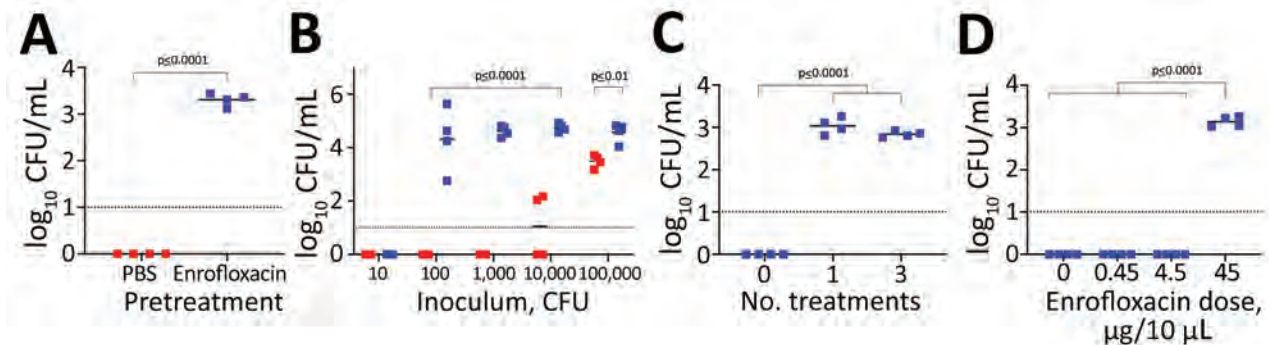
Figure 1. Susceptibility of mice to colonization by *Bordetella pertussis* after treatment with enrofloxacin. A, B) C57BL/6 mice were pretreated 3 times intranasally with 45 µg enrofloxacin in 10 µL (blue squares) or with phosphate-buffered saline (PBS; red squares) before being challenged with 5 µL PBS containing (A) 500 CFU of *B. pertussis*; or (B) *B. pertussis* ranging from 10–10,000 CFU. Colonization was assessed 3 days post inoculation by enumerating the number of *B. pertussis* CFU recovered from nasal cavities. C) Colonization and growth of *B. pertussis* at 500 CFU after 0, 1, and 2 pretreatments with 45 mg of enrofloxacin. D) *B. pertussis* colonization after intranasal enrofloxacin pretreatment at various doses. Each square represents a single biologic replicate. Dotted lines indicate limit of detection. Horizontal bars indicate mean.

HDHV pneumonic inoculation of 500,000 CFU of *B. pertussis* in 50 µL PBS. Both groups were sampled for >28 days (Figure 2, panel A). As usually observed in the HDHV pneumonic model, at day 3, *B. pertussis* had grown to large numbers in the lower respiratory tract of mice, but numbers were <10,000 CFU in the nasal cavities, and were undetectable in most HDHV mice by day 21, demonstrating more rapid clearance than is observed in human infections. In contrast, *B. pertussis* rarely reached the lungs of mice in the LDLV group (Figure 2, panel B), but *B. pertussis* numbers in the nasal cavity increased nearly 100-fold to ≈10,000 CFU and persisted at this level throughout the 28-day experiment (Figure 2, panel A). These data indicate that in the absence of lung infection, *B. pertussis* can efficiently colonize, grow, and persist in the nasopharynx.

Host Immune Response

The colonization profile of the nasopharyngeal (LDLV) model revealed profound differences in the dynamics of the infection compared with the pneumonic (HDHV) model, suggesting very different interactions with host immunity. We and others previously have shown that the large bolus of *B. pertussis* delivered into the lungs in the pneumonic infection model rapidly activates both innate and adaptive immune components to generate a robust immune response that clears *B. pertussis* infection in ≈4 weeks (*11,12*). However, this infection model is unlike natural human infection because of the extraordinarily severe pneumonic disease, the robustness of the immune response, and the speed of bacterial clearance. In contrast, delivery of low doses of *B. pertussis* limited to the nasopharynx, more like natural exposure, resulted in localized growth in the upper respiratory tract, where the pathogen persisted at higher numbers for much longer. This finding led us to hypothesize that this more natural mode of infection might enable *B. pertussis* to grow more gradually, the way it would naturally, and thereby provide a model system to study how it might avoid unnecessary stimulation

Figure 2. Growth and persistence of *Bordetella pertussis* in the nasal cavity of mice after low-dose–low-volume nasopharyngeal inoculation over time. C57BL/6 mice were inoculated intranasally with 500 CFU of *B. pertussis* in 5 µL phosphate-buffered saline for nasopharyngeal inoculations (blue squares) or 500,000 CFU in 50 µL for the pneumonic inoculations (red squares). The results were replicated in >4 study runs. *B. pertussis* colonization was assessed for the nasal cavities

(A) and the lungs (B). Dotted lines indicate limit of detection. Error bars indicate SD of the mean. Inoc., inoculation.
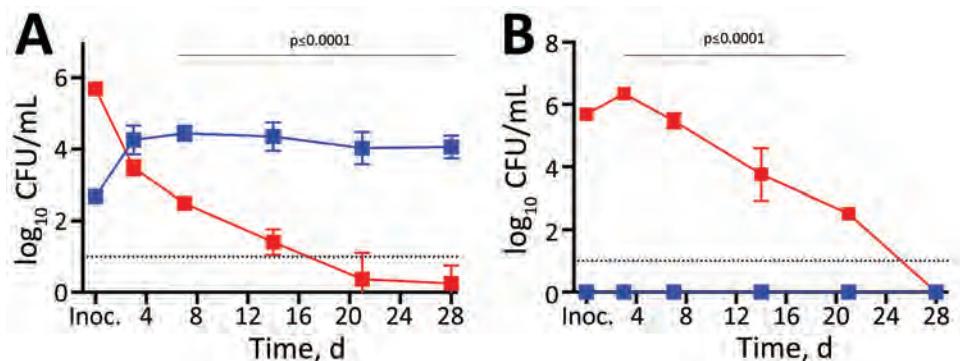
of host immunity to persist. To examine this hypothesis, we compared the relative proportions of major groups of immune cells in the lungs and nasopharyngeal washes on day 14 after HDHV pneumonic and LDLV nasopharyngeal inoculations.

Consistent with prior studies, the pneumonic infection model resulted in 5-fold to 50-fold increases in numbers of neutrophils (CD11b+/CD115–/Ly6G^{high}), T cells (CD45+/CD3+), B cells (CD45+/B220+), and natural killer cells (CD45+/CD3–/NK1.1+) in the lungs (Figure 3, panels A–D) and in the nasal cavities (Figure 3, panels E–H) relative to control mice. By comparison, we detected only modest increases (<2-fold) among some immune cell populations in LDLV-inoculated mice, despite having even higher numbers of *B. pertussis* in the nose at the time. These observations indicate that *B. pertussis* can grow from small inocula to large numbers in the nasopharynx with minimal immune response. HDHV pneumonic inoculations also resulted in a robust systemic immune response indicated by the numbers of splenocytes with significant induction of IL-17, IL-4, and IL-10 compared with uninfected naive mice (Figure 4). But low-dose nasopharyngeal inoculation did not result in measurable increases in cytokines. Together these data reveal substantial differences in the immune response to pneumonic versus nasopharyngeal infection models.

Persistent Nasopharyngeal Infection

A characteristic of pertussis in humans is the persistence of infection and disease lasting for many weeks or months; pertussis is also known as the 100-day cough. To compare persistence in the 2 contrasting infection models, we inoculated groups of C57Bl/6J mice to establish either nasopharyngeal (LDLV) or pneumonic (HDHV) infections. We then noted the presence or absence of *B. pertussis* in the nasal cavities (detection limit 10 CFU) on days 3, 7, 14, 28, 60, 90, and 120 postinoculation. For pneumonic infection models, the percentage of mice with bacteria recovered from the nasal cavities dropped from 100% on day 7 to 25% on day 28, after which bacteria were no longer detected (Figure 5, panel A). In contrast, LDLV nasopharyngeal inoculation resulted in more persistent infections; 100% of mice were still colonized at day 28 and 50% at day 60. Bacteria were still detected in 1/4 (25%) mice at day 90 and were only cleared from all mice 120 days after inoculation, highlighting the extraordinary persistence of this organism when delivered in more natural low dose and volume, and providing an experimental system in which to study its persistence.

As previously described for the HDHV pneumonic infection model, *B. pertussis* delivered to the lungs in large numbers induced a rapid increase in
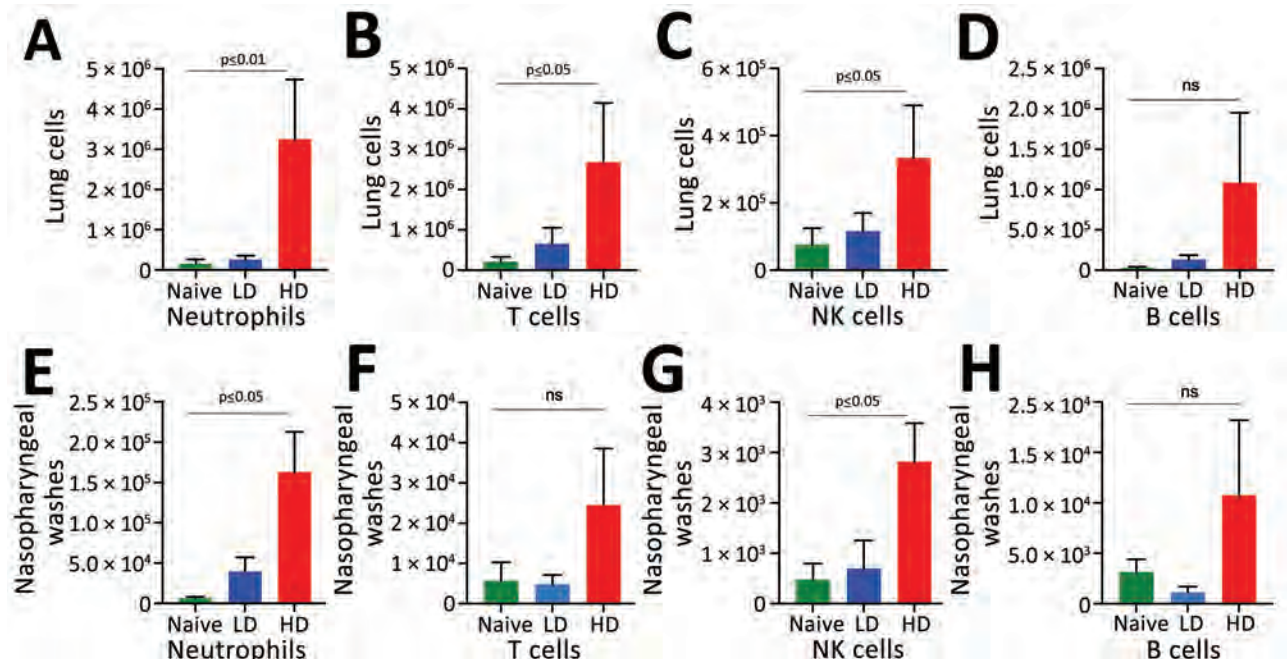
Figure 3. Host immune responses to LD and HD *Bordetella pertussis* inoculation. C57/Bl6 mice received LD of 500 CFU of *B. pertussis* in 5 µL phosphate-buffered saline (PBS) via nasopharyngeal inoculation or HD of 500,000 of *B. pertussis* CFU in 50 µL PBS via pneumonic inoculation. Naive control mice were inoculated with 50 µL of PBS. The study was conducted twice. A–D) Enumeration of immune cells in the lungs 14 days postinoculation. E–H) Enumeration of immune cells from nasopharyngeal washes. Error bars indicate SD for 4 biologic replicates HD, high-dose–high volume; LD, low-dose–low-volume; ns, no statistical significance.

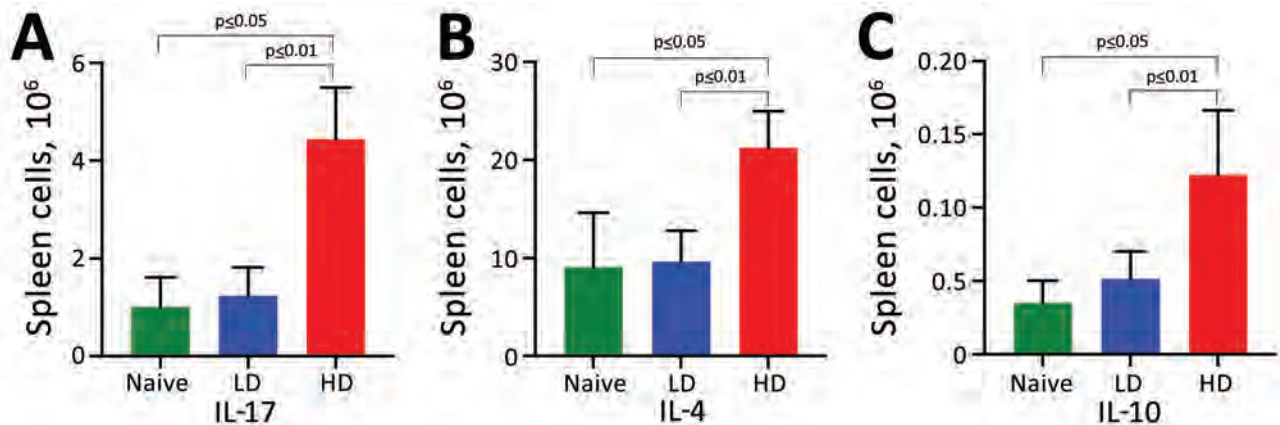**Figure 4.** Host cytokine responses to LD nasopharyngeal inoculation and HD pneumonic inoculation of *Bordetella pertussis.* C57/Bl6 mice received LD of 500 CFU of *B. pertussis* in 5 μL phosphate-buffered saline (PBS) via nasopharyngeal inoculation or HD of 500,000 of *B. pertussis* CFU in 50 μL PBS via pneumonic inoculation. Naive control mice were inoculated with 50 μL of PBS. Splenocytes were isolated from mice at day 14 postinoculation. A) IL-17; B) IL-4; and C) IL-10. Error bars indicate SD for 4 biologic replicates; analysis was conducted once. HD, high-dose–high volume; IL, interleukin; LD, low-dose–low-volume.

B. pertussis serum IgG titers to ≈10,000 by day 28 and to ≈20,000 by day 60 (Figure 5, panel B). As antibody titers rose, colonization levels dropped throughout the respiratory tract (Figure 5, panel A), consistent with the known roles of antibodies in clearing infection (*30*). Antibody titers continued to increase after the pathogen was cleared, contributing to the strong convalescent immunity associated with the conventional pneumonic model. In contrast, after LDLV nasopharyngeal inoculation, serum *B. pertussis* IgG levels were barely detectable even after months of persistent infection, reflecting the minimal induction, suppression, or both of host adaptive immunity by the pathogen. These lower antibody titers correlate with much slower control and clearance of

infection in the nasopharyngeal infection model and in natural infections.

Convalescent Immunity
Conventional HDHV pneumonic infections have been shown to induce robust protective immunity. However, LDLV nasopharyngeal inoculation resulted in more persistent infection and induced lower antibody titers, either because lower numbers of *B. pertussis* in the lungs are less immune stimulatory or because *B. pertussis* more effectively modulates the immune response when it follows this more natural course of infection. However, in both cases, infection eventually is cleared, indicating that adaptive immunity is generated and effective. To compare the
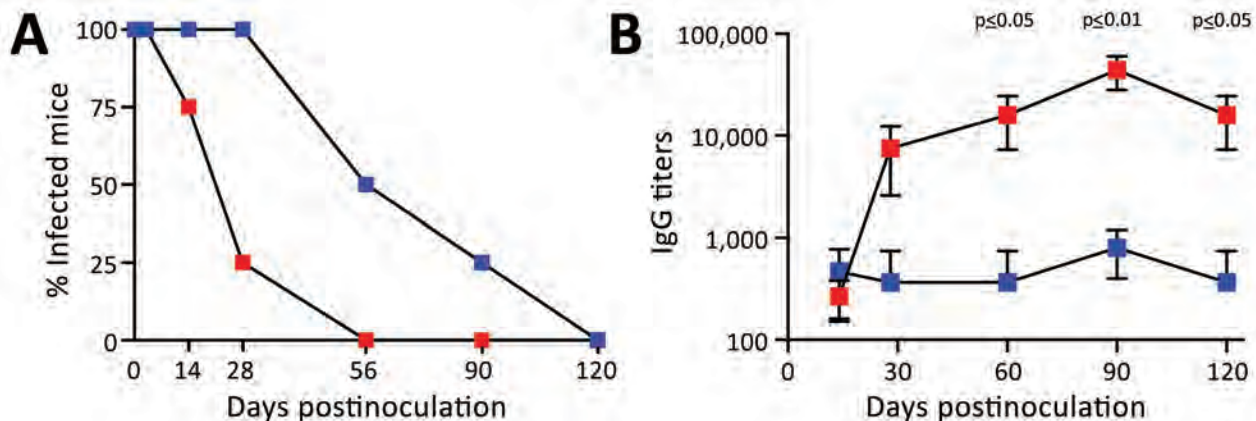
Figure 5. Comparison of serum IgG titers from mice receiving LD nasopharyngeal inoculation and HD pneumonic inoculation of *Bordetella pertussis.* Blue squares indicate LD mice; red squares indicate HD mice. C57/Bl6 mice received LD of 500 CFU of *B. pertussis* in 5 μL phosphate-buffered saline (PBS) via nasopharyngeal inoculation or HD of 500,000 of *B. pertussis* CFU in 50 μL PBS via pneumonic inoculation. Error bars indicate SD for 4 biologic replicates. A) Percentage of mice (4 per group) colonized on days 3, 7, 14, 28, 60, 90, and 120 following inoculations. Studies on days 3, 7, 14, and 28 were conducted 4 times; the 120-day experiment was conducted once. B) *B. pertussis* IgG titers in serum over time. HD, high-dose–high volume; LD, low-dose–low-volume.

Figure 6. Risk for *Bordetella pertussis* reinfection after experimental nasopharyngeal infection of mice. C57Bl/6J mice were inoculated intranasally with 500 CFU of *B. pertussis* in 5 µL PBS for nasopharyngeal inoculations (blue squares) or 500,000 CFU in 50 µL for the pneumonic inoculations (red squares). The study was conducted twice. Values are the SD of 4 biologic replicates. A) Number of *B. pertussis* bacteria in respiratory organs on day 7 after pneumonic challenge. B) *B. pertussis* IgG titers (log scale) in the serum of mice challenged via PNC or NPL inoculation. Green represents naive mice inoculated with PBS. NPL, nasopharyngeal; PBS, phosphate-buffered saline; PNC, pneumonic.
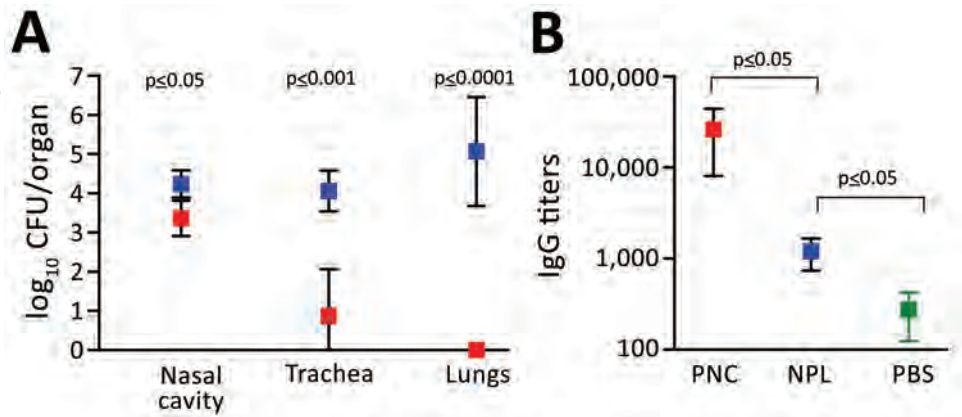
relative efficacy of convalescent immunity induced by the 2 infection models, we examined the protection each conferred against subsequent challenge.

Mice convalescing from prior pneumonic infection rapidly cleared a high-dose pneumonic challenge from the lungs and reduced numbers in the nasal cavity by >90% within 7 days (Figure 6, panel A), as previously documented (*32,33*). These mice showed no signs of disease, and bacterial numbers were far lower than those for unvaccinated mice challenged with the same dose (Figure 2, panel B), demonstrating that prior pneumonic infection confers protection against disease. In striking contrast, mice convalescing from prior low-dose nasopharyngeal inoculation had much higher numbers of *B. pertussis* in all respiratory organs. This finding shows that mice convalescing from nasopharyngeal infection fail to prevent subsequent colonization and bacterial growth when challenged with artificially large and deep lung pneumonic inoculation. These results agree with the corresponding serum antibody titers measured (Figure 6, panel B) and reveal profoundly different protective immunity induced by nasopharyngeal infection than described in previous studies that used the conventional HDHV pneumonic infection model (*24,32*).

Vaccination Effects on Colonization

Although pneumonic models were central in developing aP vaccines that prevent severe disease, these assays of extreme pneumonic virulence failed to reveal the limited protection that aP vaccines provide against less severe upper respiratory tract colonization (*6,7*). Thus, these models did not predict the current problem of *B. pertussis* reemergence. Therefore,

we set out to test whether the LDLV nasopharyngeal model might enable us to measure the failure of the aP vaccines and provide an assay system in which improved vaccines could be developed. For our vaccination experiments, we used the intraperitoneal delivery route, which is convenient and known to confer robust protection. Groups of mice that were vaccinated with either wP or aP vaccine, and unvaccinated control mice, were challenged via LDLV nasopharyngeal inoculation. wP-vaccinated mice were substantially protected against nasal colonization and had few or no bacteria remaining by day 7 after challenge (Figure 7). In contrast, *B. pertussis* colonized and
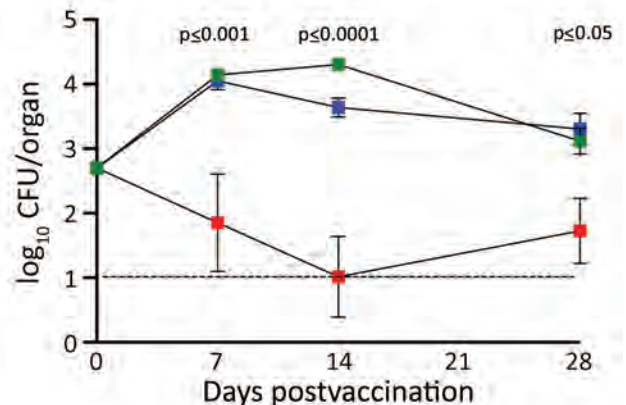
Figure 7. Comparison of nasal cavity colonization of *Bordetella pertussis* among experimentally infected mice after intraperitoneal vaccination with acellular pertussis (aP) or whole-cell pertussis (wP) vaccine. Graph compares colonization profiles over 28 days. Green squares indicate naive mice; blue squares indicate mice vaccinated with aP; red squares indicate mice vaccinated wP. Error bars indicate SD of the mean for 4 biologic replicates. The study was conducted twice; results are shown for a single experiment. Dotted line indicates limit of detection. p values indicate statistically significant differences between aP- and wP-vaccinated mice.

grew in the nasal cavities of aP-vaccinated animals nearly as efficiently as in naive animals. These results demonstrate that aP vaccination fails to prevent nasopharyngeal colonization in this experimental system. This approach can measure the differences between wP and aP vaccines in this regard, providing an assay in which to evaluate various proposed new vaccines that might prevent colonization better than current aP vaccines (*34,35*).

Discussion

Inoculating animals with high doses of *B. pertussis* delivered deep into the lungs (HDHV) induces severe pathology in the lower respiratory tract of rodents and baboons (*36*). Postmortem descriptions of lung pathology in 8 human infants who died from infantile pertussis revealed marked leukocytosis and pulmonary hypertension (*37*), features replicated in mouse and baboon pneumonic models (*36,38,39*), suggesting that these conventional pneumonic infection models reasonably replicate the most extreme form of human disease. However, these cases are extreme; pertussis generally is described as a disease of the upper respiratory tract that induces relatively little inflammation and histopathology (*40,41*) and often could occur with minimal symptoms and go undiagnosed (*25*). *B. pertussis* is highly infectious to humans, indicating that small numbers of bacteria landing in the upper respiratory tract can efficiently colonize, grow, and spread. However, conventional pneumonic infection models bypass the need to efficiently attach and establish the first microcolony, then grow and spread from there to other sites, potentially suppressing both the initial inflammatory response and the subsequent adaptive immune response. These aspects of the infectious process have not been well simulated in the HDHV pneumonic model, making it difficult to study and understand them.

We observed that localized application of antimicrobial drugs consistently enabled small numbers of *B. pertussis* to efficiently colonize, grow, and establish persistent infections in the nasopharynx of mice, mimicking the early stages of natural infection. Despite the efficient colonization and growth to higher and more sustained numbers in the nasal cavity, we detected only a modest (<2-fold) responses among immune cell populations. Furthermore, infections remained localized to the upper respiratory tract and rarely progressed to the lungs, agreeing with the notion that pertussis is primarily an upper respiratory tract infection. Of note, multiple contact tracing studies identify asymptomatic carriage as the likely source of human infections (*42*). In addition, the strong inflammatory responses and high antibody titers observed in pneumonic infection models are not routinely observed in most surveys of human infections (*43–45*).

Both wP and aP vaccines prevent severe pneumonic disease in HDHV pneumonic infection experimental models in rodents and primates, and both prevent severe disease in humans. However, consensus is growing that aP vaccines fail to prevent colonization and transmission, aspects of the infection process that are poorly simulated in the pneumonic infection model. Our findings for the novel LDLV nasopharyngeal infection system show that aP vaccines provide much less protection against colonization by small numbers of *B. pertussis* compared with wP vaccines. Thus, the LDLV nasopharyngeal infection model provides a complementary experimental system that enables the study of aspects of infection that are poorly mimicked in the HDHV pneumonic infection model. Further study of contemporary circulating *B. pertussis* strains in the context of low-dose nasopharyngeal infections could help define the factors that contribute to the diverse mechanisms by which *B. pertussis* evades immune responses. Such studies could elucidate how *B. pertussis* is able to colonize, grow, shed, and be efficiently spread from host to host within aP-vaccinated populations. Furthermore, our model can guide development of new vaccines that can overcome the limitations of current aP vaccines and better control the circulation of this reemerging pathogen.

About the Author

Dr. Soumana was a postdoctoral scholar in the laboratory of Dr. Harvill in the Department of Infectious Diseases, College of Veterinary Medicine, University of Georgia, Athens, Georgia, USA, when this work was conducted. He currently works in the Department of Medicine in the University of British Columbia, Vancouver, BC, Canada. His research interest lies in examining the contributions of respiratory microbiota on pathogenesis and disease.

References

1. Roush SW, Murphy TV; Vaccine-Preventable Disease Table Working Group. Historical comparisons of morbidity and mortality for vaccine-preventable diseases in the United States. JAMA. 2007;298:2155–63. https://doi.org/10.1001/jama.298.18.2155

2. Klein NP. Licensed pertussis vaccines in the United States. History and current state. Hum Vaccin Immunother. 2014;10:2684–90. https://doi.org/10.4161/hv.29576

3. Centers for Disease Control and Prevention. National notifiable disease surveillance, 2019 [cited 2021 Jul 2]. https://www.cdc.gov/pertussis/surv-reporting.html

4. Hozbor D, Mooi F, Flores D, Weltman G, Bottero D, Fossati S, et al. Pertussis epidemiology in Argentina: trends over 2004–2007. J Infect. 2009;59:225–31. https://doi.org/10.1016/j.jinf.2009.07.014

5. Daniels HL, Sabella C. *Bordetella pertussis* (Pertussis). Pediatr Rev. 2018;39:247–57. https://doi.org/10.1542/pir.2017-0229

6. Warfel JM, Zimmerman LI, Merkel TJ. Acellular pertussis vaccines protect against disease but fail to prevent infection and transmission in a nonhuman primate model. Proc Natl Acad Sci U S A. 2014;111:787–92. https://doi.org/10.1073/pnas.1314688110

7. Smallridge WE, Rolin OY, Jacobs NT, Harvill ET. Different effects of whole-cell and acellular vaccines on *Bordetella* transmission. J Infect Dis. 2014;209:1981–8. https://doi.org/10.1093/infdis/jiu030

8. Redhead K, Watkins J, Barnard A, Mills KH. Effective immunization against *Bordetella pertussis* respiratory infection in mice is dependent on induction of cell-mediated immunity. Infect Immun. 1993;61:3190–8. https://doi.org/10.1128/IAI.61.8.3190-3198.1993

9. Barnard A, Mahon BP, Watkins J, Redhead K, Mills KH. Th1/Th2 cell dichotomy in acquired immunity to *Bordetella pertussis*: variables in the in vivo priming and in vitro cytokine detection techniques affect the classification of T-cell subsets as Th1, Th2 or Th0. Immunology. 1996;87:372–80. https://doi.org/10.1046/j.1365-2567.1996.497560.x

10. McGuirk P, Mills KH. A regulatory role for interleukin 4 in differential inflammatory responses in the lung following infection of mice primed with Th1- or Th2-inducing pertussis vaccines. Infect Immun. 2000;68:1383–90. https://doi.org/10.1128/IAI.68.3.1383-1390.2000

11. Leef M, Elkins KL, Barbic J, Shahin RD. Protective immunity to *Bordetella pertussis* requires both B cells and CD4(+) T cells for key functions other than specific antibody production. J Exp Med. 2000;191:1841–52. https://doi.org/10.1084/jem.191.11.1841

12. Kirimanjeswara GS, Agosto LM, Kennett MJ, Bjornstad ON, Harvill ET. Pertussis toxin inhibits neutrophil recruitment to delay antibody-mediated clearance of *Bordetella pertussis*. J Clin Invest. 2005;115:3594–601. https://doi.org/10.1172/JCI24609

13. Higgins SC, Jarnicki AG, Lavelle EC, Mills KH. TLR4 mediates vaccine-induced protective cellular immunity *to Bordetella pertussis*: role of IL-17-producing T cells. J Immunol. 2006;177:7980–9. https://doi.org/10.4049/jimmunol.177.11.7980

14. Wolfe DN, Kirimanjeswara GS, Goebel EM, Harvill ET. Comparative role of immunoglobulin A in protective immunity against the Bordetellae. Infect Immun. 2007;75:4416–22. https://doi.org/10.1128/IAI.00412-07

15. Andreasen C, Powell DA, Carbonetti NH. Pertussis toxin stimulates IL-17 production in response to *Bordetella pertussis* infection in mice. PLoS One. 2009;4:e7079. https://doi.org/10.1371/journal.pone.0007079

16. Andreasen C, Carbonetti NH. Role of neutrophils in response to *Bordetella pertussis* infection in mice. Infect Immun. 2009;77:1182–8. https://doi.org/10.1128/IAI.01150-08

17. Zhang X, Goel T, Goodfield LL, Muse SJ, Harvill ET. Decreased leukocyte accumulation and delayed *Bordetella pertussis* clearance in IL-6-/- mice. J Immunol. 2011;186:4895–904. https://doi.org/10.4049/jimmunol.1000594

18. Alvarez Hayes J, Erben E, Lamberti Y, Ayala M, Maschi F, Carbone C, et al. Identification of a new protective antigen of *Bordetella pertussis*. Vaccine. 2011;29:8731–9. https://doi.org/10.1016/j.vaccine.2011.07.143

19. Henderson MW, Inatsuka CS, Sheets AJ, Williams CL, Benaron DJ, Donato GM, et al. Contribution of *Bordetella* filamentous hemagglutinin and adenylate cyclase toxin to suppression and evasion of interleukin-17-mediated inflammation. Infect Immun. 2012;80:2061–75. https://doi.org/10.1128/IAI.00148-12

20. Sato Y, Izumiya K, Sato H, Cowell JL, Manclark CR. Aerosol infection of mice with *Bordetella pertussis*. Infect Immun. 1980;29:261–6. https://doi.org/10.1128/IAI.29.1.261-266.1980

21. Xing DK, Das RG, Williams L, Canthaboo C, Tremmil J, Corbel MJ. An aerosol challenge model of *Bordetella pertussis* infection as a potential bioassay for acellular pertussis vaccines. Vaccine. 1999;17:565–76. https://doi.org/10.1016/S0264-410X(98)00235-7

22. Warfel JM, Beren J, Kelly VK, Lee G, Merkel TJ. Nonhuman primate model of pertussis. Infect Immun. 2012;80:1530–6. https://doi.org/10.1128/IAI.06310-11

23. Warfel JM, Beren J, Merkel TJ. Airborne transmission of *Bordetella pertussis*. J Infect Dis. 2012;206:902–6. https://doi.org/10.1093/infdis/jis443

24. Higgs R, Higgins SC, Ross PJ, Mills KH. Immunity to the respiratory pathogen *Bordetella pertussis*. Mucosal Immunol. 2012;5:485–500. https://doi.org/10.1038/mi.2012.54

25. Gill CJ, Gunning CE, MacLeod WB, Mwananyanda L, Thea DM, Pieciak RC, et al. Asymptomatic Bordetella pertussis infections in a longitudinal cohort of young African infants and their mothers. Elife. 2021;10:e65663. https://doi.org/10.7554/eLife.65663

26. Halim TYF, Takei F. Isolation and characterization of mouse innate lymphoid cells. Curr. Protoc. Immunol. 2014; 106:3.25.1–13. PubMed https://doi.org/10.1002/0471142735.im0325s106

27. Cossarizza A, Chang HD, Radbruch A, Akdis M, Andrä I, Annunziato F, et al. Guidelines for the use of flow cytometry and cell sorting in immunological studies. Eur J Immunol. 2017;47:1584–797. https://doi.org/10.1002/eji.201646632

28. Mann P, Goebel E, Barbarich J, Pilione M, Kennett M, Harvill E. Use of a genetically defined double mutant strain of *Bordetella bronchiseptica* lacking adenylate cyclase and type III secretion as a live vaccine. Infect Immun. 2007;75:3665–72. https://doi.org/10.1128/IAI.01648-06

29. Mattoo S, Cherry JD. Molecular pathogenesis, epidemiology, and clinical manifestations of respiratory infections due to *Bordetella pertussis* and other Bordetella subspecies. Clin Microbiol Rev. 2005;18:326–82. https://doi.org/10.1128/CMR.18.2.326-382.2005

30. Weyrich LS, Feaga HA, Park J, Muse SJ, Safi CY, Rolin OY, et al. Resident microbiota affect *Bordetella pertussis* infectious dose and host specificity. J Infect Dis. 2014;209:913–21. https://doi.org/10.1093/infdis/jit597

31. Kirimanjeswara GS, Mann PB, Harvill ET. Role of antibodies in immunity to *Bordetella* infections. Infect Immun. 2003;71:1719–24. https://doi.org/10.1128/IAI.71.4.1719-1724.2003

32. Wilk MM, Allen AC, Misiak A, Borkner L, Mills KH. The immunology of *Bordetella pertussis* infection and vaccination. In: Rohani P, Scarpino SV editors. Pertussis: epidemiology, immunology, and evolution. Oxford: Oxford University Press; 2019. p. 42–65.

33. Mills KH, Ryan M, Ryan E, Mahon BP. A murine model in which protection correlates with pertussis vaccine efficacy in children reveals complementary roles for humoral and cell-mediated immunity in protection against *Bordetella pertussis.* Infect Immun. 1998;66:594–602. https://doi.org/10.1128/IAI.66.2.594-602.1998

34. Ausiello CM, Cassone A. Acellular pertussis vaccines and pertussis resurgence: revise or replace? MBio. 2014;5: e01339-14. https://doi.org/10.1128/mBio.01339-14

35. Dewan KK, Linz B, DeRocco SE, Harvill ET. Acellular pertussis vaccine components: today and tomorrow. Vaccines (Basel). 2020;8:217. https://doi.org/10.3390/vaccines8020217

36. Zimmerman LI, Papin JF, Warfel J, Wolf RF, Kosanke SD, Merkel TJ. Histopathology of *Bordetella pertussis* in the baboon model. Infect Immun. 2018;86:e00511-18. https://doi.org/10.1128/IAI.00511-18

37. Paddock CD, Sanden GN, Cherry JD, Gal AA, Langston C, Tatti KM, et al. Pathology and pathogenesis of fatal *Bordetella pertussis* infection in infants. Clin Infect Dis. 2008;47:328–38. https://doi.org/10.1086/589753

38. Pittman M, Furman BL, Wardlaw AC. *Bordetella pertussis* respiratory tract infection in the mouse: pathophysiological responses. J Infect Dis. 1980;142:56–66. https://doi.org/10.1093/infdis/142.1.56

39. Scanlon KM, Snyder YG, Skerry C, Carbonetti NH. Fatal pertussis in the neonatal mouse model is associated with pertussis toxin-mediated pathology beyond the airways. Infect Immun. 2017;85:e00355-17. https://doi.org/10.1128/IAI.00355-17

40. Cherry JD. Pertussis: challenges today and for the future. PLoS Pathog. 2013;9:e1003418. https://doi.org/10.1371/journal.ppat.1003418

41. Cherry JD. The history of pertussis (whooping cough); 1906–2015: facts, myths, and misconceptions. Curr Epidemiol Rep. 2015;2:120–30. https://doi.org/10.1007/s40471-015-0041-9

42. Craig R, Kunkel E, Crowcroft NS, Fitzpatrick MC, de Melker H, Althouse BM, et al. Asymptomatic infection and transmission of pertussis in households: a systematic review. Clin Infect Dis. 2020;70:152–61. https://doi.org/10.1093/cid/ciz531

43. Müller FM, Hoppe JE, Wirsing von König CH. Laboratory diagnosis of pertussis: state of the art in 1997. J Clin Microbiol. 1997;35:2435–43. https://doi.org/10.1128/JCM.35.10.2435-2443.1997

44. Watanabe M, Connelly B, Weiss AA. Characterization of serological responses to pertussis. Clin Vaccine Immunol. 2006;13:341–8. https://doi.org/10.1128/CVI.13.3.341-348.2006

45. Lee AD, Cassiday PK, Pawloski LC, Tatti KM, Martin MD, Briere EC, et al.; Clinical Validation Study Group. Clinical evaluation and validation of laboratory methods for the diagnosis of *Bordetella pertussis* infection: culture, polymerase chain reaction (PCR) and anti-pertussis toxin IgG serology (IgG-PT). PLoS One. 2018;13:e0195979. https://doi.org/10.1371/journal.pone.0195979

Address for correspondence: Kalyan Dewan, Department of Infectious Diseases, College of Veterinary Medicine, University of Georgia, Athens, GA 30602, USA; email: kaldew@uga.edu

Spotted Fever Group Rickettsioses in Israel, 2010–2019

Regev Cohen, Talya Finn, Frida Babushkin, Yael Paran, Ronen Ben Ami, Alaa Atamna,
Sharon Reisfeld, Gabriel Weber, Neta Petersiel, Hiba Zayyad, Eyal Leshem, Miriam Weinberger,
Yasmin Maor, Nicola Makhoul, Lior Nesher, Galia Zaide, Dar Klein, Adi Beth-Din, Yafit Atiya-Nasagi

In a multicenter, nationwide, retrospective study of patients hospitalized with spotted fever group rickettsiosis in Israel during 2010–2019, we identified 42 cases, of which 36 were autochthonous. The most prevalent species was the *Rickettsia conorii* Israeli tick typhus strain (n = 33, 79%); infection with this species necessitated intensive care for 52% of patients and was associated with a 30% fatality rate. A history of tick bite was rare, found for only 5% of patients; eschar was found in 12%; and leukocytosis was more common than leukopenia. Most (72%) patients resided along the Mediterranean shoreline. For 3 patients, a new *Rickettsia* variant was identified and had been acquired in eastern, mountainous parts of Israel. One patient had prolonged fever before admission and clinical signs resembling tickborne lymphadenopathy. Our findings suggest that a broad range of *Rickettsia* species cause spotted fever group rickettsiosis in Israel.

Spotted fever group rickettsioses (SFGRs) are arthropodborne diseases caused by obligate intracellular, gram-negative bacteria of the genus *Rickettsia*.

Author affiliations: Laniado Hospital, Netanya, Israel (R. Cohen, T. Finn, F. Babushkin); Technion–Israel Institute of Technology, Haifa, Israel (R. Cohen, T. Finn, S. Reisfeld, G. Weber); Tel-Aviv Sourasky Medical Centre, Tel-Aviv, Israel (Y. Paran, R. Ben Ami); Tel Aviv University, Tel Aviv (Y. Paran, R. Ben Ami, A. Atamna, E. Leshem, M. Weinberger, Y. Maor); Rabin Medical Centre, Petah-Tikva, Israel (A. Atamna); Hillel Yaffe Medical Centre, Hadera, Israel (S. Reisfeld); Carmel Medical Centre, Haifa (G. Weber); Rambam Medical Centre, Haifa (N. Petersiel); Padeh Poriya Medical Centre, Tiberias, Israel (H. Zayyad); Bar Ilan University, Safed, Israel (H. Zayyad, N. Makhoul); Sheba Medical Centre, Ramat Gan, Israel (E. Leshem); Shamir (formerly Assaf Harofeh) Medical Center, Zerifin, Israel (M. Weinberger); Edith Wolfson Medical Centre, Holon, Israel (Y. Maor); Galilee Medical Centre, Nahariya, Israel (N. Makhoul); Soroka Medical Centre, Beer Sheba, Israel (L. Nesher); Ben-Gurion University of the Negev, Beer Sheba (L. Nesher); Israel Institute for Biological Research, Ness Ziona, Israel (G. Zaide, D. Klein, A. Beth-Din, Y. Atiya-Nasagi)

SFGRs are associated with ≈20 species of *Rickettsia*, of which 16 are considered human pathogens (*1,2*). Recent introduction of molecular methods provided more information about SFGR agents causing human disease and enabled their identification, for which the clinical significance of some remains lacking (*3*). *R. conorii* complex, the etiologic agent of Mediterranean spotted fever, includes 4 strains: *R. conorii* Malish (cause of Mediterranean spotted fever), *R. conorii* Astrakhan (cause of Astrakhan fever), *R. conorii* Indian tick typhu*s* (cause of Indian tick typhus), and *R. conorii* Israeli tick typhus strain (ITTS, cause of Israeli spotted fever [ISF]) (*4–7*).

ISF begins as fever followed by a maculopapular rash, usually involving the palms and soles and frequently accompanied by systemic symptoms. Most cases are self-limiting, but some may lead to organ failure and death. Clinical and epidemiologic presentations caused by other strains of rickettsiae may vary (*5,8–11*). Studies from Portugal indicate that compared with Mediterranean spotted fever, ISF is characterized by lower rates of eschar and tick-exposure history, higher frequency of gastrointestinal symptoms, and greater severity of illness with a high case-fatality rate (*10,12,13*). Case-fatality rates in Israel before 1998 were reportedly 0.7%, but incidence in some years (e.g., 1997) was higher (3.5%) (*14*). Since 1998, several case reports of fatal SFGR in Israel have been published (*9,15–17*), along with reports of 22 other patients with sepsis requiring hospitalization (*9,17–22*). Of these, isolates from only 3 patients were sequenced and identified as *R. conorii* ITTS; 2 of these patients exhibited purpura fulminans and all 3 died (*9,15*). Few studies of ISF have been conducted in Israel; most were conducted during the 1990s and relied on serologic diagnostic methods that cannot differentiate between the SFGRs (*23*). In Israel, SFGR is a notifiable disease, and in recent years, incidence has increased; 51 cases (including 7 deaths) were reported to the Israeli Ministry of Health in 2017, compared

with the average yearly incidence of 26 cases during 2014–2016 (24).

The etiology of SFGR in Israel is thought to be *R. conorii* ITTS on the basis of limited molecular identification of this strain from clinical cases and from ticks (9,15,25). However, the yearly variations in disease severity and clinical manifestations are intriguing and may suggest involvement of >1 species of spotted fever group (SFG) *Rickettsia*. Using a large database from the national reference center, we studied the specific species of *Rickettsia* that cause SFGRs in Israel and characterized their unique epidemiology and clinical features. Institutional review board approval was granted at the principal investigator site (0002-19-LND) and for each participating institute.

Methods

Study Design
We conducted a multicenter, retrospective study of hospitalized patients with an SFGR during 2010–2019. The study included SFGR diagnosed by molecular methods at the Israel Institute for Biological Research (IIBR; Ness Ziona, Israel), which serves as the national reference center for *Rickettsia*. Blood and tissue samples from hospitalized patients with a suspected SFGR are occasionally submitted to the IIBR for molecular diagnosis, at the discretion of the treating physician. For cases of successful molecular identification, the referring medical center was requested to provide patient demographic and clinical data from the medical charts at each participating site. Deidentified data were integrated into a central database.

Serology and Molecular Diagnoses
The IIBR tested serum samples for antibodies against *R. conorii* and *R. typhi* by an in-house immunofluorescence assay (cutoff for IgG of 1:100), as previously described (26). Skin biopsy samples, whole blood, cerebrospinal fluid, and other tissues were tested by PCR (17,27). Stored SFG-positive *Rickettsia* DNA samples and sequenced unique regions from 4 conserved *Rickettsia* genes were batch tested (primers listed in Table 1). *R. africae* was identified by real-time PCR targeting an internal transcribed spacer (30). These analyses enabled identification of ISF, *R. africae, R. conorii* Malish strain, and a new *Rickettsia* variant. Each set of reactions included a positive control and nontemplate as a negative control. The same primers were used for sequencing as for amplification. For species-level identification, we compared sequence results by using BLAST (http://www.ncbi.nlm.nih.gov/BLAST).

Mapping Locations of SFGR Acquisition
We recorded the site of presumed rickettsiosis acquisition for autochthonous cases. When the site was unknown, we used the patient's address.

Statistical Analyses
We used descriptive statistics to summarize patient characteristics. We calculated differences between categorical and continuous variables by using Pearson χ^2, Student t, and Mann-Whitney tests, as appropriate. We used 1-way analysis of variance to analyze differences among groups. For statistical analyses, we used SPSS Statistics 25 (https://www.ibm.com). We considered 2-sided p<0.05 to be significant.

Table 1. Oligonucleotide primers used for PCR amplification and sequencing of *Rickettsia* species in study of spotted fever group rickettsioses in Israel, 2010–2019*

Primer	Target gene	Primer sequence, 5′ → 3′
213F	*OmpA*	AATCAATATTGGAGCCGGTAA
667R	*OmpA*	ATTTGCATCAATCGTATAAGTAGC
120F	*OmpA*	AAGGAGCTATAGCAAACGGCA
760R	*OmpA*	TATCAGGGTCTATATTCGCACCTA
760newF	*OmpA*	TAGGTGCGAATATAGACCCTGATA
1231R	*OmpA*	TGGCAATAGTTACATTTCCTGCAC
373F	*gltA*	TTGTAGCTCTTCTCATCCTATGGC
1138R	*gltA*	CATTTGCGACGGTATACCCATA
Rico173F	*gltA*	CGACCCGGGTTTTATGTCTA
1179R	*gltA*	TCCAGCCTACGATTCTTGCTA
gltA_EXT_R	*gltA*	TACTCTCTATGTACATAACCGGTG
gltA_NES_F	*gltA*	ATGATTGCTAAGATACCTACCATC
1497_R	*OmpB*	CCTATATCGCCGGTAATT
3462_F	*OmpB*	CCACAGGAACTACAACCATT
4346_R	*OmpB*	CGAAGAAGTAACGCTGACTT
607_F	*OmpB*	AATATCGGTGACGGTCAAGG
D1390R	*Sca4*	CTTGCTTTTCAGCAATATCAC
D767F	*Sca4*	CGATGGTAGCATTAAAAGCT

*All primers were designed at the Israel Institute for Biological Research (Ness Ziona, Israel), except Rico173F (25), rickettsial *OmpB* primers (28), and *sca4* primers (29).

Results

SFGR Cases Diagnosed by IIBR in the Past Decade
In the 10-year study period, 1,985 cases of rickettsioses from the community and hospitals countrywide were diagnosed at IIBR by serologic testing; 811 were SFGR and 1,174 were murine typhus. Another 89 cases were positive by PCR, 66 for SFGR and 23 for murine typhus (Figure 1, panels A, B). Comparing 2010–2014 with 2015–2019 indicated an increased number of serologic tests performed yearly (from an average of ≈2,000 to ≈6,500). The percentage of positive serologic results decreased from 3% in 2010–2013 to 1.2% in 2014–2016 and then increased again to 2% in 2017–2019. Concomitantly, a 4-fold increase in total PCR tests performed was accompanied by a 7-fold increase in positive PCR results (average of 2.2–15.6 positive cases/year in the 2 periods). Of the 66 SFGR cases positive by PCR, 42 (64%) were identified to the strain level; for the other 24 cases, the classification failed, probably because of a low number of DNA copies in the original sample.

Rickettsia Strains
The most prevalent *Rickettsia* strain in this study was *R. conorii* ITTS, found in 33/42 (79%) of cases identified to the strain level. The other strains accounted for 4 cases of *R. africae* infection, 2 of *R. conorii* Malish strain infection, and 3 of the newly identified *Rickettsia* variant (27). Most (36/42, 86%) cases were autochthonous: 32/36 (89%) were caused by *R. conorii* ITTS, 1 by *R. conorii* Malish strain, and the remaining 3 by the new *Rickettsia* variant (Figure 1, panel B). The 6 imported cases included 4 infections with *R. africae*, all acquired during a safari (in South Africa, Mozambique, Zimbabwe, or Botswana); 1 *R. conorii* ITTS imported from Cyprus; and 1 *R. conorii* Malish strain imported from New Delhi, India.

Molecular diagnosis was performed from skin biopsy samples from 27 patients (19 with ISF, 3 with new *Rickettsia* variant infection, 1 with *R. conorii* Malish strain infection, and 4 with African tick bite fever [ATBF]); from the blood of 19 patients (16 with ISF, 2 with *R. conorii* Malish strain, and 1 with new *Rickettsiae* variant); and from cerebrospinal fluid, lymph node, and liver biopsy postmortem samples from 1 patient with ISF. Seven patients were positive by PCR of samples from >1 source, mostly skin biopsy and whole blood. Serologic testing was performed for 36/42 (86%) patients; results were available for 26. Of these, results were negative for 16 (61%) and the median time between disease onset to last serology test was 6.2 days (range 0–11 days); for 10 (39%), the result was either positive (5 patients) or borderline (5 patients) and median time from disease onset to last serologic test 15.5 days (range 2–29 days).

Geographic and Seasonal Distribution of Cases
The 36 autochthonous cases were reported from 12 hospitals representing most areas of Israel: 6 from central Israel, 4 from northern Israel, and 2 from southern Israel. *R. conorii* ITTS was reported from all but 1 hospital. All cases of *R. africae* infection were reported from 1 hospital. The most abundant concentration of cases (26/36, 72%, all *R. conorii* ITTS) was along the Mediterranean shoreline, with the highest aggregation of cases in the Sharon and Haifa districts (Figure 2, panel A). Ten cases were acquired inland, of which 6 were caused by *R. conorii* ITTS and 3 the new *Rickettsia* variant. Those 3 cases were presumably acquired in more mountainous areas of Israel. The *R. conorii* Malish strain was acquired in the desert region near Beer-Sheba.

Nearly half (27/61, 44%) of SFGR cases occurred during the 3 summer months, peaking in August. For the other seasons, 24% were recorded in the fall, 24% in spring, and 8% in winter.
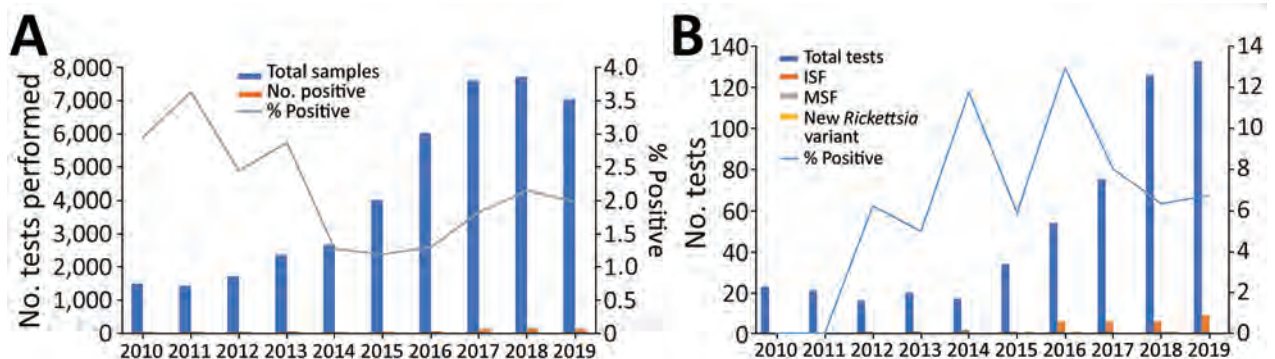

Figure 1. Spotted fever group rickettsioses, Israel, 2010–2019. A) Serologic tests performed in the Israeli central laboratory for rickettsiosis and number of positive cases per year. B) Autochthonous cases identified to the strain level. ISF, Israeli spotted fever; MSF, Mediterranean spotted fever.
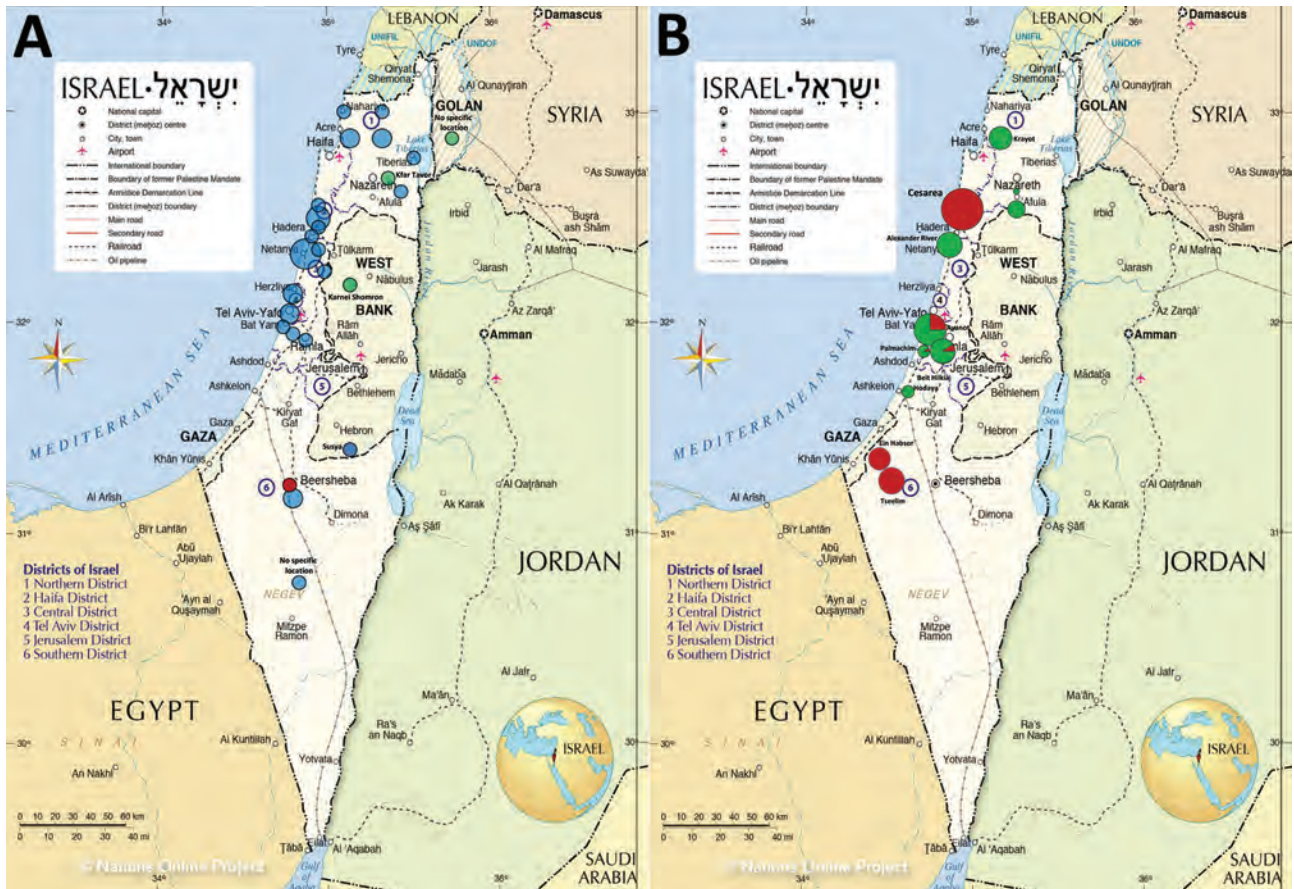
Figure 2. Geography of spotted fever group rickettsioses, Israel, 2010–2019. A) Presumed areas of autochthonous infection acquisition (n = 36 cases). B) Tick collection sites and tick species collected during 2014 by Rose et al. (*31*). ISF, Israeli spotted fever; MSF, Mediterranean spotted fever. Source: Nations Online Project (https://www.nationsonline.org).

Patient Characteristics and Demographics

Median patient age was 50.5 years (interquartile range [IQR] 26–66 years), 25/42 (60%) were male, and 21/42 (50%) had ≥1 significant previous medical conditions (diabetes mellitus and dyslipidemia were the most prevalent, at 19% each) (Table 2). We found no significant differences between the 4 groups of rickettsial infections with regard to patient age, sex, and previous medical conditions. Although a history of tick exposure was rarely reported (2/42, 5% of patients, all in the ISF group), domestic animal exposure was quite common (reported by 25/42, 60% of patients), most commonly to dogs (20/42, 48%) and cats (5/42, 12%). Few patients reported exposure to cattle, sheep, or rats.

Clinical Features

All patients were hospitalized except for 1 with ATBF, who had mild disease (Table 3). The mean duration of stay was 11.9 days, and median (IQR) was 5 (3–10) days. Fever affected 41/42 (98%) patients. The mean

number of days with fever until hospitalization was 5.2, and the median (IQR) was 5 (3–6) days; 98% of patients were hospitalized by day 9 of fever onset. For patients infected with the new *Rickettsia* variant, the mean interval was significantly longer (13.6 ± 13.3 days, range 5–29 days; p = 0.002 when compared with the other groups); 1 patient in this group had fever of unknown origin for 29 days before hospitalization.

Skin involvement in SFGR patients—either rash or eschar—was nearly universal (41/42, 98%). Systemic rash was documented for 37/42 (88%) of patients and absent for all 4 with ATBF, 1 with *R. conorii* Malish strain infection. The prevalent rash type was maculopapular (22/42, 53%), followed by macular and petechial (6/42, 15%) and macular (4/42, 10%). Involvement of palms and soles was common (30/38, 79%) for those with non-ATBF rickettsiosis. Purpura fulminans was seen in 3 patients, all within the ISF group (9% of patients in this group). Eschar was present on 12% patients with ISF, 100% with ATBF, 1 of the 2 with *R. conorii* Malish infection, and 1 of the 3

infected with the new *Rickettsia* variant. Except for 1 ISF patient who had 3 lesions, typically patients had only 1 eschar, usually on the lower limbs, including those in the ATBF group.

The time interval between fever onset and appearance of rash differed among the groups: for ISF patients, the mean (range) was 3.2 (0–8) days, and for patients infected with the new *Rickettsia* variant, the mean and median were 15 days. Of the 2 patients with *R. conorii* Malish strain infection, 1 had rash that reportedly appeared 1 day before fever onset.

Systemic symptoms (e.g., myalgia and headache) were common for all patients with non-ATBF *Rickettsia* infection, and meningoencephalitis was evident in 8/33 (24%) of patients with ISF. For ATBF patients, rates of systemic symptoms were lower. Similarly, about one third of patients with non-ATBF rickettsiosis but none with ATBF experienced severe disease with shock, multiorgan failure, need for mechanical ventilation, disseminated intravascular coagulation, acute respiratory distress syndrome, and need for intensive care.

Mortality Rate and Related Risk Factors

Of the 42 patients, 10 (23.8%) died during their hospital stay, all within 20 days of admission (mean ± SD [range] 6.3 ± 6.3 [1–20] days, median [IQR] was 3.5 [2.5–11] days). Mean age among those who died was 55 (14–95) years and among those who survived, 42.5

(1–83) years (p = 0.8). Mortality rate was remarkably high for the ISF group, reaching 30%, although none in the other 3 groups died. The only patient-related risk factor significantly associated with death was alcohol abuse (hazard ratio [HR] 5.8, 95% CI 1.14–30.4). Disease-related risk factors associated with death were hemodynamic shock at admission (HR 10.7, 95% CI 1.33–87.3), disseminated intravascular coagulation (HR 4.7, 95% CI 1.19–18.6), and jaundice (HR 6.7, 95% CI 1.4–32.2). All patients in our study received doxycycline during hospitalization; the mean ± SD (range) interval from fever onset to doxycycline receipt was 6 ± 4.3 (1–29) days. This interval did not differ between groups of patients who survived (5.7 ± 4.8 days) or died (6.9 ± 1.7 days) (p = 0.4).

Laboratory Data`

Except for ATBF, laboratory findings did not differ between the groups (Table 4). During the first 3 days of hospitalization, acute kidney injury was common (>50%); other common findings included hepatic injury accompanied with mild to moderate jaundice, mild rhabdomyolysis, mild international normalized ratio prolongation, thrombocytopenia, and lymphocytopenia. Leukocytosis was more common than leukopenia, and C-reactive protein levels were >100 mg/L (reference <5 mg/L). ATBF cases were distinctly different and patients showed much milder systemic reactions: no hepatocellular injury,

Table 2. Demographics and epidemiologic data for patients with spotted fever group rickettsiosis, according to rickettsial species, Israel, 2010–2019*

Patient data	*R. conorii* Israeli tick typhus strain	*R. conorii* Malish strain	*R. africae*	New *Rickettsia* variant	Total	p value
No. cases	33	2	4	3	42	
Age, y, median (IQR)	48 (18–64)	38	55.5 (52.5–64)	66	50.5 (26–66)	NS
Sex						
M	20 (61)	1 (50)	2 (50)	2 (67)	25 (60)	NS
F	13 (39)	1 (50)	2 (50)	1 (33)	17 (40)	NS
Any previous medical condition†	17 (51)	1 (50)	1 (25)	2 (66)	21 (50)	NS
Diabetes mellitus	6 (18)	1 (50)	0	1 (33)	8 (19)	NS
Dyslipidemia	7 (21)	0	0	1 (33)	8 (19)	NS
Hypertension	7 (21)	0	0	0	7 (17)	NS
Obesity	3 (9)	0	0	0	3 (7)	NS
COPD	1 (3)	0	1 (25)	1 (33)	3 (7)	NS
Chronic liver disease	1 (3)	1 (50)	0	0	2 (5)	NS
Alcohol abuse	3 (9)	0	0	0	3 (7)	NS
Psychiatric disorder/dementia	3 (9)	0	0	0	3 (7)	NS
Drug abuse	2 (6)	0	0	0	2 (5)	NS
Congestive heart failure	2 (6)	0	0	0	2 (5)	NS
Chronic renal failure	1 (3)	0	0	0	1 (2.5)	NS
Exposure history						
Tick	2 (6)	0	0	0	2 (5)	NS
Animals, species	20 (60), 17 dogs, 4 cats, 2 rats, 2 sheep, 1 cow	0	2 (50),1 dog, 1 African safari	3 (100), 2 dogs, 1 cat	25 (59)	NS
Recent overseas travel	1 (3), to Cyprus	1 (50), to India	4 (100), to Africa	0	6 (14)	<0.0001

*Values are no. (%) unless otherwise indicated. COPD, chronic obstructive pulmonary disease; IQR, interquartile range; NS, not significant (p>0.05).
†Includes all conditions described in the table except previous stroke, previous nonactive malignancy, atrial fibrillation, active malignancy, or immunosuppression.

Table 3. Clinical features of patients with spotted fever group rickettsiosis, according to rickettsial species, Israel, 2010–2019*

Patient data	*R. conorii* Israeli tick typhus strain	*R. conorii* Malish strain	*R. africae*	New *Rickettsia* variant	Total	p value
No. cases	33	2	4	3	42	
Fever	32 (97)	2 (100)	4 (100)	3 (100)	41 (98)	NS
Fever to admission interval, d, mean (± SD, range)	4.5 (± 2.1, 0–8)	6.5 (± 3.5, 4–9)	3.5 (± 2.4, 1–6)	13.6 (± 13.3, 5–29)	5.2 (± 4.3, 0–29)	0.002†
Systemic rash	33 (100)	1 (50)	0	3 (100)	37 (88)	<0.0001‡
Rash type						
Macular only	4 (12)	0	0	0	4 (10)	
Maculopapular	19 (58)	1 (100)	0	2 (67)	22 (53)	
Macular and petechial	5 (15)	0	0	1 (33)	6 (15)	
Petechial only	2 (6)	0	0	0	2 (5)	
Purpura fulminans	3 (9)	0	0	0	3 (7)	
Palm and sole involvement						
Yes	27 (82)	1 (100)	0	2 (67)	30 (73)	<0.0001‡
No	4 (12)	0	4 (100)	1 (33)	9 (22)	
Unknown	2 (6)	0	0	0	2 (5)	
Fever to rash interval, d, mean (± SD, range)§	3.2 (± 2.2, 0–8)	−1¶	NR	15 (± 16.9, 3–27)#	3.7 (± 4.6, 0–27)	
Eschar	4 (12)	1 (50)	4 (100)	1 (33)	10 (24)	0.011‡
>1 eschar	1 case (3 lesions)	None	None	None	None	
Location						
Lower limb	3	1	4	0	8	
Upper limb	1	0	0	0	1	
Neck	0	0	0	1	1	
Other signs/symptoms						
Lymphadenitis	2 (6)	1 (50)	1 (25)	1 (33)	5 (12)	NS
Lymphangitis	0	0	0	0	0	NS
Myalgia	13 (39)	2 (100)	1 (25)	2 (67)	18 (43)	NS
Arthralgia	5 (15)	0	0	1 (33)	6 (14)	NS
Cough	7 (21)	1 (50)	0	1 (33)	9 (21)	NS
Diarrhea	7 (21)	2 (100)	0	1 (33)	10 (24)	NS
Rigors	12 (36)	2 (100)	1 (25)	0	15 (36)	NS
Headache	14 (42)	2 (100)	1 (25)	1 (33)	18 (43)	NS
Photophobia	1 (3)	0	0	0	1 (2)	NS
Confusion	10 (30)	0	0	2 (67)	12 (28)	NS
Meningoencephalitis	8 (24)	0	0	0	8 (19)	NS
Fever of unknown origin	5 (15)	0	0	1 (33)	6 (14)	NS
ARDS	10 (30)	1 (50)	0	2 (67)	13 (31)	NS
DIC	10 (30)	1(50)	0	0	11 (26)	NS
Shock	13 (39)	2 (100)	0	1 (33)	16 (38)	NS
Hospitalization	33 (100)	2 (100)	3 (75)	3 (100)	41 (98)	NS
LOS, d, mean (± SD, range)	8.9 (± 10.4, 1–47)	12 (± 2.8, 10–14)	2.2 (± 2, 0–4)	57.6 (± 91, 5–163)	11.9 (± 25.6, 0–163)	0.01†
Intensive care admission	17 (52)	2 (100)	0	1 (33)	20 (48)	NS
Mechanical ventilation	13 (39)	2 (100)	0	1 (33)	16 (38)	NS
Death from rickettsiosis	10 (30)	0	0	0	10 (24)	NS**

*Values are no. (%) unless otherwise indicated. ARDS, acute respiratory distress syndrome; DIC, disseminated intravascular coagulation; LOS, length of stay; NS, not significant.
†Between the new *Rickettsia* group and other spotted fever groups, using 1-way analysis of variance.
‡Between *R. africae* and the other 3 *Rickettsia* spotted fever groups, using Pearson χ² tests.
§Data available for 36 patients: 1 had no fever (Israeli spotted fever), 1 had no rash (*R. conorii* Malish strain), and 4 had unknown date of rash appearance (3 Israeli spotted fever strain and 1 the new species).
¶One *R. conorii* Malish patient had no rash and the other had rash before fever.
#For 1 patient, the date of rash appearance was not documented.
**p = 0.058 for *R. conorii* Israeli tick typhus strain compared with the other *Rickettsia* groups, using Pearson χ² test.

jaundice, rhabdomyolysis, or thrombocytopenia; and significantly lower C-reactive protein levels (mean 35 mg/L; p = 0.034) (Table 4).

New *Rickettsia* Variant

In 3 epidemiologically unrelated patients, we identified a new *Rickettsia* variant of the ISF clade. Partial sequencing of the following conserved *Rickettsia* genes

indicated that the isolates were 100% identical to each other: *glt*A (GenBank accession no. MW366541), *rOmpA* (MW366542), and *sca4* (MW366543). Highest similarity (92.2%–96.9% homology) was seen with *R. conorii* Astrakhan, *R. slovaca*, *R. sibirica*, and *R. conorii* ITTS. Phylogenetic analysis could not assign the new variant to any existing strain, as previously described (27). The 3 cases were unrelated spatially or temporally (Appendix,

https://wwwnc.cdc.gov/EID/article/27/8/20-3661-App1.pdf).

Discussion

With this nationwide clinical and molecular study, we provide molecular evidence that *R. conorii* ITTS is the most commonly identified strain of SFG *Rickettsia* among hospitalized patients in Israel. Although SFGR is a reportable disease in Israel, it is underreported; of the average of 81 cases diagnosed by serologic testing each year according to the IIBR laboratory data, an average of 27 cases are reported to the Ministry of Health each year ([24]) (Figure 1, panel A). Because we lack clinical information for many of these cases, such as

Table 4. Laboratory features of 42 patients with spotted fever group rickettsiosis according to rickettsial species, during hospitalization days 1–3, Israel, 2010–2019*

Feature†	*R. conorii* Israeli tick typhus strain	*R. conorii* Malish strain	*R. africae*	New *Rickettsia* variant	Total	p value
No. cases	33	2	4	3	42	
Acute kidney injury (creatinine ≥1.3 mg/dL), no. (%)	20/32 (62.5)	0/2	1/4 (25)	1/3 (33)	22/41 (54)	NS‡
Creatinine, mg/dL, mean (range)	1.8 (0.13–6.25)	0.83 (0.7–0.9)	0.96 (0.6–1.3)	1.6 (1.17–2.4)	1.6 (0.1–6.25)	NS§
Hepatocellular injury pattern						
AST or ALT >2 ULN, no. (%)	24/33 (73)	2/2 (100)	0/4 (100)	2/3 (67)	28/42 (67)	0.02‡
AST, IU/L, mean (range)	855 (42–8,895)	249 (270–228)	27 (23–31)	83 (60–107)	728 (23–8,895)	NS§
ALT, IU/L, mean (range)	334 (12–2,881)	94 (109–80)	26 (25–29)	88 (40–164)	22/41 (54)	NS§
Cholestatic injury pattern						
Alkaline phosphatase or GGT >2 ULN, no. (%)	16/32 (48)	2/2 (100)	1/4 (25)	2/3 (67)	21/41 (51)	NS‡
Alkaline phosphatase, IU/L, mean (range)	196 (32–1,056)	109 (67–152)	64 (63–65)	265 (60–416)	190 (32–1,056)	NS§
GGT, IU/L, mean (range)	156 (15–1,026)	150 (129–171)	73 (21–125)	507	154 (15–1,026)	NS§
Jaundice, bilirubin >1.3 mg/dL, no. (%)	14/33 (42)	1/2 (50)	0/3	0/3	15/41 (36)	NS‡
Bilirubin, mg/dL, mean (range)	1.77 (0.29–10)	2.6 (1.3–4)	0.4 (0.3–0.5)	0.93 (0.6–1.3)	1.46 (0.29–10)	NS§
C-reactive protein >5 mg/L, no. (%)	30/30 (100)	1/1 (100)	4/4 (100)	3/3 (100)	38/38 (100)	NS‡
C-reactive protein, mg/L, (range)	207 (17–460)	102	35 (17–61)	223 (131–273)	187 (17–410)	0.034§
Rhabdomyolysis, creatine kinase >ULN, no. (%)	17/30 (52)	1/2 (50)	0/2	0/3	18/37 (49)	NS‡
Creatine kinase, IU/L (range)	1,345 (81–8,900)	271 (128–414)	92 (71–113)	79 (57–102)	1,119 (57–8,900)	NS§
Complete blood count						
Leukocytosis, >10,000 leukocytes/μL, no. (%)	15/33 (45)	0/2	0/4	1/3 (33)	16/42 (38)	NS‡
Leukopenia, <4,000 leukocytes/μL, no. (%)	6/33 (18)	1/2 (50)	0/4	1/3 (33)	8/42 (19)	NS‡
Leukocytes, × 10^3/μL, mean (range)	14.2 (2.5–43.3)	4.5 (2.6, 6.4)	4.5 (4–5.2)	10.2 (3.9–17.1)	13.1 (2.5–43.3)	NS§
Lymphocytopenia, ALC <1,500/μL, no. (%)	30/33 (91)	2/2 (100)	4/4 (100)	3/3 (100)	36/42 (93)	NS‡
ALC, × 10^3/μL, mean (range)	0.9 (0.2–6.9)	0.35 (0.3–0.4)	1.26 (1.2–1.3)	1.1 (0.6–2.3)	0.9 (0.2–6.9)	NS§
Thrombocytopenia, platelets <150K cells/μL, no. (%)	29/32 (88)	2/2 (100)	0/4	3/3 (100)	34/41 (83)	0.001‡
Platelets, × 10^3/μL, mean (range)	84 (15–271)	36 (26–46)	238 (164–316)	64 (37–101)	82 (15–271)	0.001§
Coagulopathy, INR >1.2, no. (%)	16/33 (48)	1/2 (50)	0/2	0/3	17/40 (42)	NS‡
INR, mean (range)	1.38 (0.9–3)	1.5 (1.1–1.9)	0.96 (0.93–1)	1.09 (1.04–1.16)	1.36 (0.9–3)	NS§
Molecular diagnosis source, no. (%)						
Skin biopsy sample/eschar	19 (58)	1 (50)	4 (100)	3 (100)	27 (64)	
Blood	16 (48)	2 (100)	0	1 (33)	19 (45)	
CSF	1 (3)	0	0	0	1 (2)	
Other organs	2 (6)¶	0	0	0	2 (5)	
Serologic diagnosis, no. (%) samples	32 (97)	2 (100)	1 (25)	1 (33)	36 (86)	
Positive	5 (16)	0	0	0	5 (14)	
Borderline	2 (6)	0	0	1 (33)	3 (8)	
Negative	25 (78)	2 (100)	1 (25)	0	28 (78)	

*ALC, absolute lymphocyte count; ALT, alanine aminotransferase; AST, aspartate aminotransferase; CSF, cerebrospinal fluid; GGT, gamma glutamyl transpeptidase; INR, international normalized ratio; NS, not significant; ULN, within upper limit of normal range.
†Highest or lowest levels reached within the time frame are reported.
‡By Pearson χ^2 test.
§By 1-way analysis of variance, conducted on day-of-admission data.
¶One from liver biopsy sample and 1 from enlarged lymph node.

severity of illness and hospitalization, we can only partially infer the role of this strain in causing SFGR among hospitalized and ambulatory patients. Although *R. conorii* ITTS was suspected as the causative agent of SFGR in Israel, this suspicion has been supported only by very limited data: rare case reports of fatal human cases (*9,15*) and a few studies of ticks (*25,32*).

Testing for spotted fever by serology and recently by PCR increased during 2017–2019 compared with the preceding 3 years. This rise probably represents increased clinical suspicion of SFGR and a true increase in disease activity. Despite missing molecular data for ambulatory patients with mild cases of SFGR, we believe that during the past 3 years, *R. conorii* ITTS has led a silent outbreak of SFGR in Israel. Similarly, an unprecedented 46% increase in SFGR was reported during 2016–2017 by the US Centers for Disease Control and Prevention from states where SFGR is known to be endemic (*33*). US authorities were faced with the dilemma of whether this increased incidence should be ascribed to a true increase, increased testing, or inappropriate use of a single serologic test instead of paired tests, reflecting past infection in a disease-endemic area.

We report the epidemiologic features of SFGR patients, although comparison between *R. conorii* ITTS with the other groups was limited because of small numbers. In Israel, SFGR affects mainly young adults and has a mild predilection for men. SFGR has been endemic to the Sharon and Haifa Districts since the 1990s (*34*); in our study, these 2 districts accounted for 44% (16/36) of all autochthonous cases. These results are similar to those reported in 2014 by Rose et al., who also investigated the association between geographic data and SFGR-positive ticks. Areas with SFG *Rickettsia*–infected ticks were associated with brown-type soil, higher land surface temperatures, and higher precipitation (*31*). We observed a wide geographic distribution of human ISF cases with aggregation in northern Israel.

Although *R. conorii* ITTS seems to be the main *Rickettsia* causing clinical disease in Israel, why this strain is rarely found in ticks collected from Israel (*25,35*) and other countries (*7,36,37*) remains unclear. Studies from Israel have found *Rickettsia massiliae* to be more prevalent (≈10 fold) than *R. conorii* ITTS among questing ticks and ticks feeding on animals (*31,35,38*). This discrepancy could be explained by underreporting of *R. massiliae* infection in humans with mild or subclinical disease. Most patients in our study were hospitalized with severe disease and may represent a reporting bias of *R. conorii* ITTS, which causes more

severe disease. Patients with milder illness, potentially caused by other rickettsiae, may not be hospitalized, and illness may resolve undiagnosed, without the need for molecular studies.

Rose et al. (*31*) collected *Rhipicephalus sanguineus* and *Rh. turanicus* ticks from geographic locations similar to the presumed areas of the clinical autochthonous cases in our study (Figure 2, panel B). However, *R. conorii* ITTS was found only rarely (1.8%) and strictly in *Rh. sanguineus* ticks. Hence, the role of *Rh. turanicus* ticks as possible vectors of *R. conorii* ITTS and *R. massiliae* as a cause of rickettsiosis in humans should be further explored. Although clearly reported as a cause of SFGR, *R. massiliae* is still rarely isolated from human patients (*39*). Deleterious effects of *R. conorii* on *Rh. sanguineus* tick fitness, resulting in infected ticks not surviving the winter, may explain its low prevalence among ticks in nature (*40,41*).

The new *Rickettsia* variant was found in the eastern and more mountainous parts of the country: the Golan Heights, the Galilee region, and the West Bank of the Palestinian Authority. This distribution may suggest a geographic niche for either this new *Rickettsia* or its vector and should be further explored in studies of tick collections from these mountainous areas. The single case of *R. conorii* Malish strain infection acquired locally in this study was in a 50-year-old man from the desert area, who had a necrotic eschar in the thigh and severe systemic disease.

Most cases were reported during the summer and peaked in August. This finding is consistent with previous reports (*12*) and may be attributed to increased activity of the vectors and to the aggressiveness and host indiscrimination of *Rh. sanguineus* ticks when exposed to higher temperatures (*42*).

Patients rarely remembered seeing or being bitten by ticks (only 2 remembered); however, exposure to animals was common (25/42, 59% of cases), mainly to dogs (20/25, 80%), the principal hosts of *Rh. sanguineus* ticks (the main reservoir of *R. conorii*). This finding implies that exposure to domestic pets is more relevant than exposure to ticks.

The clinical and laboratory features for patients in our case series were typical of SFGR, although eschar, which is considered rare in patients with ISF, was seen in 12% of patients, 1 of whom had 3 lesions. ISF caused purpura fulminans in 9% and meningoencephalitis in 24%. About half of ISF patients experienced multiorgan involvement that included kidney and liver injury, jaundice, rhabdomyolysis/myositis, and coagulopathy. Severe disease requiring intensive care was strikingly common (52%), and 30% of ISF patients died in hospital. The high mortality rate,

previously reported for ISF infection (*10*), contrasted with lower rates from historical reports from Israel during the 1990s. This discrepancy may result from reporting bias with increased awareness in recent years, as well as improved laboratory capabilities. An additional possibility is an outbreak of a more virulent strain, such as *R. conorii* ITTS. Risk factors for death included only alcohol abuse, as previously described (*12*). Admission-to-treatment (doxycycline) interval was not significant.

The small number of cases in this investigation makes drawing conclusions or comparisons difficult; however, the new *Rickettsia* variant may lead to prolonged fever before care seeking and may resemble tickborne lymphadenopathy usually related to *Rickettsia slovaca* or *Rickettsia raoultii* (*11*). Patients with ATBF had a distinct clinical syndrome of a milder clinical disease; for 25%, systemic symptoms were limited to fever, myalgia, and headache with no systemic rash.

In conclusion, we report a nationwide case series of hospitalized patients with molecularly diagnosed SFGR over a decade in Israel, of which *R. conorii* ITTS was the principal cause of severe disease, multiorgan failure, and high mortality rates. We also describe a new *Rickettsia* variant, which may be associated with unique epidemiologic and clinical features. This study suggests that a broader range of species causes SFGR in Israel and that this possibility should be explored in larger, prospective studies, especially in light of the potential candidates found in ticks.

Acknowledgments

About the Author

Dr. Cohen is the head of the infectious diseases unit and infection control unit in Sanz Medical Center, Laniado Hospital, Netanya, Israel. His research interests are zoonoses and healthcare-associated infections, including resistant microorganisms and viral respiratory infections.

References

1. Diop A, Raoult D, Fournier PE. Rickettsial genomics and the paradigm of genome reduction associated with increased virulence. Microbes Infect. 2018;20:401–9. https://doi.org/10.1016/j.micinf.2017.11.009
2. Blanton LS, Walker DH. *Rickettsia rickettsii* and other spotted fever group rickettsiae (Rocky Mountain spotted fever and other spotted fevers). In: Bennett JE, Dolin R, Blaser MJ, editors. Mandell, Douglas, and Bennett's principles and practice of infectious diseases, 9th ed. Amsterdam: Elsevier; 2020.
3. Parola P, Paddock CD, Socolovschi C, Labruna MB, Mediannikov O, Kernif T, et al. Update on tick-borne rickettsioses around the world: a geographic approach. Clin Microbiol Rev. 2013;26:657–702. https://doi.org/10.1128/CMR.00032-13
4. Bacellar F, Beati L, França A, Poças J, Regnery R, Filipe A. Israeli spotted fever rickettsia (*Rickettsia conorii* complex) associated with human disease in Portugal. Emerg Infect Dis. 1999;5:835–6. https://doi.org/10.3201/eid0506.990620
5. Colomba C, Trizzino M, Giammanco A, Bonura C, Di Bona D, Tolomeo M, et al. Israeli spotted fever in Sicily. Description of two cases and minireview. Int J Infect Dis. 2017;61:7–12. https://doi.org/10.1016/j.ijid.2017.04.003
6. Zhu Y, Fournier PE, Eremeeva M, Raoult D. Proposal to create subspecies of *Rickettsia conorii* based on multi-locus sequence typing and an emended description of *Rickettsia conorii*. BMC Microbiol. 2005;5:11. https://doi.org/10.1186/1471-2180-5-11
7. Znazen A, Hammami B, Lahiani D, Ben Jemaa M, Hammami A. Israeli spotted fever, Tunisia. Emerg Infect Dis. 2011;17:1328–30. https://doi.org/10.3201/eid1707.101648
8. Angelakis E, Richet H, Raoult D. *Rickettsia sibirica mongolitimonae* infection, France, 2010–2014. Emerg Infect Dis. 2016;22:880–2. https://doi.org/10.3201/eid2205.141989
9. Cohen R, Babushkin F, Shapiro M, Uda M, Atiya-Nasagi Y, Klein D, et al. Two cases of Israeli spotted fever with purpura fulminans, Sharon District, Israel. Emerg Infect Dis. 2018;24:835–40. https://doi.org/10.3201/eid2405.171992
10. de Sousa R, Nóbrega SD, Bacellar F, Torgal J. Mediterranean spotted fever in Portugal: risk factors for fatal outcome in 105 hospitalized patients. Ann N Y Acad Sci. 2003;990:285–94. https://doi.org/10.1111/j.1749-6632.2003.tb07378.x
11. Parola P, Rovery C, Rolain JM, Brouqui P, Davoust B, Raoult D. *Rickettsia slovaca* and *R. raoultii* in tick-borne rickettsioses. Emerg Infect Dis. 2009;15:1105–8. https://doi.org/10.3201/eid1507.081449
12. Sousa R, França A, Dória Nòbrega S, Belo A, Amaro M, Abreu T, et al. Host- and microbe-related risk factors for and pathophysiology of fatal *Rickettsia conorii* infection in Portuguese patients. J Infect Dis. 2008;198:576–85. https://doi.org/10.1086/590211
13. Raoult D, Weiller PJ, Chagnon A, Chaudet H, Gallais H, Casanova P. Mediterranean spotted fever: clinical, laboratory and epidemiological features of 199 cases. Am J Trop Med Hyg. 1986;35:845–50. https://doi.org/10.4269/ajtmh.1986.35.845
14. Aharonowitz G, Koton S, Segal S, Anis E, Green MS. Epidemiological characteristics of spotted fever in Israel over 26 years. Clin Infect Dis. 1999;29:1321–2. https://doi.org/10.1086/313432
15. Weinberger M, Keysary A, Sandbank J, Zaidenstein R, Itzhaki A, Strenger C, et al. Fatal *Rickettsia conorii* subsp. israelensis infection, Israel. Emerg Infect Dis. 2008;14:821–4. https://doi.org/10.3201/eid1405.071278
16. Paddock CD, Childs JE, Zaki SR, Berger SA. Reply. J Infect Dis. 2000;181:810–2. https://doi.org/10.1086/315288
17. Leitner M, Yitzhaki S, Rzotkiewicz S, Keysary A. Polymerase chain reaction-based diagnosis of Mediterranean spotted fever in serum and tissue samples. Am J Trop Med Hyg. 2002;67:166–9. https://doi.org/10.4269/ajtmh.2002.67.166
18. Regev-Yochay G, Segal E, Rubinstein E. Glucose-6-phosphate dehydrogenase deficiency: possible determinant for a fulminant course of Israeli spotted fever. Isr Med Assoc J. 2000;2:781–2.
19. Ergas D, Sthoeger ZM, Keysary A, Strenger C, Leitner M, Zimhony O. Early diagnosis of severe Mediterranean spotted

fever cases by nested-PCR detecting spotted fever rickettsiae 17-kD common antigen gene. Scand J Infect Dis. 2008; 40:965–7. https://doi.org/10.1080/00365540802400584

20. Cohen J, Lasri Y, Landau Z. Mediterranean spotted fever in pregnancy. Scand J Infect Dis. 1999;31:202–3. https://doi.org/10.1080/003655499750006290

21. Bentov Y, Sheiner E, Kenigsberg S, Mazor M. Mediterranean spotted fever during pregnancy: case presentation and literature review. Eur J Obstet Gynecol Reprod Biol. 2003;107:214–6. https://doi.org/10.1016/S0301-2115 (02)00303-2

22. Shazberg G, Moise J, Terespolsky N, Hurvitz H. Family outbreak of *Rickettsia conorii* infection. Emerg Infect Dis. 1999;5:723–4. https://doi.org/10.3201/eid0505.990518

23. Cwikel BJ, Ighbarieh J, Sarov I. Antigenic polypeptides of Israeli spotted fever isolates compared with other spotted fever group rickettsiae. Ann N Y Acad Sci. 1990;590(1 Rickettsiolog):381–8. https://doi.org/10.1111/ j.1749-6632.1990.tb42244.x

24. Israel Center for Disease Control Ministry of Health. Publication files, infectious diseases, notifiable infectious diseases in Israel [in Hebrew] [cited 2020 Apr 15]. https://www.health.gov.il/UnitsOffice/HD/PH/ epidemiology/Pages/epidemiology_report.aspx

25. Harrus S, Perlman-Avrahami A, Mumcuoglu KY, Morick D, Baneth G. Molecular detection of *Rickettsia massiliae*, *Rickettsia sibirica mongolitimonae* and *Rickettsia conorii israelensis* in ticks from Israel. Clin Microbiol Infect. 2011;17:176–80. https://doi.org/10.1111/j.1469-0691.2010.03224.x

26. Keysary A, Strenger C. Use of enzyme-linked immunosorbent assay techniques with cross-reacting human sera in diagnosis of murine typhus and spotted fever. J Clin Microbiol. 1997;35:1034–5. https://doi.org/10.1128/ JCM.35.4.1034-1035.1997

27. Klein D, Beth-Din A, Cohen R, Lazar S, Glinert I, Zayyad H, et al. New spotted fever group *Rickettsia* isolate, identified by sequence analysis of conserved genomic regions. Pathogens. 2019;9:E11. https://doi.org/10.3390/pathogens9010011

28. Roux V, Raoult D. Phylogenetic analysis of members of the genus *Rickettsia* using the gene encoding the outer-membrane protein rOmpB (*ompB*). Int J Syst Evol Microbiol. 2000;50:1449–55. https://doi.org/10.1099/ 00207713-50-4-1449

29. Sekeyova Z, Roux V, Raoult D. Phylogeny of *Rickettsia* spp. inferred by comparing sequences of 'gene D', which encodes an intracytoplasmic protein. Int J Syst Evol Microbiol. 2001;51:1353–60. https://doi.org/10.1099/ 00207713-51-4-1353

30. Bechah Y, Socolovschi C, Raoult D. Identification of rickettsial infections by using cutaneous swab specimens and PCR. Emerg Infect Dis. 2011;17:83–6. https://doi.org/ 10.3201/eid1701.100854

31. Rose J, Nachum-Biala Y, Mumcuoglu KY, Alkhamis MA, Ben-Nun A, Lensky I, et al. Genetic characterization of spotted fever group rickettsiae in questing ixodid ticks collected in Israel and environmental risk factors for their

infection. Parasitology. 2017;144:1088–101. https://doi.org/ 10.1017/S0031182017000336

32. Sentausa E, El Karkouri K, Robert C, Raoult D, Fournier PE. Genome sequence of *Rickettsia conorii* subsp. *israelensis*, the agent of Israeli spotted fever. J Bacteriol. 2012;194:5130–1. https://doi.org/10.1128/JB.01118-12

33. Heitman KN, Drexler NA, Cherry-Brown D, Peterson AE, Armstrong PA, Kersh GJ. National surveillance data show increase in spotted fever rickettsiosis: United States, 2016-2017. Am J Public Health. 2019;109:719–21. https://doi.org/10.2105/AJPH.2019.305038

34. Mumcuoglu KY, Keysary A, Gilead L. Mediterranean spotted fever in Israel: a tick-borne disease. Isr Med Assoc J. 2002;4:44–9.

35. Ereqat S, Nasereddin A, Al-Jawabreh A, Azmi K, Harrus S, Mumcuoglu K, et al. Molecular detection and identification of spotted fever group rickettsiae in ticks collected from the West Bank, Palestinian Territories. PLoS Negl Trop Dis. 2016;10:e0004348. https://doi.org/10.1371/ journal.pntd.0004348

36. Kamani J, Baneth G, Mumcuoglu KY, Waziri NE, Eyal O, Guthmann Y, et al. Molecular detection and characterization of tick-borne pathogens in dogs and ticks from Nigeria. PLoS Negl Trop Dis. 2013;7:e2108. https://doi.org/10.1371/ journal.pntd.0002108

37. Chisu V, Masala G, Foxi C, Socolovschi C, Raoult D, P arola P. *Rickettsia conorii israelensis* in *Rhipicephalus sanguineus* ticks, Sardinia, Italy. Ticks Tick Borne Dis. 2014;5:446–8. https://doi.org/10.1016/j.ttbdis.2014.02.003

38. Waner T, Keysary A, Eremeeva ME, Din AB, Mumcuoglu KY, King R, et al. *Rickettsia africae* and *Candidatus* Rickettsia barbariae in ticks in Israel. Am J Trop Med Hyg. 2014;90:920– 2. https://doi.org/10.4269/ajtmh.13-0697

39. Eldin C, Virgili G, Attard L, Edouard S, Viale P, Raoult D, et al. *Rickettsia massiliae* infection after a tick bite on the eyelid. Travel Med Infect Dis. 2018;26:66–8. https://doi.org/ 10.1016/j.tmaid.2018.08.002

40. Socolovschi C, Gaudart J, Bitam I, Huynh TP, Raoult D, Parola P. Why are there so few *Rickettsia conorii conorii*-infected *Rhipicephalus sanguineus* ticks in the wild? PLoS Negl Trop Dis. 2012;6:e1697. https://doi.org/10.1371/journal.pntd.0001697

41. Parola P, Socolovschi C, Raoult D. Deciphering the relationships between *Rickettsia conorii conorii* and *Rhipicephalus sanguineus* in the ecology and epidemiology of Mediterranean spotted fever. Ann N Y Acad Sci. 2009; 1166:49–54. https://doi.org/10.1111/j.1749-6632. 2009.04518.x

42. Socolovschi C, Raoult D, Parola P. Influence of temperature on the attachment of *Rhipicephalus sanguineus* ticks on rabbits. Clin Microbiol Infect. 2009;15(Suppl 2):326–7. https://doi.org/ 10.1111/j.1469-0691.2008.02260.x

Address for correspondence: Regev Cohen, Head of Infectious Diseases Unit, Sanz Medical Center, 16 Divrei Haim St, Kiryat Sanz, 42150, Netanya, Israel; email: regevco@gmail.com

Spatial, Ecologic, and Clinical Epidemiology of Community-Onset, Ceftriaxone-Resistant *Enterobacteriaceae*, Cook County, Illinois, USA

Vanessa Sardá, William E. Trick, Huiyuan Zhang, David N. Schwartz

We performed a spatial and mixed ecologic study of community-onset *Enterobacteriaceae* isolates collected from a public healthcare system in Cook County, Illinois, USA. Individual-level data were collected from the electronic medical record and census tract–level data from the US Census Bureau. Associations between individual- and population-level characteristics and presence of ceftriaxone resistance were determined by logistic regression analysis. Spatial analysis confirmed nonrandom distribution of ceftriaxone resistance across census tracts, which was associated with higher percentages of Hispanic, foreign-born, and uninsured residents. Individual-level analysis showed that ceftriaxone resistance was associated with male sex, an age range of 35–85 years, race or ethnicity other than non-Hispanic Black, inpatient encounter, and percentage of foreign-born residents in the census tract of isolate provenance. Our findings suggest that the likelihood of community-onset ceftriaxone resistance in *Enterobacteriaceae* is influenced by geographic and population-level variables. The development of effective mitigation strategies might depend on better accounting for these factors.

The continuous rise of infections secondary to extended-spectrum beta-lactamase (ESBL)–producing *Enterobacteriaceae* in the United States is a complex public health problem and considered a serious threat by the Centers for Disease Control and Prevention (*1*). Recently, the incidence of infections caused by ESBL producers in the United States was noted to have increased by 53.3% during 2019–2017, driven largely by a surge in community-onset cases (*2*). Globally, a similar trend has been described, and developing countries bear a disproportionate burden of infections secondary to these drug-resistant pathogens (*3–5*). The steady increases in rates of infections caused by ESBL-producing *Escherichia coli* and *Klebsiella pneumoniae* persist despite antimicrobial stewardship and infection control efforts (*6,7*).

Initially confined to the healthcare environment, infections caused by ESBL-producing *Enterobacteriaceae* among patients without previous healthcare exposure have been described since the mid-2000s (*8,9*). This epidemiologic shift has been largely attributed to the emergence of the CTX-M–producing *E. coli* sequence type (ST) 131 clone, which expanded rapidly throughout the United States and remains the most prevalent ESBL-producing *E. coli* clone in the community (*10*). In addition to higher virulence and transmissibility of the *E. coli* ST131 clone, its therapeutic management is particularly challenging because of its associated resistance to commonly used oral antimicrobial drugs such as quinolones and trimethoprim/sulfamethoxazole (*6,10*).

From an epidemiologic standpoint, multiple transmission pathways for community-onset ESBL-producing *Enterobacteriaceae* have been proposed. Potential sources of acquisition outside of healthcare environments include gastrointestinal colonization after international travel (*11,12*) and transmission among household members (*7,13*). In addition, ESBL-producing *Enterobacteriaceae* have been isolated from foodstuffs (*14,15*), livestock (*14*), and waterways (*16,17*), all of which have been posited as potential sources for human colonization and subsequent infection. A better understanding of the epidemiology of community-onset infections caused by ESBL-producing bacteria across geographic areas can help

identify areas with higher disease burden and suggest pathways of transmission and mitigation strategies that are potentially unique to each region. Spatial and ecologic analyses help to address the influence of geography and population-level variables on disease distribution in a given region.

We conducted an epidemiologic analysis of the distribution of community-onset, ceftriaxone-resistant (CTX-R) *Enterobacteriaceae* from a single healthcare system in Cook County, Illinois, USA. We hypothesized that population-level characteristics are contributing factors for the presence of CTX-R *Enterobacteriaceae* in a geographic area and at the individual level.

Methods

Cook County Health (CCH) is a large safety-net healthcare system in Chicago and suburban Cook County, Illinois. It consists of a 450-bed teaching hospital near downtown Chicago, a small community hospital in the South Side of Chicago, a small hospital and clinic for the treatment of detainees in the Cook County jail, and 13 community clinics distributed throughout Cook County. In 2018, CCH cared for 205,322 persons, most of whom self-identified as non-Hispanic Black (49.1%) or Hispanic (32.7%). Through electronic queries, we identified all culture isolates of the commonest *Enterobacteriaceae* species collected at CCH: E. coli, K. pneumoniae, *Enterobacter cloacae, Proteus mirabilis, Enterobacter aerogenes*, and *Klebsiella oxytoca* collected from Cook County residents during January 1, 2016–December 31, 2018. We determined antimicrobial susceptibilities by using the MicroScan Gram-negative panel (Beckman Coulter, https://www.beckmancoulter.com) and interpreted results by using Clinical and Laboratory Standards Institute breakpoints (18). We obtained antimicrobial susceptibilities retrospectively and did not retain any isolates for further analysis. We excluded isolates collected from persons <18 years of age, surveillance isolates, isolates with intermediate susceptibility to ceftriaxone or intermediate susceptibility or resistance to carbapenems, and duplicate isolates (defined as isolates from the same persons, of the same species, and collected within 30 days). To select for community-onset isolates, we included only isolates collected in the ambulatory clinic or emergency department (ED) setting and those collected during the first 2 days of hospitalization.

Demographic characteristics, collected from the electronic medical record (EMR), were patient sex and age and self-identified race and ethnicity, categorized as non-Hispanic Black, non-Hispanic White, Hispanic, or other. We classified encounter types as outpatient (ambulatory clinic), ED, or inpatient. Census-tract variables for Cook County were obtained from the 2017 US Census Bureau American Community Survey 5-year estimates (19). We extracted census tract data on race and ethnicity, immigration status (US-born or foreign-born), deprivation (households below poverty level and uninsured status), and overcrowding (>1.5 occupants per room).

Spatial Analysis

Cook County, which includes the city of Chicago, contains 1,319 land census tracts and has an estimated population of 5,149,580 residents (19). We used ArcGIS version 10.4.1 (ESRI, https://www.esri.com) to geocode isolates to their census tract of provenance by using residential addresses available in the EMR. We calculated and mapped the percentage of CTX-R isolates in each census tract (i.e., the number of CTX-R isolates divided by the number of all isolates multiplied by 100). To minimize imprecision of CTX-R percentages in census tracts with low number of isolates, we excluded from the spatial analysis census tracts that had <3 isolates collected during the study period. We used spatial autocorrelation analysis (Moran I) to identify whether *Enterobacteriaceae* CTX-R percentages were distributed at random or clustered in census tracts across Cook County. Similarly, we conducted spatial autocorrelation analysis on CTX-R percentage distribution of *E. coli* isolates alone.

Ecologic Analysis

After excluding census tracts with <3 isolates, we categorized the remaining census tracts on the basis of the presence or absence of a CTX-R isolate. We evaluated the relationship between each population-level variable and the presence of >1 CTX-R isolates in a census tract by using bivariate logistic regression, summarized by odds ratios (ORs) and corresponding 95% CIs. We conducted a similar analysis for *E. coli* isolates alone.

Individual Risk Analysis

We categorized individual *Enterobacteriaceae* isolates on the basis of the identification of ceftriaxone resistance in the susceptibility panel. We included all isolates in the analysis of individual risk. The variables of interest were the individual demographic variables collected from the EMR and the type of clinical encounter. In addition, we included an ecologic variable, the percentage of foreign-born population in the census tract of residency. We evaluated the relationship between each variable and identification of ceftriaxone resistance in an individual isolate by

using bivariate logistic regression, summarized by ORs and corresponding 95% CIs. We conducted all statistical analyses by using Stata version 14.2 (StataCorp, https://www.stata.com).

Results

We collected 12,892 *Enterobacteriaceae* isolates at CCH during the study period, 10,891 of which met the inclusion criteria and were included in the dataset. We summarized the demographic and clinical characteristics of the patients from whom *Enterobacteriaceae* isolates were collected (Table 1). Most isolates were collected from women (7,853 [72.1%]), were from urine specimens (9,315 [85.5%]), were collected in ambulatory clinics (5,889 [54.1%]), or were identified as *E. coli* (7,977 [73.2%]). A total of 1,035 (9.5%) *Enterobacteriaceae* (817 [10.2%] *E. coli* isolates) were resistant to ceftriaxone. We observed no notable trends in ceftriaxone resistance across study years.

In the 1,319 land census tracts in Cook County, we collected *Enterobacteriaceae* isolates from residents of 1,131 (85.8%) and *E. coli* alone from residents of 1,085 (82.3%). The mean number of such isolates per census tract was 9.6 (SD + 9.28, range 1–92), and the mean number of *E. coli* isolates obtained per census tract was 7.4 (SD + 7.16, range 1–62). We plotted choropleth maps depicting the geographic distribution of all *Enterobacteriaceae* isolates and *E. coli* isolates alone (Figure 1). Among census tracts from which >1 isolate was obtained, CTX-R *Enterobacteriaceae* isolates were identified in 500 (44.2%), and most CTX-R isolates (561 [54.2%]) came from only 125 (11%) census tracts. In the case of CTX-R *E. coli* isolates, 424 (39.1%) of the 1,085 census tracts had a CTX-R *E. coli* isolate reported during the study period, and only 93 (8.6%) census tracts accounted for 406 (49.7%) of all CTX-R *E. coli* isolates.

A total of 886 census tracts had >3 *Enterobacteriaceae* isolates collected during the study period and were included in the spatial and ecologic analyses. The mean CTX-R percentage among these census tracts was 8.7%. Autocorrelation analysis (Moran I) indicated that CTX-R percentages among all isolates were not distributed randomly across Cook County census tracts (index 0.02, p<0.01). A total of 776 census tracts had >3 *E. coli* isolates collected during the study period and were included in the spatial and ecologic analysis of *E. coli* isolates. The average CTX-R percentage of *E. coli* isolates among census tracts was 9.6%. Autocorrelation analysis (Moran I) of CTX-R percentages among *E. coli* isolates also found a nonrandom distribution among census tracts (index 0.03, p<0.01). We mapped the geographic distribution of

CTX-R percentages for all *Enterobacteriaceae* and for *E. coli* isolates alone (Figure 2).

We identified census tract–level characteristics reported in the 2017 American Community Survey of residents of the 886 census tracts that accounted for >3 *Enterobacteriaceae* isolates and compared census tracts with ceftriaxone resistance (461 [52.1%] of census tracts, mean 15.5 isolates/census tract) and without (425 [47.9%] of census tracts, mean 8.03 isolates/census tract). Bivariate analysis found that the presence of CTX-R isolates was negatively associated with census-tract percentages of non-Hispanic White and non-Hispanic Black populations, and positively associated with census-tract percentages of Hispanic, foreign-born, and uninsured residents. We observed no statistical associations between the outcome and percentages of households with incomes below the federal poverty level or with overcrowding (Table 2). Census tract-level characteristics were moderately correlated (r = −0.78 to 0.69).

Among the 776 census tracts with >3 *E. coli* isolates, 395 (50.9%) had no CTX-R isolates and 381

Table 1. Demographic and clinical characteristics of patients from whom selected *Enterobacteriaceae* isolates were collected, Cook County Health healthcare system, Illinois, USA, 2016–2018

Characteristic	No. isolates (%)
Total no. isolates	10,891 (100)
Sex	
F	7,853 (72.1)
M	3,038 (27.9)
Age group, y	
18–34	2,011 (18.6)
35–51	3,109 (28.5)
52–68	4,092 (37.5)
69–85	1,471 (13.5)
>85	208 (1.9)
Race and ethnicity	
Non-Hispanic White	997 (9.2)
Non-Hispanic Black	4,394 (40.4)
Hispanic	4,898 (44.9)
Other	602 (5.5)
Encounter type	
Outpatient	5,889 (54.1)
Emergency department	2,890 (26.5)
Inpatient	2,112 (19.4)
Organism	
Escherichia coli	7,977 (73.2)
Klebsiella pneumoniae	1,367 (12.6)
Proteus mirabilis	811 (7.5)
Enterobacter cloacae	376 (3.4)
Klebsiella oxytoca	197 (1.8)
Enterobacter aerogenes	163 (1.5)
Specimen type	
Urine	9,315 (85.5)
Wound	981 (9.0)
Blood	384 (3.6)
Other	211 (1.9)
Ceftriaxone susceptibility	
Susceptible	9,856 (90.5)
Resistant	1,035 (9.5)

(49.1%) had >1 resistant *E. coli* isolate collected during the study period, with an average CTX-R percentage of 19.4%. Bivariate analysis showed a negative association between presence of CTX-R *E. coli* isolates in census tracts and percentage of non-Hispanic Black population. Conversely, the odds of ceftriaxone resistance in an E.coli isolates was positively associated with the percentage of Hispanic, foreign-born, and uninsured residents and with residential overcrowding (Table 3).

All 10,891 *Enterobacteriaceae* isolates (1,035 [9.5%] of which were CTX-R) were included in the individual risk analysis of patients from whom CTX-R and CTX-susceptible *Enterobacteriaceae* were recovered (Table 4). In the bivariate logistic regression analysis, male sex, an age range of 35–85 years, race and ethnicity other than non-Hispanic Black, and inpatient encounter were found to be associated with a higher likelihood of ceftriaxone resistance in a clinical isolate. Similarly, higher odds for the outcome were associated with the percentage of foreign-born residents in the census tract of isolate provenance.

Discussion

Our study has 4 main findings. First, compared with patients from whom CTX-susceptible community-onset *Enterobacteriaceae* isolates were collected, patients with CTX-R isolates more often were male, were 35–85 years of age, had self-identified race and ethnicity other than non-Hispanic Black, were hospitalized rather than discharged from the ED or seen in clinic, and resided in Cook County census tracts with higher proportions of foreign-born residents. Second, most patients with CTX-R isolates resided in a relatively small number of census tracts, with only 11% of *Enterobacteriaceae* isolate–generating census tracts accounting for 54.2% of CTX-R isolates and 93 (8.6%) of *E. coli* isolate–generating census tracts accounting for 49.7% of all CTX-R *E. coli* isolates. Third, spatial analysis supported the nonrandom distribution of Cook County census tracts generating higher proportions of ceftriaxone resistance among *Enterobacteriaceae* and *E. coli* isolates. Fourth, the population-level characteristics of census tracts from which isolates of CTX-R *Enterobacteriaceae* and *E. coli* were obtained differed from residents of census tracts yielding susceptible isolates exclusively, with the percentage of Hispanic residents, foreign-born, and uninsured population being positively associated with the presence of CTX-R isolates on analysis in both cohorts.

Similar to our findings, spatial studies conducted abroad of drug-resistant *Enterobacteriaceae* have
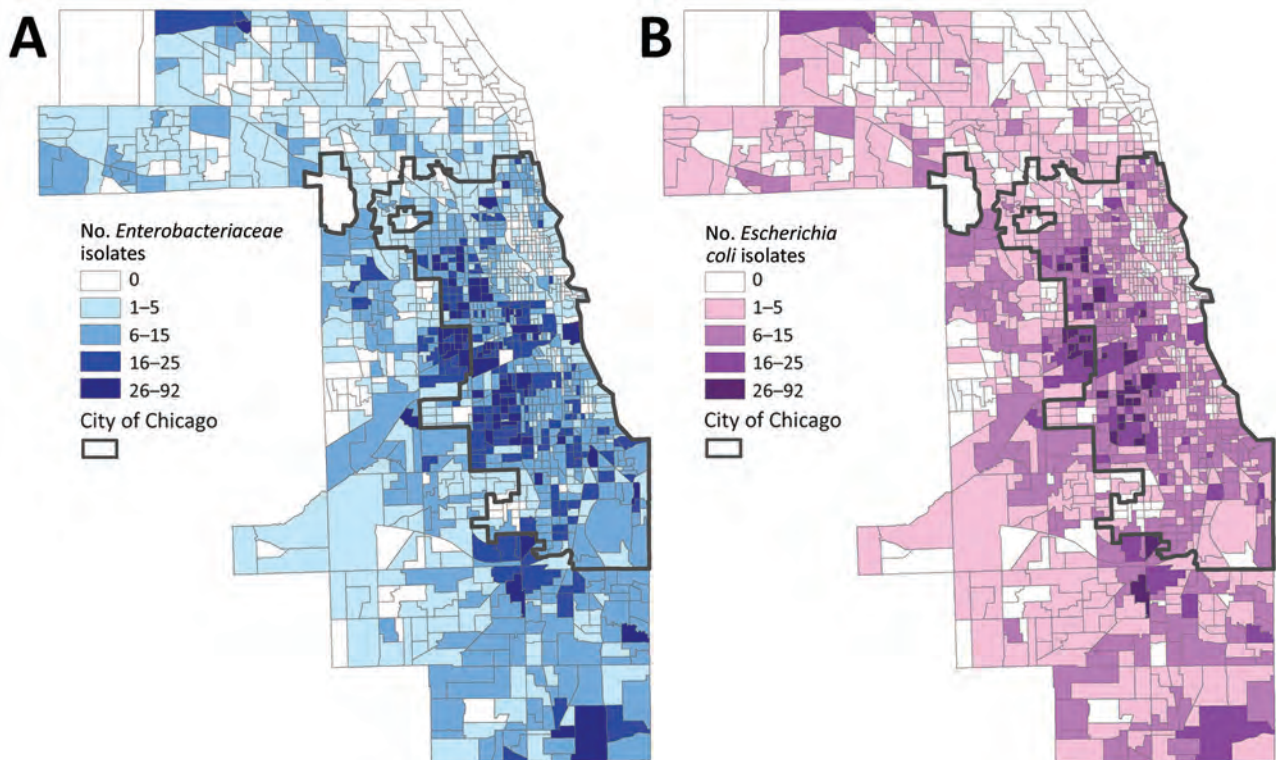
Figure 1. Number of *Enterobacteriaceae* (A) and *Escherichia coli* (B) isolates collected from patients in the Cook County Health healthcare system, by Cook County census tract, Illinois, USA, 2016–2018.
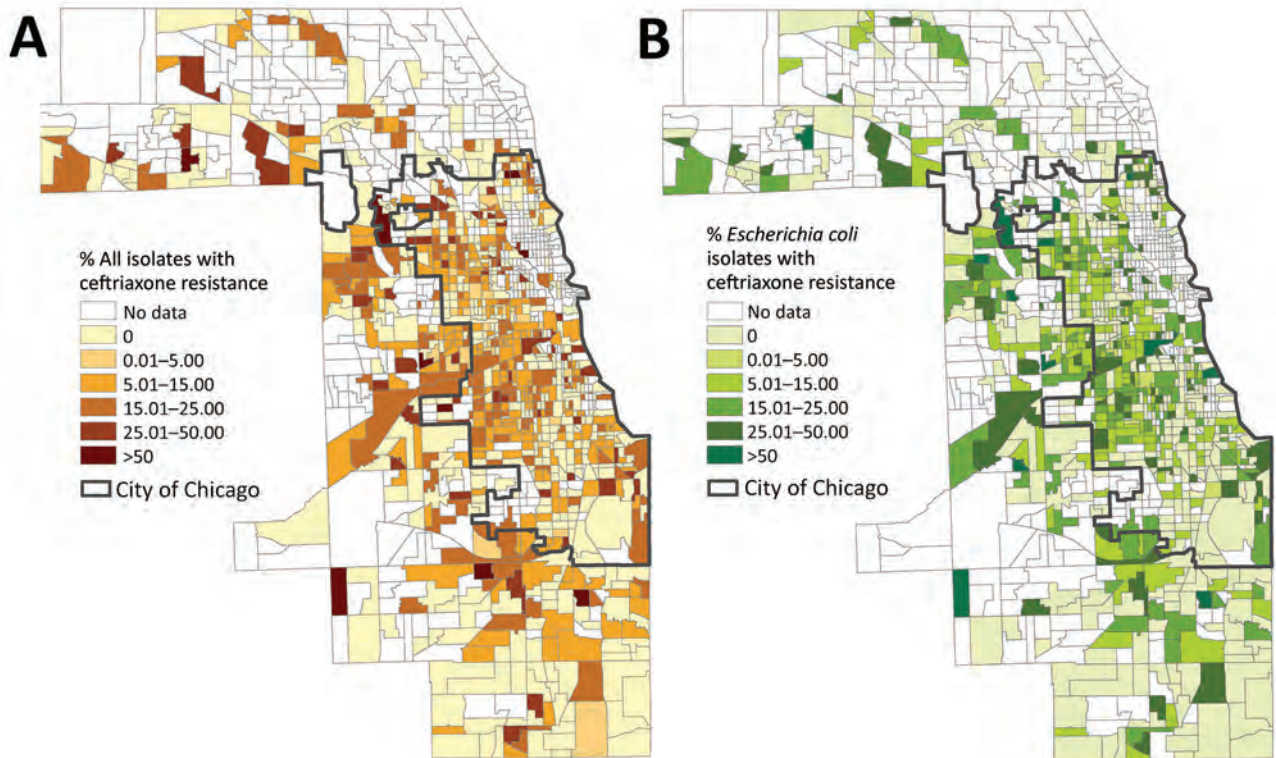
Figure 2. Percentage of ceftriaxone-resistant *Enterobacteriaceae* (A) and Escherichia coli (B) isolates collected from patients in the Cook County Health healthcare system, by Cook County census tract, Illinois, USA, 2016–2018.

shown nonrandom spatial distribution of antimicrobial-resistant *Enterobacteriaceae* in large urban areas. A study from São Paulo, Brazil (*20*), identified hotspot clusters of ciprofloxacin-resistant E.coli isolates that were associated with population-level ciprofloxacin usage. A study from Japan (*21*) also showed clustering of levofloxacin-resistant *E. coli* isolates in the western part of the country, also associated with population-level quinolone usage. In Chicago, residence in the northwest and southern region of Chicago (and adjacent suburbs) was independently associated with increased likelihood of infection by CTX-M-9 *Enterobacteriaceae* isolates in children (*22*).

Our individual-level analysis showing that ceftriaxone resistance was associated with increasing age and male sex is consistent with data reported elsewhere (*8,23*) and might reflect unmeasured associated underlying conditions, especially those involving the genitourinary tract (*8,24*) and antibiotic exposures (*8,25–27*). Unmeasured underlying conditions and associated antibiotic exposure could also account for the strong association between ceftriaxone resistance and the need for hospitalization, although the increased virulence observed in circulating ESBL-producing clones (*28*) could account for this finding.

The associations between self-reported Hispanic ethnicity and CTX-R *Enterobacteriaceae* and *E. coli* identified in the individual-level analysis and ecologic analyses merit further scrutiny. First, the correlation of Hispanic ethnicity and foreign-born status at a population level (r = 0.69) suggests that these 2 communities are highly interrelated; indeed, ≈45.6% of foreign-born persons in Cook County are noted to have emigrated from Latin America (*19*). Therefore, patients who self-identified as Hispanics also might have been foreign-born and might have become colonized by resistant organisms before emigration from or during travel to Latin American countries, some of which have reported

Table 2. Population-level risk factors for ceftriaxone-resistant *Enterobacteriaceae* identified in Cook County census tracts, Illinois, USA, 2016–2018

Risk factor	Bivariate analysis	
	Odds ratio (95% CI)	p value
Non-Hispanic White population	0.98 (0.98–0.99)	<0.01
Non-Hispanic Black population	0.99 (0.99–0.99)	<0.01
Hispanic population	1.02 (1.01–1.02)	<0.01
Foreign-born population	1.02 (1.01–1.03)	<0.01
Households below poverty	1.00 (0.99–1.39)	0.35
Overcrowding	1.16 (0.97–1.39)	0.10
Uninsured population	1.07 (1.05–1.10)	<0.01

Table 3. Population-level risk factors for ceftriaxone-resistant *Escherichia coli* identified in Cook County census tracts, Illinois, USA, 2016–2018

Risk factor	Bivariate analysis	
	Odds ratio (95% CI)	p value
Non-Hispanic White population	0.99 (0.99–1.00)	0.44
Non-Hispanic Black population	0.98 (0.98–0.99)	<0.01
Hispanic population	1.03 (1.02–1.03)	<0.01
Foreign-born population	1.04 (1.03–1.05)	<0.01
Households below poverty	0.99 (0.98–1.00)	0.24
Overcrowding	1.25 (1.04–1.53)	0.02
Uninsured population	1.08 (1.06–1.11)	<0.01

high prevalence of ESBL-producing *Enterobacteriaceae* (5,29,30). This same pathway could explain the similar association between the proportion of foreign-born population in a census tract and likelihood of ceftriaxone-resistance in the ecologic and individual-level analyses. In addition, a sizable proportion of non–US-born Cook County residents emigrated from countries in Asia (27.3%) and fewer emigrated from Africa (3.2%) (19), continents with variable but often high prevalence of drug-resistant *Enterobacteriaceae* (3,4) (We did not include other racial and ethnic population-level characteristics in our individual-level analysis because of multicollinearity with individual-level race and ethnicity). Second, Hispanics residing in the United States have been reported to use antibiotics without prescription more frequently than other racial and ethnic groups (31). Third, we cannot discount that proximity of Hispanic communities, foreign-born

communities, or both to environmental sources, such as contaminated waterways, might be an important added risk factor for colonization or infection by drug-resistant *Enterobacteriaceae* in these areas.

Although in our ecologic analysis the percentage of households beneath the poverty line was not significantly different between census tracts from which CTX-R *Enterobacteriaceae* or *E. coli* isolates were and were not generated, observed associations between the percentage of uninsured residents and the presence in census tracts of CTX-R isolates suggest that census tract-level deprivation might predispose to antimicrobial-resistant infections. In the analysis limited to *E. coli* isolates, overcrowding percentages were also associated with antimicrobial-resistant infections, suggesting possible household-level transmission. A recently published study by Otter et al. from London (27) identified associations between community-level variables, individual-level variables, and likelihood of ESBL rectal colonization among patients admitted to the hospital. In their analysis, only recent overseas travel, recent antimicrobial use, and community-level overcrowding rates were associated with ESBL rectal carriage, whereas individual- and community-level race, ethnicity, and immigration characteristics were not. The paucity of spatial and ecologic studies of antimicrobial-resistant *Enterobacteriaceae* in the United States makes it difficult to establish whether our results are representative of the urban epidemiology of these organisms in the country. Although not directly

Table 4. Individual and population-level risk factors for ceftriaxone-resistant *Enterobacteriaceae* in patients, Cook County Health healthcare system, Illinois, USA, 2016–2018*

Characteristic	No. (%) isolates			Bivariate analysis	
	All	Ceftriaxone-susceptible	Ceftriaxone-resistant	OR (95% CI)	p value
Total no. isolates	10,891 (100)	9,856 (90.5)	1,035 (9.5)		
Sex					
F	7,853 (72.1)	7,215 (66.2)	638 (5.9)	Referent	
M	3,038 (27.9)	2,641 (24.2)	397 (3.7)	1.7 (1.5–1.9)	<0.01
Age group, y					
18–34	2,011 (18.6)	1,895 (17.4)	116 (1.2)	Referent	
35–51	3,109 (28.5)	2,846 (26.1)	263 (2.4)	1.5 (1.2–1.9)	<0.01
52–68	4,092 (37.5)	3,667 (33.7)	425 (3.8)	1.9 (1.5–2.3)	<0.01
69–85	1,471 (13.5)	1,259 (11.6)	212 (1.9)	2.8 (2.2–3.5)	<0.01
>85	208 (1.9)	189 (90.9)	19 (9.1)	1.6 (0.9–2.7)	0.05
Race and ethnicity					
Non-Hispanic White	997 (9.2)	902 (8.3)	95 (0.9)	1.6 (1.2–2.0)	<0.01
Non-Hispanic Black	4,394 (40.4)	4,120 (37.8)	274 (2.6)	Referent	
Hispanic	4,898 (44.9)	4,324 (39.7)	574 (5.2)	1.9 (1.7–2.3)	<0.01
Other†	602 (5.5)	510 (4.7)	92 (0.8)	2.7 (2.1–3.5	<0.01
Encounter type					
Outpatient	5,889 (54.1)	5,419 (49.8)	470 (4.3)	Referent	
Emergency department	2,890 (26.5)	2,655 (24.4)	235 (2.1)	1.0 (0.9–1.2)	0.80
Inpatient	2,112 (19.4)	1,782 (16.4)	330 (3.0)	2.1 (1.8–2.5)	<0.01
Mean % foreign-born population (SD)‡	21.5 (17.0)	21.04 (17.0)	25.8 (16.2)	1.0 (1.0–1.1)	<0.01

*Values are no. (%) except as indicated. OR, odds ratio.
†Other refers to isolates from participants who identified as non-Hispanic and reported race as Asian (3% of all isolates), American Indian/Alaska Native (0.4%), multiple races (0.1%), or unknown race (0.8%)
‡Based on data from 2017 American Community Survey 5-year estimates (19).

comparable because of a difference in outcomes, the discrepancy of our findings and those reported by Otter et al. (27) suggest that the effect of population-level variables might remain distinct in different geographic areas.

Our findings are limited by the fact that our isolates were obtained in a single healthcare system. As a safety-net healthcare system, CCH is likely to be subject to geographic bias already because our patients do not come equitably from all census tracts in Cook County. The paucity of isolates from Cook County communities that do not obtain services from our healthcare system limits the generalizability of our findings regionally. We were unable to gather data regarding risk factors for healthcare-associated infections (such as recent hospitalization) and recent antimicrobial use, both important limitations. In addition, the relatively small sample size and high correlation between population-level factors made meaningful multivariable analysis infeasible. We were unable to perform genomic analysis of CTX-R organisms, which would have enabled us to evaluate the relatedness of isolates and make stronger inferences about whether spatial clustering was related to a point source or interpersonal transmission. Finally, the limited number of clinical and population-level variables included in the individual risk analysis prevents definite conclusions regarding individual risk for CTX-R infection among our patients. Indeed, concurrent assessment of other well-known individual risk factors, such as recent travel or antimicrobial use, could alter the effect size of ecologic variables. Nevertheless, our findings corroborate previous investigations that have identified important community-level variation in CTX-R infection risk in association with geographic (20–22), demographic (7,23–25), and population-level variables (27). Developing effective mitigation strategies, such as focusing antimicrobial stewardship efforts on affected areas, including residence as a risk factor in treatment-decision algorithms, or identifying and eradicating local environmental sources of drug-resistant pathogens, could well depend on improved understanding of these dynamics.

About the Author

Dr. Sardá is an infectious disease attending at Cook County Health, and an assistant professor of medicine at Rush Medical College in Chicago, IL. Her research interests are in antimicrobial resistance, spatial and ecological determinants of health, and the applications of machine learning in epidemiology.

References

1. CDC. Antibiotic resistance threats in the United States, 2019 [cited 2020 Oct 1]. https://www.cdc.gov/drugresistance/pdf/threats-report/2019-ar-threats-report-508.pdf
2. Jernigan JA, Hatfield KM, Wolford H, Nelson RE, Olubajo B, Reddy SC, et al. Multidrug-resistant bacterial infections in U.S. hospitalized patients, 2012–2017. N Engl J Med. 2020;382:1309–19. https://doi.org/10.1056/NEJMoa1914433
3. Flokas ME, Karanika S, Alevizakos M, Mylonakis E. Prevalence of ESBL-producing *Enterobacteriaceae* in pediatric bloodstream infections: a systematic review and meta-analysis. PLoS One. 2017;12:e0171216. https://doi.org/10.1371/journal.pone.0171216
4. Toy T, Pak GD, Duc TP, Campbell JI, El Tayeb MA, Von Kalckreuth V, et al. Multicountry distribution and characterization of extended-spectrum β-lactamase-associated Gram-negative bacteria from bloodstream infections in sub-Saharan Africa. Clin Infect Dis. 2019;69 (Suppl 6):S449–58. https://doi.org/10.1093/cid/ciz450
5. Villegas MV, Kattan JN, Quinteros MG, Casellas JM. Prevalence of extended-spectrum beta-lactamases in South America. Clin Microbiol Infect. 2008;14(Suppl 1):154–8. https://doi.org/10.1111/j.1469-0691.2007.01869.x
6. Lob SH, Nicolle LE, Hoban DJ, Kazmierczak KM, Badal RE, Sahm DF. Susceptibility patterns and ESBL rates of *Escherichia coli* from urinary tract infections in Canada and the United States, SMART 2010-2014. Diagn Microbiol Infect Dis. 2016;85:459–65. https://doi.org/10.1016/j.diagmicrobio.2016.04.022
7. Hilty M, Betsch BY, Bögli-Stuber K, Heiniger N, Stadler M, Küffer M, et al. Transmission dynamics of extended-spectrum β-lactamase-producing *Enterobacteriaceae* in the tertiary care hospital and the household setting. Clin Infect Dis. 2012;55:967–75. https://doi.org/10.1093/cid/cis581
8. Rodríguez-Baño J, Navarro MD, Romero L, Martínez-Martínez L, Muniain MA, Perea EJ, et al. Epidemiology and clinical features of infections caused by extended-spectrum beta-lactamase-producing *Escherichia coli* in nonhospitalized patients. J Clin Microbiol. 2004;42:1089–94. https://doi.org/10.1128/JCM.42.3.1089-1094.2004
9. Pitout JD, Gregson DB, Church DL, Elsayed S, Laupland KB. Community-wide outbreaks of clonally related CTX-M-14 beta-lactamase-producing *Escherichia coli* strains in the Calgary health region. J Clin Microbiol. 2005;43:2844–9. https://doi.org/10.1128/JCM.43.6.2844-2849.2005
10. Doi Y, Park YS, Rivera JI, Adams-Haduch JM, Hingwe A, Sordillo EM, et al. Community-associated extended-spectrum β-lactamase-producing *Escherichia coli* infection in the United States. Clin Infect Dis. 2013;56:641–8. https://doi.org/10.1093/cid/cis942
11. Arcilla MS, van Hattem JM, Haverkate MR, Bootsma MCJ, van Genderen PJJ, Goorhuis A, et al. Import and spread of extended-spectrum β-lactamase-producing *Enterobacteriaceae* by international travellers (COMBAT study): a prospective, multicentre cohort study. Lancet Infect Dis. 2017;17:78–85. https://doi.org/10.1016/S1473-3099(16)30319-X
12. van Duijkeren E, Wielders CCH, Dierikx CM, van Hoek AHAM, Hengeveld P, Veenman C, et al. Long-term carriage of extended-spectrum β-lactamase-producing *Escherichia coli* and Klebsiella pneumoniae in the general population in the Netherlands. Clin Infect Dis. 2018;66:1368–76. https://doi.org/10.1093/cid/cix1015
13. Martischang R, Riccio ME, Abbas M, Stewardson AJ, Kluytmans JAJW, Harbarth S. Household carriage and acquisition of extended-spectrum β-lactamase-producing

Enterobacteriaceae: A systematic review. Infect Control Hosp Epidemiol. 2020;41:286–94. https://doi.org/10.1017/ice.2019.336

14. Day MJ, Hopkins KL, Wareham DW, Toleman MA, Elviss N, Randall L, et al. Extended-spectrum β-lactamase-producing *Escherichia coli* in human-derived and foodchain-derived samples from England, Wales, and Scotland: an epidemiological surveillance and typing study. Lancet Infect Dis. 2019;19:1325–35. https://doi.org/10.1016/S1473-3099(19)30273-7

15. Johnson JR, Sannes MR, Croy C, Johnston B, Clabots C, Kuskowski MA, et al. Antimicrobial drug-resistant *Escherichia coli* from humans and poultry products, Minnesota and Wisconsin, 2002-2004. Emerg Infect Dis. 2007;13:838–46. https://doi.org/10.3201/eid1306.061576

16. Fuentes MD, Gutierrez S, Sahagun D, Gomez J, Mendoza J, Ellis CC, et al. Assessment of antibiotic levels, multi-drug resistant bacteria and genetic biomarkers in the waters of the Rio Grande River between the United States–Mexico border. J Health Pollut. 2019;9:190912. https://doi.org/10.5696/2156-9614-9.23.190912

17. Jørgensen SB, Søraas AV, Arnesen LS, Leegaard TM, Sundsfjord A, Jenum PA. A comparison of extended spectrum β-lactamase producing *Escherichia coli* from clinical, recreational water and wastewater samples associated in time and location. PLoS One. 2017;12:e0186576. https://doi.org/10.1371/journal.pone.0186576

18. Clinical and Laboratory Standards Institute. Performance standards for antimicrobial susceptibility testing, 30th edition (M100). Wayne (PA): The Institute; 2020.

19. US Census Bureau. American Community Survey 5-year estimates. 2017 [cited 2020 Oct 1]. https://data.census.gov

20. Kiffer CR, Camargo EC, Shimakura SE, Ribeiro PJ Jr, Bailey TC, Pignatari AC, et al. A spatial approach for the epidemiology of antibiotic use and resistance in community-based studies: the emergence of urban clusters of *Escherichia coli* quinolone resistance in Sao Paulo, Brasil. Int J Health Geogr. 2011;10:17. https://doi.org/10.1186/1476-072X-10-17

21. Terahara F, Nishiura H. Fluoroquinolone consumption and *Escherichia coli* resistance in Japan: an ecological study. BMC Public Health. 2019;19:426. https://doi.org/10.1186/s12889-019-6804-3

22. Logan LK, Medernach RL, Domitrovic TN, Rispens JR, Hujer AM, Qureshi NK, et al. The clinical and molecular epidemiology of CTX-M-9 group producing *Enterobacteriaceae* infections in children. Infect Dis Ther. 2019;8:243–54. https://doi.org/10.1007/s40121-019-0237-2

23. Ho PL, Chu YP, Lo WU, Chow KH, Law PY, Tse CW, et al. High prevalence of *Escherichia coli* sequence type 131 among antimicrobial-resistant *E. coli* isolates from geriatric patients.

J Med Microbiol. 2015;64:243–7. https://doi.org/10.1099/jmm.0.000012

24. Calbo E, Romaní V, Xercavins M, Gómez L, Vidal CG, Quintana S, et al. Risk factors for community-onset urinary tract infections due to *Escherichia coli* harbouring extended-spectrum beta-lactamases. J Antimicrob Chemother. 2006;57:780–3. https://doi.org/10.1093/jac/dkl035

25. Rodríguez-Baño J, Picón E, Gijón P, Hernández JR, Ruíz M, Peña C, et al.; Spanish Network for Research in Infectious Diseases (REIPI). Community-onset bacteremia due to extended-spectrum beta-lactamase-producing Escherichia coli: risk factors and prognosis. Clin Infect Dis. 2010;50:40–8. https://doi.org/10.1086/649537

26. Goodman KE, Lessler J, Cosgrove SE, Harris AD, Lautenbach E, Han JH, et al.; Antibacterial Resistance Leadership Group. A clinical decision tree to predict whether a bacteremic patient is infected with an extended-spectrum β-lactamase-producing organism. Clin Infect Dis. 2016;63:896–903. https://doi.org/10.1093/cid/ciw425

27. Otter JA, Natale A, Batra R, Tosas Auguet O, Dyakova E, Goldenberg SD, et al. Individual- and community-level risk factors for ESBL *Enterobacteriaceae* colonization identified by universal admission screening in London. Clin Microbiol Infect. 2019;25:1259–65. https://doi.org/10.1016/j.cmi.2019.02.026

28. Rottier WC, Ammerlaan HS, Bonten MJ. Effects of confounders and intermediates on the association of bacteraemia caused by extended-spectrum β-lactamase-producing *Enterobacteriaceae* and patient outcome: a meta-analysis. J Antimicrob Chemother. 2012;67:1311–20. https://doi.org/10.1093/jac/dks065

29. García C, Horna G, Linares E, Ramírez R, Tapia E, Velásquez J, et al. Antimicrobial drug resistance in Peru. Emerg Infect Dis. 2012;18:520–1. https://doi.org/10.3201/eid1803.100878

30. Winokur PL, Canton R, Casellas JM, Legakis N. Variations in the prevalence of strains expressing an extended-spectrum beta-lactamase phenotype and characterization of isolates from Europe, the Americas, and the Western Pacific region. Clin Infect Dis. 2001;32(Suppl 2):S94–103. https://doi.org/10.1086/320182

31. Mainous AG III, Cheng AY, Garr RC, Tilley BC, Everett CJ, McKee MD. Nonprescribed antimicrobial drugs in Latino community, South Carolina. Emerg Infect Dis. 2005;11:883–8. https://doi.org/10.3201/EID1106.040960

Address for correspondence: Vanessa Sardá, Cook County Health, 1900 W Polk St, Ste 643, Chicago, IL, 60611, USA; email: vanessa.sarda@cookcountyhhs.org

Social Distancing, Mask Use, and Transmission of Severe Acute Respiratory Syndrome Coronavirus 2, Brazil, April–June 2020

Marcelo Rodrigues Gonçalves, Rodrigo Citton Padilha dos Reis, Rodrigo Pedroso Tólio,
Lucia Campos Pellanda, Maria Inês Schmidt, Natan Katz, Sotero Serrate Mengue,
Pedro C. Hallal, Bernardo L. Horta, Mariangela Freitas Silveira, Roberto Nunes Umpierre,
Cynthia Goulart Bastos-Molina, Rodolfo Souza da Silva, Bruce B. Duncan

We assessed the associations of social distancing and mask use with symptomatic, laboratory-confirmed severe acute respiratory syndrome coronavirus 2 infection in Porto Alegre, Brazil. We conducted a population-based case-control study during April–June 2020. Municipal authorities furnished case-patients, and controls were taken from representative household surveys. In adjusted logistic regression analyses of 271 case-patients and 1,396 controls, those reporting moderate to greatest adherence to social distancing had 59% (odds ratio [OR] 0.41, 95% CI 0.24–0.70) to 75% (OR 0.25, 95% CI 0.15–0.42) lower odds of infection. Lesser out-of-household exposure (vs. going out every day all day) reduced odds from 52% (OR 0.48, 95% CI 0.29–0.77) to 75% (OR 0.25, 95% CI 0.18–0.36). Mask use reduced odds of infection by 87% (OR 0.13, 95% CI 0.04–0.36). In conclusion, social distancing and mask use while outside the house provided major protection against symptomatic infection.

The coronavirus disease (COVID-19) pandemic has spread worldwide (*1*). The rapid transmission of the causative agent, severe acute respiratory syndrome coronavirus 2 (SARS-CoV-2), has produced a high death toll, threatening health systems and creating huge challenges for governments and societies.

Until advances in the development and distribution of vaccines or treatments reduce the risk for COVID-19 complications to levels permitting near-normal day-to-day functioning, societies continue to require simple public health approaches to control pandemic spread, including mask use and social distancing. Several cohort studies in hospital settings have shown benefits of both interventions (*2*). However, in community settings, where these approaches have the greatest potential to limit viral spread and halt the pandemic, documented support for their use comes mostly from ecologic studies and, indirectly, from findings related to previous pandemics of other coronaviruses. Only a few studies (*3*), including a retrospective case-control study of asymptomatic contacts (*4*), a randomized trial (*5*), and a study at sea (*6*), have evaluated their effectiveness against community transmission of SARS-CoV-2 on the basis of individual-level exposure and outcome measurements. Their relevance remains embroiled in controversy. To help close this gap, we evaluated the association of mask use and social distancing with incident, symptomatic, laboratory-confirmed SARS-CoV-2 infection in a population-based case-control study.

Methods

We conducted a population-based, case-control study in Porto Alegre, the capital of Rio Grande do Sul State, Brazil, which has an estimated population of 1,483,771 (*7*). The ethics committee of the Hospital de Clínicas de Porto Alegre approved our study (approval no. 31499420.5.0000.5327), and the Brazilian National Ethics Committee (approval no. 30415520.2.0000.5313) approved the accompanying

Author affiliations: Universidade Federal do Rio Grande do Sul, Porto Alegre, Brazil (M.R. Gonçalves, R.C.P. Reis, R.P. Tólio, M.I. Schmidt, N. Katz, S.S. Mengue, R.N. Umpierre, C.G. Bastos-Molina, R.S. da Silva, B.B. Duncan); Hospital de Clínicas de Porto Alegre, Porto Alegre (M.R. Gonçalves, M.I. Schmidt, R.N. Umpierre, C.G. Bastos-Molina, R.S. da Silva, B.B. Duncan); Universidade Federal de Ciências da Saúde de Porto Alegre, Porto Alegre (L.C. Pellanda); Municipal Health Department, Porto Alegre (N. Katz); Universidade Federal de Pelotas, Pelotas, Brazil (P.C. Hallal, B.L. Horta, M.F. Silveira); Universidade do Vale dos Sinos (UNISINOS), São Leopoldo, Brazil (C.G. Bastos-Molina)

seroprevalence surveys. All participants gave prior informed consent, in written form by the controls and verbally for case-patients.

On March 19, 2020, state officials mandated school and nonessential business closure and travel restrictions and ordered citizens to stay at home unless going to essential services (8). On May 8, 2020, Porto Alegre's mayor issued a series of orders and recommendations for mask use. These mandates, with only slight alterations, remained in force in Porto Alegre throughout the period of this study. However, social distancing and mask use were not universally adopted; prominent leaders questioned their necessity and supported widely publicized gatherings, frequently without mask use.

We obtained case-patients from the Municipal Health Department, given that notification of COVID-19 cases is mandatory. The list consisted of all persons (excluding healthcare professionals) who tested positive for SARS-CoV-2 by reverse transcription PCR or antibody testing through June 19, 2020, in Porto Alegre. With rare exceptions, case-patients were receiving medical care, because testing during this period was limited and available only for symptomatic persons. Cases were identified in hospitals and primary care settings. We then contacted persons ≥18 years of age whose date of symptom onset was on or after April 28, 2020. Before deeming a case-patient nonrespondent, we attempted ≥10 calls on different days at different hours, as well as attempting contact through short message service, WhatsApp, other social media, and physical mail. We excluded persons working in healthcare settings because our focus was community transmission. We also excluded deceased persons and persons who resided outside the municipality. When the case-patient could not be interviewed, we obtained responses from a proxy (i.e., a close contact, either a family member or caretaker).

Controls were the seronegative persons in 3 representative community surveys of SARS-CoV-2 antibody prevalence in Porto Alegre conducted during May 9–11, May 23–25, and June 26–28, 2020 (9,10). For the surveys, 50 of Porto Alegre's census tracts were selected with probability proportional to size. Within each, during each survey, 10 households were selected systematically; if no one was home or residents refused participation, we used the neighboring residence. A resident of each home was then selected at random for interview.

Controls underwent a brief interview, including questions on social distancing, mask use, and sociodemographics. Seropositivity was determined by a point-of-care rapid antibody test (L.C. Pellanda et al.,

unpub. data, https://www.medrxiv.org/content/10.1101/2020.05.06.20093476v1). For case-patients, we conducted telephone interviews by using the same questions applied in the surveys.

Trained interviewers queried case-patients and controls using standardized questionnaires: "Regarding the social distancing recommended by health authorities, that is, staying at home and avoiding contact with other people, how much do you think you have managed to do?" Reply choices were 1, very little; 2, little; 3, some; 4, a great deal; and 5, practically isolated from everyone.

In response to "What has been your routine of activities?" participants opted among the following choices: 1, go out every day, all day, to work or other regular activity; 2, go out every day for some activity; 3, go out from time to time to shop and stretch my legs; 4, go out only for essential things like buying food; and 5, stay at home all the time. We created and categorized a social distancing score by summing responses to each of these questions when taken as an ordinal scale.

All case-patients were asked about mask use, but controls were asked about mask use only during the last seroprevalence survey. In response to "Do you use a mask when you leave home?" case-patients opted between yes and no and controls among yes, sometimes, and no. For modeling, we merged the replies yes and sometimes. For case-patients and controls, we defined income as mean head-of-household monthly income on the respondent's census tract.

We calculated sample size by using an α of 0.05 and 80% power: to detect an odds ratio of 2 would require 93 case-patients and 372 controls. We described continuous variables by mean (SD) or median (interquartile range) and categorical variables by frequency (percentage). When information on household size was missing, we used the mean household size of the respondent's census tract. Participants with other missing values were excluded from analyses. We investigated associations of social distancing and mask use through prespecified logistic regression analyses. We defined the pandemic moment as the date of symptom onset for case-patients and as 10 days before the date of interview for controls. We performed all analyses by using the statistical software package R version 4.0.2 (11).

Results

Of all initial case-patients, after excluding deceased persons and those who were not part of the target population, 813 case-patients were eligible for contact (Figure 1). We established contact with 467 (57.4%)
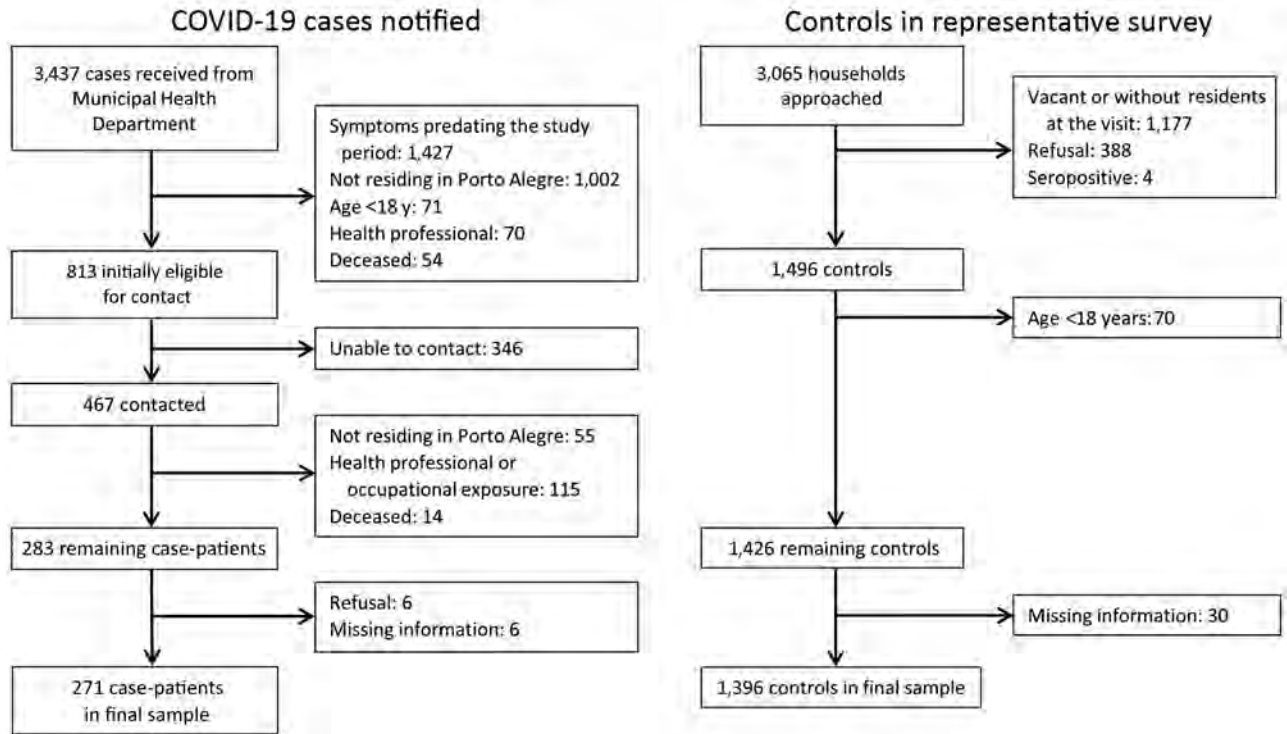
Figure 1. Flowchart of COVID-19 case-patient and controls, Porto Alegre, Brazil, April–June 2020. COVID-19, coronavirus disease.

and found an additional 184 ineligible. Of the remaining 283 persons, 12 refused participation or provided incomplete social distancing information, leaving 271 case-patients. We interviewed 237 (87.5%) directly and 34 (12.5%) by proxy. If the proportion of actual eligible case-patients among the 813 initially eligible persons was the same as among those contacted (283/467), the 271 cases represent a response rate of 55.0% among those actually eligible. Comparison of the Municipal Health Department case data showed that case-patients in the final sample differed little from those not included in terms of sex (43.9% [95% CI 37.9%–50.0%] men among those included vs. 48.3% [95% CI 44.7%–58.6%] men among those excluded) and age (46.0 [95% CI 44.0–48.0] years for those included vs. 48.0 [95% CI 46.2–49.8] years for those excluded).

For controls, of 3,065 households approached, 1,177 (38.4%) were vacant or without residents at home, residents refused in 388 (12.7%) households, and 4 seropositive persons were excluded; a total of 1,496 (48.8%) potential controls were contacted (*12*). An additional 70 were <18 years old and data on race were missing for 30, leaving 1,396 (45.5%) for analyses. Comparison of controls in the final sample with the 30 persons for whom data were missing demonstrated they were also similar in sex (38.5% [95% CI

35.9%–41.0%] men for final controls vs. 36.7% [95% CI 21.9%–54.5%] men for those with data missing) and age (49.7 [95% CI 48.8–50.6] for final controls vs. 52.3 [95% CI 44.1–60.5] years for those with data missing).

Our controls were more frequently women and were somewhat older than the average of the adult population of Porto Alegre (Table 1) (*13*). Case-patients, compared to controls, were more frequently men, Black, and younger; had a lower level of education; and lived in larger households (Table 2). Case-patients were less likely to adhere to social distancing. In the variable summarizing social distancing,

Table 1. Comparison of sociodemographic characteristics between control subjects and the population of Porto Alegre, Brazil, in study of face masks, social distancing, and transmission of severe acute respiratory syndrome coronavirus 2, April–June 2020

Characteristic	Porto Alegre, %	Controls, %
Sex		
M	47.8	38.5
F	52.2	61.5
Age group, y		
18–29	20.2	15.5
30–39	18.4	17.9
40–49	15.8	16.1
50–59	18.8	17.6
≥60	26.8	33.0
Race		
White	75.3	75.4
Nonwhite	24.7	24.6

case-patients more frequently practiced least (16.2% vs. 7.2% for controls) or little (26.6% vs. 15.5% for controls) social distancing. Mask use was commonly reported. After we excluded those reporting staying at home all the time, only 5 (1.2%) controls and 14 (7.1%) case-patients reported not using masks when out.

We compared the temporal distribution of symptom onset of case-patients and the 3 interview periods for controls (Figure 2). On average, symptom onset in case-patients was slightly less than a week before the interview date of controls (Table 2).

In crude analyses (Table 3, model 1), moderate or high adherence to social distancing and being practically isolated from everyone all reduced risk for infection. Multiple adjustments (models 2 and 3) produced little change. In model 3, those with moderate adherence to social distancing were 72% (OR 0.28, 95% CI

0.16–0.49) and those with high adherence 75% (OR 0.25, 95% CI 0.15–0.42) less likely to become infected. Persons who reported they were practically isolated from everyone were 59% (OR 0.41, 95% CI 0.24–0.70) less likely to become infected. When we excluded proxy interviews (model 4), the association of being practically isolated from everyone became stronger (OR 0.34, 95% CI 0.20–0.60).

In similar models (Table 3), lesser activity of any degree reduced the odds of infection compared to leaving home daily for the whole day. Relatively little confounding was present, and in models adjusted for all covariates, going out for some activities every day reduced odds by 74% (OR 0.26, 95% CI 0.13–0.49), going out from time to time reduced odds by 61% (OR 0.39, 95% CI 0.24–0.61), and going out just for essential activities reduced odds by 75%

Table 2. Sociodemographic and social distancing data of case-patients and controls, Porto Alegre, Brazil, April–June 2020*

Characteristic	Case-patients, n = 271	Controls, n = 1,396
Sex		
M	119 (43.9)	537 (38.5)
F	152 (56.1)	859 (61.5)
Mean age, y, ±SD	46.0 ±17.2	49.7 ±17.5
Education		
University	98 (36.2)	722 (51.7)
High school complete	88 (32.5)	388 (27.8)
High school incomplete	85 (31.4)	286 (20.5)
Race		
White	197 (72.7)	1053 (75.4)
Mixed race	35 (12.9)	182 (13.0)
Black	36 (13.3)	149 (10.7)
Other	3 (1.1)	12 (0.9)
Household size ±SD	2.9 ±1.2†	2.5 ±1.4
Monthly income, Brazilian real, head of household‡	1,575 (IQR 965–3,365)	2,205 (IQR 1,089–3,390)
Epidemiologic week ±SD	21.9 ±1.6	21.0 ±2.9
Adherence to social distancing		
Very little	32 (11.8)	56 (4.0)
Little	32 (11.8)	81 (5.8)
Moderate—some	43 (15.9)	260 (18.6)
High—a great deal	88 (32.5)	651 (46.6)
Practically isolated from everybody	76 (28.0)	348 (24.9)
Daily routine		
Go out every day, all day, to work or other regular activity	118 (43.5)	251 (18.0)
Go out every day for some activity	12 (4.4)	102 (7.3)
Go out from time to time to shop and stretch my legs	30 (11.1)	192 (13.8)
Go out only for essential things like buying food	74 (27.3)	696 (49.9)
Stay at home all the time	37 (13.7)	155 (11.1)
Social distancing score ±SD	6.2 ±2.5	7.1 ±2.0
Social distancing		
Least	44 (16.2)	100 (7.2)
Little	72 (26.6)	216 (15.5)
Much	98 (36.2)	729 (52.2)
Most	57 (21.0)	351 (25.1)
Mask use§		
No	14 (7.1)	5 (1.2)
Sometimes	NA	10 (2.4)
Always	184 (92.9)	405 (96.4)

*Values are no. (%) except as indicated. IQR, interquartile range; NA, not applicable.
†Excluding 4 case-patients living in nursing homes.
‡Median of mean head-of-household income of respondent´s census tract.
§Including only cases with pandemic moment equivalent to that of the last seroprevalence survey and excluding case-patients and controls reporting to stay at home all the time.
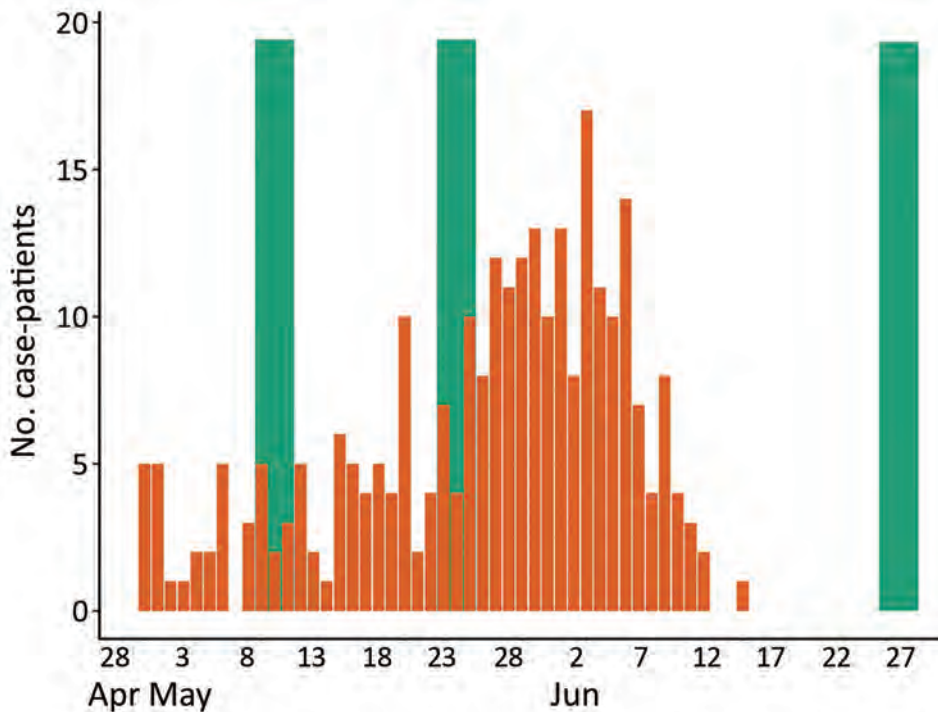
Figure 2. Number of case-patients (n = 271) by date of coronavirus disease symptom onset in study of face masks, social distancing, and transmission of severe acute respiratory syndrome coronavirus 2, Porto Alegre, Brazil, April–June 2020. Green bars indicate dates of interviews of controls (n = 1,396): May 9–11, May 23–25, and June 26–28.

(OR 0.25, 95% CI 0.18–0.36). After we excluded proxy interviews (model 4), staying home all the time also provided a major reduction in odds (OR 0.25, 95% CI 0.13–0.44).

When these 2 measures were joined in a categorical summary measure of social distancing (Table 3), practicing much distancing reduced the adjusted odds of becoming infected by 67% (OR 0.33, 95% CI 0.22–0.52) and most distancing reduced odds by 62% (OR 0.38, 95% CI 0.23–0.62), in comparison to least distancing. After excluding proxy interviews, the association became graded; odds were 73% lower (OR 0.27, 95% CI 0.16–0.46) among persons who practiced the most social distancing.

Because information on mask use was only obtained during the third seroprevalence survey, we compared use for the 464 controls in this survey with 229 case-patients of a similar pandemic moment (symptom onset <10 days before the second survey). Considering all those with mask data during this period, crude analyses demonstrated that mask use reduced odds of infection by 88% (OR 0.12, 95% CI 0.04–0.30), and after adjustments, including the summary distancing score (Table 4, model 3), by 90% (OR 0.10, 95% CI 0.03–0.25). No interaction was seen between mask use and social distancing (OR 0.96, 95% CI 0.60–1.58). The association was similar in the restricted sample, which removed those who reported staying home all the time (87%; OR 0.13, 95% CI 0.04–0.36) and, in addition, when proxy respondents

were removed (88%; OR 0.12, 95% CI 0.04–0.35). In a sensitivity analysis in which "sometimes" mask use was joined with "no" rather than with "always," mask use reduced odds of infection (model 3) by 64% (OR 0.36, 95% CI 0.17–0.74).

Finally, when we adjusted social distancing associations for mask use in an analysis limited to controls from the third survey and cases of similar pandemic moment, we found little change in associations with social distancing. There was 50% (OR 0.51, 95% CI 0.27–0.93) lesser risk for infection with little social distancing, 67% (OR 0.33, 95% CI 0.19–0.60) with much social distancing, and 59% (OR 0.41, 95% CI 0.21–0.80) with the most social distancing.

Discussion

In this population-based case-control study of COVID-19 conducted during a period of low-level to mid-level viral transmission in a major city in Brazil, mask use and adherence to social distancing resulted in major protection against symptomatic SARS-CoV-2 infection. Even after adjusting for various risk factors, adults who reported moderate or greater adherence to distancing recommendations reduced their odds of infection by one half to two thirds, and those who reported using masks when out reduced their risk by 87%. Because we excluded persons in healthcare settings, our findings directly address the use of these measures for protection against COVID-19 in the general community.

Table 3. Association of social distancing with severe acute respiratory syndrome coronavirus 2 infection, Porto Alegre, Brazil, April–June 2020

Characteristic, n = 1,667	Odds ratio (95% CI)			
	Model 1*	Model 2†	Model 3‡	Model 4§
Social distancing: How much have you managed to do?¶				
Little	0.69 (0.38–1.26)	0.72 (0.39–1.32)	0.65 (0.35–1.21)	0.65 (0.34–1.22)
Moderate (Some)	0.29 (0.17–0.50)	0.30 (0.17–0.52)	0.28 (0.16–0.49)	0.30 (0.17–0.53)
High (A great deal)	0.24 (0.15–0.39)	0.28 (0.17–0.47)	0.25 (0.15–0.42)	0.26 (0.16–0.44)
Practically isolated from everyone	0.38 (0.23–0.63)	0.44 (0.26–0.75)	0.41 (0.24–0.70)	0.34 (0.20–0.60)
What has been your routine of activities?#				
Go out every day for some activity	0.25 (0.13–0.46)	0.27 (0.14–0.50)	0.26 (0.13–0.49)	0.25 (0.12–0.48)
Go out from time to time for some activity	0.33 (0.21–0.51)	0.38 (0.24–0.59)	0.39 (0.24–0.61)	0.38 (0.23–0.60)
Go out just for essential activities	0.23 (0.16–0.31)	0.24 (0.17–0.34)	0.25 (0.18–0.36)	0.25 (0.18–0.35)
Stay at home all the time	0.51 (0.33–0.77)	0.51 (0.31–0.80)	0.48 (0.29–0.77)	0.25 (0.13–0.44)
Social distancing summary classification**				
Little	0.76 (0.49–1.19)	0.80 (0.51–1.26)	0.73 (0.46–1.16)	0.75 (0.47–1.20)
Much	0.31 (0.20–0.46)	0.35 (0.23–0.54)	0.33 (0.22–0.52)	0.33 (0.22–0.52)
Most	0.37 (0.24–0.58)	0.40 (0.25–0.65)	0.38 (0.23–0.62)	0.27 (0.16–0.46)

*Crude model.
†Model 1 with addition of sex, age, educational attainment, race, and income.
‡Model 2 with addition of household size and pandemic moment.
§Model 3 but excluding case-patients for whom a proxy provided the interview.
¶Reference category: very little.
#Reference category: go out every day, all day, to work or other regular activity.
**Reference category: least.

Evidence supporting the use of nonpharmacologic public health measures to slow viral spread of SARS-CoV-2 in communities has come mainly from ecologic studies documenting large inverse associations between greater use of these measures and viral spread (*14–17*). Evidence based on individual-level analyses, which come almost exclusively from studies of severe acute respiratory syndrome (SARS) and Middle East respiratory syndrome or from investigations in hospitals, have findings similar to ours: that risk approximately doubled with each additional meter of proximity to known infected persons, and that mask use reduced risk for transmission by 85% (OR 0.15, 95% CI 0.07–0.34) (*2*). Similar, although weaker, protection in a SARS-CoV-2 outbreak in a specific setting (the USS Roosevelt aircraft carrier) was found with greater use of face coverings (OR 0.30, 95% CI 0.17–0.52), avoidance of common areas (OR 0.56, 95% CI 0.37–0.86), and increased distance from others (OR 0.52, 95% CI 0.34–0.79) (*6*).

Very few individual-level studies have been reported on the effect of these measures on community transmission of SARS-CoV-2 (*18*). A case-control study of asymptomatic contacts in Thailand documented a risk reduction of 77% with mask use and 85% with distancing greater than 1 meter (*4*), and a study from Wuhan, China, showed mask use at home during the lockdown provided protection (*19*). An additional report ascertained that greater mask use reduced risk for predicted COVID-19 by 63% (S. Kwon et al., unpub. data, https://www. medrxiv.org/content/10.1101/2020.11.11.20229500v1). Finally, a cross-sectional study from Vermont, USA, with only 10 cases showed some protection in crude analyses (*20*).

A randomized trial in Denmark (*5*) that suggested lower, nonsignificant protection (OR 0.82, 95% CI 0.54–1.23) of mask use, although based on a potentially stronger design, had major methodologic problems (*21,22*). First, mask use was limited; only 46% reported full adherence. Second, 84% of outcomes were detected by antibody testing, leading an editorial accompanying the publication (*21*) to note that, given the extremely low incidence of cases, "all of the antibody-positive results in both intervention and control groups could have been false positives." When the study analyzed the subset of healthcare-diagnosed cases (15 participants), masks provided a greater, though not statistically significant, protection (OR 0.52, 95% CI 0.18–1.53). Third, the trial's short study periods (1 month), coupled with low antibody test sensitivity in early disease (30% ≤7 days and 72% during days 8–14) (*23*), could have resulted in the inclusion during the initial 2 weeks of case-patients who had contacted the disease before trial initiation. Similarly, during the final 2 weeks of the study period, some infections could have been missed by antibody testing, also not being detected by home-based reverse transcription PCR of uncertain sensitivity at close-out. Finally, because the intervention did not include face mask use by other household members, some cases could have resulted from home exposure, limiting the applica-

tions of the trial to current community settings, in which a greater fraction of other household members would also be using masks when out.

Our study provides estimates for easily interpretable measures—percentage effectiveness of social distancing and masking in protecting against infection—in the general community, the setting of greatest relevance for controlling the pandemic. The study occurred during a period of low to moderate transmission. Rio Grande do Sul State seroprevalence data suggest that ≈0.5% of the population became infected and 57 (3.8/100,000 population) COVID-19 deaths occurred in Porto Alegre during our ≈2-month study period (24).

The first potential limitation of our study was that response rates for case-patients (55.0%) and controls (45.5%) were low, and differential nonparticipation could introduce selection bias. Whereas not being available to participate could be associated with less social distancing, additional factors could explain the low response. Among case-patients, the frequent address changes identified when contact was achieved suggest that many case-patients on the initial list were ineligible because they were nonresidents who had furnished a false address to gain access to care. In addition, telemarketing and telephone scams lead many to ignore calls from unknown numbers. Of note, however, if these persons did not respond because they were away from their landline telephones, their inclusion would have resulted in even stronger associations. Among controls, refusal to participate was uncommon (12.7%); vacant residences were the main cause of nonresponse. Although interviews occurred on weekends, the limited attempts made to locate absent residents could have resulted in enrollment of controls who were more likely to practice social distancing. If so, this factor could have resulted in an overreport of the true effect. However, other reasons could explain the high vacancy rate, such as residents visiting vacation homes or relatives; residents, especially in apartments or other housing with restricted access, not responding to strangers; and residences being temporarily vacant. Our adjustment for age,

sex, and other covariates could have at least partially controlled for these differential responses.

Second, some exposure misclassification was possible, because questions about mask use and social distancing were unvalidated and limited in detail, having been taken from the community serology survey providing the controls. As such, we were unable to address differences in protection when indoors, outdoors, or indoors in specific settings.

Third, full adjustment for pandemic moment in analyses of mask use was not possible, because controls with data on mask use were all interviewed in a period shortly after case-patients began experiencing symptoms. However, given that this period was short and followed mandated mask use, a temporal trend in mask use would probably have been small and thus have had little effect on our estimates.

Fourth, controls could include persons who had received a misdiagnosis of false-negative. However, given low seroprevalence and our test's 86.4% sensitivity and 99.6% specificity (L.C. Pellanda, unpub. data), we estimate that misdiagnosis would likely have occurred in only 1 control.

Fifth, as the serology survey did not include occupation, we could not exclude healthcare workers among controls. Because healthcare workers would likely adhere to greater social distancing and mask use, their inclusion among controls could have falsely strengthened our findings. However, only ≈5% of the workforce in Brazil are healthcare workers (25), so we do not believe that their inclusion produced an appreciable error. In addition, errors because of lack of control for unmeasured confounding (e.g., from other occupational or residual socioeconomic differences or from recent travel) are always possible.

Sixth, a specific finding—lesser protection of those who reported being practically isolated from everyone and those who reported staying at home all the time (Table 3, model 3)—could weaken confidence in our social distancing results. However, as suggested by the additional analysis removing proxy responses (model 4), the lack of a graded dose-response in the model 3 associations could have been because of the greater risk level of case-patients who reported they

Table 4. Association of mask use with severe acute respiratory syndrome coronavirus 2 infection, Porto Alegre, Brazil, April–June 2020

Sample	Odds ratio (95% CI)		
	Model 1*	Model 2†	Model 3‡
All, n = 693	0.12 (0.04–0.30)	0.10 (0.03–0.25)	0.10 (0.03–0.25)
Restricted sample, n = 618§	0.16 (0.05–0.42)	0.12 (0.04–0.35)	0.13 (0.04–0.36)
Restricted sample, proxies removed, n = 609¶	0.16 (0.05–0.44)	0.12 (0.03–0.34)	0.12 (0.04–0.35)

*Crude model.
†Model 1 with addition of sex, age, educational attainment, race, income, and household size.
‡Model 2 with addition of social distancing score.
§Excluding those who stated that they stay at home all the time.
¶Excluding proxy responses.

were isolated but actually resided in assisted living.

Finally, application of our findings to settings with circulating virus variants or to persons who have received vaccination can only be speculated. In the case of circulating variants, risk for infection among those distancing and using masks will probably be greater, but risk among those not distancing or not using masks will also be greater. In the case of vaccination, however, risk for infection would be lower for all. We know of no a priori reason, however, to presume that the relative protection of distancing and mask use in these settings would be either lesser or greater than we report.

The primary strength of our report is that, as a population-based study, it avoids the risk for selection bias typical of less representative designs. It is sufficiently large to permit precise confidence intervals for our estimates of the benefit of protective measures. Furthermore, because our cases were detected at a time when testing was limited to symptomatic persons seeking care, the protection we found was against becoming a clinically relevant case. Finally, and perhaps most vital, our findings are based on individual-level analyses and thus permit estimation of percent reduction of risk, a direct and simple way to communicate the magnitude of individual protection afforded by these simple public health measures.

Given the hurdles faced in vaccine production, distribution, and acceptance, and the increasing emergence of virus variants, mass vaccination is unlikely to suffice to control the pandemic in the near future in many parts of the world. During this period and continuing into the future phase of maintaining viral control, simple public health measures, principally social distancing and mask use, will remain crucial options to minimize viral spread.

In conclusion, we found that social distancing and mask use while away from home provided major protection against symptomatic SARS-CoV-2 infection. Our easily grasped and generalizable estimates of protection against transmission lend support to previous, frequently less direct, assessments. Our findings support the contention that greater use of simple public health measures in the community provides major protection against symptomatic infection.

This article was preprinted at https://papers.ssrn.com/sol3/papers.cfm?abstract_id=3731445.

About the Author

Dr. Gonçalves is a family physician, epidemiologist, and associate professor of the Social Medicine Department and Postgraduate Program in Epidemiology at the Federal University of Rio Grande do Sul. Though his main research interests are health services evaluation, chronic disease, and telehealth, in recent months he has been actively engaged in clinical and research activities related to confronting the coronavirus disease pandemic.

References

1. World Health Organization. WHO coronavirus disease (COVID-19) dashboard [cited 2020 Sep 9]. https://covid19.who.int
2. Chu DK, Akl EA, Duda S, Solo K, Yaacoub S, Schünemann HJ, et al.; COVID-19 Systematic Urgent Review Group Effort (SURGE) study authors. Physical distancing, face masks, and eye protection to prevent person-to-person transmission of SARS-CoV-2 and COVID-19: a systematic review and meta-analysis. Lancet. 2020;395:1973–87. https://doi.org/10.1016/S0140-6736(20)31142-9
3. Chou R, Dana T, Jungbauer R, Weeks C. Update alert 3: masks for prevention of respiratory virus infections, including SARS-CoV-2, in health care and community settings. Ann Intern Med. 2020;173:169. https://doi.org/10.7326/L20-1292
4. Doung-Ngern P, Suphanchaimat R, Panjangampatthana A, Janekrongtham C, Ruampoom D, Daochaeng N, et al. Case-control study of use of personal protective measures and risk for SARS-CoV 2 infection, Thailand. Emerg Infect Dis. 2020;26:2607–16. https://doi.org/10.3201/eid2611.203003
5. Bundgaard H, Bundgaard JS, Raaschou-Pedersen DET, von Buchwald C, Todsen T, Norsk JB, et al. Effectiveness of adding a mask recommendation to other public health measures to prevent SARS-CoV-2 infection in Danish mask wearers: a randomized controlled trial. Ann Intern Med. 2021;174:335–43.
6. Payne DC, Smith-Jeffcoat SE, Nowak G, Chukwuma U, Geibe JR, Hawkins RJ, et al.; CDC COVID-19 Surge Laboratory Group. SARS-CoV-2 infections and serologic responses from a sample of U.S. Navy service members—USS Theodore Roosevelt, April 2020. MMWR Morb Mortal Wkly Rep. 2020;69:714–21. https://doi.org/10.15585/mmwr.mm6923e4
7. Brazilian Institute of Geography and Statistics. Porto Alegre [cited 2020 Sep 9]. https://www.ibge.gov.br/cidades-e-estados/rs/porto-alegre.html
8. PROCERGS. Decree No. 55.118, of March 16, 2020. Establishes complementary measures to prevent contagion by COVID-19 (new coronavirus) within the State. Official Register of the State of Rio Grande do Sul, Porto Alegre [in Portuguese]. 2020 Mar 17 [cited 2020 Nov 13]. https://www.diariooficial.rs.gov.br/materia?id=395443
9. Hallal PC, Horta BL, Barros AJD, Dellagostin OA, Hartwig FP, Pellanda LC, et al. Trends in the prevalence of COVID-19 infection in Rio Grande do Sul, Brazil: repeated serological surveys. Cien Saude Colet. 2020;25(suppl 1):2395–401. https://doi.org/10.1590/1413-81232020256.1.09632020
10. Barros AJD, Victora CG, Menezes AMB, Horta BL, Hartwig F, Victora G, et al. Social distancing patterns in nine municipalities of Rio Grande do Sul, Brazil: the Epicovid19/RS study. Rev Saude Publica. 2020;54:75. https://doi.org/10.11606/s1518-8787.2020054002810

11. R Core Team. R: A language and environment for statistical computing. Vienna: R Foundation for Statistical Computing; 2021 [cited 2020 Sep 19]. https://www.r-project.org

12. Silveira MF, Barros AJD, Horta BL, Pellanda LC, Victora GD, Dellagostin OA, et al. Population-based surveys of antibodies against SARS-CoV-2 in Southern Brazil. Nat Med. 2020;26:1196–9. https://doi.org/10.1038/s41591-020-0992-3

13. SIDRA: IBGE Automatic Recovery System. National Annual Continuous Household Sample Survey–PNADC/A [cited 2020 Sep 21]. https://sidra.ibge.gov.br/pesquisa/pnadca/tabelas

14. Courtemanche C, Garuccio J, Le A, Pinkston J, Yelowitz A. Strong social distancing measures in the United States reduced the COVID-19 growth rate. Health Aff (Millwood). 2020;39:1237–46. https://doi.org/10.1377/hlthaff.2020.00608

15. Lyu W, Wehby GL. Community use of face masks and COVID-19: evidence from a natural experiment of state mandates in the US. Health Aff (Millwood). 2020;39:1419–25. https://doi.org/10.1377/hlthaff.2020.00818

16. Islam N, Sharp SJ, Chowell G, Shabnam S, Kawachi I, Lacey B, et al. Physical distancing interventions and incidence of coronavirus disease 2019: natural experiment in 149 countries. BMJ. 2020;370:m2743. https://doi.org/10.1136/bmj.m2743

17. Haug N, Geyrhofer L, Londei A, Dervic E, Desvars-Larrive A, Loreto V, et al. Ranking the effectiveness of worldwide COVID-19 government interventions. Nat Hum Behav. 2020;4:1303–12. https://doi.org/10.1038/s41562-020-01009-0

18. Chou R, Dana T, Jungbauer R, Weeks C, McDonagh MS. Update alert: masks for prevention of respiratory virus infections, including SARS-CoV-2, in health care and community settings. Ann Intern Med. 2020;173:W86. https://doi.org/10.7326/L20-0948

19. Centers for Disease Control and Prevention. Coronavirus disease 2019 (COVID-19) scientific brief: community use of cloth masks to control the spread of SARS-CoV-2. 2020 [cited 2020 Nov 13]. https://www.cdc.gov/coronavirus/2019-ncov/more/masking-science-sars-cov2.html

20. van den Broek-Altenburg EM, Atherly AJ, Diehl SA, Gleason KM, Hart VC, MacLean CD, et al. Jobs, housing, and mask wearing: cross-sectional study of risk factors for COVID-19. JMIR Public Health Surveill. 2021;7:e24320. https://doi.org/10.2196/24320

21. Frieden TR, Cash-Goldwasser S. Of Masks and Methods. Ann Intern Med. 2021;174:421–2.

22. Haber NA, Wieten SE, Smith ER. Letter of concern regarding "Reduction in COVID-19 infection using surgical facial masks outside the healthcare system." Dan Med J. 2020;67:A205063.

23. Deeks JJ, Dinnes J, Takwoingi Y, Davenport C, Spijker R, Taylor-Phillips S, et al.; Cochrane COVID-19 Diagnostic Test Accuracy Group. Antibody tests for identification of current and past infection with SARS-CoV-2. Cochrane Database Syst Rev. 2020;6:CD013652.

24. Dados Covid-19 em Porto Alegre [cited 2020 Sep 10]. https://mhbarbian.shinyapps.io/covid19_poa/

25. Machado MH, Oliveira ES, Moyses NMN. Trends in the health labor market in Brazil. In: Pierantoni C, dal Poz MR, France T, editors. Working in health: quantitative and qualitative approaches. Vol. 1. Rio de Janeiro (Brazil): Center for Studies and Research in Collective Health, State University of Rio de Janeiro; 2011. p. 103–116 [cited 2021 Apr 9]. http://www.ensp.fiocruz.br/observarh/arquivos/TendenciasTrabalho.pdf

Address for correspondence: Marcelo Rodrigues Gonçalves, Postgraduate Program in Epidemiology, School of Medicine, Federal University of Rio Grande do Sul, Rua Ramiro Barcelos, 2400, Porto Alegre, Rio Grande do Sul, Brazil; email: marcelorog@gmail.com

EID Podcast
A Critique of Coronavirus
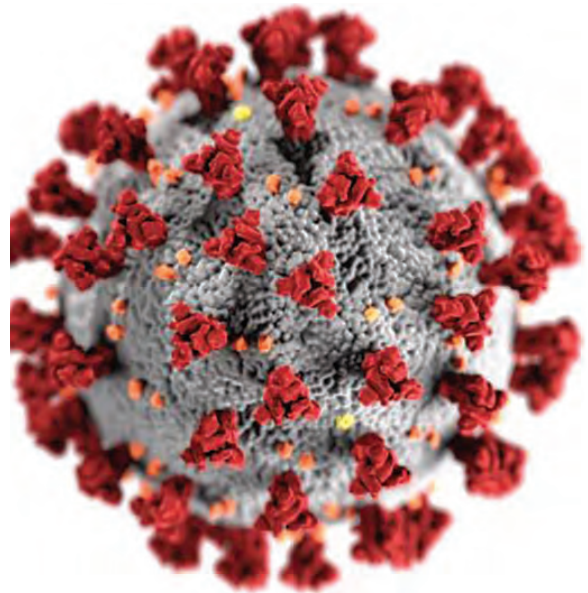
Humans have spent eons imagining—and experiencing—outbreaks of disease. Now that the COVID-19 pandemic has reached our doorstep, it's jarring to think about how this virus is eerily different from the pandemics of popular imagination.

In this EID podcast, Dr. Elana Osen, a specialty registrar at St. George's University Hospital in London, reads a poem she wrote about her experience of the COVID-19 pandemic.

Visit our website to listen:
https://go.usa.gov/xwjzs

EMERGING INFECTIOUS DISEASES®

Costs and Outcomes of Integrated Human African Trypanosomiasis Surveillance System Using Rapid Diagnostic Tests, Democratic Republic of the Congo

Rian Snijders, Alain Fukinsia, Yves Claeys, Epco Hasker, Alain Mpanya, Erick Miaka, Filip Meheus, Marleen Boelaert[1]

We integrated sleeping sickness case detection into the primary healthcare system in 2 health districts in the Democratic Republic of the Congo. We replaced a less field-friendly serologic test with a rapid diagnostic test, which was followed up by human African trypanosomiasis microscopic testing, and used a mixed costing methodology to estimate costs from a healthcare provider perspective. We screened a total of 18,225 persons and identified 27 new cases. Average financial cost (i.e., actual expenditures) was US $6.70/person screened and $4,464/case diagnosed and treated. Average economic cost (i.e., value of resources foregone that could have been used for other purposes) was $9.40/person screened and $6,138/case diagnosed and treated. Our study shows that integrating sleeping sickness surveillance into the primary healthcare system is feasible and highlights challenges in completing the diagnostic referral process and developing a context-adapted diagnostic algorithm for the large-scale implementation of this strategy in a sustainable and low-cost manner.

Sleeping sickness, or human African trypanosomiasis (HAT), is a neglected tropical disease that has killed thousands of persons in sub-Saharan Africa since the beginning of the 20th century. This disease is caused by *Trypanosoma brucei gambiense* and *T. brucei*

Author affiliations: Swiss Tropical and Public Health Institute, Basel, Switzerland (R. Snijders); University of Basel, Basel (R. Snijders); Institute of Tropical Medicine, Antwerp, Belgium (R. Snijders, Y. Claeys, E. Hasker, M. Boelaert); Programme National de Lutte contre la Trypanosomiase Humaine Africaine, Kinshasa, Democratic Republic of the Congo (A. Fukinsia, A. Mpanya, E. Miaka); International Agency for Research on Cancer, Lyon, France (F. Meheus)

rhodesiense parasites. This article focuses on *T. brucei gambiense* infections, which account for >98% of all HAT cases (*1*). After intense control efforts during the colonial period, the disease subsided but reemerged in the 1970s and peaked in the 1990s, when >30,000 new cases were reported annually in 1997 and 1998. By the end of the 20th century, increased HAT control efforts reversed the epidemic trend (*2*). This success persuaded the World Health Organization (WHO) to target HAT for elimination as a public health problem by 2020 and to eliminate transmission by 2030 (*3*). In 2018, only 977 new HAT cases were reported globally, >75% of which occurred in the Democratic Republic of the Congo (DRC) (*2,4*).

HAT control activities consist of case detection and management complemented with vector control. Case detection can be done actively through outreach campaigns or passively by screening self-reporting cases in medical facilities. The passive approach accounted for >50% of the cases detected in DRC in 2017. With the declining prevalence, and therefore a higher cost of outreach activities on a per-case-found basis, passive screening might figure more prominently in future strategies for HAT elimination (*4,5*). Moreover, the past has shown that inadequate HAT surveillance can lead to reemerging epidemics, further underscoring the need for sustained epidemiologic surveillance and case detection in the general health system (*6,7*).

Historically, passive detection of HAT in DRC was conducted mainly at designated centers for HAT diagnosis, treatment, and control because of the complexity of diagnostic procedures. Clinical diagnosis of HAT is difficult because of its nonspecific symptoms in the early stages, and HAT needs to be confirmed

because of the complex and toxic treatment regimens currently available. First, a relatively easy and cheap serologic screening test is performed, which, if positive, is followed by microscopic testing to confirm the presence of the parasite in the lymph fluid or blood. Then, a lumbar puncture is necessary to determine if the disease has advanced to the neurologic stage, given that, until 2019, the treatment regimen was different for cases in the hematolymphatic stage (stage 1) versus those in the meningoencephalitic stage (stage 2) (1,8,9).

Mitashi et al. (5) listed the preconditions for the integration of vertical disease control services as follows: a functional health system, versatile health workers, a minimum level of disease prevalence to maintain technical skills; decision-making powers for the health system combined with technical guidance by the disease program, and mutual benefits for the healthcare system and the disease program (5,10–12). This article examined 1 additional criterion, appropriate technology.

In the past, the main serologic test used for trypanosomiasis was the card agglutination test, which requires a rotator and a cold chain and is only available in 50 test dose vials with a limited shelf life once opened (1 week in a refrigerator or up to 8 hours at room temperature). The need for electric power combined with the high wastage given the low daily use, limits the usefulness of this test in first-line health services. In addition, microscopic examination to visualize the parasite requires specific laboratory skills and equipment (5,13). Recently, 2 rapid diagnostic tests (RDTs) for HAT became commercially available: the SD-Bioline HAT test (Abbot, https://www.global-pointofcare.abbott) and the HAT Sero-K-Set (Coris BioConcept, https://www.corisbio.com). These individual thermostable tests do not require equipment or cold storage and could improve the integration of case detection in the primary healthcare system (14). A study in Uganda demonstrated that RDTs would allow HAT screening to be integrated into the routine activities of health facilities (15,16). A comparison of HAT serologic tests showed that RDTs could be a cost-effective alternative to the card agglutination test in passive detection of trypanosomiasis at health facility level (17). Our study aimed to evaluate the results and costs of a HAT surveillance system that was based on RDTs, integrated into primary care facilities, and managed at the health district level.

Methods

Research Setting
Every province in the DRC is divided into health districts that consist of a network of health facilities that each serve a well-defined area of the district (11). The study took place in the HAT-endemic health districts of Mosango and Yasa Bonga in the former Bandundu Province in DRC. Both health districts together consist of 38 health areas, have a combined population of 369,393, and represent an area of 6,160 km² (Yasa Bonga, 235,696 population and an area of 2,810 km²; Mosango, 133,697 population and an area of 3,350 km²) (18,19). During 2000–2012, a total of 45% of all HAT cases in DRC were reported in Bandundu Province, and during this period, the highest annual incidence reported in both health districts was 40 cases/10,000 population (20).

Integrating HAT Case Detection and Management
During the preintervention phase, investments were made to strengthen the infrastructure, equipment, and staff skills before integrating HAT screening because the districts did not meet several integration requirements highlighted by Mitashi et al. (5). In addition, research showed that a poorly regulated fee-for-health services payment system could lead to unpredictable health costs for patients, which reduces access to quality healthcare (9). Therefore, a flat-rate payment system was introduced to improve financial access to healthcare in both districts.

Before 2015, only 5 facilities in the study area were able to perform serologic and parasitologic tests. The intervention planned for serologic screening in >1 health facility per health area and the ability to perform HAT microscopic testing nearby. The facilities were chosen on the basis of HAT incidence during 2013–2015 and population density (Figure 1).

The intervention started with training staff and reinforcing HAT management skills at the health district level. The health district management teams and the experts from the national sleeping sickness control program (Programme National de Lutte contre la Trypanosomiase Humaine Africaine en République Démocratique Du Congo) oversaw training, management, and supply.

The screening algorithm indicated that all patients with a negative malaria test or persistent fever after a malaria treatment or >1 signs or symptoms suggestive of HAT (e.g., lymphadenopathy, headache, pruritus, musculoskeletal pain, hepatomegaly, splenomegaly, sleep disorder, and neuropsychiatric symptoms) were to be screened with a HAT RDT (11,20). HAT microscopic testing was to be conducted for all patients with a positive HAT RDT, either onsite or at the nearest facility with microscopic testing capacity (Figure 2). The microscopic testing consisted of a lymph gland puncture to examine the fluid for
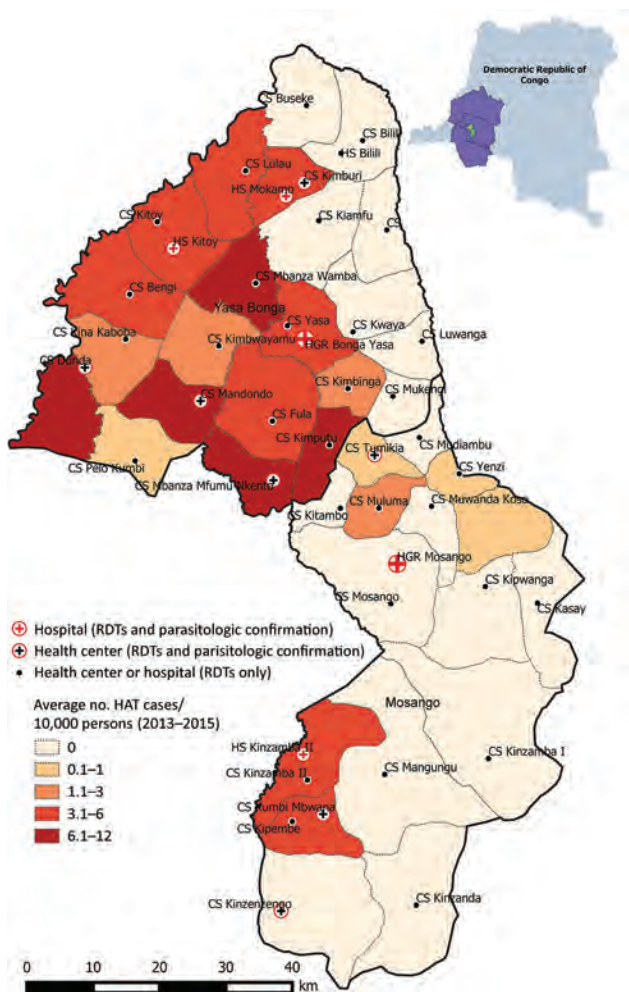
Figure 1. Health facilities performing HAT surveillance and the average human African trypanosomiasis incidence (cases/10,000 population), Democratic Republic of the Congo, 2013–2015. Inset shows location of the country in Africa. Map generated by using QGIS 3.10.1 (*4*). HAT, human African trypanosomiasis; RDT, rapid diagnostic test.

parasites if swollen glands were present, followed by the more sensitive mini anion exchange centrifugation test if no such glands were present or if the result of the lymph gland puncture was negative. Patients were considered to have a confirmed HAT case when trypanosomes were observed. The cerebrospinal fluid of patients was to be examined with a lumbar puncture because of the stage-specific treatment available at the time of the study, followed by treatment according to WHO and national guidelines (*21–24*). Stage 1 consisted of outpatient treatment with pentamidine at a health facility close to the patient's home. Stage 2 consisted of inpatient treatment in a health facility qualified to administer nifurtimox/eflornithine combination therapy.

By the end of 2016, integrated HAT surveillance was operational. HAT screening with RDTs was available in 48 facilities, and microscopic diagnostic testing was available in 11 facilities (Table 1) (*25*).

Data Collection and Analysis
We collected data during January 1, 2017–December 31, 2018. Data were based on operational and financial reports, field visits, and discussions with experts.

Number of Persons Screened, Diagnosed, and Treated
The primary indicator for measuring the output of both health districts was the number of persons screened for HAT and cases identified and treated. Of the 1,092 monthly reports expected during the study period from all participating health facilities, 91 reports (8%) were not retrieved. Most of the missing reports coincided with periods when HAT RDTs were out of stock. Therefore, we assumed that no HAT screening activities took place during the unreported months.

Because integrating disease control services requires a functional healthcare system, we tracked the utilization rate for the health district by using the number of curative consultations annually per total population. The DRC's national guidelines state that in a well-functioning health district, this rate should be ≥0.5 consultations/capita (*26*).

Financial and Economic Costs
We estimated economic and financial costs from the health provider's perspective. Financial costs represent the actual expenditure, whereas economic costs estimate the value of resources foregone that could have been used for other purposes. Costs incurred by households, research costs, and costs of activities during the preintervention phase were not included.

We recorded all costs in the currency they were incurred and converted to US dollars (USD) based on the average exchange rate during the study period (Euro to USD, 1.15; Congolese Franc to USD, 0.00067). The costs exclude the DRC's 16% value-added tax, from which the national program and donors are exempt (*27*). Transport and importation costs for goods that needed to be imported into DRC were estimated at 10% of the procurement cost on the basis of the average shipment costs between Belgium and DRC during the study period.

We used bottom-up microcosting to assess the cost of HAT tests and equipment. For capital equipment provided for HAT microscopic testing, we annualized the purchase or replacement value on the basis of the expected useful life of items and
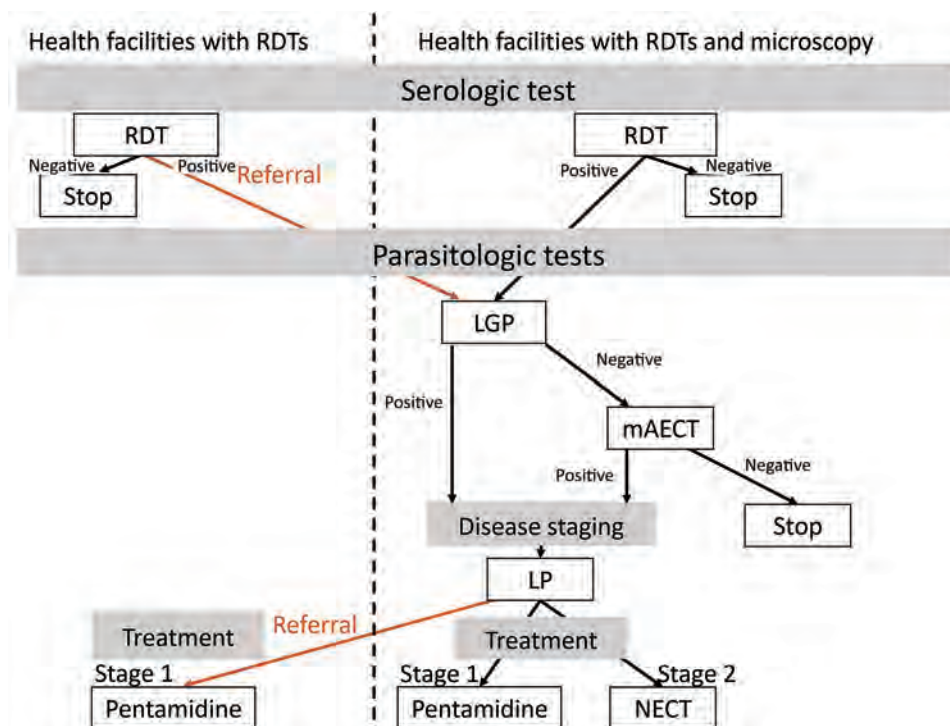
Figure 2. Diagnostic algorithm applied after a negative malaria test, persistent fever after malaria treatment, or symptoms suggestive of human African trypanosomiasis, Democratic Republic of the Congo. LGP, Lymph gland puncture; LP, lumbar puncture; mAECT, mini anion exchange centrifugation test; NEXT, nifurtimox/eflornithine combination therapy; RDT, rapid diagnostic test.

discounted them at a rate of 3% (28). We assigned a proportion of this cost to HAT testing on the basis of the expected proportion of time for which the equipment would be used for HAT tests. We estimated the cost of HAT testing by multiplying the number of persons tested by the average cost of all consumables used per test. During the study, we used only SD-Bioline HAT RDTs at a per-unit purchase price of $0.55. SD-Bioline receives a subsidy of $0.25 per test from a private donor. The per-unit price of the HAT RDT Sero-K-set was €1.79 (17).

The flat-rate payment system implemented a fixed consultation rate of 5,000 Congolese Francs (± 3.35) that enables health facilities to recover their costs with an average estimated consultation time of 15 minutes. Performing an RDT takes ≈15–20 minutes. The patients did not pay any additional fees

nor did the facilities receive any support besides the HAT tests and equipment. We included the consultation fee in the economic cost as a proxy to estimate the costs incurred by health facilities to provide the services (i.e., nurse time and use of facility resources) and the consultation fee was excluded from the financial cost estimate because no actual expenses were incurred.

For HAT treatment, we obtained outpatient follow-up and hospitalization costs from WHO and combined them with the cost for drugs used to treat side effects on the basis of the average costs of the medication during treatment in both districts in 2017. We included no HAT-specific treatment costs because pentamidine and nifurtimox/eflornithine combination therapy are donated by pharmaceutical companies (29–33).

Table 1. Number of facilities able to perform passive case detection of human African trypanosomiasis per health district before and after implementing the intervention, Democratic Republic of the Congo, 2017–2018 (25)

District and type of facility	Before the intervention		After the intervention	
	Serologic screening*	Parasitologic diagnosis†	Serologic screening	Parasitologic diagnosis
Mosango				
Hospital‡	1	1	2	2
Health center			17	2
Yasa Bonga				
Hospital	3	3	4	3
Health center	1	1	25	4
Total	5	5	48	11

*Sleeping sickness rapid diagnostic tests.
†Lymph gland puncture, mini anion exchange centrifugation test, and lumbar puncture.
‡Reference or secondary hospital.

We used top-down gross costing to estimate costs related to training and management. We annualized HAT training costs on the basis of the period between refresher training sessions. For the management costs, we included financial and in-kind support provided to the health facilities and management cost at provincial and health district level. We accounted for management costs of the national program at national level by applying a 15% markup on the activities managed by the program, which corresponds to the overhead rate the program applies for several projects to finance its role as national coordinator of HAT activities. The costs do not include transport costs of test or equipment from the capital city (Kinshasa) to the field because the districts were supplied during regular supervision visits. We estimated the cost per person screened and per case diagnosed and treated by dividing the overall cost of the intervention by the number of persons screened and treated.

Sensitivity Analysis

We used univariate sensitivity analysis to assess the impact of changes in the main cost drivers, such as the costs incurred to provide the services, including the cost of treatment and the price of RDTs. We also varied the discount rate between 0% and 5%.

Ethics

Ethics approval for this study was obtained from the institutional review board of the Institute of Tropical Medicine in Antwerp, Belgium (approval no. IRB/AB/ac/137, protocol no. 115/16) and the institutional review board of School of Public Health of the University of Kinshasa, in Kinshasa, DRC (approval no. ESP/CE/08/2017). The study evaluated costs and aggregated operational data of routine activities provided by the healthcare system. Therefore, no formal consent was needed.

Results

Number of Persons Screened, Confirmatory Tested, Diagnosed, and Treated

Both health districts were considered well-functioning during the study period; the district utilization rate was close to the national threshold of 0.5 consultations per inhabitant per year (0.53 in Yasa Bonga and 0.44 in Mosango). In 2018, only 29% (36,363/125,674) of the overall curative consultations in Yasa Bonga were done in health facilities involved in HAT screening and 77% in Mosango (46,009/59,228) (*18,34*), meaning that higher coverage of passive HAT screening

was reached in Mosango, and ≈70% of the curative consultations in Yasa Bonga took place in healthcare centers not participating in HAT screening or during periods when no HAT screening was reported. For both districts, >50% of the curative consultations involved testing with a malaria RDT, ≈60% of which tested positive.

In total, 18,225 persons were screened for HAT with a HAT RDT (i.e., ≈80% of persons that tested negative for malaria), of whom 223 [1.22%] tested positive. RDT stock-outs were the main reason that 20% of malaria-negative persons were not tested for HAT. No reports were found indicating that persons were screened for HAT on the basis of persistent fever after a malaria treatment or ≥1 signs or symptoms suggestive of HAT.

In total, 27 new HAT patients were identified through a positive mini anion exchange centrifugation test (no positive lymph gland puncture). Only 55% of the persons with a positive HAT RDT (123/223) were tested to confirm the presence of the parasite, because only 20% (25/122) of the persons with a positive HAT RDT identified in a facility without HAT microscopic testing available completed the referral. In comparison, 97% (98/101) of RDT-positive persons identified in facilities equipped to perform microscopic testing completed confirmation. Of the 27 new cases identified and treated in 2017 and 2018, a total of 9 were detected through healthcare centers and 18 by the reference and secondary hospitals (Appendix Tables 1–4, https://wwwnc.cdc.gov/EID/article/27/8/20-2399-App1.pdf).

Financial Costs

The total annual financial cost for both health districts was US $123,386 in 2017 and $28,710 in 2018; the average annual financial cost over 5 years was $62,500. The higher financial cost in the first year is attributable to staff training and equipment purchases. The financial cost is substantially lower than the economic cost because it does not consider any support for human resources or the use of other resources for the health facilities performing the tests (Appendix Table 5).

Economic Costs

We constructed an overview of the economic costs by input and activity (Table 2). The total economic cost in Mosango is ≈5% higher than in Yasa Bonga because >30% more persons were screened, leading to higher facility and RDT costs. The higher cost in Mosango is partly offset by the lower training costs, because fewer facilities were involved in HAT screening than in Yasa Bonga (Appendix Tables 6–17).

Table 2. Annual economic costs of passive human African trypanosomiasis screening in Mosango and Yasa Bonga health districts, Democratic Republic of the Congo*

Cost category and subcategory	Description	Cost, USD			Total, %
		Mosango	Yasa Bonga	Total	
Capital equipment		18,008	25,051	43,060	25
Equipment	Confirmation equipment	4,734	6,627	11,360	7
	Laboratory equipment	2,539	3,554	6,093	4
	Nonmedical equipment	2,195	3,073	5,268	3
Training	HAT diagnosis training	13,275	18,424	31.699	19
	Screening	5,079	6,950	12,029	7
	Microscopy	8,196	11,474	19,670	12
Annual recurrent costs		69,243	56,764	126,008	75
Laboratory and medical supplies	HAT tests	7,487	5,449	12,262	7
	RDTs	7,388	4,874	12,262	7
	Microscopy	99	575	673	0.4
Patient care	Staging and inpatient and outpatient care	413	1,601	2,014	1
HR and infrastructure use	Execution RDT	36,535	24,102	60,637	36
Management	Management and supervision	24,808	25,613	50,421	30
Total		87,251	81,816	169,067	100
Cost per person screened		7.95	11.29	9.28	
Cost per case diagnosed and treated		21,813	3,557	6,262	

*HAT, human African trypanosomiasis; HR, human resources; RDT, rapid diagnostic test.

Economic Cost Per Person Screened and Per Case Diagnosed and Treated

The overall cost per person screened was $9.28, and the cost per case diagnosed and treated was $6,262 (Figure 3). In Yasa Bonga, the cost per person screened is higher than in Mosango because of the higher number of facilities involved and the lower number of persons screened. However, the average cost per case diagnosed and treated is much lower in Yasa Bonga because of the higher number of cases detected and treated.

Sensitivity Analysis

We summarized the results of the univariate sensitivity analysis of several cost parameters to assess the potential impact on the cost per person screened and cost per case diagnosed and treated (Figure 4). The main cost drivers are the frequency of training and the cost at health facility level to provide this service. The economic cost per person screened or case diagnosed would be much lower if we assume that the health system can provide HAT screening by using fewer additional resources than those needed for a 15-minute consultation (the proxy used to estimate the cost at health facility level, including human resources and infrastructure); however, this approach might overestimate the health system's capacity. A lower estimated unit cost to provide this service of $1 instead of $3.55 would lower the cost per person screened and diagnosed and treated by 25%. Further, the study assumed that healthcare workers needed retraining every 3 years. Increasing the frequency of the laboratory technicians' training increases the cost per person screened and diagnosed and treated by 45%. Reducing the number of facilities where HAT microscopic testing is available decreases the cost per person screened and diagnosed and treated. Using more expensive tests or treatments increases the cost per person. Varying the discount rate from 0% to 5% had little effect on the cost estimates.
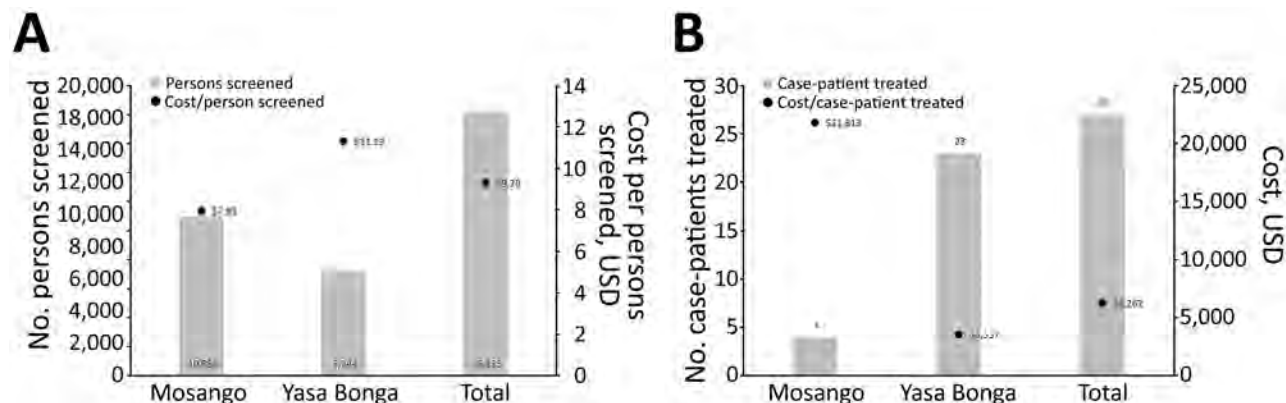
Figure 3. Cost per person screened and per human African trypanosomiasis case diagnosed and treated, Democratic Republic of the Congo.
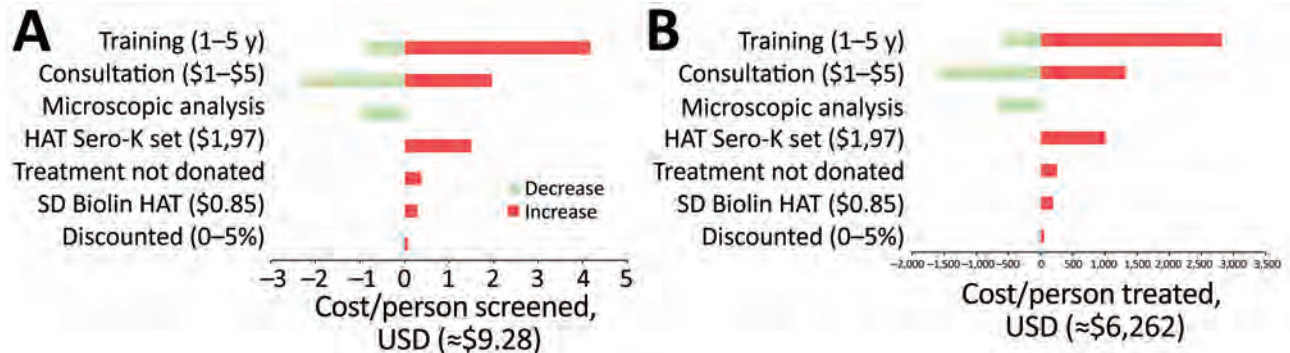
Figure 4. Sensitivity analysis on main cost drivers for HAT diagnosis and treatment, Democratic Republic of the Congo. HAT, human African trypanosomiasis.

Discussion

This study describes the development, implementation, and cost of a strategy for HAT case detection integrated into the primary healthcare system in DRC using a novel screening test. In a context of a declining number of cases combined with a need for sustained surveillance, policymakers need to reflect on the value of integrating HAT screening into the basic health service package offered by polyvalent first-line health services. Introducing HAT RDTs helped integrate HAT screening into the primary healthcare system in both health districts where the program was

piloted. Although the number of persons screened almost doubled, the number of cases identified declined, consistent with the observed overall decrease in prevalence in both districts. This decline resulted in an increased cost per person diagnosed and treated. The cost per person diagnosed and treated through passive screening estimated in this study is much higher than the cost per HAT case cured reported in an earlier study that evaluated the cost-effectiveness of screening for HAT with RDTs ($6,262 compared with $278, or $10,133/36.5 cases) (17). The earlier study modeled the use of HAT RDTs in a high-vol-
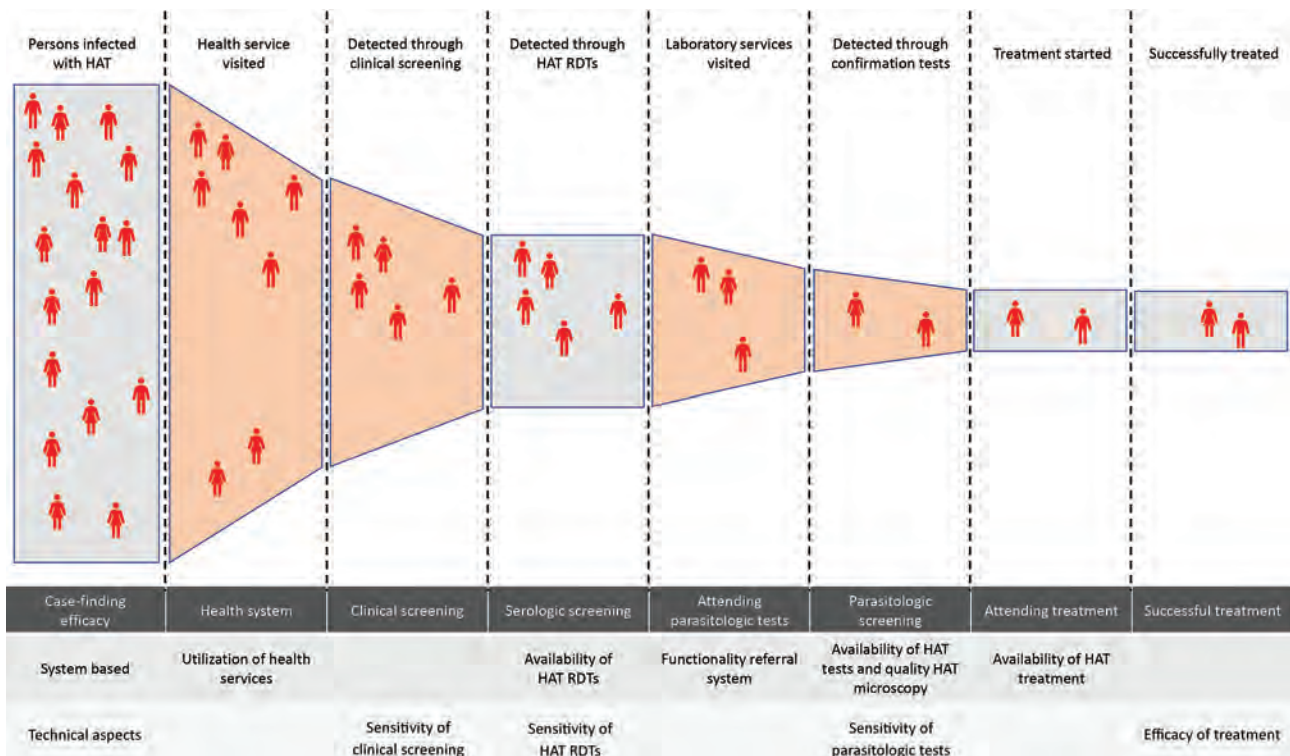
Figure 5. Illustration of potential loss in effectiveness in passive screening for HAT integrated into the primary healthcare system using an adaptation of Piot model for tuberculosis (36), Democratic Republic of the Congo. HAT, human African trypanosomiasis; RDT, rapid diagnostic test.

ume hospital that screened 2,500 patients annually for HAT and detected 36.5 HAT cases, whereas, in our study in 2018, the average number of persons screened per facility was 206 (9,892 persons/48 facilities), and the average number of cases detected per facility, 0.6 (27 cases/48 facilities), therefore incurred higher fixed facility-level costs (capital and district supervision) for services to fewer patients.

Furthermore, training and management costs were not included in previous studies, and the estimated cost of the use of the facilities' resources was much lower ($1 vs. $3.33 per person screened). The cost per person screened through passive screening in the study area is much higher than through active screening ($9.28 vs. an average of $2.1). However, the average cost per case detected is much lower ($6,318 vs. an average of $16,080) because of the higher proportion of cases detected in the population screened during passive screening than during active screening (35).

The effectiveness of this strategy should be evaluated through the number of HAT cases detected and treated. Several potential bottlenecks were identified in the process of HAT case detection (36) (Figure 5). The main challenges in the study area were the fact that potential HAT cases were not detected because the person had already tested positive on a malaria RDT or because they did not complete the referral for offsite microscopic testing. Today, a novel therapeutic, fexinidazole, has obviated the need for staging in a portion of patients and could improve the effectiveness of this system; however, there are several contraindications against this treatment (37).

The following recommendations should be considered for the scale-up of passive surveillance through RDTs. The HAT screening algorithm should be context-specific, a negative malaria test in a malaria-endemic area might not be a good preselection criterion for HAT screening. Furthermore, the system should be adapted to demand (e.g., it should be located in facilities that are most frequented, exploit the existing referral system to supply HAT test material, and take into account a minimum attendance rate). In the study setting, a separate referral and supply system for HAT was set up and closely monitored by the national program. Shifting most of these tasks to the general healthcare system will probably lower the cost and render the system more sustainable when implemented on a larger scale. The shift in service delivery might also cause a shift in the financing of the system. In this study, the costs at health facility level were borne by the health facilities because they did not receive any additional compensation for the extra time spent on HAT testing, which is reflected in the lower financial cost. Health facilities might be reluctant to participate in HAT activities without any in-kind or financial compensation. A remedy might be to include HAT formally into the performance-based financing system.

In conclusion, HAT case detection and surveillance integrated into the primary healthcare system using RDTs showed promising results but also substantial practical weaknesses. Integration is possible in a sustainable and low-cost manner if challenges regarding completing diagnostic algorithm are addressed and a context-adapted diagnostic algorithm is used.

About the Author

Miss Snijders is a researcher at the Epidemiology and Control of Neglected Tropical Diseases Unit in the Department of Public Health of the Institute of Tropical Medicine in Antwerp, Belgium. Her research interests are health economics, disease control, and epidemiology of neglected tropical diseases.

References

1. Büscher P, Cecchi G, Jamonneau V, Priotto G. Human African trypanosomiasis. Lancet. 2017;390:2397–409. https://doi.org/10.1016/S0140-6736(17)31510-6

2. World Health Organization. Factsheets: Trypanosomiasis, human African (sleeping sickness) [cited 2019 Apr 11]. https://www.who.int/news-room/fact-sheets/detail/trypanosomiasis-human-african-(sleeping-sickness)

3. Franco JR, Simarro PP, Diarra A, Jannin JG. Epidemiology of human African trypanosomiasis. Clin Epidemiol. 2014; 6:257–75.4. Programme National de Lutte contre la Trypanosomiase Humaine Africaine en République Démocratique Du Congo. Database HAT cases: 2013–2017. Kinshasa (Democratic Republic of the Congo): The Programme; 2017.

5. Mitashi P, Hasker E, Mbo F, Van Geertruyden J-P, Kaswa M, Lumbala C, et al. Integration of diagnosis and treatment of sleeping sickness in primary healthcare facilities in the Democratic Republic of the Congo. Trop Med Int Health. 2015;20:98–105. https://doi.org/10.1111/tmi.12404

6. Franco JR, Cecchi G, Priotto G, Paone M, Diarra A, Grout L, et al. Monitoring the elimination of human African trypanosomiasis: Update to 2016. PLoS Negl Trop Dis. 2018;12:e0006890. https://doi.org/10.1371/journal.pntd.0006890

7. Checchi F, Funk S, Chandramohan D, Chappuis F, Haydon DT. The impact of passive case detection on the transmission dynamics of gambiense Human African Trypanosomiasis. PLoS Negl Trop Dis. 2018;12:e0006276. https://doi.org/10.1371/journal.pntd.0006276

8. World Health Organization. Human African trypanosomiasis: symptoms, diagnosis and treatment [cited 2019 Apr 8]. https://www.who.int/trypanosomiasis_african/diagnosis/en

9. European Medcines Agency Commitee for Medicinal Products for Human Use. Assessment report: fexinidazole Winthrop [cited 2018 Nov 15]. https://www.ema.europa.eu/en/documents/medicine-outside-eu/fexinidazole-winthrop-assessment-report_en-0.pdf

10. Criel B, De Brouwere V, Dugas S. Integration of vertical programmes in multi-function health services. Studies in Health Services Organisation and Policy. 1997;3:1–48.

11. Stasse S, Vita D, Kimfuta J, da Silveira VC, Bossyns P, Criel B. Improving financial access to health care in the Kisantu district in the Democratic Republic of Congo: acting upon complexity. Glob Health Action. 2015;8:25480. https://doi.org/10.3402/gha.v8.25480

12. Pepin J, Guern C, Milord F, Bokelo M. Integration of African human trypanosomiasis control in a network of multipurpose health centers [in French]. Bull World Health Organ. 1989;67:301–8.

13. Lumbala C, Simarro PP, Cecchi G, Paone M, Franco JR, Kande Betu Ku Mesu V, et al. Human African trypanosomiasis in the Democratic Republic of the Congo: disease distribution and risk. Int J Health Geogr. 2015;14:20. https://doi.org/10.1186/s12942-015-0013-9

14. Büscher P, Gilleman Q, Lejon V. Rapid diagnostic test for sleeping sickness. N Engl J Med. 2013;368:1069–70. https://doi.org/10.1056/NEJMc1210373

15. Wamboga C, Matovu E, Bessell PR, Picado A, Biéler S, Ndung'u JM. Enhanced passive screening and diagnosis for gambiense human African trypanosomiasis in north-western Uganda—moving towards elimination. PLoS One. 2017;12:e0186429. https://doi.org/10.1371/journal.pone.0186429

16. Lee SJ, Palmer JJ. Integrating innovations: a qualitative analysis of referral non-completion among rapid diagnostic test-positive patients in Uganda's human African trypanosomiasis elimination programme. Infect Dis Poverty. 2018;7:84. https://doi.org/10.1186/s40249-018-0472-x

17. Bessell PR, Lumbala C, Lutumba P, Baloji S, Biéler S, Ndung'u JM. Cost-effectiveness of using a rapid diagnostic test to screen for human African trypanosomiasis in the Democratic Republic of the Congo. PLoS One. 2018;13:e0204335. https://doi.org/10.1371/journal.pone.0204335

18. Mubwa Mungwele N. Rapport narratif annuel des données annuelles 2018: Yasa Bonga; 2019 [cited 2019 Aug 27]. http://sante.gouv.cd/wp-content/uploads/2019/05/RAPPORT-ANNUEL-ZS-BONGA-YASA-2018.pdf

19. Rock KS, Torr SJ, Lumbala C, Keeling MJ. Predicting the impact of intervention strategies for sleeping sickness in two high-endemicity health zones of the Democratic Republic of Congo. PLoS Negl Trop Dis. 2017;11:e0005162. https://doi.org/10.1371/journal.pntd.0005162

20. World Health Organization. Control and surveillance of human African trypanosomiasis. 2013 [cited 2019 Aug 27]. https://apps.who.int/iris/handle/10665/95732

21. Checchi F, Filipe JAN, Barrett MP, Chandramohan D. The natural progression of Gambiense sleeping sickness: what is the evidence? PLoS Negl Trop Dis. 2008;2:e303. https://doi.org/10.1371/journal.pntd.0000303

22. World Health Organization. Report of a WHO meeting on elimination of African trypanosomiasis (*Trypanosoma brucei gambiense*), Geneva, 3–5 December 2012. 2013 [cited 2019 Aug 8]. http://apps.who.int/iris/bitstream/10665/79689/1/WHO_HTM_NTD_IDM_2013.4_eng.pdf

23. Steinmann P, Stone CM, Sutherland CS, Tanner M, Tediosi F. Contemporary and emerging strategies for eliminating human African trypanosomiasis due to *Trypanosoma brucei gambiense* [review]. Trop Med Int Health. 2015;20:707–18. https://doi.org/10.1111/tmi.12483

24. Programme National de Lutte contre la Trypanosomiase Humaine Africaine en République Démocratique Du Congo. Déclaration de la politique de lutte contre la trypanosomiasis humaine Africaine en République Démocratique Du Congo. Kinshasa (Democratic Republic of the Congo): The Programme; 2015.

25. Simarro PP, Cecchi G, Franco JR, Paone M, Diarra A, Ruiz-Postigo JA, et al. Mapping the capacities of fixed health facilities to cover people at risk of gambiense human African trypanosomiasis. Int J Health Geogr. 2014;13:4. https://doi.org/10.1186/1476-072X-13-4

26. Chenge MF. De la nécessité d'adapter le modèle de district sanitaire au contexte urbain: exemple de la ville de Lubumbashi en RD Congo [dissertation]. Antwerp: Institute of Tropical Medicine; 2013 [cited 2019 Aug 27]. http://dspace.itg.be/handle/10390/7467

27. des Impôts DG, Du Congo RD. Ordonnance-loi n°001/2012 du 21 septembre 2012 modifiant et completant certaines dispositions de l'ordonnance-loi n° 10/001 du 20 aout 2012 portant institution de la taxe sur la valeur ajoutee [cited 2019 Aug 27]. http://www.dgi.gouv.cd/index.php/fr/lois

28. Severens JL, Milne RJ. Discounting health outcomes in economic evaluation: the ongoing debate. Value Health. 2004;7:397–401. https://doi.org/10.1111/j.1524-4733.2004.74002.x

29. Lutumba P, Makieya E, Shaw A, Meheus F, Boelaert M. Human African trypanosomiasis in a rural community, Democratic Republic of Congo. Emerg Infect Dis. 2007;13:248–54. https://doi.org/10.3201/eid1302.060075

30. Simarro PP, Franco J, Diarra A, Postigo JA, Jannin J. Update on field use of the available drugs for the chemotherapy of human African trypanosomiasis. Parasitology. 2012;139:842–6. https://doi.org/10.1017/S0031182012000169

31. World Health Organization. Estimates of unit costs for patient services for Democratic Republic of the Congo [cited 2019 Oct 12]. https://www.who.int/choice/country/cod/cost/en

32. Babokhov P, Sanyaolu AO, Oyibo WA, Fagbenro-Beyioku AF, Iriemenam NC. A current analysis of chemotherapy strategies for the treatment of human African trypanosomiasis. Pathog Glob Health. 2013;107:242–52. https://doi.org/10.1179/2047773213Y.0000000105

33. Yun O, Priotto G, Tong J, Flevaud L, Chappuis F. NECT is next: implementing the new drug combination therapy for *Trypanosoma brucei gambiense* sleeping sickness. PLoS Negl Trop Dis. 2010;4:e720-e.

34. Anderson AD. Rapport narratif annuel Mosango: 2018. 2019 [cited 2019 Aug 27]. http://sante.gouv.cd/wp-content/uploads/2019/05/RAPPORT-ANNUEL-ZS-MOSAN-GO-2018.pdf

35. Snijders R, Fukinsia A, Claeys Y, Mpanya A, Hasker E, Meheus F, et al. Cost of a new method of active screening for human African trypanosomiasis in the Democratic Republic of the Congo. PLoS Negl Trop Dis. 2020;14:e0008832. https://doi.org/10.1371/journal.pntd.0008832

36. Piot MA. A simulation model of case finding and treatment in tuberculosis control programmes. 1967 [cited 2019 Aug 27]. https://apps.who.int/iris/handle/10665/69827

37. World Health Organization. WHO interim guidelines for the treatment of gambiense human African trypanosomiasis. 2019 [cited 2019 Aug 27]. https://apps.who.int/iris/bitstream/handle/10665/326178/9789241550567-eng.pdf

Address for correspondence: Rian Snijders, Institute of Tropical Medicine, Public Health Department, Nationalestraat 155, 2000 Antwerp, Belgium; email: riansnijders@hotmail.com

April 2021

High-Consequence Pathogens

- Blastomycosis Surveillance in 5 States, United States, 1987–2018

- Reemergence of Human Monkeypox and Declining Population Immunity in the Context of Urbanization, Nigeria, 2017–2020

- Animal Reservoirs and Hosts for Emerging Alphacoronavirsuses and Betacoronaviruses

- Difficulties in Differentiating Coronaviruses from Subcellular Structures in Human Tissues by Electron Microscopy

- Characteristics of SARS-CoV-2 Transmission among Meat Processing Workers in Nebraska, USA, and Effectiveness of Risk Mitigation Measures

- Systematic Review of Reported HIV Outbreaks, Pakistan, 2000–2019

- Infections with Tickborne Pathogens after Tick Bite, Austria, 2015–2018

- Emergence of *Burkholderia pseudomallei* Sequence Type 562, Northern Australia

- Analysis of Asymptomatic and Presymptomatic Transmission in SARS-CoV-2 Outbreak, Germany, 2020

- Histopathological Characterization of Cases of Spontaneous Fatal Feline Severe Fever with Thrombocytopenia Syndrome, Japan

- COVID-19–Associated Pulmonary Aspergillosis, March–August 2020

- Genomic Surveillance of a Globally Circulating Distinct Group W Clonal Complex 11 Meningococcal Variant, New Zealand, 2013–2018

- Dynamic Public Perceptions of the Coronavirus Disease Crisis, the Netherlands, 2020

- Evolution of Sequence Type 4821 Clonal Complex Hyperinvasive and Quinolone-Resistant Meningococci

- Epidemiologic and Genomic Reidentification of Yaws, Liberia

- Sexual Contact as Risk Factor for Campylobacter Infection

- Venezuelan Equine Encephalitis Complex Alphavirus in Bats, French Guiana

- Stability of SARS-CoV-2 RNA in Nonsupplemented Saliva

- Rare Norovirus GIV Foodborne Outbreak, Wisconsin, USA

- Experimental SARS-CoV-2 Infection of Bank Voles

- Increased SARS-Cov-2 Testing Capacity with Pooled Saliva Samples

- Persistence of SARS-CoV-2 N-Antibody Response in Healthcare Workers, London, UK

- Genomic Analysis of Novel Poxvirus Brazilian Porcupinepox Virus, Brazil, 2019

EMERGING INFECTIOUS DISEASES®

To revisit the April 2021 issue, go to:

https://wwwnc.cdc.gov/eid/articles/issue/27/4/table-of-contents

Epidemiology and Spatial Emergence of Anaplasmosis, New York, USA, 2010–2018

Alexis Russell, Melissa Prusinski, Jamie Sommer, Collin O'Connor, Jennifer White,
Richard Falco, John Kokas,[1] Vanessa Vinci, Wayne Gall,[2] Keith Tober,[1] Jamie Haight,
JoAnne Oliver, Lisa Meehan, Lee Ann Sporn, Dustin Brisson, P. Bryon Backenson

Human granulocytic anaplasmosis, a tickborne disease caused by the bacterium *Anaplasma phagocytophilum*, was first identified during 1994 and is now an emerging public health threat in the United States. New York state (NYS) has experienced a recent increase in the incidence of anaplasmosis. We analyzed human case surveillance and tick surveillance data collected by the NYS Department of Health for spatiotemporal patterns of disease emergence. We describe the epidemiology and growing incidence of anaplasmosis cases reported during 2010–2018. Spatial analysis showed an expanding hot spot of anaplasmosis in the Capital Region, where incidence increased >8-fold. The prevalence of *A. phagocytophilum* increased greatly within tick populations in the Capital Region over the same period, and entomologic risk factors were correlated with disease incidence at a local level. These results indicate that anaplasmosis is rapidly emerging in a geographically focused area of NYS, likely driven by localized changes in exposure risk.

Anaplasmosis is an emergent tickborne disease caused by the obligate intracellular bacterium *Anaplasma phagocytophilum* (*1*). Initially termed human granulocytic ehrlichiosis, human infection with *A. phagocytophilum* was first described in 1994 in patients from Minnesota and Wisconsin, USA (*1,2*). Now referred to as human granulocytic anaplasmosis or simply anaplasmosis, this infection is characterized by a nonspecific influenza-like illness marked by fever, fatigue, muscle aches, and headache (*3*). Although severe complications and death occur in rare

Author affiliations: New York State Department of Health, Albany, New York, USA (A. Russell, M. Prusinski, J. Sommer, C. O'Connor, J. White, R. Falco, J. Kokas, V. Vinci, W. Gall, K. Tober, J. Haight, J. Oliver, L. Meehan, P.B. Backenson); Paul Smith's College, Paul Smiths, New York, USA (L.A. Sporn); University of Pennsylvania, Philadelphia, Pennsylvania, USA (D. Brisson)

instances, most patients recover fully after treatment with appropriate antimicrobial drugs (*4*).

Human infection with *A. phagocytophilum* has now been documented in patients in North America, Europe, and Asia, and a notable incidence has occurred in the United States (*5*). Anaplasmosis became a nationally notifiable disease in the United States during 1999, and nationwide case counts have since increased >16-fold, from 348 cases during 2000 to 5,762 cases during 2017 (*6*). Most of these infections occur in the northeastern and upper midwestern states, where well-established populations of *Ixodes scapularis* (blacklegged or deer ticks) transmit *A. phagocytophilum* in addition to the infectious agents of Lyme disease, babesiosis, and Powassan virus disease (*7–9*).

New York State (NYS), which is situated within the northeastern United States, to which tickborne diseases are endemic, has reported the second highest number of anaplasmosis cases of any state, closely behind Minnesota (*10–12*). Surveillance of anaplasmosis cases by the NYS Department of Health (NYSDOH) indicates that since the first NYS case was reported in 1994, the burden of anaplasmosis has increased substantially, accounting for a larger proportion of NYS tickborne disease cases every year (≈4% during 2010 vs. ≈11% during 2018) (*13*). Since 2015, anaplasmosis has consistently surpassed babesiosis as the second most common tickborne disease in NYS, after Lyme disease (*13*). In addition to surveillance of tickborne disease cases, the NYSDOH also conducts routine vector surveillance to monitor the dynamics of tick populations and the prevalence of tickborne pathogens, including *A. phagocytophilum*, to estimate

tickborne disease risk across the state. We examined human case surveillance and tick surveillance data during 2010–2018 to assess the epidemiology, risk for pathogen exposure, and spatiotemporal emergence patterns of anaplasmosis in NYS.

Methods

Anaplasmosis Cases
Human anaplasmosis cases reported to the NYS-DOH were analyzed retrospectively for 2010–2018 for all NYS counties, excluding the 5 boroughs of New York City (NYC). Provider-diagnosed anaplasmosis cases and positive laboratory test results for anaplasmosis were reported to the NYSDOH as mandated by NYS public health law (14,15). Both provider-reported cases and those with positive laboratory test results were investigated by NYS local health departments; clinical and demographic information for each case was entered into the NYS-DOH Communicable Disease Electronic Surveillance System. Reports were assigned a case status on the basis of the 2008 Centers for Disease Control and Prevention case definition for anaplasmosis (16). Reports with case status of either confirmed or probable were included as cases in this study. Cases with the diagnosis of ehrlichiosis/anaplasmosis undetermined were excluded.

Tick Collection and Testing
Host-seeking ticks were collected from publicly accessible lands across NYS during 2010–2018 by using standardized drag surveys as described (17). Collection sites were selected on the basis of tick habitat suitability and risk for human exposure (e.g., presence of leaf litter and hiking trails). *I. scapularis* nymphs were collected during April–September by dragging a 1-m² piece of white flannel through leaf litter and low-lying vegetation. *I. scapularis* adults were collected during September–December by flagging a 1-m² piece of white canvas over edge ecotone and understory vegetation up to 1 m high. Ticks were stored in 100% ethanol at 4°C until they were sorted by developmental stage and identified to species by using dichotomous keys, placed into sterile microcentrifuge tubes containing 100% ethanol, and stored at −20°C until DNA extraction (18,19). Individual *I. scapularis* ticks underwent total genomic DNA extraction as previously detailed and were tested for (target gene) *A. phagocytophilum* (major surface protein 2), *Babesia microti* (18S rDNA), *Borrelia burgdorferi* (16S rDNA), and *Borrelia miyamotoi* (16S rDNA) by using a quadplex real-time PCR (17,20).

Data Analysis
We analyzed case reports meeting criteria for inclusion by using SAS version 9.2 (https://www.sas.com). Incidence rates were aggregated by NYS regions (Capital, Central, Metro, and Western), and ZIP code tabulation area (ZCTA) by using patient address and 2010 US Census population data and shapefile (21). We used ArcGIS version 10.7 (22) to map incidence at the ZCTA level. Spatial autocorrelation at the ZCTA level was determined by using Moran I analysis for each year. We determined spatial clusters by using Getis-Ord Gi* hot spot analysis (https://pro.arcgis.com) at the ZCTA level for each year. Getis-Ord Gi* analysis generated statistically significant hot spots and cold spots on the basis of the local sum of the incidence rates for each ZCTA and its neighbors within a fixed distance band at peak z-score spatial increments. We assessed temporal changes in hot spot coverage by using a 2-tailed z-test for proportions (α = 0.05).

We analyzed tick collection and pathogen testing data by using in R Studio version 1.2 (23) and mapped data by using ArcGIS. Tick population density was calculated for each collection site visit as the total number of target ticks (adult or nymphal *I. scapularis*) collected per 1,000 m² sampled. We calculated pathogen prevalence as the proportion of ticks positive for *A. phagocytophilum* among those tested by PCR for each collection site visit and region. Temporal changes in pathogen prevalence were assessed by using a 2-tailed z-test for proportions (α = 0.05).

We used the entomologic risk index (ERI), a measure of population density of pathogen-carrying ticks, to estimate human risk for an infected tick bite (24). ERI was calculated as the product of tick population density (ticks per 1,000 m² sampled) and *A. phagocytophilum* prevalence at each collection site for each life stage (nymph and adult) and each year. We calculated ZCTA-level ERI as the average ERI of all sites within the ZCTA for each life stage and year. Correlation of anaplasmosis incidence and ERI at the ZCTA level was analyzed for each year by using the Spearman rank correlation. We mapped collection sites with circles sized according to ERI magnitude and then overlaid them onto the anaplasmosis incidence Getis-Ord Gi* hot spot analysis map of the corresponding year to identify common patterns in ERI and human incidence clusters.

Results

Anaplasmosis Epidemiology
A total of 5,146 anaplasmosis cases were reported in NYS (excluding NYC) during 2010–2018, a median of 454 cases/year (range 220–1,112 cases/year) (Table 1).

Table 1. Anaplasmosis case counts and incidence by state region, New York, USA, 2010–2018

Region	No. anaplasmosis cases, incidence/100,000 persons								
	2010	2011	2012	2013	2014	2015	2016	2017	2018
Capital	65	116	135	254	231	462	420	741	547
	(4.32)	(7.70)	(8.96)	(16.87)	(15.34)	(30.68)	(27.89)	(49.21)	(36.32)
Central	1 (0.06)	2 (0.11)	2 (0.11)	3 (0.17)	5 (0.29)	8 (0.46)	8 (0.46)	24 (1.37)	27 (1.54)
Metro	154	196	178	195	183	257	304	345	273
	(3.00)	(3.82)	(3.47)	(3.80)	(3.57)	(5.01)	(5.93)	(6.72)	(5.32)
Western	0	0	0	2 (0.07)	2 (0.07)	0	1 (0.04)	2 (0.07)	3 (0.11)
New York State excluding	220	314	315	454	421	727	733	1,112	850
New York City	(1.99)	(2.83)	(2.84)	(4.10)	(3.80)	(6.56)	(6.62)	(10.04)	(7.67)

Statewide incidence increased 3.9-fold over the study period, from 2.0 cases/100,000 persons during 2010 to 7.6 cases/100,000 persons during 2018; peak incidence was 9.9 cases/100,000 persons during 2017. The most substantial increase occurred in the Capital Region, which showed an 8.4-fold increase, from 4.3 cases/100,000 persons during 2010 to 36.3 cases/100,000 persons during 2018; peak incidence was 49.2 cases/100,000 persons during 2017. Incidence tended to be higher in odd years, most notably within the Capital Region (Figure 1).

Anaplasmosis was most common among male case-patients and those identified as White and non-Hispanic (Table 2). Patients >50 years of age accounted for 72.6% of cases. Aside from fever, which is a requirement to meet confirmed or probable case status, the most commonly reported symptoms were malaise, myalgia, and chills. Rash was the least commonly reported symptom. The most common bloodwork findings were thrombocytopenia and increased levels of hepatic aminotransferases, each found in more than half of the patients. Hospitalization was reported in 35.2% of case-patients, and 0.5% (16 patients) died from anaplasmosis-related causes. Symptom onset and diagnosis occurred most often in the month of June, followed by July and May (Figure 2).

Prevalence of *A. phagocytophilum*
A total of 16,743 nymphal and 27,658 adult *I. scapularis* ticks was tested for *A. phagocytophilum* during

Figure 1. Anaplasmosis incidence by state region, New York, USA, 2010–2018.

2010–2018; a total of 721 nymphs (4.3%) and 1,789 adults (6.5%) showed positive results (Table 3). Statewide prevalence of *A. phagocytophilum* increased in nymphal and adult *I. scapularis* ticks over the study period. *A. phagocytophilum* prevalence in nymphal *I. scapularis* ticks increased in 3 of 4 geographic regions over the study period, and there was an overall statewide increase from 2.4% during 2010 to 4.5% during 2018. Statewide prevalence of *A. phagocytophilum* in adult *I. scapularis* ticks increased significantly (p<0.01) from 4.0% during 2010 to 9.2% during 2018, and we observed an increase in prevalence in all 4 regions. There was a significant (p<0.0001) 4.1-fold increase in *A. phagocytophilum* prevalence in adult *I. scapularis* ticks in the Capital Region from 2.9% during 2010 to 12.0% during 2018. Site-level ERI (*A. phagocytophilum*–carrying ticks per 1,000 m^2) ranged from 0 to 28.2 in nymphs and from 0 to 85.3 in adult *I. scapularis* ticks.

Spatial Analysis
Patient ZCTA was available for 5,138 (99.8%) cases. Yearly ZCTA-level incidence ranged from 0 to 1,818 cases/100,000 persons. Moran I analysis showed significant spatial autocorrelation (Moran index range 0.092–0.260; p<0.0001) of human incidence at the ZCTA level for all years, justifying hot spot analysis. Getis-Ord Gi* analysis yielded 1 statistically significant hot spot for each year during 2010–2018 (Figure 3). The 99% confidence hot spot for 2010 encompassed 14.2% of ZCTAs, 10.8% of the population, and 9.4% of the land area of NYS excluding NYC. All 3 of these factors increased significantly (p<0.0001) over the study period, and the 99% confidence hot spot during 2018 encompassed 30.0% of ZCTAs, 17.0% of the population, and 24.8% of the land area. The centroid of the hot spot moved 51.7 km north and 10.6 km west during 2010–2018. The hot spot expanded to include a larger portion of the Capital Region over the study period. Overlaying site-level ERI onto the hot spot analysis showed that collection sites that had high ERIs tended to be located within the anaplasmosis hot spot; however, multiple high-ERI sites across the Metro Region and sporadically throughout the
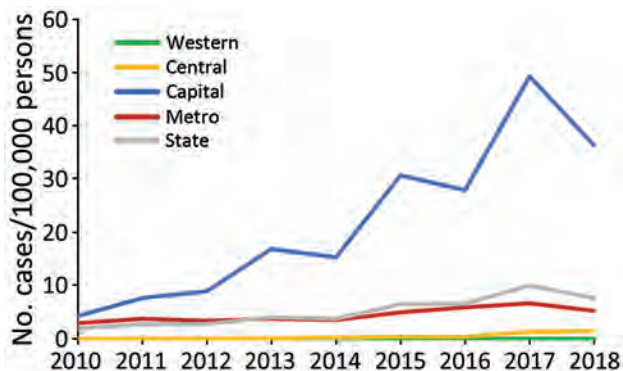
Central and Western regions were located outside the hot spot. Nymphal ERI was significantly correlated (r range 0.340–0.536; $p<0.05$) to anaplasmosis incidence at the ZCTA level for 7 of the 9 years during 2010–2018. Adult ERI was significantly correlated (r range 0.291–0.695; $p<0.01$) to anaplasmosis incidence at the ZCTA level for all years during 2010–2018.

Discussion

This 9-year study characterizes the emergence of anaplasmosis in NYS through the analysis of trends in human case and vector surveillance data over time and geography. Anaplasmosis poses an increasingly substantial public health risk in NYS, and the 2010–2018 time frame captures a dramatic increase in the burden of this newly emergent disease. A closer look at the changing epidemiology and exposure risk for this disease helps to elucidate when, where, and why anaplasmosis is rapidly expanding in NYS.

The basic epidemiologic characteristics of anaplasmosis cases in NYS are consistent with previous reports at the national level and are comparable with those of other tickborne diseases transmitted by *I. scapularis* ticks in NYS (*7,10,25,26*). Anaplasmosis, similar to Lyme disease and babesiosis, disproportionately affects White men, possibly because of residential and behavioral factors that increase the risk for tick bites in this group (*27,28*). The age distribution of patients shows a unimodal peak in the range of 60–69 years, similar to babesiosis but unlike Lyme disease, which shows bimodal peaks in the 5–9 and 50–54 year ranges (*27,28*). This finding might be related to the increased susceptibility for severe anaplasmosis infections with age, and the greater likelihood of subclinical infections in young patients (*7,29*). Anaplasmosis infection causes a constellation of nonspecific symptoms that mimic those of other tickborne diseases, but without a characteristic rash, such as erythema migrans, seen in Lyme disease (*27,28*). The hospitalization rate for anaplasmosis is higher than that for Lyme disease but lower than that of babesiosis, and the case-fatality rate of 0.5% is much lower than the 6.5% found in babesiosis patients in NYS (*26,27,29*).

The summertime peak in anaplasmosis incidence implicates *I. scapularis* nymphs, which are most active during summer months, as the developmental stage responsible for most cases, even though nymphs are approximately half as likely as adult *I. scapularis* ticks to carry *A. phagocytophilum*. This finding is consistent with other tickborne diseases and might be attributed to NYS residents spending more time outdoors during summer months and the increased difficulty of finding and removing the much smaller nymphs dur-

ing the 12–24-hour window before *A. phagocytophilum* transmission occurs (*9,25,27,30*).

Spatial assessment of the emergence of anaplasmosis indicates that the increase in cases is not occurring diffusely across NYS but is instead originating primarily within the Capital Region. The dramatic 8.4-fold increase in incidence in the Capital Region during the 9-year study period indicates a rapidly intensifying focal area of disease emergence. Hot spot analysis pinpoints an expanding focal area centered around Columbia and Rensselaer Counties, bordering the Hudson River to the west and Vermont and Massachusetts to the east. This area might be located within a local epicenter of anaplasmosis emergence in the northeastern states because case data for neighboring states indicate increasing anaplasmosis inci-

Table 2. Demographic and clinical characteristics of anaplasmosis case-patients, New York, USA, 2010–2018

Characteristic	% Cases
Case status	
Confirmed	60.3
Probable	39.7
Sex	
F	39.5
M	60.5
Age group, y	
0–9	2.1
10–19	3.0
20–29	4.2
30–39	7.0
40–49	11.1
50–59	20.5
60–69	24.9
70–79	18.0
≥80	9.2
Race	
American Indian/Alaska Native	0.0
Asian/Pacific Islander	1.1
Black	1.0
White	95.5
Other	2.3
Ethnicity	
Hispanic	3.9
Non-Hispanic	96.1
Signs/symptoms	
Arthralgia	57.9
Chills	75.9
Headache	66.8
Malaise	90.2
Myalgia	76.8
Nausea	38.6
Rash	10.7
Rigors	19.6
Stiff neck	16.5
Laboratory findings	
Anemia	29.7
Increased levels of hepatic aminotransferases	56.6
Leukopenia	42.3
Thrombocytopenia	61.8
Outcome	
Hospitalization	35.2
Death	0.5
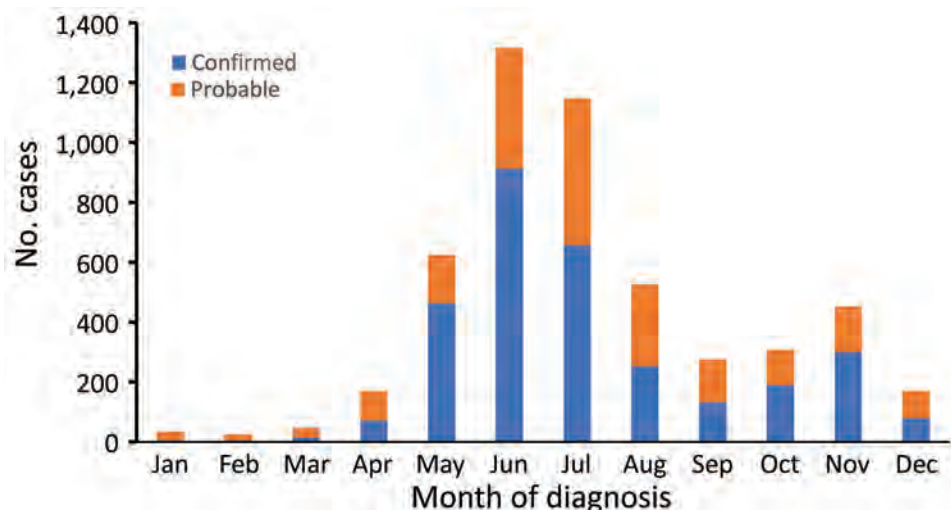
Figure 2. Anaplasmosis cases by month of diagnosis and case status, New York, USA, 2010–2018.

dence in NYS-adjacent counties over the time frame of our study (*31,32*). The geographic expansion of anaplasmosis generally mimics that of Lyme disease in NYS decades earlier, with initial emergence northward along the Hudson River (*33,34*). However, the spread of Lyme disease more closely followed the apparent range expansion of *I. scapularis* ticks from coastal areas northward and westward across NYS, whereas anaplasmosis is less common in coastal NYS and shows a more radial expansion further inland (*35*). A similar inland radial expansion pattern was seen in the emergence of anaplasmosis in Minnesota during 1996–2011 (*36*).

The hot spot defined by this study coincides with a map of seroprevalence of *Anaplasma* species in a large sample of domestic dogs across the contiguous United States during 2011–2015 (*37*). Dogs, which are affected by the same pathogenic variant of *A. phagocytophilum* as humans, might be an excellent sentinel

species in forecasting the spread of anaplasmosis, as they have been for other tickborne diseases (*38*). Many potential driving forces, including changes in land use, host density, and climate, have been implicated in the geographic spread of *I. scapularis* ticks and associated pathogens, and it is probable that a multitude of factors are shaping the spread of anaplasmosis in NYS. The rapid, geographically focused pattern of anaplasmosis emergence might also indicate recent changes in risk factors that are unique for this disease.

This study describes the changing prevalence of *A. phagocytophilum* in a large sample of host-seeking *I. scapularis* ticks collected across NYS. The overall statewide increase in pathogen prevalence over the study period, and in particular the large increase within adult *I. scapularis* ticks in the Capital Region, parallels the focal increase in human anaplasmosis incidence. The correlation of anaplasmosis ERI, which accounts for pathogen prevalence and tick population density,

Table 3. Prevalence of *Anaplasma phagocytophilum* in nymphal and adult *Ixodes scapularis* ticks by state region, New York, USA, 2010–2018

Region	Life stage	No. (%) ticks testing positive for *A. phagocytophilum*								
		2010	2011	2012	2013	2014	2015	2016	2017	2018
Capital	Nymphs	221 (4.1)	186 (3.8)	306 (6.5)	555 (5.0)	591 (8.8)	727 (3.2)	910 (4.5)	1,223 (3.5)	1,100 (5.3)
	Adults	278 (2.9)	201 (7.0)	791 (9.9)	834 (5.9)	1,689 (5.4)	1,677 (7.0)	1,462 (8.5)	1,690 (8.6)	1,617 (12.0)
Central	Nymphs	135 (2.2)	126 (3.2)	55 (0.0)	140 (2.1)	142 (4.2)	586 (1.7)	547 (2.4)	596 (0.5)	217 (1.4)
	Adults	155 (0.0)	179 (2.2)	148 (0.7)	199 (2.0)	349 (2.0)	976 (2.8)	1,329 (1.5)	401 (5.7)	401 (5.5)
Metro	Nymphs	350 (2.0)	350 (4.9)	316 (2.2)	450 (3.3)	447 (3.8)	523 (5.0)	570 (7.7)	547 (7.7)	801 (4.9)
	Adults	300 (10.0)	350 (13.7)	350 (11.7)	518 (8.1)	544 (8.8)	625 (12.0	1,103 (17.6)	889 (11.2)	874 (12.7)
Western	Nymphs	166 (1.2)	287 (4.9)	328 (7.3)	272 (8.1)	362 (7.2)	501 (3.0)	635 (6.1)	996 (3.4)	479 (3.5)
	Adults	276 (0.7)	395 (2.3)	691 (0.4)	646 (0.5)	681 (2.3)	1,243 (2.1)	1,444 (2.1)	1,234 (2.95)	1,122 (3.8)
New York State excluding New York City	Nymphs	872 (2.4)	949 (4.4)	1,005 (5.1)	1,417 (4.8)	1,542 (6.5)	2,337 (3.2)	2,662 (5.1)	3,362 (3.6)	2,597 (4.5)
	Adults	1,009 (4.0)	1,125 (6.7)	1,980 (6.2)	2,197 (4.5)	3,263 (5.0)	4,521 (5.4)	5,338 (6.9)	4,211 (7.2)	4,014 (9.2)
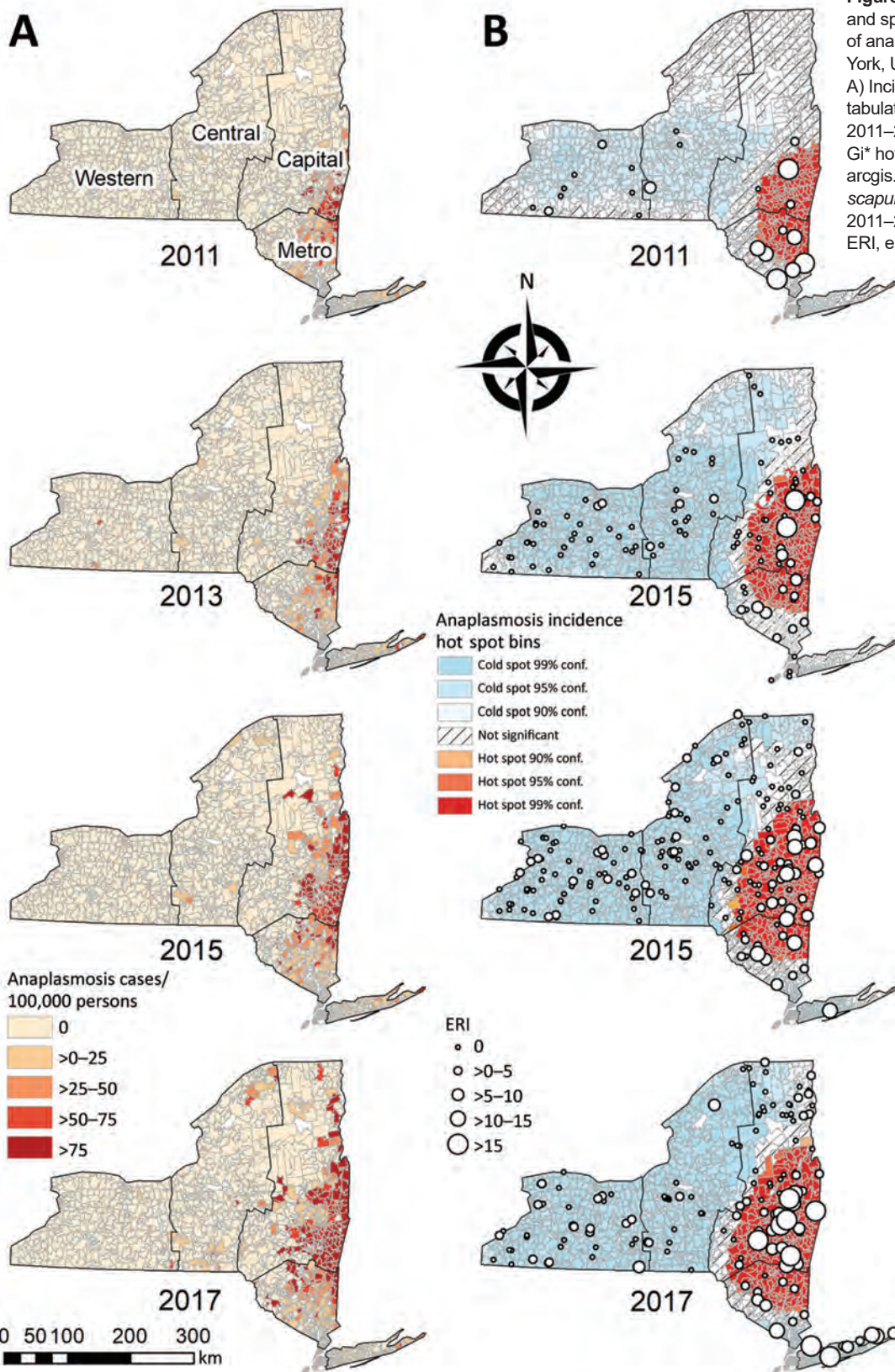
Figure 3. Epidemiology and spatial emergence of anaplasmosis, New York, USA, 2010–2018. A) Incidence by ZIP code tabulation area, odd years, 2011–2017. B) Getis-Ord Gi* hot spots (https://pro.arcgis.com) and adult *Ixodes scapularis* tick ERI, odd years, 2011–2017. Conf., confidence; ERI, entomologic risk index.

to yearly human incidence at the ZCTA-level, further supports the hypothesis that localized changes in exposure risk are driving emergence of this disease. However, the trends found in our tick surveillance data cannot fully explain the dramatic increase in anaplasmosis cases. Relatively high prevalence rates of *A. phagocytophilum* have been documented in *I. scapularis* ticks from the Metro Region of NYS as early as 1996 (*39*). A previous NYSDOH study found *A. phagocytophilum* in 6.5% of nymphs and 12.3% of adult *I. scapularis* ticks collected during 2003–2006 in the Hudson Valley, a region that overlaps most of the Metro Region and the southernmost part of the Capital Region as defined by this study, with no noted increase in pathogen prevalence over the study period (*17*). Clearly, *A. phagocytophilum* has been present at appreciable levels in the Metro Region tick population well before the recent increase in anaplasmosis cases, and although other tickborne diseases are endemic to this region, the Metro Region has not experienced a major emergence of anaplasmosis as seen in the Capital Region. The presence of multiple high-ERI tick surveillance sites, especially within the Metro Region, which were located well outside the anaplasmosis hot spot each year, underlines this discrepancy.

Some notable limitations of our host-seeking tick sampling might partially contribute to this incongruity, including greater vector surveillance coverage in some regions than others, increasing level of sampling effort over the study period, and repeated sampling of some locations but not others. Another explanation might be the distribution of pathogenic versus non-pathogenic genetic variants of *A. phagocytophilum*. The PCR used in this study does not distinguish between Ap-v1, a nonpathogenic variant that has a major reservoir in white-tailed deer (*Odocoileus virginianus*), and Ap-ha, a human pathogen that has white-footed mice (*Peromyscus leucopus*) and Eastern chipmunks (*Tamias striatus*) as major competent reservoirs (*40,41*). Studies of *I. scapularis* ticks in Ontario, Canada, which borders NYS, indicate an increase in the proportion of the pathogenic Ap-ha variant relative to the Ap-v1 variant in ticks collected after versus before 2010 (*42–44*). A similar shift in variant prevalence might be occurring in NYS and could be a driving force for human disease emergence. A follow-up study using genotyping to differentiate between variants of *A. phagocytophilum* in ticks collected across NYS, coupled with spatial analysis to examine changes in variant distribution over time and geography, is in progress and will hopefully further elucidate factors contributing to the emergence pattern of anaplasmosis in NYS.

The true burden of anaplasmosis in NYS is probably greater than that captured by our analysis of mandated case reporting. Anaplasmosis cases that are subclinical, self-limiting, misdiagnosed, or co-infections with other tickborne pathogens might be unreported or do not meet the strict case definition. In addition, the level of awareness of tickborne diseases among healthcare providers and the general public probably varies across NYS because tickborne diseases are hyperendemic in some regions and newly emergent in others. Resulting differences in patient behavior, provider diagnosis, and local health department reporting make estimating the true incidence of anaplasmosis a challenge, similar to what has been documented for Lyme disease in NYS (*45*). Lack of awareness can increase the likelihood of undiagnosed and untreated cases, which is especially relevant for a new and rapidly expanding disease such as anaplasmosis. Assessing disease epidemiology and clusters over time and geography enables us to pinpoint the populations at highest risk and anticipate when and where the disease will spread in the future so that public health efforts can be targeted toward populations who might benefit the most.

or molecular testing of ticks.

About the Author

Ms. Russell is a research scientist in the Vector Ecology Laboratory, Bureau of Communicable Disease Control, New York State Department of Health, Albany, NY. Her primary research interests are the ecology and epidemiology of tickborne diseases.

References

1. Chen SM, Dumler JS, Bakken JS, Walker DH. Identification of a granulocytotropic *Ehrlichia* species as the etiologic agent of human disease. J Clin Microbiol. 1994;32:589–95. https://doi.org/10.1128/JCM.32.3.589-595.1994
2. Bakken JS, Dumler JS, Chen SM, Eckman MR, Van Etta LL, Walker DH. Human granulocytic ehrlichiosis in the upper Midwest United States. A new species emerging? JAMA. 1994;272:212–8. https://doi.org/10.1001/jama.1994.03520030054028
3. Bakken JS, Krueth J, Wilson-Nordskog C, Tilden RL, Asanovich K, Dumler JS. Clinical and laboratory characteristics of human granulocytic ehrlichiosis. JAMA. 1996;275:199–205. https://doi.org/10.1001/jama.1996.03530270039029
4. Ramsey AH, Belongia EA, Gale CM, Davis JP. Outcomes of treated human granulocytic ehrlichiosis cases. Emerg Infect Dis. 2002;8:398–401. https://doi.org/10.3201/eid0804.010222
5. Guzman N, Yarrarapu SN, Beidas SO. *Anaplasma phagocytophilum*. Treasure Island (FL): StatPearls Publishing; 2021 [cited 2021 Mar 10]. http://www.ncbi.nlm.nih.gov/books/NBK513341
6. Centers for Disease Control and Prevention. Anaplasmosis epidemiology and statistics [cited 2019 Nov 29]. https://www.cdc.gov/anaplasmosis/stats/index.html
7. Dahlgren FS, Heitman KN, Drexler NA, Massung RF, Behravesh CB. Human granulocytic anaplasmosis in the United States from 2008 to 2012: a summary of national surveillance data. Am J Trop Med Hyg. 2015;93:66–72. https://doi.org/10.4269/ajtmh.15-0122
8. Eisen RJ, Eisen L, Beard CB. County-Scale distribution of *Ixodes scapularis* and *Ixodes pacificus* (Acari: Ixodidae) in the continental United States. J Med Entomol. 2016;53:349–86. https://doi.org/10.1093/jme/tjv237
9. Eisen L. Pathogen transmission in relation to duration of attachment by *Ixodes scapularis* ticks. Ticks Tick Borne Dis. 2018;9:535–42. https://doi.org/10.1016/j.ttbdis.2018.01.002
10. Dahlgren FS, Mandel EJ, Krebs JW, Massung RF, McQuiston JH. Increasing incidence of *Ehrlichia chaffeensis* and *Anaplasma phagocytophilum* in the United States, 2000–2007. Am J Trop Med Hyg. 2011;85:124–31. https://doi.org/10.4269/ajtmh.2011.10-0613
11. Centers for Disease Control and Prevention. MMWR summary of notifiable infectious diseases and conditions, annual summaries 2010–2015 [cited 2019 Nov 29]. https://www.cdc.gov/mmwr/mmwr_nd/index.html
12. Centers for Disease Control and Prevention. Nationally notifiable infectious diseases and conditions, United States: annual tables 2016–2018 [cited 2019 Nov 1]. https://wonder.cdc.gov/nndss/nndss_annual_tables_menu.asp
13. New York State Department of Health. Communicable disease annual reports 2000–2018 [cited 2019 Nov 29]. https://www.health.ny.gov/statistics/diseases/communicable
14. New York State. New York State Public Health Law: communicable diseases; laboratory reports and records. PHL 2102 [cited 2021 May 28]. https://newyork.public.law/laws/n.y._public_health_law_section_2102r
15. New York State. Reporting cases of suspected cases of outbreaks of communicable disease by physicians. 10NYCRR 2.10 Jul 6, 2011 [cited 2021 May 27]. https://regs.health.ny.gov/content/section-210-reporting-cases-or-suspected-cases-or-outbreaks-communicable-disease-physicians
16. Council of State and Territorial Epidemiologists. Ehrlichiosis and anaplasmosis 2008 case definition, 2008 [cited 2021 May 27]. https://wwwn.cdc.gov/nndss/conditions/ehrlichiosis-and-anaplasmosis/case-definition/2008
17. Prusinski MA, Kokas JE, Hukey KT, Kogut SJ, Lee J, Backenson PB. Prevalence of *Borrelia burgdorferi* (Spirochaetales: Spirochaetaceae), *Anaplasma phagocytophilum* (Rickettsiales: Anaplasmataceae), and *Babesia microti* (Piroplasmida: Babesiidae) in *Ixodes scapularis* (Acari: Ixodidae) collected from recreational lands in the Hudson Valley Region, New York State. J Med Entomol. 2014;51:226–36. https://doi.org/10.1603/ME13101
18. Keirans JE, Clifford CM. The genus *Ixodes* in the United States: a scanning electron microscope study and key to the adults. J Med Entomol Suppl. 1978;2(suppl_2):1–149. https://doi.org/10.1093/jmedent/15.suppl2.1
19. Durden LA, Keirans JE. Nymphs of the genus *Ixodes* (Acari: Ixodidae) of the United States: taxonomy, identification key, distribution, hosts, and medical/veterinary importance. Thomas Say Publications in Entomology. Lanham (MD): Entomological Society of America; 1996.
20. Piedmonte NP, Shaw SB, Prusinski MA, Fierke MK. Landscape features associated with blacklegged tick (Acari: Ixodidae) density and tick-borne pathogen prevalence at multiple spatial scales in central New York State. J Med Entomol. 2018;55:1496–508. https://doi.org/10.1093/jme/tjy111
21. United States Census Bureau. TIGER/Line Shapefile, 2016, 2010 nation, U.S., 2010 Census 5-Digit ZIP Code Tabulation Area (ZCTA5) national, 2019 [cited 2019 Dec 4]. https://www2.census.gov/geo/tiger/TIGER2016/ZCTA5/tl_2016_us_zcta510.zip
22. ESRI. Spatial analyst tools. Redlands (CA): ESRI; 2019 [cited 2021 Jul 3]. https://www.esri.com
23. RStudio Team. RStudio: integrated development environment for R. Boston. RStudio, PBC; 2019 [cited 2021 May 27]. https://www.rstudio.com
24. Mather TN, Nicholson MC, Donnelly EF, Matyas BT. Entomologic index for human risk of Lyme disease. Am J Epidemiol. 1996;144:1066–9. https://doi.org/10.1093/oxfordjournals.aje.a008879
25. Schwartz AM, Hinckley AF, Mead PS, Hook SA, Kugeler KJ. Surveillance for Lyme disease—United States, 2008–2015. MMWR Surveill Summ. 2017;66:1–12. https://doi.org/10.15585/mmwr.ss6622a1
26. Gray EB, Herwaldt BL. Babesiosis surveillance—United States, 2011–2015. MMWR Surveill Summ. 2019;68:1–11. https://doi.org/10.15585/mmwr.ss6806a1
27. Schotthoefer AM, Hall MC, Vittala S, Bajwa R, Frost HM. Clinical presentation and outcomes of children with human granulocytic anaplasmosis. J Pediatric Infect Dis Soc. 2018;7:e9–15. https://doi.org/10.1093/jpids/pix029
28. Nelson CA, Saha S, Kugeler KJ, Delorey MJ, Shankar MB, Hinckley AF, et al. Incidence of clinician-diagnosed

Lyme disease, United States, 2005–2010. Emerg Infect Dis. 2015;21:1625–31. https://doi.org/10.3201/eid2109.150417

29. White DJ, Talarico J, Chang HG, Birkhead GS, Heimberger T, Morse DL. Human babesiosis in New York State: review of 139 hospitalized cases and analysis of prognostic factors. Arch Intern Med. 1998;158:2149–54. https://doi.org/10.1001/archinte.158.19.2149

30. Lin S, Shrestha S, Prusinski MA, White JL, Lukacik G, Smith M, et al. The effects of multiyear and seasonal weather factors on incidence of Lyme disease and its vector in New York State. Sci Total Environ. 2019;665:1182–8. https://doi.org/10.1016/j.scitotenv.2019.02.123

31. Massachusetts Department of Public Health. Human granulocytic anaplasmosis (HGA) surveillance annual summaries 2011–2017 [cited 2019 Nov 22]. https://www.mass.gov/lists/tick-borne-disease-surveillance-summaries-and-data

32. Vermont Department of Health. Vermont tickborne disease program annual reports 2014–2017 [cited 2019 Nov 22]. https://www.healthvermont.gov/disease-control/tickborne-diseases

33. White DJ, Chang HG, Benach JL, Bosler EM, Meldrum SC, Means RG, et al. The geographic spread and temporal increase of the Lyme disease epidemic. JAMA. 1991;266:1230–6. https://doi.org/10.1001/jama.1991.03470090064033

34. Chen H, White DJ, Caraco TB, Stratton HH. Epidemic and spatial dynamics of Lyme disease in New york State, 1990–2000. J Med Entomol. 2005;42:899–908. https://doi.org/10.1603/0022-2585(2005)042[0899:EASDOL]2.0.CO;2

35. Khatchikian CE, Prusinski MA, Stone M, Backenson PB, Wang I-N, Foley E, et al. Recent and rapid population growth and range expansion of the Lyme disease tick vector, *Ixodes scapularis*, in North America. Evolution. 2015;69:1678–89. https://doi.org/10.1111/evo.12690

36. Robinson SJ, Neitzel DF, Moen RA, Craft ME, Hamilton KE, Johnson LB, et al. Disease risk in a dynamic environment: the spread of tick-borne pathogens in Minnesota, USA. EcoHealth. 2015;12:152–63. https://doi.org/10.1007/s10393-014-0979-y

37. Liu Y, Watson SC, Gettings JR, Lund RB, Nordone SK, Yabsley MJ, et al. A Bayesian spatio-temporal model for forecasting *Anaplasma* species seroprevalence in domestic dogs within the contiguous United States. PLoS One. 2017;12:e0182028. https://doi.org/10.1371/journal.pone.0182028

38. Mead P, Goel R, Kugeler K. Canine serology as adjunct to human Lyme disease surveillance. Emerg Infect Dis. 2011;17:1710–2. https://doi.org/10.3201/1709.110210

39. Daniels TJ, Boccia TM, Varde S, Marcus J, Le J, Bucher DJ, et al. Geographic risk for lyme disease and human granulocytic ehrlichiosis in southern New York state. Appl Environ Microbiol. 1998;64:4663–9. https://doi.org/10.1128/AEM.64.12.4663-4669.1998

40. Massung RF, Courtney JW, Hiratzka SL, Pitzer VE, Smith G, Dryden RL. *Anaplasma phagocytophilum* in white-tailed deer. Emerg Infect Dis. 2005;11:1604–6. https://doi.org/10.3201/eid1110.041329

41. Keesing F, McHenry DJ, Hersh M, Tibbetts M, Brunner JL, Killilea M, et al. Prevalence of human-active and variant 1 strains of the tick-borne pathogen *Anaplasma phagocytophilum* in hosts and forests of eastern North America. Am J Trop Med Hyg. 2014;91:302–9. https://doi.org/10.4269/ajtmh.13-0525

42. Werden L, Lindsay LR, Barker IK, Bowman J, Gonzales EK, Jardine CM. Prevalence of *Anaplasma phagocytophilum* and *Babesia microti* in *Ixodes scapularis* from a newly established Lyme disease endemic area, the Thousand Islands Region of Ontario, Canada. Vector Borne Zoonotic Dis. 2015;15:627–9. https://doi.org/10.1089/vbz.2015.1792

43. Krakowetz CN, Dibernardo A, Lindsay LR, Chilton NB. Two *Anaplasma phagocytophilum* strains in *Ixodes scapularis* ticks, Canada. Emerg Infect Dis. 2014;20:2064–7. https://doi.org/10.3201/eid2012.140172

44. Nelder MP, Russell CB, Lindsay LR, Dibernardo A, Brandon NC, Pritchard J, et al. Recent emergence of *Anaplasma phagocytophilum* in Ontario, Canada: early serological and entomological indicators. Am J Trop Med Hyg. 2019;101:1249–58. https://doi.org/10.4269/ajtmh.19-0166

45. White J, Noonan-Toly C, Lukacik G, Thomas N, Hinckley A, Hook S, et al. Lyme disease surveillance in New York State: an assessment of case underreporting. Zoonoses Public Health. 2018;65:238–46. https://doi.org/10.1111/zph.12307

Address for correspondence: Melissa Prusinski, New York State Department of Health, Vector Ecology Laboratory, Wadsworth Center, Biggs Laboratories C-456–C-467B, Empire State Plaza, Albany, NY 12237, USA; email: melissa.prusinski@health.ny.gov

Zoonotic Soil-Transmitted Helminths in Free-Roaming Dogs, Kiribati

Patsy A. Zendejas-Heredia, Allison Crawley, Helen Byrnes, Rebecca J. Traub, Vito Colella

Soil-transmitted helminths are highly prevalent in the Asia–Pacific region. We report a 96.5% prevalence of zoonotic soil-transmitted helminths in dogs in Kiribati. We advocate for urgent implementation of treatment and prevention programs for these zoonotic pathogens, in line with the Kiribati–World Health Organization Cooperation Strategy 2018–2022.

Soil-transmitted helminths (STHs) are a group of parasitic worms infecting both humans and animals living in resource-limited settings (*1*). STHs affect >2 billion persons worldwide, causing major physical and cognitive impairment in children and negative health outcomes in pregnant women and women of childbearing age (*2*). Hookworms alone infect nearly half a billion persons, causing iron-deficiency anemia, stunted growth, and malnutrition (*3*). In addition, iron deficiencies may increase the risk of bacterial infections, especially in children <5 years of age (*3*). Although STHs are largely considered human-specific parasites, dogs are also known to harbor STHs that cause well-documented zoonotic diseases globally (*3*). The *Ancylostoma ceylanicum* roundworm is a zoonotic STH with dogs as reservoirs and is the second most common hookworm infecting humans in many regions in Southeast Asia and the Western Pacific (*3*). In humans, canine hookworms cause cutaneous larva migrans; *A. braziliense* hookworm is the only species capable of causing creeping eruptions and *A. caninum* hookworm triggers eosinophilic enteritis and aphthous ileitis (*4*). Recently, *A. caninum* eggs have been reported in the feces of human patients, suggesting that this parasite may

complete its life cycle in humans, which can potentially result in disease transmission between hosts (*4*). In dogs, infections with hookworms are a common cause of hemorrhagic diarrhea and death in pups and chronic iron deficiency anemia in adult animals (*4*). The existence of dogs in close proximity to humans living in poor-hygiene settings, coupled with a lack of veterinary services and zoonotic awareness, exacerbates infection risks for the transmission of zoonotic STHs (*5*). In the Pacific islands, data on STH prevalence is scarce; therefore, estimates of disease burden caused by STHs cannot be accurately assessed.

Kiribati is a sovereign state in Micronesia in the central Pacific Ocean and is one of the most geographically isolated and impoverished countries in the world (*6*). Effects of poverty and climate change exert a huge toll on the ecology and health of humans and animals inhabiting the country. For instance, in the capital, South Tarawa, the high level of poverty, overcrowding, and presence of free-roaming animals influence the epidemiology of zoonotic STHs, trapping poor persons in a vicious cycle of poverty (*6,7*). Despite the Kiribati–World Health Organization Cooperation Strategy 2018–2022 (*6*), to date, no information is available on the presence and diversity of zoonotic STHs in free-roaming animals in Kiribati.

The Study

The republic of Kiribati consists of 32 atolls in the central Pacific Ocean, with a population of >110,000 persons, inhabiting mainly the Gilbert Islands. The main economic revenue comes from seafood exports and fishing. Most primary foods are imported, and safe water supplies, proper solid waste disposal, and sanitation facilities are scarce, posing major threats to public health (*6*).

We investigated the occurrence of zoonotic STHs in free-roaming dogs in Tarawa Atoll, Kiribati, as part of a dog health and population management program

Author affiliations: University of Melbourne, Parkville, Victoria, Australia (P. Zendejas-Heredia, R.J. Traub, V. Colella); independent researcher, Brisbane, Queensland, Australia (A. Crawley); Vets Beyond Borders, Brisbane (H. Byrnes)

Figure 1. Living conditions of dogs on Tarawa Atoll, Kiribati.

led by the Mardi Chi Dingo Foundation (https://farriervet.com/mardi-chi; Figure 1), which aims to seek a sustainable locally driven solution to improving animal health and overpopulation problems. The protocol of this study was approved by the Animal Ethics Committee at the Faculty of Veterinary and Agricultural Sciences (University of Melbourne, Melbourne, Victoria, Australia; ethics identification no. 1914930).

On the basis of previous surveys in regions with similar ecologic conditions (≈80% expected prevalence of enteric parasites) (5), we estimated that ≈200 dogs needed to be sampled in Kiribati to assess the prevalence of zoonotic STHs with 95% confidence and to detect a pathogen, if present, at a prevalence of $\geq$0.5% (assuming diagnostic sensitivity of 80% and specificity of 98%). To minimize animals' stress, we collected fecal samples from the rectal ampulla coinciding with the dog being anesthetized just before desexing surgery. We immediately preserved the fecal samples in Zymo DNA/RNA Shield (Zymo Research, https://www.zymoresearch.com), which renders any potential pathogen inactive or noninfective. We subjected fecal samples (200 mg each) from 198 dogs to genomic DNA extraction at the University of Melbourne using a Maxwell RSC PureFood GMO and Authentication Kit (Promega, https://www.promega.com) according to the manufacturer's instructions with modifications in that we performed an additional bead-beating step with 400 μL CTAB buffer using 0.5 mm zirconia/silica beads (Daintree Scientific, http://www.daintreescientific.com.au) using a FastPrep-24 5G Instrument (MP Biomedicals, https://www.mpbio.com). After bead-beating and cell lysis, we proceeded with DNA purification in a Maxwell RSC 48 Instrument (Promega). We stored the final eluted sample (100 μL)

at −20°C for further analyses. We subjected the extracted DNA to multiplex quantitative PCR screenings for hookworm species (4) and *Strongyloides stercoralis* (8). We analyzed and visualized the data with GraphPad Prism version 8.0 (GraphPad Software, https://www.graphpad.com).

Overall, 96.5% (95% CI 93.9–99.0) of dogs were positive for $\geq$1 of the investigated parasites. A total of 93.4% (95% CI 92.5–98.4) were positive for *A. caninum*, 26.3% (95% CI 20.1–32.4) for *A. ceylanicum*, 16.2% (95% CI 11.5–21.9) for *A. braziliense*, and 29.8% (95% CI 23.4–361) for *S. stercoralis* (Figure 2).

Conclusions

We demonstrated that dogs play a major role in contaminating the environment with zoonotic STH species, potentially serving as reservoirs for infections of humans living in Kiribati. Current control strategies against STHs in Kiribati have been based on deworming of school-age children as part of the Pacific program to eliminate lymphatic filariasis using albendazole as prophylactic treatment (9). However, this drug has limited effects against *S. stercoralis*, which requires ivermectin for its effective control and for which public health strategies are yet to be developed (10,11). Similarly, the emerging zoonotic agent *A. ceylanicum* has been reported with high prevalence, and despite ≈100 million persons currently infected with this STH (12), to date, no plan exists for its control. Given the different transmission
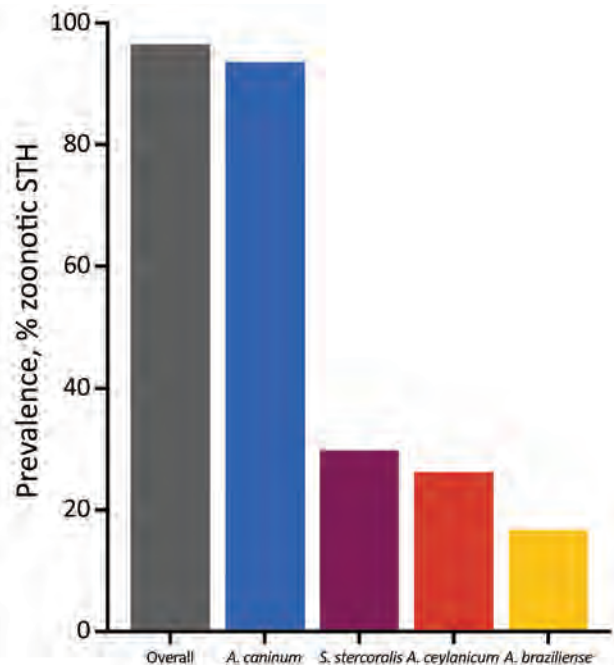
Figure 2. Prevalence of zoonotic soil-transmitted helminths in dogs on Tarawa Atoll, Kiribati.

dynamics and infection outcomes with different zoonotic STHs, accurate identification of these parasites is essential for the implementation of effective therapy and control programs (*4*,*12*). However, despite the efforts of nonprofit organizations, data on the occurrence of canine STHs in Kiribati were not previously available, hindering the understanding of the contribution of dogs in the transmission of zoonotic pathogens to humans.

Previous studies have shown an association between helminth infections and higher levels of anemia among school-age children from the Pacific region (*13*). Children with helminth infections were 3.6 times more likely to be stunted in growth and 2 times more likely to be anemic (*13*). This scenario is worsened by the absence of effective sewage systems, which contributes to the environmental contamination with animal and human feces, as demonstrated by the high levels of fecal coliforms in samples extracted from groundwater throughout South Tarawa (*14*). The lack of appropriate water, sanitation, and hygiene procedures increases the risks for infection with human and animal pathogens, including STHs. As a consequence, pneumonia and diarrhea, which have both strong links to hygiene and water, are some of the leading causes of illness and death among children in Kiribati (*14*).

In summary, we report a 96.5% prevalence of zoonotic STHs in dogs in Kiribati. Our results provide policy makers and key stakeholders with epidemiologic information that can be used for control programs to improve the health and quality of life of persons (in particular, women of reproductive age and children) and animals in the country, in line with the Kiribati–World Health Organization Cooperation Strategy 2018–2022.

About the Author

Ms. Zendejas-Heredia is a PhD candidate at the University of Melbourne, Melbourne, Australia. Her research is focused on the understanding of transmission dynamics of zoonotic soil-transmitted helminths in the Asia–Pacific region.

References

1. World Health Organization. Soil-transmitted helminth infections. Fact sheets. 2020 [cited 2021 Apr 21]. https://www.who.int/news-room/fact-sheets/detail/soil-transmitted-helminth-infections
2. World Health Organization. 2030 targets for soil-transmitted helminthiases control programmes. 2020 [cited 2021 Apr 21]. https://www.who.int/intestinal_worms/resources/9789240000315/en/
3. Loukas A, Hotez PJ, Diemert D, Yazdanbakhsh M, McCarthy JS, Correa-Oliveira R, et al. Hookworm infection. Nat Rev Dis Primers. 2016;2:16088. https://doi.org/10.1038/nrdp.2016.88
4. Massetti L, Colella V, Zendejas PA, Ng-Nguyen D, Harriott L, Marwedel L, et al. High-throughput multiplex qPCRs for the surveillance of zoonotic species of canine hookworms. PLoS Negl Trop Dis. 2020;14:e0008392. https://doi.org/10.1371/journal.pntd.0008392
5. Schär F, Inpankaew T, Traub RJ, Khieu V, Dalsgaard A, Chimnoi W, et al. The prevalence and diversity of intestinal parasitic infections in humans and domestic animals in a rural Cambodian village. Parasitol Int. 2014; 63:597–603. https://doi.org/10.1016/j.parint.2014.03.007
6. World Health Organization. Kiribati–WHO Country Cooperation Strategy 2018–2022. 2017 [cited 2021 Apr 21]. https://iris.wpro.who.int/handle/10665.1/13945
7. Storey D, Hunter S. Kiribati: An environmental "perfect storm." Aust Geogr. 2010;41:167–81. https://doi.org/10.1080/00049181003742294
8. Verweij JJ, Canales M, Polman K, Ziem J, Brienen EAT, Polderman AM, et al. Molecular diagnosis of *Strongyloides stercoralis* in faecal samples using real-time PCR. Trans R Soc Trop Med Hyg. 2009;103:342–6. https://doi.org/10.1016/j.trstmh.2008.12.001
9. Montresor A, Cong DT, Sinuon M, Tsuyuoka R, Chanthavisouk C, Strandgaard H, et al. Large-scale preventive chemotherapy for the control of helminth infection in Western Pacific countries: six years later. PLoS Negl Trop Dis. 2008;2:e278. https://doi.org/10.1371/journal.pntd.0000278
10. World Health Organization. Intestinal worms. 2020 [cited 2021 Apr 21]. https://www.who.int/intestinal_worms/epidemiology/strongyloidiasis
11. Henriquez-Camacho C, Gotuzzo E, Echevarria J, White AC Jr, Terashima A, Samalvides F, et al. Ivermectin versus albendazole or thiabendazole for *Strongyloides stercoralis* infection. Cochrane Database Syst Rev. 2016;(1):CD007745. https://doi.org/10.1002/14651858.CD007745.pub3
12. Traub RJ. *Ancylostoma ceylanicum*, a re-emerging but neglected parasitic zoonosis. Int J Parasitol. 2013;43:1009–15. https://doi.org/10.1016/j.ijpara.2013.07.006
13. Hughes RG, Sharp DS, Hughes MC, Akau'ola S, Heinsbroek P, Velayudhan R, et al. Environmental influences on helminthiasis and nutritional status among Pacific schoolchildren. Int J Environ Health Res. 2004;14:163–77. https://doi.org/10.1080/0960312042000218589
14. Government of Kiribati. Kiribati development plan 2016–19. 2016 [cited 2021 Apr 21]. http://www.mfed.gov.ki/sites/default/files/Kiribati%20Development%20Plan%202016%20-%2019.pdf

Address for correspondence: Vito Colella, Faculty of Veterinary and Agricultural Sciences, The University of Melbourne, Corner Flemington Rd and Park Dr, Parkville, VIC 3052, Australia; email: vito.colella@unimelb.edu.au

SARS-CoV-2 Prevalence among Outpatients during Community Transmission, Zambia, July 2020

Jonas Z. Hines, Sombo Fwoloshi, Davies Kampamba, Danielle T. Barradas, Dabwitso Banda, James E. Zulu, Adam Wolkon, Samuel Yingst, Mary Adetinuke Boyd, Mpanji Siwingwa, Lameck Chirwa, Muzala Kapina, Nyambe Sinyange, Victor Mukonka, Kennedy Malama, Lloyd B. Mulenga, Simon Agolory

During the July 2020 first wave of severe acute respiratory syndrome coronavirus 2 in Zambia, PCR-measured prevalence was 13.4% among outpatients at health facilities, an absolute difference of 5.7% compared with prevalence among community members. This finding suggests that facility testing might be an effective strategy during high community transmission.

The first cases of infection with severe acute respiratory syndrome coronavirus 2 (SARS-CoV-2), the virus that causes coronavirus disease (COVID-19), were reported in Zambia in March 2020 (*1*). During the first wave of infections, confirmed cases rapidly increased during July and peaked in August 2020 (Appendix, https://wwwnc.cdc.gov/EID/article/27/8/21-0502-App1.pdf). Zambia initially focused on screening travelers at points-of-entry and tracing contacts of persons with laboratory-confirmed cases. In April 2020, the Zambia Ministry of Health began SARS-CoV-2 surveillance among hospital inpatients and outpatients to identify cases of local transmission (*1,2*). It was believed that testing in health facilities would be more efficient at identifying cases than testing in the general population, which was particularly noteworthy given the severe shortage of SARS-CoV-2 tests in Africa early in the pandemic (*3,4*). A household prevalence survey conducted in

6 districts in Zambia in July 2020 found a community SARS-CoV-2 prevalence of 7.6% by using realtime PCR (rPCR) (*5*). To determine if facility testing was an effective case-finding strategy during a period of high community transmission, we compared SARS-CoV-2 prevalence among outpatients, overall and stratified by reasons for visiting the facility, with prevalence among community members in the same districts (*5*).

The Study

During July 2–31, 2020, we administered a cross-sectional prevalence survey of patients attending 20 outpatient clinics, including hospitals and health centers, in 6 districts in Zambia (Appendix). The number of facilities we selected in each district was proportional to the number of facilities in the other districts (Appendix). We recruited participants from outpatient departments regardless of their reason for visiting the facilities. Study teams were instructed to recruit ≥50 participants per facility and to attempt to show no preference in selection. We obtained consent or assent (for minors) before beginning study procedures. Participants completed an interviewer-administered questionnaire that included demographics, medical history, SARS-CoV-2 exposures, history of recent illness, and reason for visiting the facility. Concurrently, we conducted a cluster-sampled household prevalence survey in the same 6 districts (*5*). These surveys provided an opportunity to directly compare outpatient and community SARS-CoV-2 prevalence estimates. The study was approved by the Zambia National Health Research Authority and the University of Zambia Biomedical Research Ethics Committee. The activity was reviewed by the US Centers for Disease Control and Prevention (CDC) and conducted consistent with applicable US federal law and CDC policy.

Author affiliations: US Centers for Disease Control and Prevention, Lusaka, Zambia (J.Z. Hines, D.T. Barradas, A. Wolkon, S. Yingst, M.A. Boyd, S. Agolory); University Teaching Hospital, Lusaka (S. Fwoloshi, D. Kampamba, M. Siwingwa, L. Chirwa, L.B. Mulenga); Zambia Ministry of Health, Lusaka (S. Fwoloshi, K. Malama, L.B. Mulenga); Zambia Field Epidemiology Training Program, Lusaka (D. Banda, J.E. Zulu); Zambia National Public Health Institute, Lusaka (M. Kapina, N. Sinyange, V. Mukonka)

We tested nasopharyngeal specimens for SARS-CoV-2 RNA by using rPCR and plasma specimens for SARS-CoV-2 antibodies by using ELISA. We extracted RNA for rPCR using the QIAGEN Viral Mini procedure (https://www.qiagen.com). We used the Maccura SARS-CoV-2 Fluorescent PCR kit (https://www.maccura.com) on the QuantStudio 3 platform (ThermoFisher, https://www.thermofisher.com) as the primary rPCR diagnostic (6) and used the CDC assay method to confirm positive and indeterminant results (7). We performed the Euroimmun ELISA (PerkinElmer, https://www.perkinelmer.com) to test for spike protein IgG in single replicate (8). Participants could take part in any or all of the survey, rPCR testing, or serologic testing options based on personal preference.

We calculated SARS-CoV-2 prevalence as the number of positive results divided by the total number of tests conducted. Estimates were calculated separately for rPCR and ELISA results. We adjusted variance and 95% CIs for clustering by facility and seroprevalence for imperfect assay test characteristics (sensitivity 64.2%; specificity 100%; L. Steinhardt, pers. comm., email, 2021 Apr 2) using the Rogan-Gladen method (Appendix). To assess various factors associated with SARS-CoV-2 prevalence among outpatients, we used bivariate Poisson regression models to calculate prevalence ratios (PRs) and 95% CIs, with a random effects term for facility.

Of 1,975 persons representing ≈3.5% of ≈57,000 outpatients from the 20 facilities that we approached in July 2020 about participating (District Health Information System version 2; https://dhis2.org), 1,952 (98.8%) completed the questionnaire and 1,908 (97.7%) submitted either nasopharyngeal (1,490; 76.3%) or blood (1,657; 84.3%) specimens or both (Appendix). Of the 1,952 total participants, the number per district ranged from 160 (8.2%) in Nakonde District to 639 (32.8%) in Lusaka District; the median number of participants per facility was 93 (interquartile range 78–107; Table 1, https://wwwnc.cdc.gov/EID/article/27/8/21-0502-App1.pdf). Median participant age was 32 years (interquartile range 24–43 years); 60.5% were female. Overall, 34.1% of participants reported having a coexisting medical condition. Fever or respiratory complaints accounted for 28.2% of reasons for visiting the facility; 2.3% of participants were specifically seeking COVID-19 testing.

SARS-CoV-2 rPCR-measured prevalence was 13.4% (95% CI 8.3%–18.5%; Table 1); SARS-CoV-2 ELISA-measured prevalence was 8.2% (95% CI 5.1%–11.4%). Compared with community members, outpatients overall had higher rPCR-measured prevalence (PR 1.8, 95% CI 1.1–2.9; Table 2) as did those seeking COVID-19 testing (PR 3.6, 95% CI 2.2–5.9) or those without a stated reason for the visit (PR 2.0, 95% CI 1.2–3.3). Although only 2.2% of participants reported contact with confirmed COVID-19 case-patients, rPCR-measured prevalence was higher among outpatients specifically seeking COVID-19 testing compared with outpatients attending facilities for another reason (PR 2.2, 95% CI 1.4–3.3). In addition, outpatients had higher ELISA-measured prevalence than community members (PR 2.5, 95% CI 1.4–4.5) (Appendix). Among outpatients with SARS-CoV-2 infection, 45.7% did not report experiencing any symptoms associated with SARS-CoV-2.

Conclusions

Outpatients had higher SARS-CoV-2 prevalence than did community members in Zambia. Given the high SARS-CoV-2 prevalence and proportion of asymptomatic infections among outpatients, without instituting protective measures facilities might become transmission foci. Ameliorating risk requires instituting robust prevention and control strategies including universal masking in facilities (9,10). Furthermore, persons seeking testing at facilities should be quickly identified and isolated, because they might be at particularly high risk for having the virus.

One limitation of our study is that underlying condition and exposure history are subject to self-report

Table 2. Severe acute respiratory syndrome coronavirus 2 prevalence measured by PCR, prevalence ratios, and absolute prevalence differences between community members and outpatient participants, stratified by reason for attending the health facility, Zambia, July 2020

Population	Prevalence, % (95% CI)	Prevalence ratio (95% CI)	Absolute difference, % (95% CI)
Community members,† n = 2,990	7.6 (4.7–10.6)	Referent	Referent
Outpatients, n = 1,490			
Overall	13.4 (8.3–18.5)	1.8 (1.1–2.9)	5.7 (0.3–11.2)
Fever or respiratory complaint	12.9 (6.6–19.2)	1.7 (0.9–3.0)	5.3 (−1.2 to 11.7)
COVID-19 testing	27.5 (17.7–37.3)	3.6 (2.2–5.9)	19.9 (10.5–29.3)
Other acute medical complaints	10.7 (5.6–15.7)	1.4 (0.8–2.5)	3.0 (−2.4 to 8.4)
Routine health visit	12.5 (4.6–20.3)	1.6 (0.8–3.2)	4.8 (−2.9 to 12.5)
Not specified	15.5 (9.8–21.2)	2.0 (1.2–3.3)	7.9 (2.0–13.8)

*COVID-19, coronavirus disease.
†Estimates derived from a cluster-sampled household prevalence survey conducted among community members in the same 6 districts (Kabwe, Livingstone, Lusaka, Nakonde, Ndola, and Solwezi) as in the outpatient prevalence study.

and recall biases. The districts and facilities were not randomly selected and, despite our intentions to remain unbiased, may not have been representative of the population. The small sample size may have affected our ability to detect differences in factors associated with SARS-CoV-2 prevalence. The higher ELISA-measured prevalence among outpatients than community members could signal noncomparability between these 2 populations or that being an outpatient is a possible marker for other behaviors that increase SARS-CoV-2 infection risk. We assumed exact sensitivity and specificity values for the serology assay, but emerging evidence on serologic cross-reactivity (11–13) and antibody decay (14) might affect these values. However, given the timing of our study early in the outbreak, antibody decay was unlikely to substantially affect sensitivity (J. Perez-Saez, unpub. data, https://doi.org/10.1101/2021.03.16.21253710).

Countries with limited testing capacity need efficient strategies to identify persons with SARS-CoV-2 infections to interrupt transmission. In Zambia, when measured by rPCR, outpatients had 80% higher SARS-CoV-2 prevalence than persons in the surrounding community. Testing all outpatients regardless of their reasons for visiting the facility during periods of community transmission might help identify otherwise undetected SARS-CoV-2 infections. Compared with community-based SARS-CoV-2 testing, outpatient testing, which is often more convenient, might identify cases more effectively. Therefore, testing at facilities during periods of high community transmission might be an effective strategy to identify persons with SARS-CoV-2 infection, especially when testing capacity is limited.

About the Author

Dr. Hines is the surveillance advisor in the US Centers for Disease Control and Prevention Center for Global Health field office in Lusaka, Zambia. He is an internal medicine physician with 6 years of international public health experience, including in areas of surveillance methodology and public health workforce capacity building.

References

1. Chipimo PJ, Barradas DT, Kayeyi N, Zulu PM, Muzala K, Mazaba ML, et al. First 100 persons with COVID-19—Zambia, March 18–April 28, 2020. MMWR Morb Mortal Wkly Rep. 2020;69:1547–8. https://doi.org/10.15585/mmwr.mm6942a5
2. Zambia Ministry of Health. Implementation strategy—active screening for COVID-19 in health facilities. Lusaka (ZM): Zambia Ministry of Health; 2020.
3. Nkengasong J. Let Africa into the market for COVID-19 diagnostics. Nature. 2020;580:565. https://doi.org/10.1038/d41586-020-01265-0
4. Kavanagh MM, Erondu NA, Tomori O, Dzau VJ, Okiro EA, Maleche A, et al. Access to lifesaving medical resources for African countries: COVID-19 testing and response, ethics, and politics. Lancet. 2020;395:1735–8. https://doi.org/10.1016/S0140-6736(20)31093-X
5. Mulenga LB, Hines JZ, Fwoloshi S, Chirwa L, Siwingwa M, Yingst S, et al. Prevalence of SARS-CoV-2 in six districts in Zambia in July, 2020: a cross-sectional cluster sample survey. Lancet Glob Health. 2021;9:e773–81. https://doi.org/10.1016/S2214-109X(21)00053-X
6. Maccura Biotechnology. SARS-CoV-2 fluorescent PCR kit: instructions for use. 2020 [cited 27 May 2021]. https://www.fda.gov/media/137026/download
7. Centers for Disease Control and Prevention. CDC 2019-novel coronavirus (2019-nCoV) real-time RT-PCR diagnostic panel. 2020 [cited 27 May 2021] https://www.fda.gov/media/134922/download
8. U.S. Food and Drug Administration. Serology test evaluation report for "SARS-COV-2 ELISA (IgG)" from Euroimmun. 2020 [cited 27 May 2021] https://www.accessdata.fda.gov/cdrh_docs/presentations/maf/maf3246-a001.pdf
9. Wang X, Ferro EG, Zhou G, Hashimoto D, Bhatt DL. Association between universal masking in a health care system and SARS-CoV-2 positivity among health care workers. JAMA. 2020;324:703–4. https://doi.org/10.1001/jama.2020.12897
10. Kim H, Hegde S, LaFiura C, Raghavan M, Sun N, Cheng S, et al. Access to personal protective equipment in exposed healthcare workers and COVID-19 illness, severity, symptoms and duration: a population-based case-control study in six countries. BMJ Glob Health. 2021;6:e004611. https://doi.org/10.1136/bmjgh-2020-004611
11. Tso FY, Lidenge SJ, Peña PB, Clegg AA, Ngowi JR, Mwaiselage J, et al. High prevalence of pre-existing serological cross-reactivity against severe acute respiratory syndrome coronavirus-2 (SARS-CoV-2) in sub-Sahara Africa. Int J Infect Dis. 2020;102:577–83. https://doi.org/10.1016/j.ijid.2020.10.104
12. Nkuba Ndaye A, Hoxha A, Madinga J, Mariën J, Peeters M, Leendertz FH, et al. Challenges in interpreting SARS-CoV-2 serological results in African countries. Lancet Glob Health. 2021;9:e588–9. https://doi.org/10.1016/S2214-109X(21)00060-7
13. Steinhardt LC, Ige F, Iriemenam NC, Greby SM, Hamada Y, Uwandu M, et al. Cross-reactivity of two SARS-CoV-2 serological assays in a malaria-endemic setting. J Clin Microbiol. 2021 Apr 14 [Epub ahead of print]. https://doi.org/10.1128/JCM.00514-21 PMID: 33853839
14. Choe PG, Kim K-H, Kang CK, Suh HJ, Kang E, Lee SY, et al. Antibody responses 8 months after asymptomatic or mild SARS-CoV-2 infection. Emerg Infect Dis. 2021;27:928–31. https://doi.org/10.3201/eid2703.204543

Address for correspondence: Jonas Z. Hines, CDC–Zambia Office, PO Box 320065, 351 Independence Way, Woodlands, Lusaka, Zambia; email: jhines1@cdc.gov

Outbreak of SARS-CoV-2 B.1.1.7 Lineage after Vaccination in Long-Term Care Facility, Germany, February–March 2021

Pinkus Tober-Lau,[1] Tatjana Schwarz,[1] David Hillus, Jana Spieckermann, Elisa T. Helbig,
Lena J. Lippert, Charlotte Thibeault, Willi Koch, Leon Bergfeld, Daniela Niemeyer,
Barbara Mühlemann, Claudia Conrad, Stefanie Kasper, Friederike Münn, Frank Kunitz,
Terry C. Jones, Norbert Suttorp, Christian Drosten, Leif Erik Sander,[2] Florian Kurth,[2] Victor M. Corman[2]

One week after second vaccinations were administered, an outbreak of B.1.1.7 lineage severe acute respiratory syndrome coronavirus 2 infections occurred in a long-term care facility in Berlin, Germany, affecting 16/20 vaccinated and 4/4 unvaccinated residents. Despite considerable viral loads, vaccinated residents experienced mild symptoms and faster time to negative test results.

Outbreaks of severe acute respiratory syndrome coronavirus 2 (SARS-CoV-2) in long-term care facilities (LTCF) are of great concern and have been reported to have high case-fatality rates (*1*). Consequently, national vaccination strategies prioritize residents of LTCFs (*2*).

The coronavirus disease (COVID-19) mRNA vaccine BNT162b2 (Pfizer-BioNTech, https://www.pfizer.com) has demonstrated high efficacy against COVID-19 (*3*). Protection has been observed ≥12 days after the first vaccination, and reported vaccine efficacy is 52% between the first and second dose and 91% in the first week after the second dose (*3*). Although breakthrough infections have been reported, vaccinated persons were at substantially lower risk for infection and symptomatic disease (*4,5*).

The variant of concern (VOC) B.1.1.7 rapidly became the predominant lineage in Europe in 2021. Analyses estimated that B.1.1.7 has increased transmissibility and a ≤0.7 higher reproduction number (*6*). Neutralization activity of serum samples from BNT162b2-vaccinated persons has been shown to be slightly reduced against B.1.1.7 in cell culture (*7*), but observational data from Israel suggest BNT162b2 vaccination is effective against B.1.1.7 (*8*).

We investigated a SARS-CoV-2 B.1.1.7 outbreak in a LTCF, which involved 20 BNT162b2-vaccinated residents and 4 unvaccinated residents. We report on clinical outcomes, viral kinetics, and control measures applied for outbreak containment. The study was approved by the ethics committee of Charité–Universitätsmedizin Berlin (EA2/066/20) and conducted in accordance with the Declaration of Helsinki and guidelines of Good Clinical Practice (https://www.ema.europa.eu/en/documents/scientific-guideline/ich-e-6-r2-guideline-good-clinical-practice-step-5_en.pdf).

The Study

On February 4, 2021, daily SARS-CoV-2 screening of employees yielded a positive antigen point-of-care test (AgPOCT) result in 1 caregiver in a LTCF in Berlin, Germany. Among 24 residents of the unit under their responsibility, 20 (83%) residents had received the second dose of BNT162b2 on January

Author affiliations: Charité–Universitätsmedizin Berlin, Berlin, Germany (P. Tober-Lau, T. Schwarz, D. Hillus, E.T. Helbig, L.J. Lippert, C. Thibeault, W. Koch, L. Bergfeld, D. Niemeyer, B. Mühlemann, C. Conrad, S. Kasper, F. Münn, T.C. Jones, N. Suttorp, C. Drosten, L.E. Sander, F. Kurth, V.M. Corman); Paritätisches Seniorenwohnen gGmbH, Berlin (J. Spieckermann); German Centre for Infection Research (DZIF), Berlin (D. Niemeyer, B. Mühlemann, T.C. Jones, C. Drosten, V.M. Corman); Bezirksamt Lichtenberg von Berlin, Berlin (F. Kunitz); University of Cambridge, Cambridge, UK (T.C. Jones); German Center for Lung Research, Gießen, Germany (N. Suttorp, L.E. Sander); Bernhard Nocht Institute for Tropical Medicine (F. Kurth); University Medical Centre Hamburg-Eppendorf, Hamburg, Germany (F. Kurth)

[1]These authors contributed equally to this article.

[2]These senior authors contributed equally to this article.

29 or 30, 2021 (Figure 1). Four residents had not been vaccinated for nonmedical reasons (i.e., personal refusal or delayed provision of consent by legal guardian). AgPOCTs and reverse transcription PCR (RT-PCR) testing of all residents on February 4 detected SARS-CoV-2 infections in 3/4 unvaccinated and 10/20 vaccinated residents (Figure 1). At the time of testing, 2 vaccinated patients exhibited mild fatigue and one of those also had diarrhea; all other patients were asymptomatic.

The next week, testing detected 7 additional infections, resulting in 4/4 unvaccinated infected residents and 16/20 vaccinated infected residents. The remaining 4 vaccinated residents tested negative throughout the 30-day observation period (Figure 1).

In addition to residents, 11/33 (33%) staff members from the unit tested positive for SARS-Cov-2 by February 18; of those, none were twice-vaccinated staff members, 2/8 (25%) had received 1 dose of BNT162b, and 9/22 (40.9%) had not been vaccinated. No infected staff required hospital treatment.

Respiratory symptoms, including cough and shortness of breath, occurred in 5/16 (31.3%) vaccinated patients and all 4 unvaccinated patients (Figure 2, panel A; Appendix Table, https://wwwnc.cdc.gov/EID/article/27/8/21-0887-App1.pdf). All 4 unvaccinated SARS-CoV-2–infected patients and 2/16

(12.5%) vaccinated patients required hospitalization (Figure 1; Figure 2, panel A). Supplemental oxygen therapy was required by 3/4 (75.0%) unvaccinated and 1/16 (6.3%) vaccinated patients (Figure 1; Figure 2, panel A). Two patients, 1/16 (6.3%) vaccinated persons and 1/4 (25.0%) unvaccinated persons, required intermittent oxygen therapy after discharge. One vaccinated patient with a history of hypertension and microvascular dementia died 6 days after testing positive by RT-PCR because of a hypertensive crisis with intracerebral hemorrhage. Another vaccinated patient died 16 days after testing positive by RT-PCR. Neither patient experienced respiratory symptoms during the infection (Figure 1).

Containment measures in place included mandatory use of FFP2 or N95 masks and daily AgPOCT screening for anyone entering the facility. Immediately after detection, the facility was closed to visitors and additional containment measures were put in place, including designated staff and separate entrance, elevator, and changing rooms. Staff were required to change personal protective equipment before entering each room. Residents of all 7 units of the LTCF underwent weekly AgPOCT for >3 weeks, and residents in the adjacent unit underwent AgPOCT every 2–3 days. The outbreak was contained within the unit; no further cases were detected.
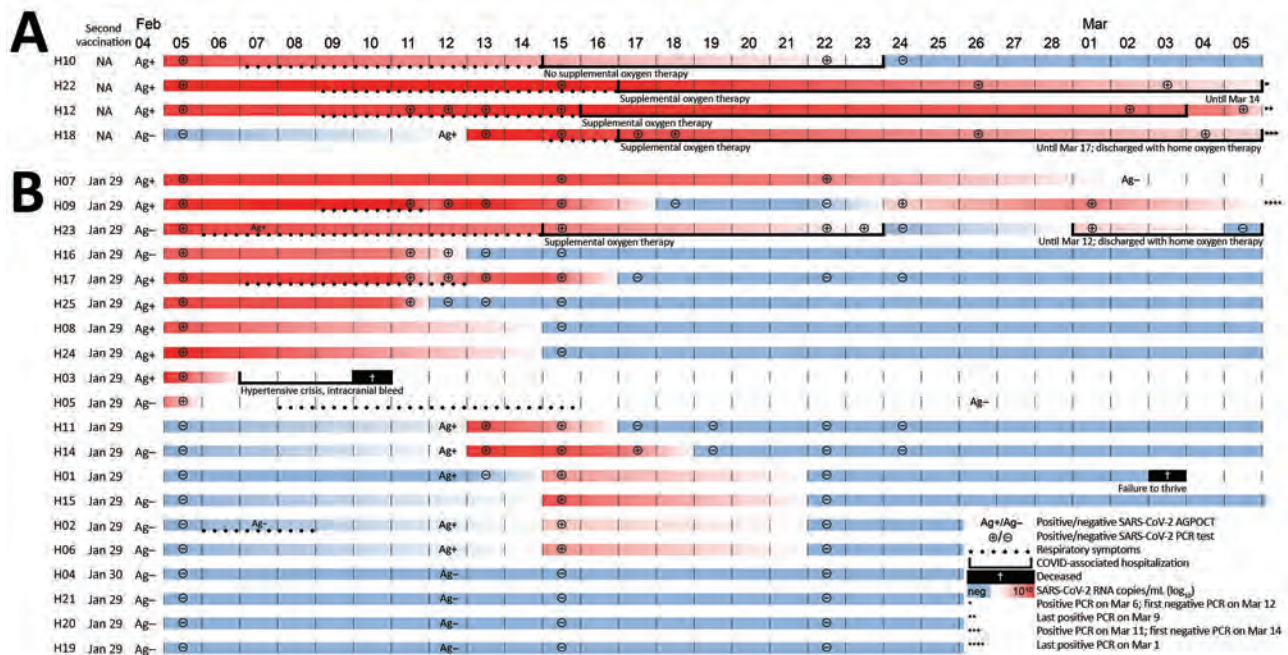
Figure 1. Individual trajectories of 24 long-term care facility residents over 30-day study period in outbreak of SARS-CoV-2 B.1.1.7 lineage infections, Germany, February–March 2021. A) Four unvaccinated residents; B) 20 residents who received their second dose of BNT162b2 COVID-19 mRNA vaccine (https://www.pfizer.com) on January 29 or 30, 2021. After a positive result in a healthcare worker, residents received AgPOCT and subsequently underwent regular RT-PCR testing for SARS-CoV-2. Dotted lines indicate respiratory symptoms, and continuous lines indicate hospitalization. AgPOCT, antigen point-of-care test; COVID-19, coronavirus disease; RT-PCR, reverse transcription PCR; SARS-CoV-2, severe acute respiratory syndrome coronavirus 2.

Figure 2. Characteristics of outbreak of SARS-CoV-2 B.1.1.7 lineage infections after vaccination in long-term care facility, Germany, February–March 2021. A) After a positive test result in a healthcare worker, 16/20 (80.0%) vaccinated residents and 4/4 (100.0%) unvaccinated residents subsequently tested positive for SARS-CoV-2. Among infected patients, 5/16 (31.25%) vaccinated and all 4 (100.0%) unvaccinated patients exhibited respiratory symptoms (i.e., cough or shortness of breath) during the course of disease. All 4 unvaccinated patients required hospital treatment; 3 (75.0%) received supplemental oxygen therapy and a standard course of dexamethasone. Two (12.5%) vaccinated patients also required hospital treatment, including 1 patient who experienced hypertensive crisis and intracranial bleeding and died 4 days after admission, and 1 patient with secondary bacterial pneumonia and urinary tract infection. B) Peak SARS-CoV-2 RNA concentrations in infected vaccinated residents (n = 16) and infected unvaccinated residents (n = 4), as well as SARS-CoV-2 B.1.1.7 RNA concentrations of an independent group of age-matched persons (n = 48) without known vaccination status whose infections were diagnosed during routine care. C) Time between first positive and first negative reverse transcription PCR or antigen point-of-care test result in vaccinated (n = 16) and unvaccinated (n = 4) residents. In 3 residents (2 vaccinated and 1 unvaccinated), negativity was determined by antigen point-of-care test only. D) Anti-SARS-CoV-2 receptor binding domain–specific IgG. E) IFN-γ release assay of SARS-CoV-2 specific T cells measured in 10/20 (50.00%) vaccinated and 2/4 (50.00%) unvaccinated residents 5 weeks after initial testing. IFN-γ, interferon-γ; SARS-CoV-2, severe acute respiratory syndrome coronavirus 2; S/CO, signal-to-cutoff ratio.
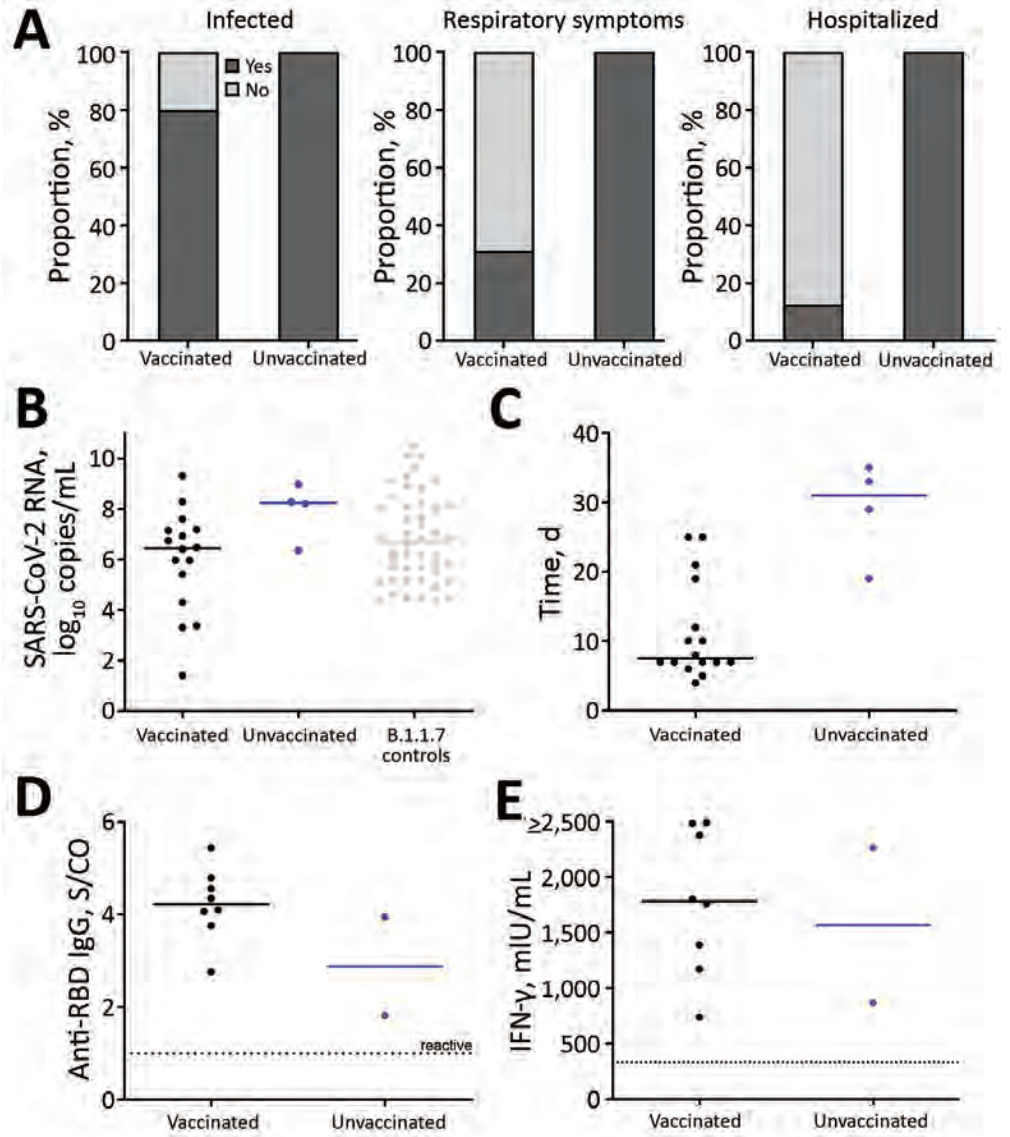
All SARS-CoV-2 RNA-positive samples were tested for presence of SARS-CoV-2 VOCs by RT-PCR and complete genome sequencing (Appendix). RT-PCR suggested the presence of B.1.1.7, which was confirmed by sequencing in 11 patients for whom sufficient sequence information was available. In phylogenetic analysis, sequences form a monophyletic clade with additional sequences from Berlin interspersed (Appendix Figure 1), suggesting a common outbreak source, including infections outside the unit.

We performed serial RT-PCR testing of nasopharyngeal swab specimens from 22 patients. SARS-CoV-2 RNA concentrations peaked within 5 days (Appendix Figure 2). The median peak SARS-CoV-2 RNA concentration in vaccinated and unvaccinated patients overlapped concentrations detected at time of diagnosis in B.1.1.7 patients of similar

ages (Figure 2, panel B). However, SARS-CoV-2 RNA concentration was lower among vaccinated residents than unvaccinated residents, although the difference was not statistically significant (6.45 vs. 8.15 $\log_{10}$ copies/mL; p = 0.10). Furthermore, duration of SARS-CoV-2 RNA shedding was considerably shorter in vaccinated patients than in unvaccinated patients (7.5 [95% CI 7–17.3] days vs. 31 [95% CI 21.5–34.5] days; p = 0.003) (Figure 2, panel C). Peak SARS-CoV-2 RNA concentrations above 10^6 copies per mL, below which virus isolation in cell culture is usually not successful, were detected in all 4 unvaccinated patients but only in 7/16 vaccinated patients (9).

We further assessed the level of infectiousness in 22 samples from 14 patients by virus cell culture (Appendix). One sample obtained from a vaccinated patient 7 days after the first positive RT-PCR test, which showed 9.32 $\log_{10}$ SARS-CoV-2 RNA copies/mL, yielded a positive isolation outcome. Isolation attempts from samples of the same patient taken in the next 4 days and from 21 samples taken from 13 other patients were unsuccessful.

Five weeks after initial testing, 8/8 vaccinated and infected residents and 2/2 unvaccinated and infected residents showed robust antibody responses against SARS-CoV-2 spike antigens, virus neutralization capacity, and interferon-γ release of SARS-CoV-2–specific T cells (Figure 2, panels D, E; Appendix Figure 3). These results confirm the immune response capability in these patients.

Conclusions

We performed a longitudinal study of SARS-CoV-2 infections in a LTCF unit. Nearly all infected residents were symptomatic, including most residents that had received a second BNT162b2 dose the week before. The outbreak was caused by SARS-CoV-2 VOC lineage B.1.1.7, which might partly explain the high attack rate and lack of protection in vaccinated residents. Nevertheless, we reported a lower attack rate, a shorter duration of SARS-CoV-2 RNA shedding, and a lower proportion of symptomatic COVID-19 requiring hospitalization and oxygen support for vaccinated patients. However, despite the limited sample size and the short interval between second vaccination and infection, this outbreak raises questions about the effectiveness of the vaccination regimen in the elderly (3,8,10–12). A delayed and overall reduced immune response to BNT162b2 vaccination has been described in elderly persons (13,14), which might explain the reported outbreak and infections in LTCF described elsewhere (4,5).

This outbreak highlights that older adults have reduced protection ≤ 2 weeks after second BNT162b2 vaccination. Therefore, single-dose regimens and extended dosing intervals might be insufficient for fully protecting this population (15). Vaccination of LTCF residents and staff is likely effective in reducing the spread of SARS-CoV-2. However, regular SARS-CoV-2 screening, prompt outbreak containment, and nonpharmaceutical interventions (16) remain necessary for optimal protection in this setting.

About the Author

Dr. Tober-Lau is a physician and doctoral researcher in the Department of Infectious Diseases and Respiratory Medicine at Charité–Universitätsmedizin Berlin, Germany. His research interests focus on infectious diseases and global health.

References

1. Arons MM, Hatfield KM, Reddy SC, Kimball A, James A, Jacobs JR, et al.; Public Health–Seattle and King County and CDC COVID-19 Investigation Team. Presymptomatic SARS-CoV-2 infections and transmission in a skilled nursing facility. N Engl J Med. 2020;382:2081–90. https://doi.org/10.1056/NEJMoa2008457

2. European Centre for Disease Prevention and Control. Overview of COVID-19 vaccination strategies and vaccine deployment plans in the EU/EEA and the UK. 2020 [cited 2021 Apr 14]. https://www.ecdc.europa.eu/en/publications-data/overview-current-eu-eea-uk-plans-covid-19-vaccines

3. Polack FP, Thomas SJ, Kitchin N, Absalon J, Gurtman A, Lockhart S, et al.; C4591001 Clinical Trial Group. Safety and efficacy of the BNT162b2 mRNA Covid-19 vaccine. N Engl J Med. 2020;383:2603–15. https://doi.org/10.1056/NEJMoa2034577

4. White EM, Yang X, Blackman C, Feifer RA, Gravenstein S, Mor V. Incident SARS-CoV-2 infection among mRNA-vaccinated and unvaccinated nursing home residents. N Engl J Med. 2021 May 19 [Epub ahead of print].

5. Teran RA, Walblay KA, Shane EL, Xydis S, Gretsch S, Gagner A, et al. Postvaccination SARS-CoV-2 infections among skilled nursing facility residents and staff members—Chicago, Illinois, December 2020–March 2021. MMWR Morb Mortal Wkly Rep. 2021;70:632–8. https://doi.org/10.15585/mmwr.mm7017e1

6. Davies NG, Abbott S, Barnard RC, Jarvis CI, Kucharski AJ, Munday JD, et al.; CMMID COVID-19 Working Group; COVID-19 Genomics UK (COG-UK) Consortium. Estimated transmissibility and impact of SARS-CoV-2 lineage B.1.1.7 in England. Science. 2021;372:eabg3055. https://doi.org/10.1126/science.abg3055

7. Muik A, Wallisch A-K, Sänger B, Swanson KA, Mühl J, Chen W, et al. Neutralization of SARS-CoV-2 lineage B.1.1.7 pseudovirus by BNT162b2 vaccine-elicited human sera. Science. 2021;371:1152–3. https://doi.org/10.1126/science.abg6105

8. Dagan N, Barda N, Kepten E, Miron O, Perchik S, Katz MA, et al. BNT162b2 mRNA Covid-19 vaccine in a nationwide mass vaccination setting. N Engl J Med. 2021;384:1412–23. https://doi.org/10.1056/NEJMoa2101765

9. Wölfel R, Corman VM, Guggemos W, Seilmaier M, Zange S, Müller MA, et al. Virological assessment of hospitalized patients with COVID-2019. Nature. 2020;581:465–9. https://doi.org/10.1038/s41586-020-2196-x

10. Baden LR, El Sahly HM, Essink B, Kotloff K, Frey S, Novak R, et al.; COVE Study Group. Efficacy and safety of the mRNA-1273 SARS-CoV-2 vaccine. N Engl J Med. 2021;384:403–16. https://doi.org/10.1056/NEJMoa2035389

11. Thompson MG, Burgess JL, Naleway AL, Tyner HL, Yoon SK, Meece J, et al. Interim estimates of vaccine effectiveness of BNT162b2 and mRNA-1273 COVID-19 vaccines in preventing SARS-CoV-2 infection among health care personnel, first responders, and other essential and frontline workers—eight U.S. locations, December 2020–March 2021. MMWR Morb Mortal Wkly Rep. 2021;70:495–500. https://doi.org/10.15585/mmwr.mm7013e3

12. Tenforde MW, Olson SM, Self WH, Talbot HK, Lindsell CJ, Steingrub JS, et al.; IVY Network; HAIVEN Investigators. IVY Network; HAIVEN Investigators. Effectiveness of Pfizer-BioNTech and Moderna vaccines against COVID-19 among hospitalized adults aged ≥65 years—United States, January–March 2021. MMWR Morb Mortal Wkly Rep. 2021;70:674–9. https://doi.org/10.15585/mmwr.mm7018e1

13. Müller L, Andrée M, Moskorz W, Drexler I, Walotka L, Grothmann R, et al. Age-dependent immune response to the Biontech/Pfizer BNT162b2 COVID-19 vaccination. Clin Infect Dis. 2021 Apr 27 [Epub ahead of print]. https://doi.org/10.1093/cid/ciab381

14. Schwarz T, Tober-Lau P, Hillus D, Helbig ET, Lippert LJ, Thibeault C, et al. Delayed antibody and T-cell response to BNT162b2 vaccination in the elderly, Germany. Emerg Infect Dis. 2021 Jun XX [Epub ahead of print]. https://doi.org/10.3201/eid2708.211145

15. Jeyanathan M, Afkhami S, Smaill F, Miller MS, Lichty BD, Xing Z. Immunological considerations for COVID-19 vaccine strategies. Nat Rev Immunol. 2020;20:615–32. https://doi.org/10.1038/s41577-020-00434-6

16. Gmehlin CG, Munoz-Price LS. Coronavirus disease 2019 (COVID-19) in long-term care facilities: A review of epidemiology, clinical presentations, and containment interventions. Infect Control Hosp Epidemiol. 2020 Oct 26 [Epub ahead of print]. https://doi.org/10.1017/ice.2020.1292

Address for correspondence: Victor M. Corman, Leif Erik Sander, and Florian Kurth, Charité–Universitätsmedizin Berlin, Charfieplatz 1, D-10117, Berlin, Germany; email: victor.corman@charite.de, leif-erik.sander@charite.de, florian.kurth@charite.de

Delayed Antibody and T-Cell Response to BNT162b2 Vaccination in the Elderly, Germany

Tatjana Schwarz,[1] Pinkus Tober-Lau,[1] David Hillus, Elisa T. Helbig, Lena J. Lippert, Charlotte Thibeault, Willi Koch, Irmgard Landgraf, Janine Michel, Leon Bergfeld, Daniela Niemeyer, Barbara Mühlemann, Claudia Conrad, Chantip Dang-Heine, Stefanie Kasper, Friederike Münn, Kai Kappert, Andreas Nitsche, Rudolf Tauber, Sein Schmidt, Piotr Kopankiewicz, Harald Bias, Joachim Seybold, Christof von Kalle, Terry C. Jones, Norbert Suttorp, Christian Drosten, Leif Erik Sander,[2] Victor M. Corman,[2] Florian Kurth[2]

We detected delayed and reduced antibody and T-cell responses after BNT162b2 vaccination in 71 elderly persons (median age 81 years) compared with 123 healthcare workers (median age 34 years) in Germany. These data emphasize that nonpharmaceutical interventions for coronavirus disease remain crucial and that additional immunizations for the elderly might become necessary.

The severe acute respiratory syndrome coronavirus 2 (SARS-CoV-2) pandemic has led to an urgent need for vaccines, particularly among persons at high risk for severe disease and death, such as the elderly (*1*). Efficacy against severe coronavirus disease (COVID-19) of mRNA vaccine BNT162b2 (Pfizer-BioNTech, https://www.pfizer.com) is reported to be >90% starting 7 days after the second vaccination; robust antibody and T-cell response has been demonstrated

consistently across age groups (*2–4*). However, only 4.3% of participants in the BNT162b2 efficacy trial were ≥75 years of age (*4*). Given the elderly generally have weaker immune responses after vaccination, more detailed investigation is necessary (*4,5*).

The Study

In a prospective observational cohort study, we investigated SARS-CoV-2–specific antibodies, maturation of IgG avidity, and interferon-γ (IFN-γ) release of SARS-CoV-2–specific T cells in 2 cohorts of young and elderly BNT162b2-vaccinated persons (Table). Participants were recruited from 2 studies conducted at Charité–Universitätsmedizin Berlin, both conducted in accordance with the Declaration of Helsinki and Good Clinical Practice (https://www.ema.europa.eu/en/documents/scientific-guideline/ich-e-6-r2-guideline-good-clinical-practice-step-5_en.pdf) and approved by the local ethics committee (EA4/244/20 and EA4/245/20)

The first cohort consisted of 123 healthcare workers; median age was 34 (interquartile range [IQR] 20–64) years. The second cohort consisted of 71 elderly residents of an assisted living facility; median age was 81 (IQR 70–96) years. Blood samples were taken before the first vaccination (week 0), just before the second vaccination (week 3), and 4 weeks after the second vaccination (week 7). To discriminate between vaccine-induced antibody response and convalescent SARS-CoV-2 infection, we used the SeraSpot Anti-SARS-CoV-2 IgG microarray-based immunoassay including nucleocapsid and spike as antigens (Seramun Diagnostica GmbH, https://www.seramun.com) (Appendix, https://wwwnc.cdc.gov/EID/article/27/8/21-1145-

Author affiliations: Charité–Universitätsmedizin Berlin, Berlin, Germany (T. Schwarz, P. Tober-Lau, D. Hillus, E.T. Helbig, L.J. Lippert, C. Thibeault, W. Koch, L. Bergfeld, D. Niemeyer, B. Mühlemann, C. Conrad, C. Dang-Heine, S. Kasper, F. Münn, K. Kappert, R. Tauber, S. Schmidt, P. Kopankiewicz, H. Bias, J. Seybold, C. von Kalle, T.C. Jones, N. Suttorp, C. Drosten, L.E. Sander, V.M. Corman, F. Kurth); Hausarztpraxis am Agaplesion Bethanien Sophienhaus, Berlin (I. Landgraf); Robert Koch Institute, Berlin (J. Michel, A. Nitsche); German Centre for Infection Research, Berlin (D. Niemeyer, B. Mühlemann, T.C. Jones, C. Drosten, V.M. Corman); Berlin Institute of Health, Berlin (C. Dang-Heine, K. Kappert, R. Tauber, S. Schmidt, J. Seybold, C. von Kalle); Labor Berlin–Charité Vivantes GmbH, Berlin (K. Kappert, R. Tauber); University of Cambridge, Cambridge, UK (T.C. Jones); German Center for Lung Research, Gießen, Germany (N. Suttorp, L.E. Sander, F. Kurth); Bernhard Nocht Institute for Tropical Medicine, Hamburg, Germany (F. Kurth); University Medical Centre Hamburg-Eppendorf, Hamburg (F. Kurth)

[1]These authors contributed equally to this article.

[2]These senior authors contributed equally to this article.

App1.pdf). Ten of 123 healthcare workers and 1 of 71 elderly participants showed reactive anti-nucleocapsid or anti-spike IgG before the first vaccination and were excluded from further analyses.

At week 3, in the younger cohort, 93/107 (86.9%, 95% CI 79.2%–92.0%) participants showed reactive SARS-CoV-2 receptor-binding domain (RBD) IgG, compared with only 16/52 elderly participants (30.8%, 95% CI 19.9%–44.3%). At week 7, the antibody response rate had increased in both cohorts, to 112/113 in younger participants (99.1%, 95% CI 95.2%–100.0%) and 64/70 in the elderly cohort (91.4%, 95% CI 82.5%–96.0%) (Figure, panel A; Appendix Table). The comparison of SARS-CoV-2 RBD IgG levels demonstrated a significant difference in the 2 cohorts at both week 3 (p<0.0001) and week 7 (p = 0.0003) (Appendix Table), indicating a substantial delay and overall reduced antibody response in elderly participants. We observed similar kinetics and differences between cohorts for antibody responses to 2 further SARS-CoV-2 spike antigens: the S1 subdomain and the full spike protein (Appendix Table, Figure).

We further confirmed the delayed and reduced antibody response in the elderly by measurement of the functional neutralization capacity using the surrogate virus neutralization test (sVNT) cPass (medac GmbH, https://international.medac.de) (Appendix) (6). At week 3, only 24/52 elderly participants (46.2%, 95% CI 33.3%–59.5%) had neutralizing capacity in serum, compared with 97/107 younger participants (90.7%, 95% CI 83.7%–94.8%; p<0.0001 (Figure). In addition, the median sVNT titer for elderly participants was significantly lower than the young cohort (26.4% [IQR 6.8%–40.9%] vs. 60.2% [IQR 45.0%–76.4%]; p<0.0001) (Appendix Table). Although the neutralizing antibody response rate increased to 63/70 (90.0%, 95% CI 80.8%–95.1%) in elderly participants by week 7, the median sVNT titer remained significantly lower than in the younger cohort (89.6% [IQR 70.9%–95.2%] vs. 96.7% [IQR 95.6%–97.2%]; p<0.0001) (Appendix Table).

To characterize the maturation of IgG avidity in all 16 elderly and 30 randomly selected younger participants who were seroreactive at week 3, we applied a modified SARS-CoV-2 S1 IgG ELISA (Euroimmun, https://www.euroimmun.com) (Appendix Figure 2). The delayed antibody response in the elderly is reflected in results: at week 7, only 8/16 elderly (50.0%, 95% CI 28.0%–72.0%) exhibited high S1 IgG avidity indices (≥60) compared with 28/30 young participants (93.3%, 95% CI 78.7%–98.8%) (Figure, panel C). Consequently, the median relative avidity index of IgG was significantly higher in

Table. Cohort characteristics in study of delayed antibody and T-cell response to BNT162b2 vaccination in the elderly, Germany*

Characteristic	Healthcare workers	Elderly
No. patients	123	71
Sex		
F	65 (52.9)	54 (76.1)
M	58 (47.2)	17 (23.9)
Median age, y (IQR)	34 (20–64)	81 (70–96)
Underlying conditions		
Cardiovascular disease	15 (12.2)	56 (78.9)
Type 2 diabetes	1 (0.8)	13 (18.3)
Respiratory disease	16 (13.0)	11 (15.5)
Dyslipidemia	5 (4.1)	21 (29.6)
Thyroid dysfunction	0	16 (22.5)
Chronic kidney disease	0	12 (16.9)
Chronic liver or GI disease	2 (1.6)	18 (25.4)
Rheumatic disease	6 (4.9)	7 (9.9)
Active solid malignancy	2 (1.6)	4 (5.6)
Active hematological malignancy	0	4 (5.6)
Neurologic disease	1 (0.8)	18 (25.4)
Immunodeficiency	1 (0.8)	0
Others	9 (7.3)	29 (40.9)
Outpatient medication		
No	79 (64.2)	5 (7.0)
Yes	39 (31.7)	64 (90.1)
Unknown	5 (4.1)	2 (2.8)

*Values are no. (%) except as indicated. BNT162b2 is manufactured by Pfizer-BioNTech (https://www.pfizer.com). GI, gastrointestinal; IQR, interquartile range.

the younger cohort than the elderly cohort (76.2% [IQR 67.6%–82.9%] vs. 59.3% [IQR 55.3%–68.9%]; p = 0.0002) (Figure, panel C).

In addition to antibody responses, we assessed SARS-CoV-2 spike-specific T cell responses by an IFN-γ release assay (IGRA) (Euroimmun) (Appendix) of S1 peptide-stimulated T cells at week 7. The proportion of persons with IGRA results above the defined threshold (Appendix) was significantly lower in the elderly than in younger participants (51.2% [95% CI 36.8%–65.4%] vs. 84.5% [95% CI 74.4%–91.1%]; p = 0.0002). Accordingly, median S1-induced IFN-γ release was significantly decreased in the elderly compared to younger participants (707.3 mIU/mL [IQR 216–1,392] vs. 2184 mIU/mL [IQR 1,274–2,484]; p<0.0001) (Figure, panel D). In contrast, we detected no significant difference in IFN-γ release after mitogen stimulation between the 2 cohorts, indicating no general impairment of IFN-γ responses in the elderly (p = 0.77) (Figure, panel D; Appendix Table).

In summary, vaccination with BNT162b2 induces both arms of adaptive immunity: SARS-CoV-2–specific antibodies and SARS-CoV-2–specific T cells. However, we observed delayed and less robust cellular and humoral immune response among the elderly than among younger adults. A limitation of our study is the lack of data on other COVID-19 vaccines. Furthermore, we cannot exclude that underlying diseases or medications, which are more common in the
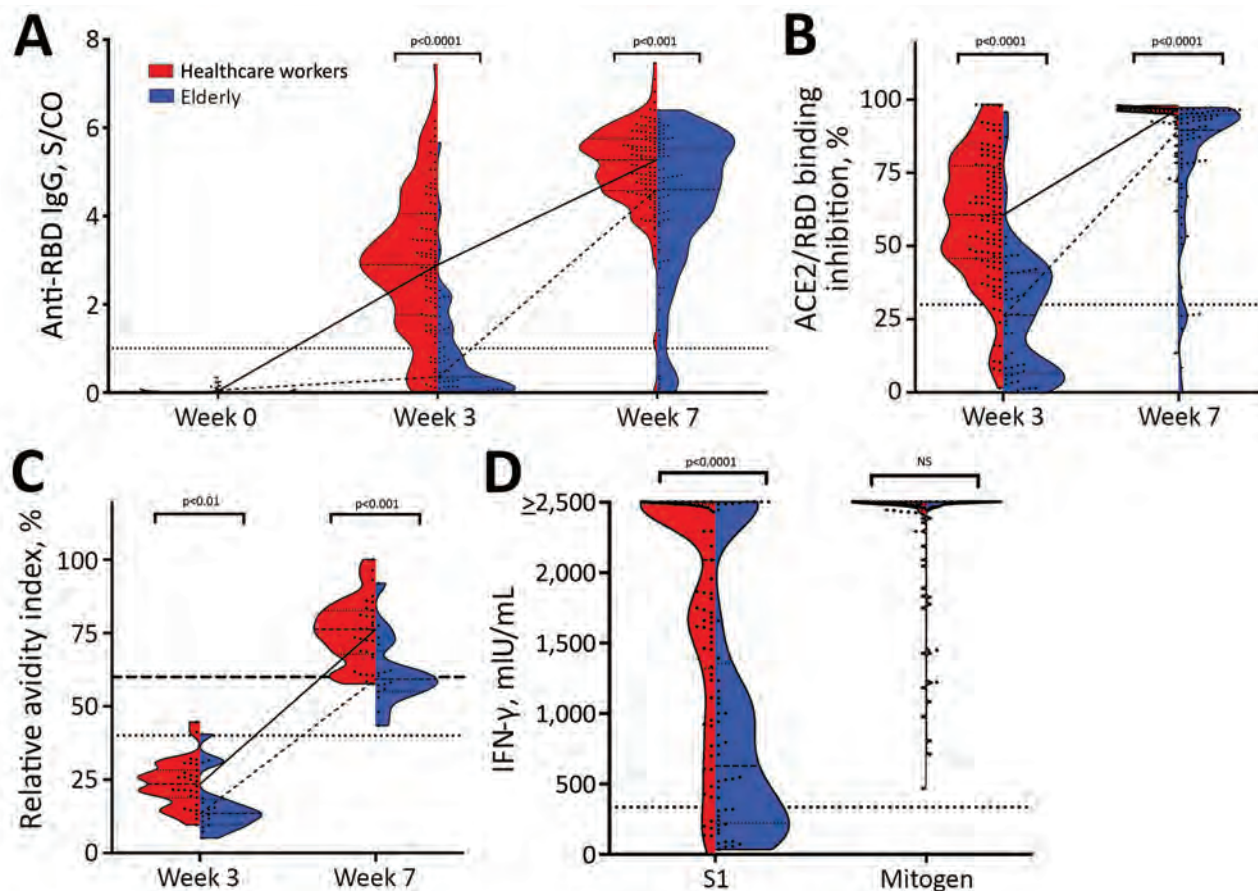
Figure. Severe acute respiratory syndrome coronavirus 2 (SARS-CoV-2)–specific antibody and T-cell response after vaccination with BNT162b2 (Pfizer-BioNTech, https://www.pfizer.com) in the elderly, Germany. A) SARS-CoV-2 RBD IgG measured in serum of BNT162b2-vaccinated younger participants (healthcare workers) before the first vaccination (n = 100, week 0), 3 weeks after the first vaccination (n = 107, week 3), and 4 weeks after the second vaccination (n = 113, week 7) and from elderly participants at week 0 (n = 70), week 3 (n = 52), and week 7 (n = 70) using the SeraSpot Anti-SARS-CoV-2 IgG assay (Seramun Diagnostica GmbH, https://www.seramun.com). B) Neutralizing capacity of antibodies measured at week 3 and 7 in the young and elderly cohorts using the ELISA-based surrogate virus neutralization test (sVNT) cPass (medac GmbH, https://international.medac.de). C) SARS-CoV-2 spike IgG avidity analyzed in the healthcare workers cohort (n = 30) and elderly cohort (n = 16) at week 3 and 7. D) At week 7, whole blood from vaccinated elderly participants (n = 43) and young participants (n = 71) was stimulated ex vivo with components of the S1 domain of the spike protein for 24 h, and IFN-γ concentration in the supernatant was detected by ELISA. Dotted lines indicate the manufacturer's specified threshold for RBD IgG >1 S/Co, for sVNT >30%, and for avidity 40–60% borderline avidity and >60% high avidity. For IGRA, we defined an arbitrary threshold at 334.2 mIU/mL. p value was calculated by the nonparametric Mann Whitney U test, and the median and interquartile range are depicted. ACE2, angiotensin-converting enzyme 2; IFN-γ, interferon-γ; IU, international units; NS, not significant; RBD, receptor-binding domain; S/CO, signal-to-cutoff ratio; sVNT, surrogate virus neutralization test.

elderly (Table), might impair the vaccine-induced immune response. For example, patients on dialysis have significantly lower antibody response than vaccinated same-age patients not on dialysis (E. Schrezenmeier et al., unpub. data, http://medrxiv.org/lookup/doi/10.1101/2021.03.31.21254683). In line with our observations for BNT162b2, an effect of age-dependent decrease of

Our data are supported by other real-world observations suggesting a delayed and reduced immunogenicity of BNT162b2 in the elderly (*5,7*; D.A. Collier et al., unpub. data, http://medrxiv.org/lookup/doi/10.1101/2021.02.03.21251054). In line with our observations for BNT162b2, an effect of age-dependent decrease of

immune function, referred to as immunosenescence, is well known and contributes to increased prevalence of infectious disease and vaccine failure in the elderly (*8*). A lower vaccine-induced immune response to influenza and hepatitis B viruses is well documented (*9,10*); however, such data are scarce for mRNA vaccines.

Of note, vaccination with 2 doses of BNT162b2 might not fully prevent SARS-CoV-2 outbreaks among elderly persons in congregate settings, such as long-term care facilities, possibly because of delayed and reduced immune response. However, vaccination protects against severe disease (*11–13*).

Conclusions

Although the immune response of elderly participants 4 weeks after the second dose of BNT162b2 nearly reached the level of younger participants, a small fraction of elderly participants did not demonstrate robust antibody and T-cell response. However, the immunologic correlates of protection remain unknown, and identification of persons with no or incomplete protection after vaccination remains challenging. Therefore, strategies focused solely on vaccinating high-risk groups might be insufficient to protect those at risk for severe disease. For the elderly, vaccinating caregivers and close contacts should be prioritized. Moreover, a booster vaccination, altered vaccine dose, or different COVID-19 vaccines should be considered for the elderly if further evidence demonstrates high rates of breakthrough infections despite 2-dose BNT162b2 vaccination.

These results are particularly relevant for vaccination strategies focused on broad administration of the first dose of a 2-dose vaccine while postponing the second vaccination. This practice might leave a relevant proportion of elderly with comparatively low levels of immunity for a prolonged period, emphasizing the need for nonpharmaceutical interventions, such as mask use and regular testing.

About the Author

Dr. Schwarz is a postdoctoral researcher in the Institute of Virology, Charité–Universitätsmedizin Berlin, Berlin, Germany. Her research interests include infectious disease surveillance and immunologic testing.

References

1. Brown AE, Heinsbroek E, Kall MM, Allen H, Beebeejaun K, Blomquist P, et al.; PHE COVID-19 Mortality Working Group. Epidemiology of confirmed COVID-19 deaths in adults, England, March–December 2020. Emerg Infect Dis. 2021;27:1468–71. https://doi.org/10.3201/eid2705.203524
2. Walsh EE, Frenck RW Jr, Falsey AR, Kitchin N, Absalon J, Gurtman A, et al. Safety and immunogenicity of two RNA-based Covid-19 vaccine candidates. N Engl J Med. 2020;383:2439–50. https://doi.org/10.1056/NEJMoa2027906
3. Dagan N, Barda N, Kepten E, Miron O, Perchik S, Katz MA, et al. BNT162b2 mRNA Covid-19 vaccine in a nationwide mass vaccination setting. N Engl J Med. 2021;384:1412–23. https://doi.org/10.1056/NEJMoa2101765
4. Polack FP, Thomas SJ, Kitchin N, Absalon J, Gurtman A, Lockhart S, et al.; C4591001 Clinical Trial Group. Safety and Efficacy of the BNT162b2 mRNA Covid-19 Vaccine. N Engl J Med. 2020;383:2603–15. https://doi.org/10.1056/NEJMoa2034577
5. Van Praet JT, Vandecasteele S, De Roo A, De Vriese AS, Reynders M. Humoral and cellular immunogenicity of the BNT162b2 mRNA Covid-19 Vaccine in nursing home residents. Clin Infect Dis. 2021 Apr 7 [Epub ahead of print]. https://doi.org/10.1093/cid/ciab300
6. Tan CW, Chia WN, Qin X, Liu P, Chen MI-C, Tiu C, et al. A SARS-CoV-2 surrogate virus neutralization test based on antibody-mediated blockage of ACE2-spike protein-protein interaction. Nat Biotechnol. 2020;38:1073–8. https://doi.org/10.1038/s41587-020-0631-z
7. Müller L, Andrée M, Moskorz W, Drexler I, Walotka L, Grothmann R, et al. Age-dependent immune response to the Biontech/Pfizer BNT162b2 COVID-19 vaccination. Clin Infect Dis. 2021 Apr 27 [Epub ahead of print]. https://doi.org/10.1093/cid/ciab381
8. Crooke SN, Ovsyannikova IG, Poland GA, Kennedy RB. Immunosenescence and human vaccine immune responses. Immun Ageing. 2019;16:25. https://doi.org/10.1186/s12979-019-0164-9
9. Fisman DN, Agrawal D, Leder K. The effect of age on immunologic response to recombinant hepatitis B vaccine: a meta-analysis. Clin Infect Dis. 2002;35:1368–75. https://doi.org/10.1086/344271
10. McElhaney JE, Verschoor CP, Andrew MK, Haynes L, Kuchel GA, Pawelec G. The immune response to influenza in older humans: beyond immune senescence. Immun Ageing. 2020;17:10. https://doi.org/10.1186/s12979-020-00181-1
11. Cavanaugh AM, Fortier S, Lewis P, Arora V, Johnson M, George K, et al. COVID-19 outbreak associated with a SARS-CoV-2 R.1 lineage variant in a skilled nursing facility after vaccination program—Kentucky, March 2021. MMWR Morb Mortal Wkly Rep. 2021;70:639–43. https://doi.org/10.15585/mmwr.mm7017e2

12. Teran RA, Walblay KA, Shane EL, Xydis S, Gretsch S, Gagner A, et al. Postvaccination SARS-CoV-2 infections among skilled nursing facility residents and staff members—Chicago, Illinois, December 2020–March 2021. MMWR Morb Mortal Wkly Rep. 2021;70:632–8. https://doi.org/10.15585/mmwr.mm7017e1

13. Tober-Lau P, Schwarz T, Hillus D, Spieckermann J, Helbig ET, Lippert LJ, et al. Outbreak of SARS-CoV-2 B.1.1.7 lineage after vaccination in long-term care facility, Germany, February–March 2021. Emerg Infect Dis. 2021 Jun XX [Epub ahead of print]. https://doi.org/10.3201/eid2708.210087

Address for correspondence: Victor M. Corman, Leif Erik Sander, and Florian Kurth, Charité–Universitätsmedizin Berlin, Charitéplatz 1, D-10117, Berlin, Germany; email: victor.corman@charite.de, leif-erik.sander@charite.de, florian.kurth@charite.de

May 2021

COVID-19

- Coordinated Strategy for a Modeling-Based Decision Support Tool for COVID-19, Utah, USA

- Clinical Laboratory Perspective on Human Infections Caused by Unusual Nonhemolytic, Lancefield Group B *Streptococcus halichoeri*

- Case Series of Laboratory-Associated Zika Virus Disease, United States, 2016–2019

- Successful Control of an Onboard COVID-19 outbreak Using the Cruise Ship as a Quarantine Facility, Western Australia T

- Coccidioidomycosis and COVID-19 Co-Infection, United States, 2020

- Epidemiologic Findings From Case Investigations and Contact Tracing of the First 200 Cases of Coronavirus Disease 2019 (COVID-19) identified in Santa Clara County, California, USA

- SARS-CoV-2 in Nursing Homes after 3 Months of Serial, Facility-Wide Point Prevalence Testing, Connecticut, USA

- Transmission of Severe Acute Respiratory Syndrome Coronavirus 2 during Border Quarantine and Air Travel, New Zealand (Aotearoa)

- Engineered NS1 Provides Sensitive and Specific Zika Diagnosis from Patient Serology

- Monitoring SARS-CoV-2 Circulation and Diversity through Community Wastewater Sequencing, the Netherlands and Belgium

- Characteristics and Clinical Implications of Carbapenemase-Producing *Klebsiella pneumoniae* Colonization and Infection, Italy

- Serologic Screening of Severe Acute Respiratory Syndrome Coronavirus 2 Infection in Cats and Dogs during First Coronavirus Disease Wave, the Netherlands

- Epidemiologic History and Genetic Diversity Origins of Chikungunya and Dengue Viruses, Paraguay

- Herd Immunity against Severe Acute Respiratory Syndrome Coronavirus 2 Infection in 10 Communities, Qatar

- Active Case Finding of Current Bornavirus Infections in Human Encephalitis Cases of Unknown Etiology, Germany, 2018–2020

- Susceptibility to SARS-CoV-2 of Cell Lines and Substrates Commonly used to Diagnose and Isolate Influenza and Other Viruses

- Symptom Diary–Based Analysis of COVID-19 Disease Course, Germany, 2020

- Use of Genomics to Track Coronavirus Disease Outbreaks, New Zealand

- Global Trends in Norovirus Genotype Distribution among Children with Acute Gastroenteritis

- Genetic Evidence and Host Immune Response in Persons Reinfected with SARS-CoV-2, Brazil

- Prevalence and Clinical Profile of SARS-CoV-2 Infection among Farmworkers, California, June–November 2020

- Epidemiology of Confirmed COVID-19 Deaths in Adults, England, March–December 2020

- Prescribing Antimicrobial Drugs for Acute Gastroenteritis, Primary Care, Australia, 2013–2018

- Evaluating Differences in Whole Blood, Serum, and Urine Screening Tests for Zika Virus, Puerto Rico 2016

- Longevity of Middle East Respiratory Syndrome Coronavirus Antibody Responses in Patients, Saudi Arabia

- Whole-Genome Sequencing of Shiga Toxin–Producing Escherichia coli OX18 from a Fatal Hemolytic Uremic Syndrome Case

- COVID-19–Associated Mold Infection in Critically ill Patients, Chile

EMERGING INFECTIOUS DISEASES®

To revisit the May 2021 issue, go to:

https://wwwnc.cdc.gov/eid/articles/issue/27/5/table-of-contents

Autochthonous Cases of Tick-Borne Encephalitis, Belgium, 2020

Anke Stoefs, Leo Heyndrickx, Jonathan De Winter, Evelien Coeckelbergh, Barbara Willekens, Alicia Alonso-Jiménez, Anne-Marie Tuttino, Yvette Geerts, Kevin K. Ariën, Marjan Van Esbroeck

We report 3 confirmed autochthonous tick-borne encephalitis cases in Belgium diagnosed during summer 2020. Clinicians should include this viral infection in the differential diagnosis for patients with etiologically unexplained neurologic manifestations, even for persons without recent travel history.

Tick-borne encephalitis (TBE) is a severe viral zoonosis caused by TBE virus (TBEV) (*1*). To date, confirmed locally acquired human TBEV infections have not been reported in Belgium, although the most common vector, the tick *Ixodes ricinus*, is abundant in Belgium and seroprevalence studies have revealed the presence of TBEV antibodies in dogs, cattle, roe deer, and wild boar (*2*,*3*). We report 3 confirmed autochthonous TBE cases, diagnosed at the National Reference Centre (NRC) for Arboviruses (Antwerp, Belgium) during summer 2020.

The Study

A 48-year-old woman had muscle pain and an elevated body temperature 2 weeks after a tick bite on her right hip. She tested negative for coronavirus disease (COVID-19), and her general practitioner prescribed antimicrobial drugs. A few days later, the patient was hospitalized with asthenia, tremor, drowsiness, and fever. A neurologist determined signs of peripheral facial palsy with brachial weakness and nuchal rigidity. Cerebrospinal fluid (CSF) showed an elevated leukocyte count (37 cells/µL; reference range 0–5 cells/µL). *Borrelia* serology and PCR results were negative. Magnetic resonance imaging

(MRI) showed demyelinating lesions and encephalopathy and electroencephalography showed diffuse slow activity. Serum collected on day 5 after illness onset tested positive for TBEV IgM and IgG by immunofluorescence assay (IFA) performed at the NRC. Several months later, the patient still had weakness of her right arm, loss of cognitive function, inability to concentrate, fatigue, and tremor.

A 59-year-old man was admitted to the neurology department of a hospital in Belgium with paraparesis and meningitis. Influenza-like symptoms, including fever, fatigue, myalgia, and headache, had occurred a few days earlier. CSF showed an elevated leukocyte count (371 cells/µL; reference range 0–5 cells/µL). Positron emission tomography (PET) and MRI showed no signs of underlying malignancies or encephalopathy. Infectious diseases screening did not reveal the etiology. The patient recalled a tick bite after a walk in a forest in his neighborhood 2 weeks before symptom onset. *Borrelia* and TBEV serology were added to the differential diagnosis, and TBEV antibodies were detected by IFA performed on serum collected on day 20 after illness onset. The patient went through a severe motor polyradiculitis and was using a wheelchair at discharge. At his last clinical evaluation, 9 months after hospitalization, the patient's motor skills had clearly improved.

A 58-year-old man sought medical attention 48 hours after onset of dyspnea, cough, and fever. A COVID-19 test was done and repeated a week later; results of both were negative. The symptoms subsided for a week, but then fever returned, accompanied by severe and persistent headaches, weakness, decreased appetite, and diarrhea. The patient lived in the woods and enjoyed outdoor activities, such as biking and hiking. He recalled multiple tick bites and a bite by a sick squirrel in the weeks before symptom onset. A transesophageal echocardiogram and PET scan were normal, and screening for expected infectious diseases was negative. TBE was diagnosed by IFA performed on serum collected on day 18 after

illness onset. Except for occasional headaches, he recovered without residual symptoms.

The NRC used Flavivirus Profile 2 (EUROIMMUN AG, https://www.euroimmun.com) mosaic IFA to detect TBEV IgM and IgG antibodies in serum from the 3 patients and in CSF from 2 of them (no CSF was available for case 3). TBEV-specific antibodies were confirmed in all patients by plaque-reduction neutralization test (PRNT) with a 90% PRNT at titer ≥1:25. Retrospective real-time reverse transcription PCR (rRT-PCR), adapted from M. Schwaiger (*4*), on acute-phase serum collected from case-patient 3 revealed the presence of TBEV RNA, but the viral load was too low for further analysis (Table).

Conclusions

We describe 3 cases of confirmed autochthonous TBE in Belgium. TBEV IgM and IgG were detected in serum samples from all 3 cases. TBE was confirmed by PRNT. Intrathecally produced TBEV IgM were detected in 2 cases. In the third case, for which no CSF was available, TBE infection was confirmed by detection of TBEV RNA in an acute-phase serum sample. Because the virus typically is not detectable in serum or CSF by the time patients undergo TBE testing, rRT-PCR was not performed on convalescent samples from the other 2 cases (*4,5*). PCR testing on urine can be useful 1–2 weeks after symptom onset (*6*), but urine samples were not available from these cases.

The 3 cases we describe met the current European Centre for Disease Prevention and Control case definition for confirmed TBE (*7*). None of the patients had been vaccinated against TBEV or other flaviviruses, and none had traveled abroad in the months before symptom onset. Belgium closed its borders during March 20 through mid-June 2020 as part of measures to contain the COVID-19 pandemic. These regulations greatly increased outdoor activities, such as walking in forests, among the population in early spring 2020, probably leading to higher

exposure to ticks (*8*). The increased incidence of tick bites also was illustrated through the online platform TekenNet (*9*), a project of the Belgian Institute of Public Health that monitors tick exposure among the population by inviting citizens to voluntarily report tick bites. The 3 patients had been exposed in geographically separate regions of the country, 2 of which were adjacent to an area with known TBEV seropositivity in animals (Figure).

TBE occurs after an incubation period of a median of 8 (range 4–28) days after a bite from an infected tick (*1*). Serologic diagnosis of TBE is hampered by a degree of cross reactivity with the antibodies against other flaviviruses in nearly all assays (*5*). The flavivirus IFA used by the NRC can determine the predominant flavivirus antibody response because it combines 8 different flavivirus substrates on different biochips. Unlike IgG, IgM responses generally are type-specific; therefore, IFA IgM is a useful tool for identification of infections during the acute phase of disease (*1*).

The incidence of TBE in Europe has increased in recent years, and the infection emerged in the Netherlands in 2016 and the United Kingdom in 2019 (*10,11*). The occurrence of autochthonous cases in the Netherlands in 2016, not far from the border with Belgium, led to a 26% increase in TBE serology inquiries at the NRC in 2017 compared with those for 2016 and a 143% increase in 2018 compared with those for 2016 (M. Van Esbroeck, unpub. data). In Belgium, the virus has been shown to circulate in animals, but human infections have been limited to a few imported cases until now (*2,12*). In 2018, two human cases of autochthonous TBE were suspected but not confirmed because both patients also spent time abroad during the incubation period (*3,13,14*). In a study on the prevalence of pathogens in ticks collected from humans in Belgium, none of the examined ticks were infected with TBEV (*14,15*). Studies to determine the geographic spread and genetic diversity of TBEV in ticks were put on hold in 2020 due to the COVID-19

Table. Laboratory results confirming TBEV infections in 3 autochthonous human cases, Belgium, 2020

Case no.	Symptom onset date	Exposure Likely site, postal code	Exposure Likely route, time	Sample type, days after symptom onset	Flavivirus IFA IgM†	Flavivirus IFA IgG‡	PRNT$_{90}$ titer	rRT-PCR
1	Jun 5	Oostkamp, 8020	Tick bite, 2 wk before symptom onset	Serum, 5	TBEV+	TBEV+	1:25	ND
				CSF, 6	TBEV+	TBEV+	ND	ND
2	Jun 21	Lille, 2275	Tick bite, 2 wk before symptom onset	CSF, 18	TBEV+	TBEV+	ND	ND
				Serum, 20	TBEV+	TBEV+	1:60	ND
3	Jul 20	Wanze, 4520	Multiple tick bites in the weeks before symptom onset	Serum, 2	–	–	ND	+
				Serum, 18	TBEV+	TBEV+	1:194	ND

*CSF, cerebrospinal fluid; IFA, immunofluorescence assay; ND, not done; PRNT$_{90}$, plaque reduction neutralization testing at 90% sensitivity; rRT-PCR, real-time reverse transcription PCR; TBEV, tick-borne encephalitis virus; +, positive; –, negative.
†Only TBEV-positive on the flavivirus mosaic IFA.
‡Also positive signal for ≥1 other flavivirus on the mosaic IFA, including West Nile virus, Japanese encephalitis virus, yellow fever virus, and dengue virus serotypes 1–4.

Figure. Geographic distribution of autochthonous human cases of tick-borne encephalitis, Belgium and the Netherlands (adapted from National Institute of Public Health and Environment [10]). Grey shading indicates communities in Belgium in which antibodies against tick-borne encephalitis virus have been detected in animals (adapted from S. Roelandt [2]).

pandemic. During the 2021 tick season, ticks will be collected by flagging in areas where TBEV exposure most likely occurred for the 3 described patients.

Confirmed TBE cases involving the central nervous system are reported to the European Surveillance System (3). Because approximately two thirds of human TBEV infections are asymptomatic, TBE probably is underdiagnosed in Europe (15).

Vaccination against TBEV is not recommended for the general population (3). However, persons living in Belgium should be aware of the risk for exposure to ticks and protect themselves against tick bites when engaging in outdoor activities. Clinicians also should include TBE in the differential diagnosis in patients with etiologically unexplained neurologic manifestations, even without a recent travel history.

About the Author

Ms. Stoefs is completing a postgraduate specialization in clinical biology at the University of Louvain and is an intern at the Institute of Tropical Medicine, Antwerp. Her current research interest includes arboviral diseases.

References

1. Lindquist L, Vapalahti O. Tick-borne encephalitis. Lancet. 2008; 371:1861–71. https://doi.org/10.1016/S0140-6736(08)60800-4
2. Roelandt S. Questing for tick-borne encephalitis virus in Belgium using veterinary sentinel surveys and risk factor mapping [dissertation]. Ghent (Belgium): Ghent University; 2016.
3. Superior Health Council. Vaccination against tick-borne encephalitis (TBE). Report no. 9435. Brussels: SHC; 2019 [cited 2021 Apr 24]. https://healthpr.belgium.be/sites/default/files/uploads/fields/fpshealth_theme_file/shc_9435_tbe.pdf
4. Schwaiger M, Cassinotti P. Development of a quantitative real-time RT-PCR assay with internal control for the laboratory detection of tick borne encephalitis virus (TBEV) RNA. J Clin Virol. 2003;27:136–45. https://doi.org/10.1016/s1386-6532(02)00168-3
5. Holzmann H. Diagnosis of tick-borne encephalitis. Vaccine. 2003;21:S36–40. https://doi.org/10.1016/S0264-410X(02)00819-8
6. Veje M, Studahl M, Norberg P, Roth A, Möbius U, Brink M, et al. Detection of tick-borne encephalitis virus RNA in urine. J Clin Microbiol. 2014;52:4111–2. https://doi.org/10.1128/JCM.02428-14
7. European Centre for Disease Prevention and Control. EU case definitions: European Commission; 2018 [cited 2021 Apr 15]. https://www.ecdc.europa.eu/en/surveillance-and-disease-data/eu-case-definitions
8. Geebelen L, Leroy M, Lernout T. TickNet 2020: surveillance of tick bites in Belgium. Report number D/2021/14.440/24 [in Dutch]. Brussels: Sciensano; 2021 [cited 2021 Apr 24]. https://tekennet.wiv-isp.be/reports/Final_Surveillance%20van%20tekenbeten_TekenNet%202020.pdf </eref>
9. Sciensano. TickNet [in Dutch] [cited 2021 Apr 26]. https://tekennet.wiv-isp.be
10. National Institute for Public Health and the Environment. Spread of tick-borne encephalitis virus in the Netherlands; 2020 [cited 2021 May 31]. https://www.rivm.nl/en/news/spread-of-tick-borne-encephalitis-virus-in-netherlands
11. Kreusch TM, Holding M, Hewson R, Harder T, Medlock JM, Hansford KM, et al. A probable case of tick-borne encephalitis (TBE) acquired in England, July 2019. Euro Surveill. 2019;24:1900679. https://doi.org/10.2807/1560-7917.ES.2019.24.47.1900679
12. Gils S, Frans J, Ho E, Smismans A, Vermylen P, Dewil M, et al. Case report: tick-borne encephalitis (TBE) in a Belgian traveller returning from Germany. J Travel Med. 2018;25. https://doi.org/10.1093/jtm/tay078
13. Lernout T, Litzroth A, Rebolledo J, Tersago K. Zoonoses and vector-transmitted diseases: summary annual review 2018. Report no. D/2019/14.440/97 [in Dutch]. Brussel: Sciensano; 2019 [cited 2021 Apr 24]. https://epidemio.wiv-isp.be/ID/reports/Zo%C3%B6nosen%20en%20vectoroverdraagbare%20ziekten%202018.pdf
14. Suin V, Lernout T, Van Esbroeck M, Van Gucht S. TBE in Belgium. In: Dobler G, Erber W, Bröker M, Schmitt HJ, eds. The TBE Book. 3rd ed. Singapore: Global Health Press; 2020. https://doi.org/10.33442/26613980_12b3-3
15. Lernout T, De Regge N, Tersago K, Fonville M, Suin V, Sprong H. Prevalence of pathogens in ticks collected from humans through citizen science in Belgium. Parasit Vectors. 2019;12:550. https://doi.org/10.1186/s13071-019-3806-z

Address for correspondence: Marjan Van Esbroeck, Institute of Tropical Medicine, Kronenburgstraat 43/3, 2000 Antwerp, Belgium; email: mvesbroeck@itg.be

Epidemiology of COVID-19 in Prisons, England, 2020

Wendy M. Rice, Dimple Y. Chudasama, James Lewis, Francis Senyah, Isaac Florence, Simon Thelwall,
Lisa Glaser, Maciej Czachorowski, Emma Plugge, Hilary Kirkbride, Gavin Dabrera, Theresa Lamagni

Using laboratory data and a novel address matching methodology, we identified 734 cases of coronavirus disease in 88 prisons in England during March 16–October 12, 2020. An additional 412 cases were identified in prison staff and household members. We identified 84 prison outbreaks involving 86% of all prison-associated cases.

Incarcerated persons are at an increased risk for severe acute respiratory syndrome coronavirus 2 (SARS-CoV-2) transmission and illness because of both the prison environment and the vulnerability of the residents (*1,2*). To limit spread in prisons in England, visitation restrictions were introduced, the population was compartmentalized to limit movement, and an early release scheme was put in place (*3,4*). As in the general population, only those admitted to a hospital were tested for SARS-CoV-2 initially, but testing was expanded to all symptomatic cases in late May 2020, specifically persons with cough, fever, or anosmia.

Outbreaks of coronavirus disease (COVID-19) have been reported in correctional facilities (*5–8*). We describe characteristics and outcomes for prison-associated COVID-19 cases in England reported to Public Health England (PHE) in March 16–October 12, 2020.

The Study

COVID-19 cases confirmed by real-time PCR in England must be reported to PHE's laboratory reporting system (Second Generation Surveillance System [SGSS]) in accordance with statutory legislation (*9*). Prison residence was identified from case addresses reported by laboratories or the NHS database–registered address (*9*).

We used a previously described process to match case data against a national database of properties (AddressBase Premium; Ordnance Survey, https://www.ordnancesurvey.co.uk) listed by Unique Property

Author affiliation: Public Health England, London, UK

Reference Number (UPRN) (*2*). We identified prisons using the property classes designated by UPRN. We used ESRI LocatorHub software (https://www.esriuk.com) for exact matching of case addresses to AddressBase. We used fuzzy matching on failed records and manually matched remaining records.

Laboratory records from national key worker testing were the sources for identifying prison staff and of symptomatic household members of key workers also eligible for testing. We were not able to link prison staff–associated cases to specific facilities because workers' residential addresses and not workplace addresses were provided; we could not extrapolate workplace on the basis of residence given the regional prison distribution (Figure 1).

We defined associated deaths as deaths in cases occurring <60 days from first positive specimen date or in cases for which COVID-19 was on the death certificate. We calculated incidence in incarcerated persons using official prison denominators for September 2020 (*10*).

We defined outbreaks in prisons as >2 cases within 14 days (by specimen date) residing at the same location (UPRN). We extracted records for cases identified March 16–October 12, 2020, and analyzed them using Stata version 15 (StataCorp, https://www.stata.com). The first laboratory-confirmed COVID-19 case in an incarcerated person in England was identified on March 16, 2020, in a high-security prison. We identified 734 incarcerated case-patients, accounting for 0.14% of all cases reported through October 12, 2020 in England (N = 527,225); we also identified 412 cases in prison staff and their households.

Most (52%, 380/734) incarcerated cases were reported before June 6; a second wave was reported in mid-September (Figure 1). The crude incidence in incarcerated persons in England was 988.1/100,000 population, which was not significantly different than incidence in the general population, at 935.3/100,000
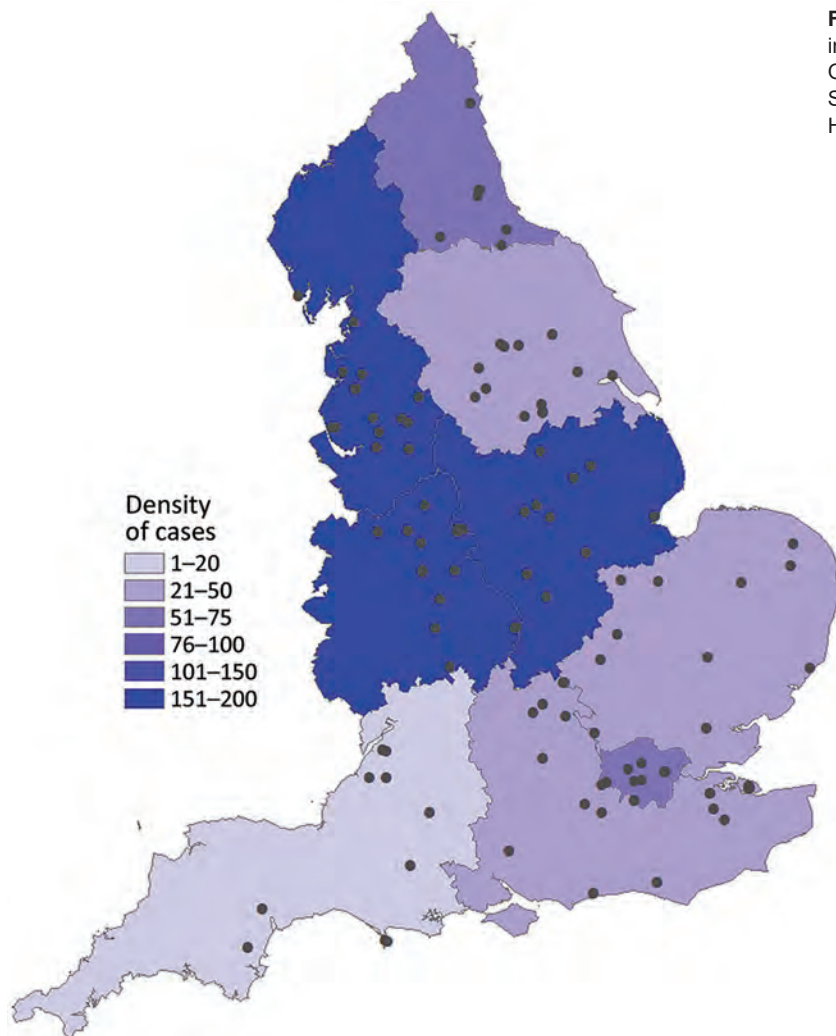
Figure 1. Cases of coronavirus disease in incarcerated persons, England, March 16–October 12, 2020. Dots indicate prison locations. Shading indicates density of cases by Public Health England center.

Density of cases
- 1–20
- 21–50
- 51–75
- 76–100
- 101–150
- 151–200

population (relative risk 1.05; p = 0.14). Incidence rates varied between prisons, from 0 to 14,171.4/100,000 population. Of the 112 prisons in England, 88 (78.6%) were identified as having ≥1 confirmed case (Figure 1). Most prison staff–associated cases were identified after the introduction of key worker testing in April 2020, a total of 303 (74%) staff cases during April 28–May 31, mirroring the trend in England (Figure 2).

Ethnicity data were available for 652 incarcerated cases. Of those, 74.3% (n = 507) identified as White, 7.9% (n = 54) Asian, and 6.4% (n = 44) Black, compared with the general population that was 86% White, 7.5% Asian, and 3.3% Black (*11*). Most staff-associated case-patients identified as White (86.6%, 367/412) (Table).

Twenty-three COVID-19-related deaths were identified, giving a case-fatality ratio (CFR) of 3.13%; the CFR for England was 8.0% over the study period. The CFR was highest for those reported to be White

(3.94%, 20/507); differences by ethnicity were not statistically significant (p = 0.32) (Table).

The number of cases at each prison was 1–124 (IQR 3–7); the upper range resulted from a single outbreak. Overall, 87% of incarcerated cases (n = 638) were associated with an outbreak; we identified a total of 84 prison outbreaks. Eighteen deaths occurred across all outbreaks. For staff-associated cases, clustering by time and place was seen within the same household for 73 cases, including 14 children >18 years of age.

Conclusions

In this study, we aimed to use routine laboratory surveillance data to describe the first wave of COVID-19 cases associated with prisons in England. Because nearly half the prisons in England are overcrowded (*12*), cases in these environments require monitoring and prompt response. Nearly all cases in incarcerated persons were associated with an outbreak. Future
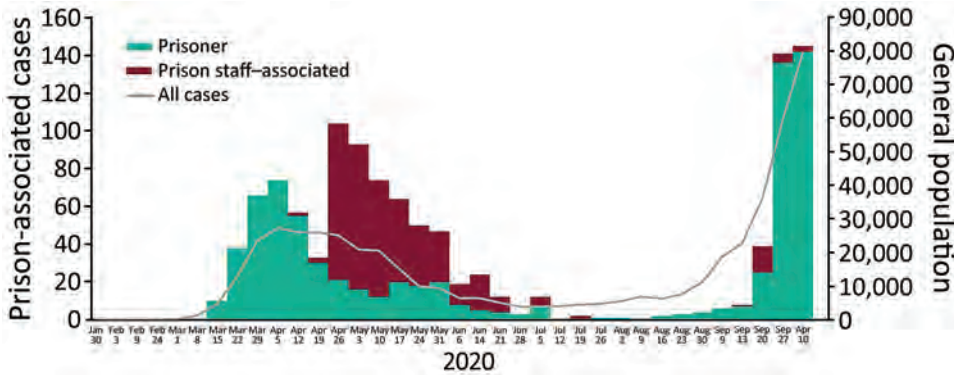
Figure 2. Laboratory-confirmed coronavirus disease cases associated with prisons in England (incarcerated persons, prison staff, and families) by testing date compared to all cases in England, March 16–October 12, 2020. Scales for the y-axes differ substantially to underscore patterns but do not permit direct comparisons.

work should examine the value of genome sequencing to link outbreak cases molecularly.

Although we saw no difference in the crude incidence rates between incarcerated persons and the general population, infection rates were likely underestimated because asymptomatic persons were not tested. In prisons, testing of asymptomatic persons could be employed at the discretion of local government but was usually only done in larger or more severe outbreaks. Other studies have demonstrated asymptomatic detections during outbreaks in other institutional settings (13); wider asymptomatic testing was not introduced in England until 2021.

Testing hesitancy has been reported elsewhere (6), which could also affect the crude rates we report.

Inaccurate address information for incarcerated case-patients could also lead to underestimation. Trends in deaths among the incarcerated differs from reports elsewhere (7). Calculating and comparing CFRs in subsequent waves in these facilities could help to understand this trend.

Sixteen percent of case-patients were from a Black, Asian, or other minority ethnic background, despite making up over a quarter of the prison population and 13% of the general population (12) (Table 1). The differences in infection rates observed by ethnicity may relate to age-related conditions in this population. We noted a higher proportion of White incarcerated cases >65 years of age; increased age is a known risk factor for severe COVID-19 infection (12,14). Older age

Table. Demographic characteristics of COVID-19 cases in incarcerated persons and in persons associated with prison staff, England, March 16–October 12, 2020 *

Characteristic	Incarcerated persons	Prison staff–associated	No. deaths	CFR† (95% CI)
Total, N = 1,157	734 (63.5%)	412 (35.6%)	23 (1.99%)	3.13 (2.00–4.67)
Age group, y				
0–17	5	14	0	0.00‡
18–21	31	12	0	0.00
22–45	435	223	4	0.92 (0.02–2.34)
46–65	192	153	8	4.17 (1.82–8.04)
>66	71	10	11	15.5 (8.0–26.03)
Sex				
F	46	166	2	4.35 (0.05–14.84)
M	688	242	22	3.05 (1.9–4.63)
Unknown	0	4	0	0.00
Race/ethnicity‡				
White/White British	507	318	20	3.94 (2.43–6.03)
Asian/Asian British	54	33	NA	‡
Black/Black British	44	9	NA	‡
Mixed	20	4	NA	0.00
Other	27	3	NA	0.00
Unknown	82	45	NA	0.00
Prison type				
Category C (trainer)	259	NA	7	2.70 (1.09–5.49)
Local	193	NA	8	4.15 (1.81–8.0)
Category B (high security, trainer)	138	NA	2	1.45 (0.18–5.14)
Female	43	NA	2	4.65 (0.57–15.81)
Category A (maximum security)	40	NA	2	5.00 (0.61–24.29)
Open	27	NA	2	7.41 (0.91–24.29)
Youth detention	15	NA	0	0.00

*No deaths were reported among prison staff or their associated cases. CFR, case-fatality rate; COVID-19, coronavirus disease; NA, not available.
†CFR calculated using only incarcerated case data.
‡CFR and 95% CIs for non-White groups not included due to small numbers reported in other categories (<5 cases).

groups also experience a high burden of noncommunicable diseases, putting them at increased risk for more severe infection (*14*). Possible differences in acceptance of testing by age or ethnicity should also be considered relating to these different rates.

The inability to distinguish key workers from household members using these data limited our ability to determine household transmission direction but indicates spread. We were unable to assess the potential role of prison staff–associated cases in seeding prison outbreaks on the basis of routine laboratory data. Other studies have indicated that cases associated with correctional facilities can contribute to additional spread in local communities (*15*), supporting the potential benefit of routine screening of staff to prevent seeding of COVID-19.

Despite limitations, this study adds to the growing evidence base addressing the impact of COVID-19 in prisons. We demonstrate the utility of a highly sensitive address matching methodology to help enhance COVID-19 surveillance. Prison-associated cases make up <1% of COVID-19 cases in England. Because of the increased risk for rapid spread in these environments and the effects of outbreak management on the health of the incarcerated population, being able to identify early signals of increasing case numbers is of great importance for protecting these vulnerable groups.

Acknowledgments

About the Author

Ms. Rice is a Field Epidemiology Training Programme fellow based in the Yorkshire and Humber Field Service team in Leeds, UK. Her research interests include outbreak analysis; healthcare-associated infections and antimicrobial resistance; and health equity.

References

1. Montoya-Barthelemy AG, Lee CD, Cundiff DR, Smith EB. COVID-19 and the correctional environment: the American prison as a focal point for public health. Am J Prev Med. 2020;58:888–91. https://doi.org/10.1016/j.amepre.2020.04.001

2. Chudasama DY, Flannagan J, Collin SM, Charlett A, Twohig KA, Lamagni T, et al. Household clustering of SARS-CoV-2 variant of concern B.1.1.7 (VOC-202012-01) in

England. J Infect. 2021 Apr 29 S0163-4453(21)00216-4 (Epub ahead of print). https://doi.org/10.1016/j.jinf.2021.04.029

3. O'Moore E. Briefing paper—interim assessment of impact of various population management strategies in prisons in response to COVID-19 pandemic in England. 2020 Apr 24 [cited 2020 Dec 16]. https://assets.publishing.service.gov.uk/government/uploads/system/uploads/attachment_data/file/882622/covid-19-population-management-strategy-prisons.pdf

4. HM Prison and Probation Service. COVID-19 official statistics. 2020 Aug 31 [cited 2020 Dec 16]. https://assets.publishing.service.gov.uk/government/uploads/system/uploads/attachment_data/file/919130/HMPPS_COVID19_AUG20_Pub_Doc.pdf

5. Wallace M, Hagan L, Curran KG, Williams SP, Handanagic S, Bjork A, et al. COVID-19 in correctional and detention facilities—United States, February–April 2020. MMWR Morb Mortal Wkly Rep. 2020;69:587–90. https://doi.org/10.15585/mmwr.mm6919e1

6. Wallace M, Marlow M, Simonson S, Walker M, Christophe N, Dominguez O, et al. Public health response to COVID-19 cases in correctional and detention facilities—Louisiana, March–April 2020. MMWR Morb Mortal Wkly Rep. 2020;69:594–8. https://doi.org/10.15585/mmwr.mm6919e3

7. Saloner B, Parish K, Ward JA, DiLaura G, Dolovich S. COVID-19 cases and deaths in federal and state prisons. JAMA. 2020;324:602–3. https://doi.org/10.1001/jama.2020.12528

8. Pringle JC, Leikauskas J, Ransom-Kelley S, Webster B, Santos S, Fox H, et al. COVID-19 in a correctional facility employee following multiple brief exposures to persons with COVID-19—Vermont, July–August 2020. MMWR Morb Mortal Wkly Rep. 2020;69:1569–70. https://doi.org/10.15585/mmwr.mm6943e1

9. Clare T, Twohig KA, O'Connell A-M, Dabrera G. Timeliness and completeness of laboratory-based surveillance of COVID-19 cases in England. Public Health. 2021;194:163–6. PubMed https://doi.org/10.1016/j.puhe.2021.03.012

10. Ministry of Justice. Population bulletin monthly: September 2020. 2020 Sep 25 [cited 2020 Oct 14]. https://www.gov.uk/government/statistics/prison-population-figures-2020

11. UK Government. Population of England and Wales. 2018 [updated August 2020; cited 2021 May 15]. https://www.ethnicity-facts-figures.service.gov.uk/uk-population-by-ethnicity/national-and-regional-populations/population-of-england-and-wales/latest

12. Sturge G. UK prison population statistics. 2020 Jul 3 [cited 2020 Oct 14]. https://commonslibrary.parliament.uk/research-briefings/sn04334

13. Arons MM, Hatfield KM, Reddy SC, Kimball A, James A, Jacobs JR, et al. Presymptomatic SARS-CoV-2 infections and transmission in a skilled nursing facility. N Eng J Med 2020;382:2081–90. https://doi.org/10.1056/NEJMoa2008457

14. Munday D, Leaman J, O'Moore É, Plugge E. The prevalence of non-communicable disease in older people in prison: a systematic review and meta-analysis. Age Ageing. 2019;48:204–12. https://doi.org/10.1093/ageing/afy186

15. Reinhart E, Chen DL. Incarceration and its disseminations: COVID-19 pandemic lessons from Chicago's Cook County Jail. Health Aff (Millwood). 2020;39:1412–8. https://doi.org/10.1377/hlthaff.2020.00652

Address for correspondence: Wendy Rice, Public Health England, Field Service, National Infection Service, Blenheim House, West One, Duncombe Street, Leeds LS1 4PL, UK; email: wendy.rice@phe.gov.uk

Natural Human Infections with *Plasmodium cynomolgi*, *P. inui*, and 4 other Simian Malaria Parasites, Malaysia

Nan Jiun Yap,[1] Hanisah Hossain,[1] Thamayanthi Nada-Raja, Romano Ngui,
Azdayanti Muslim, Boon-Peng Hoh, Loke Tim Khaw, Khamisah Abdul Kadir,
Paul Cliff Simon Divis, Indra Vythilingam, Balbir Singh, Yvonne Ai-Lian Lim

We detected the simian malaria parasites *Plasmodium knowlesi*, *P. cynomolgi*, *P. inui*, *P. coatneyi*, *P. inui*–like, and *P. simiovale* among forest fringe–living indigenous communities from various locations in Malaysia. Our findings underscore the importance of using molecular tools to identify newly emergent malaria parasites in humans.

Zoonotic malaria caused by *Plasmodium knowlesi*, commonly found in long-tailed macaques (*Macaca fascicularis*) and pig-tailed macaques (*M. nemestrina*), is now a major emerging disease, particularly in Malaysia (*1,2*). Two other simian malaria parasites, *P. cynomolgi* (*2–4*) and *P. inui* (*2*), have also been shown to have the potential of zoonotic transmission to humans through the bites of infected mosquitoes under natural and experimental conditions. The risk of acquiring zoonotic malaria is highest for persons living at the forest fringe and working or venturing into the forest because of their proximity with the monkey reservoir hosts and the mosquito vectors (*5,6*). With the aid of molecular methods, we aimed to investigate whether human infections with simian malaria parasites were present among indigenous communities in Malaysia whose villages are situated in the forest or at the forest fringe.

Author affiliations: Universiti Malaya, Kuala Lumpur, Malaysia (N.J. Yap, R. Ngui, A. Muslim, I. Vythilingam, Y.A.-L. Lim); Universiti Malaysia Sarawak, Kota Samarahan, Sarawak, Malaysia (H. Hossain, T. Nada-Raja, K.A. Kadir, P.C.S. Divis, B. Singh); Universiti Teknologi MARA (Sungai Buloh Campus), Selangor, Malaysia (A. Muslim); UCSI University, Kuala Lumpur, Malaysia (B.-P. Hoh); International Medical University, Kuala Lumpur, Malaysia (L.T. Khaw)

The Study

We examined 645 archived blood samples that we had collected during 2011–2014 among indigenous populations of various subtribes from 14 villages in 7 states in Malaysia (Appendix Table 1, https://wwwnc.cdc.gov/EID/article/27/8/20-4502-App1.pdf). We first screened the extracted DNA samples at Universiti Malaya (UM) for the presence of *Plasmodium* with the aid of genus-specific primers (rPLU1 and rPLU5; rPLU3 and rPLU4) (Appendix). Of the 645 indigenous community samples, 102 (15.8%) were positive for *Plasmodium*. Using species-specific nested PCR assays (Appendix), we identified these infections as monoinfections with *P. knowlesi* (n = 40), *P. vivax* (n = 21), *P. cynomolgi* (n = 9), *P. falciparum* (n = 6), *P. coatneyi* (n = 3), *P. inui* (n = 3), *P. malariae* (n = 2), and *P. ovale curtisi* (n = 1) (Table 1). In 17 samples, the species could not be identified despite repeated attempts. Our species-specific primer pairs were designed on the basis of either the asexually (A) or sexually (S) transcribed forms of *Plasmodium* small subunit (SSU) rRNA genes (*7*); the genus-specific primer pairs anneal to both asexual and sexual forms of the SSU rRNA genes, and therefore the genus-specific assay is more sensitive.

We further characterized the 55 samples that tested positive for simian malaria parasites by amplifying a longer fragment of the SSU rRNA gene (914 bp–950 bp) for direct sequencing. Phylogenetic analysis using the neighbor-joining method (Figure 1) revealed the presence of *P. knowlesi* (samples PK1–40), *P. coatneyi* (UM1–3), *P. cynomolgi* (UM9, UM11, UM12, UM14, UM15, UM17, UM18), and *P. inui* (UM5–7). Meanwhile, 2 sequences derived from

Table 1. Human and simian *Plasmodium* malaria species identified by nested PCR at UM targeting SSU rRNA genes among indigenous community blood samples, by state, Malaysia*

State	No. samples tested	No. positive samples	Human and simian malaria species							
			P. falciparum	*P. vivax*	*P. malariae*	*P. ovale curtisi*	*P. knowlesi*	*P. coatneyi*	*P. cynomolgi*	*P. inui*
Pahang	109	5	0	2	0	1	2	0	0	0
Perak	61	55	3	10	2	0	26	3	5	0
Selangor	49	0	0	0	0	0	0	0	0	0
Negeri Sembilan	163	13	1	2	0	0	2	0	2	0
Melaka	32	13	2	3	0	0	1	0	1	1
Kelantan	32	9	0	2	0	0	6	0	1	0
Sarawak	199	7	0	2	0	0	3	0	0	2
Total/overall prevalence	645	102† (of 645; 15.8%)	6 (of 102; 5.9%)	21 (20.6%)	2 (2.0%)	1 (1.0%)	40 (39.2%)	3 (2.9%)	9 (8.8%)	3 (2.9%)

*SSU, small subunit; UM, Universiti Malaya.
†102 of 645 (15.8%) indigenous community samples were found positive with *Plasmodium* genus-specific primers; 17 *Plasmodium* genus-positive samples could not be identified up to species level despite repeated attempts.

samples UM10 and UM16 were found to be closely related to *P. simiovale*.

We then reextracted DNA from 15 blood samples that were positive for *P. coatneyi*, *P. cynomolgi*, and *P. inui* and sent these samples (blinded) together with 5 *Plasmodium*-negative samples to Universiti Malaysia Sarawak (UNIMAS) to confirm their identities by PCR and sequencing of part of the cytochrome c oxidase subunit 1 (COX1) gene. At UNIMAS, using nested PCR assays based on SSU rRNA genes, we found 1 single and 9 double species infections. We could not identify the species of *Plasmodium* for sample UM6, 4 of the *Plasmodium*-positive samples from UM were *Plasmodium* negative, and all 5 *Plasmodium*-negative samples from UM (UM4, 8, 13, 19, 20) tested negative (Table 2). Furthermore, because both laboratories at UM and UNIMAS had previously extracted DNA from macaque blood to examine for simian malaria parasites, we tested the samples for macaque DNA to rule out the possibility that the simian malaria

parasites detected were the result of contamination with macaque blood. We obtained negative results using nested PCR for detection of macaque DNA for the 20 DNA samples when they were first received at UNIMAS and also when we repeated testing after completing the sequencing of COX1 genes, indicating that these samples were not contaminated with macaque blood upon receipt or during subsequent experiments at UNIMAS.

We then subjected the PCR-positive samples (UM6–7, UM9–12, UM14–18) to amplification and sequencing of partial COX1 genes. Neighbor-joining (Figure 2) phylogenetic inference of these sequences, together with available referral sequences from GenBank, indicated that 32 haplotypes from samples UM9–12 and UM14–18 were genetically indistinguishable from *P. cynomolgi*. Our phylogenetic analyses also demonstrated that sample UM7 had a single infection with *P. inui*–like parasites, whereas UM6 had a double infection with *P. simiovale* and *P. inui*–like

Table 2. Comparison between results of nested PCR and sequencing at UM and UNIMAS for identification of *Plasmodium* malaria species from indigenous community blood samples, Malaysia*

Sample ID	Identification at UM		Identification at UNIMAS	
	PCR assays based on SSU rRNA genes	Phylogenetic analysis of SSU rRNA genes	PCR assays based on SSU rRNA genes	Phylogenetic analysis of COX1 genes
UM1	*P. coatneyi*	*P. coatneyi*	Negative	ND
UM2	*P. coatneyi*	*P. coatneyi*	Negative	ND
UM3	*P. coatneyi*	*P. coatneyi*	Negative	ND
UM5	*P. inui*	*P. inui*	Negative	ND
UM6	*P. inui*	*P. inui*	Positive	*P. inui*–like, *P. simiovale*
UM7	*P. inui*	*P. inui*	*P. inui*	*P. inui*-like
UM9	*P. cynomolgi*	*P. cynomolgi*	*P. cynomolgi, P. inui*	*P. cynomolgi*
UM10	*P. cynomolgi*	*Plasmodium* spp.	*P. cynomolgi, P. inui*	*P. cynomolgi*
UM11	*P. cynomolgi*	*P. cynomolgi*	*P. cynomolgi, P. inui*	*P. cynomolgi*
UM12	*P. cynomolgi*	*P. cynomolgi*	*P. cynomolgi, P. inui*	*P. cynomolgi*
UM14	*P. cynomolgi*	*P. cynomolgi*	*P. cynomolgi, P. inui*	*P. cynomolgi*
UM15	*P. cynomolgi*	*P. cynomolgi*	*P. cynomolgi, P. inui*	*P. cynomolgi*
UM16	*P. cynomolgi*	*Plasmodium* spp.	*P. cynomolgi, P. inui*	*P. cynomolgi, P. inui*–like, *P. simiovale*
UM17	*P. cynomolgi*	*P. cynomolgi*	*P. cynomolgi, P. inui*	*P. cynomolgi*
UM18	*P. cynomolgi*	*P. cynomolgi*	*P. cynomolgi, P. inui*	*P. cynomolgi*

*Negative, negative for *Plasmodium* DNA and not examined by species-specific nested PCR assays; ND, not done; positive, positive for *Plasmodium* DNA but negative with species-specific nested PCR assays. SSU, small subunit; UM, Universiti Malaya; UNIMAS, Universiti Malaysia Sarawak.

parasites and UM16 had a triple infection with *P. cynomolgi, P. simiovale*, and *P. inui*–like parasites.

We generated phylogenetic trees of similar topology by the maximum-likelihood method for the SSU rRNA genes (Appendix Figure 1) and by the Bayesian maximum clade credibility method for the COX1 genes (Appendix Figure 2). There were discrepancies between the nested PCR assay results and the sequencing results between our 2 laboratories; mixed species of *Plasmodium* were identified only at UNIMAS. A possible explanation is that the DNA samples analyzed at UNIMAS were newly extracted and were different from the ones used in the experiments at UM. There might also be a compromise of the sensitivity in detecting the species with lower parasitemia in mixed infections as a result of competition for nest 1 primers by the species with higher parasite loads. Furthermore, for sequencing of the SSU rRNA genes at UM, primers that were specific for the species identified by nested PCR assays were used, whereas for the COX1 genes, both *P. cynomolgi*–specific primers and primers that could amplify other species of *Plasmodium* were used. Therefore, additional species of *Plasmodium* were identified at UNIMAS in these samples, such as *P. simiovale* and *P. inui*–like, for which no species-specific PCR primers exist.

Conclusions

The 40 *P. knowlesi* infections we detected originated from 6 states in Malaysia, thereby confirming the widespread distribution of human *P. knowlesi* malaria cases in Malaysia (*1*). We detected *P. cynomolgi* infections among indigenous communities in 4 states in Malaysia. Taken together with previous reports of naturally acquired *P. cynomolgi* infections in humans in the states of Terengganu, Sabah, and Sarawak (*3,8,9*), our findings indicate that human infections caused by *P. cynomolgi* are also widely distributed in Malaysia.

Our study highlights the occurrence of naturally acquired human infections with *P. inui, P. inui*–like, *P. coatneyi*, and *P. simiovale*. Natural human *P. inui* infections have not been described (*10*), although the parasite is experimentally transmissible to humans (*2*). For *P. coatneyi*, attempts to infect humans with blood from an infected rhesus monkey and through infected mosquitoes were unsuccessful (*2*). *P. simiovale* is a lesser-studied simian malaria parasite that was previously described only in toque macaques (*Macaca sinica*) of Sri Lanka (*2*) until it was recently identified, together with *P. inui*–like parasites, in long-tailed macaques from Sarawak in Malaysian Borneo (*11*). All these simian malaria parasites would have been diagnosed by microsco-
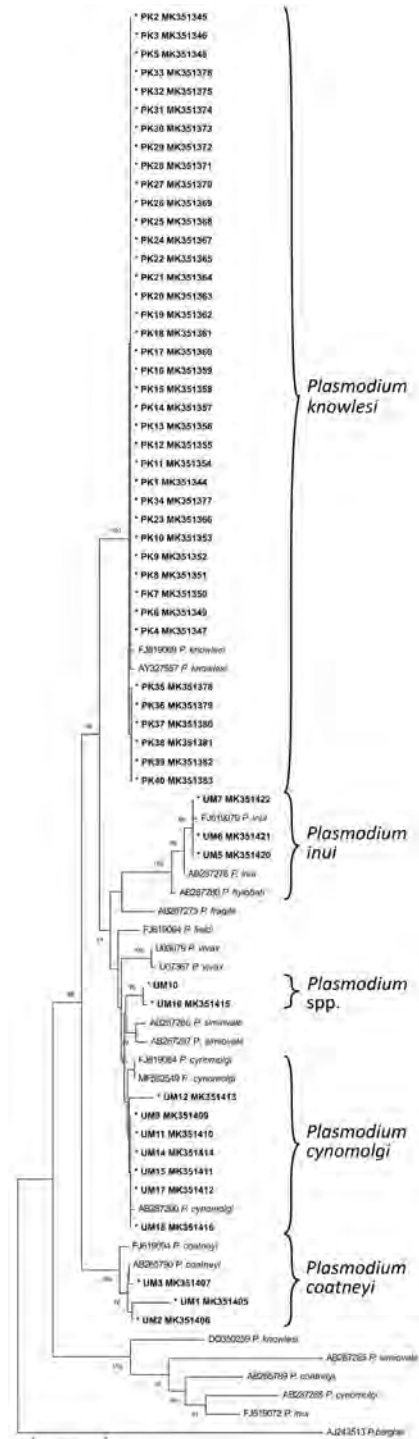
Figure 1. Neighbor-joining phylogenetic tree of *Plasmodium* species based on partial sequence of SSU rRNA genes for identification of *Plasmodium* malaria species from indigenous community blood samples, Malaysia. Nucleotide sequences generated from this study are marked with asterisks and are in bold. GenBank accession numbers are provided for all sequences. Numbers at nodes indicate percentage support of 1,000 bootstrap replicates; only bootstrap values above 70% are displayed. Scale bar indicates branch length.
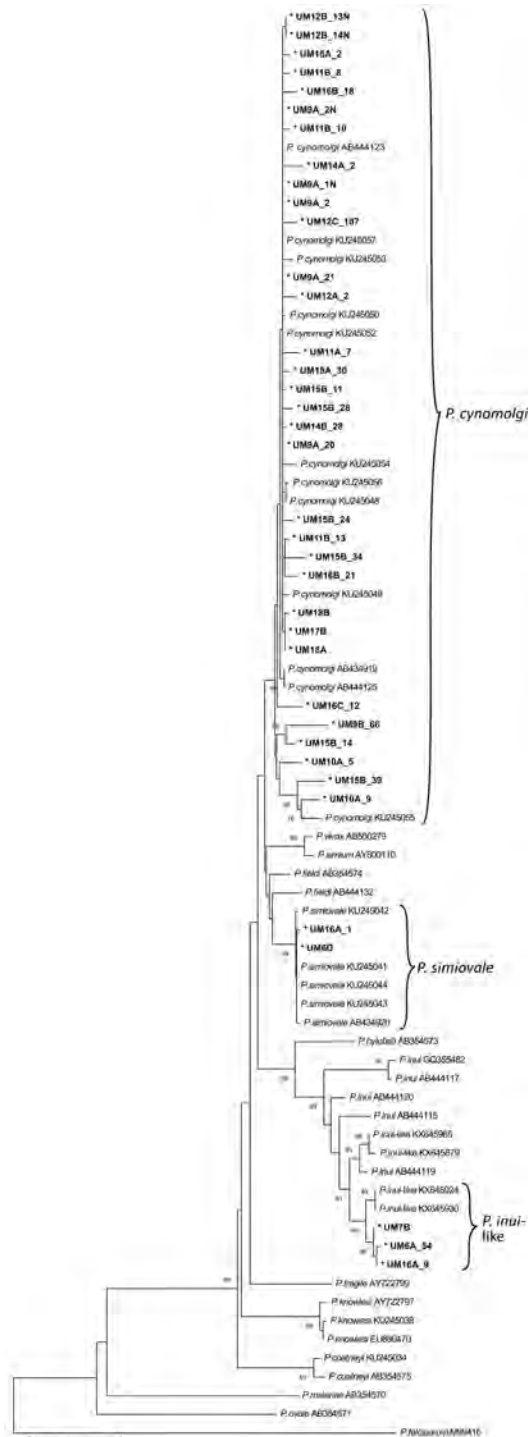
Figure 2. Neighbor-joining phylogenetic tree of *Plasmodium* species based on partial sequence of COX1 genes for identification of *Plasmodium* malaria species from indigenous community blood samples, Malaysia. Nucleotide sequences generated from this study are marked with asterisks and are in bold. GenBank accession numbers are provided for all sequences. Numbers at nodes indicate percentage support of 1,000 bootstrap replicates; only bootstrap values above 70% are displayed. Scale bar indicates branch length.

py as human malaria parasites because they share morphological similarities with human malaria parasites. The early blood stages of *P. knowlesi* resemble those of *P. falciparum*, and the other forms are similar to *P. malariae* (*2,6*). *P. cynomolgi* is morphologically similar to *P. vivax* (*2*), and both *P. inui* and *P. inui*–like parasites are morphologically identical to *P. malariae* (*2,11*), whereas *P. coatneyi* bears morphologic similarities to *P. falciparum* and *P. simiovale* bears morphologic similarities to *P. ovale* (*2,12*). Besides misdiagnosis of simian malaria parasites as human malaria parasites, there are other limitations of microscopy for diagnosis of malaria; thus, using molecular tools is paramount in generating accurate epidemiology data (*6*). It is envisaged that screening with molecular tools of other communities living at the forest fringes will demonstrate the widespread distribution of zoonotic malaria and uncover more newly emergent malaria parasites.

About the Author

Dr. Yap is a postdoctoral researcher at the Department of Parasitology, Faculty of Medicine, Universiti Malaya, Kuala Lumpur, Malaysia. Her primary research interests include epidemiology and molecular characterization of zoonotic malaria species.

References

1. Jeyaprakasam NK, Liew JWK, Low VL, Wan-Sulaiman WY, Vythilingam I. *Plasmodium knowlesi* infecting humans in Southeast Asia: what's next? PLoS Negl Trop Dis. 2020;14:e0008900. https://doi.org/10.1371/journal.pntd.0008900
2. Coatney GR, Collins WE, Warren M, Contacos PG. The primate malarias. Washington (DC): US National Institute of Allergy and Infectious Diseases; 1971
3. Ta TH, Hisam S, Lanza M, Jiram AI, Ismail N, Rubio JM. First case of a naturally acquired human infection with *Plasmodium cynomolgi*. Malar J. 2014;13:68. https://doi.org/10.1186/1475-2875-13-68
4. Imwong M, Madmanee W, Suwannasin K, Kunasol C, Peto TJ, Tripura R, et al. Asymptomatic natural human infections with the simian malaria parasites *Plasmodium*

cynomolgi and *Plasmodium knowlesi.* J Infect Dis. 2019;219:695–702. https://doi.org/10.1093/infdis/jiy519

5. Anstey NM, Grigg MJ. Zoonotic malaria: the better you look, the more you find. J Infect Dis. 2019;219:679–81. https://doi.org/10.1093/infdis/jiy520

6. Singh B, Daneshvar C. Human infections and detection of *Plasmodium knowlesi.* Clin Microbiol Rev. 2013;26:165–84. https://doi.org/10.1128/CMR.00079-12

7. Li J, Gutell RR, Damberger SH, Wirtz RA, Kissinger JC, Rogers MJ, et al. Regulation and trafficking of three distinct 18 S ribosomal RNAs during development of the malaria parasite. J Mol Biol. 1997;269:203–13. https://doi.org/10.1006/jmbi.1997.1038

8. Grignard L, Shah S, Chua TH, William T, Drakeley CJ, Fornace KM. Natural human infections with *Plasmodium cynomolgi* and other malaria species in an elimination setting in Sabah, Malaysia. J Infect Dis. 2019;220:1946–9. https://doi.org/10.1093/infdis/jiz397

9. Raja TN, Hu TH, Kadir KA, Mohamad DSA, Divis PCS, Wong LL, et al. Naturally acquired human *Plasmodium cynomolgi* and *P. knowlesi* infections, Malaysian Borneo. Emerg Infect Dis. 2020;26:1801–9. https://doi.org/10.3201/eid2608.200343

10. Siner A, Liew ST, Kadir KA, Mohamad DSA, Thomas FK, Zulkarnaen M, et al. Absence of *Plasmodium inui* and *Plasmodium cynomolgi*, but detection of *Plasmodium knowlesi* and *Plasmodium vivax* infections in asymptomatic humans in the Betong division of Sarawak, Malaysian Borneo. Malar J. 2017;16:417. https://doi.org/10.1186/s12936-017-2064-9

11. Nada Raja T, Hu TH, Zainudin R, Lee KS, Perkins SL, Singh B. Malaria parasites of long-tailed macaques in Sarawak, Malaysian Borneo: a novel species and demographic and evolutionary histories. BMC Evol Biol. 2018;18:49. https://doi.org/10.1186/s12862-018-1170-9

12. Dissanaike AS. Simian malaria parasites of Ceylon. Bull World Health Organ. 1965;32:593–7.

Addresses for correspondence: Yvonne Ai-Lian Lim, Department of Parasitology, Faculty of Medicine, Universiti Malaya, Kuala Lumpur, Malaysia; email: limailian@um.edu.my; Balbir Singh, Malaria Research Centre, Faculty of Medicine and Health Sciences, Universiti Malaysia Sarawak, Kota Samarahan, Sarawak, Malaysia; email: bsingh@unimas.my
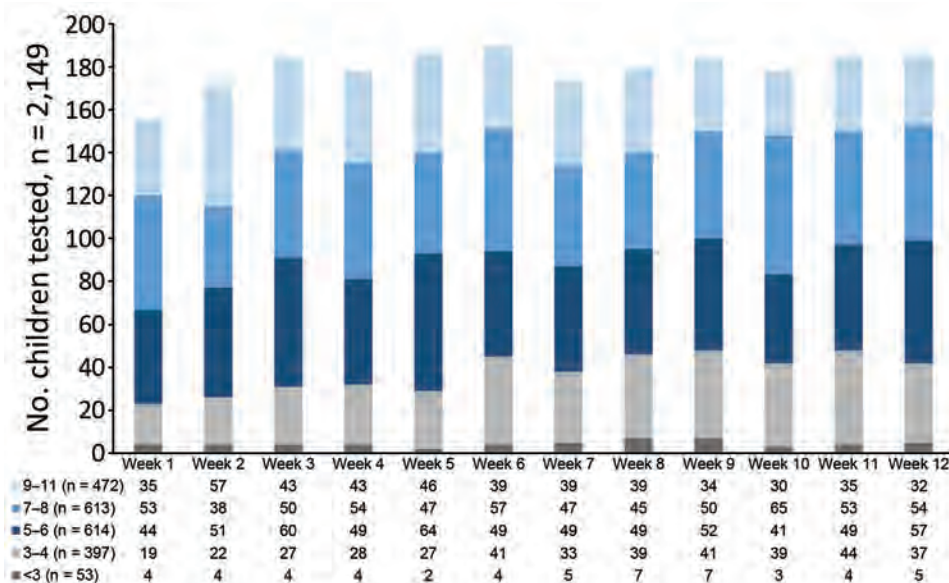
Weekly SARS-CoV-2 Sentinel Surveillance in Primary Schools, Kindergartens, and Nurseries, Germany, June–November 2020

Martin Hoch,[1] Sebastian Vogel,[1] Laura Kolberg, Elisabeth Dick, Volker Fingerle, Ute Eberle, Nikolaus Ackermann, Andreas Sing, Johannes Huebner, Anita Rack-Hoch, Tilmann Schober, Ulrich von Both

We investigated severe acute respiratory syndrome coronavirus 2 infections in primary schools, kindergartens, and nurseries in Germany. Of 3,169 oropharyngeal swab specimens, only 2 were positive by real-time reverse transcription PCR. Asymptomatic children attending these institutions do not appear to be driving the pandemic when appropriate infection control measures are used.

Children have been disproportionately affected by public health measures in the current coronavirus disease (COVID-19) pandemic (*1*). In contrast to other age groups, children have shown lower rates of severe acute respiratory syndrome coronavirus 2 (SARS-CoV-2)–positive cases; lower risk for symptomatic, acute, COVID-19; a generally milder course of disease with the exception of some rare manifestations and the post–COVID-19 multisystem inflammatory syndrome in children; and lower secondary attack rates (*2–4*). Susceptibility to infection in ≤10 years of age is estimated to be lower than that for teenagers. Accumulating evidence shows that, given limited infection control measures, SARS-CoV-2 might spread sustainably in secondary/high schools but to a lesser degree in primary schools and nurseries (*2,5*).

Closure of childcare facilities and schools has been shown to negatively affect the physical and emotional well-being of children, teenagers, and parents, potentially having a long-term impact on their lives (*6*). Thus, various expert groups called for avoiding

closing of these institutions (*7,8*). Against the background of presymptomatic transmission found in adults, it is critical to public health authorities to be able to rely on real-life data monitoring the number of asymptomatic yet infected children attending educational institutions (*9*). Some studies have reported low numbers of infected cases in primary schools or childcare facilities but were conducted during a lockdown or semi-lockdown period (*5,10*). The aim of our study (the Münchner Virenwächter Study) was to implement a real-time sentinel program in a representative number of 5 primary schools and 5 (6 in phase 2) nurseries/kindergartens in Munich, Germany.

The Study

This study was approved by the ethics committee of the Ludwig-Maximilians University under project no. 20-484. We intended to accomplish a timely detection of infected cases and offer an additional level of safety to participating institutions during regular operating mode. The study spanned over 2 phases (Figure 1): phase 1, June 15–July 26, 2020; and phase 2, September 7–November 1, 2020. Participating institutions were randomly selected, and written informed consent was obtained in the first week of each phase. To correct for underrepresentation of younger children (≤5 years of age), we included an additional nursery/kindergarten into phase 2.

We tested oropharyngeal swab specimens for SARS-CoV-2 by using real-time reverse transcription PCR (rRT-PCR); weekly samples were obtained from randomly selected children (n = 20) and staff (n = 5) in each institution. Swab specimens were taken on-site by trained medical personnel, and results were timely reported. For rRT-PCR, we processed specimens

Author affiliations: Bavarian Health and Food Safety Authority, Oberschleissheim, Germany (M. Hoch, S. Vogel, V. Fingerle, U. Eberle, N. Ackermann, A. Sing); Ludwig-Maximilians-University, Munich, Germany (L. Kolberg, E. Dick, J. Huebner, A. Rack-Hoch, T. Schober, U. von Both); German Center for Infection Research, Munich (U. von Both)

[1]These authors contributed equally to this article.
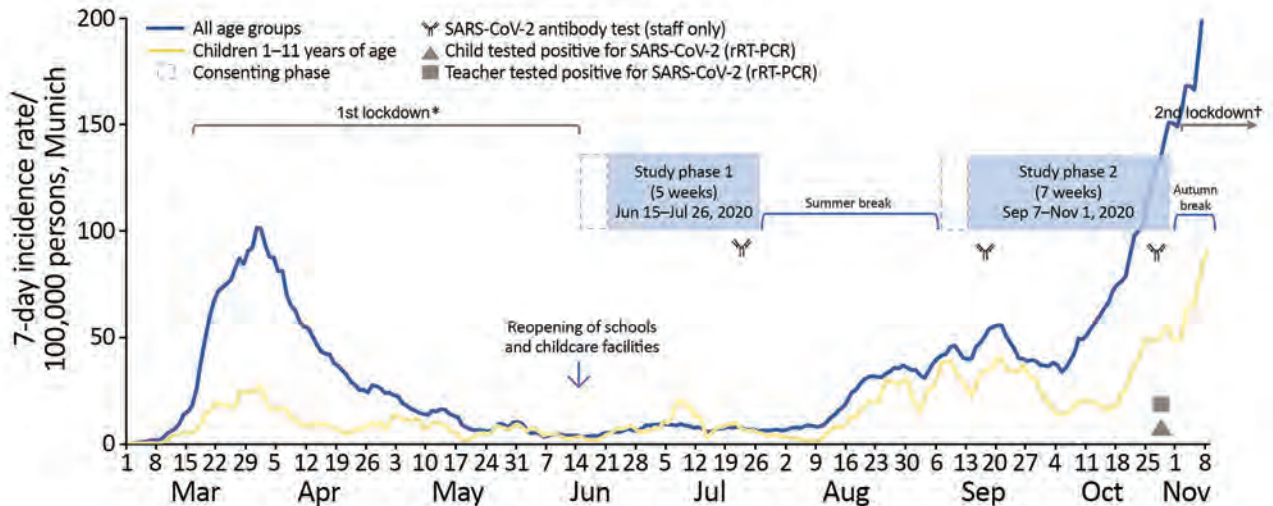
Figure 1. Weekly SARS-CoV-2 sentinel surveillance in primary schools, kindergartens, and nurseries, Germany, June–November 2020. Timeline of Münchner Virenwächter study in context of pandemic activity in Munich, Germany. The 7-day incidence rates were derived from the national surveillance system according to the German Infection Protection Act, Bavarian Health and Food Safety Authority as of November 28th, 2020. rRT-PCR, real-time reverse transcription PCR; SARS-CoV-2, severe acute respiratory syndrome coronavirus 2. *Included closure of schools and childcare facilities. †Schools, childcare facilities, and shops/businesses kept open.

by using the AmpliCube Coronavirus SARS-CoV-2 Panel (Mikrogen, https://www.mikrogen.de) on a CFX96 Touch rRT-PCR Detection System (Bio-Rad, https://www.bio-rad.com). We retested single gene results by using the Xpert Xpress SARS-CoV-2 Test (Cepheid, https://www.cepheid.com).

We performed SARS-CoV-2 IgG screening at 3 sequential time points for samples from consenting staff members by using the Liaison SARS-CoV-2 S1/ S2 IgG System (DiaSorin, https://www.diasorin. com) (Figure 1). We confirmed active results by using the RecomLine SARS-CoV-2 IgG Lineblot (Mikrogen). Antibody screening was complemented by obtaining a throat swab specimen at the same time to exclude active infection. Institutions were asked to respond to a questionnaire assessing implementation of infection control measures for phases 1 and 2.

We processed 3,169 oropharyngeal swab specimens during the 12-week testing period, 2,149 from children (median age 7 years, range 1–11 years, male:female ratio 1.03) and 1,020 from staff (median age 41 years, range 17–76 years, male:female ratio 0.13). We also obtained 493 swab specimens from staff during weekly testing and 527 swab specimens to complement serologic testing. We also tested 527 blood samples from staff for SARS-CoV-2 IgG. We determined pediatric sample distribution per study week (Figure 2).

No SARS-CoV-2 infections were detected during phase 1 of the study. During phase 2, only week 12 yielded 2 positive samples from 1 primary school.

All SARS-CoV-2 IgG test results were negative at timepoints 1 and 2; only 1 positive serologic result was detected at timepoint 3. We identified some changes for implemented infection control measures between study phases and for individual facets between schools and childcare facilities (Table). All children attending primary schools were wearing face masks on school premises, except when seated for classes. Regular ventilation was begun as a daily routine in all institutions, as per national infection prevention and control guidance (Robert Koch Institute, https://www.rki.de).

Designed during the first lockdown in Munich, our study was intended to determine a feasible SARS-CoV-2 sentinel program in primary schools and childcare facilities in anticipation of a second pandemic wave and increasing incidence rates. Although public health and political authorities were concerned that childcare institutions would be major drivers of the pandemic, our results suggest that this did not happen. This result was consistent with those of another report suggesting that it was unlikely that children are major drivers of the pandemic even if attending schools (11).

Our study was not powered to accurately illustrate changes in incidences during low-incidence periods because of small sample sizes. However, we detected 2 cases in a primary school, 1 child and 1 teacher, during a high, local, 7-day incidence rate of 50 cases/100,000 children 1–11 years of age and 150 cases/100,000 persons in the general population.

Figure 2. Weekly SARS-CoV-2 sentinel surveillance in primary schools, kindergartens, and nurseries, Germany, June–November 2020. Distribution of weekly pediatric oropharyngeal swab samples for SARS-CoV-2 testing by real-time reverse transcription PCR. Color code indicates individual age groups. Age stratification is per week of children tested for SARS-CoV-2. SARS-CoV-2, severe acute respiratory syndrome coronavirus 2.

	Week 1	Week 2	Week 3	Week 4	Week 5	Week 6	Week 7	Week 8	Week 9	Week 10	Week 11	Week 12
9–11 (n = 472)	35	57	43	43	46	39	39	39	34	30	35	32
7–8 (n = 613)	53	38	50	54	47	57	47	45	50	65	53	54
5–6 (n = 614)	44	51	60	49	64	49	49	49	52	41	49	57
3–4 (n = 397)	19	22	27	28	27	41	33	39	41	39	44	37
<3 (n = 53)	4	4	4	4	2	4	5	7	7	3	4	5

Tracing of 36 close contacts (33 classmates and 3 private contacts) identified only 1 additional case in another asymptomatic child in the same class. Telephone interview–based contact tracing showed that the teacher reported to have experienced unspecific symptoms of headache and malaise 6 days before testing. Thus, it seems reasonable to deduce that transmission occurred from staff to both children.

Conclusions

Several reports have assessed the role of children in the dynamics of SARS-CoV-2 transmission. A study conducted in day care centers in Germany that used buccal mucosal and anal swabs for SARS-CoV-2 detection concluded that day care centers are not relevant reservoirs in a low prevalence setting (*12*). However, this study used self-testing, lacked oropharyngeal swab specimens, and was conducted during a minimal local incidence rate. Our study covered both low and high 7-day incidence periods while obtaining oropharyngeal swab specimens from children 1–11 years of age. Ismail et al. reported complementary data from the United Kingdom, which showed that staff members had an increased risk for SARS-CoV-2

Table. Comparison of implementation of infection control measures for phase 1 and 2 during weekly SARS-CoV-2 sentinel surveillance in primary schools, kindergartens, and nurseries, Germany, June–November 2020*

	Childcare facilities		Primary school	
Infection control measure	Phase 1	Phase 2	Phase 1	Phase 2
Reduced number of supervised children	0/5	0/6	5/5	0/5
Supervision of children by rotating groups/classes	0/5	0/6	5/5	0/5
Physical distancing between staff members inside	5/5	6/6	5/5	5/5
Physical distancing between staff members outside	5/5	6/6	5/5	4/5
Physical distancing between children inside	1/5	2/6	5/5	5/5
Physical distancing between children outside	2/5	2/6	5/5	1/5
Face mask for staff members inside	0/5	6/6	4/5	5/5
Face mask for staff members outside	0/5	2/6	4/5	4/5
Face mask for staff members during drop-off/collection of children	3/5	6/6	4/5	5/5
Face mask for parents during drop-off/collection of children	5/5	6/6	4/5	5/5
Parents allowed to enter premises when dropping off or collecting children	5/5	4/6	1/5	2/5
Washing hands before collection of children by parents	3/5	5/6	1/5	1/5
Use of bathroom facilities separate for individual groups/classes	5/5	5/6	2/5	2/5
Closure of garden/playground areas	0/5	0/6	0/5	0/5
Use of garden/playground areas separate for individual groups/classes	4/5	4/6	5/5	5/5
Handwashing before meals	5/5	6/6	5/5	5/5
Handwashing before entering classes/groups	5/5	5/5	5/5	5/5
Hand disinfectant dispensers provided on premises	4/5	6/6	4/5	3/5
Cancellation of common activities	5/5	6/6	5/5	5/5

*Values indicate number of participating childcare facilities or primary schools that implemented a specific infection control measure, which ranged from 0/5 to 5/5 or 0/6 to 6/6. Phase 1, June 15–July 26, 2020; phase 2, September 7–November 1, 2020. SARS-CoV-2, severe acute respiratory syndrome coronavirus 2.

infection compared with students in any educational setting and that most cases linked to outbreaks were in staff (*13*).

Secondary attack rate analysis of the cases in our study also suggests that infections were transmitted from staff to children. In addition, low prevalence for SARS-CoV-2 antibodies in staff over the 3-month study period suggests no relevant infection activity in either work or private setting. Another recent report highlighted the need for maintaining low infection rates in the community to keep schools open during the pandemic (*14*).

Our study was conducted before the emergence of SARS-CoV-2 variants, such as B.1.1.7. Thus, the effect of this variant on children could not be addressed in our study. However, recent data from the United Kingdom found no evidence of more severe disease in children during the second wave, suggesting that infection with the B.1.1.7 variant does not result in a greatly different clinical course than the original strain (*15*).

We conclude that asymptomatic children attending primary schools, kindergartens, and nurseries are not greatly contributing to pandemic distribution of SARS-CoV-2 while adhering to infection control measures described above, even during high local background incidence. Thus, these children are unlikely to initiate clusters or outbreaks in the community when these institutions continue to play their critical role for the physical and emotional well-being of children and their families.

About the Author

Dr. Hoch is head of the department of Infectious Diseases Epidemiology and Task Force Infectiology at the Bavarian Health and Food Safety Authority, Oberschleissheim, Germany. His primary research interests are pediatric infectious diseases and their impact on public health, and emerging and reemerging infectious diseases.

References

1. Snape MD, Viner RM. COVID-19 in children and young people. Science. 2020;370:286–8. https://doi.org/10.1126/science.abd6165
2. Goldstein E, Lipsitch M, Cevik M. On the effect of age on the transmission of SARS-CoV-2 in households, schools, and the community. J Infect Dis. 2021;223:362–9. https://doi.org/10.1093/infdis/jiaa691
3. Kim-Hellmuth S, Hermann M, Eilenberger J, Ley-Zaporozhan J, Fischer M, Hauck F, et al. SARS-CoV-2 triggering severe acute respiratory distress syndrome and secondary hemophagocytic lymphohistiocytosis in a 3-year-old child with Down syndrome. J Pediatric Infect Dis Soc. 2021;10:543–6. https://doi.org/10.1093/jpids/piaa148
4. Whittaker E, Bamford A, Kenny J, Kaforou M, Jones CE, Shah P, et al.; PIMS-TS Study Group and EUCLIDS and PERFORM Consortia. Clinical characteristics of 58 children with a pediatric inflammatory multisystem syndrome temporally associated with SARS-CoV-2. JAMA. 2020;324:259–69. https://doi.org/10.1001/jama.2020.10369
5. Ladhani SN, Baawuah F, Beckmann J, Okike IO, Ahmad S, Garstang J, et al. SARS-CoV-2 infection and transmission in primary schools in England in June–December, 2020 (sKIDs): an active, prospective surveillance study. Lancet Child Adolesc Health. 2021;5:417–27. https://doi.org/10.1016/S2352-4642(21)00061-4
6. Buonsenso D, Roland D, De Rose C, Vásquez-Hoyos P, Ramly B, Chakakala-Chaziya JN, et al. Schools closures during the COVID-19 pandemic: a catastrophic global situation. Pediatr Infect Dis J. 2021;40:e146–50. https://doi.org/10.1097/INF.0000000000003052
7. Levinson M, Cevik M, Lipsitch M. Reopening primary schools during the pandemic. N Engl J Med. 2020;383:981–5. https://doi.org/10.1056/NEJMms2024920
8. Patrick SW, Henkhaus LE, Zickafoose JS, Lovell K, Halvorson A, Loch S, et al. Well-being of parents and children during the COVID-19 pandemic: a national survey. Pediatrics. 2020;146:e2020016824. https://doi.org/10.1542/peds.2020-016824
9. L'Huillier AG, Torriani G, Pigny F, Kaiser L, Eckerle I. Culture-competent SARS-CoV-2 in nasopharynx of symptomatic neonates, children, and adolescents. Emerg Infect Dis. 2020;26:2494–7. https://doi.org/10.3201/eid2610.202403
10. Otte Im Kampe E, Lehfeld A-S, Buda S, Buchholz U, Haas W. Surveillance of COVID-19 school outbreaks, Germany, March to August 2020. Euro Surveill. 2020;25. https://doi.org/10.2807/1560-7917.ES.2020.25.38.2001645
11. Soriano-Arandes A, Gatell A, Serrano P, Biosca M, Campillo F, Capdevila R et al.; the COPEDI-CAT Research Group. Household SARS-CoV-2 transmission and children: a network prospective study. Clib Dis. 20210;Mar 12:ciaa228 [Online ahead of print]. https://doi.org/10.1093/cid/ciab228
12. Hoehl S, Kreutzer E, Schenk B, Westhaus S, Foppa I, Herrmann E et al. Longitudinal testing for respiratory and gastrointestinal shedding of SARS-CoV-2 in day care centres in Hesse, Germany. Clin Infect Dis. 2021;Jan 3:ciaa1912 [Online ahead of print]. https://doi.org/10.1093/cid/ciaa1912
13. Ismail SA, Saliba V, Lopez Bernal J, Ramsay ME, Ladhani SN. SARS-CoV-2 infection and transmission in educational settings: a prospective, cross-sectional analysis of infection clusters and outbreaks in England. Lancet Infect Dis. 2021;21:344–53. https://doi.org/10.1016/S1473-3099(20)30882-3

14. Mensah AA, Sinnathamby M, Zaidi A, Coughlan L, Simmons R, Ismail SA, et al. SARS-CoV-2 infections in children following the full re-opening of schools and the impact of national lockdown: prospective, national observational cohort surveillance, July-December 2020, England. J Infect. 2021;82:67–74. https://doi.org/10.1016/j.jinf.2021.02.022

15. Brookman S, Cook J, Zucherman M, Broughton S, Harman K, Gupta A. Effect of the new SARS-CoV-2 variant B.1.1.7 on children and young people. Lancet Child Adolesc Health. 2021;5:e9–10. https://doi.org/10.1016/S2352-4642(21)00030-4

Address for correspondence: Ulrich von Both, Hauner Children's Hospital, Ludwig-Maximilians-University, Lindwurmstrasse 4, 80337 Munich, Germany; email: ulrich.von.both@med.lmu.de

March 2021

Mycobacterial Infections

- Parallels and Mutual Lessons in Tuberculosis and COVID-19 Transmission, Prevention, and Control

- Genomic Evidence of In-Flight Transmission of SARS-CoV-2 Despite Predeparture Testing

- Evaluation of National Event-Based Surveillance, Nigeria, 2016–2018

- Clinical Features and Comparison of Kingella and Non-*Kingella* Endocarditis in Children, Israel

- Use of US Public Health Travel Restrictions during COVID-19 Outbreak on Diamond Princess Ship, Japan, February–April 2020

- Systematic Review of Pooling Sputum as an Efficient Method for Xpert MTB/RIF Tuberculosis

- Testing during COVID-19 Pandemic Decentralized Care for Rifampicin-Resistant Tuberculosis, Western Cape, South Africa

- Transmission of Antimicrobial-Resistant *Staphylococcus aureus* Clonal Complex 9 between Pigs and Humans, United States

- Epidemiology and Clinical Course of First Wave Coronavirus Disease Cases, Faroe Islands Oral Human Papillomavirus Infection in Children during the First 6 Years of Life, Finland

- Clusters of Drug-Resistant *Mycobacterium tuberculosis* Detected by Whole-Genome Sequence Analysis of Nationwide Sample, Thailand, 2014–2017

- Daily Forecasting of Regional Epidemics of Coronavirus Disease with Bayesian Uncertainty

- Quantification, United States Fluconazole-Resistant *Candida glabrata* Bloodstream Isolates, South Korea, 2008–2018

- Excess All-Cause Deaths during Coronavirus Disease Pandemic, Japan, January–May 2020

- *Mycoplasma genitalium* and Other Reproductive Tract Infections in Pregnant Women, Papua New Guinea, 2015–2017

- Effectiveness of Preventive Therapy for Persons Exposed at Home to Drug-Resistant Tuberculosis, Karachi, Pakistan

- Familial Clusters of Coronavirus Disease in 10 Prefectures, Japan, February–May 2020

- Population-Based Geospatial and Molecular Epidemiologic Study of Tuberculosis Transmission Dynamics, Botswana, 2012–2016

- Extrapulmonary Nontuberculous *Mycobacteria* Infections in Hospitalized Patients, United States, 2010–2014

- Genomic Characterization of *hlyF*-positive Shiga Toxin–Producing *Escherichia coli*, Italy and the Netherlands, 2000–2019

- Isolate-Based Surveillance of *Bordetella pertussis*, Austria, 2018–2020

- Decline of Tuberculosis Burden in Vietnam Measured by Consecutive National Surveys, 2007–2017

- Foodborne Origin and Local and Global Spread of *Staphylococcus saprophyticus* Causing Human Urinary Tract Infections

- Prevalence of SARS-CoV-2 Antibodies in First Responders and Public Safety Personnel, New York City, New York, USA, May–July 2020

- Local and Travel-Associated Transmission of Tuberculosis at Central Western Border of Brazil, 2014–2017

- Antibody Responses 8 Months after Asymptomatic or Mild SARS-CoV-2 Infection

- Lung Pathology of Mutually Exclusive Co-infection with SARS-CoV-2 and *Streptococcus pneumoniae*

EMERGING INFECTIOUS DISEASES®

To revisit the March 2021 issue, go to:

https://wwwnc.cdc.gov/eid/articles/issue/27/3/table-of-contents

Genomic Detection of Schmallenberg Virus, Israel

Adi Behar, Omer Izhaki, Asael Rot, Tzvika Benor, Mario Yankilevich,
Monica Leszkowicz-Mazuz, Jacob Brenner

We discuss genomic detection of Schmallenberg virus in both *Culicoides* midges and affected ruminants during June 2018–December 2019, demonstrating its circulation in Israel. This region is a geographic bridge between 3 continents and may serve as an epidemiologic bridge for potential Schmallenberg virus spread into Asia.

Simbu serogroup viruses form one of the largest serogroups in the genus *Orthobunyavirus* of the family *Peribunyaviridae*, comprising $\geq$25 antigenically different, but serologically related, negative-sense single-stranded RNA viruses. These viruses are transmitted mainly by *Culicoides* biting midges; they persist in the environment by cycling between infected mammalian hosts and *Culicoides* vectors. Notable examples from the Simbu serogroup are Akabane virus (AKAV), Aino virus, Schmallenberg virus (SBV), Sathuperi virus (SATV), Shamonda virus (SHAV), Peaton virus (PEAV), and Shuni virus (SHUV, which is also suspected of infecting humans.). These viruses are known to cross the placenta of ruminants to the developing fetus, causing abortion, stillbirth, and neonatal malformations that are seen only at birth. The congenital malformations are termed arthrogryposis-hydranencephaly syndrome. Given that the clinical signs can be observed only months after viremia has occurred, field and laboratory practitioners are at a huge disadvantage when facing epidemics caused by these viruses (*1–7*).

Until recently, the most studied viruses of the Simbu serogroup were AKAV and Aino virus, both known to be present in Israel (*1,3*). In 2011, a new Simbu virus emerged in Europe and was named Schmallenberg virus (SBV) (*8*). Studies suggested that SBV is a reassortant virus, deriving the medium (M)

Author affiliations: Kimron Veterinary Institute, Beit Dagan, Israel (A. Behar, O. Izhaki, A. Rot, M. Leszkowicz-Mazuz, J. Brenner); Veterinary Field Services, Beit Dagan, Israel (T. Benor, M. Yankilevich)

RNA segment from SATV and the small (S) and large (L) RNA segments from SHAV, probably as a result of co-infection of these viruses in either *Culicoides* vectors or the ruminant hosts (*1,9,10*).

Once SBV emerged in Europe, it was clear to our team in Israel that this virus was either already present in Israel or would be introduced in the future. After AKAV and SHUV outbreaks (*3,11*) and virus neutralization test assays showing the additional presence of SATV, SHAV, and PEAV in Israel (*12*), a systematic monitoring system for arboviruses was established in 2015. Serum samples and vectors are collected every month from 13 selected dairy farms representing different geographic regions in Israel (Figure). Specific PEAV, SHUV, and SATV RNA fragments were also detected by nested quantitative PCR (qPCR) from different *Culicoides* species during 2015–2017 (*13*). Furthermore, in 2017, RNA fragments of a specific PEAV were detected in the cerebrospinal fluid (CSF) and testicles of a malformed calf exhibiting hydranencephaly (*14*). SBV was not found in all the studies conducted during 2011–2017, nor was it detected passively in Israel (*3,11–14*). We report the detection of SBV RNA in Israel in both vectors and affected ruminants.

The Study

During June 2018–December 2019, we trapped 13 pools of *Culicoides imicola*, 8 pools of *C. oxystoma*, 5 pools of *C. puncticollis*, and 5 pools of *C. newsteadii* midges (each pool containing 50 midges) around livestock farms, and we tested CSF from 3 malformed 1-day-old lambs (born on July 3, 2019) and 1 malformed 11-day-old calf (born on November 1, 2019) (Figure; Appendix, https://wwwnc.cdc.gov/EID/article/27/8/20-3705-App1.pdf). We extracted RNA from *Culicoides* homogenates and CSF using Maxwell 16 Viral Total Nucleic Acid Purification Kit (Promega, https://www.promega.com) according to the manufacturer's instructions. We used total viral nucleic acids (0.4 µg) for cDNA synthesis

Figure. Locations and types of farms sampled in study of Schmallenberg virus (SBV), Israel. Farm numbers match those listed in Table 2. Green, farms from which SBV-positive *Culicoides* pools were collected; red, farms on which SBV-positive malformed progeny were detected.

by UltraScript Reverse transcription (PCR Biosystems, https://www.promega.com) according to the manufacturer's instructions. We performed reverse transcription (RT) nested qPCR targeting the L RNA segment of Simbu serogroup viruses according to Behar et al. (*13*). We further subjected samples suspected of being Simbu serogroup positive to RT-nested and seminested PCRs performed using S, M, and L segment-specific primer sets (Table 1; Appendix).

Of the 31 species-specific pools from the 4 *Culicoides* midge species that are known or suspected to be vectors of Simbu serogroup viruses (i.e., *C. imicola*, *C. oxystoma*, *C. puncticollis*, *C. newsteadii*) (*2*,*12*,*15*), we found that 11 contained RNA of Simbu serogroup viruses in 2018 and 2019 (35% of the total pools tested) (Table 2; Figure; Appendix Table). We identified partial nucleotide sequences of the S (370/830 bp) and L (370/6,882 bp) segments. Phylogenetic analysis of the samples showed that all positive samples were virtually identical to SBV (GenBank accession nos. MT816474–82, MT816485–95) (Appendix Figure, panels A, C). These samples were collected from several different geographic regions in Israel (Table 2, lines 1 and 3–12 in the Samples column; Figure; Appendix Table). In addition, we detected SBV RNA-specific fragments of the S (370/850 bp), M (430/4,373 bp), and L segments (370/6,882 bp) in a CSF sample from a malformed lamb born in July 2019 on a farm in southern Israel (Negev desert) and a malformed calf born in November 2019 on a farm in northern Israel (Galilee) (GenBank accession nos. MT816472, MT816473, MT816483, MT816484, MT816496, MT816497) (Table 2, lines 2 and 13 in the Samples column; Appendix Figure).

In general, the most susceptible period for induction of congenital malformations by Simbu serogroup viruses is 65–70 days of gestation in lambs and 150 days of gestation in calves (*1*,*7*). Thus, SBV detection

Table 1. Primer sets used for the amplification of Schmallenberg virus RNA-specific fragments of the S, medium M, and L segments by reverse transcription nested PCR*

Segment	External primer sequence, 5′ → 3′	Internal primer sequence, 5′ → 3′	Expected product size, bp	Reference
S	AKAI206F: CAC AAC CAA GTG TCG ATC TTA	S_nestF: TGG TTA ATA ACC ATT TTC CCC A	370	External: (*4*); internal: this study
	SimbuS637: GAG AAT CCA GAT TTA GCC CA	S_nestR: GTC ATC CAY TST TCW GCA GTC A		
M	924F: CCG AAA ACA AGG AAA TTG TG	1899F: TAT AGT CCC TGG ATT AGG TC	430	Forward primers: (*8*); reverse primers: this study
	2331R: GGT TCA AAC ATC TCT AGG C	2331R: GGT TCA AAC ATC TCT AGG C		
L	SNL_F: GCA AAC CCA GAA TTT GYW GA	panOBV-L-2959 F: TTG GAG ART ATG ARG CTA ARA TGT G	370	External: this study; internal: (*6*)
	SNL_R: ATT SCC TTG NAR CCA RTT YC	panOBV-L-3274R: TGA GCA CTC CAT TTN GAC ATR TC		

*L, large; M, medium; S, small.

Table 2. Samples that tested positive for Schmallenberg virus by reverse transcription nested PCR, Israel*

Geographic region	Sample source	Collection date	Infected farm type (farm no.)
Golan Heights (latitude 34.1)	*Culicoides oxystoma* midge	2018 Sep	Beef cattle (1)
Galilee (latitude 32.7–33.5)	Malformed calf	2019 Nov	Beef cattle (2)†
Sharon plain (latitude 32.2)	*C. imicola* midge‡	2018 Jun	Beef cattle (3)§
	C. puncticollis midge	2018 Jun	Beef cattle (3)§
	C. newsteadii midge	2018 Jun	Beef cattle (3)§
	C. imicola midge	2018 Jul	Dairy cattle (4)
Interior plain (latitude 31.89)	*C. imicola* midge‡	2018 Nov	Small ruminant farm (5)†§
	C. imicola midge	2018 Nov	Small ruminant farm (5)†§
	C. imicola midge‡	2019 Dec	Small ruminant farm (6)§
Coastal plain (latitude 31.89)	*C. oxystoma* midge	2018 Jun	Dairy cattle (7)
Negev desert (latitude 29.7–30.714)	*C. oxystoma* midge	2018 Nov	Small ruminant farm (8)§
	C. puncticollis midge	2019 Jul	Small ruminant farm (9)†¶
	Malformed lamb	2019 Jul	Small ruminant farm (9)†¶
South Jordan Valley (latitude 31.56)	NA	NA	NA

*NA, not applicable.
†Farms on which dams and ewes gave birth to stillborn and malformed neonates.
‡Samples were confirmed positive at Friedrich Loeffler Institute, Greifswald, Germany.
§Farms expecting a rate of 80%–85% prolificacy, but during calving season showed only 50%–65% prolificacy.
¶Sheep farm from which both insects and malformed lambs were sampled.

in the respective ruminants fits with viral infection in March–April 2019, suggesting exposure to SBV in Israel in early spring 2019. Nevertheless, reports on severe decline in progeny prolificacy, stillbirths, and malformed lambs were reported by farmers to the Veterinary Field Services from autumn 2018 through December 2019 (Table 2). The detection of SBV in *Culicoides* pools collected from several of those farms (Table 2, lines 3–5, 7–9, and 11–12 in the Sample column; Figure; Appendix Table) suggests that SBV might have been clinically affecting ruminants in Israel as early as June 2018.

Conclusions

Our results demonstrate the circulation of SBV outside Europe. Future studies are needed to determine the seroprevalence of SBV in the Middle East, because this information is essential for understanding the risk of SBV spread into countries in Asia. Because SATV is found in the Middle East (*12,13*), virus neutralization tests will probably not be able to properly distinguish between antibodies against SBV and those against SATV. Therefore, developing a competitive ELISA system using SBV-specific antibodies is crucial. Finally, the presence of both SATV and SBV in Israel provides a unique opportunity for comparative studies on possible cross-protection of SBV commercial vaccines between these viruses.

About the Author

Dr. Behar is a researcher working in the parasitology division of Kimron Veterinary Institute in Beit Dagan, Israel. She established and is running the arbovirus systematic monitoring system of the Israeli Veterinary Services. Her research interests include the interactions among bloodsucking insects, their microbiota, and the pathogens that they transmit.

References

1. De Regge N. Akabane, Aino and Schmallenberg virus—where do we stand and what do we know about the role of domestic ruminant hosts and *Culicoides* vectors in virus transmission and overwintering? Curr Opin Virol. 2017;27:15–30. https://doi.org/10.1016/j.coviro.2017.10.004
2. Sick F, Beer M, Kampen H, Wernike K. *Culicoides* biting midges—underestimated vectors for arboviruses of public health and veterinary importance. Viruses. 2019;11:376–94. https://doi.org/10.3390/v11040376
3. Brenner J, Rotenberg D, Jaakobi S, Stram Y, Guini-Rubinstein M, Menasherov S, et al. What can Akabane disease teach us about other arboviral diseases. Vet Ital. 2016;52:353–62. https://doi.org/10.12834/VetIt.547.2587.2
4. Hirashima Y, Kitahara S, Kato T, Shirafuji H, Tanaka S, Yanase T. Congenital malformations of calves infected with Shamonda virus, Southern Japan. Emerg Infect Dis. 2017;23:993–6. https://doi.org/10.3201/eid2306.161946
5. Yanase T, Murota K, Hayama Y. Endemic and emerging arboviruses in domestic ruminants in East Asia. Front Vet Sci. 2020;7:168. https://doi.org/10.3389/fvets.2020.00168
6. Steyn J, Motlou P, van Eeden C, Pretorius M, Stivaktas VI, Williams J, et al. Shuni virus in wildlife and nonequine domestic animals, South Africa. Emerg Infect Dis. 2020;26:1521–5. https://doi.org/10.3201/eid2607.190770
7. St George TD, Standfast HA. Simbu group viruses with teratogenic potential. In: Monath TP, editor. The arboviruses: epidemiology and ecology. Boca Raton (FL): CRC Press; 1989. p. 146–66.
8. Hoffmann B, Scheuch M, Höper D, Jungblut R, Holsteg M, Schirrmeier H, et al. Novel orthobunyavirus in cattle, Europe,

2011. Emerg Infect Dis. 2012;18:469–72. https://doi.org/10.3201/eid1803.111905

9. Yanase T, Kato T, Aizawa M, Shuto Y, Shirafuji H, Yamakawa M, et al. Genetic reassortment between Sathuperi and Shamonda viruses of the genus Orthobunyavirus in nature: implications for their genetic relationship to Schmallenberg virus. Arch Virol. 2012;157:1611–6. https://doi.org/10.1007/s00705-012-1341-8

10. Coupeau D, Bayrou C, Baillieux P, Marichal A, Lenaerts AC, Caty C, et al. Host-dependence of in vitro reassortment dynamics among the Sathuperi and Shamonda simbuviruses. Emerg Microbes Infect. 2019;8:381–95. https://doi.org/10.1080/22221751.2019.1586410

11. Golender N, Brenner J, Valdman M, Khinich Y, Bumbarov V, Panshin A, et al. Malformations caused by Shuni virus in ruminants, Israel, 2014–2015. Emerg Infect Dis. 2015;21:2267–8. https://doi.org/10.3201/eid2112.150804

12. Brenner J, Yanase T, Kato T, Yaakobi S, Khinich E, Paz R, et al. Serological evidence suggests that several Simbu serogroup viruses circulated in Israel. Vet Ital. 2019;55:81–9.

13. Behar A, Rot A, Lavon Y, Izhaki O, Gur N, Brenner J. Seasonal and spatial variation in Culicoides community structure and their potential role in transmitting Simbu serogroup viruses in Israel. Transbound Emerg Dis. 2020;67:1222–30. https://doi.org/10.1111/tbed.13457

14. Behar A, Leibovich BB, Edery N, Yanase T, Brenner J. First genomic detection of Peaton virus in a calf with hydranencephaly in Israel. Vet Med Sci. 2019;5:87–92. https://doi.org/10.1002/vms3.129

15. Kato T, Shirafuji H, Tanaka S, Sato M, Yamakawa M, Tsuda T, et al. Bovine arboviruses in Culicoides biting midges and sentinel cattle in southern Japan from 2003 to 2013. Transbound Emerg Dis. 2016;63:e160–72. https://doi.org/10.1111/tbed.12324

Address for correspondence: Adi Behar, Department of Parasitology, Kimron Veterinary Institute, PO Box 12, Beit Dagan 50250, Israel; email: adib@moag.gov.il, adibehar@gmail.com.

EMERGING INFECTIOUS DISEASES®

Parasitic Disease Surveillance, Mississippi, USA

Richard S. Bradbury,[1] Meredith Lane, Irene Arguello, Sukwan Handali,
Gretchen Cooley, Nils Pilotte, John M. Williams, Sam Jameson, Susan P. Montgomery,
Kathryn Hellmann, Michelle Tharp, Lisa Haynie, Regina Galloway, Bruce Brackin,
Brian Kirmse, Lisa Stempak, Paul Byers, Steven Williams, Fazlay Faruque, Charlotte V. Hobbs[1]

Surveillance for soil-transmitted helminths, strongyloidiasis, cryptosporidiosis, and giardiasis was conducted in Mississippi, USA. PCR performed on 224 fecal samples for all soil-transmitted helminths and on 370 samples for only *Necator americanus* and *Strongyloides stercoralis* identified 1 *S. stercoralis* infection. Seroprevalences were 8.8% for *Toxocara*, 27.4% for *Cryptosporidium*, 5.7% for *Giardia*, and 0.2% for *Strongyloides* parasites.

Human populations in the state of Mississippi and the rest of the southeastern United States have historically been at risk for hookworm and other parasitic diseases (*1,2*). With improved sanitation and economic development, soil-transmitted helminths (STH), including the species *Ascaris lumbricoides* and *Trichuris trichiura*, were presumed to have been eliminated. However, a recent report of continued hookworm and strongyloidiasis transmission in a community without access to proper sanitation in Alabama, USA, has challenged this assumption (*3*).

The Study

To investigate the current prevalence of these infections, we conducted a pilot study to identify STH and other potentially endemic parasitic infections in convenience samples of specimens collected from patients in Mississippi. We deidentified fresh fecal samples submitted for diagnostic testing from

Author affiliations: Centers for Disease Control and Prevention, Atlanta, Georgia, USA (R.S. Bradbury, M. Lane, S. Handali, G. Cooley, S.P. Montgomery); Synergy America, Inc., Atlanta (M. Lane); University of Mississippi Medical Center, Jackson, Mississippi, USA (I. Arguello, J.M. Williams, S. Jameson, K. Hellmann, M. Tharp, L. Haynie, R. Galloway, B. Kirmse, L. Stempak, F. Faruque, C.V. Hobbs); Smith College, North Hampton, Massachusetts, USA (N. Pilotte, S. Williams); Mississippi State Department of Health, Jackson (B. Brackin, P. Byers)

patients at the University of Mississippi Medical Center (UMMC; Jackson, Mississippi, USA) during March 30, 2017–February 22, 2018, and serum samples submitted during October 28, 2017–March 29, 2018. This study was approved by the UMMC Institutional Review Board; the Centers for Disease Control and Prevention (CDC) was determined to be nonengaged and therefore did not undertake a separate institutional review board review.

We froze two 250-mg aliquots of feces for later DNA extraction. Where sample volume allowed, we performed microscopic examination using the saturated salt (specific gravity 1.2) passive flotation method as previously described (*4*). We extracted DNA by using the SurePrep Soil DNA isolation kit (ThermoFisher, https://www.thermofisher.com) after conducting initial bead beating for 3 minutes using zirconium beads. We stored DNA extracts at −80°C and sent them to the CDC for real-time PCR analysis. At CDC, each sample was initially tested for inhibition and poor DNA extraction by a real-time PCR assay targeting the human cytochrome B gene (*5*). Samples positive by this inhibition and extraction control were then tested by multiparallel real-time PCR for STH (*6*). A cycle threshold (C_t) ≤ 35 was considered to represent a positive result. Any positive PCR results were confirmed by duplicate testing.

We froze the deidentified serum samples at –80°C and sent them to CDC, where they were tested for antibodies to *Toxocara* spp., *S. stercoralis*, *Cryptosporidium* spp., and *G. duodenalis* using MAGPIX multiplex serology (ThermoFisher) (Appendix, https://wwwnc.cdc.gov/EID/article/27/8/20-4318-App1.pdf) to detect evidence of prior exposure. For statistical calculations, we used Excel (Microsoft, https://www.microsoft.com) and R version 3.3.1 (https://www.r-project.org).

Table 1. Results of microscopic examination and real-time PCR testing for soil-transmitted helminth and *Strongyloides stercoralis* infection on postdiagnostic fecal samples from patients at University of Mississippi Medical Center, Jackson, Mississippi, USA*

Method	Inhibition and extraction control	*S. stercoralis*	*Necator americanus*	*Ascaris lumbricoides*	*Trichuris trichiura*	*Ancylostoma* spp.	Other parasite species
Saturated salt centrifugal flotation	NA	0/507 (0)	0/507 (0)	0/507 (0)	0/507 (0)	0/507 (0)	0/507 (0)
Real-time PCR	594/631 (94.1)	1/594 (0.2)	0/594 (0)	0/224 (0)	0/224 (0)	0/224 (0)	NA
*Values are no. (%) unless indicated. NA, not applicable.							

A total of 650 fecal samples were obtained from UMMC patients. The median age of patients providing fecal samples for this analysis was 56 years (range 2–95 years). We obtained samples sufficient to perform saturated salt centrifugal flotation on 507 samples (80%). We found no samples to contain helminth eggs or larvae. Sufficient sample for DNA extraction was available for 631 (99.5%) samples. Of these fecal DNA extracts, a negative inhibition and extraction control excluded 37 samples. We tested 224 DNA extracts for *Ancylostoma* spp., *N. americanus*, *S. stercoralis*, *A. lumbricoides*, and *T. trichiura* by real-time PCR. (Table 1)

Because prior work in Alabama (*3*) detected only *N. americanus* and *S. stercoralis* infections, we screened an additional 370 DNA extracts for these helminths only. Of these 370 samples, 2 DNA extracts yielded positive amplicons for *S. stercoralis*

(C_t 29.57 and 30.48). The first of these samples (C_t 29.57) yielded no amplification curve on repeat testing and was interpreted as representing an initial false-positive result. The second sample (C_t 30.48) was positive upon confirmatory retesting (C_t 28.52 and 30.49). (Table 1)

A total of 1,960 postdiagnostic serum samples from Mississippi residents were available for multiplex serologic testing. The median age of patients providing serum samples for this analysis was 38 years (range 0–94 years). Of the 1,960 samples, 646 (33.0%) reacted with the Cp17 antigen of *C. parvum* (range 87–48,448 mean fluorescence intensity [MFI]), and 1,076 (54.9%) reacted with Cp23 (range 377–56,727 MFI). Of those samples, 538 (27.4%) reacted with both *C. parvum* antigens (Figure 1, panel A), suggesting prior *Cryptosporidium* species infection. A total of
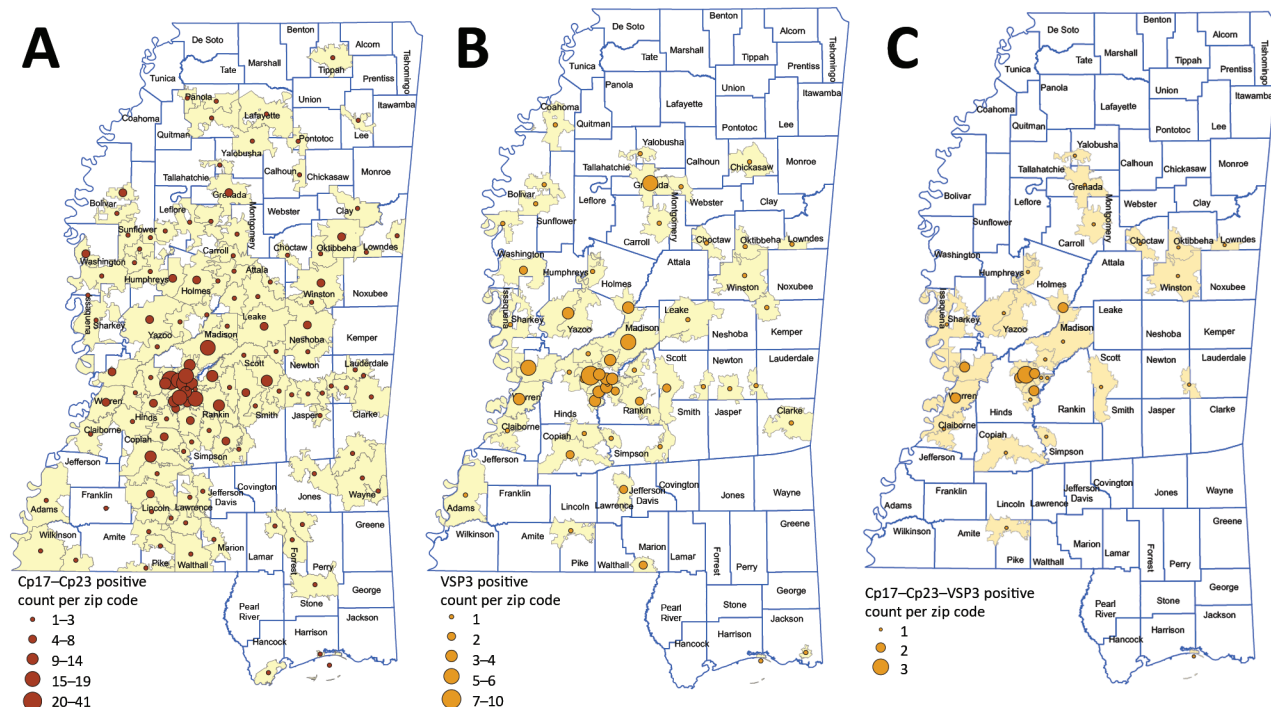
Figure 1. Places of residence of participants with antibody levels suggesting prior exposure to *Cryptosporidium* spp. Cp17 and Cp23 (n = 538) (A), *Giardia duodenalis* VSP3 (n = 111) (B), and *Cryptosporidium* spp. Cp17 and Cp23 and *Giardia duodenalis* VSP3 (combined) (n = 38) (C), Mississippi, USA. All serologic assays were performed using MAGPIX multiplex recombinant antigen beads (ThermoFisher, https://www.thermofisher.com) on convenience serum samples collected at the University of Mississippi Medical Center (Jackson, MS, USA) during October 28, 2017–March 29, 2018.

Table 2. Results of multiplex serologic testing for antibodies suggesting prior exposure to *Toxocara* spp., *Giardia duodenalis*, and *Cryptosporidium* spp. on 1,960 postdiagnostic serum samples from patients at University of Mississippi Medical Center, Jackson, Mississippi, USA*

Parasite antigen used						
Toxocara spp. Tc-CTL-1	*S. stercoralis* rSs-NIE-1 plus CrAg-ELISA†	*G. duodenalis* VSP3	*C. parvum* Cp17	*C. parvum* Cp23	*C. parvum* Cp17 + Cp23‡	*C. parvum* Cp17 + Cp23 and *G. duodenalis* VSP3
172 (8.8)	4 (0.2)	111 (5.7)	646 (33.0)	1,076 (54.9)	538 (27.4)	38 (1.9)

*All values are no. (%).
†8 samples were found to be positive by the rSs-NIE-1 MAGPIX multiplex serologic assay (ThermoFisher, https://www.thermofisher.com), but only 4 reacted in the confirmatory *S. stercoralis* crude L3 larval antigen (CrAg) ELISA.
‡Only samples reactive to both Cp17 and Cp23 were considered positive for *Cryptosporidium* spp. exposure.

111 samples (5.7%) reacted with the *G. duodenalis* VSP3 antigen (range 84–48,547 MFI) (Figure 1, panel B). A total of 38 (1.9%) samples contained antibodies to the Cp17, Cp23 and VSP3 antigens (Figure 1, panel C), demonstrating prior exposure to both *Cryptosporidium* and *G. duodenalis* infections. A total of 172 (8.8%) samples contained antibodies to *Toxocara* spp. Tc-CTL-1 antigen (range 23.2–33,814 MFI) (Table 2; Figure 2, panel A). When *Toxocara*-seropositive participants ≤6 years of age were excluded, 167/1,814 (9.2%) of UMMC patient samples were seropositive. A total of 9 (0.4%) samples contained antibodies reacting with the recombinant *S. stercoralis* NIE-1 antigen (range 16.2–11248 MFI) in MAGPIX serologic testing, of which 4 (0.2%) were positive in the confirmatory *S. stercoralis* CrAg-ELISA (range 9.94–57.7 IU/mL) (Figure 2, panel B).

Conclusions

The results of this limited pilot study suggest a low prevalence of STH infections in Mississippi but that rare infections with *S. stercoralis* might be found in Mississippi residents. The single case confirmed by real-time PCR tests likely represents active infection. Because >80% of patients with strongyloidiasis serorevert within 18 months after successful treatment (7), the 4 confirmed antibody-positive serum samples also likely represent active cases of strongyloidiasis. No linked immigration or travel history data on patients providing these samples were available, so whether these infections were acquired within the United States is unknown. Combined with the recent finding of strongyloidiasis in a rural community from Alabama (3), these data should encourage more focused sampling of areas with poor sanitation and
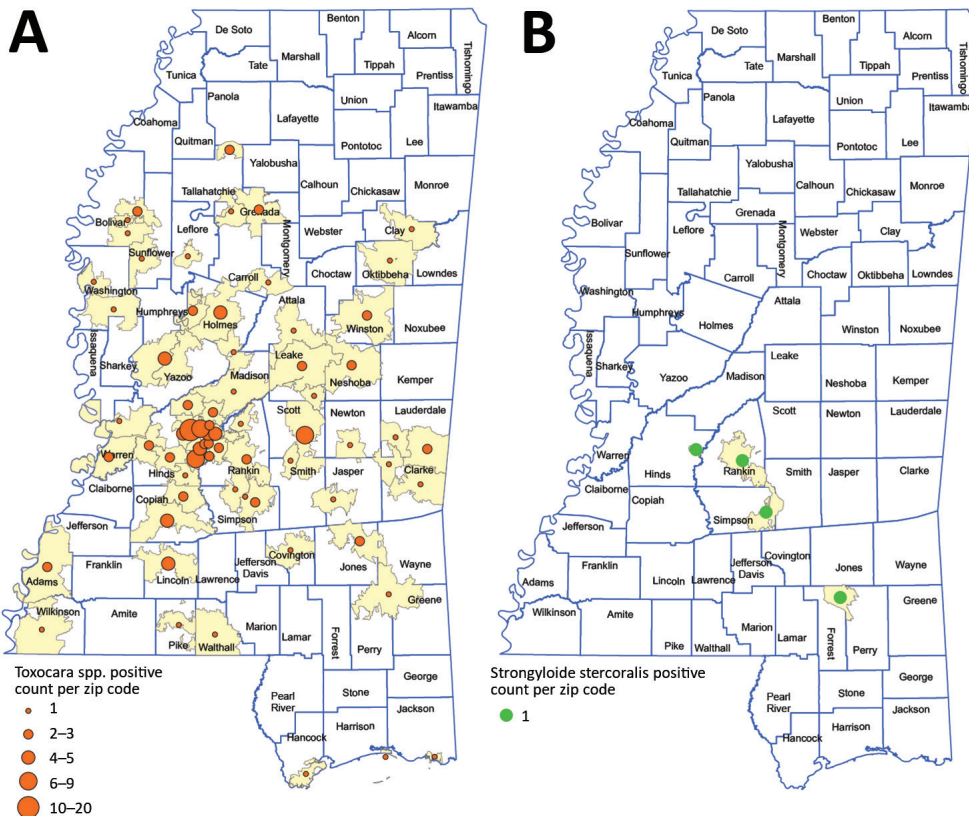
Figure 2. Places of residence of participants with antibody levels suggesting prior exposure to *Toxocara* spp. Tc-CTL-1 (n = 172) (A) and *Strongyloides stercoralis* Ss-NIE-1 (n = 4) (B), Mississippi, USA. All serologic assays were performed using MAGPIX multiplex recombinant antigen beads (ThermoFisher, https://www.thermofisher.com) on convenience serum samples collected at the University of Mississippi Medical Center (Jackson, MS, USA) during October 28, 2017–March 29, 2018. Only those samples confirmed by a subsequent *S. stercoralis* crude L3 larval antigen (CrAg) ELISA are included.

hygiene, high levels of poverty, and poor access to healthcare for potential residual foci of endemic STH and strongyloidiasis transmission in Mississippi and the wider southeastern United States.

The total *Toxocara* spp. seroprevalence in all participants in this study was 8.8%, which is higher than the average prevalence reported by the most recent National Health and Nutrition Examination Survey study (*8*). Although these results are not directly comparable because of different sampling methods, the potentially high *Toxocara* spp. seroprevalence in Mississippi warrants further investigation.

The seroprevalence results of this study suggest that prior exposure to *Cryptosporidium* spp. is common in Mississippi. Only 5.7% of the postdiagnostic serum samples were found to have serologic evidence of prior exposure to *G. duodenalis* infection. A small number of samples (1.9%) contained antibodies reacting with the 3 antigens Cp17, Cp23, and VSP3, indicating prior exposure to *Cryptosporidium* spp. and *G. duodenalis* infection. Further investigation of the epidemiology of waterborne protozoan infection in Mississippi, including determination of the actual prevalence and distribution using systematic sampling and determination of the species and subtypes infecting persons, is warranted.

The absence of any positive findings by microscopic examination or PCR for the STH suggests that such infections are uncommon in the general Mississippi population. We found high seroprevalence of antibodies to *Toxocara* spp. in Mississippi. Although this finding could indicate increased exposure to this infectious agent compared with the national average, our data do not enable determination of the sources of increased infection or overall annual incidence of disease. Further studies on the epidemiology and prevalence of parasitic diseases in the state of Mississippi are indicated.

In conclusion, this convenience sampling study did not find evidence of high STH prevalence in Mississippi. However, we did identify several likely current cases of strongyloidiasis and relatively high rates of *Toxocara* exposure. We recommend further investigation with larger sample sizes to more clearly define the true extent of STH infection in this region.

About the Author

Dr. Bradbury is a senior lecturer in microbiology and molecular biology at Federation University in Berwick, Victoria, Australia, and is a microbiologist with expertise in laboratory diagnostics and parasitic diseases. His research interests include strongyloidiasis, soil-transmitted helminths, zoonoses, and emerging parasitic diseases. Dr. Hobbs is a professor of pediatric infectious disease and attending physician at Children's of Mississippi, University of Mississippi Medical Center, Jackson, Mississippi, USA. Her research interests include parasitic diseases in children in resource-limited settings.

References

1. Elman C, McGuire RA, Wittman B. Extending public health: the Rockefeller Sanitary Commission and hookworm in the American South. Am J Public Health. 2014;104:47–58. https://doi.org/10.2105/AJPH.2013.301472
2. Stiles, CW. Report upon the prevalence and geographic distribution of hookworm disease (uncinariasis or anchylostomiasis) in the United States. Washington: US Government Printing Office; 1903.
3. McKenna ML, McAtee S, Bryan PE, Jeun R, Ward T, Kraus J, et al. Human intestinal parasite burden and poor sanitation in rural Alabama. Am J Trop Med Hyg. 2017;97:1623–8. https://doi.org/10.4269/ajtmh.17-0396
4. Gillespie S, Bradbury RS. A survey of intestinal parasites of domestic dogs in central Queensland. Trop Med Infect Dis. 2017;2:60. https://doi.org/10.3390/tropicalmed2040060
5. Bradbury RS, Arguello I, Lane M, Cooley G, Handali S, Dimitrova SD, et al. Parasitic infection surveillance in Mississippi Delta children. Am J Trop Med Hyg. 2020;103:1150–3. https://doi.org/10.4269/ajtmh.20-0026
6. Pilotte N, Papaiakovou M, Grant JR, Bierwert LA, Llewellyn S, McCarthy JS, et al. Improved PCR-based detection of soil transmitted helminth infections using a next-generation sequencing approach to assay design. PLoS Negl Trop Dis. 2016;10:e0004578. https://doi.org/10.1371/journal.pntd.0004578
7. Kearns TM, Currie BJ, Cheng AC, McCarthy J, Carapetis JR, Holt DC, et al. *Strongyloides* seroprevalence before and after an ivermectin mass drug administration in a remote Australian aboriginal community. PLoS Negl Trop Dis. 2017;11:e0005607. https://doi.org/10.1371/journal.pntd.0005607
8. Liu EW, Chastain HM, Shin SH, Wiegand RE, Kruszon-Moran D, Handali S, et al. Seroprevalence of antibodies to *Toxocara* species in the United States and associated risk factors, 2011–2014. Clin Infect Dis. 2018;66:206–12. https://doi.org/10.1093/cid/cix784

Address for correspondence: Richard S. Bradbury, School of Health and Life Sciences, Federation University, Berwick, 3806, VIC, Australia; email: r.bradbury@federation.edu.au; Charlotte V. Hobbs, Department of Pediatrics, Division of Infectious Disease, Department of Microbiology, University of Mississippi Medical Center, Batson Children's Hospital, 2500 N State St, Jackson, MS 39216, USA; email: chobbs@umc.edu

Screening for Q Fever in Patients Undergoing Transcatheter Aortic Valve Implantation, Israel, June 2018–May 2020

Nesrin Ghanem-Zoubi, Mical Paul, Moran Szwarcwort, Yoram Agmon, Arthur Kerner

Q fever infective endocarditis frequently mimics degenerative valvular disease. We tested for *Coxiella burnettii* antibodies in 155 patients in Israel who underwent transcatheter aortic valve implantation. Q fever infective endocarditis was diagnosed and treated in 4 (2.6%) patients; follow-up at a median 12 months after valve implantation indicated preserved prosthetic valvular function.

Q fever is a zoonotic infection caused by the bacterium *Coxiella burnettii* that occurs worldwide. Q fever has been endemic in Israel for many years; several superimposed outbreaks have occurred in the past 2 decades (*1–3*).

A clinical observation of 2 patients with severe prosthetic Q fever infective endocarditis (IE) diagnosed several months after transcatheter aortic valve implantation (TAVI) indicated that Q fever IE could have been the underlying valve disease but was not detected before TAVI. We considered this possibility, because Q fever IE typically manifests as a chronic disease, frequently in the absence of fever and inflammatory markers, as well as absent or small fine vegetations (*4,5*).

Considering the epidemiology of Q fever in Israel and the ominous prognosis of Q fever endocarditis after TAVI, we began routine screening of patients undergoing TAVI for antibodies to *C. burnettii* to identify and treat Q fever IE as soon as possible after TAVI. In this study, we review a 2-year period of serologic screening and discuss the value of Q fever screening in this setting.

The Study

Beginning in June 2018, serologic screening for Q fever was ordered for all patients admitted for TAVI

Author affiliations: Rambam Health Care Campus, Haifa, Israel (N. Ghanem-Zoubi, M. Paul, M. Szwarcwort, Y. Agmon, A. Kerner); Technion–Israel Institute of Technology, Haifa (N. Ghanem-Zoubi, M. Paul, Y. Agmon, A. Kerner)

at Rambam Health Care Campus, a 960-bed primary and tertiary university-affiliated hospital in northern Israel. We tested serum samples for *C. burnettii* phase 2 IgM and phase I or phase II IgG by using ELISA (Institute Virion/Serion GmbH, https://www.virion-serion.de). For samples that tested positive, we then conducted an indirect immunofluorescence assay (IFA) for confirmation and titer determination. We performed the IFA locally using a commercial kit (Focus Diagnostics, https://www.focusdx.com) or an in-house test at The National Reference Laboratory for Rickettsiosis (Nes Ziona, Israel). An infectious diseases specialist evaluated patients with positive IgG for *C. burnettii* chronic infection. IE was diagnosed according to the modified Duke criteria (*6*) or the Dutch consensus guidelines of chronic Q fever infection (*7*) with an IFA phase I IgG of $\geq$800. Patients began treatment and follow-up was conducted at the infectious disease and cardiology outpatient clinics. Diagnostic testing was performed as a part of a clinical routine, and anonymous data collection was approved by the hospital's ethics committee with a waiver of informed consent.

During June 1, 2018–May 31, 2020, a total of 197 TAVI procedures were performed at Rambam Health Care Campus. Serologic testing for Q fever was conducted in 155 patients. Nine patients tested positive for $\geq$1 Q fever IgG by ELISA: 7 had phase I IgG and 2 patients had only phase II IgG. On IFA, 4 patients (2.6%) had a phase I IgG titer of >800 and were further evaluated for Q fever IE (Table). All 4 patients had underlying conditions, but none had fever or vegetations on echocardiography. None of the patients had a specific high-risk exposure for Q fever. We recommended treatment with doxycycline and hydroxychloroquine for $\geq$24 months (as recommended for Q fever IE in the presence of prosthetic valve). In 3 of 4 patients, treatment was modified to an alternative regimen because of intolerance or side effects. We did not perform

Table. Characteristics of identified patients with Q fever infective endocarditis, Israel, June 1, 2018–May 31, 2020*

Variable	Patient 1	Patient 2	Patient 3	Patient 4
Age, y/sex	77/M	52/F	73/F	79/M
Underlying conditions	Hypertension, CAD, s/p CABG, and AVR (7 y)	s/p Hodgkin lymphoma (30 y), DM, CAD, and s/p CABG (8 y)	Scleroderma	DM, hypertension, asthma
Habitat/exposure risk factor†	Urban/none	Urban/none	Urban/none	Urban/none
Indication for TAVI	Symptomatic aortic insufficiency, NYHA 3/4	Symptomatic aortic stenosis and insufficiency (moderate to severe); chest pain and dyspnea with minimal effort	Symptomatic severe aortic stenosis; recurrent syncope	Symptomatic severe aortic stenosis, NYHA 3/4
Echo findings before TAVI	Moderate aortic stenosis and severe regurgitation with thickened leaflets	Severe aortic stenosis	Severe aortic stenosis with severe calcifications and moderate mitral regurgitation with leaflets sclerosis	Severe aortic stenosis
Coxiella burnettii phase I IgG	1:32,00	1:25,600	1:3,200	1:1,024
C. burnettii PCR in blood	Not performed	Not performed	Negative	Not performed
Q fever IE according to modified Duke criteria	Possible	Possible	Possible	Possible
Q fever IE according to Dutch consensus guidelines	Probable	Probable	Probable	Probable
Treatment	Doxycycline and hydroxychloroquine, changed to doxycycline and ciprofloxacin	Doxycycline and hydroxychloroquine, changed to doxycyline monotherapy	Doxycycline and hydroxychloroquine, changed to ciprofloxacin	Doxycycline and hydroxychloroquine
Timing of and status at last follow-up	18 mo, asymptomatic, preserved valve function, and stable serologic results	8 mo, asymptomatic, preserved valve function, and stable serologic results	12 mo, severe fatigue, preserved aortic valve function, and stable serologic results	12 mo, asymptomatic, preserved valve function, and decreasing serologic results

*AVR, aortic valve replacement; CABG, coronary artery bypass grafting; CAD, coronary artery disease; DM, diabetes mellitus; IE, infective endocarditis; NYHA, New York Heart Association (classification); s/p, status post; TAVI, transcatheter aortic valve implantation.
†Risk factors for Q fever are employment as a veterinarian, farmer, abattoir worker, or any contact with farm animals.

fluorodeoxyglucose positron emission tomography-computed tomography for diagnosis, because it would not have led to a change in management. Patient 2 underwent fluorodeoxyglucose positron emission tomography–computed tomography 2 months before TAVI as part of lymphoma follow-up; it showed no evidence of pathologic uptake in the valve or elsewhere. As of the last follow-up visit (median 12 months, range 8–18 months), all 4 patients had preserved prosthetic valve function, and none experienced symptomatic Q fever infection. One patient reported severe fatigue, likely related to underlying scleroderma.

Conclusions

During a 2-year period of routine serologic screening for Q fever among patients undergoing TAVI, we identified 4 case-patients with Q fever IE, affecting 2.6% of patients screened. None of the 4 case-patients experienced fever or echocardiographic findings that were suggestive of IE.

Diagnosing Q fever IE can be challenging, especially in the absence of tissue samples, as in the case of patients undergoing TAVI. Several studies have highlighted the difficulties of the diagnosis of Q fever IE (Appendix Table 1). The diagnostic criteria used in the absence of tissue samples are based on the modified Duke criteria (6), the Dutch consensus guidelines for chronic Q fever (7), and the recently revised definition of "persistent *C. burnettii* infection" by Melenotte et al. (8) (Appendix Table 2). For definitive diagnosis, all 3 definitions are based mainly on serologic tests and echocardiography, PET, or CT findings to prove valve infection. Both imaging modalities have poor sensitivity in the case of *C. burnettii* IE (9–11). The alternative minor diagnostic criteria consist also of infrequent findings, such as embolic and immunologic phenomena. We recommended treatment for patients with possible or probable IE (Table), recognizing the significant consequences of a delayed diagnosis and treatment of prosthetic Q fever IE among patients at very high risk for surgery a priori.

In a study conducted in 2 centers in the United Kingdom, routine serologic screening for Q fever before valve surgery was performed in 139 patients. In this low-endemicity setting, no patient with Q fever IE was identified (12). In our study conducted in a Q fever–endemic region, the yield of such a strategy seems clinically significant. The incidence of Q fever in Israel according to reported cases to the Ministry of Health

is ≈2.2/100,000 population (https://www.health.gov.il/UnitsOffice/HD/PH/epidemiology/Pages/epidemiology_report.aspx). In comparison, data from countries in the European Union from 2018 showed the highest incidence was 0.7/100,000 population in Spain. An alternative indicator of Q fever endemicity is the percentage of IE caused by Q fever out of all IE cases. According to the International Collaboration on Endocarditis registry data, *C. burnettii* was responsible for almost 1% of all IE cases in 25 countries (*13*). This rate reaches almost 5% in Q fever–endemic regions, such as southern France (*14*). A similar rate was observed at our hospital; Q fever IE was diagnosed in 5 (5.3%) of 95 cases of definitive IE during 2013–2016, according to local data from a prospective registry.

The primary limitation of our study is that, as a single-center study, it reflects the epidemiology of a limited geographic area. The short-term follow-up of patients with Q fever IE does not enable a description of the long-term benefit of our strategy. We did not evaluate the cost-effectiveness of our surveillance strategy. In addition, we might have missed cases of Q fever IE by conducting serologic screening only, since Q fever IE with low phase I IgG titers (<800) (*9*) or even negative serologic results (*15*) has been described. Nevertheless, as a screening strategy, serologic testing seems to be sufficient. Early diagnosis and appropriate treatment as soon as possible after prosthetic valve implantation contributed substantially to preserve valve function and prevented potential ongoing infection. Therefore, we suggest screening for Q fever in TAVI patients in settings in which Q fever incidence is >0.5 per 100,000 (nationally or in Q fever–endemic regions within countries), after Q fever outbreaks regardless of baseline incidence, or in places in which Q fever causes >2% of all cases of IE.

About the Author

Dr. Ghanem-Zoubi is an infectious diseases and internal medicine specialist; deputy director of the Infectious Diseases Institute, Rambam Health Care Campus, Haifa, Israel; and, with others, leads the endocarditis team at Rambam Health Care Campus. Her primary research interests in recent years have been infective endocarditis and zoonoses, including brucellosis and Q fever.

References

1. Steiner HA, Raveh D, Rudensky B, Paz E, Jerassi Z, Schlesinger Y, et al. Outbreak of Q fever among kitchen employees in an urban hospital. Eur J Clin Microbiol Infect Dis. 2001;20:898–900. https://doi.org/10.1007/s10096-001-0641-9
2. Oren I, Kraoz Z, Hadani Y, Kassis I, Zaltzman-Bershadsky N, Finkelstein R. An outbreak of Q fever in an urban area in Israel. Eur J Clin Microbiol Infect Dis. 2005;24:338–41. https://doi.org/10.1007/s10096-005-1324-8
3. Amitai Z, Bromberg M, Bernstein M, Raveh D, Keysary A, David D, et al. A large Q fever outbreak in an urban school in central Israel. Clin Infect Dis. 2010;50:1433–8. https://doi.org/10.1086/652442
4. Million M, Thuny F, Richet H, Raoult D. Long-term outcome of Q fever endocarditis: a 26-year personal survey. Lancet Infect Dis. 2010;10:527–35. https://doi.org/10.1016/S1473-3099(10)70135-3
5. Houpikian P, Habib G, Mesana T, Raoult D. Changing clinical presentation of Q fever endocarditis. Clin Infect Dis. 2002;34:E28–31. https://doi.org/10.1086/338873
6. Li JS, Sexton DJ, Mick N, Nettles R, Fowler VG Jr, Ryan T, et al. Proposed modifications to the Duke criteria for the diagnosis of infective endocarditis. Clin Infect Dis. 2000;30:633–8. https://doi.org/10.1086/313753
7. Kampschreur LM, Wegdam-Blans MCA, Wever PC, Renders NHM, Delsing CE, Sprong T, et al.; Dutch Q Fever Consensus Group. Chronic Q fever diagnosis— consensus guideline versus expert opinion. Emerg Infect Dis. 2015;21:1183–8. https://doi.org/10.3201/eid2107.130955
8. Melenotte C, Protopopescu C, Million M, Edouard S, Carrieri MP, Eldin C, et al. Clinical features and complications of *Coxiella burnetii* infections from the French National Reference Center for Q Fever. JAMA Netw Open. 2018;1:e181580. https://doi.org/10.1001/jamanetworkopen.2018.1580
9. Melenotte C, Million M, Raoult D. New insights in *Coxiella burnetii* infection: diagnosis and therapeutic update. Expert Rev Anti Infect Ther. 2020;18:75–86. https://doi.org/10.1080/14787210.2020.1699055
10. Eldin C, Melenotte C, Million M, Cammilleri S, Sotto A, Elsendoorn A, et al. 18F-FDG PET/CT as a central tool in the shift from chronic Q fever to *Coxiella burnetii* persistent focalized infection: a consecutive case series. Medicine (Baltimore). 2016;95:e4287. https://doi.org/10.1097/MD.0000000000004287
11. Kouijzer IJE, Kampschreur LM, Wever PC, Hoekstra C, van Kasteren MEE, de Jager-Leclercq MGL, et al. The value of 18 F-FDG PET/CT in diagnosis and during follow-up in 273 patients with chronic Q fever. J Nucl Med. 2018;59:127–33. https://doi.org/10.2967/jnumed.117.192492
12. Seddon O, Ashrafi R, Duggan J, Rees R, Tan C, Williams J, et al. Seroprevalence of Q Fever in patients undergoing heart valve replacement surgery. J Heart Valve Dis. 2016;25:375–9.
13. Murdoch DR, Corey GR, Hoen B, Miró JM, Fowler VG Jr, Bayer AS, et al.; International Collaboration on Endocarditis-Prospective Cohort Study (ICE-PCS) Investigators. Clinical presentation, etiology, and outcome of infective endocarditis in the 21st century: the International Collaboration on Endocarditis-Prospective Cohort Study. Arch Intern Med. 2009;169:463–73. https://doi.org/10.1001/archinternmed.2008.603
14. Casalta JP, Gouriet F, Richet H, Thuny F, Habib G, Raoult D. Prevalence of Coxiella burnetii and Bartonella species as cases of infective endocarditis in Marseilles (1994-2007). Clin Microbiol Infect. 2009;15(Suppl 2):152–3. https://doi.org/10.1111/j.1469-0691.2008.02185.x
15. Melenotte C, Loukil A, Rico A, Lepidi H, Raoult D. Blood culture-negative cardiovascular infection in a patient with multiple sclerosis. Open Forum Infect Dis. 2019;6:ofz429. https://doi.org/10.1093/ofid/ofz429

Address for correspondence: Nesrin Ghanem-Zoubi, Infectious Diseases Institute, Rambam Health Care Campus, Ha-Aliya 8 St, Haifa 3109601, Israel; email: n_ghanem@rambam.health.gov.il

African Horse Sickness Virus Serotype 1 on Horse Farm, Thailand, 2020

Napawan Bunpapong, Kamonpan Charoenkul, Chanakarn Nasamran, Ekkapat Chamsai,
Kitikhun Udom, Supanat Boonyapisitsopa, Rachod Tantilertcharoen, Sawang Kesdangsakonwut,
Navapon Techakriengkrai, Sanipa Suradhat, Roongroje Thanawongnuwech, Alongkorn Amonsin

To investigate an outbreak of African horse sickness (AHS) on a horse farm in northeastern Thailand, we used whole-genome sequencing to detect and characterize the virus. The viruses belonged to serotype 1 and contained unique amino acids (95V,166S, 660I in virus capsid protein 2), suggesting a single virus introduction to Thailand.

African horse sickness virus (AHSV) is an RNA virus of the family *Reoviridae*, genus *Orbivirus*. AHSV can be classified into 9 serotypes according to virus capsid protein (VP) 2 (*1*). Serotypes 1–8 have been reported from restricted areas of sub-Saharan Africa only. Serotype 9 is more widespread and causes epidemics outside Africa. Serotype 4 caused outbreaks in Spain and Portugal during 1987–1990 (*2*).

In Thailand, the first AHS outbreak was reported in March 2020 in northeastern Thailand (*3–5*). AHS outbreaks have been reported in 17 provinces of Thailand, affecting ≈2,700 horses (Appendix Table 1, https://wwwnc.cdc.gov/EID/article/27/8/21-0004-App1.pdf) (*6*). We report a comprehensive outbreak investigation of emerging AHSV and whole-genome characterization of AHSV recovered from a horse farm in northeastern Thailand.

The Study

In March 2020, the Veterinary Diagnostic Laboratory at Chulalongkorn University (Bangkok, Thailand) was notified of unusual horse deaths on a recreational horse farm, which encompasses up to 6,400 m², in Nakhon Ratchasima Province, northeastern Thailand. A total of 49 horses (2 thoroughbred, 21 miniature, 26 native horses) were kept on free range. Other animals on the farm were 3 dogs, 3 rabbits, 3 pigs, and

Author affiliation: Chulalongkorn University, Bangkok, Thailand

8 peacocks. The outbreak investigation and sample collection were conducted under the approval of Institutional Animal Care and Use Committee protocol no. 2031050.

On March 20, 2020, the outbreak began when horses showed severe clinical signs including depression, fever, dyspnea, and subcutaneous edema in the temporal or supraorbital area, followed by sudden death within 48 hours. On March 28, we visited the horse farm, implemented insect-proof housing, and collected a blood sample from a horse with clinical signs (horse CU-1), which died the next day. We performed necropsies on 2 horse carcasses (CU-2 and CU-3) and collected 7 tissue samples. Gross lesions showed frothy exudate in the bronchial lumen and mild edema of the supraorbital sinus and conjunctiva. We observed intermuscular and perineural edema at the axillary region and subcutaneous muscle, periaortic edema, and subendocardial hemorrhage (Figure 1). Histopathologic slides showed congestion of the spleen, liver, lymph nodes, and lung; no other remarkable lesions were observed. The outbreak lasted 3 weeks and affected 30 horses (last case on April 10). On April 26, horses on the farm were vaccinated with polyvalent, live-attenuated AHSV vaccine (Ondersterpoort Biological Products, https://www.obpvaccines.co.za); no horses showed clinical signs after vaccination and implementation of insect-proof housing. In total, during the 3 weeks of the outbreak, the mortality rate for horses on the farm was 61.22% (30 deaths/49 horses) (Appendix Table 2). Mortality rates by breed were 100% (2/2) for thoroughbreds, 76.19% (16/21) for miniature horses, and 46.15% (12/26) for native horses. The same management practices were applied for horses of all breeds.

We visited the horse farm again on May 30 (1 month after vaccination) and August 1 (3 months after vaccination). From the remaining horses we collected 18 serum samples at each visit (total 36). All
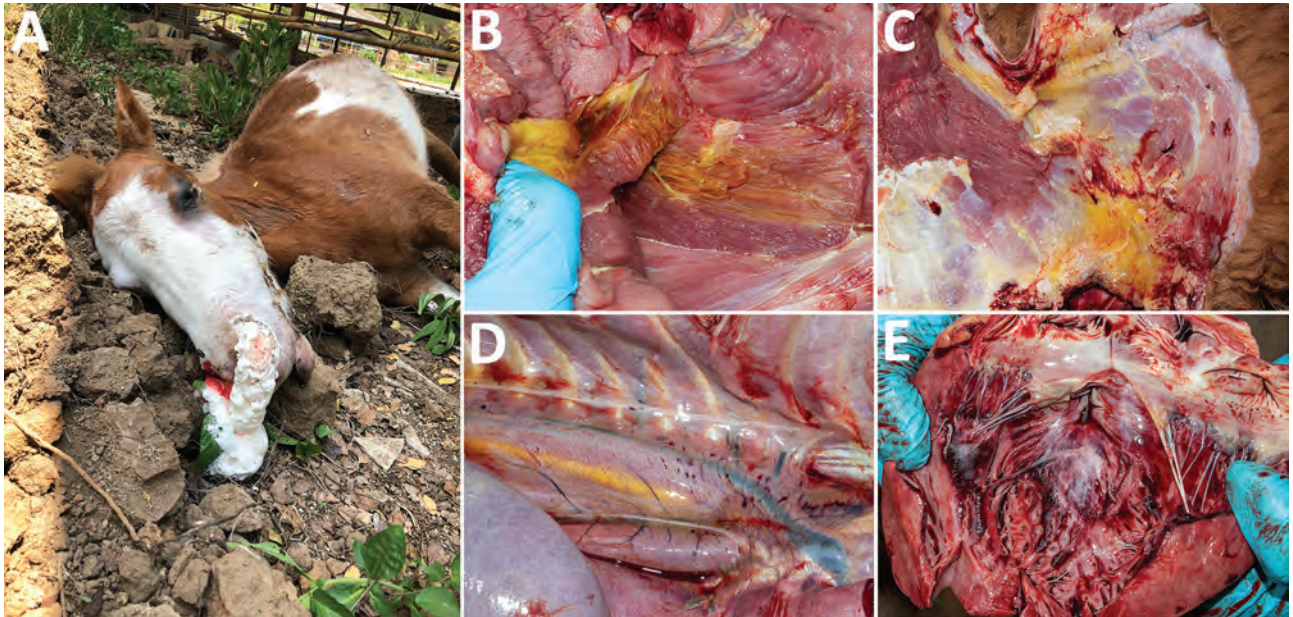
Figure 1. Gross lesions from horses affected by African horse sickness, Thailand, 2020. A) Mild edema at the supraorbital fossa with frothy exudate from the nostrils; B) yellow, gelatinous infiltrations and perineural edema of the intramuscular tissues; C) right axillary subcutaneous edema; D) periaortic edema and hemorrhage; E) subendocardial petechiae and ecchymoses of the heart.

samples were tested for antibodies against AHSV by blocking ELISA specific to VP7 (INgezim AHSV Compac Plus; Eurofins Technologies, https://ingenasa.eurofins-technologies.com) (Appendix). All 36 serum samples were positive for AHSV antibodies (Appendix Table 3).

To identify AHSV, we extracted viral RNA from 8 blood and tissue samples by using the GeneAll GENTi Viral DNA/RNA Extraction Kit (GeneAll, http://www.geneall.com). We performed real-time reverse transcription PCR (RT-PCR) with VP7 gene–specific primers and probes by using the SuperScript III Platinum One-Step qRT-PCR System (Thermo Fisher, https://www.thermofisher.com) (Appendix) (7). All 8 samples were positive for AHSV (cycle threshold 28.29–33.91). In detail, blood samples from horse CU-1; lymph nodes from CU-2; and lymph node, lung, spleen, heart, liver, and kidney samples from CU-3 were positive for AHSV (Appendix Table 4). To further characterize AHSV from Thailand, we performed VP2 gene-specific RT-PCR, which showed that the AHSVs from Thailand belong to AHSV serotype 1 (8). We next subjected the spleen from horse CU-3

to whole-genome sequencing and 2 additional viruses (from CU-1 and CU-2) to VP2 and nonstructural gene (NS) 3 gene sequencing (Table). We conducted whole-genome sequencing by amplifying viral fragments and sequencing by using MinION Oxford Nanopore technologies (https://nanoporetech.com) (Appendix Table 5) (9). The nucleotide sequences of the AHSVs from Thailand were submitted to GenBank (accession nos. MW387422–35). Nucleotide sequences of AHSV from Thailand were pairwise compared against those of vaccine and reference viruses. We found that the whole genome of Thailand AHSV (virus CU-3) possessed high nucleotide identities (99.40%–100%) to the reference Thailand AHSV-1 (110983/63 and TAI2020/01). For the VP2 gene, Thailand AHSV possessed 99.90% nucleotide identities among them; the highest nucleotide identity (99.90%) was to the reference Thailand AHSV-1 (110983/63 and TAI2020/01, 02, and 03). The nucleotide identities of VP2 between Thailand AHSV and the reference AHSV of serotypes 2–9 were low (54.60%–67.10%). For the NS3 gene, Thailand AHSV had 99.90% nucleotide identities; the highest nucleotide

Table. Characterization of African horse sickness virus isolated during study of African horse sickness on horse farm, Thailand, 2020*

| Virus | Host horse | | | Nucleotide sequences, GenBank accession nos. | | |
	Sex	Age	Breed	WGS	VP2	NS3
CU-1	F	3	Miniature	NA	MW387422	MW387423
CU-2	F	3	Miniature	NA	MW387424	MW387425
CU-3	F	2	Miniature	MW387426–35	MW387427	MW387435

*NA, not available; NS, nonstructural gene; VP, viral capsid protein; WGS, whole-genome sequences (10 segments).

identity was to the reference South Africa AHSV of clade gamma (97.10%–99.90%) (Appendix Table 6).

For phylogenetic analysis, we included the VP2 sequences of the Thailand AHSV and reference viruses (AHSV-1 vaccine strains and AHSV serotypes 1–9). For phylogenetic analysis of NS3, we included the NS3 sequences of Thailand AHSV and reference viruses of alpha, beta, and gamma clades. The maximum clade credibility trees for VP2 and NS3 genes were constructed by using BEAST 2.0 (https://beast.community) with the Bayesian Markov chain Monte Carlo algorithm (Appendix). Phylogenetic analysis of the VP2 gene showed that Thailand AHSV was clustered in AHSV serotype 1 but not in other clusters (serotypes 2–9). For NS3, the Thailand AHSVs were grouped within the gamma clade, similar to the references AHSV-1 and AHSV-2 (Figure 2). We analyzed amino acid determinants of VP2 and NS3 at 2 neutralizing epitopes (residues 321–339 and 377–400) (10). Thailand

AHSV had identical amino acids at positions 321–339 and 377–400 among Thailand AHSVs and some reference AHSV-1 but differed from the reference vaccine strains (HS29/62 and OBP-116). The deduced amino acids related to the virulence of AHSV at positions 357 of VP2 and 165–168 and 201 of NS3 were also analyzed (1,11). Thailand AHSV contained virulence-related amino acids at VP2–357N and NS3–201M, which were not observed in some reference AHSV-1 and AHSV vaccines (Appendix Table 7). Of note, all Thailand AHSVs contained unique amino acids at positions 95V, 166S, and 660I, suggesting a single introduction from the same AHSV ancestor into Thailand.

Conclusions

We speculate that AHSV serotype 1 potentially spread outside Africa from imported subclinically infected animals, such as zebras. The Thailand government implemented control measures to prevent further spread,
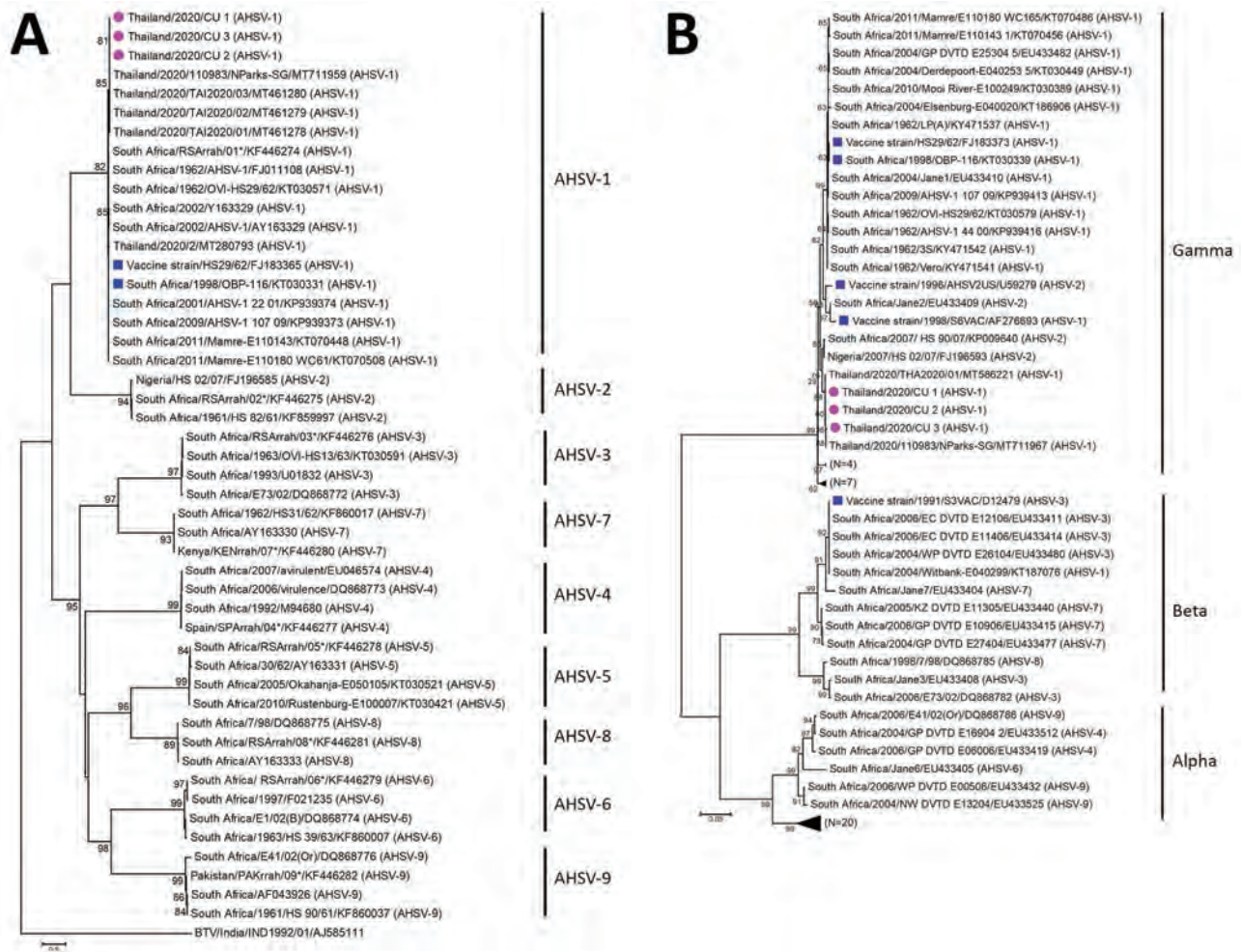
Figure 2. Phylogenetic trees for AHSV, Thailand, 2020. A) Viral capsid protein 2; B) nonstructural gene 3. Purple circles indicate Thailand AHSV characterized in this study; blue squares indicate AHSV vaccine strains; numbers after AHSV indicate serotypes. Scale bars indicate nucleotide substitutions per site. AHSV, African horse sickness virus.

including movement restrictions, quarantine, disinfection, and vector control. Moreover, to prevent spread in Thailand and neighboring countries, mass vaccination of equids with a live-attenuated AHSV vaccine was conducted. The AHSV from Thailand possessed unique amino acids, suggesting a single introduction of the virus to the country. This information will be useful for strategic planning for disease prevention and control, vaccine selection, and diagnostic assay development.

About the Author

Dr. Bunpapong is a PhD candidate at the Department of Veterinary Public Health and a senior veterinarian at the Veterinary Diagnostic Laboratory, Faculty of Veterinary Science, Chulalongkorn University, Bangkok, Thailand. Her research interests include emerging and reemerging infectious diseases in animals.

References

1. Potgieter AC, Wright IM, van Dijk AA. Consensus sequence of 27 African horse sickness virus genomes from viruses collected over a 76-year period (1933 to 2009). Genome Announc. 2015;3:e00921-15. https://doi.org/10.1128/genomeA.00921-15
2. Mellor PS, Hamblin C. African horse sickness. Vet Res. 2004;35:445–66. https://doi.org/10.1051/vetres:2004021
3. King S, Rajko-Nenow P, Ashby M, Frost L, Carpenter S, Batten C. Outbreak of African horse sickness in Thailand, 2020. Transbound Emerg Dis. 2020;tbed.13701. https://doi.org/10.1111/tbed.13701
4. Lu G, Pan J, Ou J, Shao R, Hu X, Wang C, et al. African horse sickness: its emergence in Thailand and potential threat to other Asian countries. Transbound Emerg Dis. 2020 May 14 [Epub ahead of print]. https://doi.org/10.1111/tbed.13625
5. Castillo-Olivares J. African horse sickness in Thailand: challenges of controlling an outbreak by vaccination. Equine Vet J. 2021;53:9–14. https://doi.org/10.1111/evj.13353
6. World Animal Health Information System, World Organisation for Animal Health. Animal disease events. African horse sickness, Thailand [cited 2020 Dec 30]. https://wahis.oie.int/#/events
7. Guthrie AJ, Maclachlan NJ, Joone C, Lourens CW, Weyer CT, Quan M, et al. Diagnostic accuracy of a duplex real-time reverse transcription quantitative PCR assay for detection of African horse sickness virus. J Virol Methods. 2013;189:30–5. https://doi.org/10.1016/j.jviromet.2012.12.014
8. Maan NS, Maan S, Nomikou K, Belaganahalli MN, Bachanek-Bankowska K, Mertens PP. Serotype specific primers and gel-based RT-PCR assays for 'typing' African horse sickness virus: identification of strains from Africa. PLoS One. 2011;6:e25686. https://doi.org/10.1371/journal.pone.0025686
9. Quan M, van Vuuren M, Howell PG, Groenewald D, Guthrie AJ. Molecular epidemiology of the African horse sickness virus S10 gene. J Gen Virol. 2008;89:1159–68. https://doi.org/10.1099/vir.0.83502-0
10. Martínez-Torrecuadrada JL, Langeveld JPM, Meloen RH, Casal JI. Definition of neutralizing sites on African horse sickness virus serotype 4 VP2 at the level of peptides. J Gen Virol. 2001;82:2415–24. https://doi.org/10.1099/0022-1317-82-10-2415
11. van Staden V, Smit CC, Stoltz MA, Maree FF, Huismans H. Characterization of two African horse sickness virus nonstructural proteins, NS1 and NS3. Arch Virol Suppl. 1998;14:251–8. https://doi.org/10.1007/978-3-7091-6823-3_22

Address for correspondence: Alongkorn Amonsin, Center of Excellence for Emerging and Reemerging Infectious Diseases in Animals (CUEIDAs) and One Health Research Cluster, Chulalongkorn University, Bangkok 10330, Thailand; email: alongkornamonsin1@gmail.com

Replication in Human Intestinal Enteroids of Infectious Norovirus from Vomit Samples

Marie Hagbom, Jenny Lin, Tina Falkeborn, Lena Serrander, Jan Albert, Johan Nordgren, Sumit Sharma

A typical clinical symptom of human norovirus infection is projectile vomiting. Although norovirus RNA and viral particles have been detected in vomitus, infectivity has not yet been reported. We detected replication-competent norovirus in 25% of vomit samples with a 13-fold to 714-fold increase in genomic equivalents, confirming infectious norovirus.

Human noroviruses are positive-sense RNA viruses that cause nearly 685 million cases of acute gastroenteritis worldwide per year, including ≈200 million cases in children, resulting in 50,000 child deaths (1). The disease is a substantial burden to healthcare systems and carries a global economic cost of ≈US $65 billion each year (2). Noroviruses are shed and usually transmitted through the fecal–oral route. However, outbreak investigations have suggested vomiting is a major contributor to transmission; norovirus has been detected in vomitus (3–5) and oral mouthwash samples (6). Despite this documented role in transmission, data on viral loads are limited, and information about infectivity in vomit is lacking (3–5,7).

A Norwalk virus (genus *Norovirus*) human challenge trial found that 56% of vomit samples contained detectable virus, and the median titer was 4.1×10^4 genomic equivalents (GEq)/mL (7). Another study reported that nearly half of the participants suffered vomiting postchallenge and on average shed up to 8.0×10^5 GEq/mL in vomit for the Norwalk virus and 3.9×10^4 GEq/mL in vomit for the 2 GII strains studied (4). The presence of intact virions in vomit was also reported in an early human challenge study with the Norwalk virus (8). These intact virions were detected by immune electron microscopy in concentrated

Author affiliations: Linköping University, Linköping, Sweden (M. Hagbom, J. Lin, L. Serrander, J. Nordgren, S. Sharma); Linköping University Hospital, Linköping (T. Falkeborn, L. Serrander); Karolinska University Hospital, Stockholm, Sweden (J. Albert); Karolinska Institutet, Stockholm (J. Albert)

vomit from 1 of the 5 challenge volunteers. These studies indicate that vomit could be a source of major spread of noroviruses, but the presence of infectious virus in vomit has not been reported.

The Study

To determine the presence of infectious virus in vomit, we used the human intestinal enteroid (HIE) culture system to culture vomit samples positive for norovirus. The system was previously used to replicate human noroviruses from fecal samples (9). HIE cultures were established using biopsy specimens from patients who underwent gastric bypass (ethics permission no. 2019–00600, Linköping Ethical Board, Linköping, Sweden). Written informed consent was obtained from all participants. We obtained 28 PCR-positive norovirus vomit samples collected for routine diagnosis from persons with acute gastroenteritis from Karolinska University Hospital (Stockholm, Sweden) and University Hospital of Linköping. The vomit samples were anonymized when received, and only information regarding the initial cycle threshold (C_t) value was provided. Decoded clinical samples without person-related data and traceability that have not been taken for research purposes do not require ethics or legal clearance according to The Swedish Ethics Review Authority.

The norovirus C_t values in the diagnostic PCRs ranged from 13.4 to 31.7. A previous study using fecal samples observed that the replication rate dropped substantially when 1.9×10^3 GEq were used as inoculum for infection (10), whereas another study reported loss of infectivity at higher C_t values (11). Of 28 vomit samples, 20 that had C_t values of ≤26 had 8.9×10^6 to 1.6×10^{10} GEq/mL (Table); the remaining 8 vomit samples had $<1 \times 10^6$ GEq/mL (in undiluted vomit) and were excluded from further evaluation.

Infectivity was tested on 5-day-old differentiated HIEs established from the jejunum of persons who had undergone gastric bypass surgery. Initial screening to determine infectivity of vomit samples was done with 2 different HIEs (HIE 003 and HIE 004) isolated from

secretor-positive persons (i.e., having a functional fucosyltransferase 2 gene). Both HIEs showed similar replication for the same 5 vomit samples. Next, we used HIE 003 for infection in triplicates with 2 technical repeats during quantitative reverse transcription PCR (qRT-PCR) (Figure). Norovirus genotypes in the vomit samples were determined by nucleotide sequencing. We defined infection as a >10-fold increase in GEq 72 hours postinfection (hpi) compared with 2 hpi, determined by qRT-PCR. We compiled details regarding the qRT-PCR method and the isolation, culturing, genotyping or phenotyping, and infection of HIEs (Appendix, https://wwwnc.cdc.gov/EID/article/27/8/21-0011-App1.pdf).

Partial nucleotide sequencing of the norovirus capsid region showed that 16 of the 20 vomit samples contained GII.4 norovirus genotype (belonging to GII.4 genotype Sydney 2012 variant), 3 contained GII.2, and 1 contained GII.17 norovirus genotype (Table). In the HIE infectivity assay, 5 of the vomit samples resulted in an increase in GEq, ranging from 13-fold to 714-fold at 72 hpi compared with 2 hpi; all these samples contained GII.4 noroviruses (Figure). The percentage of vomit samples (31.2%) containing GII.4 norovirus that successfully replicated is similar to that reported by Constantini et al. (10) using fecal samples positive for norovirus by PCR (25.6%). Of the 4 vomit samples containing GII.2 (n = 3) and GII.17 (n = 1), none demonstrated any replication in HIE, despite 2 GII.2 and 1 GII.17 vomit samples having similar or higher GEq in the inoculum compared to the fecal samples that could be successfully replicated in Constantini et al. (10). Of note, this finding might be because of the small number of GII.2-containing vomit samples and GII.17-containing vomit samples tested; not all fecal samples with high viral loads can be successfully replicated (10).

Conclusions

A previous study reported that fecal suspensions that showed successful norovirus replication in HIE cultures contained 1.9×10^3 to 1.7×10^7 GEq in the inoculum, regardless of genogroup or genotype (10). In our study, the GII.4 norovirus that could be successfully replicated contained a similar viral load (9.55×10^4 to 1.61×10^7 GEq) in the inoculum used for infection. Vomit samples that failed to show norovirus replication had of 8.91×10^3 to 1.66×10^6 GEq in the inoculum used for infection (Table), which suggests that viral load is not the sole criterion for successful infection in HIEs, as has been reported for norovirus cultured from feces (10). Because the vomit samples in this study were anonymized, no information beside the initial norovirus C_t value was available.

Table. Details of the norovirus genotypes and titers in the 20 vomit samples tested for norovirus infectivity in human intestinal enteroids*

Sample name	Genotype†	Titer, GEq/mL‡
V1	GII.4§	7.86×10^9
V2	GII.4	1.36×10^9
V3	GII.4	5.28×10^8
V5	GII.4	1.44×10^8
V6	GII.2	8.55×10^7
V8	GII.4	1.16×10^8
V11	GII.17	1.21×10^8
V12	GII.4	1.25×10^7
V18	GII.2	5.41×10^7
V19	GII.4	2.00×10^8
V20	GII.2	8.73×10^8
V21	GII.4	5.92×10^7
V22	GII.4	1.91×10^7
V23	GII.4	2.83×10^8
V24	GII.4	1.66×10^9
V25	GII.4	1.61×10^{10}
V29	GII.4	1.51×10^8
V30	GII.4	8.91×10^6
V32	GII.4	9.55×10^7
V33	GII.4	3.52×10^8

*Bold indicates vomit samples that showed successful norovirus replication. GEq, genomic equivalent.
†Norovirus genotype determined by partial sequencing of the VP1 gene encoding the major capsid protein.
‡Norovirus titer (GEq/mL) in undiluted vomit used to infect human intestinal enteroids. 100μL of 1:100 diluted sample was used as inoculum.
§All GII.4 norovirus detected belonged to the GII.4 Sydney 2012 variant.

Factors such as long-term storage (12) and the time of collection postinfection (13) might affect infectivity and cannot be ruled out. Repeated freeze-thaw cycles could also influence the infectivity of viruses, possibly because of the disruption of the capsid proteins, which could degrade the viral genome. However, Richards et al. (12) reported that norovirus capsid integrity is not compromised after repeated freeze-thaw cycles. Therefore, despite not knowing the exact long-term storage conditions in the 2 hospitals that provided the vomit samples (although most were stored at −70°C for ≤3 years), variation in infectivity should not have been caused by multiple freeze-thaw cycles. The time of sample collection also might influence infectivity. Samples should be collected within the first 24 hours after symptom onset. Norovirus can be shed in feces for ≥7 days, but no studies report infectivity after the initial 48–72 hours after symptom onset (13). Although qRT-PCR is standard for detecting norovirus RNA, it does not distinguish infectious virus particles from noninfectious virus particles (10).

Although an estimate of the 50% human infectious dose (HID_{50}) in vomit containing virus is unknown, it has been calculated to be ≈2,800 GEq for secretor-positive persons challenged with the Norwalk virus (7). Comparing the RNA levels in vomit and feces (on the basis of human challenge
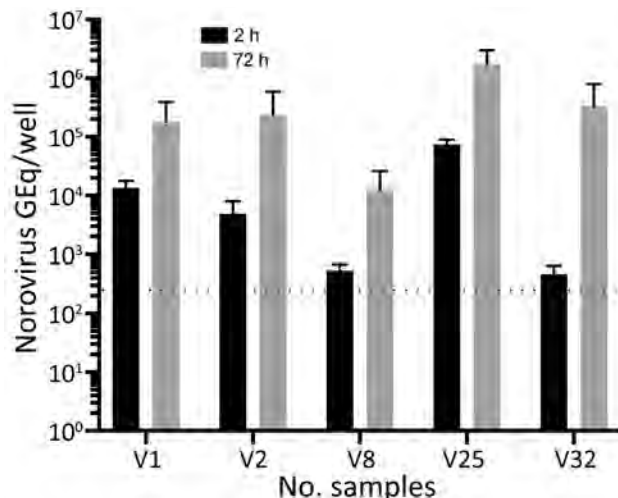
Figure. Replication in human intestinal enteroids of norovirus from vomit samples. Differentiated human intestinal enteroid monolayers were inoculated with norovirus-positive vomit samples. The number of norovirus GEq was quantified by reverse transcription quantitative PCR, 2 hours and 72 hours postinfection. Five of 20 vomit samples showed viral replication (defined as a >10-fold increase in the GEq). Data are presented as the mean ±SD of biologic triplicates. The inoculum for vomit samples that demonstrated viral replication were as follows: V1, 7.9×10^6 GEq/well; V2, 1.4×10^6 GEq/well; V8, 1.2×10^5 GEq/well; V25, 1.6×10^7 GEq/well; and V32, 9.6×10^4 GEq/well. The dotted lines represent quantitative reverse transcription PCR limit of detection. GEq, genomic equivalent.

studies with the Norwalk virus), it was estimated that 1 mL of vomitus contained up to 9,000 HID_{50} of virus (*7*). The combination of a low infectious dose and a large quantity of virus in vomit led to the suggestion that each vomiting event has the potential to infect >150,000 persons (*4*). In our study, we found that ≥95,500 GEq per inoculum was sufficient for infection of HIEs. Considering the different models studied (human vs. in vitro), the use of strains from different genogroups, and fecal versus vomit inoculum, the similarity in infectious dose is noteworthy.

In conclusion, this study demonstrates that norovirus contained in vomit is infectious. Aerosols and droplets from vomiting could be a source of norovirus transmission.

About the Author

Dr. Hagbom works primarily with enteric viruses in the Division of Molecular Medicine and Virology, Linköping University, Sweden. Her main research interests are pathophysiology and disease mechanisms of rotaviruses and noroviruses.

References

1. Centers for Disease Control and Prevention. Norovirus worldwide [cited 2020 Sep 10]. https://www.cdc.gov/norovirus/trends-outbreaks/worldwide.html
2. Bartsch SM, Lopman BA, Ozawa S, Hall AJ, Lee BY. Global economic burden of norovirus gastroenteritis. PLoS One. 2016;11:e0151219. https://doi.org/10.1371/journal.pone.0151219
3. Kirby A, Ashton L, Hart IJ. Detection of norovirus infection in the hospital setting using vomit samples. J Clin Virol. 2011;51:86–7. https://doi.org/10.1016/j.jcv.2011.02.007
4. Kirby AE, Streby A, Moe CL. Vomiting as a symptom and transmission risk in norovirus illness: evidence from human challenge studies. PLoS One. 2016;11:e0143759. https://doi.org/10.1371/journal.pone.0143759
5. Magill-Collins A, Gaither M, Gerba CP, Kitajima M, Iker BC, Stoehr JD. Norovirus outbreaks among Colorado River rafters in the Grand Canyon, summer 2012. Wilderness Environ Med. 2015;26:312–8. https://doi.org/10.1016/j.wem.2015.02.007
6. Kirby A, Dove W, Ashton L, Hopkins M, Cunliffe NA. Detection of norovirus in mouthwash samples from patients with acute gastroenteritis. J Clin Virol. 2010;48:285–7. https://doi.org/10.1016/j.jcv.2010.05.009
7. Atmar RL, Opekun AR, Gilger MA, Estes MK, Crawford SE, Neill FH, et al. Determination of the 50% human infectious dose for Norwalk virus. J Infect Dis. 2014;209:1016–22. https://doi.org/10.1093/infdis/jit620
8. Greenberg HB, Wyatt RG, Kapikian AZ. Norwalk virus in vomitus. Lancet. 1979;1:55. https://doi.org/10.1016/S0140-6736(79)90508-7
9. Ettayebi K, Crawford SE, Murakami K, Broughman JR, Karandikar U, Tenge VR, et al. Replication of human noroviruses in stem cell-derived human enteroids. Science. 2016;353:1387–93. https://doi.org/10.1126/science.aaf5211
10. Costantini V, Morantz EK, Browne H, Ettayebi K, Zeng XL, Atmar RL, et al. Human norovirus replication in human intestinal enteroids as model to evaluate virus inactivation. Emerg Infect Dis. 2018;24:1453–64. https://doi.org/10.3201/eid2408.180126
11. Chan MCW, Cheung SKC, Mohammad KN, Chan JCM, Estes MK, Chan PKS. Use of human intestinal enteroids to detect human norovirus infectivity. Emerg Infect Dis. 2019;25:1730–5. https://doi.org/10.3201/eid2509.190205
12. Richards GP, Watson MA, Meade GK, Hovan GL, Kingsley DH. Resilience of norovirus GII.4 to freezing and thawing: implications for virus infectivity. Food Environ Virol. 2012;4:192–7. https://doi.org/10.1007/s12560-012-9089-6
13. Robilotti E, Deresinski S, Pinsky BA. Norovirus. Clin Microbiol Rev. 2015;28:134–64. https://doi.org/10.1128/CMR.00075-14

Address for correspondence: Sumit Sharma, Division of Molecular Medicine and Virology, Department of Biomedical and Clinical Sciences, Linköping University, 581 83 Linköping, Sweden; email: sumit.sharma@liu.se

Endogenous Endophthalmitis Caused by ST66-K2 Hypervirulent *Klebsiella pneumoniae*, United States

Edwin Kamau, Paul R. Allyn, Omer E. Beaird, Kevin W. Ward, Nancy Kwan, Omai B. Garner, Shangxin Yang

We describe a case of endogenous endophthalmitis caused by sequence type 66-K2 hypervirulent *Klebsiella pneumoniae* in a diabetic patient with no travel history outside the United States. Genomic analysis showed the pathogen has remained highly conserved, retaining >98% genetic similarity to the original strain described in Indonesia in 1935.

Hypervirulent *Klebsiella pneumoniae* (hvKp) strains are mostly community-acquired and can cause invasive infections such as liver abscess with metastatic spread (*1,2*). The genetic determinants of hypervirulence are found on chromosomal mobile genetic elements, large plasmids, or both. The most common virulence determinants of hvKp include siderophore systems for iron acquisition, increased capsule production, K1 and K2 serotypes, and the colibactin toxin (*1*). In addition, these hvKp strains demonstrate hypermucoviscosity, as indicated by a positive string test, and are usually susceptible to antimicrobial drugs (*1*). However, multidrug–resistant hypervirulent strains have emerged in Asia, a region to which hvKp is endemic (*1,3*). Kp52.145 (laboratory strain B5055), which belongs to sequence type (ST) 66, is one of the most virulent and widely studied K2 strains. The ST66-K2 sublineage contains virulence genes in its chromosome and 2 large plasmids (*4,5*). ST66-K2 was isolated in Indonesia in 1935; since then, cases have been reported in Australia in 2002 (caused by strain AJ210), Germany in 2017 (caused by strain 18-0005) and France in 2018 (caused by strain SB5881) (*6–8*).

The most common hvKp infection metastatic sites are the eyes, lungs, and central nervous system (*1*).

Author affiliation: University of California, Los Angeles, California, USA

Endogenous endophthalmitis (EE) caused by hvKp is associated with risk factors such as diabetes mellitus, Asian ancestry, and infection with the K1 serotype (*2*). Although the prevalence of hvKp is increasing in the United States and Europe (*1,2,9*), where EE has been documented in patients of Asian and non-Asian descent (*9,10*), these infections are not well-recognized. Ocular prognoses and clinical outcomes for EE are usually poor and exacerbated by late or missed diagnosis (*2*). We describe a case of EE caused by a hvKp strain of the ST66-K2 sublineage in the United States.

The Study

A 30-year-old Caucasian man who had a history of poorly controlled type 1 diabetes mellitus and recreational use of methamphetamine and intravenous heroin sought treatment at the emergency department of a local hospital in California, USA, for progressive right eye and ear pain, which had lasted ≈1 week, and vision loss. Hospital staff noted substantial edema and tenderness of the right external auditory canal with otorrhea, along with suspected orbital cellulitis. Computed tomography scans revealed complete opacification of the right middle ear cavity and mastoid air cells, prominent thickening and hyperenhancement of the right posterolateral sclera, and a cystic and necrotic lesion in the left parotid region. He was prescribed vancomycin and cefepime and then transferred to Ronald Reagan UCLA Medical Center (Los Angeles, CA, USA) for ophthalmologic evaluation.

At admission, he had a perforated right tympanic membrane with external otitis media and mastoiditis, a left parotid abscess, and right endogenous endophthalmitis with subretinal abscess. A transthoracic echocardiogram showed no signs of valvular vegetations; an abdominal ultrasound showed no signs of hepatic lesions. Results of blood cultures were negative. Cultures from the parotid abscess and ear

Figure. Comparative genetic analysis of sequence type 66-K2 hypervirulent *Klebsiella pneumoniae* isolate (UCLA353) from a 30-year-old man in California, USA, who had endogenous endophthalmitis and 4 other isolates: AJ210 (Australia, 2002 [*6*]), 18-0005 (Germany, 2017 [*7*]), SB5881 (France, 2018 [*8*]), and Kp52.145 (Indonesia, 1935 [[*11*]]). Maximum-likelihood tree based on single-nucleotide polymorphisms and not drawn to scale. Colors indicate different loci; shades indicate different
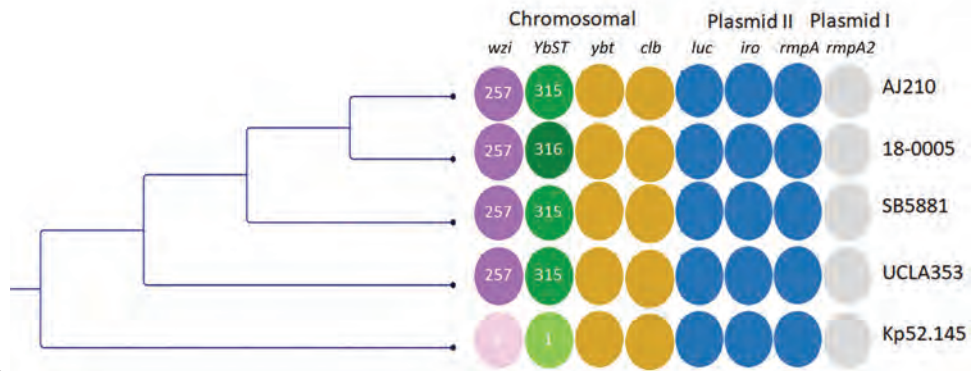
alleles. Colored columns show the capsular sequence type of the *wzi* gene, which codes for the outer membrane protein WZI; YbST; the chromosomal virulence loci y*ybt* and *clb*; the plasmid II–associated virulence loci *iuc*, *iro*, and *rmpA*; and the plasmid I–associated virulence locus *rmpA2*. AJ210, 18-0005, SB5881 and UCLA353 share the *wzi* 257 allele (dark purple). AJ210, SB5881 and UCLA353 share the YbST 315 allele, whereas 18-0005 has the YbST 316 allele (dark green). The *wzi* and YbST alleles for strain Kp52.145 are shown in lighter colors. *clb*, colibactin; *iro*, salmochelin; *iuc*, aerobactin; *rmpA*, regulator of mucoid phenotype; YbST, yersiniabactin sequence type; *ybt*, yersiniabactin.

drainage grew hypermucoviscous K. pneumoniae (Appendix Figure 1, https://wwwnc.cdc.gov/EID/article/27/8/21-0234-App1.pdf) and methicillin-susceptible Staphylococcus aureus. The K. pnuemoniae isolate was susceptible to all drugs tested, including ampicillin (Appendix Table 1).

We prescribed intravitreal injections of vancomycin, ceftazidime, and voriconazole every other day in addition to intravenous ceftriaxone (2 g 2×/d), intravenous voriconazole (4 mg/kg 2×/d), and oral metronidazole (500 mg 3×/d) for ≈2 weeks. We conducted a pars plana vitrectomy to drain the subretinal abscess in the patient's right eye. We sent the vitreous and aqueous samples for bacterial and fungal culturing, which returned negative results. After the surgery, the patient continued to take ceftriaxone, metronidazole, and voriconazole in addition to using eye drops containing prednisolone, ciloxan, and atropine. He was discharged 15 days after admission. Two weeks after discharge, he reported that his pain had resolved but his vision loss continued with minimal light perception.

We sequenced the isolate (UCLA353) using the Miseq platform (Illumina, https://www.illumina.com) with 2 × 250 bp protocol; long-read sequenc-

ing was conducted using MinION (Oxford Nanopore Technologies, https://nanoporetech.com) according to the manufacturer's recommendations. The sequence files were submitted to the National Center for Biotechnology Information Sequence Read Archive (https://www.ncbi.nlm.nih.gov/sra) under BioProject accession no. PRJNA729785. We analyzed the sequences using the CLC Genomics Workbench (QIAGEN, https://www.qiagen.com) and Geneious Prime (Geneious, https://www.geneious.com). We identified multilocus sequence types and virulence factors using BIGSdb (http://bigsdb.pasteur.fr/klebsiella). In addition, we used the default settings of ResFinder to identify antimicrobial resistance genes, CSI Phylogeny to identify single-nucleotide polymorphisms (SNPs), and PlasmidFinder to identify plasmid replicons (Center for Genomic Epidemiology, https://cge.cbs.dtu.dk/services). Genomic analyses revealed UCLA353 to be closely related to Kp52.145 (GenBank accession no. FO834906) with 99.7% genomic coverage and 98.8% pairwise identity. UCLA353 and Kp52.145 had all identical chromosomal hypervirulent genes and genomic islands, including the K2 capsular gene cluster, colibactin gene, yersiniabactin gene on an ICE*Kp*10 mobile genetic element, and the

Table. Single-nucleotide polymorphism matrix of 5 ST66-K2 hypervirulent *Klebsiella pneumoniae* strains

Strain (country, year [reference])	18-0005	AJ210	Kp52.145	SB5881	UCLA353
18-0005 (Germany, 2017 [*7*])	0	65	219	56	796
AJ210 (Australia, 2002 [*6*])	65	0	208	71	785
Kp52.145 (Indonesia, 1935 [*11*])	219	208	0	225	775
SB5881 (France, 2018 [*8*])	56	71	225	0	802
UCLA353 (United States, 2020, this study)*	796	785	775	802	0

*Isolate from a 30-year-old man in California who had endogenous endophthalmitis.

recently described phospholipase D family protein gene (Figure) (*11*). In addition, UCLA353 carried 2 plasmids (with lengths of 95,157 bp and 164,217 bp) nearly identical to those present in the SB5881 isolate documented in 2018 in France (GenBank accession nos. LR792629 and LR792630), with 100% genomic coverage and 99.9% pairwise identity (Appendix Figure 2). The 95-kb plasmid I in UCLA353 was also nearly identical to the Kp52.145 plasmid I (GenBank accession no. FO834904); the 164-kb plasmid II shared 100% genome coverage with Kp52.145 plasmid II (FO834905) but had a 39-kb sequence insertion previously described in SB5881 (*8*) (Appendix Figure 2). SNP analysis of the chromosomal sequences of UCLA353 and the other 4 ST66-K2 strains revealed that UCLA353 was genetically distinct, with 775 SNPs compared with Kp52.145 and 785–802 compared with AJ210, 18-0005, and SB5881 (Table 1). UCLA353 did not carry any resistance genes. Similar to other ST66-K2 strains, UCLA353 did not have the bla_{SHV} gene, and was therefore susceptible to β-lactams including ampicillin (Appendix Table 1). Further analysis showed all the ST66-K2 strains carried highly similar virulence factors (Appendix Table 2).

Conclusions

Ocular prognoses and clinical outcomes for EE are usually poor, often entailing partial or complete vision loss, enucleation or evisceration, or death (*2*). Late or missed diagnosis delays the initiation of specialized ocular therapy (e.g., intravitreal or source control) and can worsen outcomes. Early treatment is crucial to preserving full or partial vision (*1–3,10*). A pooled analysis of clinical studies revealed that most (83.2%) EE infections caused by hvKp were detected >24 hours after admission (*2*). These data indicate that patients at high risk for EE, especially those with underlying conditions such as diabetes mellitus or *K. pneumoniae*–associated pyogenic liver abscess, should be monitored closely for EE even when it is not initially apparent. Detection of K1 or K2 capsular serotypes, hypermucoviscous phenotype, and ampicillin susceptibility might suggest disseminated EE caused by hvKp. Although bacteremia is usually a prerequisite for metastatic dissemination, it may not always be detectable (*1,2*).

This infection probably began as otitis externa complicated by otitis media caused by perforated tympanic membrane and otomastoiditis, conditions that subsequently spread to the sinuses and right orbit. In a similar scenario, strain SB5881 also caused invasive infection including acute otitis media in a patient with type 1 diabetes mellitus and chronic alcoholism (*8*). Despite its emergence in or before 1935, ST66-K2 hvKp infections were not reported until 2002, probably because of the limited availability of high-resolution genomic sequencing tools in the 20th century (*8,11*). Thus, the prevalence of ST66-K2 hvKp might be largely underestimated.

In summary, we describe a case of EE caused by ST66-K2 hvKp in a Caucasian diabetic man with no travel history outside the United States. This lineage has remained highly conserved, preserving all of its virulence factors and >98% of its genome. Clinicians should be aware of the threat and challenges of EE caused hvKp infections.

About the Author

Dr. Yang is the assistant medical director of Clinical Microbiology Laboratory at the UCLA School of Medicine, Los Angeles, California, USA. His research interests include molecular diagnostics and innovation, clinical applications of next-generation sequencing, clinical virology, transplant-related infectious diseases testing, genomic epidemiology, and antimicrobial resistance mechanisms and genotypic prediction for resistance.

References

1. Choby JE, Howard-Anderson J, Weiss DS. Hypervirulent *Klebsiella pneumoniae*—clinical and molecular perspectives. J Intern Med. 2020;287:283–300. https://doi.org/10.1111/joim.13007
2. Hussain I, Ishrat S, Ho DCW, Khan SR, Veeraraghavan MA, Palraj BR, et al. Endogenous endophthalmitis in *Klebsiella pneumoniae* pyogenic liver abscess: systematic review and meta-analysis. Int J Infect Dis. 2020;101:259–68. https://doi.org/10.1016/j.ijid.2020.09.1485
3. Xu M, Li A, Kong H, Zhang W, Chen H, Fu Y, et al. Endogenous endophthalmitis caused by a multidrug-resistant hypervirulent *Klebsiella pneumoniae* strain belonging to a novel single locus variant of ST23: first case report in China. BMC Infect Dis. 2018;18:669. https://doi.org/10.1186/s12879-018-3543-5
4. Bialek-Davenet S, Criscuolo A, Ailloud F, Passet V, Jones L, Delannoy-Vieillard AS, et al. Genomic definition of hypervirulent and multidrug-resistant *Klebsiella pneumoniae* clonal groups. Emerg Infect Dis. 2014;20:1812–20. https://doi.org/10.3201/eid2011.140206
5. Struve C, Roe CC, Stegger M, Stahlhut SG, Hansen DS, Engelthaler DM, et al. Mapping the evolution of hypervirulent *Klebsiella pneumoniae*. MBio. 2015;6:e00630. https://doi.org/10.1128/mBio.00630-15
6. Holt KE, Wertheim H, Zadoks RN, Baker S, Whitehouse CA, Dance D, et al. Genomic analysis of diversity, population

structure, virulence, and antimicrobial resistance in *Klebsiella pneumoniae*, an urgent threat to public health. Proc Natl Acad Sci U S A. 2015;112:E3574–81. https://doi.org/10.1073/pnas.1501049112

7. Klaper K, Wendt S, Lübbert C, Lippmann N, Pfeifer Y, Werner G. Hypervirulent *Klebsiella pneumoniae* of lineage ST66-K2 caused tonsillopharyngitis in a German patient. Microorganisms. 2021;9:133. https://doi.org/10.3390/microorganisms9010133

8. Rodrigues C, d'Humières C, Papin G, Passet V, Ruppé E, Brisse S. Community-acquired infection caused by the uncommon hypervirulent *Klebsiella pneumoniae* ST66-K2 lineage. Microb Genom. 2020;6:mgen000419. https://doi.org/10.1099/mgen.0.000419

9. Baekby M, Hegedüs N, Sandahl TD, Krogfelt KA, Struve C. Hypervirulent *Klebsiella pneumoniae* K1 liver abscess and endogenous endophthalmitis in a Caucasian man. Clin Case Rep. 2018;6:1618–23. https://doi.org/10.1002/ccr3.1696

10. Kashani AH, Eliott D. The emergence of *Klebsiella pneumoniae* endogenous endophthalmitis in the USA: basic and clinical advances. J Ophthalmic Inflamm Infect. 2013;3:28. https://doi.org/10.1186/1869-5760-3-28

11. Lery LM, Frangeul L, Tomas A, Passet V, Almeida AS, Bialek-Davenet S, et al. Comparative analysis of *Klebsiella pneumoniae* genomes identifies a phospholipase D family protein as a novel virulence factor. BMC Biol. 2014;12:41. https://doi.org/10.1186/1741-7007-12-41

Address for correspondence: Shangxin Yang, UCLA Clinical Microbiology Laboratory, 11633 San Vicente Blvd, Los Angeles, CA 90049, USA; email: shangxinyang@mednet.ucla.edu

April 2020

Vectorborne Infections

EMERGING INFECTIOUS DISEASES®

To revisit the April 2020 issue, go to:

Whole-Genome Sequencing of SARS-CoV-2 from Quarantine Hotel Outbreak

Lex E.X. Leong, Julien Soubrier, Mark Turra, Emma Denehy, Luke Walters, Karin Kassahn, Geoff Higgins, Tom Dodd, Robert Hall, Katina D'Onise, Nicola Spurrier, Ivan Bastian, Chuan K. Lim

Author affiliations: University of South Australia, Adelaide, South Australia, Australia (L.E.X. Leong); South Australian Health and Medical Research Institute, Adelaide (L.E.X. Leong); SA Pathology, Adelaide (L.E.X. Leong, J. Soubrier, M. Turra, L. Walters, K. Kassahn, G. Higgins, T. Dodd, I. Bastian, C.K. Lim); University of Adelaide, Adelaide (J. Soubrier, G. Higgins, I. Bastian, C.K. Lim); Department for Health and Wellbeing, Adelaide (E. Denehy, R. Hall, K. D'Onise, N. Spurrier); Royal Adelaide Hospital, Adelaide (C.K. Lim)

Hotel quarantine for international travelers has been used to prevent coronavirus disease spread into Australia. A quarantine hotel–associated community outbreak was detected in South Australia. Real-time genomic sequencing enabled rapid confirmation tracking the outbreak to a recently returned traveler and linked 2 cases of infection in travelers at the same facility.

Since November 2019, community outbreaks of coronavirus disease (COVID-19), seeded by uncontrolled local transmission of severe acute respiratory syndrome coronavirus 2 (SARS-CoV-2) after importations, have overwhelmed the healthcare systems in many countries (*1*). Australia, including the state of South Australia, has largely controlled local transmission through early public health control measures such as rapid contact tracing and extensive nucleic acid amplification testing (NAAT). To limit introduction of SARS-CoV-2 into Australia, state and territory governments mandated 14-day quarantine in dedicated facilities for returning international travelers, including SARS-CoV-2 testing on arrival and before release. The clinically supervised hotel system enables containment of the risk for transmission associated with these travelers, especially those coming from countries experiencing SARS-CoV-2 resurgence (*2*) and asymptomatic or presymptomatic viral shedding carriers (*3*).

No local transmission had been recorded in the state since August 2020 until a community outbreak was identified in early November; the outbreak numbered 33 epidemiologically clustered cases as of December 2020. The first identified positive case in the outbreak was a family member of a housekeeping attendant at one of the quarantine hotels. Immediate screening of close contacts rapidly identified 14 additional cases, including 2 security guards working in the same hotel. The suspected source case was a traveler returned from the United Kingdom. Two additional cases were in travelers who stayed in rooms adjacent to that source patient. We hypothesized that this outbreak might have been caused by an inadequate ventilation system of the quarantine hotel.

Our study detailed the laboratory aspect of the quarantine hotel–associated outbreak, highlighting the utility of genomic sequencing for detecting the source of infection in locally acquired cases. Before this outbreak, all SARS-CoV-2–positive isolates in South Australia, including those from internationally returned travelers, had been prospectively sequenced on the Illumina platform (https://www.illumina.com) using the tiled amplicon ARTIC primers (https://github.com/artic-network/artic-ncov2019/tree/master/primer_schemes/nCoV-2019/V1) directly on clinical specimens. Sequencing reads were then aligned to the reference genome (Wuhan-Hu-1, RefSeq NC_045512.2) for construction of consensus genomes. A comprehensive database of high-quality SARS-CoV-2 genomes, representing >81% of positive isolates in South Australia, was thus available for comparison. Most (28/33) consensus genomes from this outbreak comprised >1,000× read depth and ≥95% coverage of the reference genome.

We designated the quarantine hotel–associated outbreak variant as B.1.36.1 lineage using the pangolin nomenclature system (*4*) (pangolin version 2.3.8, pangoLEARN v2021-04-01; https://github.com/cov-lineages/pangolin). The phylogenetic tree with genomes from its parental lineage B.1.36 (n = 3,010) suggested that this lineage and its sublineages potentially emerged from its ancestral lineage in February 2020 (Figure). To date, the B.1.36 lineage in GISAID has a large representation of genome sequences from the United Kingdom (n = 1,864, 62%), South Asia (n = 445, 15%), Europe (n = 324, 11%) and the Middle East (n = 155, 5%) (*5*).

Phylogenetic analysis using the 3,038 consensus genomes from the B.1.36 lineage, including those from this outbreak, demonstrated that the outbreak cluster represented 1 highly supported distinct clade consisting of all genomes from the quarantine hotel–associated cases (Figure). Although the source case was asymptomatic at the time of arrival, their mandatory nasopharyngeal swab showed relatively high viral loads by quantitative PCR (E-gene cycle threshold
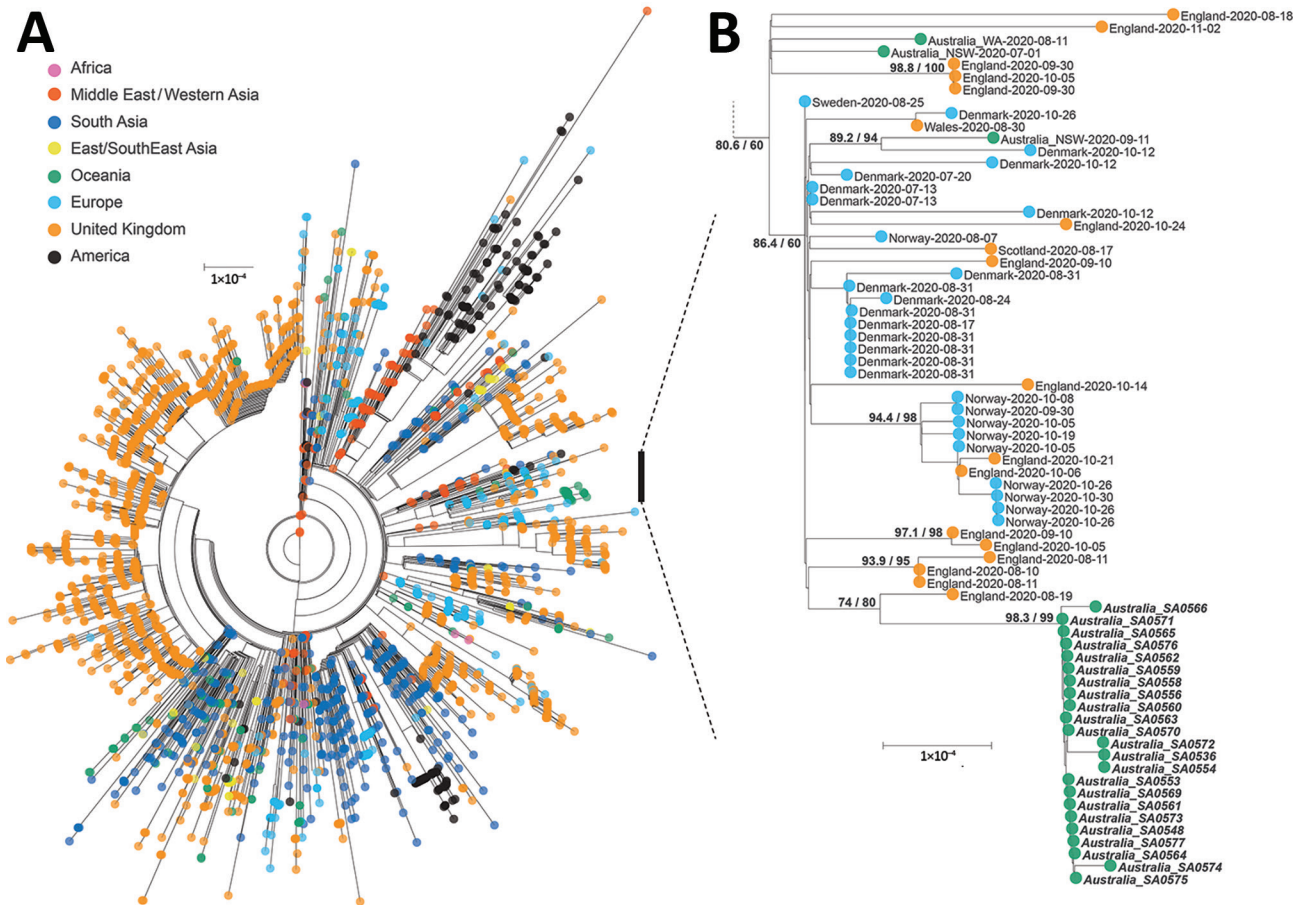
Figure. Maximum-likelihood phylogenetic tree of severe acute respiratory syndrome coronavirus 2 genomes from a quarantine hotel–associated community outbreak of coronavirus disease in South Australia, Australia. A) Genomes from lineage B.1.36 (n = 3,038). B) Subtree of lineage B.1.36.1 focusing on the quarantine hotel clusters and a returned traveler from the United Kingdom; bold type indicates those strains. Consensus genomes were profile-aligned using COVID-Align (*5*), and phylogenetic trees were constructed using IQ-TREE with general time reversible plus invariate plus gamma 4 sites model (*6*). SH-like approximate likelihood ratio test score was 98.3%, ultrafast bootstrap approximation 99%. Scale bar indicates substitutions per site.

= 27.52); antinucleocapsid antibody seroconversion 14 days later confirmed the timing of infection.

Transmission within the initial large family group with a high infection rate demonstrated the overdispersion characteristics of SARS-CoV-2 (*6*). The short viral incubation period and generation time for this clonal SARS-CoV-2 cluster reduced our capacity to predict the transmission chain within this outbreak. Another limitation for a thorough epidemiologic investigation of the source case is the extended distance between the South Australia cluster and other UK cases on the phylogenetic tree, which is likely due to gaps in global sequencing effort.

Mutational profile analysis showed limited evidence in this outbreak variant to support enhanced infection or transmission from a single site mutation (*7*). Apart from the most notable D614G mutation for enhanced replication, this cluster does not have the

mutations at the receptor binding motif of the spike protein that are common to several variants of concern (N417K/T, L452R, E484K/Q, N501Y/T).

Our study demonstrated that, in addition to hotel quarantine to prevent introduction of SARS-CoV-2 into the community, NAAT testing and rapid genomic sequencing are essential components of an effective public health response. In contrast to epidemiology-guided sequencing approaches, a comprehensive sequencing of all COVID-19 positive cases is important in discovering previously unidentified links. Sequencing enabled us to identify 2 additional case-patients who were guests in the quarantine hotel, which led to further improvements and policy changes in the quarantine system. This outbreak in the context of no recent local transmission highlights the transmissibility of SARS-CoV-2 and the risk for transmission chains that are occurring unchecked in countries with a high incidence of SARS-CoV-2.

Acknowledgments

We acknowledge the contributions of genome sequences from other laboratories to GISAID (https://www.gisaid.org). We thank the Australian Cancer Research Foundation Cancer Genomics Facility, and Microbiological Diagnostic Unit Public Health Laboratory for their helpful discussions.

About the Author

Dr. Leong is a senior medical scientist at SA Pathology. His research interests include pathogen genomes in public health, epidemiology, and infection outbreaks.

References

1. Miller IF, Becker AD, Grenfell BT, Metcalf CJE. Disease and healthcare burden of COVID-19 in the United States. Nat Med. 2020;26:1212–7. https://doi.org/10.1038/s41591-020-0952-y
2. Speake H, Phillips A, Chong T, Sikazwe C, Levy A, Lang J, et al. Flight-associated transmission of severe acute respiratory syndrome coronavirus 2 corroborated by whole-genome sequencing. Emerg Infect Dis. 2020;26:2872–80. https://doi.org/10.3201/eid2612.203910
3. Zhou F, Li J, Lu M, Ma L, Pan Y, Liu X, et al. Tracing asymptomatic SARS-CoV-2 carriers among 3,674 hospital staff: a cross-sectional survey. EClinicalMedicine. 2020;26:100510. https://doi.org/10.1016/j.eclinm.2020.100510
4. Rambaut A, Holmes EC, O'Toole Á, Hill V, McCrone JT, Ruis C, et al. A dynamic nomenclature proposal for SARS-CoV-2 lineages to assist genomic epidemiology. Nat Microbiol. 2020;5:1403–7. https://doi.org/10.1038/s41564-020-0770-5
5. Lemoine F, Blassel L, Voznica J, Gascuel O. COVID-Align: accurate online alignment of hCoV-19 genomes using a profile HMM. Bioinform. 2020;btaa871. https://doi.org/10.1093/bioinformatics/btaa871
6. Nguyen LT, Schmidt HA, von Haeseler A, Minh BQ. IQ-TREE: A fast and effective stochastic algorithm for estimating maximum likelihood phylogenies. Mol Biol Evol. 2015;32:268–74. https://doi.org/10.1093/molbev/msu300
7. Elbe S, Buckland-Merrett G. Data, disease and diplomacy: GISAID's innovative contribution to global health. Glob Chall. 2017;1:33–46. https://doi.org/10.1002/gch2.1018
8. Endo A, Abbott S, Kucharski AJ, Funk S. Estimating the overdispersion in COVID-19 transmission using outbreak sizes outside China. Wellcome Open Res. 2020;5:67. https://doi.org/10.12688/wellcomeopenres.15842.3
9. van Dorp L, Richard D, Tan CCS, Shaw LP, Acman M, Balloux F. No evidence for increased transmissibility from recurrent mutations in SARS-CoV-2. Nat Commun. 2020;11:5986. https://doi.org/10.1038/s41467-020-19818-2

Address for correspondence: Lex Leong, Public Health and Epidemiology, Microbiology and Infectious Disease, SA Pathology, Frome Rd, Adelaide 5000, South Australia, Australia; email: lex.leong@sa.gov.au

Linezolid- and Multidrug-Resistant Enterococci in Raw Commercial Dog Food, Europe, 2019–2020

Ana R. Freitas,[1,2] Liliana Finisterra, Ana P. Tedim,[2] Bárbara Duarte, Carla Novais,[1,2] Luísa Peixe[1,2] from the ESCMID Study Group on Food- and Water-borne Infections (EFWISG)

Author affiliations: Instituto Universitário de Ciências da Saúde (IUCS) Departamento de Ciências, Cooperativa de Ensino Superior Politécnico e Universitário (CESPU), CRL, Gandra, Portugal (A.R. Freitas); UCIBIO, Faculdade de Farmácia, Universidade do Porto, Porto, Portugal (A.R. Freitas, L. Finisterra, B. Duarte, C. Novais, L. Peixe); Hospital Universitario Rio Hortega/Instituto de Investigación Biomédica de Salamanca, Valladolid/Salamanca, Spain (A.P. Tedim)

We describe enterococci in raw-frozen dog food commercialized in Europe as a source of genes encoding resistance to the antibiotic drug linezolid and of strains and plasmids enriched in antibiotic-resistance and virulence genes in hospitalized patients. Whole-genome sequencing was fundamental to linking isolates from dog food to human cases across Europe.

Raw meat–based diets are increasingly popular for feeding dogs, but the extent of antimicrobial-resistant bacteria in raw dog food is rarely addressed globally (1). The Centers for Disease Control and Prevention does not recommend feeding raw diets to pets because of frequent contamination with *Salmonella* and *Listeria* (https://www.cdc.gov/healthypets/publications/pet-food-safety.html), but awareness about this issue is not as evident in Europe. Eating raw meat has been considered a risk factor for carriage of clinically relevant ampicillin-resistant (AmpR) *Enterococcus faecium* and *optrA*-positive linezolid-resistant *E. faecalis* in dogs (2,3), but data for commercial pet food are not available. We evaluated multidrug-resistant (MDR) *Enterococcus* in raw-frozen dog food commercialized in countries in Europe; we focused on transferable linezolid resistance (LinR) genes because linezolid is a last-resort drug to treat gram-positive infections (4).

We purchased 14 raw-frozen dog food samples from the 2 commercially available brands in Portugal in specialized stores (September 2019–January 2020). Brand A (produced in Europe) is available in specialized

Table. Characterization of *Enterococcus* isolates obtained from raw dog food samples, Porto, Portugal, 2019–2020*

Species	cgMLST†	MLST‡	Sample (brand)§	Antimicrobial drug resistance profile#	Antibiotic resistance genotype	MIC LIN, mg/L	Transfer of LinR genes
E. faecalis	CT1206	ST40	Duck (B)	ERY, TET, CHL, LIN	*optrA, fexA, cat, erm(B), lsa(A), tet(M), dfr(G)*	8	–
	CT1207	ST674	Salmon (A)	CIP, ERY, TET, STR, CHL, LIN	*optrA, cfrD, fexA, cat, ant(6)-Ia, aph(3')-III, erm(B), lsa(A), tet(M), tet(L), dfr(G)*	8	++
	CT1205	ST1008	Turkey (A)¶	ERY, TET, GEN, STR, CHL	*optrA, poxtB, fexB, cat, aac(6')-aph(2"), ant(6)-Ia, ant(9)-Ia, aph(3')-III, erm(B), lnu(B), lsa(A), lsa(E), tet(M), tet(L), dfr(G)*	4	–
	CT1205	ST1008	Turkey (A)¶	ERY, TET, STR, CHL	*optrA, poxtA, fexB, cat, aac(6')-aph(2"), ant(6)-Ia, ant(9)-Ia, aph(3')-III, erm(B), lnu(B), lsa(A), lsa(E), tet(M), tet(L), dfr(G)*	4	–
	CT1209	ST1008	Chicken + lamb (A)	ERY, TET, STR, CHL, LIN	*optrA, poxtA, fexB, cat, aac(6')-aph(2"), ant(6)-Ia, ant(9)-Ia, aph(3')-III, erm(B), lnu(B), lsa(A), lsa(E), tet(M), tet(L), dfr(G)*	8	–
	CT1208	ST1009	Turkey + goose (B)	ERY, CHL, LIN	*optrA, cfrD, fexA, cat, erm(B), lsa(A), dfr(G)*	8	–
E. faecium	CT106	ST80	Salmon (A)	<u>AMP</u> (>256 mg/L), CIP, ERY, TET, GEN, STR, QD	*aac(6')-aph(2"), ant(6)-Ia, aph(3')-III, erm(B), msr(C), tet(M), tet(L), dfr(G)*	ND	NA
	CT284	ST25	Beef (A)	AMP (32 mg/L), CIP, ERY, TET, GEN, STR, QD, CHL	*poxtA, fexB, aac(6')-aph(2"), ant(6)-Ia, ant(9)-Ia, aph(3')-III, erm(A), erm(B), msr(C), lnu(B), lsa(E), tet(M), tet(L), dfr(G)*	4	–
	CT374	ST264	Beef (A)	AMP (32 mg/L), CIP, TET, STR, QD	*cat, ant(6)-Ia, lnu(G), tet(M), tet(L), dfr(G)*	ND	NA
	CT272	ST1091	Duck (B)	<u>AMP</u> (>256 mg/L), CIP, ERY, TET, STR, QD	*ant(9)-Ia, erm(A), erm(B), msr(C), tet(M), tet(L), dfr(G)*	ND	NA
	CT3399	ST1263	Deer (B)	<u>AMP</u>, ERY, TET, STR, QD, CHL	*poxtA, fexB, cat, ant(6)-Ia, ant(9)-Ia, aph(3')-III, erm(A), msr(C), lnu(B), lsa(E), tet(L), dfr(G)*	4	+

*AMP, ampicillin; cgMLST, core-genome MLST; CIP, ciprofloxacin; CHL, chloramphenicol; CT, complex type; ERY, erythromycin; GEN, high-level resistance to gentamicin; LIN, linezolid; LinR, linezolid-resistant; MLST, multilocus sequence typing; NA, not applicable; ND, not done: QD, quinupristin/dalfopristin; STR, high-level resistance to streptomycin; ST, sequence type: +, positive (transfer frequency of 10^{-8}); ++, positive (transfer frequency of 10^{-7}); –, negative.
†The *E. faecalis* CT1205-CT1209 and the *E. faecium* CT3399 were identified in this study by submitting them to the cgMLST database (https://www.cgMLST.org) through Ridom SeqSphere⁺ version 7.2 software (https://www.ridom.de/seqsphere).
‡The novel *E. faecalis* ST1008–ST1009 were submitted to the MLST database (https://www.pubmlst.org).
§Brand A is produced in Europe; Brand B is produced in the United Kingdom.
¶These 2 samples correspond to 2 different batches and were acquired at different times (October 2019 and January 2020).
#QD resistance was tested only against *E. faecium* isolates. Successful transfer of ampicillin resistance is underlined (<u>AMP</u>) and all transconjugants exhibited high values of ampicillin resistance (16–256 mg/L).

stores, brand B (produced in the United Kingdom) in specialized stores and online; both are commercialized across different countries in Europe. We enriched samples (25 g) in buffered peptone water (1:10), then in brain–heart infusion broth with or without different antibiotic drugs (ampicillin [16 μg/mL], vancomycin [6 μg/mL], chloramphenicol [16 μg/mL]), and plated them onto Slanetz-Bartley agar with and without the same drug concentrations. We identified isolates with different morphologies per plate by PCR. We performed antibiotic susceptibility testing by disk diffusion using European Committee on Antimicrobial Susceptibility Testing (EUCAST) (5) or Clinical and Laboratory Standards Institute (6) guidelines. We used broth microdilution for linezolid and Etest for ampicillin. We searched acquired LinR genes (*optrA/poxtA/cfrA-E*) and

typed representative isolates by multilocus sequence typing (n = 20; https://www.pubmlst.org) and whole-genome sequencing (LinR *E. faecalis* [n = 6] and AmpR/LinR *E. faecium* [n = 5]) using the Hi Seq 2500 Sequencing System (Illumina, https://www.illumina.com). We deposited assemblies (SPAdes version 3.11.1; https://cab.spbu.ru/software/spades) in GenBank (Bioproject PRJNA663240) and characterized them using in silico tools (http://www.genomicepidemiology.org) and in-house databases (7).

All samples carried enterococci resistant to erythromycin, streptomycin, chloramphenicol, and tetracycline; 93% resistant to ampicillin, ciprofloxacin, and quinupristin/dalfopristin; 79% resistant to gentamicin; and 50% resistant to linezolid. We detected acquired LinR genes among 20 MDR isolates from

64% of samples from both brands and with different types of ingredients (Table): *optrA* (4 *E. faecalis*, 1 *E. faecium*), *poxtA* (2 *E. faecium*), *optrA+poxtA* (8 *E. faecalis*, 3 *E. faecium*) or *optrA+cfrD* (2 *E. faecalis*). Of those, 15 expressed LinR (MIC = 8 mg/L), whereas 5 were susceptible (MIC = 4 mg/L) (Table).

The *E. faecium* isolates (n = 39) were mostly MDR (70%), expressing resistance to tetracycline (85%), quinupristin/dalfopristin (72%), erythromycin (64%), ciprofloxacin (59%), streptomycin (57%), ampicillin (56%), gentamicin (23%), chloramphenicol (21%), or linezolid (10%). We compared selected dog food AmpR *E. faecium* genomes with 7,660 available GenBank *E. faecium* genomes by complex types (CTs) through core-genome multilocus sequence typing (Ridom SeqSphere⁺ version 7.2, https://www.ridom.de/seqsphere). Those data (Figure) and data from single-nucleotide polymorphisms (Appendix Figure 1, https://wwwnc.cdc.gov/EID/article/27/8/20-4933-App1.pdf) showed different clusters grouping related isolates obtained from dog food and hospitalized patients (sequence type [ST] 80/CT106; ST264/CT374) or from pet food and livestock or wastewaters (ST1091/CT284; ST1263/CT3399) in different countries. Dog food *E. faecium* was enriched in acquired antibiotic-resistant and virulence genes as strains from different sources (Appendix Figure 1). ST80 *E. faecium* from brand A was phylogenetically related to other strains from Germany and Netherlands; ST1091 and ST1263 from brand B were phylogenetically related to UK strains (Figure). By filter-mating (*8*), we found that 3 (ST25, ST80, ST1263) of 5 AmpR *E. faecium* isolates transferred a chromosomal genetic platform containing *pbp5* to GE1 *E. faecium* strain

(Table). Following our previous description of a large transferable *pbp5*-containing platform in a clinical isolate (*8*), we partly identified highly similar genetic platforms carrying different adaptive features including virulence genes (e.g., *sgrA*) in ST80 and ST1263 dog food AmpR *E. faecium* (Appendix Figure 2). ST1263 *E. faecium* was able to transfer *poxtA* by conjugation (Table).

The *E. faecalis* isolates (n = 52) recovered were mostly MDR (75%), resistant to chloramphenicol (83%), tetracycline (79%), erythromycin (75%), streptomycin (63%), gentamicin (31%), linezolid (21%), or ciprofloxacin (10%). ST40, ST674, ST1008, and ST1009 sequences corresponded to novel complex types carrying antimicrobial resistance (*aac(6′)-aph(2″)/ant(6)-Ia/aph3″-III/erm(B)/tet(M),tet(L),dfr(G)*) and virulence (*ace/gelE/elrA*) genes linked to clinically relevant MDR lineages (Table) (*7,9*). ST674 *E. faecalis* carried *optrA* on a pheromone-responsive plasmid (pAPT110) identical to others from non–clonally related *E. faecalis* in hospitalized patients in Spain and China (Appendix Figure 3). Similarly to pAPT110 in this study transferring *optrA* in high rates (Table), pEF10748 (China) is an *optrA* highly transferable plasmid with a complete sex-pheromone response module (*10*).

In conclusion, the diversity and rate of *E. faecium* and *E. faecalis* with linezolid-resistance genes (*optrA/poxtA/cfrD*) we identified were unexpectedly high. Our data suggest that raw dog food could be a sentinel of emerging antimicrobial resistance traits because this type of food may accumulate raw ingredients of different origins, namely from animals associated with intensive farming, adding a new concern to the global health burden of antimicrobial resistance.

Figure. Minimum-spanning tree based on the core-genome multilocus sequence typing (cgMLST) data from *Enterococcus faecium* isolates (n = 15) from different sources in Europe. The tree is based on cgMLST (1,423 genes) analyses made with Ridom SeqSphere⁺ version 7.2 software (https://www.ridom.de/seqsphere). Each circle represents 1 allele profile. The numbers on the connecting lines represent the number of cgMLST allelic differences between 2 isolates. Sequence types are shown in colored circles (see key); numbers in circles are isolate identifications. Gray shading around nodes indicates clusters of closely related isolates (≤20). CK, chicken; DE, Denmark; DF, dog food; HP, hospitalized patient; PT, Portugal; ST, sequence type; SW, swine; UK, United Kingdom; WW, wastewater.

About the Author
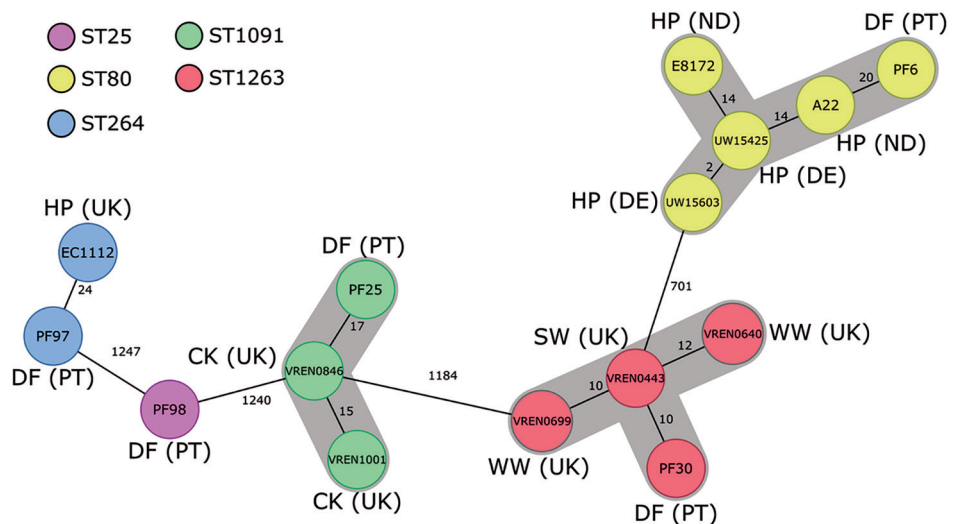
Dr. Freitas is a contracted investigator at the Research Unit on Applied Molecular Biosciences (UCIBIO@REQUIMTE) in the Faculty of Pharmacy of the University of Porto, Portugal. She is currently the secretary of the Food- and Water-borne Infections Study Group from the European Society of Clinical Microbiology and Infectious Diseases. Her main research interests are in the molecular epidemiology, genomics, and evolution of antimicrobial-resistant *Enterococcus*.

References

1. Davies RH, Lawes JR, Wales AD. Raw diets for dogs and cats: a review, with particular reference to microbiological hazards. J Small Anim Pract. 2019;60:329–39. https://doi.org/10.1111/jsap.13000
2. van den Bunt G, Top J, Hordijk J, de Greeff SC, Mughini-Gras L, Corander J, et al. Intestinal carriage of ampicillin- and vancomycin-resistant *Enterococcus faecium* in humans, dogs and cats in the Netherlands. J Antimicrob Chemother. 2018;73:607–14. https://doi.org/10.1093/jac/dkx455
3. Wu Y, Fan R, Wang Y, Lei L, Feßler AT, Wang Z, et al. Analysis of combined resistance to oxazolidinones and phenicols among bacteria from dogs fed with raw meat/vegetables and the respective food items. Sci Rep. 2019;9:15500. https://doi.org/10.1038/s41598-019-51918-y
4. Bender JK, Cattoir V, Hegstad K, Sadowy E, Coque TM, Westh H, et al. Update on prevalence and mechanisms of resistance to linezolid, tigecycline and daptomycin in enterococci in Europe: Towards a common nomenclature. Drug Resist Updat. 2018;40:25–39. https://doi.org/10.1016/j.drup.2018.10.002
5. European Committee on Antimicrobial Susceptibility Testing (EUCAST). Breakpoint tables for interpretation of MICs and zone diameters. EUCAST version 10.0; 2020 [cited 2020 Dec 1]. https://www.eucast.org/fileadmin/src/media/PDFs/EUCAST_files/Breakpoint_tables/v_11.0_Breakpoint_Tables.pdf
6. Clinical and Laboratory Standards Institute. Performance standards for antimicrobial susceptibility testing: twenty-eighth informational supplement M100. Annapolis Junction (MD): The Institute; 2018.
7. Freitas AR, Tedim AP, Novais C, Lanza VF, Peixe L. Comparative genomics of global *optrA*-carrying *Enterococcus faecalis* uncovers a common chromosomal hotspot for *optrA* acquisition within a diversity of core and accessory genomes. Microb Genom. 2020;6:e000350. https://doi.org/10.1099/mgen.0.000350
8. Novais C, Tedim AP, Lanza VF, Freitas AR, Silveira E, Escada R, et al. Co-diversification of *Enterococcus faecium* core genomes and PBP5: evidences of *pbp5* horizontal transfer. Front Microbiol. 2016;7:1581. https://doi.org/10.3389/fmicb.2016.01581
9. Raven KE, Reuter S, Gouliouris T, Reynolds R, Russell JE, Brown NM, et al. Genome-based characterization of hospital-adapted *Enterococcus faecalis* lineages. Nat Microbiol. 2016;1:15033. https://doi.org/10.1038/nmicrobiol.2015.33
10. Zou J, Tang Z, Yan J, Liu H, Chen Y, Zhang D, et al. Dissemination of linezolid resistance through sex pheromone plasmid transfer in *Enterococcus faecalis.* Front Microbiol. 2020;11:1185. https://doi.org/10.3389/fmicb.2020.01185

Address for correspondence: Luísa Peixe, UCIBIO, Departamento de Ciências Biológicas, Laboratório de Microbiologia, Faculdade de Farmácia, Universidade do Porto, Rua Jorge de Viterbo Ferreira, n. 228, 4050-313 Porto, Portugal; email: lpeixe@ff.up.pt

Highly Pathogenic Avian Influenza A(H5N8) Virus Clade 2.3.4.4b, Western Siberia, Russia, 2020

Ivan Sobolev, Kirill Sharshov, Nikita Dubovitskiy, Olga Kurskaya, Alexander Alekseev, Sergey Leonov, Yuriy Yushkov, Victor Irza, Andrey Komissarov, Artem Fadeev, Daria Danilenko, Junki Mine, Ryota Tsunekuni, Yuko Uchida, Takehiko Saito, Alexander Shestopalov

Author affiliations: Federal Research Center of Fundamental and Translational Medicine, Novosibirsk, Russia (I. Sobolev, K. Sharshov, N. Dubovitskiy, O. Kurskaya, A. Alekseev, A. Shestopalov); Siberian Federal Scientific Centre of Agro-BioTechnologies, Krasnoobsk, Russia (S. Leonov, Y. Yushkov); Federal Governmental State-Financed Institution Federal Centre for Animal Health, Vladimir, Russia (V. Irza); Smorodintsev Research Institute of Influenza, St. Petersburg,

Russia (A. Komissarov, A. Fadeev, D. Danilenko); Division of Transboundary Animal Disease, National Institute of Animal Health, Tsukuba, Japan (J. Mine, R. Tsunekuni, Y. Uchida, T. Saito)

Two variants of highly pathogenic avian influenza A(H5N8) virus were detected in dead poultry in Western Siberia, Russia, during August and September 2020. One variant was represented by viruses of clade 2.3.4.4b and the other by a novel reassortant between clade 2.3.4.4b and Eurasian low pathogenicity avian influenza viruses circulating in wild birds.

In 1996, the highly pathogenic avian influenza (HPAI) A(H5N1) virus subtype of the A/goose/Guangdong/1/1996 lineage was detected in domestic geese in China (1). Since 2014, H5Nx HPAI viruses belonging to clade 2.3.4.4 of A/goose/Guangdong/1/1996 lineage have spread internationally, posing a threat to the health of poultry and wild birds. Viruses of clade 2.3.4.4b have been detected in China (2013) and South Korea (2014); in 2016, reassortant strains between 2.3.4.4b and the Eurasian low pathogenicity avian influenza (LPAI) virus, for polymerase basic protein 2 (PB2), polymerase basic protein 1 (PB1), polymerase acidic gene (PA), nucleoprotein (NP), and matrix gene (M) segments, were reported in China (Qinghai Lake) and Russia (Uvs–Nuur Lake) (2). Thereafter, 2.3.4.4b viruses and their reassortant strains have spread worldwide and have been identified in poultry and wild birds in multiple countries (3).

In January and February 2020, a novel HPAI H5N8 clade 2.3.4.4b virus was detected in Germany. This virus shares 6 gene segments with the HPAI H5N8 virus in Eurasia, Asia, and Africa and 2 gene segments with LPAI virus A(H3N8), which has recently been detected in wild birds of Russia (4). HPAI virus strains closely related to isolates from Germany have also been identified in other countries of Europe, according to GISAID (https://www.gisaid. org). In October 2020, HPAI virus related to the variant from Germany has also been isolated in Japan (5) and South Korea (6).

Other variants of HPAI H5Nx virus were detected in the fall of 2020. Viruses of genetic group B of clade 2.3.4.4 and subtypes H5N8, H5N5, and H5N1 were found in Russia, Kazakhstan, and a number of countries in Europe (3,7,8). These viruses are genetically related to strains isolated in Egypt during 2017–2019 (7) and in Iraq in May 2020 (8).

The previous cases of H5 HPAI virus in Russia occurred at the end of 2018. In 2019 and the first half of 2020 H5Nx viruses had not been detected in Russia. In August and September 2020, we collected 58 samples from dead domestic birds on private rural farms in Western Siberia. We characterized 7 strains by using complete genome sequencing, phylogenetic analysis, and intravenous pathogenicity index testing. We identified all 7 strains as HPAI viruses on the basis of the amino acid sequence of the hemagglutinin (HA) proteolytic cleavage site (PLREKRRKR|G) and intravenous pathogenicity index values of 2.92–2.93 in chickens (Table).

We divided the isolated strains into 2 groups according to the sequences of the genome segments. Group 1 consists of 4 strains, whereas group 2 consists of 3 strains (Table). By using BLAST analysis (http:// blast.ncbi.nlm.nih.gov/Blast.cgi), we found all 8 genome segments of group 1 and the 3 genome segments (HA, M, and NS) of group 2 to be closely related (99.01%–100% nucleotide identity) to the genome segments of HPAI clade 2.3.4.4b virus strains isolated in Russia, Kazakhstan, and Europe in the summer and fall of 2020. We found the genome segments of neuraminidase, PB2, PB1, PA, and NP in group 2 to be related (98.38%–99.06% nucleotide identity) to different LPAI viruses from Eurasia.

Phylogenetic analysis showed that the whole genome of group 1 and HA, M, and nonstructural gene genome segments of group 2 clustered with HPAI H5N8 clade 2.3.4.4b virus. They were also related to H5N8 viruses from Egypt (2019) and Iraq (May 2020) but were not related to the H5N8 variants from Germany in early 2020 (Figure; Appendix 1 Figures 1–7, https://wwwnc.cdc.gov/EID/article/27/8/20-4969-App1.pdf). The neuraminidase, PB2, PB1, PA, and NP segments of group 2 viruses clustered with

Table. Highly pathogenic avian influenza A viruses subtype H5N8 isolated from birds, Novosibirsk, Western Siberia, Russia, 2020*

Group	Isolate ID	Site	Collection date	IVPI value
1	A/goose/Russia_Novosibirsk region/1-12/2020	Intestine	2020 Sep 15	2.92
1	A/goose/Russia_Omsk region/55-1/2020	Intestine	2020 Aug 29	2.92
1	A/chicken/Russia_Novosibirsk region/1910-1/2020	Liver	2020 Sep 22	2.92
1	A/chicken/Russia_Novosibirsk region/1910-2/2020	Intestine	2020 Sep 22	2.92
2	A/chicken/Russia_Novosibirsk region/3-1/2020	Intestine	2020 Sep 20	2.93
2	A/chicken/Russia_Novosibirsk region/3-15/2020	Intestine	2020 Sep 20	2.93
2	A/chicken/Russia_Novosibirsk region/3-29/2020	Brain	2020 Sep 20	2.93

*ID, identification; IVPI, intravenous pathogenicity index.
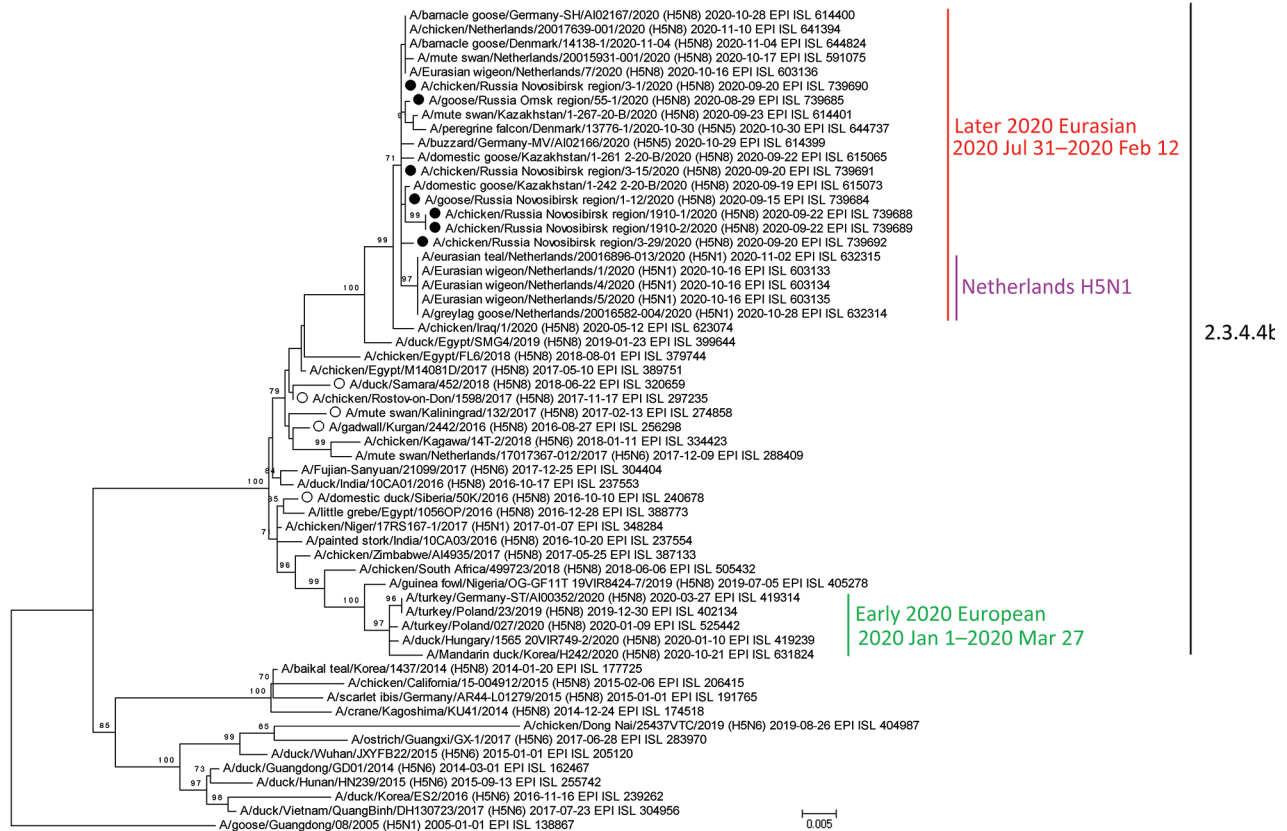
Figure. Maximum-likelihood phylogenetic tree of the hemagglutinin segment of HPAI subtype H5N8 virus isolated from birds, Novosibirsk, Western Siberia, Russia, 2020, and reference segments from GISAID (http://www.gisaid.org). Filled circles indicate HPAI H5N8 virus strains from Russia isolated in 2020; open circles indicate strains from Russia isolated during 2016–2018. Virus identification number, date of identification, and GISAID accession number are provided for all sequences. HPAI, highly pathogenic avian influenza.

LPAI viruses identified in Eurasia. Consequently, group 2 strains are reassortant strains between Egyptian-like HPAI and LPAI viruses from Eurasia (Appendix 1 Figure 8). Of note, PB2, PA, and NP segments of group 2 isolates clustered on phylogenetic trees (nucleotide identity of 97.32%–97.45% for PB2, 98.98%–99.02% for PA, and 98.86%–99.00% for NP) with the HPAI H5N1 reassortants isolated in the fall of 2020 in the Netherlands (*8*). PB1 segments showed a lower level of identity (96.21%–96.26%).

On the basis of our phylogenetic data, chronology of virus isolations, general birds' flyways, and previously described patterns of HPAI viruses spreading from Siberia during 2005–2006, 2014, and 2016–2017 (*3,9,10*), we suggest that new H5N8 viral strain from Eurasia in late 2020 possibly descended from the H5N8 virus circulating in Egypt during 2017–2019 and then disseminated through Iraq into Western Siberia and North Kazakhstan during the spring migration. Egyptian-like HPAI H5N8 virus possibly reached breeding and staging areas in Siberia

in early 2020, spread in wild bird populations, and reassorted with LPAI viruses. During fall migration, standard Egyptian-like HPAI H5N8 virus and novel reassortant strains spread to the European part of Eurasia, leading to a reassortment event, which has been detected in Netherlands. However, further studies of 2020–2021 European H5Nx viruses are needed to verify this hypothesis.

Acknowledgments

Forestry and Fisheries of Japan (project no. JPJ008837) as part of its program for funding commissioned projects for promotion of strategic international collaborative research.

About the Author

References

1. Duan L, Campitelli L, Fan XH, Leung YH, Vijaykrishna D, Zhang JX, et al. Characterization of low-pathogenic H5 subtype influenza viruses from Eurasia: implications for the origin of highly pathogenic H5N1 viruses. J Virol. 2007;81:7529–39. https://doi.org/10.1128/JVI.00327-07
2. Lee DH, Sharshov K, Swayne DE, Kurskaya O, Sobolev I, Kabilov M, et al. Novel reassortant clade 2.3.4.4 avian influenza A(H5N8) virus in wild aquatic birds, Russia, 2016. Emerg Infect Dis. 2017;23:359–60. https://doi.org/10.3201/eid2302.161252
3. Verhagen JH, Fouchier RAM, Lewis N. Highly pathogenic avian influenza viruses at the wild-domestic bird interface in Europe: future directions for research and surveillance. Viruses. 2021;13:212. https://doi.org/10.3390/v13020212
4. King J, Schulze C, Engelhardt A, Hlinak A, Lennermann SL, Rigbers K, et al. Novel HPAIV H5N8 reassortant (clade 2.3.4.4b) detected in Germany. Viruses. 2020;12:281. https://doi.org/10.3390/v12030281
5. Isoda N, Twabela AT, Bazarragchaa E, Ogasawara K, Hayashi H, Wang ZJ, et al. Re-invasion of H5N8 high pathogenicity avian influenza virus clade 2.3.4.4b in Hokkaido, Japan, 2020. Viruses. 2020;12:1439. https://doi.org/10.3390/v12121439
6. Jeong S, Lee DH, Kwon JH, Kim YJ, Lee SH, Cho AY, et al. Highly pathogenic avian influenza clade 2.3.4.4b subtype H5N8 virus isolated from Mandarin Duck in South Korea, 2020. Viruses. 2020;12:1389. https://doi.org/10.3390/v12121389
7. Beerens N, Heutink R, Harders F, Roose M, Pritz-Verschuren S, Germeraad E, et al. Novel incursion of a highly pathogenic avian influenza subtype H5N8 virus in the Netherlands, October 2020. Emerg Infect Dis. 2021;27:1750–3. https://doi.org/10.3201/eid2706.204464
8. Lewis NS, Banyard AC, Whittard E, Karibayev T, Al Kafagi T, Chvala I, et al. Emergence and spread of novel H5N8, H5N5 and H5N1 clade 2.3.4.4 highly pathogenic avian influenza in 2020. Emerg Microbes Infect. 2021;10:148–51. https://doi.org/10.1080/22221751.2021.1872355
9. Olsen B, Munster VJ, Wallensten A, Waldenström J, Osterhaus AD, Fouchier RA. Global patterns of influenza a virus in wild birds. Science. 2006;312:384–8. https://doi.org/10.1126/science.1122438
10. Marchenko V, Goncharova N, Susloparov I, Kolosova N, Gudymo A, Svyatchenko S, et al. Isolation and characterization of H5Nx highly pathogenic avian influenza viruses of clade 2.3.4.4 in Russia. Virology. 2018;525:216–23. https://doi.org/10.1016/j.virol.2018.09.024

Tuberculosis-Associated Hospitalizations and Deaths after COVID-19 Shelter-In-Place, San Francisco, California, USA

Janice K. Louie, Rocio Agraz-Lara, Laura Romo, Felix Crespin, Lisa Chen,[1] Susannah Graves[1]

Author affiliations: San Francisco Department of Public Health Tuberculosis Prevention and Control Program, San Francisco, California, USA (J.K. Louie, R. Agraz-Lara, L. Romo, F. Crespin, S. Graves); University of California, San Francisco (J.K. Louie, L. Chen)

A mandated shelter-in-place and other restrictions associated with the coronavirus disease pandemic precipitated a decline in tuberculosis diagnoses in San Francisco, California, USA. Several months into the pandemic, severe illness resulting in hospitalization or death increased compared with prepandemic levels, warranting heightened vigilance for tuberculosis in at-risk populations.

Since the emergence of a novel coronavirus, severe acute respiratory syndrome coronavirus 2 (SARS-CoV-2), which causes coronavirus disease (COVID-19), unprecedented measures have been recommended to reduce transmission. In San Francisco, California, USA, progressively restrictive health officer orders implemented since early 2020 have included travel quarantines, shelter-in-place (SIP), deferral of routine medical appointments and elective surgeries, closure of public-facing events and businesses, and isolation and quarantine when appropriate (1). Nationwide, disruptions in medical services have contributed to delaying or avoiding routine care and a decrease in non–COVID-19-related hospital admissions and emergency department visits (2). Similarly, worldwide tuberculosis (TB) case reports have declined, including in San Francisco, where a ≈60% decrease in newly diagnosed TB cases compared with prior years was observed in the first 4 months of the pandemic (3,4).

The San Francisco Department of Public Health (SFDPH) Tuberculosis Prevention and Control Program manages all cases of active TB in San Francisco residents (≈881,549 population). In 2019, San Francisco had a high incidence of TB, with rates >4-fold higher (11.9 cases/100,000 persons) than the national rate. The affected population is predominantly

---

[1]These senior authors contributed equally to this article.

Figure. Comparison of TB cases pre-SIP (January 1, 2019–March 15, 2020) and after SIP (March 16, 2020–January 31, 2021), San Francisco, California, USA. Scales for the y-axes differ substantially to underscore patterns but do not permit direct comparisons. Total TB cases indicates total number of case-patients receiving TB treatment, by month. Cases were counted according to the month when TB was diagnosed. In the first months of the pandemic after SIP was implemented (March 16–June 30, 2020), numbers of patients newly diagnosed with TB decreased compared with the 14.5 months prior. In early July 2020, the number of patients newly diagnosed with TB began to increase, with a higher proportion requiring hospitalization or having a TB-related death. SIP, shelter-in-place; TB, tuberculosis.
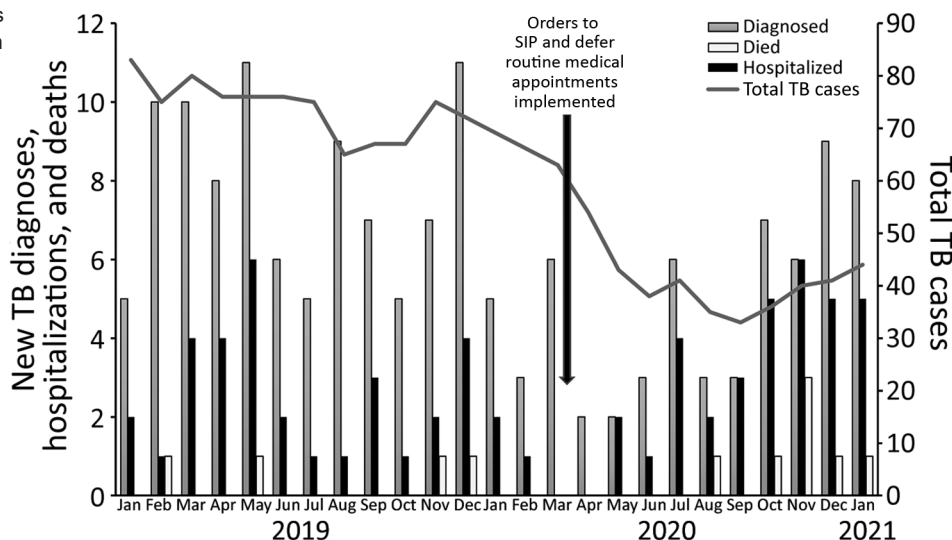
non–US-born (86%) with >80% residing in the United States >5 years (5). We reviewed overall numbers of active TB case-patients in San Francisco and newly diagnosed cases including those resulting in hospitalization, intensive care unit admission, and death. We divided our analysis into 2 periods: pre-SIP (January 1, 2019–March 15, 2020) and during SIP (March 16, 2020–January 31, 2021). TB was reportable within 1 working day of diagnosis. Cases were diagnosed by microbiologic testing or medical assessment for consistent clinical and radiographic findings. All patients who received a TB diagnosis after SIP began were tested for SARS-CoV-2 co-infection at the time of TB diagnosis, except for 7 patients during March–May 2020, when testing was less available. For all fatalities, we used a standardized algorithm to review medical records and death certificates to determine whether cause of death was TB-related. Because

these activities were public health surveillance and not research, review by institutional review board was not requested.

During the 14.5-month pre-SIP period, the monthly average number of patients receiving TB treatment was 73.0 persons, compared with 42.7 persons during the 10.5-month SIP period, resulting in a 42% reduction. The initial SIP period was marked by low numbers of new TB diagnoses during mid-March through June; increasing numbers starting in July, when more case-patients had TB diagnosed while they were hospitalized or dying from TB (Figure). Pre-SIP, a total of 114 patients (average 7.9 patients/month) were newly diagnosed with TB. A total of 38 (33.3%) patients were hospitalized, including 5 (4.4%) who required intensive care. A total of 4 (3.5%) patients died with cause of death assessed as TB-related. In comparison, after SIP

Table. New diagnoses of TB pre-SIP compared with during SIP during the coronavirus disease pandemic, San Francisco, California, USA, January 1, 2020–January 30, 2021*

Variable	Pre-SIP: 2019 Jan 1–2020 Mar 15	SIP: 2020 Mar 16–2021 Jan 30	p value†
New diagnoses of active TB	114 (100)	52 (100)‡	NA
Average no. new TB cases/month	7.9	5.0	NA
Median age of case-patients, y (range)	64.0 (3–101)	66.0 (15–97)	NS
New case-patients with cavitary TB	33 (28.9)	11 (21.2)	NS
New TB case-patients requiring hospitalization	38 (33.3)	33 (63.5)	0.0003
New TB case-patients requiring intensive care	5 (4.4)	12 (23.1)	0.0002
New TB case-patients who died	15 (13.2)	10 (19.2)	NS
New TB case-patients with TB-related deaths§	4 (3.5)	7 (13.5)	0.017

*Values are no. (%) unless indicated. Cases were counted according to the month when TB was diagnosed. NA, not applicable; NS, not significant (p≥0.05); SIP, shelter-in-place; TB, tuberculosis.
†By Pearson χ^2 test.
‡All patients were tested for severe acute respiratory syndrome coronavirus 2 co-infection at time of TB diagnosis, except for 7 patients for whom testing was not routinely available in the first 3 months of the pandemic (March–May 2020); no patients were positive.
§Cause of death was evaluated by standardized algorithm and review of medical records and death certificate, when available. Deaths were counted as TB-related when TB was assessed as an immediate or contributing cause of death.

began, 52 patients (average 5.0 patients/month) were newly diagnosed with TB. A total of 33 (63.5%) patients were hospitalized, including 12 (23.1%) patients who required intensive care; 7 (13.5%) patients died with cause of death assessed as TB-related. No patients diagnosed with TB during SIP reported having previous SARS-CoV-2 infection; all patients screened for SARS-CoV-2 had negative results. One patient experienced new-onset low-grade fever and cough 37 days after starting TB treatment and subsequently tested SARS-CoV-2 positive; this patient had no new radiographic abnormalities or COVID-19–related complications. More patients during SIP than before SIP required hospitalization, received intensive care, or had a TB-related death ($p<0.05$ by Pearson χ^2 test (Table). We found no difference in duration of TB symptoms pre-SIP (median 1 month, range 0–120 months) than that during SIP (median 1.5 months, range 0–24 months).

Our preliminary findings suggest that delayed TB diagnosis early in the pandemic, coinciding with implementation of SIP and other restrictive measures, might have contributed to an increasing proportion of patients who later experienced severe illness or death. Although we used SIP as a proxy, other factors probably contributed to the trend. The same racial, ethnic, and socioeconomic inequities that contributed to limited healthcare access during the COVID-19 pandemic are prevalent in TB-infected populations (6). Symptomatic patients might have been reluctant or unable to seek medical evaluation, thereby leading to worsening TB disease. The overlap of signs, symptoms, and abnormal radiographic findings for COVID-19 and TB could have resulted in prioritizing COVID-19 screening over TB diagnosis.

Our observations are a snapshot in time and are not representative of TB activity in other cities or regions where COVID-19 transmission rates and corresponding SIP and public health responses differ. Nevertheless, we collected real-world data consistent with the Stop-TB Partnership modeling studies predicting that prolonged disruption of TB activities could result in an excess of millions of TB cases and deaths through 2025 (7). As vaccination rates increase and restrictions ease, continued vigilance and public messaging about the importance of early diagnosis of TB in high-risk populations remain critical.

About the Author

Dr. Louie is the medical director of the San Francisco Department of Public Health's Tuberculosis Prevention and Control Program. Her research interests include the epidemiology, clinical management, and treatment of tuberculosis in older populations.

References

1. San Francisco Department of Public Health. Coronavirus (COVID-19) health orders [cited 2021 Mar 22]. https://www.sfdph.org/dph/alerts/coronavirus-healthorders.asp
2. Czeisler ME, Marynak K, Clarke KEN, Salah Z, Shakya I, Thierry JM, et al. Delay or avoidance of medical care because of COVID-19-related concerns—United States, June 2020. MMWR Morb Mortal Wkly Rep. 2020;69:1250–7. https://doi.org/10.15585/mmwr.mm6936a4
3. World Health Organization. Global tuberculosis report 2020 [cited 2021 Mar 22]. https://apps.who.int/iris/bitstream/handle/10665/336069/9789240013131-eng.pdf
4. Louie JK, Reid M, Stella J, Agraz-Lara R, Graves S, Chen L, et al. A decrease in tuberculosis evaluations and diagnoses during the COVID-19 pandemic. Int J Tuberc Lung Dis. 2020;24:860–2. https://doi.org/10.5588/ijtld.20.0364
5. California Department of Public Health Tuberculosis Control Branch. Tuberculosis disease data and publications [cited 2021 Mar 22]. https://www.cdph.ca.gov/Programs/CID/DCDC/Pages/TB-Disease-Data.aspx
6. Anderson KE, McGinty EE, Presskreischer R, Barry CL. Reports of forgone medical care among US adults during the initial phase of the COVID-19 pandemic. JAMA Netw Open. 2021;4:e2034882. https://doi.org/10.1001/jamanetworkopen.2020.34882
7. Stop TB Partnership. The potential impact of the COVID-19 response on tuberculosis in high-burden countries: a modeling analysis [cited 2021 Mar 22]. http://www.stoptb.org/assets/documents/news/Modeling%20Report_1%20May%202020_FINAL.pdf

Address for correspondence: Janice Louie, San Francisco Department of Public Health Tuberculosis Prevention and Control Program, 2460 22nd St, Bldg 90, 4th Fl, San Francisco, CA 94110, USA; email: janice.louie@sfdph.org

SARS-CoV-2 Superspread in Fitness Center, Hong Kong, China, March 2021

Daniel K.W. Chu,[1] Haogao Gu,[1] Lydia D.J. Chang, Sammi S.Y. Cheuk, Shreya Gurung, Pavithra Krishnan, Daisy Y.M. Ng, Gigi Y.Z. Liu, Carrie K.C. Wan, Dominic N.C. Tsang, Malik Peiris, Leo L.M. Poon

Author affiliations: The University of Hong Kong, Hong Kong, China (D.K.W. Chu, H. Gu, L.D.J. Chang, S.S.Y. Cheuk, S. Gurung, P. Krishnan, D.Y.M. Ng, G.Y.Z. Liu, C.K.C. Wan, M. Peiris, L.L.M. Poon); The Government of Hong Kong Special Administrative Region, Hong Kong (D.N.C. Tsang)

To investigate a superspreading event at a fitness center in Hong Kong, China, we used genomic sequencing to analyze 102 reverse transcription PCR–confirmed cases of severe acute respiratory syndrome coronavirus 2 infection. Our finding highlights the risk for virus transmission in confined spaces with poor ventilation and limited public health interventions.

Hong Kong, China, is at the end of a fourth wave of severe acute respiratory syndrome coronavirus 2 (SARS-CoV-2) infection. The virus causing this wave was introduced in September 2020 (GISAID clade GH) (1) and has continued to evolve in Hong Kong. As of April 30, 2021, a total of 11,771 SARS-CoV-2 cases had been laboratory confirmed; more than half (56%) were detected during the fourth wave. We describe a superspreading event that occurred in a 3,000-ft^2 fitness center in March 2021 (Appendix Figure 1, https://wwwnc.cdc.gov/EID/article/27/8/21-0833-App1.pdf).

On March 10, 2021, an asymptomatic 27-year-old male fitness trainer (patient FC1) received a positive reverse transcription PCR (RT-PCR) test result as part of a voluntary coronavirus disease (COVID-19) screening program. This program provided services to persons for community or private purposes (e.g., for work or travel). The fitness trainer had previously received a negative COVID-19 test result on February 17, 2021. He taught small group classes in the fitness center every day from February 28 through March 8, except March 4, 2021.

His positive test result triggered a local health authority to conduct epidemiologic investigation and contact tracing. The fitness center was immediately closed to the public. The local government also issued a compulsory testing notice to those who had visited this center from February 25 through March 10. About 300 visitors were tested and 101 cases were confirmed (7 staff members and 94 customers; case-patients FC2–FC102) (Appendix Table 1). All case-patients had recently visited this center; >80% of cases were detected within 3 days of the first case (Appendix Figure 2). Another 53 SARS-CoV-2–positive persons were subsequently identified; they had had close contact with the 102 case-patients but no epidemiologic link to the fitness center.

Of the 102 case-patients, all were hospitalized according to local standard practice, recovered uneventfully, and were discharged. None had received COVID-19 vaccination before this outbreak. A total of 46 case-patients were asymptomatic at the time of testing. The percentage of asymptomatic case-patients in this cluster (45%) is higher than that of all persons with confirmed cases in Hong Kong (30%; p<0.005). It is not known whether the general physical well-being of case-patients in this cluster affected their clinical status. Their ages, on average, were lower than that of all persons with confirmed cases in Hong Kong (38 vs. 44 years; p<0.005).

Among the 56 symptomatic case-patients, signs and symptoms started to develop for 36 of them during March 9–11; the earliest onset date was March 6 (case-patient FC46). Assuming the average incubation period of COVID-19 to be ≈5 days (2), the superspreading event might have occurred around March 5. Because SARS-CoV-2 can be transmitted by asymptomatic and presymptomatic persons (3), our data did not enable us to identify the index case-patient of this cluster.

To exclude unrelated transmission chains in this fitness center, we used next-generation sequencing to study respiratory samples from 59 of the case-patients (1,4). We used 5 epidemiologically unrelated local case-patients, including 4 detected in the same period, as controls. All virus sequences from the fitness center outbreak genetically clustered together and were genetically distinct from the controls (Figure), demonstrating that this superspreading event was caused by a single virus introduction.

Many case-patients, including FC1 and FC46, were located at the root of this phylogenetic branch. There are a few minor clades in this phylogenetic branch, suggesting that the initial introduction triggered multiple independent transmission chains thereafter in this setting.

SARS-CoV-2 transmission in fitness centers/gyms has been reported (5–8). SARS-CoV-2 can be

---
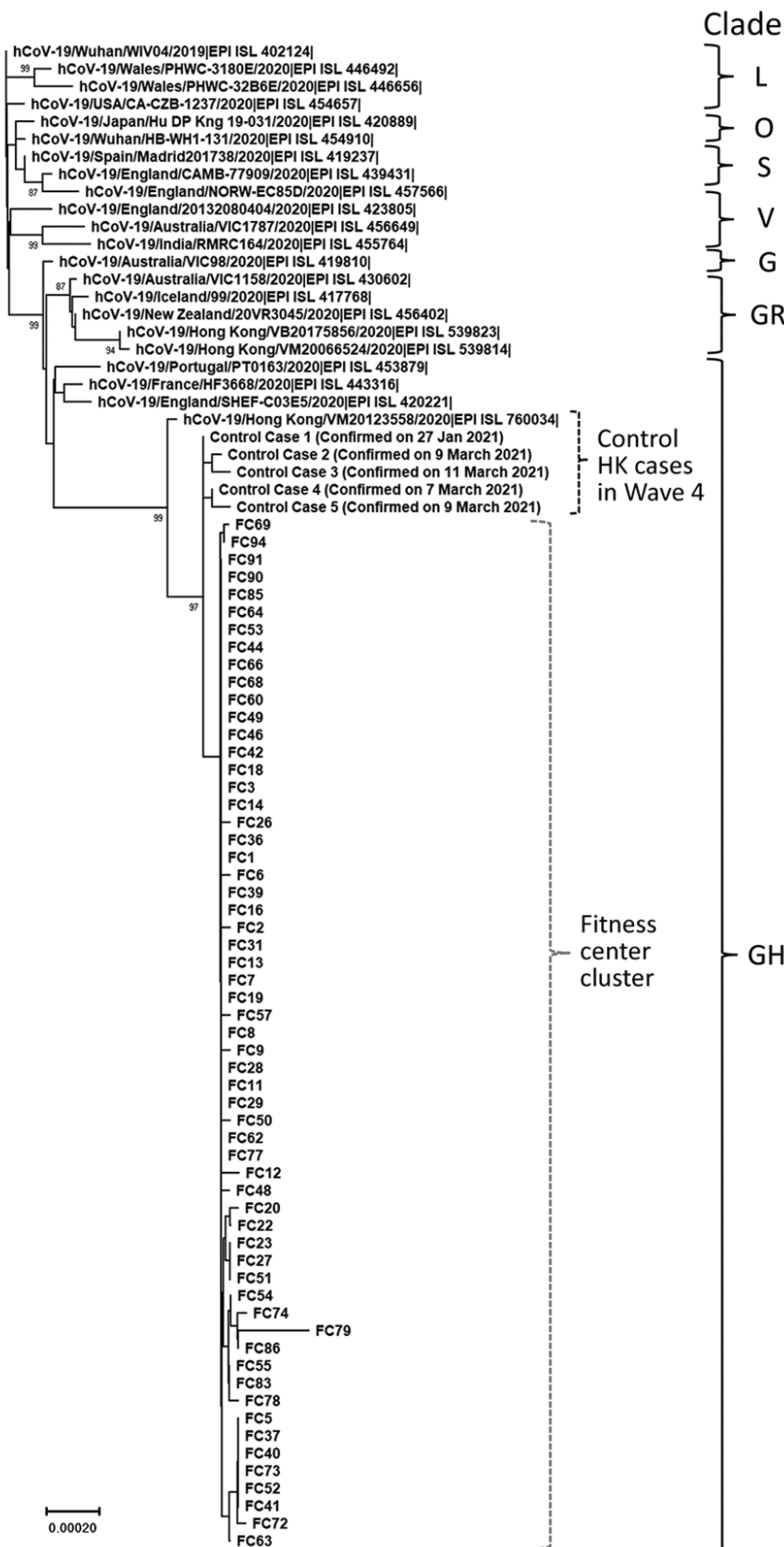
Figure. Phylogenetic tree of the severe acute respiratory syndrome coronavirus 2 (SARS-CoV-2) viruses detected in a fitness club in Hong Kong, China, in March 2021. Viruses from clades L, S, V, G, GH, GR, and O (others) are also included in the analysis. Near full-length genomes of studied samples were deduced by a previously described Illumina (https://www.illumina.com) sequencing protocol (sequence coverage >100) (*1,4*). Human SARS-CoV-2 WIV04 is selected to be the root of this phylogenetic tree. The tree was constructed by using the neighbor-joining method. Only bootstrap values >80 are shown. EPI ISL accession nos. for sequences retrieved in GISAID (https://www.gisaid.org) are provided. Scale bar indicates estimated genetic distance.

transmitted by close contact, droplets, or fomites (*9*). Uncontrolled physical activities in a fitness center might produce any or all of these transmission modes (e.g., increased physical contact, increased levels of exhaled respiratory droplets in a confined space because of vigorous breathing, and shared communal space and equipment). Although in this study we were unable to identify the predominant transmission mode accounting for this superspreading event, a recent report indicates that physical activities in a fitness center can create a pronounced level of saliva aerosol (*10*). An air change rate of 2.2/hour in a fitness center is insufficient to dilute the amount of saliva aerosol generated from physical activities (*10*). Of note, mask wearing during exercise was not compulsory by law at the time of this outbreak. Many case-patients in our study reported not wearing a mask while training at that time (e.g., weight training, high-intensity circuit training, and boxing). A follow-up investigation revealed that this center has air conditioning units but lacks a fresh air and exhaust duct system. This finding suggests that poor ventilation might have played a major role in this outbreak.

After this outbreak, new recommendations were issued to prevent superspreading events at fitness centers in Hong Kong. For staff in these settings, RT-PCR testing for SARS-CoV-2 every 2 weeks is compulsory, and staff are prioritized to receive COVID-19 vaccination. For all persons in fitness settings, mask wearing at all times is now mandatory, except when showering or eating. Recommendations for air ventilation in all fitness centers are under investigation.

About the Author

Dr. Chu is a research assistant professor at The University of Hong Kong, China. His research interests focus on diagnostic virology, molecular diagnostics, and virus evolution.

References

1. Chu DKW, Hui KPY, Gu H, Ko RLW, Krishnan P, Ng DYM, et al. Introduction of ORF3a-Q57H SARS-CoV-2 variant causing fourth epidemic wave of COVID-19, Hong Kong, China. Emerg Infect Dis. 2021;27:1492–5. https://doi.org/10.3201/eid2705.210015
2. Li Q, Guan X, Wu P, Wang X, Zhou L, Tong Y, et al. Early transmission dynamics in Wuhan, China, of novel coronavirus-infected pneumonia. N Engl J Med. 2020;382:1199–207. https://doi.org/10.1056/NEJMoa2001316
3. Wu P, Liu F, Chang Z, Lin Y, Ren M, Zheng C, et al. Assessing asymptomatic, pre-symptomatic and symptomatic transmission risk of SARS-CoV-2. Clin Infect Dis. 2021;ciab271. https://doi.org/10.1093/cid/ciab271
4. Choi EM, Chu DKW, Cheng PKC, Tsang DNC, Peiris M, Bausch DG, et al. In-flight transmission of SARS-CoV-2. Emerg Infect Dis. 2020;26:2713–6. https://doi.org/10.3201/eid2611.203254
5. Groves LM, Usagawa L, Elm J, Low E, Manuzak A, Quint J, et al. Community transmission of SARS-CoV-2 at three fitness facilities—Hawaii, June–July 2020. MMWR Morb Mortal Wkly Rep. 2021;70:316–20. https://doi.org/10.15585/mmwr.mm7009e1
6. Bae S, Kim H, Jung TY, Lim JA, Jo DH, Kang GS, et al. Epidemiological characteristics of COVID-19 outbreak at fitness centers in Cheonan, Korea. J Korean Med Sci. 2020;35:e288. https://doi.org/10.3346/jkms.2020.35.e288
7. Lendacki FR, Teran RA, Gretsch S, Fricchione MJ, Kerins JL. COVID-19 outbreak among attendees of an exercise facility—Chicago, Illinois, August–September 2020. MMWR Morb Mortal Wkly Rep. 2021;70:321–5. https://doi.org/10.15585/mmwr.mm7009e2
8. Jang S, Han SH, Rhee JY. Cluster of coronavirus disease associated with fitness dance classes, South Korea. Emerg Infect Dis. 2020;26:1917–20. https://doi.org/10.3201/eid2608.200633
9. Sia SF, Yan LM, Chin AWH, Fung K, Choy KT, Wong AYL, et al. Pathogenesis and transmission of SARS-CoV-2 in golden hamsters. Nature. 2020;583:834–8. https://doi.org/10.1038/s41586-020-2342-5
10. Blocken B, van Druenen T, Ricci A, Kang L, van Hooff T, Qin P, et al. Ventilation and air cleaning to limit aerosol particle concentrations in a gym during the COVID-19 pandemic. Build Environ. 2021;193:107659. https://doi.org/10.1016/j.buildenv.2021.107659

Address for correspondence: Leo Poon, School of Public Health, The University of Hong Kong, Rm 528, Lab Block 21, Sassoon Rd, Pokfulam, Hong Kong, China; email: llmpoon@hku.hk

Persistence of SARS-CoV-2–Specific IgG in Children 6 Months After Infection, Australia

Zheng Quan Toh, Rachel A. Higgins, Lien Anh Ha Do, Karin Rautenbacher, Francesca L. Mordant, Kanta Subbarao, Kate Dohle, Jill Nguyen, Andrew C. Steer, Shidan Tosif, Nigel W. Crawford, Kim Mulholland, Paul V. Licciardi

Author affiliations: Murdoch Children's Research Institute, Melbourne, Victoria, Australia (Z.Q. Toh, R.A. Higgins, L.A.H. Do, K. Dohle, J. Nguyen, A.C. Steer, S. Tosif, N.W. Crawford, K. Mulholland, P.V. Licciardi); The University of Melbourne, Melbourne (Z.Q. Toh, L.A.H. Do, A.C. Steer, S. Tosif, N.W. Crawford, K. Mullholland, P.V. Licciardi); The Royal Children's Hospital, Melbourne (K. Rautenbacher, A.C. Steer, S. Tosif, N.W. Crawford); World Health Organization Collaborating Centre for Reference and Research on Influenza, The Peter Doherty Institute for Infection and Immunity, Melbourne (F.L. Mordant, K. Subbarao); London School of Hygiene and Tropical Medicine, London, UK (K. Mulholland)

The duration of the humoral immune response in children infected with severe acute respiratory syndrome coronavirus 2 is unknown. We detected specific IgG 6 months after infection in children who were asymptomatic or had mild symptoms of coronavirus disease. These findings will inform vaccination strategies and other prevention measures.

Children <18 years of age account for ≈3% of coronavirus disease (COVID-19) cases worldwide (1). Most (70%) children with COVID-19 are asymptomatic or have mild illness; very few require hospitalization (2,3). The nature and persistence of the immune response generated by children after infection with severe acute respiratory syndrome coronavirus 2 (SARS-CoV-2), the causative agent of COVID-19, is unknown. We investigated the humoral immune response to SARS-CoV-2 in children and adults as part of a longitudinal cohort study in Melbourne, Victoria, Australia.

Nasopharyngeal swab samples of persons with suspected SARS-CoV-2 infection and their close contacts were tested by reverse transcription PCR at The Royal Children's Hospital in Melbourne during May–October 2020. We invited SARS-CoV-2–positive patients and their household members to participate in this cohort study. We collected blood samples at the time of enrollment, as well as ≈28 days, 3 months, and 6 months later. We obtained written informed consent from parents/guardians and assent from children. The study was conducted with the approval of the Human Research Ethics Committee at The Royal Children's Hospital (approval no. HREC/63666/RCHM-2019).

To measure IgG, we used a modified 2-step ELISA based on the method described by Amanat et al. (4) and the LIAISON SARS-CoV-2 S1/S2 IgG assay (DiaSorin, https://www.diasorin.com). We also conducted a SARS-CoV-2 microneutralization assay on an available subset of samples. For the ELISA, we screened samples using the SARS-CoV-2 receptor-binding domain as the antigen; for potential positive samples, we confirmed results that tested positive by additional ELISA using S1 antigen. We calculated the results of S1-positive samples according to the World Health Organization SARS-CoV-2 pooled serum standard (standard provided by the National Institute for Biological Standards and Control, South Mimms, UK) and reported data as ELISA units per milliliter. We set a seropositivity cutoff at 1.5 ELISA units/mL on the basis of results of archived serum samples taken before the pandemic. We then conducted the LIAISON assay according to the manufacturer's instructions and the microneutralization assay as described by Tosif et al. (5) (Appendix, https://wwwnc.cdc.gov/EID/article/27/8/21-0965-App1.pdf).

During May 10, 2020–October 28, 2020, we recruited a cohort of 134 children (0–18 years of age) and 160 adults (19–73 years of age). We included only participants with a positive PCR result for SARS-CoV-2 or who were seropositive at the first timepoint (median 11 days after diagnosis, range 5–13 days) and had blood samples for ≥2 timepoints. At the first timepoint, 4 adults had negative PCR results but positive serologic results; of these adults, 3 had borderline seropositive antibody levels.

By February 2021, we had identified 54 SARS-CoV-2–positive participants: 22 children (median age of 4 years, range 0–18 years) and 32 adults (median age of 37 years, range 22–73 years). In total, 5 (23%) children and 2 (6%) adults were asymptomatic; the rest had mild symptoms, and none were hospitalized. The median duration of follow-up after diagnosis was 195 days (range 188–213 days) for children and 194 days (range 183–212 days) for adults.

By day 43 (range 27–79), 15/19 (79%) children and 26/28 (93%) adults had seroconverted. These participants remained seropositive for ≥90 days (Figure, panels A, B). By day 195 (≈6 months), 14/17 (82%) of children and 18/21 (86%) of adults were seropositive; however, from day 43 to 195, geometric mean antibody
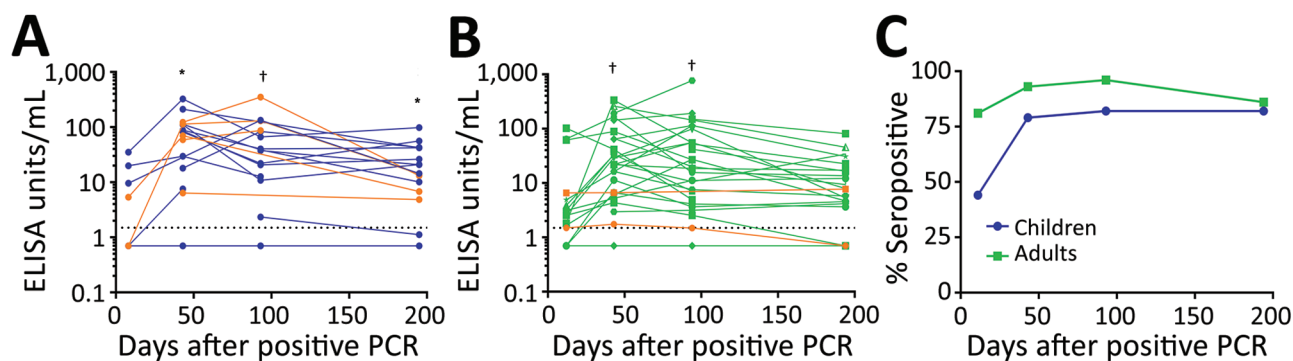
Figure. Persistence of IgG responses against severe acute respiratory syndrome coronavirus 2 in children and adults, Australia, 2020–2021. Patients tested positive by PCR, ELISA, or both. A) Antibody responses of 22 children 0–18 years of age. B) Antibody responses of 32 adults 22–73 years of age. Orange points and lines indicate asymptomatic cases; blue points and lines indicate symptomatic cases in children; green points and lines indicate symptomatic cases in adults. Dotted lines indicate seropositivity cutoff. C) Seropositivity rates in 22 children and 32 adults. Blue points and lines indicate all children, regardless of symptoms; green points and lines indicate all adults, regardless of symptoms. *p<0.05; †p<0.01 (compared with the fist timepoint [day 11]).

concentration decreased ≈2-fold in both groups (Figure, panel C). We observed no significant differences in geometric mean antibody concentration from day 43 (range 27–79) to day 194 (range 183–212), nor from 93 (range 27–79) to day 194 (range 183–212), for either children or adults (Figure, panels A, B). The seropositivity and antibody levels were also not significantly different between children and adults at all timepoints (Figure 1, panel C; Appendix Figure 1). Seropositive samples defined by our in-house ELISA correlated with results from the LIAISON assay and neutralizing antibody assay (Appendix Figures 2, 3). In total, 4/19 (21%) children and 2/28 (7%) adults did not seroconvert; however, we could not rule out other SARS-CoV-2–related immune responses, such as cellular or mucosal mechanisms (5,6).

We found that, similar to the adults in this cohort and those in previous studies (7,8), SARS-CoV-2–positive children with no or mild symptoms mounted strong and durable humoral responses that persisted for ≥6 months. Our study was limited by the relatively small sample size; in addition, only a subset of samples was available for the microneutralization assay. In conclusion, our data indicate that SARS-CoV-2–positive children have a persistent antibody response for ≥6 months. The roles and durations of other components of the immune system (such as the cellular and mucosal responses) during SARS-CoV-2 infection remain undetermined. These results will inform vaccination strategies and other public health measures.

About the Author

Dr. Toh is a research officer based at the Murdoch Children's Research Institute, Melbourne, Victoria, Australia. His primary research interests include infectious diseases, immunology, and vaccinology.

References

1. Dawood FS, Ricks P, Njie GJ, Daugherty M, Davis W, Fuller JA, et al. Observations of the global epidemiology of COVID-19 from the prepandemic period using web-based surveillance: a cross-sectional analysis. Lancet Infect Dis. 2020;20:1255–62. https://doi.org/10.1016/S1473-3099(20)30581-8
2. Qiu H, Wu J, Hong L, Luo Y, Song Q, Chen D. Clinical and epidemiological features of 36 children with coronavirus

disease 2019 (COVID-19) in Zhejiang, China: an observational cohort study. Lancet Infect Dis. 2020;20:689–96. https://doi.org/10.1016/S1473-3099(20)30198-5

3. Zimmermann P, Curtis N. Why is COVID-19 less severe in children? A review of the proposed mechanisms underlying the age-related difference in severity of SARS-CoV-2 infections. Arch Dis Child. 2020 Dec 1 [Epub ahead of print].

4. Amanat F, Stadlbauer D, Strohmeier S, Nguyen THO, Chromikova V, McMahon M, et al. A serological assay to detect SARS-CoV-2 seroconversion in humans. Nat Med. 2020;26:1033–6. https://doi.org/10.1038/s41591-020-0913-5

5. Tosif S, Neeland MR, Sutton P, Licciardi PV, Sarkar S, Selva KJ, et al. Immune responses to SARS-CoV-2 in three children of parents with symptomatic COVID-19. Nat Commun. 2020;11:5703. https://doi.org/10.1038/s41467-020-19545-8

6. Sekine T, Perez-Potti A, Rivera-Ballesteros O, Strålin K, Gorin JB, Olsson A, et al.; Karolinska COVID-19 Study Group. Robust T cell immunity in convalescent individuals with asymptomatic or mild COVID-19. Cell. 2020;183:158–168.e14. https://doi.org/10.1016/j.cell.2020.08.017

7. Duysburgh E, Mortgat L, Barbezange C, Dierick K, Fischer N, Heyndrickx L, et al. Persistence of IgG response to SARS-CoV-2 [Erratum in: Lancet Infect Dis. 2021;21:e16; 2021;21:e36]. Lancet Infect Dis. 2021;21:163–164.

8. Choe PG, Kim KH, Kang CK, Suh HJ, Kang E, Lee SY, et al. Antibody responses 8 months after asymptomatic or mild SARS-CoV-2 infection. Emerg Infect Dis. 2021;27:928–31. https://doi.org/10.3201/eid2703.204543

COVID-19 and the Consequences of Anchoring Bias

Harold W. Horowitz, Caren Behar, Jeffrey Greene

Author affiliations: Weill Cornell Medicine, New York, New York, USA (H.W. Horowitz); New York-Presbyterian Brooklyn Methodist Hospital, Brooklyn, New York, USA (H.W. Horowitz); New York University Langone School of Medicine, New York (C. Behar, J. Greene)

Suspicion of coronavirus disease in febrile patients might lead to anchoring bias, causing misdiagnosis of other infections for which epidemiologic risks are present. This bias has potentially severe consequences, illustrated by cases of human granulocytic anaplasmosis and Lyme disease in a pregnant woman and human granulocytic anaplasmosis in another person.

Coronavirus disease (COVID-19) took the United States by force during the first quarter of 2020, affecting the economy, societal norms, and the delivery of medical care (*1,2*). As fear of COVID-19 has spread, diagnosing COVID-19 in febrile persons has been prioritized, and patients may be presumed to have COVID-19 pending results of testing for severe acute respiratory syndrome coronavirus 2 (SARS-CoV-2). This mindset has had unintended consequences, including delaying evaluations for other infectious diseases, potentially leading to adverse outcomes. We describe 2 cases that illustrate this point.

In the first case, a 35-year-old man left New York, New York, USA, to go hiking in Maryland during June 5–June 7, 2020. He experienced fever, body aches, and fatigue during June 10–13 that resolved but left him fatigued and weak. He was seen on June 19; laboratory results were unremarkable, but lymphopenia was detected. He tested negative for SARS-CoV-2 on June 19 and June 25 by PCR. On June 25, ELISA for Lyme disease was positive, and reflex to Western blot revealed IgM 41-kD, 39-kD, and 23-kD bands but no IgG bands. Fever up to 38°C recurred on June 22 and lasted until June 29; he also experienced persistent fatigue and myalgia. Further testing on July 6 revealed serologic results for Lyme similar to results from June 25 and *Anaplasma phagocytophilum* titers of IgM 1:320 and IgG 1:1260. Anaplasma PCR was negative on that date. He was treated with doxycycline for 10 days and recovered.

In the second case, a 31-year-old woman who was 6 months pregnant left New York at the end of May 2020 to rent a house in Ulster County, New York. On June 3, she removed a tick from her neck. On June 9, she experienced severe headaches and the next day had low-grade fever, chills, and body aches. She had no cough, shortness of breath, or sore throat. On June 10, she tested negative for SARS-CoV-2 by PCR. She continued to have extreme fatigue, myalgia, and low-grade fever. She was prescribed oseltamivir by her obstetrician on June 11. On June 14, she felt better. Repeat PCR testing for SARS-CoV-2 on June 15 was negative. She continued to improve until June 23, when she experienced recurrent fever up to 38.9°C, chills, and lethargy. She contacted her obstetrician and was told she had

a presumptive diagnosis of COVID-19. On June 30, she saw her internist and underwent laboratory testing for tickborne illnesses; she was treated empirically with amoxicillin because of her risks for Lyme disease. PCR for *A. phagocytophilum* was positive, as was a second test on July 8. Serologic results for Lyme were positive for 41-kD, 39-kD, and 23-kD bands with no IgG bands. Platelets were 140,000 (previously 336,000), aspartate aminotransferase was 95, and alanine aminotransferase was 81. Several weeks later, studies revealed anaplasma IgM 1:256 and IgG 1:1,280. Lyme disease C6 antibody was positive. After discussion, the patient and her physicians chose not to treat for anaplasmosis because she was clinically improving. The patient has remained well, and the child was born healthy by normal spontaneous vaginal delivery.

COVID-19 has had devastating effects on the medical system and led to widespread changes in the practice of medicine. We believe that the imperative to rule out COVID-19 led to diagnostic anchoring bias in these cases. Such biases are among the most common in the heuristic decision-making process (3,4). Of note, in these 2 cases (case 1, human granulocytic anaplasmosis [HGA]; case 2, co-infection with Lyme disease and HGA), COVID-19 was ruled out without considering other diagnoses, even though the patients were visiting areas to which tickborne diseases are endemic. Given the incidence of such diseases in these areas and widespread attempts to educate healthcare providers about these diseases, failure to evaluate for tickborne infections would be difficult to imagine before COVID-19. Although both of these patients have done well, serious consequences to the fetus could have occurred if Lyme disease had gone undiagnosed and untreated (5). Although transmission of *A. phagocytophilum* during pregnancy has been reported (6) and treatment during pregnancy in a limited number of cases has possibly prevented transmission (7), in this instance the patient cleared the anaplasma without treatment, and the child was born disease-free. Clearance of infection without treatment has been reported in other studies, but we are unaware of cases describing the outcome of pregnancy in untreated women with acute HGA (8).

We appreciate the devastating effects that a missed COVID-19 diagnosis can have on a person, as well as the epidemiologic implications thereof. However, failing to diagnose tickborne illnesses and other infections also can have serious consequences. Healthcare providers must keep an open mind to diagnoses other than COVID-19 in febrile patients and not fall prey to misdiagnosis because of current pressures to evaluate for COVID-19.

About the Author

Dr. Horowitz is clinical professor of medicine at Weill Cornell Medicine and chief of infectious diseases at New York-Presbyterian Brooklyn Methodist Hospital. He has been involved in clinical practice for the past 38 years, and his research has focused on immune-suppressed patients, tickborne diseases, and, more recently, antimicrobial stewardship and hospital-acquired infections.

References

1. CDC COVID-19 Response Team. Severe outcomes among patients with coronavirus disease 2019 (COVID-19)—United States, February 12–March 16, 2020. MMWR Morb Wkly Rep. 2020;69:343–6.
2. Hollander JE, Carr BG. Virtually Perfect? Telemedicine for Covid-19. N Engl J Med. 2020;382:1679–81. https://doi.org/10.1056/NEJMp2003539
3. Sapersnik G, Redelmeier D, Ruff CC, et a. Cognitive biases associated with medical decisions: a systematic review. BMC Med Inform Decis Mak. 2016;16:138. https://doi.org/10.1186/s12911-016-0377-1
4. Ogdie AR, Reilly JB, Pang WG, Keddem S, Barg FK, Von Feldt JM, et al. Seen through their eyes: residents' reflections on the cognitive and contextual components of diagnostic errors in medicine. Acad Med. 2012;87:1361–7. https://doi.org/10.1097/ACM.0b013e31826742c9
5. Waddell LA, Greig J, Lindsay LR, Hinckley AF, Ogden NH. A systematic review on the impact of gestational Lyme disease in humans on the fetus and newborn. PLoS One. 2018;13:e0207067. https://doi.org/10.1371/journal.pone.0207067
6. Horowitz HW, Kilchevski E, Haber S, et al. Brief report: Perinatal transmission of the human granulocytic ehrlichiosis agent. N Engl J Med. 1998;339:375–8. https://doi.org/10.1056/NEJM199808063390604
7. Dhand A, Nadelman RB, Aguero-Rosenfeld ME, Haddad F, Stokes D, Horowitz HW. Human granulocytic anaplasmosis in pregnancy: case series and review of literature. Clin Infect Dis. 2007;45:589–93. https://doi.org/10.1086/520659
8. Bakken JS, Haller I, Riddell D, Walls JJ, Dumler JS. The serological response of patients infected with the agent of human granulocytic ehrlichiosis. Clin Infect Dis. 2002;34:22–7. https://doi.org/10.1086/323811

Address for correspondence: Harold Horowitz, New York Presbyterian-Brooklyn Methodist Hospital, 506 6th St, Brooklyn, New York, NY 11215, USA; email: hwh2002@med.cornell.

Molecular Detection and Characterization of *Rickettsia asembonensis* in Human Blood, Zambia

Lavel C. Moonga, Kyoko Hayashida,
Namwiinga R. Mulunda, Yukiko Nakamura, James Chipeta,[1] Hawela B. Moonga,
Boniface Namangala, Chihiro Sugimoto,
Zephaniah Mtonga, Mable Mutengo, Junya Yamagishi

Author affiliations: Hokkaido University, Sapporo, Japan
(L.C. Moonga, K. Hayashida, Y. Nakamura, C. Sugimoto,
J. Yamagishi); University of Zambia, Lusaka, Zambia
(N.R. Mulunda, J. Chipeta, B. Namangala, M. Mutengo); National
Malaria Control Center, Lusaka (H.B. Moonga); Chongwe District
Hospital, Lusaka (Z. Mtonga); Levy Mwanawasa Medical
University, Lusaka (M. Mutengo)

Rickettsia asembonensis is a flea-related *Rickettsia* with unknown pathogenicity to humans. We detected *R. asembonensis* DNA in 2 of 1,153 human blood samples in Zambia. Our findings suggest the possibility of *R. asembonensis* infection in humans despite its unknown pathogenicity.

*R*ickettsia asembonensis is a fleaborne rickettsia closely related to *Rickettsia felis* and is thus referred to as an *R. felis*–like organism. *R. asembonensis* was first detected in cat fleas in Kenya and subsequently reported worldwide (*1,2*). Although *R. felis* has been increasingly recognized as a human infective agent that can cause human febrile disease, the infectivity and pathogenicity of *R. asembonensis* in humans is largely unknown. Recent investigations in patients with febrile illness and petechial lesions identified *R. asembonensis* DNA and antibodies for rickettsial antigens in Malaysia (*3,4*). Furthermore, *R. asembonensis* was isolated in cellular cultures from patients in Peru with acute febrile illness and confirmed by sequencing (*5*). These reports suggest the possibility of *R. asembonensis* as a human infective agent. However, no direct evidence of *R. felis* and *R. asembonensis* as an etiologic agent of human illness has been established. A previous study in Zambia revealed the predominant existence of *R. asembonensis* and *R. felis* in cat fleas (*6*). Our study investigates the presence of these rickettsiae in human blood in Zambia.

We obtained 753 residual patient blood samples from hospitals in urban Lusaka (n = 519) and the

Chongwe District (n = 234) of Zambia. Approximately half of the samples (303/753) were traceable to clinical records of patients. The common clinical conditions among those patients included fever, anemia, meningitis, septicemia, and sickle cell anemia (Appendix Table 1, https://wwwnc.cdc.gov/EID/article/27/8/20-3467-App1.pdf). In addition, we obtained dried blood spots on Whatman FTA classic cards (Millipore Sigma, https://www.sigmaaldrich.com) from healthy volunteers from rural eastern (n = 200) and central (n = 200) provinces to assess rickettsia infection in healthy rural persons. The study was approved by the National Health Research Authority of Zambia through the Biomedical Research Ethics Committee (reference no. 007-10-18).

We extracted genomic DNA and subjected it to PCR screening that targeted the citrate synthase gene (*gltA*) of *Rickettsia*. We subjected the positive samples to multiple-gene sequencing analysis targeting the 17-kDa common antigen (*htrA*), outer membrane protein A (*OmpA*), and outer membrane protein B (*OmpB*) genes using previously described primers (Appendix Table 2). We aligned the sequences using MAFFT (https://mafft.cbrc.jp/alignment/server) and performed phylogenetic analysis by the neighbor-joining method using MEGA7 (https://www.megasoftware.net). We determined the estimated *Rickettsia* bacterial burden in *Rickettsia*-positive blood samples by *OmpA* quantitative PCR by using published primers. We further testsed the *gltA* PCR-positive samples for malaria by nested PCR (Appendix Table 2).

We detected *R. asembonensis* in 0.39% (2/519) samples from the urban Lusaka District by *gltA* PCR. The samples from the Chongwe District and the rural areas of the eastern and central provinces were all negative, although the possibility that dried blood spot samples from rural areas might have lower detection sensitivity cannot be ruled out. BLAST analysis (https://blast.ncbi.nlm.nih.gov/Blast.cgi) of the *gltA* sequences obtained (GenBank accession nos. LC557154 and LC557155) showed 100% homology to *R. asembonensis* identified in cat fleas from human dwellings and domestic dogs in 3 countries: Senegal (GenBank accession no. JF966774), Kenya (accession no. JN315968), and Zambia (accession no. LC431490) (*6,7*). Comparing the sequenced *gltA* with those detected in fleas from Peru (GenBank accession no. KY650697) and other regions in the Americas showed 99.8% similarity. Phylogenetic analysis of *gltA* confirmed the detected sequences' closer relatedness by clustering with genes from cat fleas from sub-Saharan Africa, a distinct cluster from other regions (Figure). The *OmpA*, *OmpB*, and *htrA* sequences showed clustering without regional

[1]Deceased.
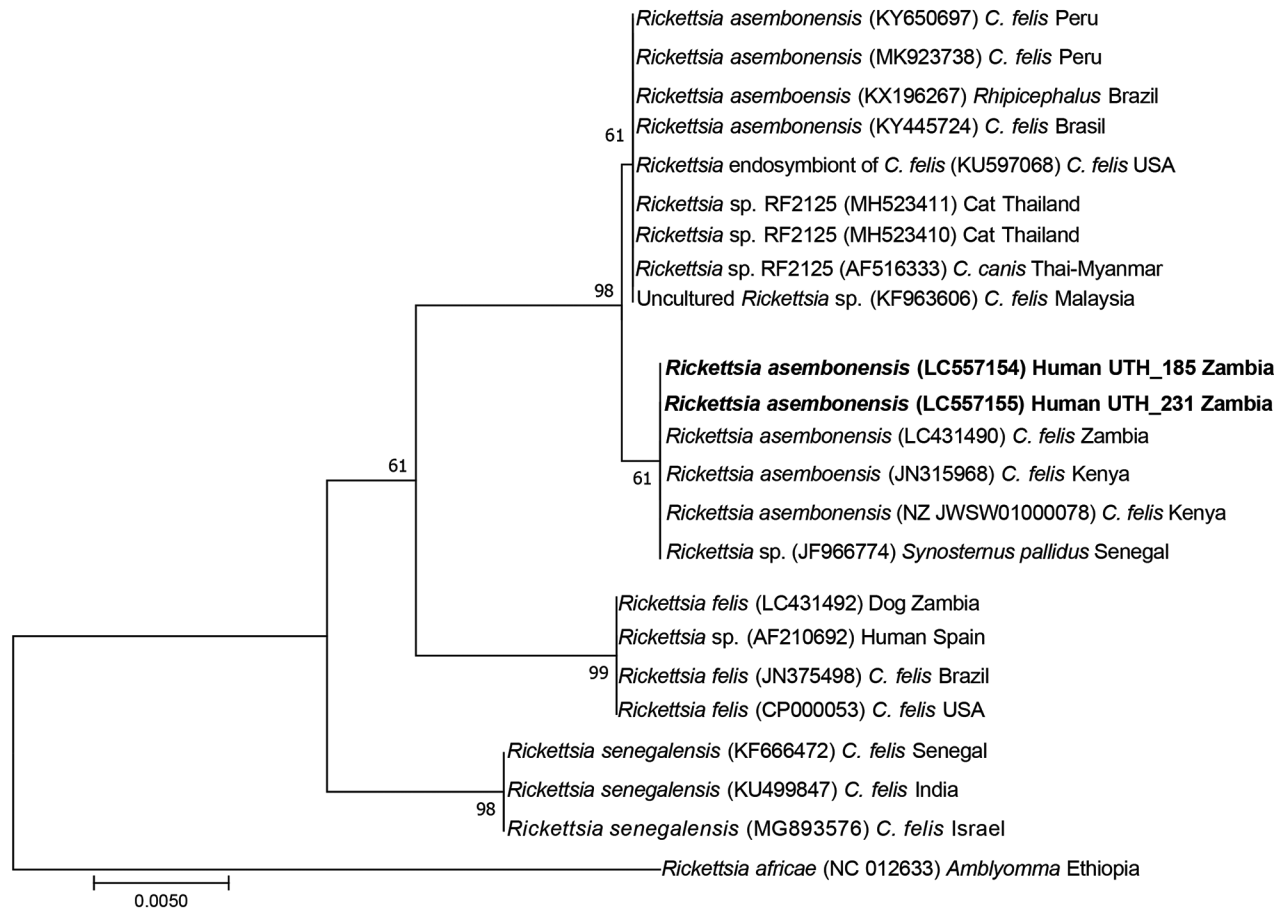
Figure. Phylogenetic tree of *Rickettsia felis* and *R. felis*–like organisms based on the sequences of the *gltA* gene (581 bp) from human blood samples collected from Zambia, 2019 (in bold). The tree was constructed using the neighbor-joining method with the maximum-likelihood model. Bootstrap values are shown on nodes based on 1,000 replicates. Sequences are identified by species name, GenBank accession number, host, and country of detection. Scale bar indicates nucleotide substitutions per site.

discrimination (data not shown). The obtained nucleotides are available in GenBank under accession nos. LC557154–61. Detection of genotypically similar *R. asembonensis* in persons and cat fleas in Zambia suggests possible human infection by *R. asembonensis* through cat flea bites. Nevertheless, the epidemiologic cycle and pathogenicity of *R. asembonensis* and other related *R. felis*–like organisms remain to be elucidated.

The patient identified as UTH_185 in whom *R. asembonensis* was detected had a medical record of anemia and weight loss (Table). The malaria test was

negative. Despite the limited association of *Rickettsia* infection with anemia, severe *R. felis* infection has been reported with severe anemia, possibly attributable to hemorrhage from vascular damage in rickettsial disease (*8*). However, the observed evidence was limited and could not establish *R. asembonensis* as the cause of these symptoms. The second *R. asembonensis*–positive sample from the patient identified as UTH_231 had limited clinical information, which did not allow for further interpretation. The 2 *R. asembonensis*–positive blood samples showed estimated

Table. Selected demographic and clinical characteristics of 2 persons in whom *Rickettsia asembonensis* was detected from blood samples collected in Zambia

Characteristic	Patient UTH_185	Patient UTH_231
Age, y	42	45
Sex	Female	Female
Residential area	Lusaka	Lusaka
Clinical manifestation	Anemia and weight loss	No information
Estimated rickettsia genome copies/mL blood	890,000	2,150,000
Malaria test	Negative	Negative

DNA quantities of 890,000 copies/mL of blood from patient UTH_185 and 2,100,000 copies/mL of blood from patient UTH_231 (Table). These results are within the same range as a previous study for *Rickettsia rickettsii* estimated rickettsial burden (*9*).

In conclusion, detection of *R. asembonensis* of identical genotype in cat fleas and human blood in Zambia suggests possible transmission from cat fleas to humans. Given the worldwide distribution of *R. asembonensis*, further studies to elucidate its pathogenicity and epidemiologic cycle are warranted.

About the Author

Dr. Moonga is a postdoctoral research fellow at Hokkaido University. His research interests include arthropodborne zoonoses, specifically fleaborne rickettsia infections as a possible cause of febrile illness, and developing of rapid molecular diagnostic tools.

References

1. Jiang J, Maina AN, Knobel DL, Cleaveland S, Laudisoit A, Wamburu K, et al. Molecular detection of *Rickettsia felis* and *Candidatus* Rickettsia asemboensis in fleas from human habitats, Asembo, Kenya. Vector Borne Zoonotic Dis. 2013;13:550–8. https://doi.org/10.1089/vbz.2012.1123
2. Maina AN, Jiang J, Luce-Fedrow A, St John HK, Farris CM, Richards AL. Worldwide presence and features of flea-borne *Rickettsia asembonensis.* Front Vet Sci. 2019;5:334. https://doi.org/10.3389/fvets.2018.00334
3. Kho KL, Koh FX, Singh HKL, Zan HAM, Kukreja A, Ponnampalavanar S, et al. Case report: spotted fever group rickettsioses and murine typhus in a Malaysian teaching hospital. Am J Trop Med Hyg. 2016;95:765–8. https://doi.org/10.4269/ajtmh.16-0199
4. Tay ST, Kho KL, Vythilingam I, Ooi CH, Lau YL. Investigation of possible rickettsial infection in patients with malaria. Trop Biomed. 2019;36:257–62.
5. Palacios-Salvatierra R, Cáceres-Rey O, Vásquez-Domínguez A, Mosquera-Visaloth P, Anaya-Ramírez E. Rickettsial species in human cases with non-specific acute febrile syndrome in Peru [in Spanish]. Rev Peru Med Exp Salud Publica. 2018;35:630–5. https://doi.org/10.17843/rpmesp.2018.354.3646
6. Moonga LC, Hayashida K, Nakao R, Lisulo M, Kaneko C, Nakamura I, et al. Molecular detection of *Rickettsia felis* in dogs, rodents and cat fleas in Zambia. Parasit Vectors. 2019;12:168. https://doi.org/10.1186/s13071-019-3435-6
7. Roucher C, Mediannikov O, Diatta G, Trape J-FF, Raoult D. A new *Rickettsia* species found in fleas collected from human dwellings and from domestic cats and dogs in Senegal. Vector Borne Zoonotic Dis. 2012;12:360–5. https://doi.org/10.1089/vbz.2011.0734
8. Zavala-Castro J, Zavala-Velázquez J, Walker D, Pérez-Osorio J, Peniche-Lara G. Severe human infection with *Rickettsia felis* associated with hepatitis in Yucatan, Mexico. Int J Med Microbiol. 2009;299:529–33. https://doi.org/10.1016/j.ijmm.2009.03.002
9. Kato C, Chung I, Paddock C. Estimation of *Rickettsia rickettsii* copy number in the blood of patients with Rocky Mountain spotted fever suggests cyclic diurnal trends in bacteraemia. Clin Microbiol Infect. 2016;22:394–6. https://doi.org/10.1016/j.cmi.2015.12.019

Address for correspondence: Kyoko Hayashida, Hokkaido University, International Institute for Zoonosis Control, Division of Collaboration and Education, Kita 20 Nishi 10, Kita-Ku, Sapporo 001-0020, Hokkaido, Japan; email: kyouko-h@czc.hokudai.ac.jp

Post–13-Valent Pneumococcal Conjugate Vaccine Dynamics in Young Children

Corinne Levy, Naim Ouldali, Emmanuelle Varon, Stéphane Béchet, Stéphane Bonacorsi, Robert Cohen

Author affiliations: Association Clinique et Thérapeutique Infantile du Val-de-Marne, Créteil, France (C. Levy, N. Ouldali, S. Béchet, R. Cohen); Groupe de Pathologie Infectieuse Pédiatrique, Paris, France (C. Levy, N. Ouldali, E. Varon, S. Bonacorsi, R. Cohen); Université Paris Est, IMRB-GRC GEMINI, Créteil (C. Levy, E. Varon, R. Cohen); Centre Hospitalier Intercommunal de Créteil, Créteil (C. Levy, E. Varon, R. Cohen); Association Française de Pédiatrie Ambulatoire, Saint-Germain-en-Laye, France (C. Levy, R. Cohen); Assistance Publique-Hôpitaux de Paris, Hôpital Robert Debré, ECEVE INSERM UMR 1123, Paris (N. Ouldali, S. Bonacorsi); Université de Paris, IAME, UMR 1137, INSERM, Paris (S. Bonacorsi)

To the Editor: We read with interest the article by Ben-Shimol et al. (1), which described the disproportionate increase of non–13-valent pneumococcal conjugate vaccine (PCV) additional PCV20 serotypes (vaccine type [VT] 20–13) in patients who had respiratory infections or invasive pneumococcal disease (IPD) after PCV13 implementation in Israel. The authors emphasized the higher disease potential of VT20–13 serotypes compared with non-VT20 serotypes. We would like to complement their results with data from France and highlight the similarities and the differences in serotype distribution. Our long-term prospective population-based surveillance comprises pneumococcal isolates from 793 healthy carriers, 4,474 acute otitis media patients, and 441 IPD patients, all of whom were children <24 months of age (2–4). We found that VT13 serotypes accounted for 8%, VT20–13 for 30%, and non-VT20 for 60% of infections in healthy carriers and acute otitis media patients during 2015–2018. Like Ben-Shimol et al. (1), we found that the most common VT20–13 serotypes were 15B/C and 11A, and the most common non-VT20 serotypes were 23B, 15A, and 35B.

From the early PCV13 (2009–2011 in both countries) to late PCV13 period (2015–2017 in Israel and 2015–2018 in France), the prevalence of IPD caused by VT13 serotypes declined by ≈90% in both countries. However, VT20–13 serotypes predominated in Israel, whereas non-VT20 serotypes predominated in France. Although Israel had higher proportions of serotypes 12F (26.9% vs. 0.9%) and 33F (10.6% vs. 4.4%) than France (1), France saw the emergence of the non-VT20 serotype 24F (27.4%) during 2015–2018. This emergent serotype led to a higher proportion of PCV20 serotypes in Israel (62%) than in France (41.6%). The differences in vaccine type distribution between the 2 countries were mainly based on the very high rates of serotypes 12F and 33F in Israel and the emerging serotype 24F in France (5). Apart from these serotypes, the serotype distribution in IPD was very similar (Table).

In conclusion, data from Israel and France show a similar effect of PCV13 on the distribution of VT13 serotypes. The role of emerging non-PCV13 serotypes in carriage was also similar. However, we observed unexpected discrepancies in the serotype replacement pattern, driven by few highly invasive non-PCV13 serotypes. This finding suggests that serotype replacement during the PCV13 era is complex and multifactorial, and has implications for the expected effects of next-generation PCVs. Finally, France and Israel had similar serotype distributions that differed in only the late PCV13 period as a result of the emergence of some invasive specific clones (5–8).

Table. Comparison of pneumococcal serotypes in children <24 mo of age in Israel, 2015–2017, and France, 2015–2018*

Serotypes	Cases of invasive pneumococcal disease, no. (%)	
	Israel	France
Total	216 (100.0)	113 (100.0)
PCV13 serotypes	22 (10.2)	5 (4.4)
22F	8 (3.7)	8 (7.1)
33F	23 (10.6)	5 (4.4)
PCV15 serotypes†	53 (24.5)	18 (15.9)
8	2 (0.9)	2 (1.8)
10A	8 (3.7)	11 (9.7)
11A	3 (1.4)	2 (1.8)
12F	58 (26.9)	1 (0.9)
15B/C	10 (4.6)	13 (11.5)
PCV20 serotypes‡	134 (62.0)	47 (41.6)
Non-VT20	82 (38.0)	66 (58.4)
24F	7 (3.2)	31 (27.4)
VT20–13	112 (51.9)	42 (37.2)
Non-PCV13	194 (89.8)	108 (95.6)

*Non-VT20, serotypes in PCV20; PCV13, 13-valent PCV; PCV15, 15-valent PCV; PCV20, 20-valent PCV; PCV, pneumococcal conjugate vaccine; VT20–13, vaccine types in PCV20 but not PCV13.
†Comprises PCV13 serotypes as well as 22F and 33F.
‡Comprises PCV15 serotypes as well as 8, 10A, 11A, 12F, and 15B/C.

R.C., C.L., and E.V. received personal fees and nonfinancial support from Pfizer. R.C. reports personal fees from AstraZeneca GSK, Merck Sharp & Dohme, and Sanofi outside of the context of the submitted work.

References

1. Ben-Shimol S, Givon-Lavi N, Kotler L, Adriaan van der Beek B, Greenberg D, Dagan R. Post-13-valent pneumococcal conjugate vaccine dynamics in young children of serotypes included in candidate extended-spectrum conjugate vaccines. Emerg Infect Dis. 2021;27:150–60. https://doi.org/10.3201/eid2701.201178
2. Cohen R, Levy C, Ouldali N, Goldrey M, Béchet S, Bonacorsi S, et al. Invasive disease potential of pneumococcal serotypes in children after PCV13 implementation. Clin Infect Dis. 2021;72:1453–6. https://doi.org/10.1093/cid/ciaa917
3. Levy C, Vie le Sage F, Varon E, Chalumeau M, Grimprel E, Cohen R. Pediatric ambulatory and hospital networks for surveillance and clinical epidemiology of community-acquired infections. J Pediatr. 2018;194:269–270.e2. https://doi.org/10.1016/j.jpeds.2017.11.050
4. Ouldali N, Cohen R, Levy C, Gelbert-Baudino N, Seror E, Corrard F, et al. Pneumococcal susceptibility to antibiotics in carriage: a 17 year time series analysis of the adaptive evolution of non-vaccine emerging serotypes to a new selective pressure environment. J Antimicrob Chemother. 2019;74:3077–86. https://doi.org/10.1093/jac/dkz281
5. Rokney A, Ben-Shimol S, Korenman Z, Porat N, Gorodnitzky Z, Givon-Lavi N, et al. Emergence of *Streptococcus pneumoniae* serotype 12F after sequential introduction of 7- and 13-valent vaccines, Israel. Emerg Infect Dis. 2018;24:453–61. https://doi.org/10.3201/eid2403.170769
6. Janoir C, Lepoutre A, Gutmann L, Varon E. Insight into resistance phenotypes of emergent non 13-valent pneumococcal conjugate vaccine type pneumococci isolated from invasive disease after 13-valent pneumococcal conjugate vaccine implementation in France. Open Forum Infect Dis. 2016;3:ofw020. https://doi.org/10.1093/ofid/ofw020
7. Lo SW, Gladstone RA, van Tonder AJ, Lees JA, du Plessis M, Benisty R, et al.; Global Pneumococcal Sequencing Consortium. Pneumococcal lineages associated with serotype replacement and antibiotic resistance in childhood invasive pneumococcal disease in the post-PCV13 era: an international whole-genome sequencing study. Lancet Infect Dis. 2019;19:759–69. https://doi.org/10.1016/S1473-3099(19)30297-X
8. Ouldali N, Levy C, Varon E, Bonacorsi S, Béchet S, Cohen R, et al.; French Pediatric Meningitis Network. Incidence of paediatric pneumococcal meningitis and emergence of new serotypes: a time-series analysis of a 16-year French national survey. Lancet Infect Dis. 2018;18:983–91. https://doi.org/10.1016/S1473-3099(18)30349-9

Estimate of Burden and Direct Healthcare Cost of Infectious Waterborne Disease in the United States

Stephanie DeFlorio-Barker, Abhilasha Shrestha, Samuel Dorevitch

Author affiliations: US Environmental Protection Agency, Research Triangle Park, North Carolina, USA (S. DeFlorio-Barker); University of Illinois–Chicago School of Public Health, Chicago, Illinois, USA (A. Shrestha, S. Dorevitch)

To the Editors: We read with interest an article by S.A. Collier et al. (*1*) estimating the economic burden of waterborne illnesses in the United States. Although we found the study noteworthy, the burden estimates differ greatly from those in our 2018 study (*2*) of the economic burden from recreational waterborne illness in the United States. The studies estimated very different numbers of cases: Collier et al. estimated ≈7.1 million total waterborne illnesses, but we estimated ≈90 million recreational waterborne illnesses in untreated water. Collier et al. estimated $3.3 billion in total direct costs from all waterborne illness caused by 17 pathogens, but we estimated $2.9 billion from recreational waterborne illness alone. Both studies used similar methods to address underreporting and underdiagnosis of illness. Key differences between studies include that Collier et al. summarized healthcare costs associated with infections caused by 17 pathogens that might be waterborne, then relied heavily on expert judgment (*3*) to estimate the proportion attributable to water exposure. In contrast, our study used data from large cohort studies of water recreation to estimate the burden from mild and moderate illnesses and outbreak data to estimate the burden from severe illnesses from water recreation. Collier et al. estimated the direct costs of illness, whereas our study estimated both direct and indirect costs (e.g., workplace absence). Enteric pathogens responsible for gastrointestinal symptoms after water recreation are generally not identified in clinical testing (*4*); because Collier et al. used economic burden estimates from waterborne illness based only on 17 pathogens, the study substantially underestimates the overall number of cases and associated economic burden. Future research should consider cohort and outbreak data for treated and untreated recreational water and drinking water to estimate the total economic burden from waterborne illness.

References

1. Collier SA, Deng L, Adam EA, Benedict KM, Beshearse EM, Blackstock AJ, et al. Estimate of burden and direct healthcare cost of infectious waterborne disease in the United States. Emerg Infect Dis. 2021;27:140–9. https://doi.org/10.3201/eid2701.190676

2. DeFlorio-Barker S, Wing C, Jones RM, Dorevitch S. Estimate of incidence and cost of recreational waterborne illness on United States surface waters. Environ Health. 2018;17:3. https://doi.org/10.1186/s12940-017-0347-9

3. Beshearse E, Bruce BB, Nane GF, Cooke RM, Aspinall W, Hald T, et al. Attribution of illnesses transmitted by food and water to comprehensive transmission pathways using structured expert judgment, United States. Emerg Infect Dis. 2021;27:182–95. https://doi.org/10.3201/eid2701.200316

4. Dorevitch S, Dworkin MS, Deflorio SA, Janda WM, Wuellner J, Hershow RC. Enteric pathogens in stool samples of Chicago-area water recreators with new-onset gastrointestinal symptoms. Water Res. 2012;46:4961–72. https://doi.org/10.1016/j.watres.2012.06.030

Address for correspondence: Stephanie DeFlorio-Barker, US Environmental Protection Agency, 109 TW Alexander Dr M/D B243-01, Research Triangle Park, NC 27709, USA; email: Deflorio-Barker.Stephanie@epa.gov

October 2020
Bacterial Infections

EMERGING INFECTIOUS DISEASES

To revisit the October 2020 issue, go to:

https://wwwnc.cdc.gov/eid/articles/issue/26/10/table-of-contents

The Yellow Flag: Quarantine and the British Mediterranean World, 1780–1860

In reading the Centers for Disease Control and Prevention's February 2021 order (*1*) requiring passengers to wear face masks while on conveyances, I learned a new concept: "free pratique," the permission granted by a government to an international vessel (ship, plane, or other) to disembark its passengers once it has been deemed clear of contagion. That same day, opening *The Yellow Flag: Quarantine and the British Mediterranean World, 1780–1860*, by Alex Chase-Levenson, I encountered the concept again, in the same context: 18th-century travelers freed from quarantine's constraints were considered to be in "free pratique" (p. 15). History may not repeat itself, but it does rhyme.

When we think of the history of how one nation defines itself in relation to others (e.g., borders, trade, diplomacy), we do not usually include communicable disease control in the list. *The Yellow Flag* describes the administrative practices requiring quarantine of travelers and goods arriving in ports by ship (and, in some cases, at land crossings) from places considered "foul." Ships flying the yellow flag were deemed "plague smitten" and their passengers and cargo were subject to a range of complex, changeable rules.

Chase-Levenson focuses on Britain, a country perceived in the early 1800s as still at the geographic, political, and economic edge of Mediterranean power and politics. The edge case is illuminating. The anxieties accompanying increasing "globalism" in the 18th century (even if "global," for the purposes of *The Yellow Flag*'s era, meant the Mediterranean basin) so perfectly rhyme with those of the 21st: efforts to exclude or expedite the passage of persons and goods, but also collaboration among health and medical experts across many countries and jurisdictions to form coherent and defensible policy. Scientists, bureaucrats, and citizens stumbling in understanding cause and effect, prevention and efficacy. The fervor with which anticontagionists (persons who denied that the diseases of concern were spread from person to person) defended their position, including an account of an anticontagionist who injected himself with blood from a plague victim to disprove the theory of contagion, with tragically predictable results. Social media, in the form of mass-produced pamphlets, warning of secret plans, conspiracy, and perfidy. The performative aspects of infection control, such as fumigating with a few pinches of nitre on a tray of charcoal.
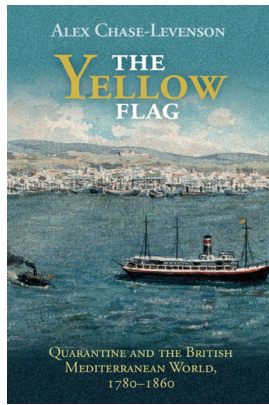
Chase-Levenson lays out these stories clearly and systematically. The narratives of individual travelers, written while in quarantine, were particularly entertaining, although the depth of detail may engage the historian more than the epidemiologist. I have but one criticism: the index seems incomplete. For example, the term "pratique" is not included. That is not the author's fault, but the publisher's.

The purpose of reading history has, to me, always been to both bring our ancestors closer—they were truly just like us in their triumphs and tragedies—and to learn what we can from their experiences to illuminate our present day. When future historians examine the COVID-19 pandemic, what will they marvel at? And shake their heads at? I have thought about that again and again during the past year and a half. Let us hope the historians are as insightful, and the results as readable, as Chase-Levenson's inquiry.

Reference

1. Requirement for persons to wear masks while on conveyances and at transportation hubs. 86 Fed. Reg. 8025, February 3, 2021 [cited 2021 May 11]. https://www.federalregister.gov/documents/2021/02/03/2021-02340/requirement-for-persons-to-wear-masks-while-on-conveyances-and-at-transportation-hubs

Rebecca Wurtz

Author affiliation: University of Minnesota School of Public Health, Minneapolis, Minnesota, USA

Address for correspondence: Rebecca Wurtz, University of Minnesota School of Public Health, 420 Delaware St SE, Minneapolis, MN 55455, USA; email: rwurtz@umn.edu

Jonas Lie (1880−1940). *The Conquerors (Culebra Cut, Panama Canal)*, **1913.** Oil on canvas, 60 in x 50 in/152.4 cm x 127 cm. Image copyright © The Metropolitan Museum of Art, New York, NY, USA. Image source: Art Resource, New York, NY, USA.

Special Wonders of the Canal

Byron Breedlove

The official opening of the Panama Canal in August 1914 marked the culmination of an idea that Charles V, Holy Roman Emperor and King of Spain, proposed in 1534, two decades after Spanish explorer Vasco Nunez de Balboa had visited the Isthmus of Panama. After an attempt by France to forge a canal connecting the Atlantic and Pacific Oceans was abandoned—in large measure because yellow fever and

Author affiliation: Centers for Disease Control and Prevention, Atlanta, Georgia, USA

malaria devastated its workforce—the United States arranged to continue the work in 1904. The US undertaking was enormous and lasted another decade, moved enough earth and rubble to create a 16-foot-wide tunnel reaching the center of the Earth, and was deemed by the American Society of Civil Engineers to be among the 7 greatest civil engineering achievements of the 20th century.

The Culebra Cut,[1] a 9-mile stretch through the Continental Divide from Gamboa on the Chagres River in the north to Pedro Miguel in the south between Bas Obispo and Pedro Miguel, proved to be the most

challenging section to finish, and this project was dubbed "the special wonder of the canal." Historian David McCullough notes the Culebra Cut "was the great focus of attention, regardless of whatever else was happening at Panama. The building of Gatun Dam or the construction of the locks, projects of colossal scale and expense, were always of secondary interest so long as the battle raged in that nine-mile stretch."

Construction in the cut continued day and night under unforgiving conditions and involving as many as 6,000 workers, including Panamanians, West Indians, and African Americans. Blistering tropical heat that could reach up to 120°F was compounded by a rainy season that lasted 9 months and by miserably high humidity. Reverberating off the canyon walls was an unrelenting cacophony created by up to 300 drills, 60 to 70 shovels each loading several trains, whistles and shouts from the workers, and countless explosions. McCullough writes, "For seven years Culebra Cut was never silent, not even for an hour." Deadly landslides occurred without warning, becoming larger and more frequent as work progressed and destroying machinery, burying workers, and reversing months of momentum. Deaths caused by trains, construction equipment, falls, and explosions occurred daily.

The Isthmus of Panama was also a perfect environment for mosquitoes. However, because the mosquitoborne illnesses of yellow fever and malaria that waylaid the effort by France had been controlled by the time work started on the cut, the Panama Canal was eventually completed ahead of schedule and under budget.

Credit centers on the work of Colonel William C. Gorgas, who after his successful efforts to control yellow fever in Cuba in 1901 was appointed chief sanitation officer for the Panama Canal project in 1904. He and his team of sanitary engineers enacted strictly enforced, integrated measures—including draining sources of standing water, applying larvicides, and screening windows—that virtually eliminated yellow fever and greatly reduced the toll of malaria, diseases that Carlos Finlay and Ronald Ross, respectively, had only a few years earlier shown were transmitted by mosquitoes. Gorgas drew upon the pioneering work of Walter Reed, James Carroll, Aristides Agramonte,

and Jesse Lazear (Lazear died of yellow fever in Cuba in September 1900), who had elucidated the role of the mosquito in yellow fever transmission. They paved the way for Gorgas to implement the assiduous and extraordinarily effective prevention/control program. According to Centers for Disease Control and Prevention, the malaria death rate for employees dropped from 11.59 per 1,000 in November 1906 to 1.23 per 1,000 in December 1909, and deaths from malaria in the total population decreased from 16.21 per 1,000 in July 1906 to 2.58 per 1,000 in December 1909.

Near the end of 1912 artist Jonas Lie viewed—and was captivated by—an early color movie, *The Making of the Panama Canal*. In early 1913, Lie made a 3-month sojourn to Panama, where he completed an estimated 30 paintings of the work. Lie witnessed the final stages of work as the excavation of Culebra Cut was completed on May 20, 1913. According to the Hudson River Museum, Lie "was enthralled by the feats of engineering required to dig the Culebra Cut, as well as the sublime visual qualities of the massive trench being carved across the Isthmus of Panama. Working tirelessly in the intense tropical heat, he produced oil sketches and drawings and took careful notes on the technical aspects of the canal construction." Lie's *The Conquerors (Culebra Cut, Panama Canal)*, featured on this month's cover, is among the best-known depictions of the canal's construction and the most celebrated painting from his excursion.

Although the painting is interspersed with earth tones, flecks of red, and smudges of green, the tones that dominate the palette are blue, black, gray, and white. Along the gorge's floor, coal-fired locomotives traverse parallel train tracks, belching black plumes of smoke that rise like sooty geysers and churning hazy clouds of bluish steam into the humid air. The bulging slope of the cut on the left, its facets captured in bold strokes, and a sheer vertical rock wall on the right, provide scale and perspective. Vestiges of native flora clinging to the right wall offer a reminder that this area was once verdant. Workers trudge the steep path from the bottom, engulfed by their surroundings. Bartholomew F. Bland, deputy director of the Hudson River Museum, says of *The Conquerors*: "It looks like hell, like an inferno . . . there's all this black smoke."

During the effort to build the canal in the 1880s, more than 22,000 workers from France died, many from malaria and yellow fever, before the etiologies of those tropical diseases were understood. Records indicate that during the period of US construction, more than 55,000 people were employed and an estimated 5,600 died of injury and disease. The death

---

[1]From 1915 to 2000, this section of the canal was named the Gaillard Cut after US Major David du Bose Gaillard, who had supervised much of the construction. After the United States transferred control of the canal to Panama In 2000, the name was changed back to the Culebra Cut (its original name from 1914–1915). Culebra is also the name of the mountain ridge that this artificial valley cuts through.

toll would have been higher without effective protocols to control vectorborne diseases, in effect a second "special wonder of the canal." Many of those practices Gorgas instituted continue to be important in global efforts to control mosquitoborne illnesses.

Bibliography
1. American Society of Civil Engineers. Seven wonders [cited 2021 Jun 16]. http://www.asce.org/Content.aspx?id=2147487311
2. Cadbury D. Seven wonders of the industrial world. London and New York: 4th Estate, 2003 p. 252–60.
3. Centers for Disease Control and Prevention. Malaria. The Panama Canal [cited 2021 Jun 8]. https://www.cdc.gov/malaria/about/history/panama_canal.html
4. Hudson River Museum. Oh Panama!: Jonas Lie paints the Panama Canal [cited 2021 Jun 4]. https://www.hrm.org/exhibitions/oh-panama
5. La Gorce T. Artist's greatest subject was the Panama Canal. The New York Times [cited 2021 Jun 4]. https://www.nytimes.com/2016/02/28/nyregion/artists-greatest-subject-was-the-panama-canal.html
6. Linda Hall Library Exhibition. Fighting the fever [cited 2021 Jun 10]. https://panama.lindahall.org/fighting-fever
7. Linda Hall Library Exhibition. Somebody dying every day [cited 2021 Jun 10]. https://panama.lindahall.org/somebody-dying-every-day
8. McCullough D. The path between the seas: the creation of the Panama Canal 1870–1914. New York: Simon and Schuster, 1977. p. 405–26; 543.
9. Public Broadcast System. American Experience. Culebra Cut [cited 2021 Jun 10]. https://www.pbs.org/video/american-experience-culebra-cut
10. Reed W, Carroll J, Agramonte A, Lazear JW. The etiology of yellow fever—a preliminary note. Public Health Pap Rep. 1900;26:37–53. [cited 2021 Jun 10] https://www.ncbi.nlm.nih.gov/pmc/articles/PMC2329228/pdf/pubhealth-pap00031-0042.pdf
11. Stern AM. The Public Health Service in the Panama Canal: a forgotten chapter of U.S. public health. Public Health Rep. 2005;120:675–9.

Address for correspondence: Byron Breedlove, EID Journal, Centers for Disease Control and Prevention, 1600 Clifton Rd NE, Mailstop H16-2, Atlanta, GA 30329-4027, USA; email: wbb1@cdc.gov

EMERGING INFECTIOUS DISEASES®

Upcoming Issue • Vol.27 No.9

**Complete list of articles in the September issue at
http://www.cdc.gov/eid/upcoming.htm**

Earning CME Credit

To obtain credit, you should first read the journal article. After reading the article, you should be able to answer the following, related, multiple-choice questions. To complete the questions (with a minimum 75% passing score) and earn continuing medical education (CME) credit, please go to http://www.medscape.org/journal/eid. Credit cannot be obtained for tests completed on paper, although you may use the worksheet below to keep a record of your answers.

You must be a registered user on http://www.medscape.org. If you are not registered on http://www.medscape.org, please click on the "Register" link on the right hand side of the website.

Only one answer is correct for each question. Once you successfully answer all post-test questions, you will be able to view and/or print your certificate. For questions regarding this activity, contact the accredited provider, CME@medscape. net. For technical assistance, contact CME@medscape.net. American Medical Association's Physician's Recognition Award (AMA PRA) credits are accepted in the US as evidence of participation in CME activities. For further information on this award, please go to https://www.ama-assn.org. The AMA has determined that physicians not licensed in the US who participate in this CME activity are eligible for AMA PRA Category 1 Credits™. Through agreements that the AMA has made with agencies in some countries, AMA PRA credit may be acceptable as evidence of participation in CME activities. If you are not licensed in the US, please complete the questions online, print the AMA PRA CME credit certificate, and present it to your national medical association for review.

Article Title
Four Human Cases of Eastern Equine Encephalitis in Connecticut, USA, during a Larger Regional Outbreak, 2019

CME Questions

1. You are advising a Northeast US public health department about the potential challenges of an eastern equine encephalitis (EEE) outbreak. On the basis of the case series by Brown and colleagues, which one of the following statements about clinical findings and diagnostic challenges in an outbreak of 4 EEE cases seen at a single Connecticut institution within a 3-week period in 2019 is correct?

A. Seizures and cerebral edema were uncommon
B. Underrecognized elements of critical neuroinvasive EEE include refractory shock with adrenergic insensitivity and neuromuscular instability with flaccid paralysis or rigidity
C. Cerebrospinal fluid (CSF) profiles rapidly shifted from lymphocytic to myeloid predominance
D. Immunofluorescence assay antibody results through a national commercial reference laboratory were positive in all cases

2. According to the case series by Brown and colleagues, which one of the following statements about epidemiologic patterns in an outbreak of 4 EEE cases seen at a single Connecticut institution within a 3-week period in 2019 is correct?

A. The 4 EEE cases were diagnosed within a 3-week period coinciding with notable shifts in vector-host infection patterns in the Northeast, showing a striking change in EEE incidence
B. The 4 EEE cases were spread out in in different geographic regions of Connecticut
C. Numbers of primary-vector and bridge-vector mosquitoes were increased by 25% over usual levels
D. An unusual feature of this outbreak was that EEE virus was detected in dairy cows

3. On the basis of the case series by Brown and colleagues, which one of the following statements about clinical and public health implications of diagnostic challenges, clinical findings, and epidemiologic patterns in an outbreak of 4 EEE cases seen at a single Connecticut institution within a 3-week period in 2019 is correct?

A. Climate change is unlikely to affect the incidence of arboviral infection
B. This outbreak did not necessitate any changes in diagnostic testing protocols
C. The timing of diagnosis did not affect decision-making regarding treatment and public health measures
D. Coordination between public health and hospital settings to improve surveillance, clinical detection, and community education is essential to control future EEE outbreaks

Earning CME Credit

To obtain credit, you should first read the journal article. After reading the article, you should be able to answer the following, related, multiple-choice questions. To complete the questions (with a minimum 75% passing score) and earn continuing medical education (CME) credit, please go to http://www.medscape.org/journal/eid. Credit cannot be obtained for tests completed on paper, although you may use the worksheet below to keep a record of your answers.

You must be a registered user on http://www.medscape.org. If you are not registered on http://www.medscape.org, please click on the "Register" link on the right hand side of the website.

Only one answer is correct for each question. Once you successfully answer all post-test questions, you will be able to view and/or print your certificate. For questions regarding this activity, contact the accredited provider, CME@medscape.net. For technical assistance, contact CME@medscape.net. American Medical Association's Physician's Recognition Award (AMA PRA) credits are accepted in the US as evidence of participation in CME activities. For further information on this award, please go to https://www.ama-assn.org. The AMA has determined that physicians not licensed in the US who participate in this CME activity are eligible for AMA PRA Category 1 Credits™. Through agreements that the AMA has made with agencies in some countries, AMA PRA credit may be acceptable as evidence of participation in CME activities. If you are not licensed in the US, please complete the questions online, print the AMA PRA CME credit certificate, and present it to your national medical association for review.

Article Title

Fungemia and Other Fungal Infections Associated with Use of *Saccharomyces boulardii* Probiotic Supplements

CME Questions

1. Your patient is a 67-year-old man taking *Saccharomyces boulardii* (Sb) probiotic yeast for irritable bowel syndrome. According to the retrospective registry study by Rannikko and colleagues, which of the following statements about use of Sb probiotic yeast and clinical characteristics among patients with *Saccharomyces* fungemia is correct?
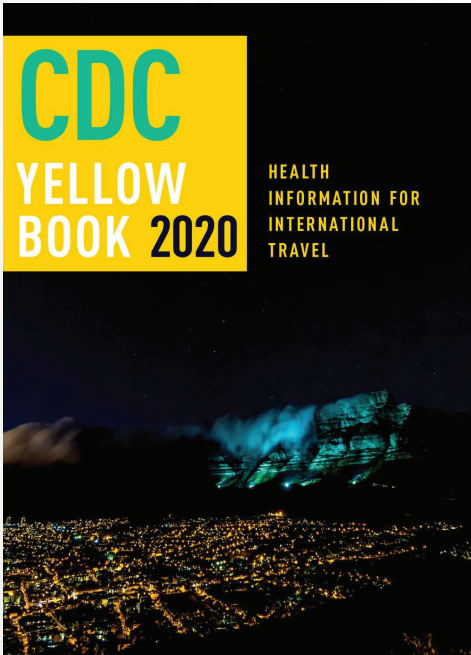
A. 20% of patients with *Saccharomyces* fungemia were using Sb probiotic yeast
B. Compared with control participants with bacteremia or candidemia, odds of Sb use by patients with *Saccharomyces* fungemia were doubled
C. 72% of patients with *Saccharomyces* fungemia had used antibiotics during the preceding 4 weeks, and 59% had a gastrointestinal disease
D. 12% of patients with *Saccharomyces* fungemia died

2. According to the retrospective registry study by Rannikko and colleagues, which of the following statements about the use of Sb probiotic yeast among patients with positive *Saccharomyces* culture findings in samples other than blood is correct?

A. Of 125 cases with known history regarding probiotic use, at least 24 (19%) were using Sb probiotic yeast, as were 2% (3/123) of control participants (OR = 10 [95% CI: 3, 32])
B. Most nonblood cultures positive for *Saccharomyces* were from the respiratory tract
C. Antifungal medication was already in use at the time of the positive culture in 18%
D. Nonblood cultures positive for *Saccharomyces* resulted in changes in antifungal therapy in 16%

3. According to the retrospective registry study by Rannikko and colleagues, which of the following statements about clinical implications of the use of Sb probiotic yeast among patients with *Saccharomyces* fungemia or other positive *Saccharomyces* culture findings is correct?

A. No safety issues were previously reported with probiotics
B. A 2017 meta-analysis of 5 studies of Sb use in adults showed significant prevention of *Clostridioides difficile* infection (CDI)
C. Sb probiotics are safe and effective for patients with possible compromise of gastrointestinal tract integrity
D. Sb probiotics are currently not recommended for patients who have indwelling catheters or who are immunocompromised or critically ill